Sustainable Approaches in the Synthesis of Organosulfur Compounds

By

Ashis Mathuri

CHEM11201904005

National Institute of Science Education and Research Bhubaneswar, Odisha – 752050

A thesis submitted to the
Board of Studies in Chemical Sciences
In partial fulfillment of requirements
for the Degree of

DOCTOR OF PHILOSOPHY

of

HOMI BHABHA NATIONAL INSTITUTE

April, 2023

Homi Bhabha National Institute[1]
Recommendations of the Viva Voce Committee

As members of the Viva Voce Committee, we certify that we have read the dissertation prepared by **Ashis Mathuri** entitled **"Sustainable Approaches in the Synthesis of Organosulfur Compounds"** and recommend that it may be accepted as fulfilling the thesis requirement for the award of Degree of Doctor of Philosophy.

Chairman - Dr. Sudip Barman	Sudip Barman	**Date:**	26.06.2023
Guide / Convener - Dr. Prasenjit Mal	Prasenjit Mal	**Date:**	26.06.23
Examiner - Prof. Ganesh Venkataraman		**Date:**	26.06.23
Member 1- Dr. Bidraha Bagh	Bidraha Bagh	**Date:**	26.06.23
Member 2- Dr. Subhadip Ghosh	Sghosh	**Date:**	26/6/23
Member 3- Dr. Ashis Biswas	Ashis Biswas	**Date:**	26/6/23

Final approval and acceptance of this thesis is contingent upon the candidate's submission of the final copies of the thesis to HBNI.
I/We hereby certify that I/we have read this thesis prepared under my/our direction and recommend that it may be accepted as fulfilling the thesis requirement.

Date: 26.06.23

Place:

Prasenjit Mal
(Dr. Prasenjit Mal)
Guide

Dr. Prasenjit Mal
Associate Professor
School of Chemical Sciences
National Institute of Science Education & Research
Jatni, Bhubaneswar-752050, Odisha, India

[1] This page is to be included only for final submission after successful completion of viva voce.

2

STATEMENT BY AUTHOR

This dissertation has been submitted in partial fulfillment of requirements for an advanced degree at Homi Bhabha National Institute (HBNI) and is deposited in the library to be made available to borrowers under rules of the HBNI.

Brief quotations from this dissertation are allowable without special permission, provided that accurate acknowledgement of source is made. Requests for permission for extended quotation from or reproduction of this manuscript in whole or in part may be granted by the Competent Authority of HBNI when in his or her judgment the proposed use of the material is in the interests of scholarship. In all other instances, however, permission must be obtained from the author.

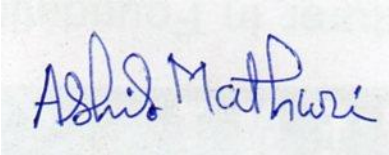

Ashis Mathuri

DECLARATION

I, hereby declare that the investigation presented in the thesis has been carried out by me. The work is original and has not been submitted earlier as a whole or in part for a degree / diploma at this or any other Institution / University.

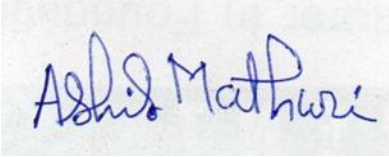

Ashis Mathuri

List of Publications arising from the thesis: (# Pertaining to The Thesis)

Journal Published

1. # **Mathuri, A.**; Pramanik, M.; Mal, P.; *J. Org. Chem.* **2022,** *87* (10), 6812-6823.

2. # **Mathuri, A.**; Pramanik, M.; Parida, A.; Mal, P. *Org. Biomol. Chem.,**2021***, 19, 8539-8543.

3. Pramanik, M. †; # **Mathuri, A.** †; Mal, *P.; Org. Biomol. Chem.* **2022,** *20* (13), 2671-2680.

. († Equal Contributed)

4. Pramanik, M.; **Mathuri, A**.; Mal, P., *Chem. Commun.* **2021,** *57*, 5698-5701.

5. Pramanik, M.; **Mathuri, A.**; Sau, S.; Das, M.; Mal, P.; *Org. Lett.* **2021,** *23* (20), 8088-8092.

6. Pramanik, M.; Choudhuri, K.; **Mathuri, A.**; Mal, P., *Chem. Commun.* **2020,** *56*, 10211-10214.

Manuscript Communicated

7. # **Mathuri, A.**; Pramanik, M.; Pal, B.; Mal, P., "Chemodivergent Chalcogenation of Aryl Alkynoates or *N*-Arylpropynamides using 9-Mesityl-10-Methylacridinium Perchlorate Photocatalyst" **(*manuscript submitted*)**

8. # **Mathuri, A.**;† Pal, B.†; Pramanik, M.; Manna, A.; Mal, P.; "C-H Chalcogenation by a Bromide Rich and Environmentally Benign Orthorhombic $CsPbBr_3$ under Visible Light, Polar Media and Aerobic Condition" **(*manuscript submitted*)**

CONFERENCE AND PRESENTATIONS

1. **Oral Presentation:** Emerging Infectious Diseases & Therapeutics Strategies (MedChem-2021) at department of chemistry in Indian Institute of Technology, Madras, on (1-3)th December 2021, Title: 'Disulfide Metathesis *via* Sulfur…Iodine Interaction and Photoswitchability'
2. **Oral Presentation:** International Conference on the Ancient Indian Knowledge System for Holistic Development (CVRU-CON-2022) at Science and Technology (Chemical Sciences) Department of Chemistry, Dr. C. V. Raman University, Chhattisgarh (India) on (28-29)th January 2022, Got the 1st Position, Title: 'Disulfide Metathesis *via* Sulfur…Iodine Interaction and Photoswitchability.'
3. **Oral Presentation:** International Conference on Indo-German Higher Education Partnerships Development (IGP-2023) at Department of Chemistry, IIT Indore, India on (22-23)th February 2023, Got the Best Award, Title: 'Controlling Reactivity of Alkynes for C-X(S, O, Cl) Bond Formations'

4. **Poster Presentation:** International Conference on Materials for the Millennium (MatCon-2021) at Department of Applied Chemistry in the Cochin University of Science and Technology on (15-19)th March 2021, Title: 'Visible Light Mediated Oxidative C-O bond Functionalization of Benzyl Alcohols'

5. **Poster Presentation:** International Conference on Recent Development of Chemistry (RDC-2021) at Department of Chemistry in NIT Durgapur on (3-5)th March 2021, Title: 'Dithioacetalization or Thioetherification of Benzyl Alcohols by Visible Light Photocatalyst'

6. **Poster Presentation:** International Conference on the Present and Future of Excellence in Organic Synthesis (PFEOS-2021) at Department of Chemistry, Tezpur University, Assam on (7-8)th January 2021, Title: 'Dithioacetalization or Thioetherification of Benzyl Alcohols by Visible Light Photocatalyst'

7. **Poster Presentation:** 1st HBNI Interaction Meeting in Chemical Sciences, NISER, Bhubaneswar on (18-20)th January 2023, Title: 'Controlling Reactivity of Alkynes for C-X(S, O, Cl) Bond Formations.'

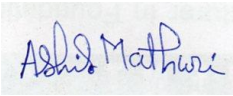

Ashis Mathuri

Dedicated
To

My Parents

ACKNOWLEDGEMENTS

I owe an unfathomable sense of gratitude to everybody who supports me throughout my work. I am sincerely thankful for their valuable guidance and constructive suggestion during the work. I am grateful to them for expressing their enlightening views and innovative idea to stabilize the work.

First of all, from the core of my heart, I would like to convey my earnest gratitude to my mentor Dr. Prasenjit Mal for his constant support, valuable guidance, and prompt suggestions throughout my research career. His judicious advice, scholarly presentation, meticulous inspection have helped me to accomplish my research work to a great extent. I want to express my gratefulness to Prof. Dr. Sudip Barman, Dr. Subhadip Ghosh, Dr. Bidraha Bagh and Dr. Ashis Biswas, who stand for the doctoral committee.

I also wish to express my sincere thanks to Prof. T. K. Chandrashekar, founder Director, NISER, and Prof. Sudhakar Panda, Director, NISER, for the laboratory facilities and off course, Department of Atomic Energy (DAE) India, for CSIR financial support.

It is my great privilege to thank Dr. Himanshu Sekhar Biswal and Sharnappa Nembenna Chairperson of SCS. I would also like to thank all other faculty members and staff profusely. I am also greatly obliged to Prof. T. K. Chandrashekar, Dr. Sudip Barman, Dr. Bidraha Bagh, Dr. N. K. Sharma, Dr. C. S. Purohit, Dr. P.C Ravikumar, Dr. Moloy Sarkar and Dr. Chidambaram Gunanathan who taught me the subject very well.

I express my warm thanks to my lab mates Dr. Debdeep Maiti, Dr. Saikat Maity, Dr. Anima Bose, Dr. Khokan Choudhuri, Dr.Anupam Manna, Dr. Toufique Alam, Dr. Ankita Bal, Dr. Shyamal Kanti Bera, Dr. Sudip Sau, Dr. Amarchand Parida, Dr. Monojit Das, Dr. Soumya Maiti,

Keshab, Himangshu, Vrittik, Soumya, Ankit, Supratim, Kushal (M.Sc) for their constant encouragement, cheerful company and thoughtful discussions. I thank all my NISER friends, especially Dr.Milan Pramanik for sharing frustration and happy moment.

I wish to express my special appreciation to my elder brother, Debdas Mathuri, who has always been a source of my strength, inspiration, and my achievements throughout my career endeavor.

Finally, I would like to convey sincere tribute to my beloved parents (Anjan Mathuri, Tara Rani Mathuri) for their constant support, unmatchable love, faith, affection, and encouragement all through the years, all the time, all the moment.

…….Ashis Mathuri

CONTENTS

SUMMARY

Organosulfur compounds are widely found in agrochemicals, pharmaceuticals, pesticides, medical chemistry, and material science. Therefore, the research area on carbon–sulfur bond formation reaction is becoming an attractive research field in organic chemistry. In this context, the central focus of this thesis describes the sustainable approaches towards C-S bond formation and metathesis reactions in organic synthesis. However, various sustainable tactics like (i) using ^{t}BuOLi (tert-butoxide) in ethanol can act as radical initiators for the thiols, (ii) cascaded oxidative sulfonylation of *N*-propargylamine *via* a three-component coupling reaction using DABCO·$(SO_2)_2$ (DABSO). 3-Arylsulfonylquinolines were obtained by mixing diazonium tetrafluoroborate, *N*-propargylamine, and DABSO under argon atmosphere in dichloroethane (DCE) for 1 h, (iii) The synthesis of diaryl sulfides and a diaryl selenide using orthorhombic $CsPbBr_3$ perovskite nano-crystal (NC) obtained from bromide precursor dibromoisocyanuric acid, can work efficiently as a visible light photocatalyst (blue LED, 5 mol % and TON ~ 18.11) under O_2 atmosphere and in acetonitrile (dielectric constant ε ~ 37.5), and (iv) cascaded chalcogenation of aryl alkynoates or *N*-arylpropynamides using 9-mesityl-10-methylacridinium perchlorate as a visible light photocatalyst to obtain selectively, either 3-sulfenylated/selenylated coumarins or spiro[4,5]trienones, and (v) *N*-Iodosuccinimide (NIS) promoted Sulfur…Iodine (S…I) interaction controlled a cross-metathesis reaction of symmetrical disulfides to unsymmetrical disulfides.

	LIST OF TABLES	**Page No.**

List of Abbreviations Used

Å	Angstrom
Ac	Acetyl
AcOH	Acetic Acid
Anhyd	Anhydrous
aq	Aqueous
Bn	benzyl
br	Broad

Bz	Benzoyl
ºC	Degree Celcius
Calcd	Calculated
cm	Centimeter
Conc	Concentrated
Cy	Cyclohexyl
d	Doublet, Days
DCE	1,2-Dichloroethane
DCM	Dichloromethane
dd	Doublet of a Doublet
dil	Dilute
DTBP	Di-tert-butyl peroxide
DMF	*N*,*N*-Dimethyl Formamide
DMSO	Dimethyl Sulfoxide
DTBP	Di-tert-butyl peroxide
DFT	Density Functional Theory
equiv	Equivalent
ESI-TOF	Electrospray ionization time-of-flight
Et	Ethyl
EtOAC	Ethyl Acetate
g	Grams
h	Hours
HFIP	1,1,1,3,3,3-Hexafluoro-2-propanol
HRMS	High-Resolution Mass Spectrometry
Hz	Hertz
IR	Infrared
lit	Liter
m	Multiplet
NIS	*N*-iodosuccinimide
NCS	N-chlorosuccinimide
M	Molar

MeCN	Acetonitrile
mp	Melting point
Me	Methyl
Min	Minutes
mL	Milliliter
mmol	Millimole
mol	Mole
MS	Mass Spectra, Molecular Sieves
M/Z	Mass to charge ratio
nm	Nanometer
NMR	Nuclear Magnetic Resonance
PIDA	Phenyliodine(III) diacetate
Py	Pyridine
rt	Room Temperature
s	Singlet, Seconds
t	*tert*
TBHP	Tert-Butylhydroperoxide
TEMPO	(2,2,6,6-Tetramethylpiperidin-1-yl)oxyl
TEC	Thiol-Ene-Click
TFE	2,2,2-Trifluoroethanol
TLC	Thin Layer Chromatography
TMS	Trimethylsilyl
Ts	*p*-Toluenesulfonyl
TFA	Trifluoroacetic acid
TYC	Thiol-Yne-Click
XRD	X-Ray Diffraction

CHAPTER 1

An Overview of C-S Bond Formation Reactions and Visible-light Photocatalysis

1.1 ABSTRACT

The chapter is divided into three major sections: (i) sulfur's Importance in daily life (ii) Using various reagents and how they work in C-S bond formations (iii) Disulfide metathesis reactions. Based on the sustainable strategies, the second part is similarly divided into sub-categories. (i) Some common organo-sulfur reagent mediated C-S bond formations (ii) iodine reagent mediated C-S bond formations (iii) C-S bond formation through electrochemistry (iv) importance of visible-light-driven photocatalytic to C-S bond formations. An overview of the present thesis' research area is provided as a brief conclusion to the chapter.

.

1.2 INTRODUCTION

It has been known from the beginning of time that sulfur is the fifth-highest element on earth[1] and the tenth most abundant element overall. It is found on earth as a sulfate mineral and also exited in a pure native form. Hot springs, hydrothermal vents, salt domes, volcanic emissions, and other places on Earth contain mainly elemental sulfur.[2] The sulfur-containing substance that is produced in the greatest amounts worldwide is sulfuric acid, which has a wide range of uses outside of the chemical industry.[3-4] Sulfur was employed as a source of fire in religious rituals in ancient India, China, Greece, and Egypt. Also known as brimstone[5], or burn stone. Antoine Lavoisier, an alchemist, discovered in 1777 that sulphur is an element but is not a compound due to the combustibility principle. Subsequently, Joseph Gay-Lussac and Louis

Thenard, two French chemists, imagined its elemental characteristics. Sulfur is an element with the atomic number 16 and the letter "S" as its symbol. It mainly fit in to p-block, group 16 in the periodic table with electronic configuration [Ne] $3S^2\ 3P^4$. As a result, the usual oxidation state of sulphur ranges from -2 to +6. Nonetheless, with the exception of noble gas, Sulphur can form a stable compound due to its electropositivity, size, and amphoteric behaviour. The ability of sulphur to mix with Xenon to create at least meta-stable molecules has been also established.[6] Sulfur can also combine with electronegative elements to generate multivalent compounds containing oxygen[7], nitrogen[8], pseudo halide[9,] or sulfur[10] as well as form pseudohalides such as sulfonates ((tosylates, mesylates, triflates and flurosulfates amongst others).[11-13] As an allotrope, sulphur produces octasulfur and Sulfur dioxide is produced during its burning when a blue flame is present. In addition, application of photoredox-organocatalysis for C-S bond synthesis will be discussed.

1.3 SULFUR IN DAILY LIFE

All living things contain sulphur, one of the fundamental components. It is also the third most prevalent mineral in the human body after calcium (Ca) and phosphorus (P). Organosulfur compounds, which can be found inside the body, like proteins[14], amino acids[15], etc. Cysteine and methionine are two of the twenty amino acids that contain sulfur. Biotin and Thiamine are two vitamins that include sulphur. According to the National Academics Food and Nutrition Board, an adult need between 0.2 and 1.5 g of sulfur daily. Our natural environment always provides us with an abundant amount of sulfur[16] in the form of fruits and vegetables. (Figure 1.1).

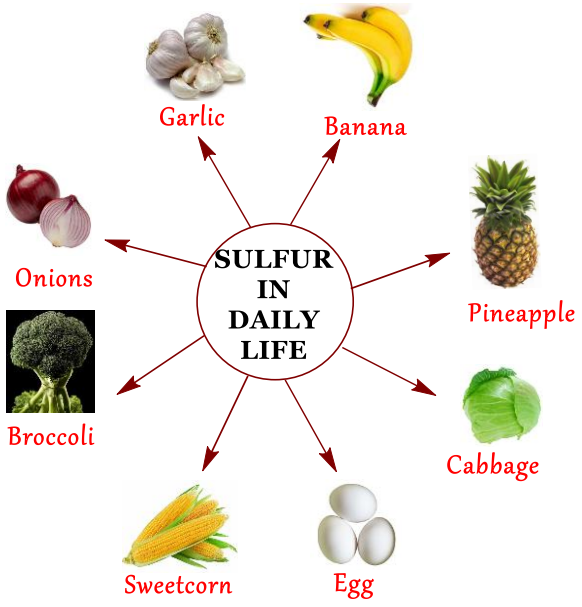

Figure 1.1. Examples of natural organo-sulfur compound used in daily life.

Furthermore, organosulfur compounds are pervasive in a wide range of natural products and are extensively utilized in the pharmaceutical sector, agrochemicals, material sciences, and medical sciences.[17-19] Some of the commercial drug candidates, such as omeprazole, penicillin V, amoxicillin, ATI2 (Ativan), and Nelfinavir, etc., are used to treat conditions including bacterial infection, anxiety, HIV, and gastric illness, etc. (Figure 1.2).

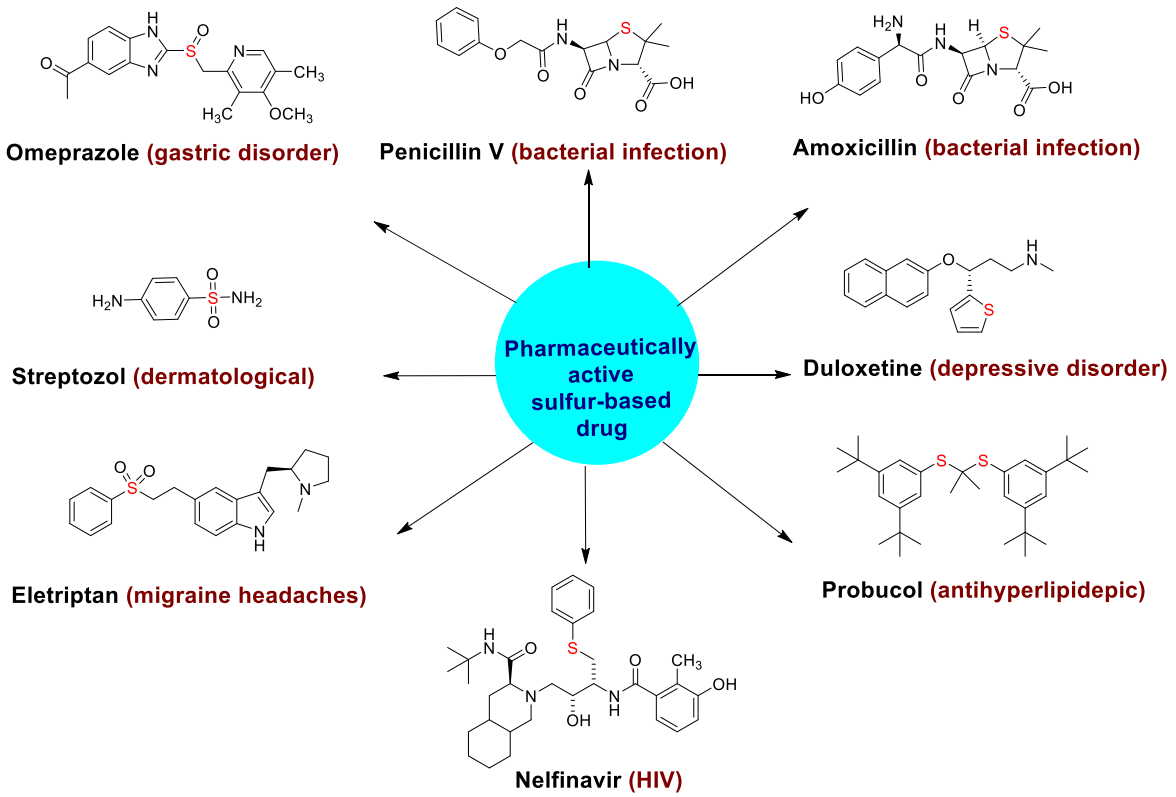

Figure 1.2. few examples of sulfur-based medicines with pharmacological activity.

1.4 PRECURSORS OF SULPHUR AND THEIR APPLICATION IN C-S BOND FORMATION REACTIONS

Precursors for the preparation of organosulfur compounds are mainly classified into two categories: a) organo-sulfur reagents such as thiophenol, disulfide, and aryl sulfonyl hydrazide, etc. b) salt of sulfur such as $PhSO_2Na$, Na_2S, and NH_4SCN etc. Herein, we've mostly talked about the organo-sulfur precursors that are employed to create C-S bonds under benign reaction condition.[20] Figure 1.3 displays examples of organo-sulfur reagents (diphenyl disulfide, thiophenol, elemental sulfur, thiosuccinimide, DABSO, sulfonyl hydrazide, thiobenzoic acid, sulfonyl chloride, dimethyl sulfoxide, sulfonic acid etc.) used in C-S bond formation reaction. However, we chose at random a few samples of organo-sulfur precursors that are readily available commercially or that are very simple to make.

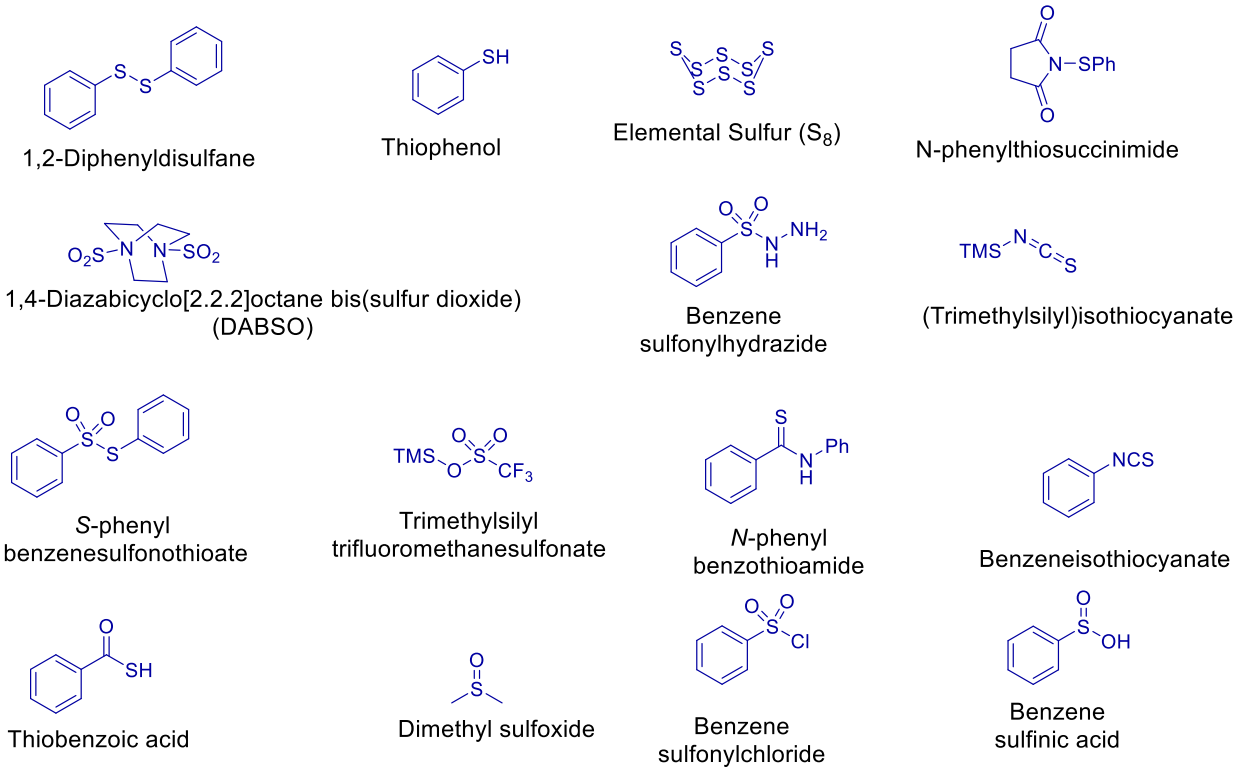

Figure 1.3. Commonly used sulfur precursors for C-S bond formation reactions.

The usage of dangerous chemicals in the chemical industry is one kind of pollution that constantly poses serious problems for our world. Finding new sustainable resources that can reduce global pollution is therefore urgently needed. In order to create greener techniques of creating an organic molecule, the experimental chemist is making an unrelieved attempt to imagine a novel reactivity archetype.[21-22] Therefore, we have herein considered methodologies for C-S bond formation reaction in terms of sustainable chemistry. The examples are classified into four categories: (i) Some common organo-sulfur reagent mediated C-S bond formations (ii) iodine reagent mediated C-S bond formations (iii) C-S bond formation through electrochemistry (iv) importance of visible-light-driven photocatalytic to C-S bond formations.

1.4.1 Some common organo-sulfur reagent mediated C-S bond formations

1.4.1.1 Elemental Sulfur

The odourless, colourless solid form of elemental sulphur[2, 23] dissolves in carbon disulfide. In general, it is employed to create C-S bonds since it is readily available and affordable. Typically, natural sources like crude petroleum, minerals, etc. contain the elemental sulphur. The allotropic forms of elemental sulphur include rhombic, octahedral, monoclinic, prismatic, and α or β-sulfur. According to several literature publications, a lot of organic reactions have utilized elemental sulphur (S8). Many studies show that elemental sulphur (S8) has been widely used in a variety of organic reactions.[8]

Retailleau and coworkers have synthesized 2-benzoylbenzothiophenes derivative from 2-nitrochalcones by using elemental sulfur and diisopropyl ethylamine (DIPEA) as activator under heating at 80 °C (Scheme 1.1).[24]

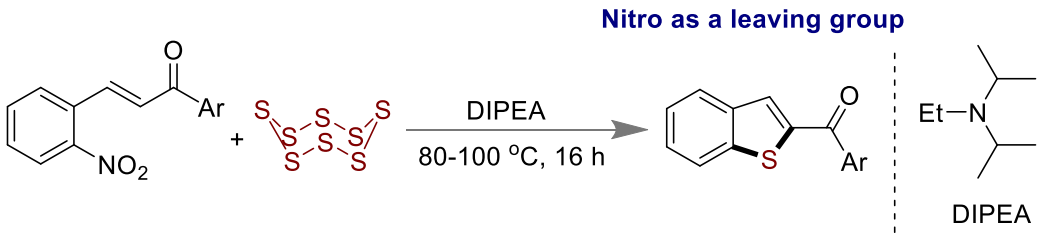

Scheme 1.1 Retailleau's approach for substituted benzothiophenes formation.

1.4.1.2 Thiophenol

Thiophenol is foul smelling colorless liquid, acidic in nature with Pk_a value 6.62.[25] The oxidation state of sulfur in thiophenol is +2. It can possess nucleophilic as well as electrophilic character[26] due to the presence of two sets of lone pair of electrons and vacant 3d orbital. Thiophenol could be easily prepared by the reduction of sulfonyl chloride with metallic zinc in acidic medium.

1.4.1.3 *N*-phenylthio-succinimide

N-Phenylthio-succinimide is a colorless solid. It is used as sulfur precursor for the cleavage of N-S bond *via* single electron transfer (SET) in acidic condition. It is prepared by the reaction of thiophenol and succinimide in presence of sulfuryl chloride and triethyl amine in anhydrous DCM at 0 ^{o}C (Scheme 1.2).

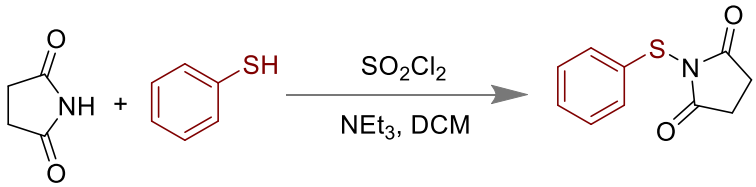

Scheme 1.2 Preparation of *N*-phenylthio-succinimide.

Cossy and coworkers developed TFA (Trifluoro acetic acid) promoted regioselective C(Sp^2)-H sulfenylation of electron rich arene by using *N*-(arylthio)-succinimides as sulfur surrogate at room temperature (Scheme 1.3).[8]

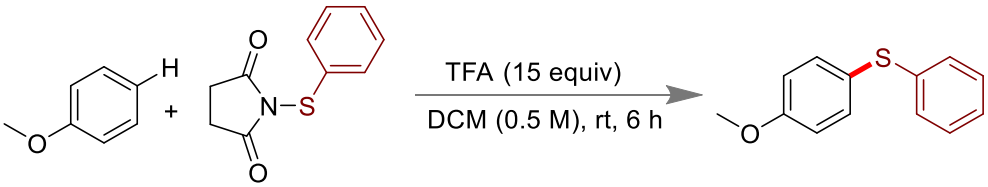

Scheme 1.3 Cossy's regioselective C-H sulfenylation.

1.4.1.4 1,4-Diazabicyclo[2,2,2]octane bis(sulfur dioxide) adduct (DABSO)

DABSO is a white, crystalline solid that is bench stable and mostly soluble in organic solvents.[27] The oxidation state of sulfur in DABSO is +4. It is typically utilized as a substitute source of gaseous SO_2 in Synthesis. DABSO was prepared by the combination of DABCO and gaseous SO_2 to form a charge transfer white crystalline solid.

Wu and his group Wu and his team developed a three-component tandem technique for the Synthesis of 3-sulfonated coumarins derivatives by combining aryldiazonium salt, DABSO,

and aryl propiolates in a DCE solvent at 60 °C (Scheme 1.8).[28] According to kinetics and experimental studies, the reaction was carried out by the treatment of aryldiazonium tetrafluoroborates and DABSO via the production of charge-transfer complexes.

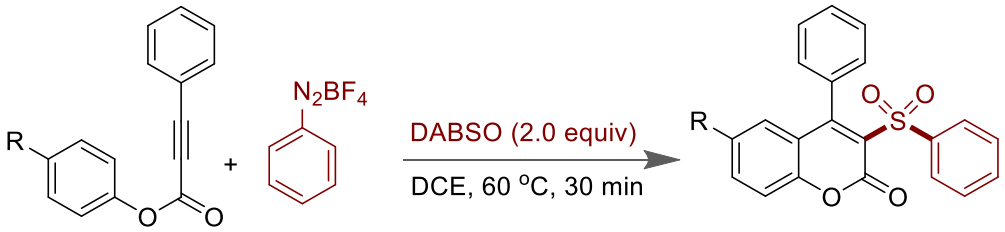

Scheme 1.4 Wu's report for 3-sulfonated coumarins synthesis.

1.4.1.5 Sulfonyl Hydrazide

Sulfonyl Hydrazide is a colorless crystalline solid and basic in nature with pKa of 17.1.[29] The oxidation state of sulfur in sulfonyl hydrazide is +6. Sulfonyl hydrazides are readily accessible, have been utilized as thiyl source for sulfonylating reactions[30] by the breaking of S-N bond. It can be easily prepared by the combination with sulfonyl chloride and hydrazide hydrate solution in THF at 0 °C (Scheme 1.5).

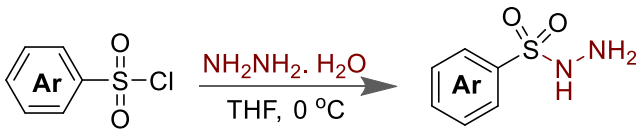

Scheme 1.5 Preparation of sulfonyl hydrazide.

Tian and coworkers created a method for selectively sulfenylating indoles utilising molecular iodine and sulfonyl hydrazide as the sulphur precursor. (Scheme 1.6).[31] Sulfonyl hydrazide decided to break down into a sulfenium ion intermediate when catalytic amounts of iodine were present, and this intermediate was then trapped by indole at the 3 positions via an electrophilic aromatic substitution reaction to create a variety of structurally different indole thioether derivatives.

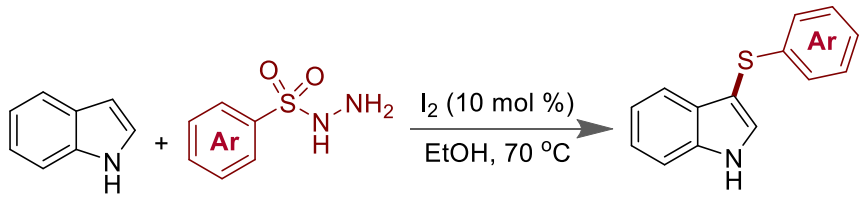

Scheme 1.6 Tian's approach for regioselective sulfenylation of indoles.

1.4.1.6 (Trimethylsilyl)isothiocyanate (TMSNCS)

(Trimethylsilyl)isothiocyanate (TMSNCS) is a light-yellow liquid that decomposes when it comes into contact with water. It has an offensive strong smell. TMSNCS is used as a versatile reagent in organic Synthesis. The -NCS being an ambidentate chelating ligand, generally used for the introduction of thiocyanate or isothiocyanate groups in Synthesis. Also, it can be utilized to make nitrogen-containing heterocycles by co-coordinating with both the chelating center (N, S). It can be prepared by the treatment of trimethylchlorosilane (TMSCl) with excess of silver isothiocyanate in inert solvents at 80 °C.

Fu and coworkers developed isothiocyanatoalkylthiation of olefins using *N*-phenylthio-succinimide and trimethylsilyl isothiocyanate in DMF under inert condition heating at 90 °C (Scheme 1.13).[32] The transformation starts with the formation classical sulfenium ion intermediate by the treatment of *N*-phenylthio-succinimide with styrene, which was trapped by TMSNCS through the hard nucleophilic center (-NCS) to afford isothiocyanatoalkylthiation product.

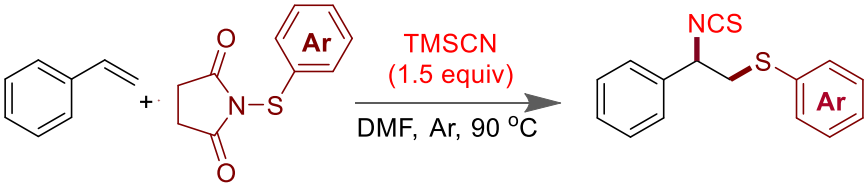

Scheme 1.7 Fu's approach for isothiocyanatoalkylthiation of styrene.

1.4.2. C-S bond formation processes under the influence of iodine reagents.

Since 1960[17], the synthetic toolbox for organic research has greatly increased due to the development of transition metal-catalyzed carbon-sulfur (C-S) bond forming reactions. Here, the main emphasis has been on the C-S coupling reaction's usage of several iodine reagents. Also, we have listed some of the iodine reagents that are frequently employed in oxidative C-S coupling. (Figure 1.4).

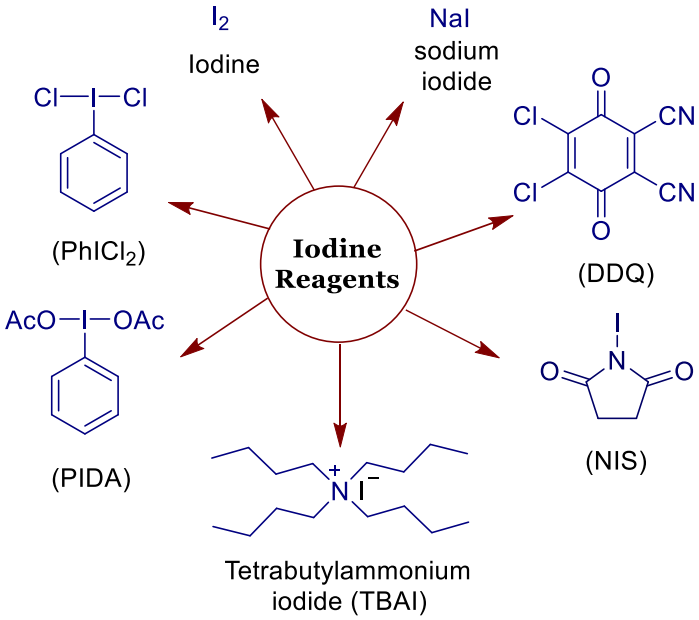

Figure 1.4. Iodine reagents used for C-S coupling reactions.

1.4.2.1. $PhICl_2$ mediated Synthesis of sulfenylated isocoumarins.

A regioselective synthesis of sulfenylated isocumarins using disulfides as sulfenylating agents and $PhICl_2$ as an oxidant was recently demonstrated by the Du group (Scheme 1.1)[33]. In the presence of the iodine reagent, aryl sulfenyl chloride generated a cyclic intermediate as explained below. After then, the creation of the finished product could result via intramolecular cyclization by a nearby oxygen.

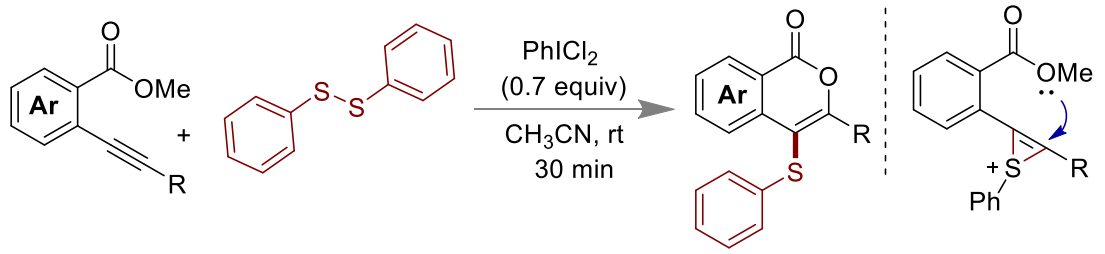

Scheme 1.8 Lei's approach for Synthesis of sulfenylated isocoumarin.

1.4.2.2 NIS mediated Synthesis of vinyl sulfone

Mal and coworkers developed extremely regio- and stereoselective C(sp2)-H sulfonylation of styrenes utilising sulfonyl hydrazide as a sulphur substitute. NIS performs two functions in this reaction. By the cleavage of the S-N bond, it was used to produce sulfonyl radical from sulfonyl hydrazides, and in the last step, it serves as the iodine source to create *β*-iodosulfone intermediate which would decomposed to formed vinyl sulfone in presence of K_2CO_3 .[34]

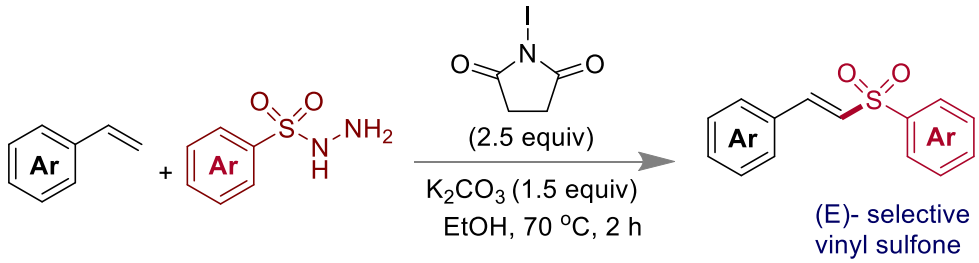

Scheme 1.9 Mal's approach for stereoselective C(sp2)-H sulfonylation of styrenes

1.4.2.3 TBAI mediated thioesterification of a methyl ketone.

A direct C_{sp3}-H thioesterification of methyl ketones was demonstrated by Yan and co-worker using TBAI/ $K_2S_2O_8$ as reaction controller (Scheme 1.5)[35]. They have demonstrated that the addition of TBAI and $K_2S_2O_8$ to the SET process could aid in producing the target product, -keto thioesterification, which then underwent oxidation and produced a C-S linked product

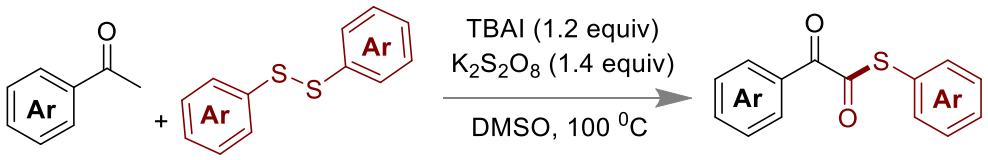

Scheme 1.10. Yu's report for oxidative thioesterification of methyl ketones.

1.4.2.4 Iodine catalyzed Synthesis of thioethers.

Iodine mediated C(Sp^2)-H bond functionalization of naphthols is developed by Huang and coworkers, for the Synthesis of thioether by using sulfonyl hydrazide as sulfur precursor in THF at 100 ^{o}C (Scheme 1.11).[36] This reaction was started with the *in-situ* generation of thiyl cationic intermediate from sulfonyl hydrazide *via* cleavage of S-O and S-N bond, and followed by nucleophilic attack of naphthol's to obtain the products.

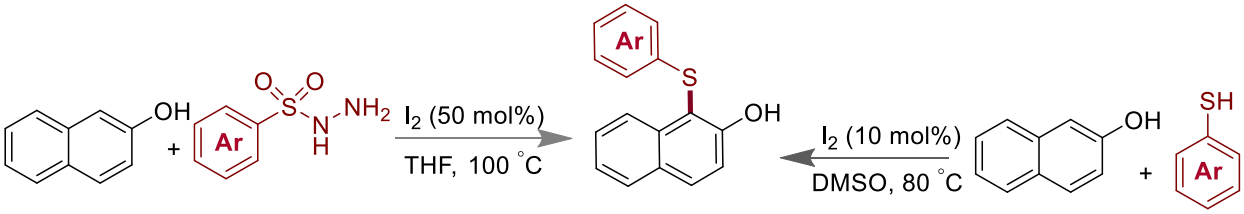

Scheme 1.11. Iodine catalyzed thioether synthesis.

Later, Peddinti group have expanded the scope, for the Synthesis of thioether by using thiophenol as sulfur precursor *via* umpolung strategy form readily available thiophenol derivative and electron rich scaffold.[37]

1.4.2.5 PIDA mediated Synthesis of arylthioer and aryl sulfoxide.

Mal and coworkers have demonstrated that the production of the intermediate sulfenium ion allows for the Synthesis of either thioethers or diaryl sulfoxides from electron-rich arenes and thiophenols. (Scheme 1.12).[38] However when thiols and the iodine(III) reagent PhI(OAc)$_2$ (PIDA) were combined in HFIP, sulfenium ions were produced. Diaryl sulphide was produced as a result of aromatic electrophilic substitution (EArS) between the sulfenium ion and an electron-rich arene. The subsequent addition of too much PIDA aided in the oxidation of the

sulphur core, resulting in the production of diaryl sulfoxides as a byproduct. Also, they believed that HFIP maintained the sulfenium ion intermediate by hydrogen bonding. The fact that HFIP could ionise PIDA in addition to possessing an excellent hydrogen bonding capability aided in the acceleration of the EArS reaction with electron-rich arenes.

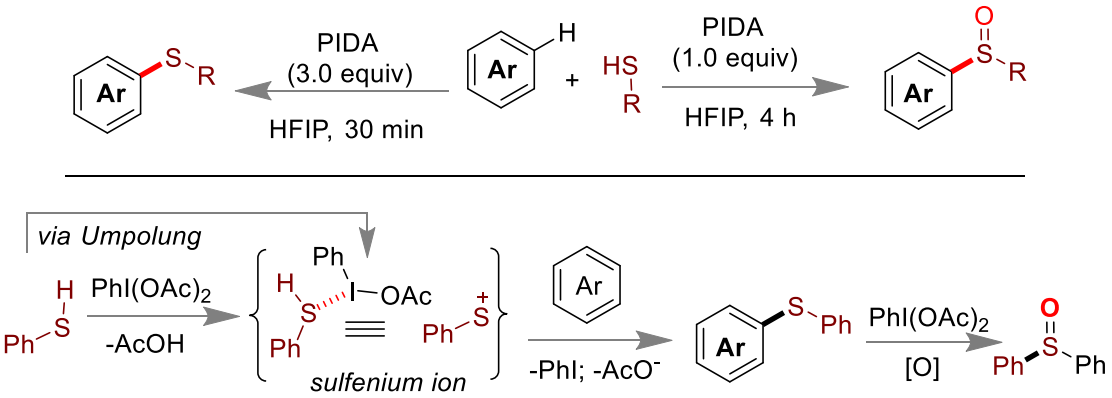

Scheme 1.12. Mal's approach for dehydrogenative C-S coupling of arene and thiol.

1.4.2.6 NaI mediated Sulfenylation of arenes or heteroarene

demonstrated an air-based oxidant-catalyzed NaI catalysed technique for the sulfenylation of arenes and heteroarenes. Controlled investigations proved that the transition requires both NaI and air. A wide variety of aryl thiols were produced in excellent yields throughout the 16-hour reaction in DMSO at 120°C.

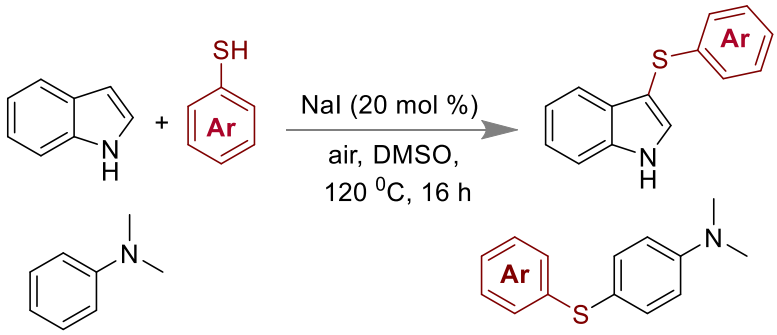

Scheme1.13. Wang's approach NaI mediated Sulfenylation of arenes or heteroarenes

.

1.4.2.7 DDQ mediated cross coupling reactions.

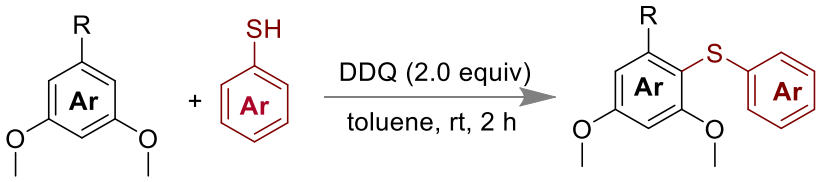

Scheme1.14. Lei's approach DDQ mediated cross coupling reactions

The Lei group revealed in 2016 that 2,3-dichloro-5,6-dicyano-1,4-benzoquinone (DDQ) mediated a radical–radical cross-coupling reaction between electron-rich arenes and thiols via cation-radical intermediates for the Synthesis of diaryl thioethers.[39] A wide variety of aryl thiols were produced in excellent yields throughout the 2 h reaction in toluene at room temperature.

1.4.3 Electrochemical oxidative C-S bond formation reaction.

Since that more people are becoming conscious of the need to conserve renewable energy due to global warming, it is crucial to cut down on chemical waste in organic synthetic methods. Electrochemical synthesis is a viable approach to reduce the use of chemicals, especially dangerous ones. Here is a discussion of a few recent electrochemical oxidative reactions that create C-S bonds.

1.4.3.1 Vicinal di-functionalization of olefin.

In 2018, Lei's group demonstrated an electrochemical oxidative oxysulfenylation and aminosulfenylation of olefins using thiophenol as a C-S coupling partner under 12 mA current in an undivided cell (Scheme 1.29)[40]. This oxidative strategy could be applied for hydroxysulfenylation and acyloxysulfenylation of alkenes, as shown in the scheme. Authors have suggested that oxidation of thiophenol at carbon anode helped to generated thiyl radical. Subsequently, the addition of thiyl radical to olefin produces a radical intermediate, which was

oxidized to generate a cationic benzyl intermediate. Finally, the nucleophilic attack by a nucleophile on carbocationic intermediate helped to get the desired product. On the other hand, concomitant cathodic reduction at platinum electrodes led to H_2 evaluation.

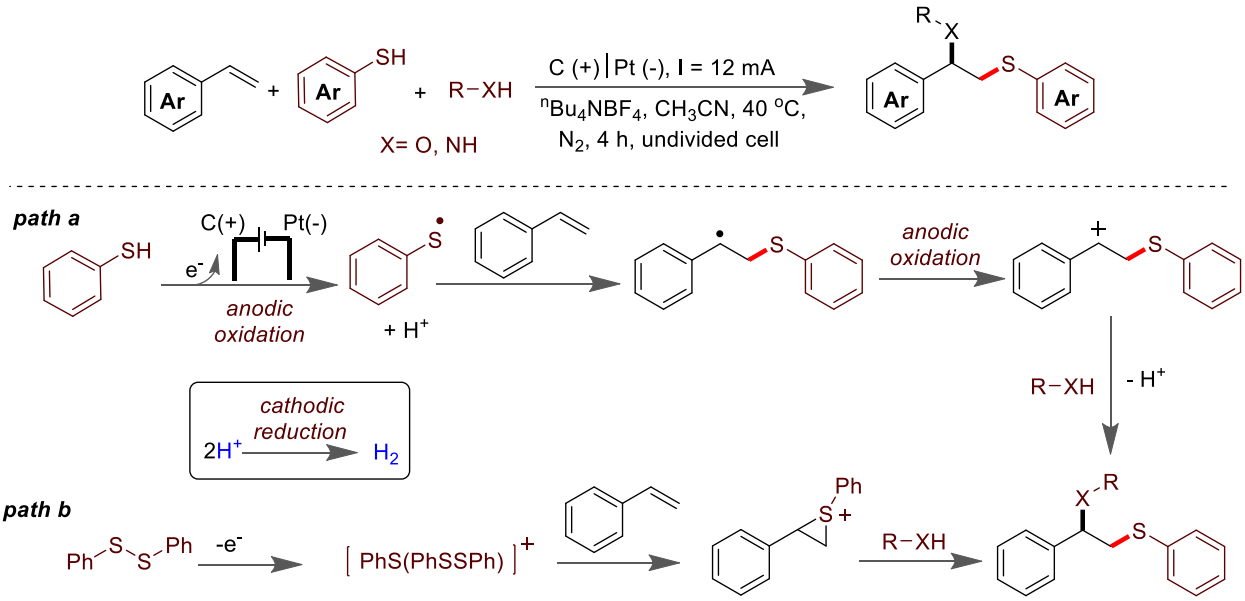

Scheme 1.15. Electrochemical difunctionalization of olefins.

1.4.3.2 Benzothiazole synthesis from α-keto acid.

Benzothiazoles are recognized as an important category of scaffold which is found in many biologically active molecules. Therefore, synthesis of benzothiazole using mild reaction conditions is always desirable. In 2016 Huang's group realized an electrochemical decarboxylative synthesis of substituted benzothiazoles from α-keto acids when 2-amino thiophenol was used as another coupling partner (Scheme 1.33)[41]. In this work, the authors have used Pt-Pt combination as cathode and anode in 0.2 M ammonium perchlorate as an electrolyte in the presence of 5 mA current for this oxidative cyclization reaction.

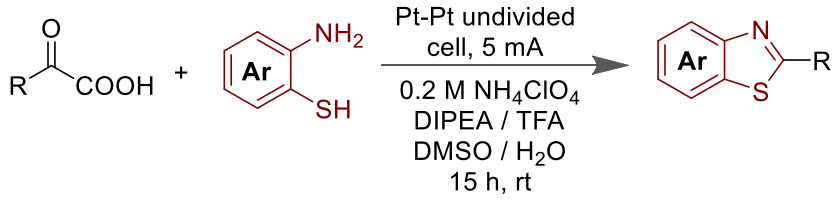

Scheme 1.16. Electrochemical decarboxylative benzothiazole synthesis.

1.4.4 Visible light-driven photocatalytic C-S bond formation reaction.

Visible-light-driven photocatalysis has been regarded as one of the key techniques in organic Synthesis because photons' energy may be easily transformed into chemical energy.[42-43] Moreover, the photocatalyst participates in the single electron transfer (SET) process, a promising alternative approach for green chemistry. Many of the photocatalysts such as eosin Y, rose bengal, benzophenone, riboflavin, etc. has been employed for a wide range of elegant C-S bond formation reaction (Figure 1.5). The majority of the photocatalyst displayed below possesses substantial visual absorption, a lengthy lifetime in the excited state, and stability in photolytic conditions.

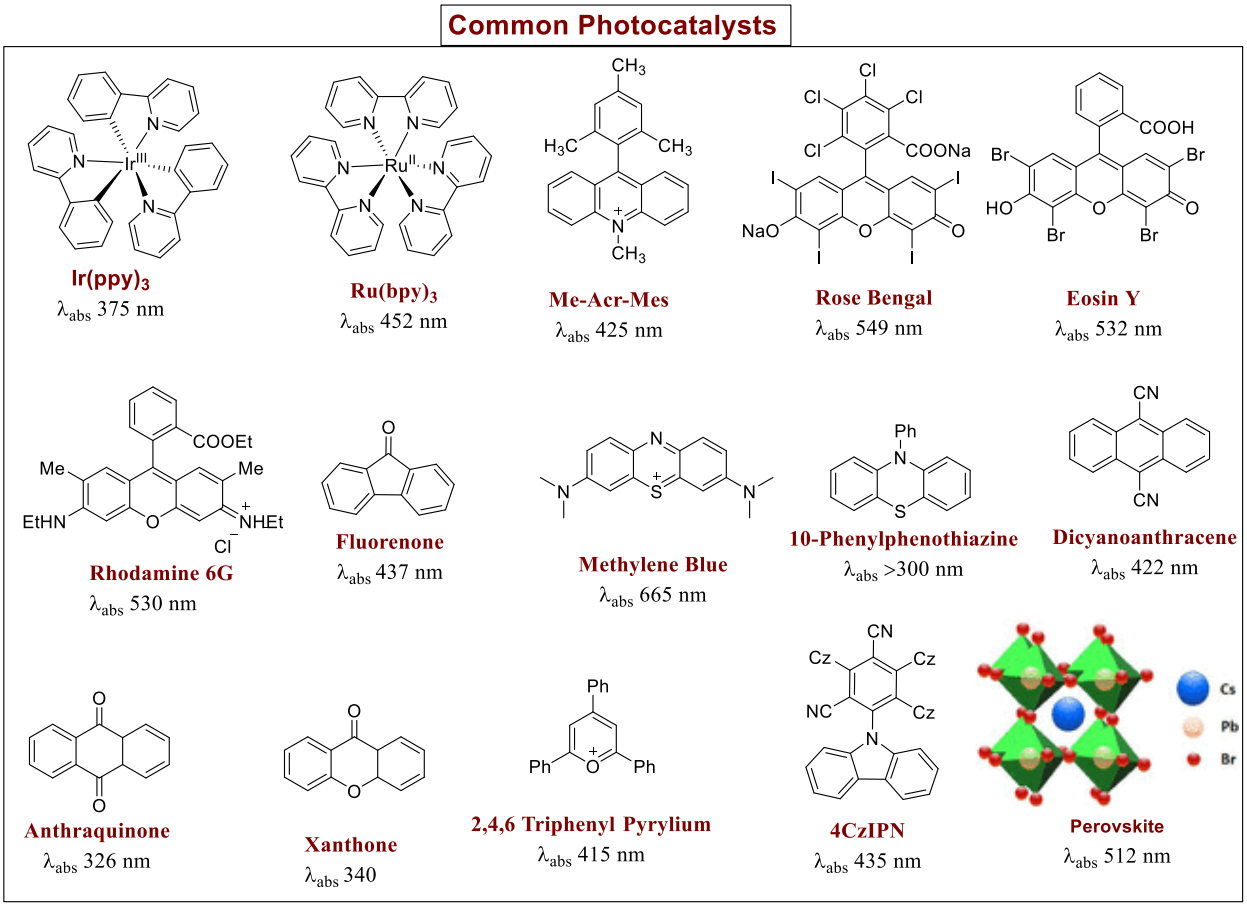

Figure 1.5. Common photocatalyst used in C-S bond formation reaction.

A photocatalyst's typical function is to either transfer energy to a substrate or assist in a single electron transfer process. (Figure 1.6). However, it needs to be excited initially by irradiation of visible light, which can therefore participate in the oxidative-reductive or energy transfer process. During an oxidative cycle, the excited state photocatalyst (PC*) can be oxidized by an acceptor, which can take one electron from the photocatalyst. Following this, oxidized PC can acquire one electron from the substrate and returns to its ground state. Notably, the substrate, now short of one electron, can quickly react through a single electron transfer process.

Similarly, a photocatalyst also involves in a reductive cycle. In this case, the excited photocatalyst (PC*) can take up one electron from a donor and itself reduced. Reduced PC can give one electron to the substrate, making one extra electron available for reaction.

Simultaneously, the photocatalyst is regenerated. However, some recent photocatalytic oxidative and reductive C-S bond formation reactions are summarized below.

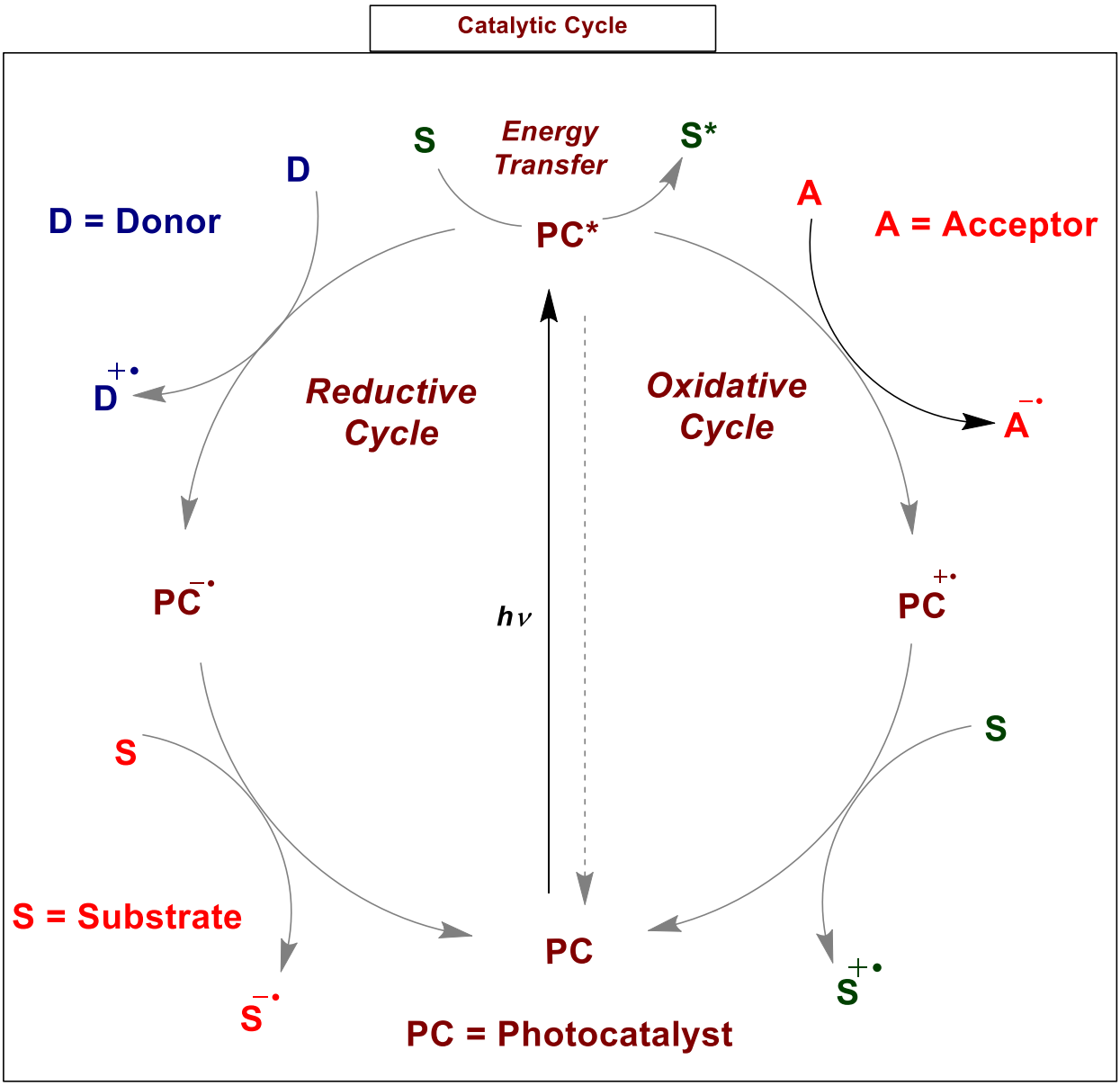

Figure 1.6. Function of a photocatalyst in the catalytic cycle.

1.4.4.1 Eosin Y as photocatalyst for *β*-ketosulfoxide from styrene.

In 2014, L.D.S Yadav group also introduced Eosin Y as a photocatalyst for the Synthesis of *β*-keto-sulfoxide from a radical addition reaction between thiols and styrenes (Scheme 1.21)[44]. In this reaction, molecular oxygen played a dual role: i) it was installed at the *β*-position of styrene ii) oxidation of sulfur center.

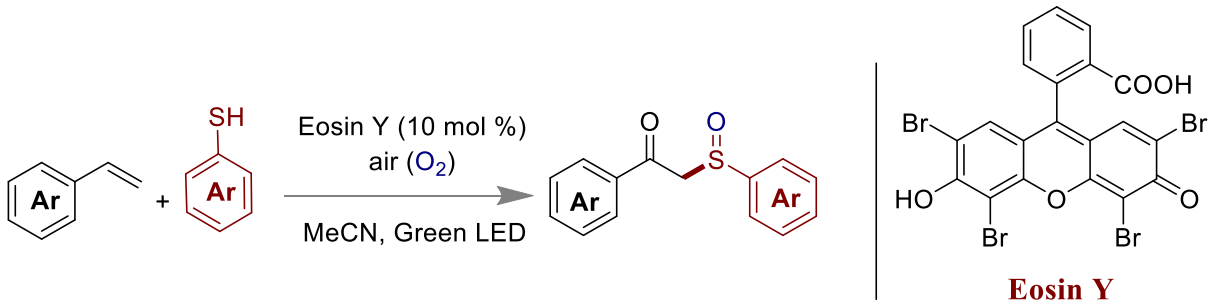

Scheme 1.17. *β*-Ketosulfoxide from styrene and thiols.

1.4.4.2 Benzophenone as photocatalyst for thiol-ene reaction.

Later on the same group envisioned that visible light-mediated thiol ene reaction was catalyzed by 10 mol % benzophenone as catalyst without any additional external oxidant (Scheme 1.22)[45]. However, the reaction proceeded *via* a radical pathway to afford various anti-Markovnikov selective products with good yield.

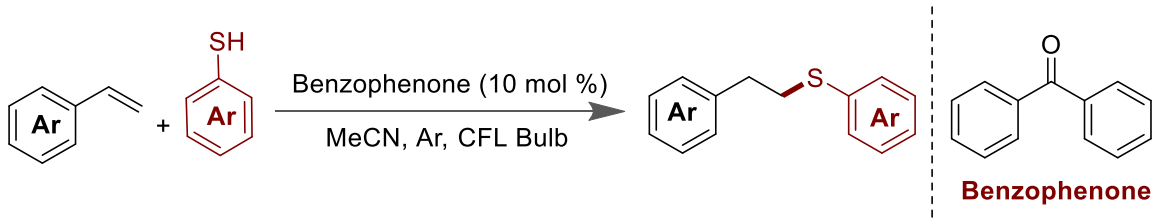

Scheme 1.18. Thiol-ene reaction by benzophenone.

1.4.4.3 Rose bengal as photocatalyst for Synthesis of vinyl sulfoxide.

Wei group has also illustrated that Synthesis of vinyl sulfoxide could be achieved from styrene and thiols under irradiation of 5 mol% Rose Bengal by white LED in air (Scheme 1.23)[46]. However, radical-mediated reactions delivered vinyl sulfoxides with reasonable yields.

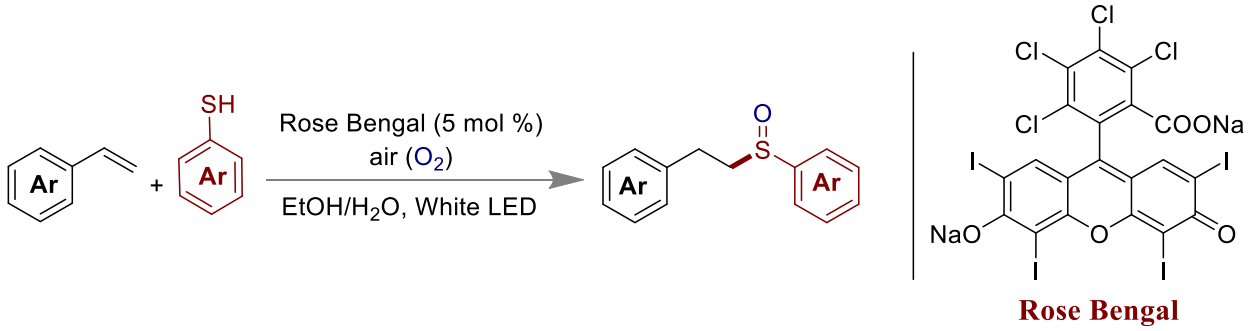

Scheme 1.19. Synthesis of vinyl sulfoxide by Rose bengal.

1.4.4.4 Ruthenium catalyzed methylsulfoxidation using diazonium salt.

N. Rastogi and co-worker showed that dimethylsulfoxide (DMSO) was used as methyl sulfinyl source for the synthesis of methylarylsulfoxide (Scheme 1.26)[47]. In this particular reaction, they have shown that $Ru(bpy)_3Cl_2$ was used for the generation of the aryl radical from aryl diazonium salt *via* single electron transfer (SET) process.

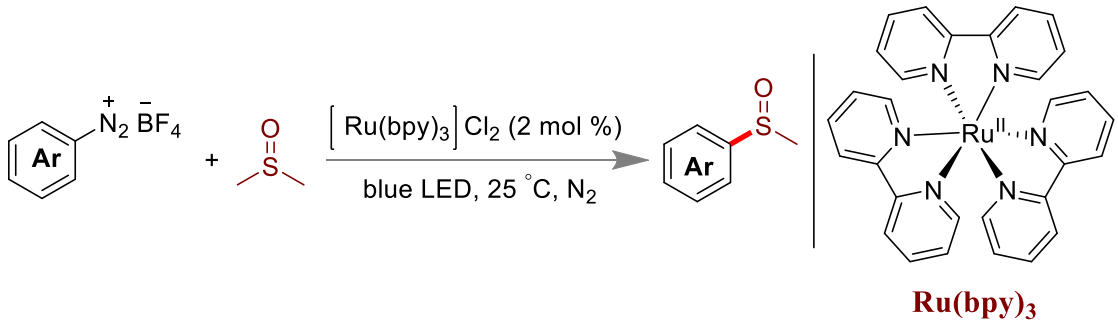

Scheme 1.20. Synthesis of vinyl sulfoxide by Ruthenium catalyzed.

1.4.4.5 Visible light-initiated Synthesis of 3-sulfonated coumarin from phenylpropiolate.

Wang's group also experienced Synthesis of 3-sulfonated coumarin from aryl propiolate and sulfinic acid using Eosin Y as photocatalyst and TBHP as terminal oxidant (Scheme 1.28) [48]. However, the internal alkyne could be functionalized to afford 3-sulfonated coumarin via cascaded formation of C-C and C-S bond in a single step.

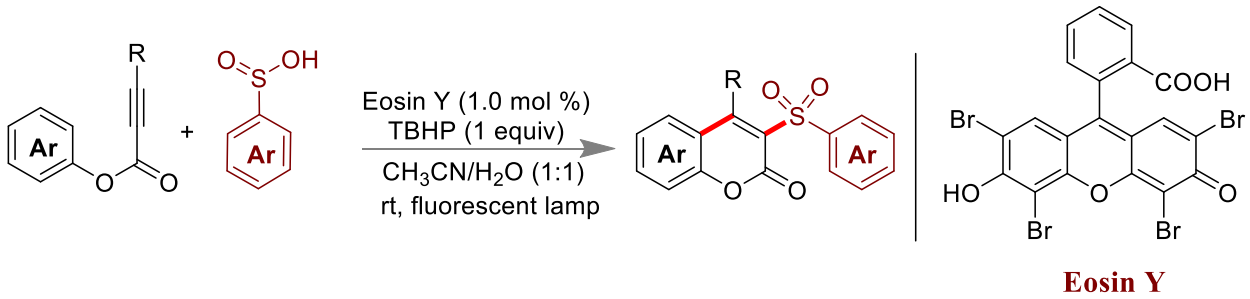

Scheme 1.21. Wang's report for visible light-initiated Synthesis of coumarin from phenylpropiolate.

1.4.4.6 Benzylic C-O Bond Functionalization

Under our previously optimized reaction conditions, irradiation of a mixture of benzyl alcohol and thiophenol under 3W blue LEDs in O_2 atmosphere and CH_3CN as solvent, thioacetals as well as thioethers were selectively isolated after 24 hours (Figure 1a). However, no sacrificial by-product other than water was observed and the excess thiophenol was recovered as such after the reaction.

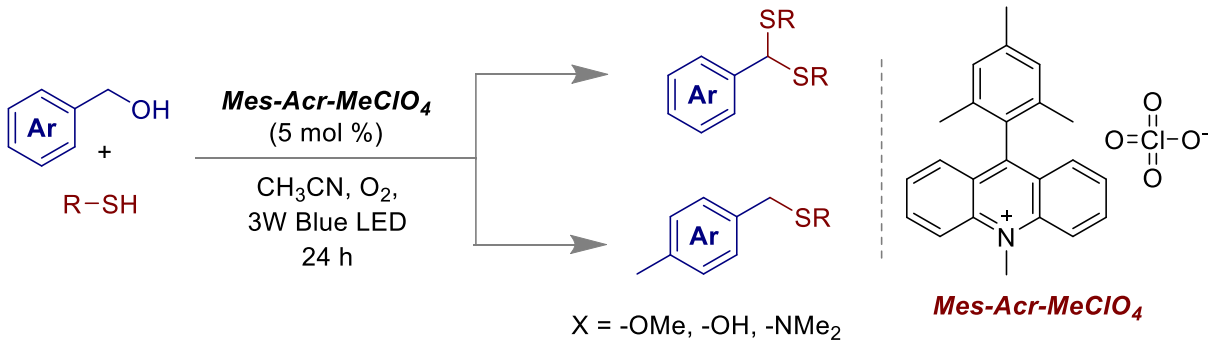

Scheme 1.22. Oxidation of benzyl alcohols and followed by C-S bond formation by photocatalysis.[49]

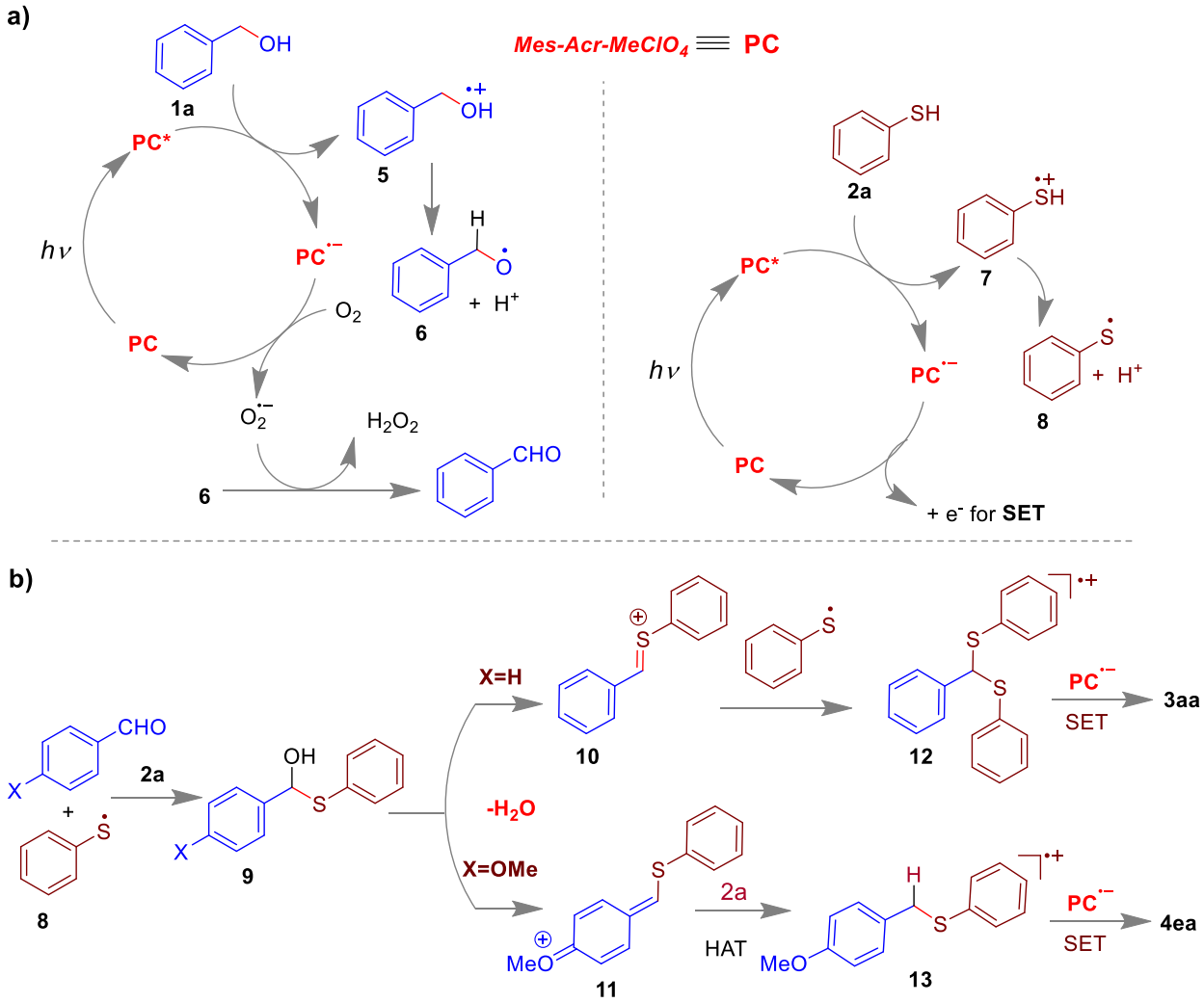

Figure 1.7. Function of a photocatalyst in the catalytic cycle.

Based on literature reports,[50-51] a plausible mechanism is given in Figure 4. At first, the photocatalyst Mes-Acr-MeClO4 (**PC**) was excited to [Mes-Acr-MeClO4]* under visible light and the excited **PC** (**PC***) produced intermediate 5 from benzyl alcohol *via* single electron transfer (SET) [52] and itself got reduced to **PC**$^{\bullet-}$. Now, The intermediate 5 possibly converted to **6** after releasing H^+. Following, the **PC**$^{\bullet-}$ generated the superoxide radical which oxidized **6** to the corresponding aldehyde and **PC** was regenerated. In a similar manner, thiophenol **2a** produced thiyl radical **8** (Figure 4a). In the second step (Figure 4b), thiyl radical reacted with benzaldehyde to give hemithioacetal intermediate 9 with the help of thiophenol **2a**.[51] Following, hemithioacetal **9** led to either **10** or **11**,

depending upon the substitution at benzyl alcohol (groups like -OMe or -NMe_2 favours the formation of **11**). In the presence of thiyl radical, intermediate **10** was further converted to **12** which led to the product dithioacetal **3aa** *via* one electron reduction by **PC**$^{\bullet-}$. However, the intermediate **11** which is well electronic rich, was further led to cation radical **13** *via* hydrogen atom transfer (HAT) from thiophenol **2a**.[53] Following, **4ea** was formed by SET from **PC**$^{\bullet-}$.

1.5 DISULFIDE METATHESIS REACTIONS

Disulfide metathesis is a type of chemical reaction that involves the exchange of disulfide bond (-S-S-) between two different molecule or within the same molecule. This reaction is typically catalyzed by a small molecule called a thiol-disulfide exchange catalyst or by enzymes called disulfide isomerases.

Disulfide metathesis can be use in various applications,[54] such as protein engineering and chemical synthesis. It is particularly useful in the production of biologically active molecules, as disulfide bonds are critical for the structure and function of many proteins and peptides.

In this reaction, two molecules with thiol (-SH) groups react with each other, leading to the forming of a new disulfide bond between them.

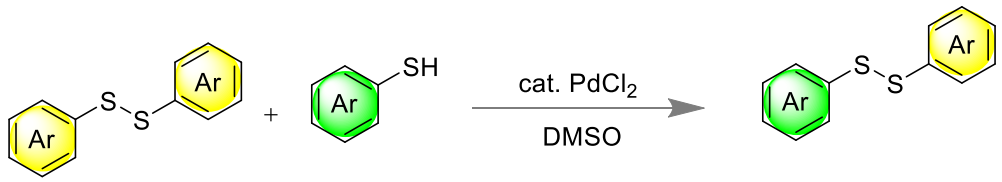

Figure 1.8. Unsymmetrical Disulfides Synthesis.[55]

1.6 OBJECTIVE

In summary, we have discussed the historical background of C-S bond formation reaction using various sustainable strategies. Most of the reports include control of the reactivity of sulfur compounds with various types of olefins, alkynes, carbonyls, functionalization, and formation of a heterocyclic core containing C-S bonds. The goal of the current thesis was to create environmentally friendly processes for C-S bond formation reactions, whether they were conducted photochemically or at room temperature.

1.6 NOTES AND REFERENCES

(1) Brasted, R. C. *Encyclopedia Britannica, inc.* **2021**.

(2) Meyer, B. Elemental Sulfur. *Chem. Rev.* **1976**, *76*, 367-388.

(3) Chenier, P. J., *Survey of Industrial Chemistry*; Springer US, 2012.

(4) Müller, H., Sulfuric Acid and Sulfur Trioxide. In *Ullmann's Encyclopedia of Industrial Chemistry*, Wiley-VCH, Weinheim. 2000.

(5) 15 - Sulfur. In *Chemistry of the Elements (Second Edition)*, Greenwood, N. N.; Earnshaw, A., Eds. Butterworth-Heinemann: Oxford, **1997**; pp 645-746.

(6) Pettersson, M.; Lundell, J.; Khriachtchev, L.; Isoniemi, E.; Räsänen, M. Hxesh, the First Example of a Xenon−Sulfur Bond. *J. Am. Chem. Soc.* **1998**, *120*, 7979-7980.

(7) Choudhuri, K.; Pramanik, M.; Mal, P. Λ^3-Iodanes as Visible Light Photocatalyst in Thioacetalization of Aldehydes. *Eur. J. Org. Chem.* **2019**, *2019*, 4822-4826.

(8) Nguyen, T. B. Recent Advances in Organic Reactions Involving Elemental Sulfur. *Adv. Synth. Catal.* **2017**, *359*, 1066-1130.

(9) Castanheiro, T.; Suffert, J.; Donnard, M.; Gulea, M. Recent Advances in the Chemistry of Organic Thiocyanates. *Chem. Soc. Rev.* **2016**, *45*, 494-505.

(10) Parida, A.; Choudhuri, K.; Mal, P. Unsymmetrical Disulfides Synthesis Via Sulfenium Ion. *Chem. Asian J.* **2019**, *14*, 2579-2583.

(11) Roth, G. P.; Fuller, C. E. Palladium Cross-Coupling Reactions of Aryl Fluorosulfonates: An Alternative to Triflate Chemistry. *J. Org. Chem.* **1991**, *56*, 3493-3496.

(12) Dixon, N. E.; Lawrance, G. A.; Lay, P. A.; Sargeson, A. M.; Taube, H., Trifluoromethanesulfonates and Trifluoromethanesulfonato-O Complexes. In *Inorg. Synth.* **1990**; pp 70-76.

(13) Kobayashi, S.; Sugiura, M.; Kitagawa, H.; Lam, W. W. L. Rare-Earth Metal Triflates in Organic Synthesis. *Chem. Rev.* **2002**, *102*, 2227-2302.

(14) Oshimura, E.; Sakamoto, K., Chapter 19 - Amino Acids, Peptides, and Proteins. In *Cosmetic Science and Technology*, Sakamoto, K.; Lochhead, R. Y.; Maibach, H. I.; Yamashita, Y., Eds. Elsevier: Amsterdam, **2017**; pp 285-303.

(15) Brosnan, J. T.; Brosnan, M. E. The Sulfur-Containing Amino Acids: An Overview. *J. Nutr.* **2006**, *136*, 1636S-1640S.

(16) Metzner, P.; Thuillier, A., 3 - Functional Modifications with Organosulfur Compounds. In *Sulfur Reagents in Organic Synthesis*, Metzner, P.; Thuillier, A., Eds. Academic Press: San Diego, **1994**; pp 53-73.

(17) Lee, C.-F.; Liu, Y.-C.; Badsara, S. S. Transition-Metal-Catalyzed C-S Bond Coupling Reaction. *Chem. Asian J.* **2014**, *9*, 706-722.

(18) Cremlyn, R. J. W., *An Introduction to Organosulfur Chemistry*; Wiley, **1996**.

(19) Suter, C. M., *The Organic Chemistry of Sulfur, Tetracovalent Sulfur Compounds, by Chester Merle Suter*; J. Wiley & sons, inc; Chapman & Hall, ltd: New York, London, **1944**.

(20) Chauhan, P.; Mahajan, S.; Enders, D. Organocatalytic Carbon–Sulfur Bond-Forming Reactions. *Chem. Rev.* **2014**, *114*, 8807-8864.

(21) Anastas, P.; Eghbali, N. Green Chemistry: Principles and Practice. *Chem. Soc. Rev.* **2010**, *39*, 301-312.

(22) Etzkorn, F. A.; Ferguson, J. L. Integrating Green Chemistry into Chemistry Education. *Angew. Chem. Int. Ed.* **2023**, *62*, e202209768.

(23) Morrison, J. A., Sulfur. In *Encyclopedia of Reagents for Organic Synthesis (Eros)*; Jhon Wiley & Sons, Ltd, **2001**.

(24) Nguyen, T. B.; Retailleau, P. Dipea-Promoted Reaction of 2-Nitrochalcones with Elemental Sulfur: An Unusual Approach to 2-Benzoylbenzothiophenes. *Org. Lett.* **2017**, *19*, 4858-4860.

(25) Campopiano, O.; Minassian, F., Thiophenol. In *Encyclopedia of Reagents for Organic Synthesis (Eros)*; Jhon Wiley & Sons, Ltd, **2001.**

(26) Choudhuri, K.; Mandal, A.; Mal, P. Aerial Dioxygen Activation Vs. Thiol–Ene Click Reaction within a System. *Chem. Commun.* **2018**, *54*, 3759-3762.

(27) Deeming, A. S.; Willis, M. C.; Lu, T.; Xiang, Y.; Wu, J., 1,4-Disulfino-1,4-Diazabicyclo [2.2.2]Octane, Bis(Inner Salt). In *Encyclopedia of Reagents for Organic Synthesis (Eros)*; Jhon Wiley & Sons, Ltd, **2018**.

(28) Zheng, D.; Yu, J.; Wu, J. Generation of Sulfonyl Radicals from Aryldiazonium Tetrafluoroborates and Sulfur Dioxide: The Synthesis of 3-Sulfonated Coumarins. *Angew. Chem. Int. Ed.* **2016**, *55*, 11925-11929.

(29) Chamberlin, A. R.; Sheppeck II, J. E.; Goess, B.; Lee, C., P-Toluenesulfonylhydrazide. In *Encyclopedia of Reagents for Organic Synthesis (Eros)*; Jhon Wiley & Sons, Ltd, **2007**.

(30) Singh, R.; Allam, B. K.; Singh, N.; Kumari, K.; Singh, S. K.; Singh, K. N. A Direct Metal-Free Decarboxylative Sulfono Functionalization (Dsf) of Cinnamic Acids to A,B-Unsaturated Phenyl Sulfones. *Org. Lett.* **2015**, *17*, 2656-2659.

(31) Yang, F.-L.; Tian, S.-K. Iodine-Catalyzed Regioselective Sulfenylation of Indoles with Sulfonyl Hydrazides. *Angew. Chem. Int. Ed.* **2013**, *52*, 4929-4932.

(32) Tian, H.; Yu, J.; Yang, H.; Zhu, C.; Fu, H. Catalyst-Free Isothiocyanatoalkylthiation of Styrenes with (Alkylthio)Pyrrolidine-2,5-Diones and Trimethylsilyl Isothiocyanate. *Adv. Synth. Catal.* **2016**, *358*, 1794-1800.

(33) Xing, L.; Zhang, Y.; Li, B.; Du, Y. In Situ Formation of Rscl/Arsecl and Their Application to the Synthesis of 4-Chalcogenylisocumarins/Pyrones from O-(1-Alkynyl)Benzoates and (Z)-2-Alken-4-Ynoates. *Org. Lett.* **2019**, *21*, 3620-3624.

(34) Pramanik, M.; Choudhuri, K.; Mal, P. N-Iodosuccinimide as Bifunctional Reagent in (E)-Selective C(Sp2)−H Sulfonylation of Styrenes. *Asian J. Org. Chem.* **2019**, *8*, 144-150.

(35) Hu, B.; Zhou, P.; Zhang, Q.; Wang, Y.; Zhao, S.; Lu, L.; Yan, S.; Yu, F. Metal-Free Oxidative Thioesterification of Methyl Ketones with Thiols/Disulfides for the Synthesis of A-Ketothioesters. *J. Org. Chem.* **2018**, *83*, 14978-14986.

(36) Kang, X.; Yan, R.; Yu, G.; Pang, X.; Liu, X.; Li, X.; Xiang, L.; Huang, G. Iodine-Mediated Thiolation of Substituted Naphthols/Naphthylamines and Arylsulfonyl Hydrazides Via C(Sp2)–H Bond Functionalization. *J. Org. Chem.* **2014**, *79*, 10605-10610.

(37) Parumala, S. K. R.; Peddinti, R. K. Iodine Catalyzed Cross-Dehydrogenative C–S Coupling by C(Sp2)–H Bond Activation: Direct Access to Aryl Sulfides from Aryl Thiols. *Green Chem.* **2015**, *17*, 4068-4072.

(38) Choudhuri, K.; Maiti, S.; Mal, P. Iodine(Iii) Enabled Dehydrogenative Aryl C−S Coupling by in Situ Generated Sulfenium Ion. *Adv. Synth. Catal.* **2019**, *361*, 1092-1101.

(39) Huang, Z.; Zhang, D.; Qi, X.; Yan, Z.; Wang, M.; Yan, H.; Lei, A. Radical–Radical Cross-Coupling for C–S Bond Formation. *Org. Lett.* **2016**, *18*, 2351-2354.

(40) Yuan, Y.; Chen, Y.; Tang, S.; Huang, Z.; Lei, A. Electrochemical Oxidative Oxysulfenylation and Aminosulfenylation of Alkenes with Hydrogen Evolution. *Sci. Adv.* **2018**, *4*, eaat5312.

(41) Wang, H.-B.; Huang, J.-M. Decarboxylative Coupling of A-Keto Acids with Ortho-Phenylenediamines Promoted by an Electrochemical Method in Aqueous Media. *Adv. Synth. Catal.* **2016**, *358*, 1975-1981.

(42) Romero, N. A.; Nicewicz, D. A. Organic Photoredox Catalysis. *Chem. Rev.* **2016**, *116*, 10075-10166.

(43) Bogdos, M. K.; Pinard, E.; Murphy, J. A. Applications of Organocatalysed Visible-Light Photoredox Reactions for Medicinal Chemistry. *Beilstein J. Org. Chem.* **2018**, *14*, 2035-2064.

(44) Keshari, T.; Yadav, V. K.; Srivastava, V. P.; Yadav, L. D. S. Visible Light Organophotoredox Catalysis: A General Approach to β-Keto Sulfoxidation of Alkenes. *Green Chem.* **2014**, *16*, 3986-3992.

(45) Singh, M.; Yadav, A. K.; Yadav, L. D. S.; Singh, R. K. P. Visible Light Photocatalysis with Benzophenone for Radical Thiol-Ene Reactions. *Tetrahedron Lett.* **2017**, *58*, 2206-2208.

(46) Cui, H.; Wei, W.; Yang, D.; Zhang, Y.; Zhao, H.; Wang, L.; Wang, H. Visible-Light-Induced Selective Synthesis of Sulfoxides from Alkenes and Thiols Using Air as the Oxidant. *Green Chem.* **2017**, *19*, 3520-3524.

(47) Pramanik, M. M. D.; Rastogi, N. Visible Light Catalyzed Methylsulfoxidation of (Het)Aryl Diazonium Salts Using Dmso. *Chem. Commun.* **2016**, *52*, 8557-8560.

(48) Yang, W.; Yang, S.; Li, P.; Wang, L. Visible-Light Initiated Oxidative Cyclization of Phenyl Propiolates with Sulfinic Acids to Coumarin Derivatives under Metal-Free Conditions. *Chem. Commun.* **2015**, *51*, 7520-7523.

(49) Pramanik, M.; Choudhuri, K.; Mathuri, A.; Mal, P. Dithioacetalization or Thioetherification of Benzyl Alcohols Using 9-Mesityl-10-Methylacridinium Perchlorate Photocatalyst. *Chem. Commun.* **2020**, *56*, 10211-10214.

(50) Schilling, W.; Riemer, D.; Zhang, Y.; Hatami, N.; Das, S. Metal-Free Catalyst for Visible-Light-Induced Oxidation of Unactivated Alcohols Using Air/Oxygen as an Oxidant. *ACS Catal.* **2018**, *8*, 5425-5430.

(51) Du, K.; Wang, S.-C.; Basha, R. S.; Lee, C.-F. Visible-Light Photoredox-Catalyzed Thioacetalization of Aldehydes under Metal-Free and Solvent-Free Conditions. *Adv. Synth. Catal.* **2019**, *361*, 1597-1605.

(52) Ohkubo, K.; Suga, K.; Fukuzumi, S. Solvent-Free Selective Photocatalytic Oxidation of Benzyl Alcohol to Benzaldehyde by Molecular Oxygen Using 9-Phenyl-10-Methylacridinium. *Chem. Commun.* **2006**, 2018-2020.

(53) Romero, N. A.; Nicewicz, D. A. Mechanistic Insight into the Photoredox Catalysis of Anti-Markovnikov Alkene Hydrofunctionalization Reactions. *J. Am. Chem. Soc.* **2014**, *136*, 17024-17035.

(54) Fritze, U. F.; von Delius, M. Dynamic Disulfide Metathesis Induced by Ultrasound. *Chem. Commun.* **2016**, *52*, 6363-6366.

(55) Guo, J.; Zha, J.; Zhang, T.; Ding, C.-H.; Tan, Q.; Xu, B. $PdCl_2$/Dmso-Catalyzed Thiol–Disulfide Exchange: Synthesis of Unsymmetrical Disulfide. *Org. Lett.* **2021**, *23*, 3167-3172.

CHAPTER 2

^{t}BuOLi Promoted Terminal Alkynes Functionalizations by Aliphatic Thiols and Alcohols

2.1 ABSTRACT

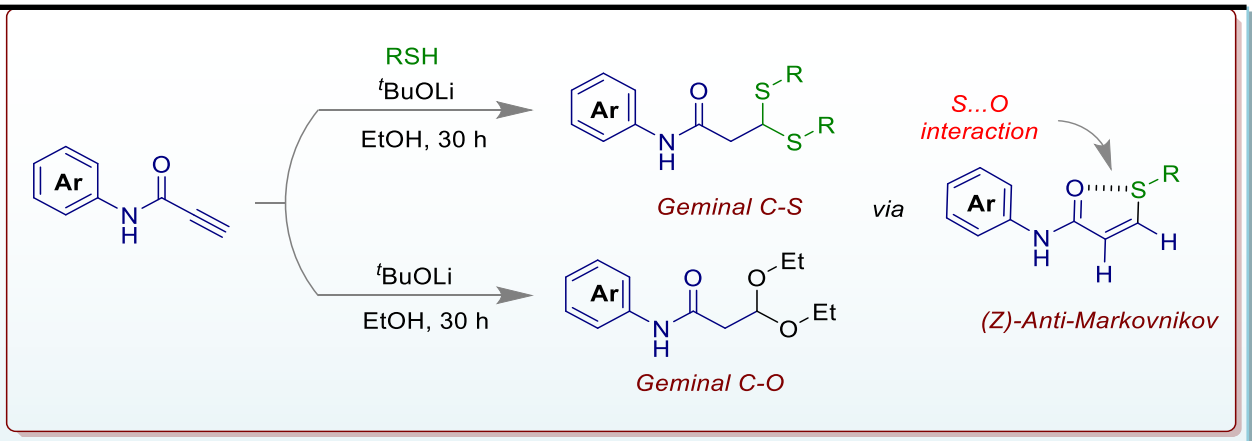

Selective radical addition to terminal alkynes is always a difficult task to achieve because it gives a mixture of stereo- and regioisomers. Herein we disclose the selective addition of aliphatic thiols or alcohols to *N*-phenylpropiolamides (terminal alkynes) using lithium *tert*-butoxide (^{t}BuOLi) in ethanol as a promoter. Mechanistically, it has been shown that the reaction proceeded through generation of thiyl radical intermediate and amide group in *N*-phenylpropiolamide could help in the activation of alkyne which led to thioacetalization *via* the formation of (*Z*)-selective *anti*-Markovnikov vinyl sulfide. The (*Z*)-selectivity for the formation of vinyl sulfides was controlled by an intramolecular sulfur…oxygen interaction.

2.2 INTRODUCTION

Towards the synthesis of novel materials based on certain requirements, it is important to select appropriate noncovalent or weak or supramolecular interactions.[1-2] Use of these weak or noncovalent interactions like cation-π,[3] anion-π,[4] H-bonding,[5] halogen bonding,[6-8] S–H···π[9] sulfur…oxygen,[10] hydrophobic effects,[11] etc., that have useful functions in the organic synthesis is also developing at a firm pace.[12-13] Especially, the non-covalent interactions like S–H···S, S–H···O, O–H···S and N–H···S etc. relating to the sulfur centers are still under consideration from both experimental[14] and theoretical[15] viewpoint because the carbon-sulfur (C-S) bonds are universally found in non-natural and natural products.[16] Interestingly, controlling the stability of radicals is one of the important tasks to perform any selectivity in a chemical reaction.[17-18] The concept like radical hydrogen bonding[19-20] has been explored as well in organic synthesis.[10]

Dithioacetals are widely employed as synthons exhibiting umpolung reactivity for many organic transformations.[21] Particularly, they acted as protecting group in the total synthesis of bioactive natural products and also used as directing group for C-H functionalization reaction.[22-23] The dithioacetals are obtained from aldehydes and non-conventional starting materials using Lewis acids, iodine catalyst and visible light.[24-26] However, selective dithioacetalization of alkyne by dithiol is challenging because it led to both Markovnikov and *anti*-Markovnikov products with poor stereoselectivity.

Recently, radical-mediated addition reaction in alkynes has become an important tool for organic synthesis.[27-29] In particular, the stereo- and regioselective difunctionalization of terminal alkynes is challenging.[30] Though the reactivity of alkyne hydrothiolation reaction is well introduced using various catalysis,[31] but suffers from lack of stereo-selectivity, formation of unwanted by-product, harsh reaction conditions, etc.[32-38] Indeed, radical addition to terminal

alkynes always gives either mono functionalized product with Markovnikov selectivity or *anti*-Markovnikov selective products with (*E*)- and (*Z*)-mixture.[14, 39] In addition, it also provides various types of geminal or vicinal coupling products (Figure 1a). Preferentially, the addition of thiyl radical to alkyne leads to (*E*)- and (*Z*)-isomeric mixture of *anti*-Markovnikov vinyl sulfides (Figure 1a).[40] However, the second thiol addition generally leads to either vicinal dithioetherification or geminal dithioacetalization.[14, 39] The reports on the synthesis of geminal dithioacetalization from terminal alkyne is limited in the literature[22, 41-44] and most of them required metal catalyst.[45-47] Our previous report on hydrothiolation of alkynes could reveal exclusive control on the *anti*-Markovnikov product using S–H···π interaction[9] as an appropriate driving force for the formation of regioselective product (Figure 1b).[40] Next, activation of terminal alkyne by introducing amide linkage in the terminal as well as internal alkyne could result in exclusive control on stereo and regioselectivity *via* S···O interaction or N–H···S hydrogen bonding interaction.[5] Inspiring by this result, we also attempted for geminal difunctionalization of terminal alkynes.[48] However, we speculated that the installation of amide skeleton in terminal alkyne could help for the formation of selective geminal addition product over vicinal addition in the presence of aliphatic thiols (Figure 1c). Interestingly, *N*-phenylpropiolamide led to dithioacetal in the presence of thiol and ^{t}BuOLi in EtOH. Again it was converted to acetals in absence of thiol.

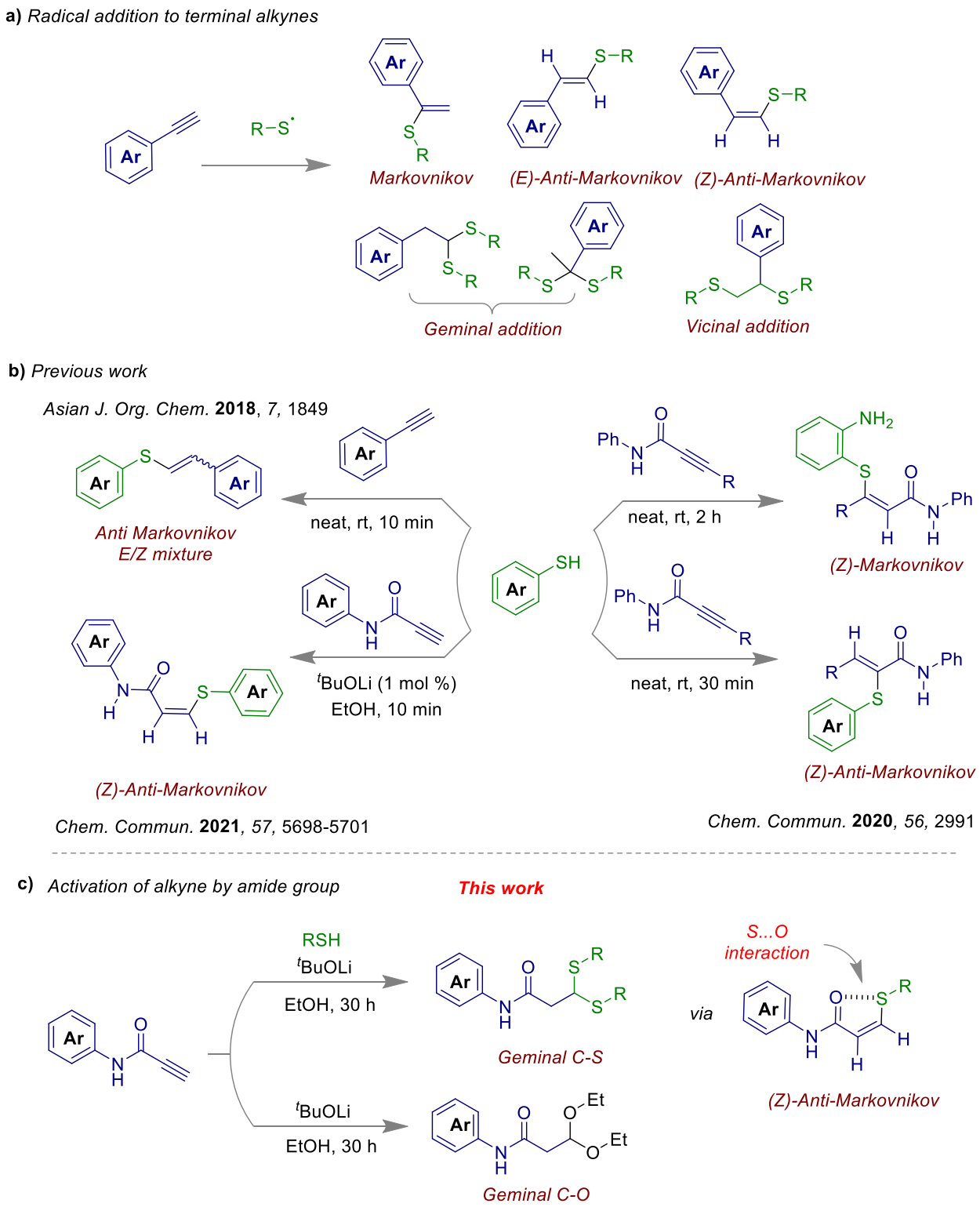

Figure 2.1. a) Various mono- and bis-functionalized products from terminal alkynes. b) Our previous approaches for selective thiol addition to various alkynes are shown.[5, 10, 40] c) This work is based on ^{t}BuOLi initiated selective bis-functionalization of *N*-phenylpropiolamide by aliphatic thiols or alcohols.

2.3 RESULT AND DISCUSSION

Initially all the reaction parameters like solvents, bases and time were altered to optimize the reaction condition. However, 5 mol % of lithium *tert*-butoxide (^{t}BuOLi) was considered for the generation of thiyl radical to conduct addition reaction between *N*-phenylpropiolamide and aliphatic thiol in ethanol. Delightfully, thioacetal **3ad** was isolated with 80% yield in EtOH after 30 h (Table 1, entry 1). During solvent study among EtOH, $CHCl_3$, Toluene, and CH_3CN, EtOH was most efficient for this transformation (entries 1-4). Yield of the product **3ad** was retained when 1 mol % of ^{t}BuOLi was loaded instead of 5 mol % (entry 5). However, others bases like ^{t}BuOK and K_2CO_3 did not make any improvement in the yield rather than ^{t}BuOLi (entries 6-7). The reaction was unsuccessful in the absence of ^{t}BuOLi (entry 8). Again, dithioacetal was produced in 69% yield in the absence of any solvent (entry 9). The yield of **3ad** was decreased to 73% when the reaction was carried out for 24 h (entry 10). Finally, maximum yield (92%) was obtained when dry EtOH and inert atmosphere condition was used (entry 11). When other alcohols like *tert*-butanol and methanol were used instead of ethanol, 77% and 74% yields of dithioacetals **3ad** were found (entries 12-13).

Table 2.1. The reaction condition optimization. [a]

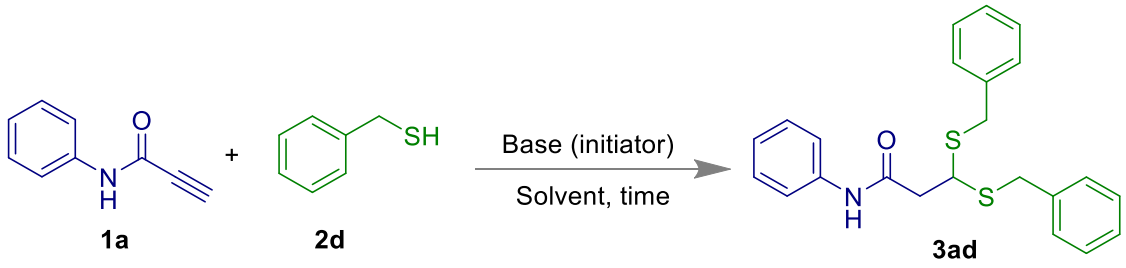

Entry	Solvent	Initiator (mol %)	Yield of 3aa (%)[a]
1	EtOH	^{t}BuOLi (5.0)	80
2	$CHCl_3$	^{t}BuOLi (5.0)	40
3	Toluene	^{t}BuOLi (5.0)	45
4	CH_3CN	^{t}BuOLi (5.0)	76
5	EtOH	^{t}BuOLi (1.0)	81
6	EtOH	^{t}BuOK (1.0)	80
7	EtOH	K_2CO_3 (1.0)	58
8	EtOH	-	0
9	-	^{t}BuOLi (1.0)	69
10	EtOH	^{t}BuOLi (1.0)	73[b]
11	EtOH	^{t}BuOLi (1.0)	92[c]
12	^{t}BuOH	^{t}BuOLi (1.0)	77
13	MeOH	^{t}BuOLi (1.0)	74

[a]Isolated yields after column chromatography, Reaction conditions: **1a** (60 mg, 0.413 mmol), **2d** (153 mg, 1.239 mmol) and ^{t}BuOLi (0.33mg, 0.00413 mmol) in 1.0 mL of EtOH under inert atmosphere for 30 h. [b]at 24 h, [c]at inert atmosphere in 1.0 mL of dry EtOH.

Under the optimized condition, the thiols were producing geminal C-S coupled products (**3aa-3ij**) with good to excellent yields (52 - 92%) (Figure 2). Heterocycle containing aliphatic thiol like furan-2-ylmethanethiol **2a**, reacted with *N*-phenylpropiolamide **1a** to produce dithioacetal **3aa** with 89% yield. Isobutyl mercaptans were also responded satisfactorily to give **3ab** and **3bb** with 69% and 75% yields. Again, dithioacetals (**3ac**, **3cc**) obtained from phenyl ethane thiol **2c**, were also well productive in this mild reaction condition. Benzyl mercaptan **2d** also yielded the geminal C-S addition product **3ad** and **3bd** with 92% and 78% yields, respectively. Likewise, compounds **3de** and **3ee** were isolated in 66% and 83% yields, respectively. Again, *para*-fluoro and ethoxy phenyl propiolamides reacted smoothly to deliver **3ff**, **3gg,** and **3ge** with 52-81% yields. Long-chain aliphatic thiol like dodecanethiol also afforded desired product **3ai** and **3hi** with 77% and 56% yields, respectively. *Para*-bromo phenylpropiolamide **1i** and ethanethiol **2j** yielded compound **3ij** with a 90% yield. Again, *N*-butylpropiolamide **1j** reacted with a thiol to give compound **3je** with a 14% yield. On the other hand, *N*-phenylpropiolamide having electron withdrawing group like -NO_2 and -CF_3 also exhibited thioacetals **3kd** and **3ld** with 55% and 84% yields, respectively. 2-Thiophenemethanethiol also yielded the corresponding thioacetal **3ak** with 76% yield. Again, scale-up synthesis of compound **3ad** was carried out which produced 79% yield. Other non-conjugated alkynes (**1m-1o**) were unable to give the desired dithioacetals in this reaction condition. Again, internal alkyne like *N*-phenylpropiolamide **1p** also produced very complex reaction mixture (Supporting Information).

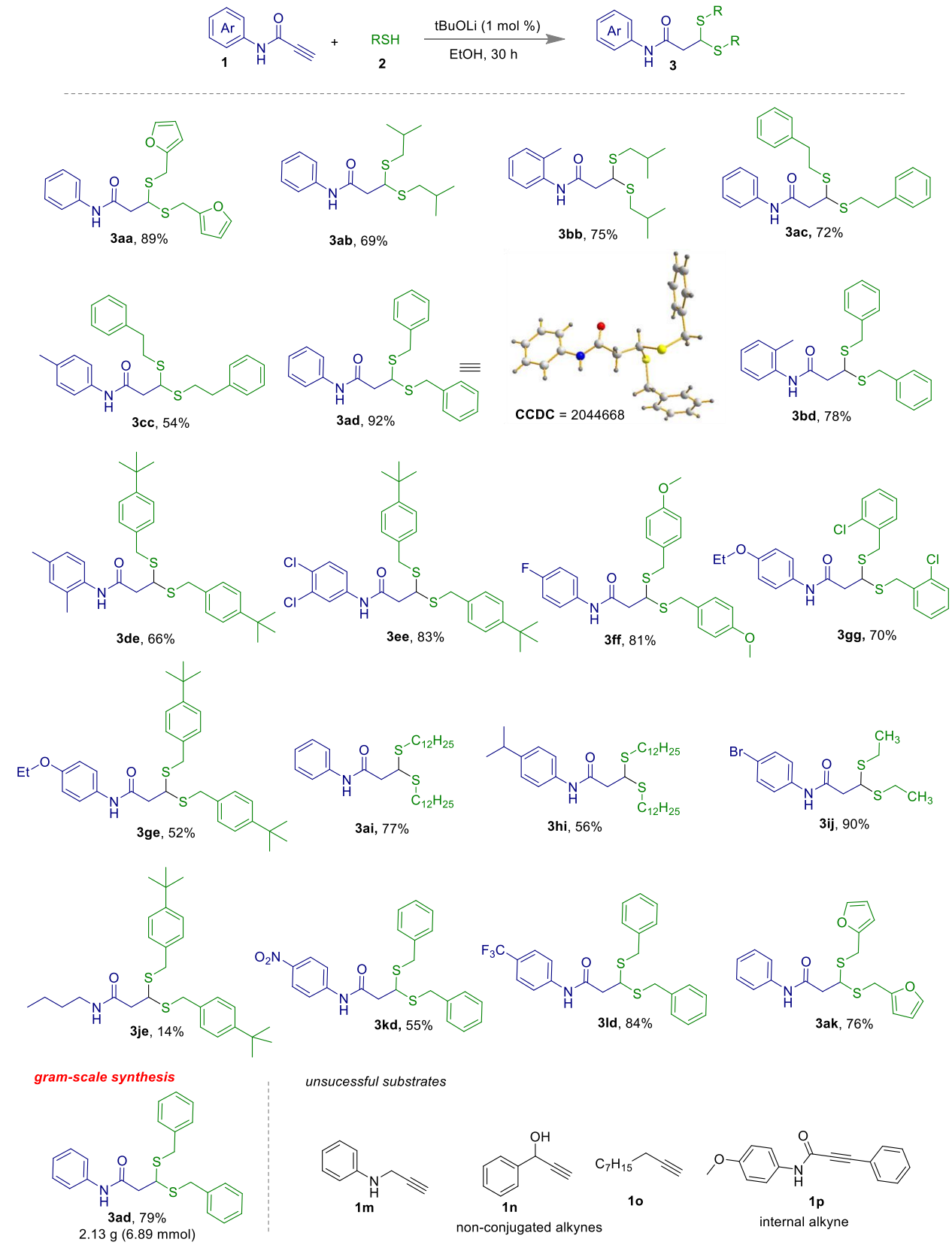

Figure 2.2. Reaction scope for various *N*-phenylpropiolamide and aliphatic thiols.

To our delight, we could also observe the switching of product to acetals **4** in the absence of aliphatic thiols when *N*-phenylpropiolamide was allowed to react with different types of alcohols (Figure 3). However, various types of acetals like **4aa**, **4ab** and **4ac** were isolated in 59-78% yields when methanol (MeOH), ethanol (EtOH) and trifluroethanol (TFE) were used as the solvent and C-O coupling partner. Again, aliphatic primary alcohols like 1-propanol and 1-butanol were also reacted with propiolamide **1a** to produce corresponding acetals **4ad** and **4ae** in 59% and 75% yields, respectively. Other long chain alcohols like 1-hexamol, 1-octanol, 1-nonanol and 1-decanol also produced desired acetals (**4af-4ai**) with satisfactory yields (60%-72%). Unfortunately, secondary alcohols such as isopropanol and hexafluoroisopropanol and tertiary alcohol like *tert*-butyl alcohol were unreacted to deliver acetals (**4aj-4al**) under standard reaction conditions.

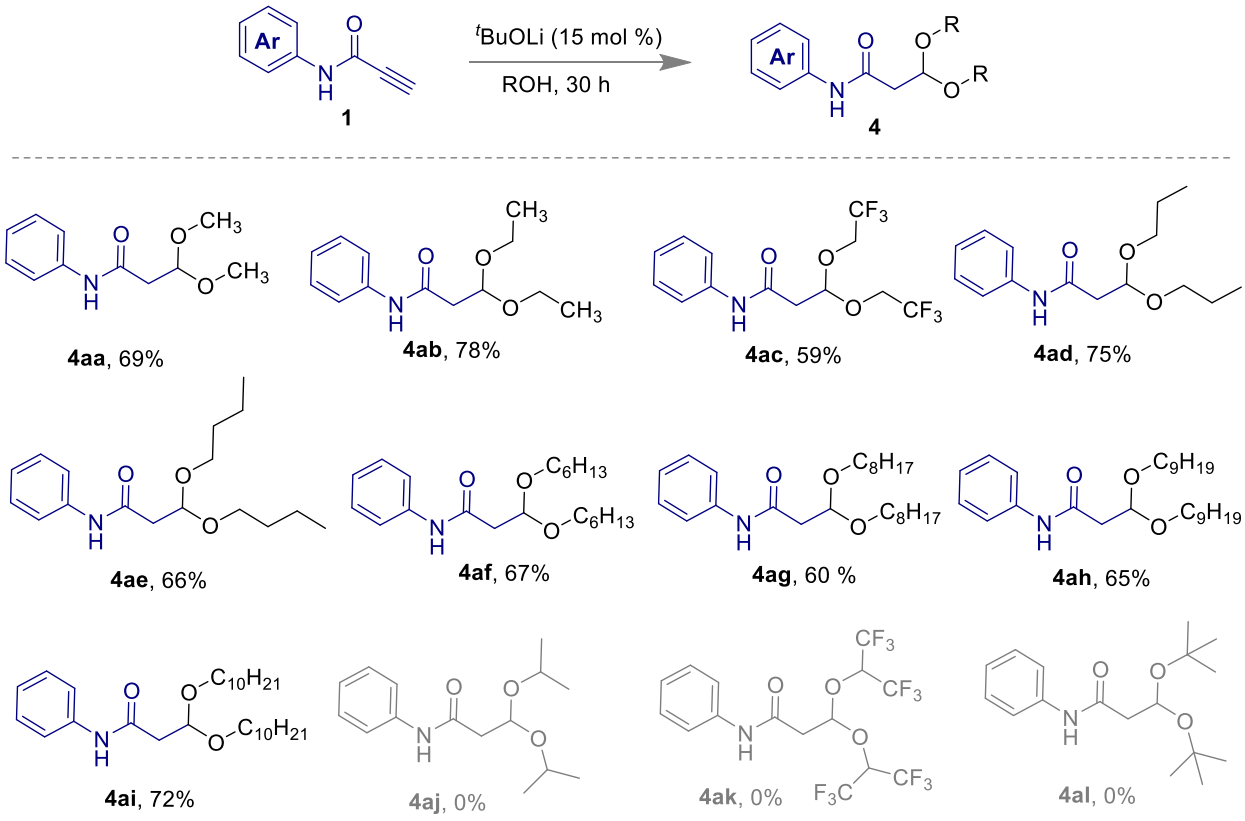

Figure 2.3. Reaction scopes of *N*-phenylpropiolamide with aliphatic alcohols.

In addition, several control experiments (Figure 4) were performed to understand the mechanism of the reaction. It was found that thioacetic acid did not produce the desired thioacetal; rather it yielded Z-vinyl sulfides **5** in 63% yield after 30 h reaction time. Again, the addition of thiophenol instead of aliphatic thiols could deliver (*Z*)-selective vinyl sulfide **6** after standard reaction time. This phenomenon can be rationalized through the stability of thiyl radical and the electron rich double bond by sulfur in vinyl sulfide which could not allow second addition of thiyl radical for the formation of geminal C-S coupling product (Figure 4a).[10] Again, when propiolate ester **7** was taken instead of propiolamide **1a**, the desired thioacetal **8** could not be identified (Figure 4b). The reaction of phenylacetylene **9** and benzyl mercaptan **2d** led to (*E*)- and (*Z*)-isomeric mixture of vinyl sulfide **10** with the formation of disulfide (Figure 4c). The observed isomeric mixture is due to absence of S···O interaction over here, which might lead to the exclusive control on Z-selectivity, and the second addition of thiyl radical was not occurred because of the inactivated alkyne **8** (as acheived by propiolamide). Again, (*Z*)-vinyl sulfide **11** was converted to thioacetals **3aa** under standard conditions, which indicated that (*Z*)-vinyl sulfide might be one of the intermediates (Figure 4d). Here, vinyl sulfide **10** was still activated by amide group which led to regio-selective formation of dithioacetals after the second addition of thiyl radical. Ethanol did not form acetal in the presence of thiols because thiols are more reactive than ethanol to form thiyl radical in the presence of lithium *tert*-butoxide. A radical trapping experiment was carried out with the help of 4 equiv TEMPO (2,2,6,6-tetramethylpiperidine 1-oxyl) as a radical scavenger which inhibited the product formation for the reaction *N*-phenylpropiolamide and benzyl mercaptan, indicating the involvement of radical intermediate in this transformation (Figure 4e).[9] On the other hand, when a similar reaction was performed with trifluoroethanol, the product yield of the compound **4ac** was retained, thus assuming the non-involvement of radical intermediate.[49]

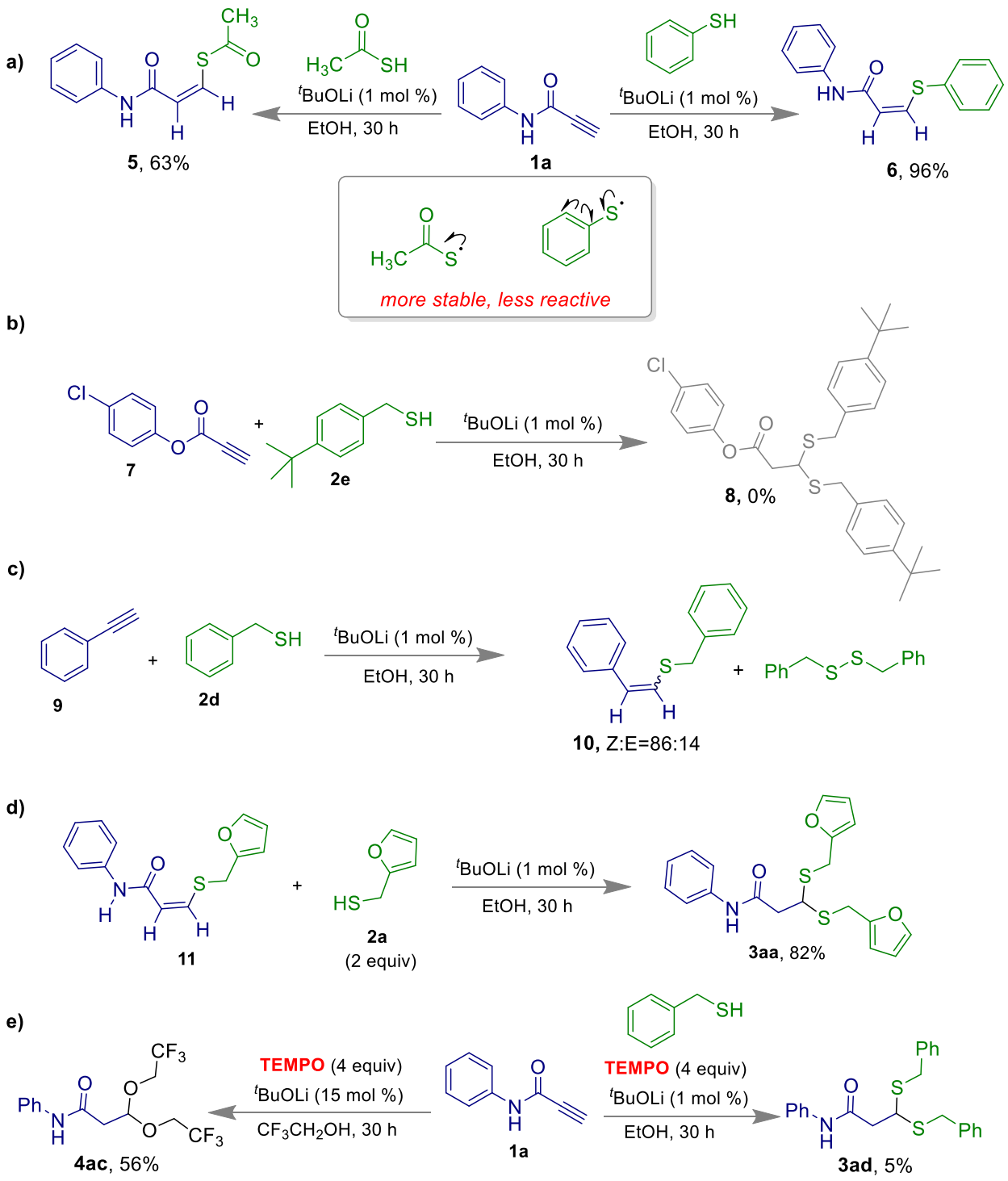

Figure 2.4. Control experiments: a) reaction of N-phenylpropiolamide **1a** with thioacetic acid and thiophenol; b) reaction of 4-chlorophenyl propiolate **7** and 4-tert-butyl benzyl mercaptan **2e**; c) reaction of phenyl acetylene **9** and benzyl mercaptan **2d**; d) reaction of (*Z*)-selective vinyl sulfide **11** and thiol **2a**; e) radical trapping experiment in the presence of TEMPO.

Based on the previous literature reports[10] and control experiment, a plausible mechanism is outlined in Figure 5. Initially, Initially, ^{t}BuOLi and thiol formed a complex **I** which underwent single electron transfer (SET) with another thiol to generate thiyl radical **II**.[9, 50-51] Consequently, thiyl radical **I** reacted with *N*-phenylpropiolamide to generate vinylic radical **II,** which was stabilized by S⋯O interaction.[10] Following, hydrogen atom transfer (HAT)[9] from thiols helped to attain Z-selective vinyl sulfides and a thiyl radical. Again, generated thiyl radical took part in a chain reaction to deliver thioacetal as a product. On the other hand, a base catalyzed ionic mechanism could be assumed for acetalization reaction.

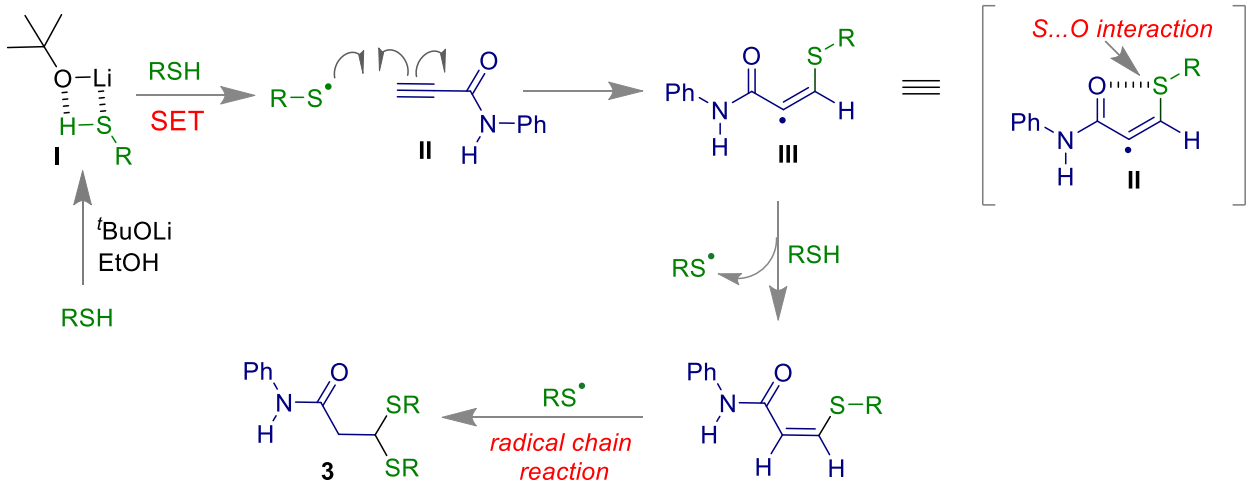

Figure 2.5. Plausible mechanism.

2.4 CONCLUSION

In conclusion, we have shown that the reactivity of *N*-phenylpropiolamide could be controlled by the presence of an amide group as a reaction controller for selective formation of thioacetals or acetals. Synthesis of various types of dithioacetals and acetals was achieved in the presence of lithium *tert*-butoxide as a reaction initiator from the reactions of *N*-phenylpropiolamide and aliphatic thiols. Overall, this work offers an excellent guideline for a stereoselective radical addition to terminal alkynes. We expect that the presented work will create a significant impact

in organic chemistry by connecting the research areas like supramolecular chemistry and organic synthesis.

2.5 EXPERIMENTAL SECTION

General aspects

All the chemicals were purchased commercially and used as received. All the reactions were performed under open atmosphere unless otherwise noted. The reactions were monitored by TLC on aluminum sheets pre-coated with silica gel. Chromatographic purifications of the compounds were performed using silica gel (mesh 230-400) and ethyl acetate/hexane as an eluent. ^{1}H and ^{13}C spectra of the compounds were recorded on Bruker 400 and 700 MHz instrument at 25 ºC. The chemical shift value (δ, ppm) were reported with respect to the residual chloroform (7.26 for ^{1}H and 77.16 ppm for ^{13}C). Mass spectra were recorded as ESI-TOF (HRMS). Infrared spectra were recorded on neat solids using KBr pellets and described in wave number (cm^{-1}). Digital melting point apparatus were used to record the Melting Point of the compound in degree centigrade (°C) and are uncorrected.

Synthesis

All *N*-phenylpropiolamide derivatives were synthesized based on literature report.[10]

Representative procedure for synthesis of 3ad. In a round bottom flask, the benzyl mercaptan (**2d**) (153 mg, 1.239 mmol) was dissolved in 0.5 mL dry EtOH and lithium *tert* butoxide (0.33 mg, 0.00413 mmol) was added to the solution at inert atmosphere. After that, a 0.5 mL solution of compound (**1a**) (60 mg, 0.413 mmol) was added and the reaction mixture was allowed to stir at inert atmosphere for 30 h. The progress of the reaction was monitored by TLC. After completion of the reaction, excess EtOH was removed under reduced pressure and column chromatography was done in EtOAc/Hexane to isolate the desired product **3ad**.

.

Gram scale synthesis for the synthesis of 3ad. In a 25 mL round bottom flask, the benzyl mercaptan (**2d**) (2.56 g, 20.7 mmol) was dissolved in 4 mL dry EtOH and lithium *tert*-butoxide (6 mg, 0.069 mmol) was added to the solution at inert atmosphere. After that, a 1 mL solution of compound (**1a**) (1 g, 6.89 mmol) was added and the reaction mixture was allowed to stir at inert atmosphere for 30 h. The progress of the reaction was monitored by TLC. After completion of the reaction, excess EtOH was removed under reduced pressure and column chromatography was done in EtOAc/Hexane to isolate the desired product **3ad** with 79% yield (2.13 g).

Representative procedure for synthesis of 4aa. In a round bottom flask, compound (**1a**) (60 mg, 0.413 mmol) and lithium *tert*-butoxide (5 mg, 0.06206 mmol) were added in 1.0 mL MeOH. Reaction mixture was allowed to react under inert atmosphere for 30 h. After completion of the reaction, excess MeOH was removed under reduced pressure and column chromatography was done in EtOAc/Hexane to isolate the desired product **4aa**.

Table 2.2. Optimization of base for **4ab**

Entry	Base (mol %)	Yield of 4ab (%)[a]
1	^{t}BuOLi (10.0)	51
2	^{t}BuOLi (15.0)	69
3	^{t}BuOLi (20.0)	62

[a]Isolated yields after column chromatography, Standard reaction conditions: **1a** (60 mg, 0.413 mmol), and ^{t}BuOLi (5 mg, 0.062 mmol) in 1 mL dry EtOH at inert atmosphere for 30 h.

Crystallographic Investigation

The compound **3ad** was recrystallized by the slow evaporation of ethanol and water mixture (ca. 50%). The crystals data were collected with Bruker SMART D8 goniometer equipped with an APEX CCD detector and with an INCOATEC micro source (Cu-Kα radiation, λ = 1.54184 Å). SAINT+[52] and SADABS[53] were used to integrate the intensities and to correct the absorption respectively The structure was resolved by direct methods and refined on F^2 with SHELXL-97.[54]

Compound (3ad) (CCDC 2044668)

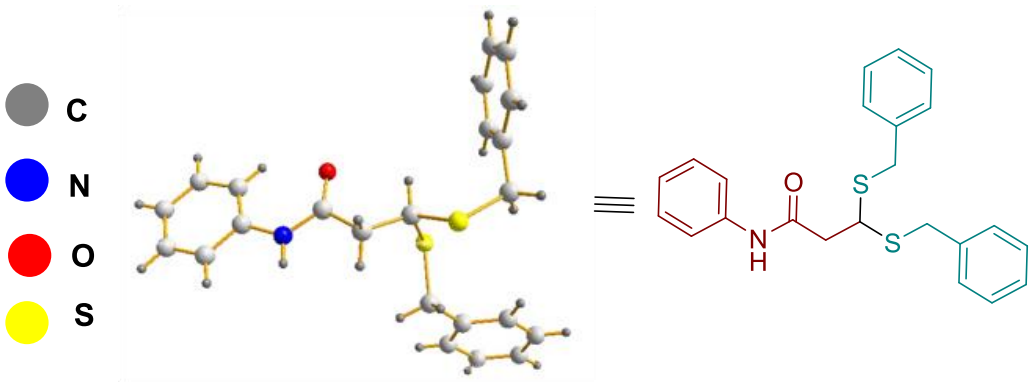

Figure 2.6. Crystal structure of (**3ad**) (CCDC 2044668).

Crystallographic Data for (**3ad**)

Empirical formula	$C_{23}H_{23}NOS_2$
Formula weight	393.54
Temperature/K	298.85(10)
Crystal system	Monoclinic
Space group	$P2_1/c$
a/Å	12.4011(2)
b/Å	18.3334(4)

c/Å	9.57886(15)
α/°	90
β/°	91.0519(16)
γ/°	90
Volume/Å3	2177.43(7)
Z	4
ρcalcg/cm^3	1.200
μ/mm^{-1}	2.296
F(000)	832.0
Crystal size/mm^3	0.2 × 0.17 × 0.18
Radiation	CuKα (λ = 1.54184)
Reflections collected	33898
Independent reflections	4456 [Rint = 0.0417, Rsigma = 0.0221]
Goodness-of-fit on F2	1.061
Final R indexes [I>=2σ (I)]	R1 = 0.0484, wR2 = 0.1314
Final R indexes [all data]	R1 = 0.0563, wR2 = 0.1371
Largest diff. peak/hole / e Å^{-3}	0.27/-0.31

3,3-Bis((furan-2-ylmethyl)thio)-N-phenylpropanamide (3aa): R_f = 0.75 (20% ethyl acetate in hexane); white solid; yield 89% (138 mg); mp 85-89 ºC; ^{1}H NMR (400 MHz, $CDCl_3$) δ 7.46 (d, *J* = 7.8 Hz, 3H), 7.34 (d, *J* = 1.2 Hz, 2H), 7.31 (t, *J* = 7.8 Hz, 2H), 7.11 (t, *J* = 7.4 Hz, 1H), 6.32-6.30 (m, 2H), 6.20 (d, *J* = 3.2 Hz, 2H), 4.27 (t, *J* = 7.2 Hz, 1H), 3.94-3.86 (m, 4H), 2.73 (d, *J* = 7.2 Hz, 2H); ^{13}C NMR (100 MHz, $CDCl_3$) δ 167.4, 151.0, 142.4, 137.7, 129.1, 124.6, 120.2, 110.8, 108.3, 47.6, 44.3, 27.5; IR (KBr) ῡ 3303, 3051, 2944, 1616, 692; HRMS (ESI/Q-TOF) m/z: [M + Na]$^+$ calcd for $C_{19}H_{19}NO_3S_2Na$ 396.0699; found 396.0684.

3,3-Bis(isobutylthio)-N-phenylpropanamide (3ab): R_f = 0.8 (20% ethyl acetate in hexane); colorless liquid; yield 69% (93 mg); ^{1}H NMR (400 MHz, $CDCl_3$) δ 7.88 (s, 1H), 7.52 (d, *J* = 7.8 Hz, 2H), 7.32 (t, *J* = 7.8 Hz, 2H), 7.11 (t, *J* = 7.4 Hz, 1H), 4.24 (t, *J* = 7.0 Hz, 1H), 2.83 (d, *J* = 7.0 Hz, 2H), 2.62 (m, 2H), 2.51 (m, 2H), 1.84 (t, 2H), 1.00 (d, *J* = 6.6 Hz, 12H); ^{13}C NMR (100 MHz, $CDCl_3$) δ 167.9, 137.8, 129.1, 124.6, 120.2, 48.4, 45.4, 40.3, 28.6, 22.2; IR (KBr) ῡ 3309, 3075, 2921, 1624, 697; HRMS (ESI/Q-TOF) m/z: $[M + Na]^+$ calcd for $C_{17}H_{27}NOS_2Na$ 348.1426; found 348.1415.

3,3-Bis(isobutylthio)-N-(o-tolyl)propanamide (3bb): R_f = 0.65 (20% ethyl acetate in hexane); White solid, yield 75% (96 mg); mp 76-79 ºC; ^{1}H NMR (400 MHz, $CDCl_3$) δ 7.77 (s, 1H), 7.70 (d, *J* = 8.0 Hz, 1H), 7.18-7.15 (m, 2H), 7.06 (t, *J* = 7.3 Hz, 1H), 4.22 (t, *J* = 7.0 Hz, 1H), 2.84 (d, *J* = 7.0 Hz, 2H), 2.62 (dd, *J* = 12.3, 6.7 Hz, 2H), 2.52 (dd, *J* = 12.3, 7.0 Hz, 2H), 2.27 (s, 3H), 1.89-1.79 (m, 2H), 1.03-0.97 (m, 12H); ^{13}C NMR (100 MHz, $CDCl_3$) δ 168.0, 135.6, 130.5, 130.0, 126.6, 125.5, 123.8, 48.4, 44.8, 40.2, 28.5, 22.3, 18.1; IR (KBr) ῡ 3294, 2967, 1651, 1301, 690; HRMS (ESI/Q-TOF) m/z: $[M + Na]^+$ calcd for $C_{18}H_{29}NOS_2Na$ 362.1588; found 362.1517.

3,3-Bis(phenethylthio)-N-phenylpropanamide (3ac): R_f = 0.85 (10% ethyl acetate in hexane); white solid; yield 75% (125 mg); mp 85-90 ºC; ^{1}H NMR (400 MHz, $CDCl_3$) δ 7.70 (s, 1H), 7.49 (d, *J* = 7.8 Hz, 2H), 7.34-7.26 (m, 6H), 7.23-7.19 (m, 6H), 7.13 (t, *J* = 7.4 Hz, 1H), 4.30 (t, *J* = 7.0 Hz, 1H), 2.99-2.95 (m, 2H), 2.92-2.85 (m, 6H), 2.78 (d, *J* = 7.0 Hz, 2H); ^{13}C NMR (100 MHz, $CDCl_3$) δ 167.7, 140.3, 137.7, 129.1, 128.7, 128.6, 126.6, 124.7, 120.2, 47.9, 45.2, 35.8, 32.6; IR (KBr) ῡ 3303, 3024, 2917, 2341, 1652, 668; HRMS (ESI/Q-TOF) m/z: $[M + H]^+$ calcd for $C_{25}H_{28}NOS_2$ 422.1607; found 422.1592.

3,3-Bis(phenethylthio)-N-(p-tolyl)propanamide (3cc): R_f = 0.75 (10% ethyl acetate in hexane); yellow solid; yield 54% (89 mg); mp 102-105 ºC; ^{1}H NMR (400 MHz, $CDCl_3$) δ 7.58 (s, 1H), 7.37 (d, *J* = 8.2 Hz, 2H), 7.30-7.26 (m, 4H), 7.23-7.19 (m, 6H), 7.12 (d, *J* = 8.2 Hz, 2H), 4.30 (t, *J* = 7.0 Hz, 1H), 2.99-2.91 (m, 3H), 2.90-2.83 (m, 5H), 2.76 (d, *J* = 7.0 Hz, 2H), 2.32 (s, 3H); ^{13}C NMR (100 MHz, $CDCl_3$) δ 167.5, 140.3, 135.1, 134.3, 129.6, 128.7, 128.6, 126.6, 120.3, 47.9, 45.2, 35.9, 32.6, 21.0; IR (KBr) ῡ 3366, 3025, 29218, 1649, 696; HRMS (ESI/Q-TOF) m/z: $[M + K]^+$ calcd for $C_{26}H_{29}NOS_2K$ 474.1322; found 474.1320.

3,3-Bis(benzylthio)-N-phenylpropanamide (3ad): R_f = 0.65 (20% ethyl acetate in hexane); white solid; yield 92% (150 mg); mp 182-185 ºC; ^{1}H NMR (400 MHz, $CDCl_3$) δ 7.39 (d, *J* = 7.8 Hz, 2H), 7.32-7.29 (m, 5H), 7.28-7.23 (m, 7H), 7.12-7.09 (m, 2H), 4.10 (t, *J* = 7.2 Hz, 1H), 3.89-3.80 (m, 4H), 2.66 (d, *J* = 7.2 Hz, 2H); ^{13}C NMR (100 MHz, $CDCl_3$) δ 167.4, 138.1, 137.6, 129.2, 129.1, 128.8, 127.4, 124.6, 120.1, 46.9, 44.5, 35.4; IR (KBr) ῡ 3303, 3077, 2921, 1683, 677; HRMS (ESI/Q-TOF) m/z: $[M + Na]^+$ calcd for $C_{23}H_{23}NOS_2Na$ 416.1113; found 416.1100.

3,3-Bis(benzylthio)-N-(o-tolyl)propanamide (3bd): R_f = 0.3 (10% ethyl acetate in hexane); white solid; yield 78% (128 mg); mp 115-119 ºC; ^{1}H NMR (400 MHz, $CDCl_3$) δ 7.66 (d, *J* = 7.9 Hz, 1H), 7.30-7.20 (m, 10H), 7.20-7.16 (m, 2H), 7.13 (s, 1H), 7.08 (t, *J* = 7.2 Hz, 1H), 4.08 (t, *J* = 7.0 Hz, 1H), 3.88-3.81 (m, 4H), 2.74 (d, *J* = 7.0 Hz, 2H), 2.17 (s, 3H); ^{13}C NMR (100 MHz, $CDCl_3$) δ 167.5, 137.9, 135.5, 130.6, 129.9, 129.2, 128.8, 127.4, 126.7, 125.6, 123.7, 46.7, 44.3, 35.6, 18.1; IR (KBr) ῡ 3263, 3027, 2918, 1620, 700; HRMS (ESI/Q-TOF) m/z: $[M + Na]^+$ calcd for $C_{24}H_{25}NOS_2Na$ 430.1270; found 430.1266.

3,3-Bis((4-(tert-butyl)benzyl)thio)-N-(2,4-dimethylphenyl)propanamide (3de): R_f = 0.65 (20% ethyl acetate in hexane); white solid; yield 66% (123mg); mp 114-116 ºC; ^{1}H NMR (700 MHz, $CDCl_3$) δ 7.43 (d, *J* = 8.6 Hz, 1H), 7.30 (d, *J* = 8.2 Hz, 4H), 7.21 (d, *J* = 8.2 Hz, 4H), 7.08 (s, 1H), 6.98-6.97(m, 2H), 4.12 (t, *J* = 7.0 Hz, 1H), 3.84-3.80 (m, 4H), 2.76 (d, *J* = 7.1 Hz, 2H), 2.28 (s, 3H), 2.12 (s, 3H), 1.29 (s, 18H); ^{13}C NMR (175 MHz, $CDCl_3$) δ 167.8, 150.4, 135.5, 134.9, 132.8, 131.2, 130.6, 128.9, 127.2, 125.7, 124.2, 47.0, 44.2, 35.1, 34.6, 31.5, 21.0, 18.2; IR (KBr) ῡ 3248, 2960, 2848, 1650, 834; HRMS (ESI/Q-TOF) m/z: $[M + H]^+$ calcd for $C_{33}H_{44}NOS_2$ 534.2860; found 534.2859.

3,3-Bis((4-(tert-butyl)benzyl)thio)-N-(3,4-dichlorophenyl)propenamide (3ee): R_f = 0.7 (20% ethyl acetate in hexane); semi solid; yield 83% (134mg); ^{1}H NMR (700 MHz, $CDCl_3$) δ 7.59 (s, 1H), 7.50 (s, 1H), 7.34-7.31 (m, 5H), 7.23-7.20 (m, 5H), 4.09 (t, *J* = 7.0 Hz, 1H), 3.86-3.80 (m, 4H), 2.71 (d, *J* = 7.1 Hz, 2H), 1.31 (s, 18H); ^{13}C NMR (175 MHz, $CDCl_3$) δ 167.9, 150.5, 137.0, 134.9, 132.7, 130.5, 128.9, 125.8, 124.7, 121.9, 119.5, 46.8, 44.2, 34.9, 34.6, 31.4; IR (KBr) ῡ 3298, 2961, 1660, 689; HRMS (ESI/Q-TOF) m/z: $[M + Na]^+$ calcd for $C_{31}H_{37}Cl_2NOS_2Na$ 596.1591; found 596.1517.

N-(4-Fluorophenyl)-3,3-bis((4-methoxybenzyl)thio)propanamide (3ff): R_f = 0.45 (20% ethyl acetate in hexane); pale yellow solid; yield 81% (140 mg); mp 108-110 ºC; ^{1}H NMR (400 MHz, $CDCl_3$) δ 7.37-7.33 (m, 2H), 7.26 (s, 1H), 7.21 (d, *J* = 8.4 Hz, 4H), 7.00 (t, *J* = 8.4 Hz, 2H), 6.83 (d, *J* = 8.4 Hz, 4H), 4.05 (t, *J* = 7.0 Hz, 1H), 3.84 (s, 6H), 3.85-3.78 (m, 4H), 2.69 (d, *J* = 7.0 Hz, 2H); ^{13}C NMR (100 MHz, $CDCl_3$) δ 167.5, 159.5 (d, $^1J_{CF}$ = 243.8 Hz), 158.9, 133.6 (d, $^4J_{CF}$ = 2.8 Hz), 130.3, 130.0, 122.0 (d, $^3J_{CF}$ = 8.0 Hz), 115.6 (d, $^2J_{CF}$ = 22.4 Hz), 114.2, 55.4, 46.3, 44.2, 34.8; IR (KBr) ῡ 3302, 2928, 2347, 1658, 833; HRMS (ESI/Q-TOF) m/z: $[M + Na]^+$ calcd for $C_{25}H_{26}FNO_3S_2Na$ 494.1230; found 494.1229.

3,3-Bis((2-chlorobenzyl)thio)-N-(4-ethoxyphenyl)propanamide (3gg): R_f = 0.45 (10% ethyl acetate in hexane); white solid; yield 70% (111 mg); mp 112-116 ºC; ^{1}H NMR (400 MHz, $CDCl_3$) δ 7.45 (s, 1H), 7.35 (dd, *J* = 7.4, 1.6 Hz, 2H), 7.30-7.21 (m, 4H), 7.21-7.12 (m, 4H), 6.81 (d, *J* = 8.8 Hz, 2H), 4.19 (t, *J* = 7 .0 Hz, 1H), 4.02-3.98 (m, 2H), 3.96-3.91 (m, 4H), 2.77 (d, *J* = 7.0 Hz, 2H), 1.39 (t, *J* = 7.0 Hz, 3H); ^{13}C NMR (100 MHz, $CDCl_3$) δ 167.3, 156.1, 135.5, 134.2, 131.1, 130.6, 130.0, 128.8, 127.1, 122.2, 114.8, 63.8, 47.4, 44.4, 33.4, 14.9; IR (KBr) ῡ 3295, 2977, 2925, 2359, 1651, 740, 697; HRMS (ESI/Q-TOF) m/z: $[M + Na]^+$ calcd for $C_{25}H_{25}Cl_2NO_2S_2Na$ 528.0596; found 528.0579.

3,3-Bis((4-(tert-butyl)benzyl)thio)-N-(4-ethoxyphenyl)propanamide (3ge): R_f = 0.55 (10% ethyl acetate in hexane); white solid; yield 52% (90 mg); mp 144-148 ºC; ^{1}H NMR (400 MHz, $CDCl_3$) δ 7.32 (d, *J* = 8.2 Hz, 4H), 7.23 (t, *J* = 7.8 Hz, 6H), 7.01 (s, 1H), 6.81 (d, *J* = 8.8 Hz, 2H), 4.12 (t, *J* = 7.2 Hz, 1H), 4.00 (q, *J* = 7.0 Hz, 2H), 3.87-3.79 (m, 4H), 2.66 (d, *J* = 7.2 Hz, 2H), 1.40 (t, *J* = 7.0 Hz, 3H), 1.29 (d, *J* = 7.2 Hz, 18H); ^{13}C NMR (100 MHz, $CDCl_3$) δ 167.4, 156.1, 150.4, 135.1, 130.6, 128.9, 125.8, 122.2, 114.8, 63.8, 47.3, 44.3, 34.9, 34.7, 31.5, 15.0; IR (KBr) ῡ 3420, 2960, 2359, 1652, 668; HRMS (ESI/Q-TOF) m/z: $[M + Na]^+$ calcd for $C_{33}H_{43}NO_2S_2Na$ 572.2627; found 572.2625.

3,3-Bis(dodecylthio)-N-phenylpropanamide (3ai): R_f = 0.85 (20% ethyl acetate in hexane); white solid; yield 77% (174 mg); mp 64-66 ºC; ^{1}H NMR (400 MHz, $CDCl_3$) δ 7.75 (s, 1H), 7.52 (d, *J* = 7.8 Hz, 2H), 7.32 (t, *J* = 7.8 Hz, 2H), 7.11 (t, *J* = 7.4 Hz, 1H), 4.26 (t, *J* = 7.0 Hz, 1H), 2.84 (d, *J* = 7.0 Hz, 2H), 2.75-2.68 (m, 2H), 2.67-2.60 (m, 2H), 1.64-1.57 (m, 4H), 1.39-1.36 (m, 4H), 1.30-1.25 (m, 32H), 0.88 (t, *J* = 6.8 Hz, 6H); ^{13}C NMR (100 MHz, $CDCl_3$) δ ^{13}C NMR (100 MHz, $CDCl_3$) δ 167.8, 137.8, 129.2, 124.6, 120.1, 47.7, 45.4, 32.1, 31.5, 29.8,

29.78, 29.76, 29.72, 29.7, 29.5, 29.4, 29.1, 22.8, 14.3; IR (KBr) ῡ 3320, 3033, 2848, 1656, 691; HRMS (ESI/Q-TOF) m/z: $[M + Na]^+$ calcd for $C_{33}H_{59}NOS_2Na$ 572.3930; found 572.3939.

3,3-Bis(dodecylthio)-N-(4-isopropylphenyl)propenamide (3hi) : R_f = 0.75 (20% ethyl acetate in hexane); white solid; yield 56% (107mg); mp 63-65 ºC; ^{1}H NMR (700 MHz, $CDCl_3$) δ 7.88 (s, 1H), 7.44 (d, *J* = 8.4 Hz, 2H), 7.17 (d, *J* = 8.4 Hz, 2H), 4.27 (t, *J* = 7.1 Hz, 1H), 2.90-2.85 (m, 1H), 2.82 (d, *J* = 7.1 Hz, 2H), 2.72-2.68(m, 2H),2.64-2.60 (m, 2H), 1.61-1.57 (m, 4H), 1.41-1.35 (m, 4H), 1.30-1.22 (m,38H); 0.88 (t, *J* =7.2 Hz, 6H); ^{13}C NMR (176 MHz, $CDCl_3$) δ 167.8, 145.3, 135.5, 127.0, 120.3, 47.8, 45.3, 33.7, 32.04, 31.4, 29.80, 29.77, 29.74, 29.67, 29.5, 29.4, 29.3, 29.1, 24.1, 22.8, 14.2; IR (KBr) ῡ 3298, 2922, 1652, 839; HRMS (ESI/Q-TOF) m/z: $[M + H]^+$ calcd for $C_{36}H_{65}NOS_2$ 592.4531; found 592.4580.

N-(4-Bromophenyl)-3,3-bis(ethylthio)propanamide (3ij): R_f = 0.4 (10% ethyl acetate in hexane); pale yellow solid; yield 90% (84 mg); mp 104-107 ºC; ^{1}H NMR (400 MHz, DMSO-D_6) δ 10.14 (s, 1H), 7.56 (d, *J* = 8.8 Hz, 2H), 7.48 (d, *J* = 8.8 Hz, 2H), 4.33 (t, *J* = 7.4 Hz, 1H), 2.81 (d, *J* = 7.4 Hz, 2H), 2.7 0-2.58 (m, 4H), 1.19 (t, *J* = 7.4 Hz, 6H); ^{13}C NMR (100 MHz, $CDCl_3$) δ 168.0, 136.8, 132.1, 121.8, 117.3, 46.9, 45.2, 25.4, 14.6; IR (KBr) ῡ 3294, 2967, 1651, 1301, 712; HRMS (ESI/Q-TOF) m/z: $[M + Na]^+$ calcd for $C_{13}H_{18}BrNOS_2Na$ 369.9905; found 369.9895.

N-butyl-3,3-bis((4-(tert-butyl)benzyl)thio)propanamide (3je): R_f = 0.35 (10% ethyl acetate in hexane); liquid; yield 14% (27 mg); ^{1}H NMR (700 MHz, $CDCl_3$) δ 7.33 (d, *J* = 8.1 Hz, 4H), 7.22 (d, *J* = 8.1 Hz, 4H), 5.32 (s, 1H), 4.05 (t, *J* = 7.2 Hz, 1H), 3.82-3.77 (m, 4H), 2.49 (d, *J* = 7.2 Hz, 2H), 1.82-1.80 (m, 2H), 1.67-1.65 (m, 3H), 1.60-1.59 (m, 1H), 1.31 (s, 18H), 1.16-1.10 (m, 1H), 1.02-0.97 (m, 2H); ^{13}C NMR (175 MHz, $CDCl_3$) δ 168.2, 150.1, 135.1, 128.8, 125.6,

48.3, 47.3, 43.6, 34.6, 34.5, 33.0, 31.4, 25.6, 24.8; IR (KBr) ῡ 3300, 2967, 1688, 1351, 766; HRMS (ESI/Q-TOF) m/z: [M + Na]$^{+}$ calcd for $C_{18}H_{29}NOS_2Na$ (-$C_{11}H_{16}$) 362.1583; found 362.0492.

3,3-Bis(benzylthio)-N-(4-nitrophenyl)propanamide (3kd): R_f = 0.35 (30% ethyl acetate in hexane); yellow solid; yield 55% (105 mg); mp 135-140 ºC; ^{1}H NMR (400 MHz, CDCl3) δ 8.18-8.16 (m, 2H), 7.54-7.52 (m, 3H), 7.32-7.28 (m, 5H), 7.28-7.26 (m, 5H), 4.03 (t, J = 7.1 Hz, 1H), 3.89-3.81 (m, 4H), 2.69 (d, J = 7.1 Hz, 2H); ^{13}C NMR (100 MHz, $CDCl_3$) δ 167.8, 143.7, 143.4, 138.0, 129.2, 128.9, 127.6, 125.1, 119.3, 46.3, 44.3, 35.3; IR (KBr) ῡ 3309, 2941, 1611, 1402, 722; HRMS (ESI/Q-TOF) m/z: [M + Na]$^{+}$ calcd for $C_{23}H_{22}N_2O_3S_2Na$ 461.0964; found 461.1005.

3,3-Bis(benzylthio)-N-(4-(trifluoromethyl)phenyl)propanamide (3ld): R_f = 0.5 (10% ethyl acetate in hexane); white solid; yield 84% (141 mg); mp 125-128 ºC ^{1}H NMR (400 MHz, $CDCl_3$) δ 7.52 (d, *J* = 8.6 Hz, 2H), 7.45 (d, *J* = 8.5 Hz, 2H), 7.30-7.27 (m, 5H), 7.26-7.21 (m, 6H), 4.03 (t, *J* = 7.1 Hz, 1H), 3.87-3.78 (m, 4H), 2.64 (d, *J* = 7.1 Hz, 2H); ^{13}C NMR (175 MHz, $CDCl_3$) δ 167.8, 140.6, 138.0, 129.2, 128.8, 127.5, 126.4, 126.26 (q, *J* = 3.4 Hz), 124.15 (q, *J* = 271.0 Hz), 119.7, 46.7, 44.4, 35.4; IR (KBr) ῡ 3314, 2950, 1673, 1131, 693; HRMS (ESI/Q-TOF) m/z: [M + Na]$^{+}$ calcd for $C_{24}H_{22}F_3NOS_2Na$ 484.0987; found 484.1317.

N-Phenyl-3,3-bis((thiophen-2-ylmethyl)thio)propanamide (3ak): R_f = 0.55 (10% ethyl acetate in hexane); semi solid; yield 76% (128 mg); ^{1}H NMR (700 MHz, $CDCl_3$) δ 7.45 (d, *J* = 8.0 Hz, 2H), 7.37-7.29 (m, 3H), 7.22-7.19 (m, 2H), 7.11 (t, *J* = 7.3 Hz, 1H), 6.93-6.89 (m, 4H), 4.25 (t, *J* = 7.1 Hz, 1H), 4.11-4.06 (m, 4H), 2.74 (d, *J* = 7.2 Hz, 2H); ^{13}C NMR (175 MHz, $CDCl_3$) δ 167.3, 141.1, 137.6, 129.1, 127.1, 126.9, 125.5, 124.6, 120.2, 47.3, 44.4, 29.9; IR

(KBr) ῡ 3355, 2971, 1645, 1299, 676; HRMS (ESI/Q-TOF) m/z: $[M + H]^+$ calcd for $C_{19}H_{20}NOS_4$ 406.0422; found 406.0443.

3,3-Dimethoxy-N-phenylpropanamide (4aa):[55] R_f = 0.4 (20% ethyl acetate in hexane); semi solid; yield 69% (54 mg); ^{1}H NMR (700 MHz, $CDCl_3$) δ 8.19 (s, 1H), 7.51 (d, *J* = 8.0 Hz, 2H), 7.30 (t, *J* = 7.4 Hz, 2H), 7.09 (t, *J* = 7.3 Hz, 1H), 4.76 (t, *J* = 5.1 Hz, 1H), 3.43 (s, 6H), 2.71 (d, *J* = 5.2 Hz, 2H); ^{13}C NMR (175 MHz, $CDCl_3$) δ 167.4, 137.9, 129.0, 124.4, 120.0, 102.2, 54.4, 42.1.

3,3-Diethoxy-N-phenylpropanamide (4ab):[56] R_f = 0.45 (20% ethyl acetate in hexane); white semi solid; yield 78% (76 mg); ^{1}H NMR (700 MHz, $CDCl_3$) δ 8.18 (s, 1H), 7.50 (d, *J* = 8.0 Hz, 2H), 7.31 (t, *J* = 7.8 Hz, 2H), 7.09 (t, *J* = 7.4 Hz, 1H), 4.86 (t, *J* = 5.1 Hz, 1H), 3.77-3.73 (m, 2H), 3.61-3.57 (m, 2H), 2.72 (d, *J* = 5.1 Hz, 2H), 1.26 (t, 7.0 Hz, 6H); ^{13}C NMR (175 MHz, $CDCl_3$) δ 167.6, 138.1, 129.1, 124.2, 119.8, 100.2, 62.9, 43.2, 15.4.

N-Phenyl-3,3-bis(2,2,2-trifluoroethoxy)propanamide (4ac): R_f = 0.7 (20% ethyl acetate in hexane); semi solid; yield 59% (84 mg); ^{1}H NMR (700 MHz, $CDCl_3$) δ 7.89 (s, 1H), 7.46 (d, *J* = 8.1 Hz, 2H), 7.31 (t, *J* = 7.7 Hz, 2H), 7.13 (t, *J* = 7.4 Hz, 1H), 5.22 (t, *J* = 5.4 Hz, 1H), 4.02-3.91 (m, 4H), 2.77 (d, *J* = 5.5 Hz, 2H); ^{13}C NMR (175 MHz, $CDCl_3$) δ 165.9, 137.3, 129.2, 125.0, 123.5 (q, $^1J_{CF3}$ = 277.8 Hz), 120.4, 101.2, 63.8 (q, $^2J_{CF3}$ = 35.2 Hz), 42.1; IR (KBr) ῡ 3289, 2926, 2108, 1597, 1321; HRMS (ESI/Q-TOF) m/z: $[M + H]^+$ calcd for $C_{13}H_{13}F_6NO_3$ 346.0881; found 346.0872.

N-Phenyl-3,3-dipropoxypropanamide (4ad): R_f = 0.65 (10% ethyl acetate in hexane); liquid; yield 75% (83 mg); ^{1}H NMR (400 MHz, $CDCl_3$) δ 8.28 (s, 1H), 7.50 (d, *J* = 8.1 Hz, 2H), 7.33-7.26 (m, 2H), 7.09 (t, *J* = 7.4 Hz, 1H), 4.85 (t, *J* = 5.0 Hz, 1H), 3.68-3.59 (m, 2H), 3.51-3.46 (m, 2H), 2.74-2.72 (m, 2H), 1.68-1.61 (m, 2H), 1.33-1.25 (m, 2H), 0.96 (t, *J* = 7.4 Hz, 6H); ^{13}C NMR (100 MHz, $CDCl_3$) δ 167.6, 138.1, 129.1, 124.2, 119.8, 100.3, 69.0, 43.0, 23.2, 10.8; IR (KBr) ῡ 3323, 2940, 1677, 1299, 785; HRMS (ESI/Q-TOF) m/z: $[M + Na]^+$ calcd for $C_{15}H_{23}NO_3Na$ 288.1570; found 288.1586.

3,3-Dibutoxy-N-phenylpropanamide (4ae): R_f = 0.65 (10% ethyl acetate in hexane); liquid; yield 66% (80 mg); ^{1}H NMR (400 MHz, $CDCl_3$) δ 8.37 (s, 1H), 7.50 (d, *J* = 8.0 Hz, 2H), 7.32-7.26 (m, 2H), 7.08 (t, *J* = 7.4 Hz, 1H), 4.84 (t, *J* = 5.0 Hz, 1H), 3.70-3.65 (m, 2H), 3.54-3.48 (m, 2H), 2.72 (d, *J* = 5.1 Hz, 2H), 1.61-1.56 (m, 4H), 1.44-1.35 (m, 4H), 0.92 (t, *J* = 7.4 Hz, 6H); ^{13}C NMR (100 MHz, $CDCl_3$) δ 167.7, 138.1, 129.0, 124.2, 119.8, 100.4, 67.1, 42.9, 31.9, 19.4, 13.9; IR (KBr) ῡ 3332, 2960, 1699, 1544, 670; HRMS (ESI/Q-TOF) m/z: $[M + Na]^+$ calcd for $C_{17}H_{27}NO_3Na$ 316.1883; found 316.1882.

3,3-Bis(hexyloxy)-N-phenylpropanamide (4af): R_f = 0.65 (10% ethyl acetate in hexane); liquid; yield 67% (97 mg); ^{1}H NMR (400 MHz, $CDCl_3$) δ 8.29 (s, 1H), 7.50 (d, *J* = 8.1 Hz, 2H), 7.33-7.26 (m, 2H), 7.11-6.95 (m, 1H), 4.84 (t, *J* = 5.3 Hz, 1H), 3.70-3.65 (m, 2H), 3.54-348 (m, 2H), 2.72 (d, *J* = 5.1 Hz, 2H), 1.68-1.58 (m, 6H), 1.38-1.25 (m, 10H), 0.88 (t, *J* = 7.05 Hz, 6H); ^{13}C NMR (100 MHz, $CDCl_3$) δ 167.6, 129.8, 129.1, 124.2, 119.8, 100.4, 67.4, 43.0, 31.7, 29.9, 26.0, 22.7, 14.1; IR (KBr) ῡ 3389, 2959, 1650, 1456, 710; HRMS (ESI/Q-TOF) m/z: $[M + Na]^+$ calcd for $C_{21}H_{35}NO_3Na$ 372.2509; found 372.2491.

3,3-Bis(octyloxy)-N-phenylpropanamide (4ag): R_f = 0.65 (10% ethyl acetate in hexane); liquid; yield 60% (101 mg); ^{1}H NMR (400 MHz, $CDCl_3$) δ 8.62 (s, 1H), 7.50 (d, *J* = 8.1 Hz, 2H), 7.30-7.26 (m, 2H), 7.06 (t, *J* = 7.4 Hz, 1H), 4.85 (t, *J* = 5.2 Hz, 1H), 3.68-3.58 (m, 2H), 3.52-3.46 (m, 2H), 2.70-2.55 (m, 6H), 1.60-1.51 (m, 6H), 1.29-1.26 (m, 14H), 0.87 (t, *J* = 7.01, 6H); ^{13}C NMR (100 MHz, $CDCl_3$) δ 167.9, 138.1, 128.9, 124.1, 119.9, 100.7, 67.6, 62.8, 32.8, 31.9, 29.4, 26.2, 25.8, 22.7, 14.1; IR (KBr) ῡ 3334, 2976, 1680, 1354, 761; HRMS (ESI/Q-TOF) m/z: $[M + Na]^+$ calcd for $C_{25}H_{43}NO_3Na$ 428.3135; found 428.3193.

3,3-Bis(nonyloxy)-N-phenylpropanamide (4ah): R_f = 0.7 (10% ethyl acetate in hexane); liquid; yield 65% (117 mg); ^{1}H NMR (400 MHz, $CDCl_3$) δ 8.38 (s, 1H), 7.50 (d, *J* = 8.0 Hz, 2H), 7.31-7.26 (m, 2H), 7.07 (t, *J* = 7.4 Hz, 1H), 4.83 (t, *J* = 5.0 Hz, 1H), 3.69-3.60 (m, 2H), 3.52-3.47 (m, 2H), 2.71 (d, *J* = 5.0 Hz, 2H), 1.63-1.52(m, 4H), 1.35-1.24 (m 24H), 0.87 (t, *J* = 7.01 Hz, 6H); ^{13}C NMR (100 MHz, $CDCl_3$) δ 167.7, 138.1, 129.0, 124.2, 119.8, 100.4, 67.4, 63.1, 42.9, 32.9, 32.0, 29.9, 29.4, 26.3, 22.7, 14.2; IR (KBr) ῡ 3340, 2956, 1608, 1142, 756; HRMS (ESI/Q-TOF) m/z: $[M + Na]^+$ calcd for $C_{27}H_{47}NO_3Na$ 456.3448; found 456.3435.

3,3-Bis(decyloxy)-N-phenylpropanamide (4ai): R_f = 0.7 (10% ethyl acetate in hexane); liquid; yield 72% (126 mg); ^{1}H NMR (400 MHz, $CDCl_3$) δ 8.63 (s, 1H), 7.50 (d, *J* = 8.1 Hz, 2H), 7.30-7.26 (m, 2H), 7.06 (t, *J* = 7.3 Hz, 1H), 4.84 (t, *J* = 5.1 Hz, 1H), 3.61-6.57(m, 4H), 2.69-2.57 (m, 4H), 1.55-1.52 (m, 4H), 1.29-1.25 (m, 26H), 0.87 (t, *J* = 7.01 Hz, 6H); ^{13}C NMR (100 MHz, $CDCl_3$) δ 167.9, 138.2, 128.9, 124.1, 119.8, 100.7, 67.6, 62.8, 32.8, 32.0, 29.7, 29.6, 29.5, 29.4, 25.8, 22.7, 14.1; IR (KBr) ῡ 3345, 2947, 1678, 1355, 789; HRMS (ESI/Q-TOF) m/z: $[M + Na]^+$ calcd for $C_{29}H_{51}NO_3Na$ 484.3761; found 484.3800.

(Z)-S-(3-Oxo-3-(phenylamino)prop-1-en-1-yl) ethanethioate (5): R_f = 0.30 (20% ethyl acetate in hexane); white solid; yield 63% (57 mg); ^{1}H NMR (700 MHz, $CDCl_3$) δ 7.72 (d, *J* = 10.0 Hz, 2H), 7.57 (d, *J* = 7.8 Hz, 2H), 7.30 (t, *J* = 7.6 Hz, 2H), 7.11 (t, *J* = 7.2 Hz, 1H), 6.18 (d, *J* = 10.0 Hz, 1H), 2.43 (s, 3H); ^{13}C NMR (175 MHz, $CDCl_3$) δ 193.2, 163.7, 137.7, 134.5, 129.1, 124.8, 120.0, 118.9, 30.8 ; IR (KBr) ʊ̄ 3342, 3285, 2941, 1599, 1144, 752; HRMS (ESI/Q-TOF) m/z: $[M + H]^+$ calcd for $C_{11}H_{12}BrNO_2S$ 222.0583; found 222.0585.

(Z)-N-Phenyl-3-(phenylthio)acrylamide (6):[10] R_f = 0.45 (20% ethyl acetate in hexane); white solid; yield 96% (102 mg); ^{1}H NMR (400 MHz, DMSO-d_6) δ 10.13 (s, 1H), 7.65 (d, *J* = 7.9 Hz, 2H), 7.53 (d, *J* = 7.4 Hz, 2H), 7.44-7.39 (m, 3H), 7.37-7.29 (m, 3H), 7.05 (t, *J* = 7.4 Hz, 1H), 6.25 (d, *J* = 9.8 Hz, 1H).

2.6 NOTES AND REFERENCES

(1) Yamashina, M.; Tanaka, Y.; Lavendomme, R.; Ronson, T. K.; Pittelkow, M.; Nitschke, J. R. An Antiaromatic-Walled Nanospace. *Nature* **2019**, *574*, 511-515.

(2) Ghosh, A.; Schmittel, M. Using Multiple Self-Sorting for Switching Functions in Discrete Multicomponent Systems. *Beilstein J. Org. Chem.* **2020**, *16*, 2831-2853.

(3) Dougherty, D. A. The Cation−Π Interaction. *Acc. Chem. Res.* **2013**, *46*, 885-893.

(4) Giese, M.; Albrecht, M.; Rissanen, K. Anion−Π Interactions with Fluoroarenes. *Chem. Rev.* **2015**, *115*, 8867-8895.

(5) Pramanik, M.; Choudhuri, K.; Chakraborty, S.; Ghosh, A.; Mal, P. (Z)-Selective Anti-Markovnikov or Markovnikov Thiol–Yne-Click Reactions of an Internal Alkyne by Amide Hydrogen Bond Control. *Chem. Commun.* **2020**, *56*, 2991-2994.

(6) Turunen, L.; Erdélyi, M. Halogen Bonds of Halonium Ions. *Chem. Soc. Rev.* **2020**, *49*, 2688-2700.

(7) Twum, K.; Rissanen, K.; Beyeh, N. K. Recent Advances in Halogen Bonded Assemblies with Resorcin[4]Arenes. *Chem. Rec.* **2021**, *21*, 386-395.

(8) Nandy, A.; Kazi, I.; Guha, S.; Sekar, G. Visible-Light-Driven Halogen-Bond-Assisted Direct Synthesis of Heteroaryl Thioethers Using Transition-Metal-Free One-Pot C–I Bond Formation/C–S Cross-Coupling Reaction. *J. Org. Chem.* **2021**, *86*, 2570-2581.

(9) Choudhuri, K.; Mandal, A.; Mal, P. Aerial Dioxygen Activation Vs. Thiol-Ene Click Reaction within a System. *Chem. Commun.* **2018**, *54*, 3759-3762.

(10) Pramanik, M.; Mathuri, A.; Mal, P. Sulfur···Oxygen Interaction-Controlled (Z)-Selective Anti-Markovnikov Vinyl Sulfides. *Chem. Commun.* **2021**, *57*, 5698-5701.

(11) Raynal, M.; Ballester, P.; Vidal-Ferran, A.; van Leeuwen, P. W. N. M. Supramolecular Catalysis. Part 1: Non-Covalent Interactions as a Tool for Building and Modifying Homogeneous Catalysts. *Chem. Soc. Rev.* **2014**, *43*, 1660-1733.

(12) Mahadevi, A. S.; Sastry, G. N. Cooperativity in Noncovalent Interactions. *Chem. Rev.* **2016**, *116*, 2775-2825.

(13) Kennedy, C. R.; Lin, S.; Jacobsen, E. N. The Cation–Π Interaction in Small-Molecule Catalysis. *Angew. Chem. Int. Ed.* **2016**, *55*, 12596-12624.

(14) Choudhuri, K.; Pramanik, M.; Mal, P. Noncovalent Interactions in C–S Bond Formation Reactions. *J. Org. Chem.* **2020**, *85*, 11997-12011.

(15) Juanes, M.; Saragi, R. T.; Pinacho, R.; Rubio, J. E.; Lesarri, A. Sulfur Hydrogen Bonding and Internal Dynamics in the Monohydrates of Thenyl Mercaptan and Thenyl Alcohol. *Phys. Chem. Chem. Phys.* **2020**, *22*, 12412-12421.

(16) Kaiser, D.; Klose, I.; Oost, R.; Neuhaus, J.; Maulide, N. Bond-Forming and -Breaking Reactions at Sulfur(Iv): Sulfoxides, Sulfonium Salts, Sulfur Ylides, and Sulfinate Salts. *Chem. Rev.* **2019**, *119*, 8701-8780.

(17) Hioe, J.; Zipse, H. Radical Stability and Its Role in Synthesis and Catalysis. *Org. Biomol. Chem.* **2010**, *8*, 3609-3617.

(18) Sowndarya S. V, S.; St. John, P. C.; Paton, R. S. A Quantitative Metric for Organic Radical Stability and Persistence Using Thermodynamic and Kinetic Features. *Chem. Sci.* **2021**, *12*, 13158-13166.

(19) Hernández-Soto, H.; Weinhold, F.; Francisco, J. S. Radical Hydrogen Bonding: Origin of Stability of Radical-Molecule Complexes. *J. Chem. Phys.* **2007**, *127*, 164102.

(20) Johnson, E. R.; Dilabio, G. A. Radicals as Hydrogen Bond Donors and Acceptors. *Interdiscip. Sci. Comput. Life Sci.* **2009**, *1*, 133-140.

(21) Zou, J.-x.; Wang, Y.-q.; Huang, L.-t.; Jiang, Y.; Chen, J.-h.; Zhu, L.-q.; Yang, Y.-h.; Feng, Y.-y.; Peng, X.; Wang, Z. One Pot Preparation of A-Dithioacetal/A-Diselenoacetal Amides Via a Dual-C–S/C–Se Bond Formation and C–C Bond Cleavage Cascade of 3-Oxo-Butanamides. *Org. Chem. Front.* **2018**, *5*, 2317-2321.

(22) Gaunt, M. J.; Sneddon, H. F.; Hewitt, P. R.; Orsini, P.; Hook, D. F.; Ley, S. V. Development of B-Keto 1,3-Dithianes as Versatile Intermediates for Organic Synthesis. *Org. Biomol. Chem.* **2003**, *1*, 15-16.

(23) Zhu, L.; Yu, H.; Guo, Q.; Chen, Q.; Xu, Z.; Wang, R. C–H Bonds Phosphorylation of Ketene Dithioacetals. *Org. Lett.* **2015**, *17*, 1978-1981.

(24) Pramanik, M.; Choudhuri, K.; Mathuri, A.; Mal, P. Dithioacetalization or Thioetherification of Benzyl Alcohols Using 9-Mesityl-10-Methylacridinium Perchlorate Photocatalyst. *Chem. Commun.* **2020**, *56*, 10211-10214.

(25) Arunprasath, D.; Sekar, G. A Transition-Metal-Free and Base-Mediated Carbene Insertion into Sulfur-Sulfur and Selenium-Selenium Bonds: An Easy Access to Thio- and Selenoacetals. *Adv. Synth. Catal.* **2017**, *359*, 698-708.

(26) Choudhuri, K.; Pramanik, M.; Mal, P. Λ3-Iodanes as Visible Light Photocatalyst in Thioacetalization of Aldehydes. *Eur. J. Org. Chem.* **2019**, 4822-4826.

(27) Lowe, A. B.; Hoyle, C. E.; Bowman, C. N. Thiol-Yne Click Chemistry: A Powerful and Versatile Methodology for Materials Synthesis. *J. Mater. Chem.* **2010**, *20*, 4745-4750.

(28) Worch, J. C.; Stubbs, C. J.; Price, M. J.; Dove, A. P. Click Nucleophilic Conjugate Additions to Activated Alkynes: Exploring Thiol-Yne, Amino-Yne, and Hydroxyl-Yne Reactions from (Bio)Organic to Polymer Chemistry. *Chem. Rev.* **2021**, *121*, 6744-6776.

(29) Ghosh, S.; Lai, D.; Hajra, A. Trifunctionalization of Alkenes and Alkynes. *Org. Biomol. Chem.* **2020**, *18*, 7948-7976.

(30) Nishino, S.; Hirano, K.; Miura, M. Cu-Catalyzed Reductive Gem-Difunctionalization of Terminal Alkynes Via Hydrosilylation/Hydroamination Cascade: Concise Synthesis of A-Aminosilanes. *Chem. Eur. J.* **2020**, *26*, 8725-8728.

(31) Dondoni, A.; Marra, A. Metal-Catalyzed and Metal-Free Alkyne Hydrothiolation: Synthetic Aspects and Application Trends. *Eur. J. Org. Chem.* **2014**, 3955-3969.

(32) Ogawa, A.; Ikeda, T.; Kimura, K.; Hirao, T. Highly Regio- and Stereocontrolled Synthesis of Vinyl Sulfides Via Transition-Metal-Catalyzed Hydrothiolation of Alkynes with Thiols. *J. Am. Chem. Soc.* **1999**, *121*, 5108-5114.

(33) Kondoh, A.; Takami, K.; Yorimitsu, H.; Oshima, K. Stereoselective Hydrothiolation of Alkynes Catalyzed by Cesium Base: Facile Access to (Z)-1-Alkenyl Sulfides. *J. Org. Chem.* **2005**, *70*, 6468-6473.

(34) Ranjit, S.; Duan, Z.; Zhang, P.; Liu, X. Synthesis of Vinyl Sulfides by Copper-Catalyzed Decarboxylative C−S Cross-Coupling. *Org. Lett.* **2010**, *12*, 4134-4136.

(35) Nurhanna Riduan, S.; Ying, J. Y.; Zhang, Y. Carbon Dioxide Mediated Stereoselective Copper-Catalyzed Reductive Coupling of Alkynes and Thiols. *Org. Lett.* **2012**, *14*, 1780-1783.

(36) Singh, R.; Raghuvanshi, D. S.; Singh, K. N. Regioselective Hydrothiolation of Alkynes by Sulfonyl Hydrazides Using Organic Ionic Base–Brønsted Acid. *Org. Lett.* **2013**, *15*, 4202-4205.

(37) Shard, A.; Kumar, R.; Saima; Sharma, N.; Sinha, A. K. Amino Acid and Water-Driven Tunable Green Protocol to Access S–S/C–S Bonds Via Aerobic Oxidative Coupling and Hydrothiolation. *RSC Adv* **2014**, *4*, 33399-33407.

(38) Li, Y.; Cai, J.; Hao, M.; Li, Z. Visible Light Initiated Hydrothiolation of Alkenes and Alkynes over Znin2s4. *Green Chem.* **2019**, *21*, 2345-2351.

(39) Pramanik, M.; Choudhuri, K.; Mal, P. Metal-Free C–S Coupling of Thiols and Disulfides. *Org. Biomol. Chem.* **2020**, *18*, 8771-8792.

(40) Choudhuri, K.; Pramanik, M.; Mandal, A.; Mal, P. S−H···Π Driven Anti-Markovnikov Thiol-Yne Click Reaction. *Asian J. Org. Chem.* **2018**, *7*, 1849–1855.

(41) Hut'ka, M.; Tsubogo, T.; Kobayashi, S. Calcium-Catalyzed Bis-Hydrothiolation of Unactivated Alkynes Providing Dithioacetals. *Organomet.* **2014**, *33*, 5626-5629.

(42) Taniguchi, N.; Kitayama, K. Zn-Catalyzed Dihydrosulfenylation of Alkynes Using Thiols. *Phosphorus, Sulfur, and Silicon and the Related Elements* **2019**, *194*, 739-741.

(43) Manzer Manhas, F.; Kumar, J.; Raheem, S.; Thakur, P.; Rizvi, M. A.; Shah, B. A. Photoredox-Mediated Synthesis of B-Hydroxydithioacetals from Terminal Alkynes. *ChemPhotoChem* **2021**, *5*, 235-239.

(44) Khade, V. V.; Thube, A. S.; Dharpure, P. D.; Bhat, R. G. Direct Synthesis of 1,3-Dithiolanes from Terminal Alkynes via Visible Light Photoredox Catalysis. *Org. Biomol. Chem.* **2022**, *20*, 1315-1319.

(45) Yadav, J. S.; Reddy, B. V. S.; Raju, A.; Ravindar, K.; Baishya, G. Hydrothiolation of Unactivated Alkynes Catalyzed by Indium(Iii) Bromide. *Chem. Lett.* **2007**, *36*, 1474-1475.

(46) Mitamura, T.; Daitou, M.; Nomoto, A.; Ogawa, A. Highly Regioselective Double Hydrothiolation of Terminal Acetylenes with Thiols Catalyzed by Palladium Diacetate. *Bull. Chem. Soc. Jpn.* **2011**, *84*, 413-415.

(47) Taniguchi, N.; Kitayama, K. Dihydrosulfenylation of Alkynes with Thiols Using a Nickel Catalyst through a Radical Process. *Asian J. Org. Chem.* **2019**, *8*, 1468-1471.

(48) Ranu, B. C.; Banerjee, S.; Jana, R. Ionic Liquid as Catalyst and Solvent: The Remarkable Effect of a Basic Ionic Liquid, [Bmim]Oh on Michael Addition and Alkylation of Active Methylene Compounds. *Tetrahedron* **2007**, *63*, 776-782.

(49) Thiyagarajan, S.; Krishnakumar, V.; Gunanathan, C. Kotbu-Catalyzed Michael Addition Reactions under Mild and Solvent-Free Conditions. *Chem. Asian J.* **2020**, *15*, 518-523.

(50) Zhou, S.; Anderson, G. M.; Mondal, B.; Doni, E.; Ironmonger, V.; Kranz, M.; Tuttle, T.; Murphy, J. A. Organic Super-Electron-Donors: Initiators in Transition Metal-Free Haloarene–Arene Coupling. *Chem. Sci.* **2014**, *5*, 476-482.

(51) Pichette Drapeau, M.; Fabre, I.; Grimaud, L.; Ciofini, I.; Ollevier, T.; Taillefer, M. Transition-Metal-Free Alpha-Arylation of Enolizable Aryl Ketones and Mechanistic Evidence for a Radical Process. *Angew. Chem. Int. Ed.* **2015**, *54*, 10587-10591.

(52) SAINT+, Bruker AXS Inc., Madison, Wisconsin, USA, 1999 (Program for Reduction of Data collected on Bruker CCD Area Detector Diffractometer V. 6.02.)

(53) SADABS, Bruker AXS, Madison, Wisconsin, USA, 2004

(54) Sheldrick, G. A Short History of Shelx. *Acta Crystallogr. Sect. A* **2008**, *64*, 112-122.

(55) Graziano, M. L.; Cimminiello, G. A Simple Route to 4,4-Dialkoxy-2-Azetidinones: Useful Intermediates for Organic Synthesis. *Synthesis* **1989**, 54-56.

(56) Stumpf, T.-D. J.; Steinbach, M.; Höltke, M.; Heuger, G.; Grasemann, F.; Fröhlich, R.; Schindler, S.; Göttlich, R. C-Bridged Bispyrrolidines and Bispiperidines as New Ligands. *Eur. J. Org. Chem.* **2018**, 5538-5547.

NMR Spectrum of Selected Compounds

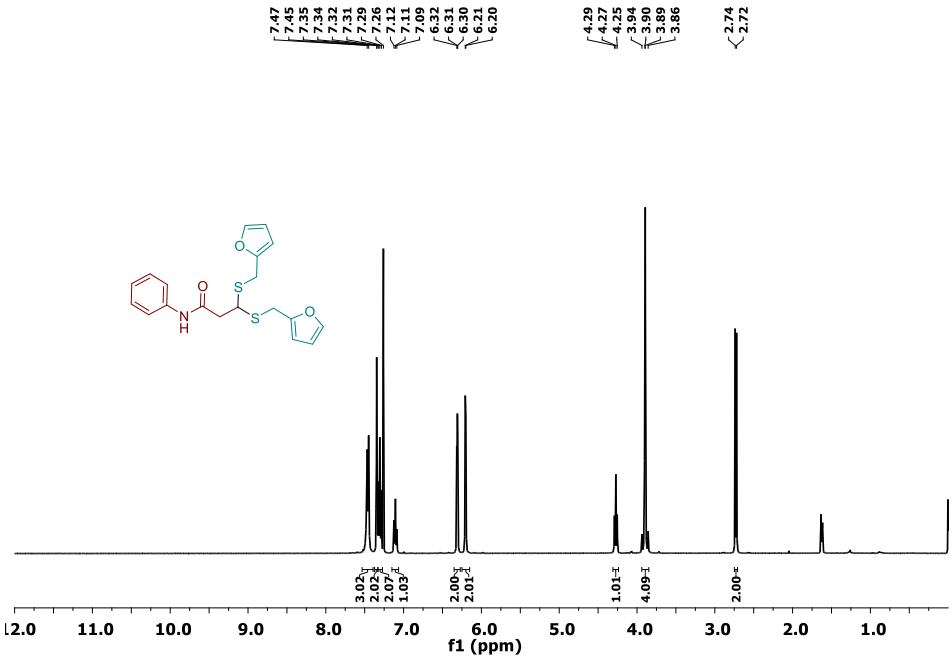

Figure 2.7. ^{1}H NMR spectrum of 3,3-bis((furan-2-ylmethyl)thio)-N-phenylpropanamide (**3aa**)

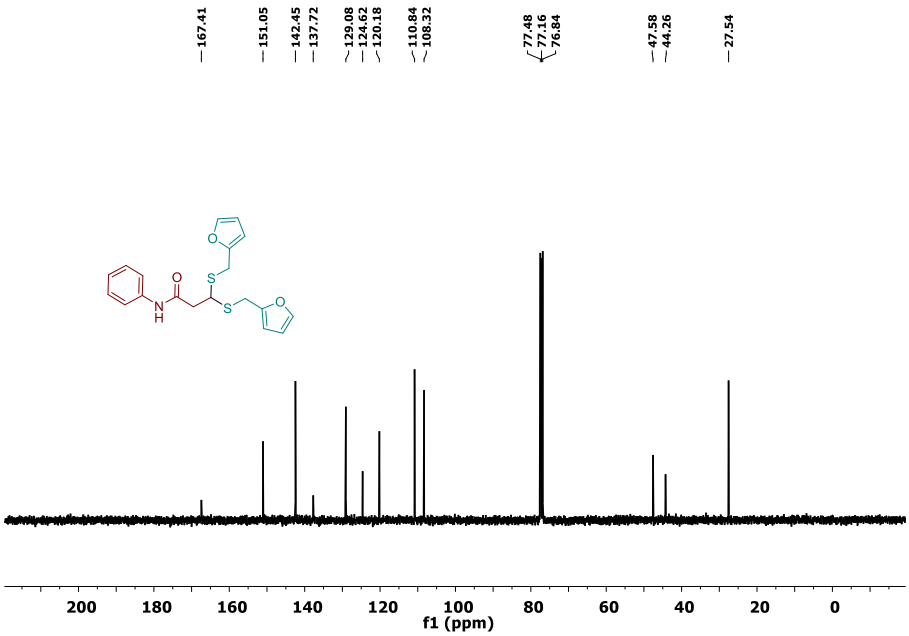

Figure 2.8. ^{13}C NMR spectrum of 3,3-bis((furan-2-ylmethyl)thio)-N-phenylpropanamide (**3aa**)

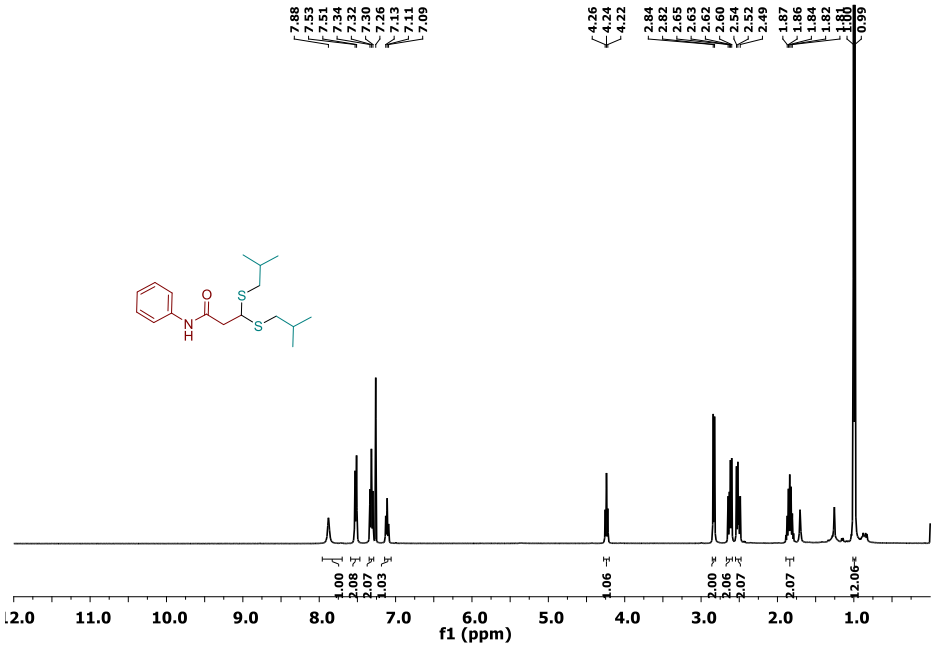

Figure 2.9. ^{1}H NMR spectrum of 3,3-bis(isobutylthio)-N-phenylpropanamide (**3ab**)

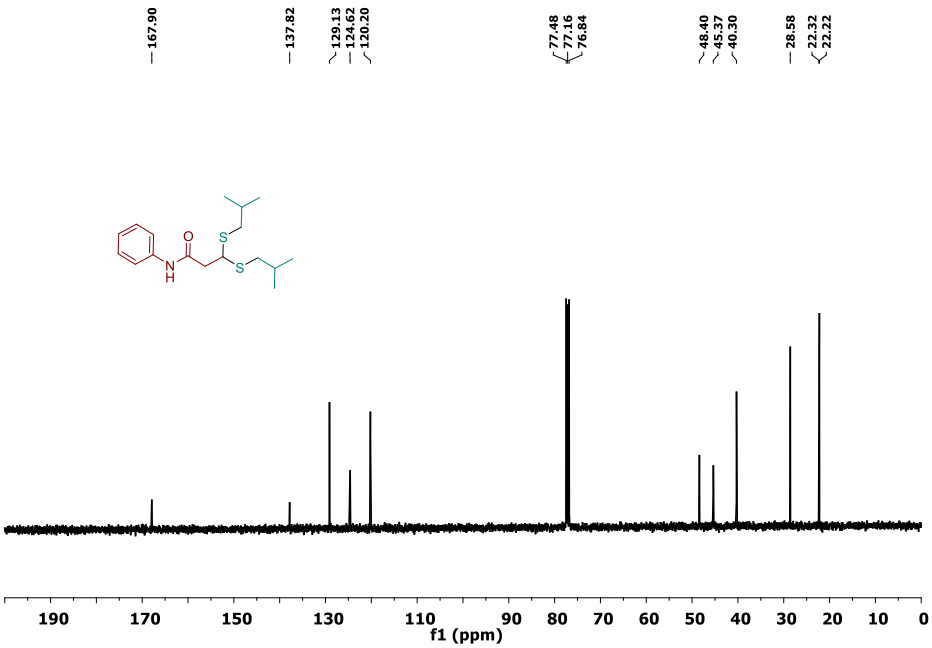

Figure 2.10. ^{13}C NMR spectrum of 3,3-bis(isobutylthio)-N-phenylpropanamide (**3ab**)

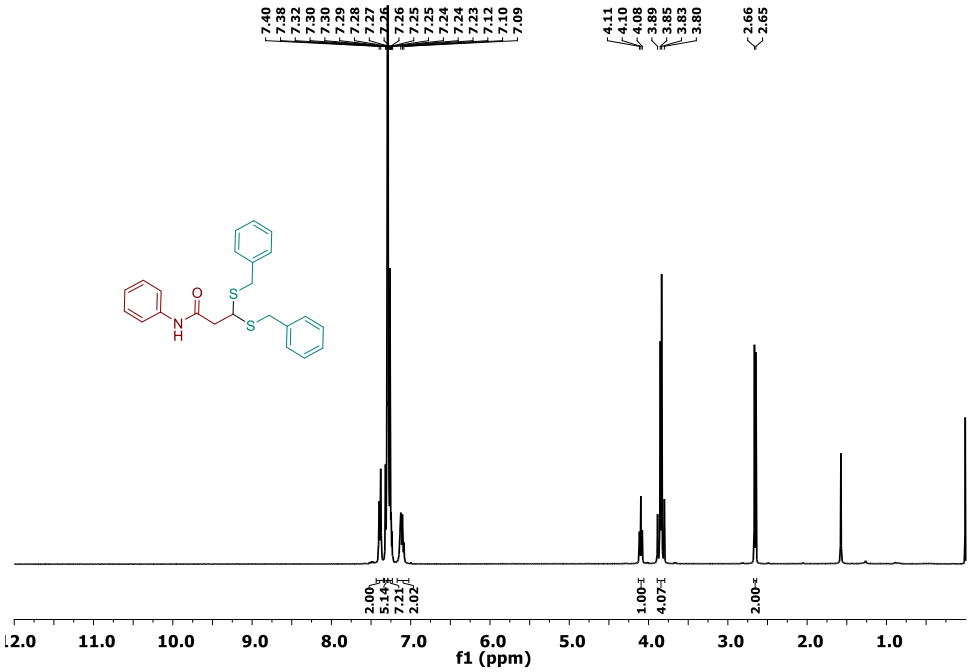

Figure 2.11. ^{1}H NMR spectrum of 3,3-bis(benzylthio)-N-phenylpropanamide (**3ad**)

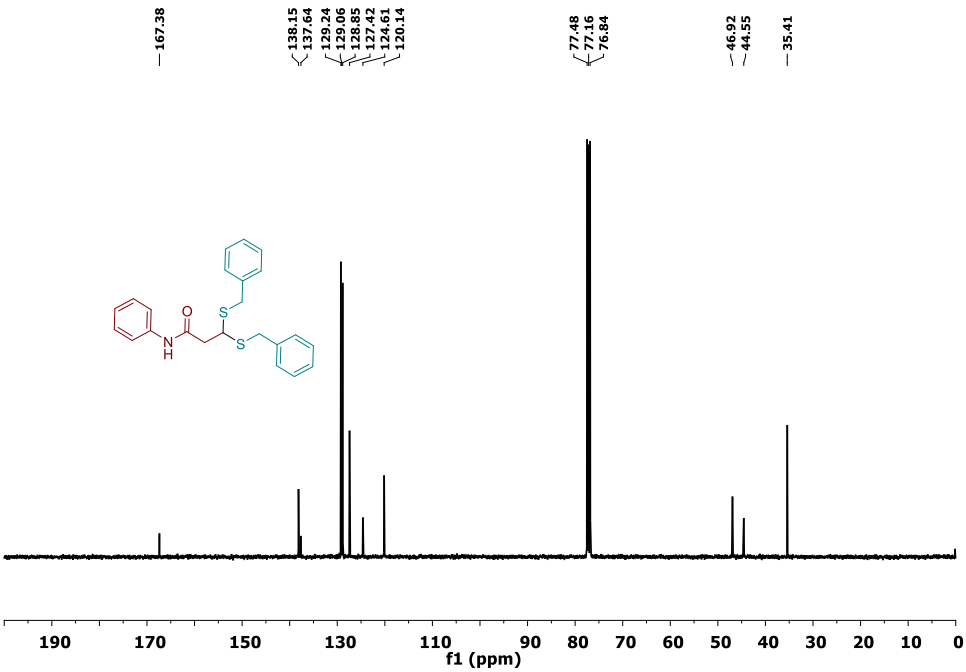

Figure 2.12. ^{13}C NMR spectrum of 3,3-bis(benzylthio)-N-phenylpropanamide (**3ad**)

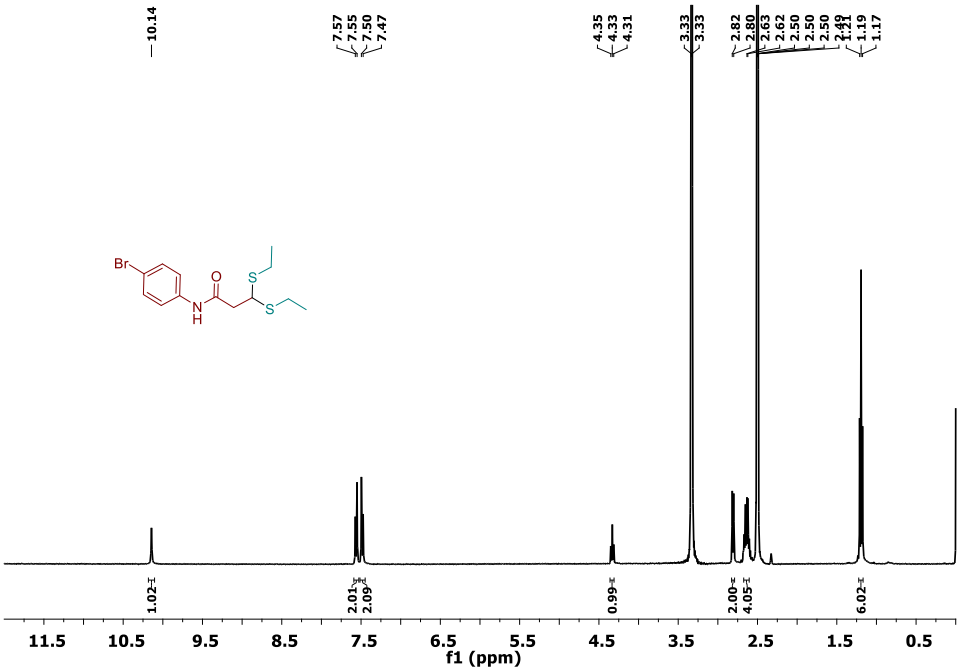

Figure 2.13. ^{1}H NMR spectrum of N-(4-bromophenyl)-3,3-bis(ethylthio)propanamide (**3ij**)

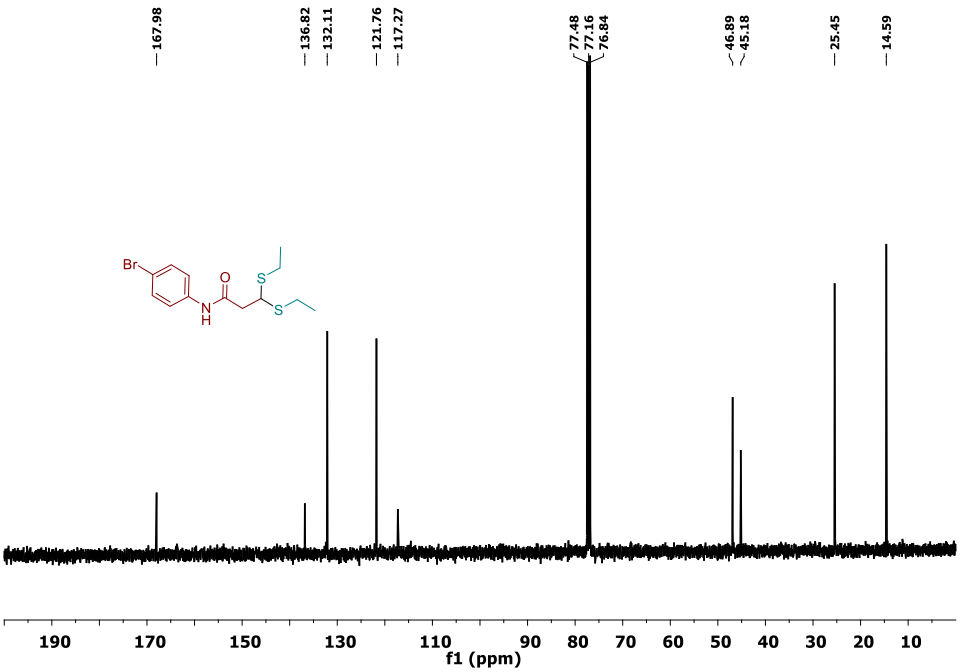

Figure 2.14. ^{13}C NMR spectrum of N-(4-bromophenyl)-3,3-bis(ethylthio)propanamide (**3ij**)

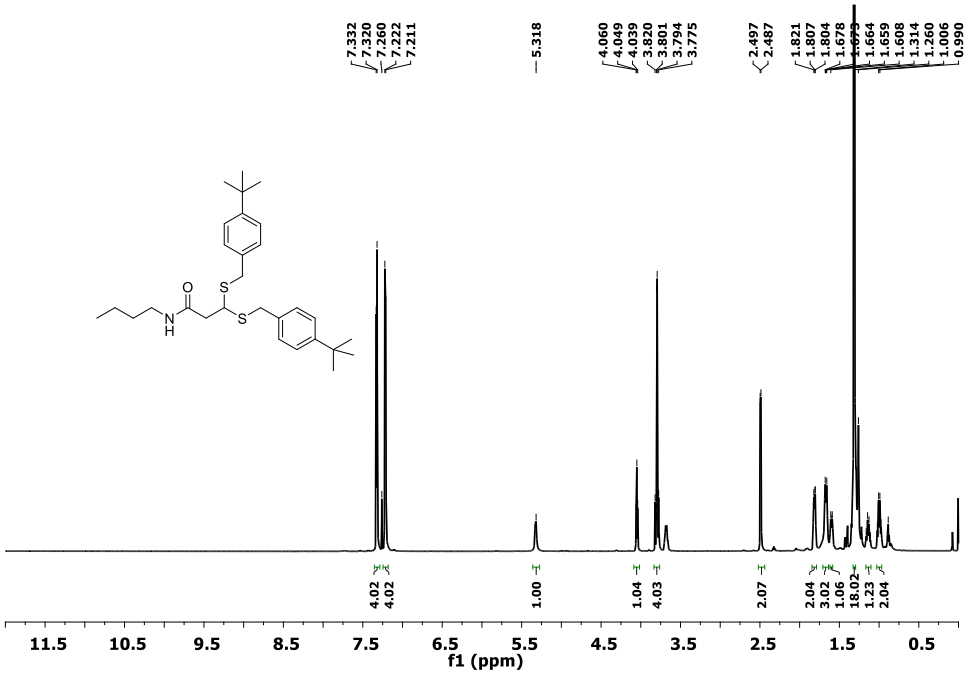

Figure 2.15. ^{1}H NMR spectrum of N-butyl-3,3-bis((4-(tert-butyl)benzyl)thio)propanamide (**3je**)

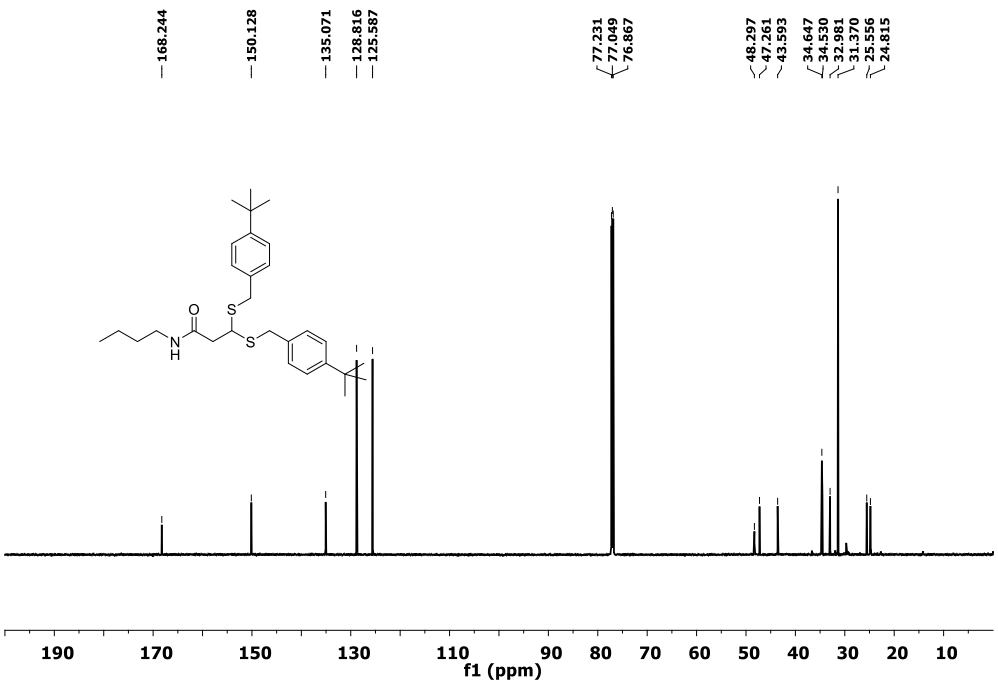

Figure 2.16. ^{13}C NMR spectrum of N-butyl-3,3-bis((4-(tert-butyl)benzyl)thio)propanamide (**3je**)

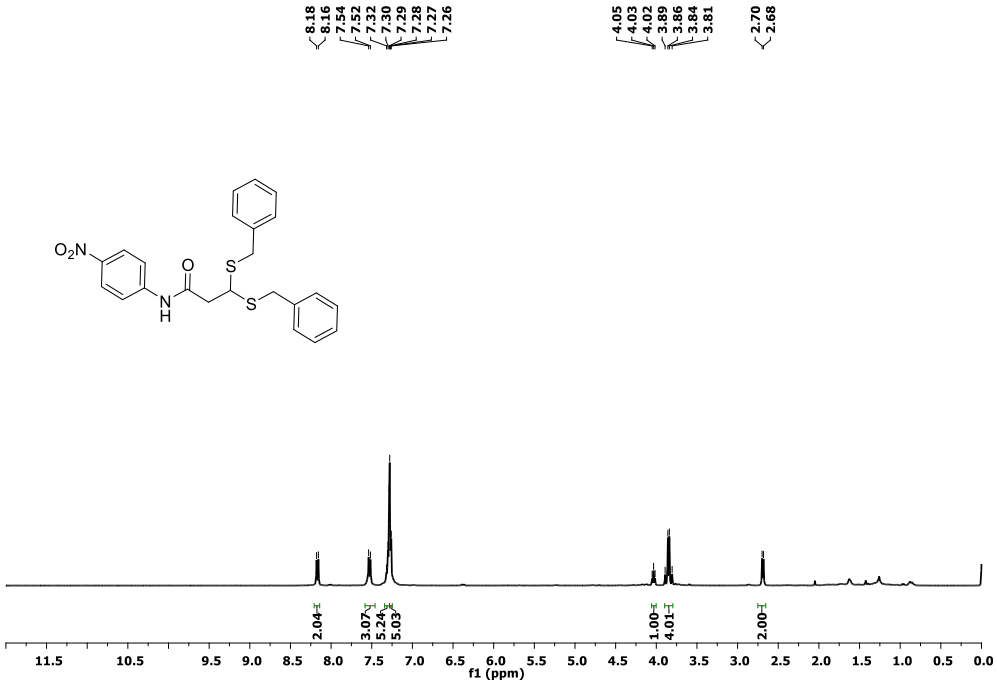

Figure 2.17. ^{1}H NMR spectrum of 3,3-bis(benzylthio)-N-(4-nitrophenyl)propanamide **(3kd)**

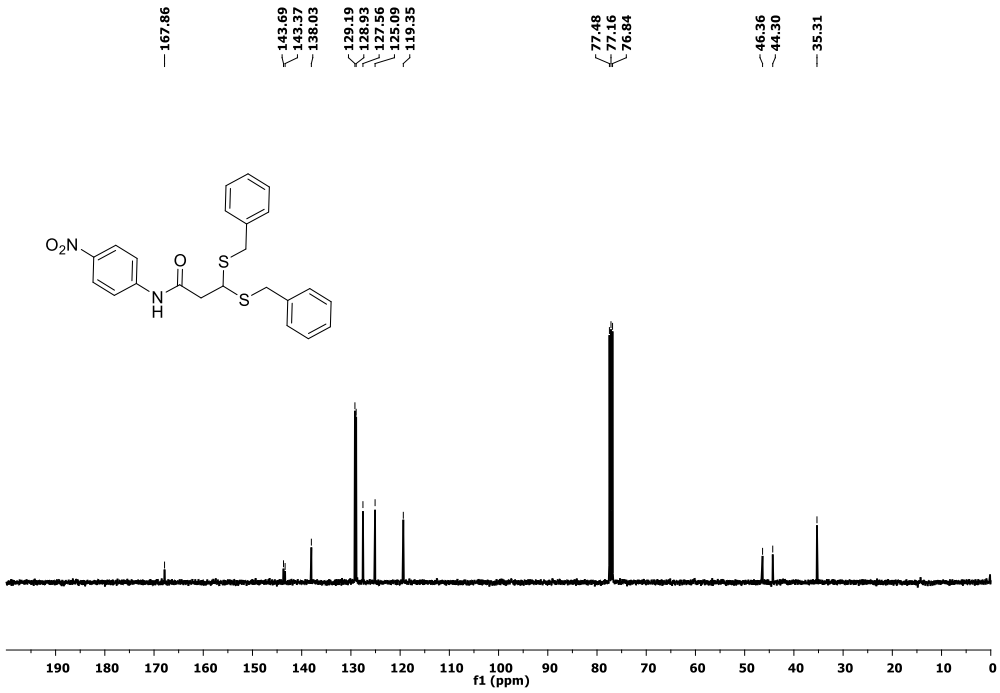

Figure 2.18. ^{13}C NMR spectrum of 3,3-bis(benzylthio)-N-(4-nitrophenyl)propanamide **(3kd)**

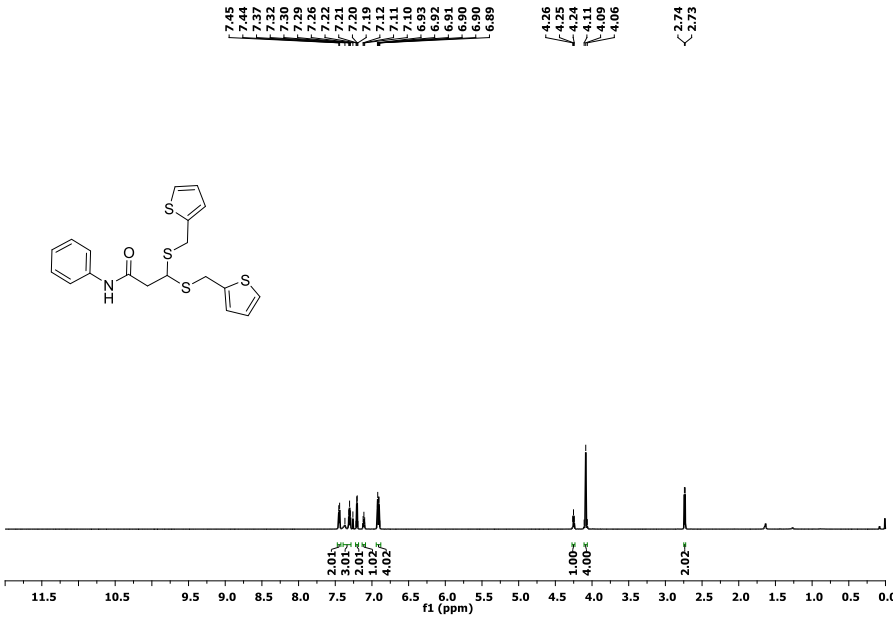

Figure 2.19. ^{1}H NMR spectrum of N-phenyl-3,3-bis((thiophen-2-ylmethyl)thio)propanamide **(3ak)**

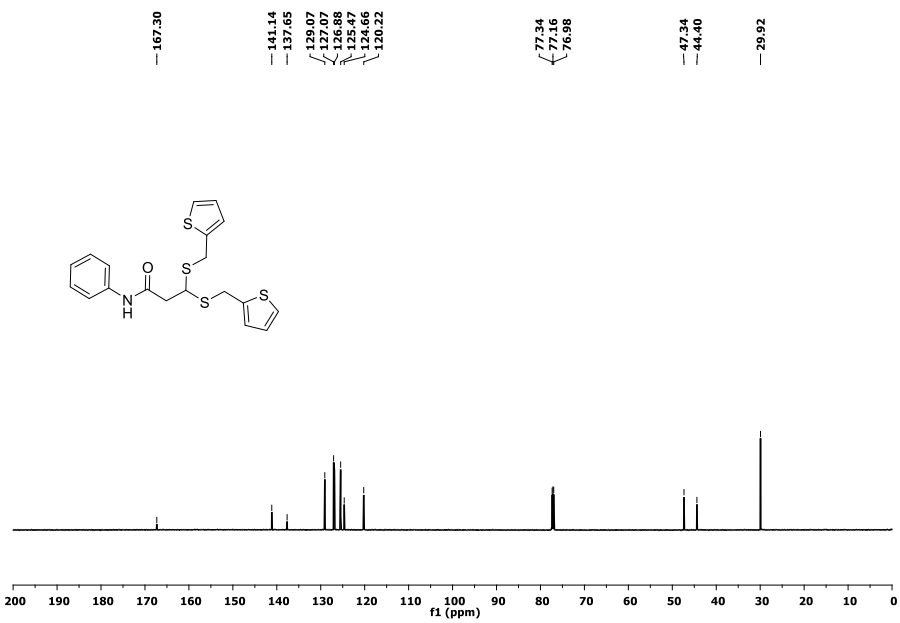

Figure 2.20. ^{13}C NMR spectrum of N-phenyl-3,3-bis((thiophen-2-ylmethyl)thio)propanamide **(3ak)**

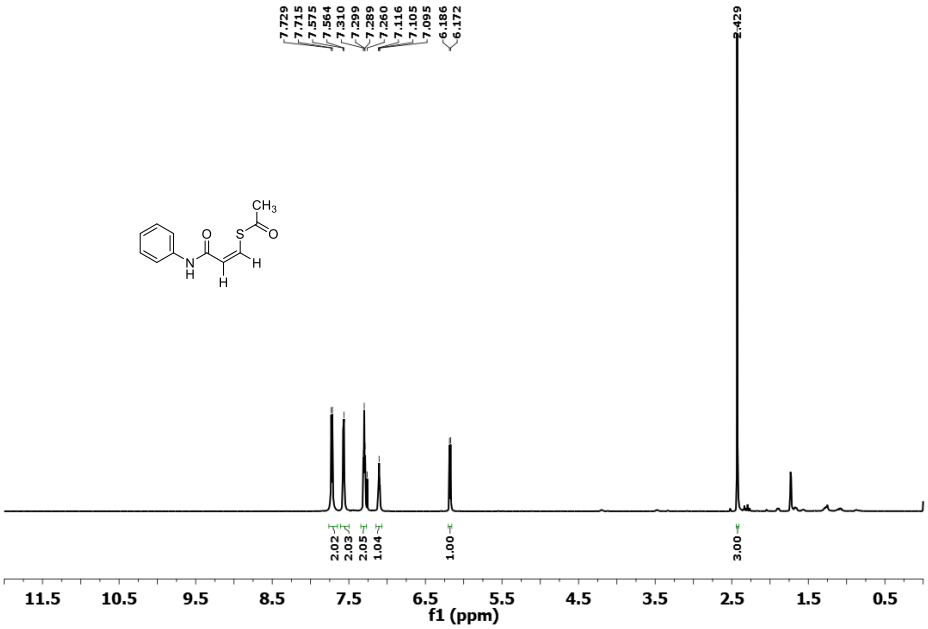

Figure 2.21. ^{1}H NMR spectrum of (Z)-S-(3-oxo-3-(phenylamino)prop-1-en-1-yl) ethanethioate (**5**)

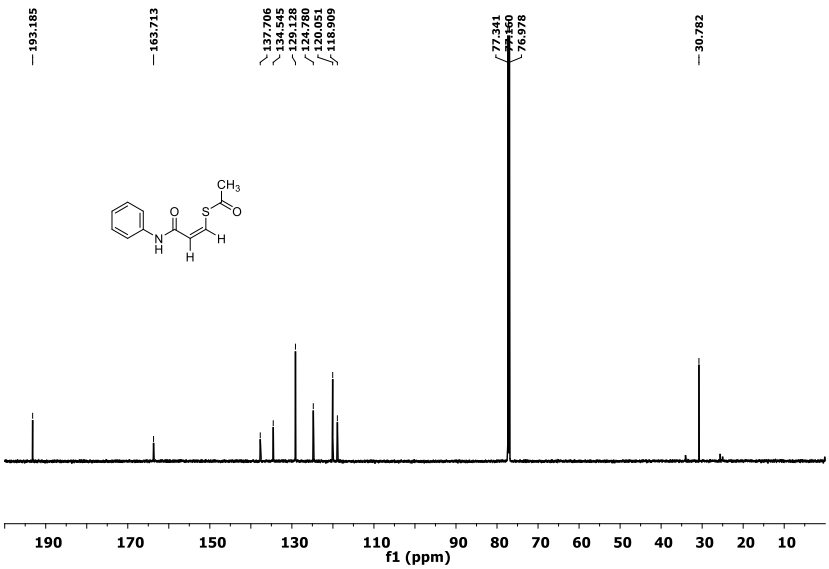

Figure 2.22. ^{13}C NMR spectrum of (Z)-S-(3-oxo-3-(phenylamino)prop-1-en-1-yl) ethanethioate (**5**)

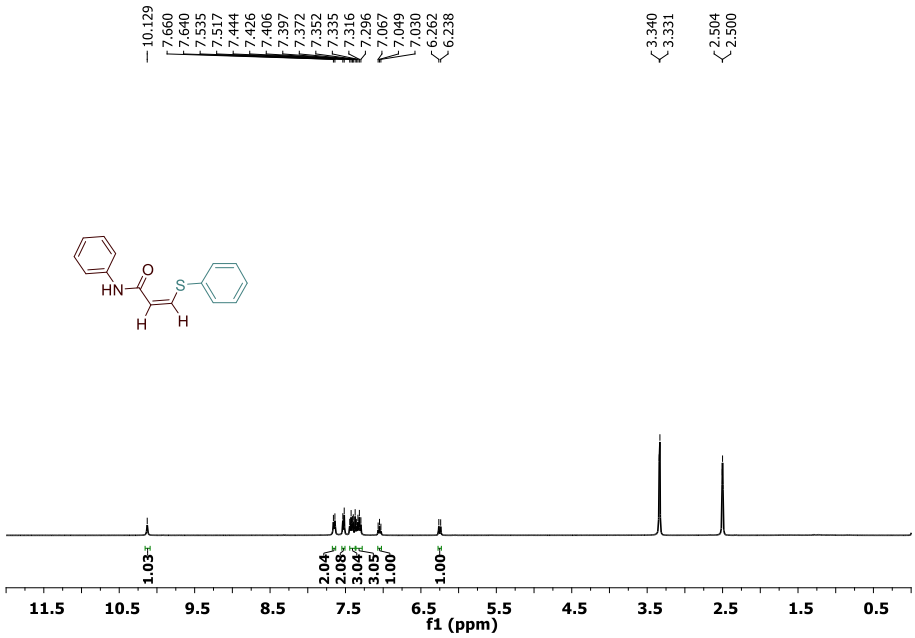

Figure 2.23. ^{1}H NMR spectrum of (Z)-N-Phenyl-3-(phenylthio)acrylamide (**6**)

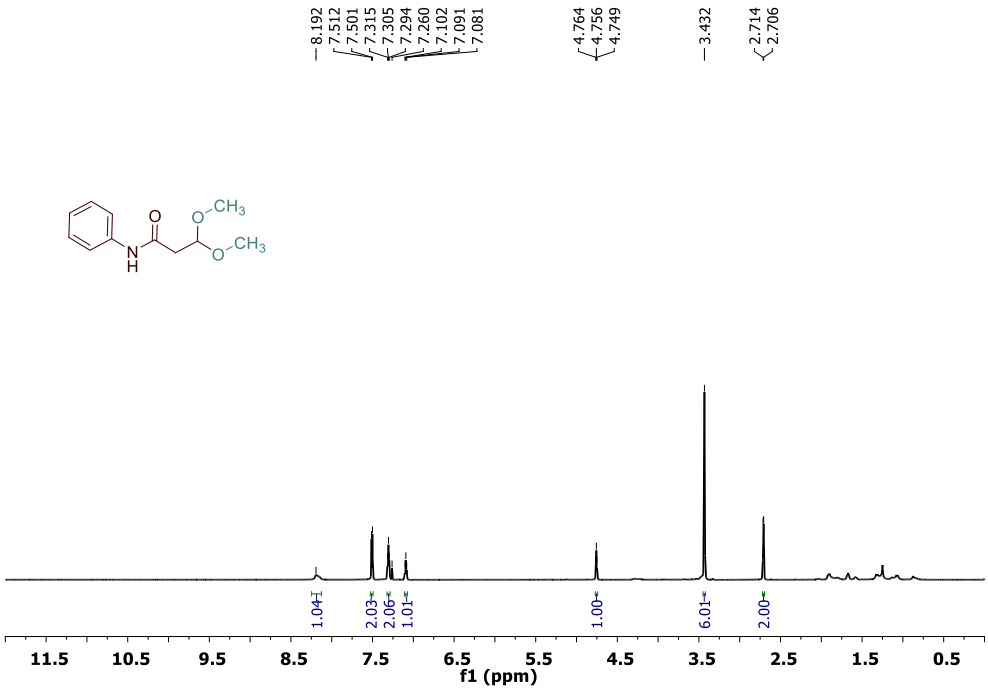

Fig. 2.24. ^{1}H NMR spectrum of 3,3-dimethoxy-N-phenylpropanamide (**4aa**)

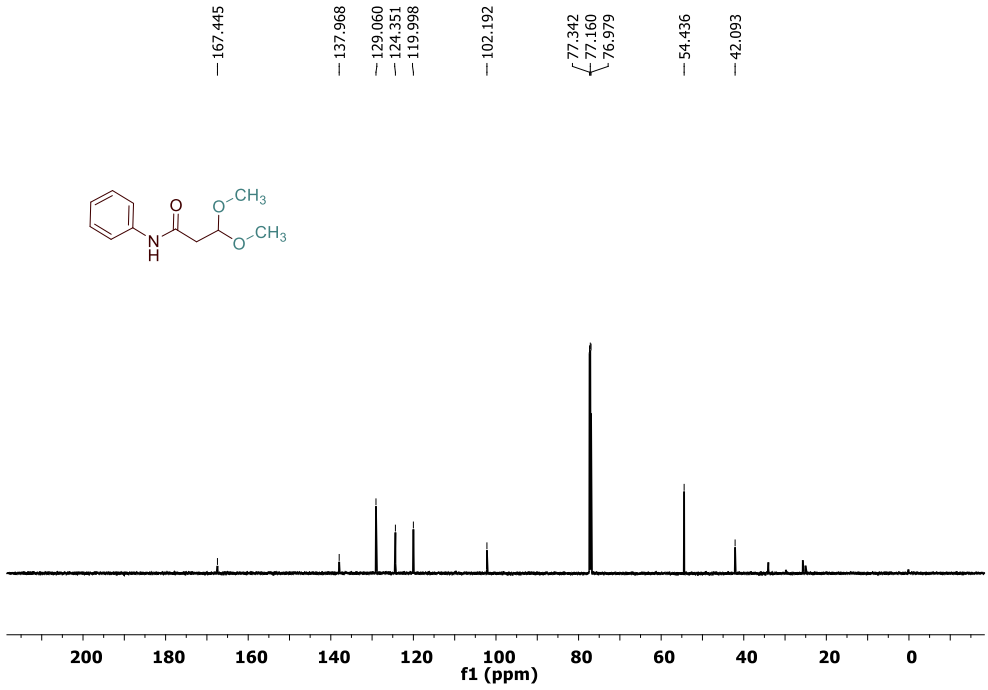

Fig. 2.25. ^{13}C NMR spectrum of 3,3-dimethoxy-N-phenylpropanamide (**4aa**)

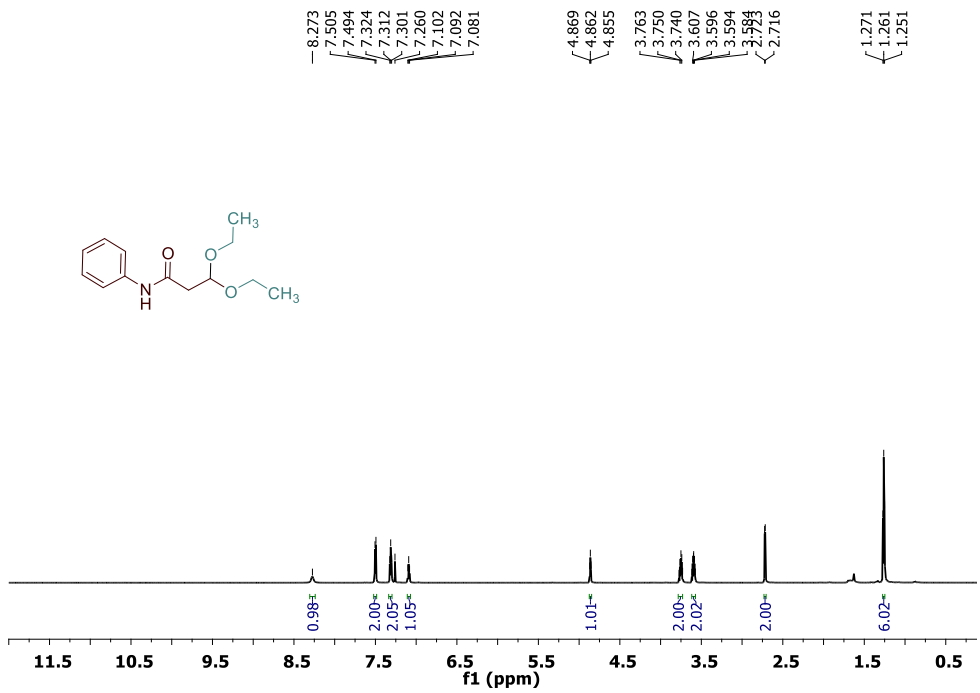

Fig. 2.26. ^{1}H NMR spectrum of 3,3-diethoxy-N-phenylpropanamide (**4ab**)

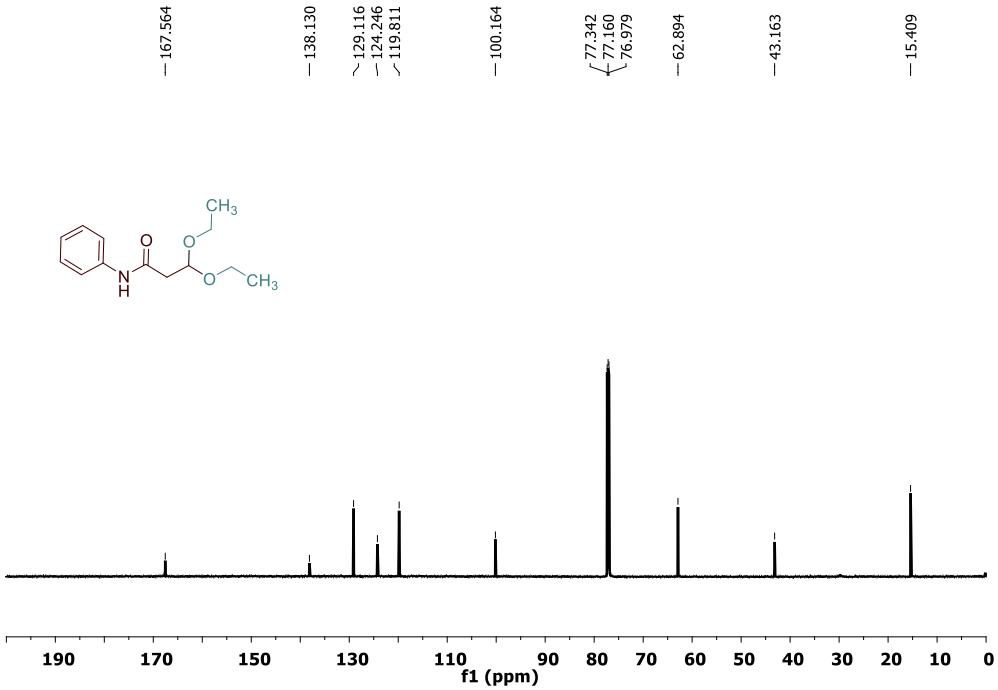

Fig. 2.27. ^{13}C NMR spectrum of 3,3-diethoxy-N-phenylpropanamide (**4ab**)

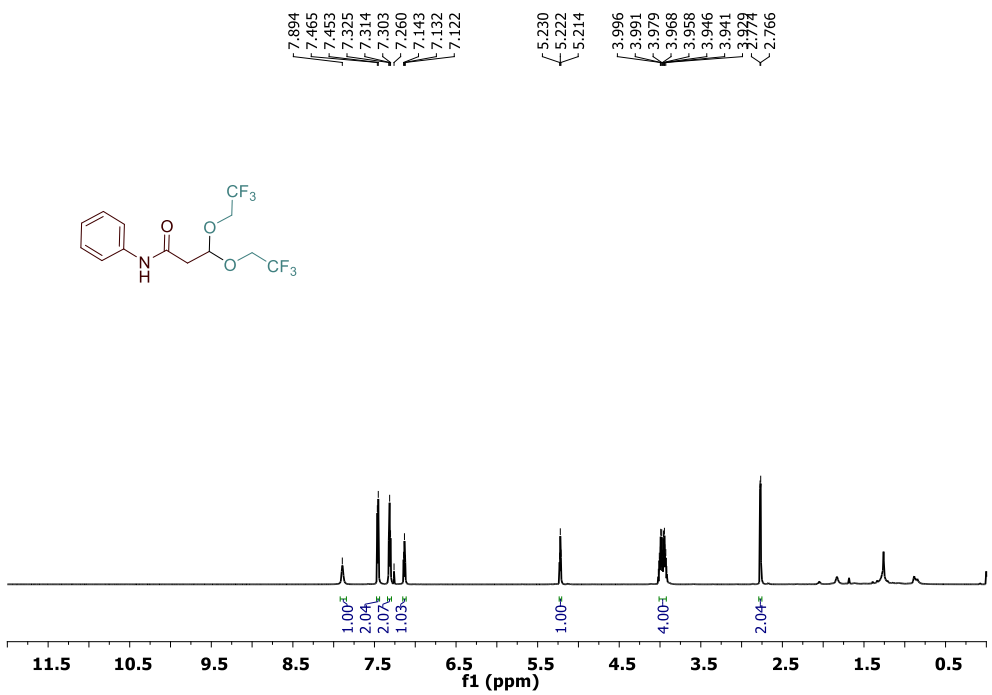

Fig. 2.28. ^{1}H NMR spectrum of N-phenyl-3,3-bis(2,2,2-trifluoroethoxy)propanamide (**4ac**)

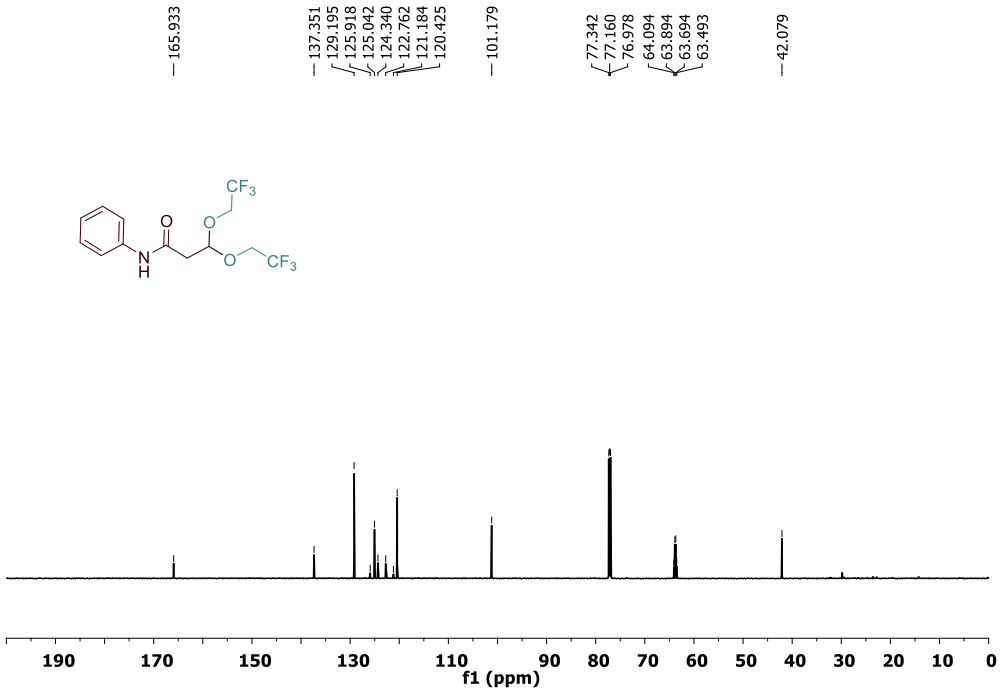

Fig. 2.29. ^{13}C NMR spectrum of N-phenyl-3,3-bis(2,2,2-trifluoroethoxy)propanamide (**4ac**)

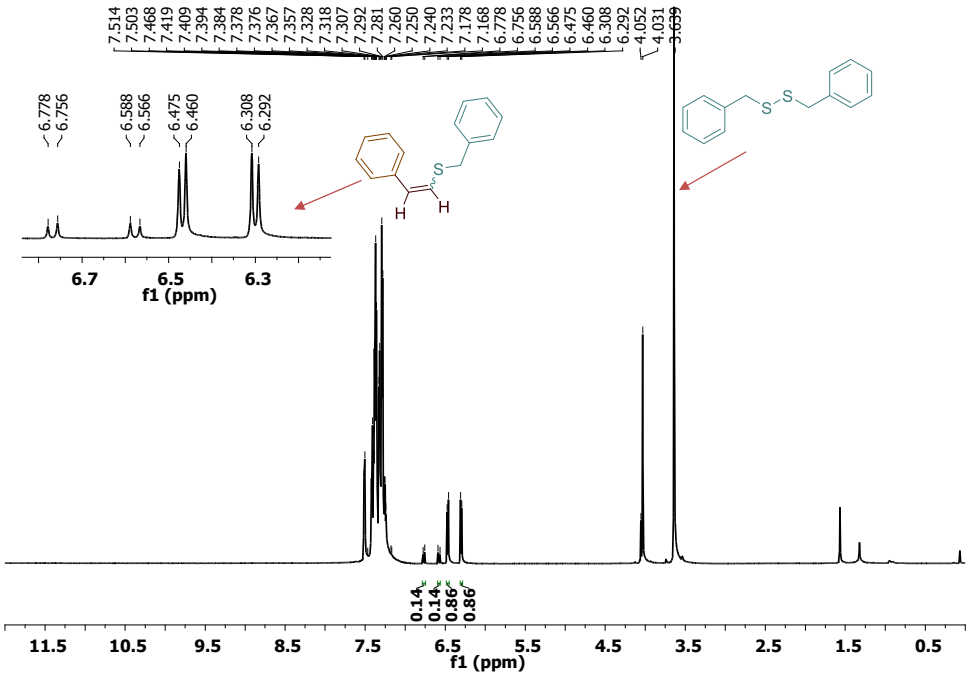

Figure 2.30. ^{1}H NMR spectrum for the mixture of benzyl (styryl)sulfane and disulfide.

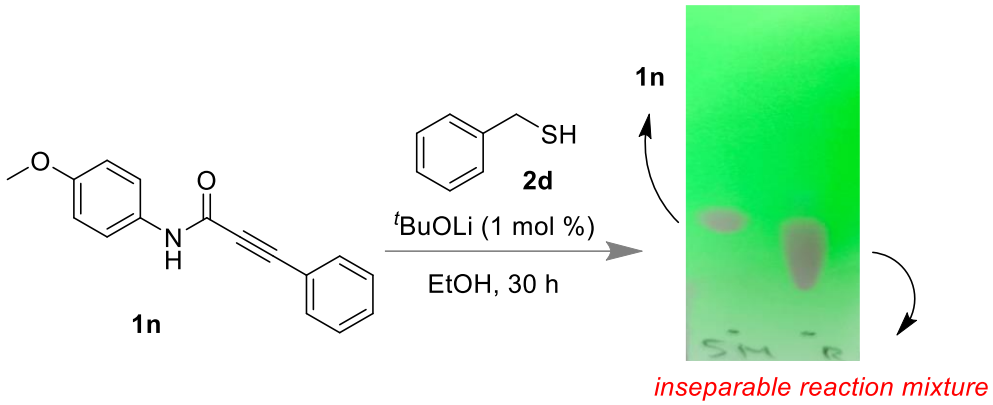

Scheme 2.1. Reaction of internal alkyne **1n** and benzyl mercaptan 2d shows complex reaction mixture.

CHAPTER 3

3-Arylsulfonylquinolines from *N*-Propargylamines *via* Cascaded Oxidative Sulfonylation using DABSO

3.1 ABSTRACT

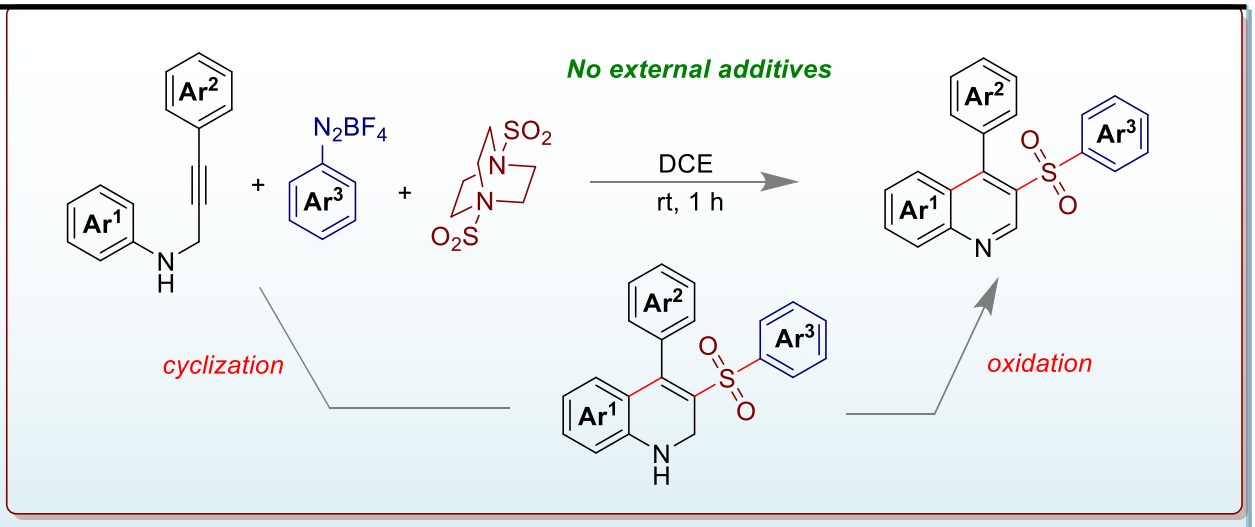

We report a cascaded oxidative sulfonylation of *N*-propargylamine *via* a three-component coupling reaction using DABCO·$(SO_2)_2$ (DABSO). 3-Arylsulfonylquinolines were obtained by mixing diazonium tetrafluoroborate, *N*-propargylamine, and DABSO under argon atmosphere in dichloroethane (DCE) for 1 h. In a radical pathway, DABSO was utilized as the -SO_2 source affording the sulfone functionality in our target products, as well as serving as an oxidant in this cascaded reaction.

3.2 INTRODUCTION

The efficient methodology of synthesizing complex molecular architecture is one of the popular research topics in organic chemistry.[1-2] Again, controlling multicomponent reactions

is highly desirable in C-S bond construction reaction[3-6] to address a well-defined system from molecular complexity.[7] Recently, the direct installation of sulfur dioxide (SO_2) in organic compounds[8-10] through a multicomponent reaction strategy has gained enormous attention in organic synthesis.[11-13] Indeed, radical-mediated cascaded insertion of SO_2 is highly advantageous over other known approaches because of the high reactivity of sulfonyl radicals.[14] Among the familiar SO_2 sources, gaseous SO_2 surrogates are generally not recommended for organic reactions due to the handling issues and unmeasurable concentration.[15-16] Again, other solids surrogates like sodium dithionites ($Na_2S_2O_4$), thiourea dioxide, potassium metabisulfite ($K_2S_2O_5$), and DABCO.$(SO_2)_2$ (DABSO) are commonly used.[17-18] Due to the air stability and easy handling procedure, DABSO is preferable as the SO_2 source.[19-22] However, other solids surrogates have poor solubility in organic solvents.[7, 15, 23] Recently, Waldvogel[15] and Wu[7] groups have individually shown the insertion of SO_2 using photochemical and electrochemical strategies. In addition, oxidative sulfonylation reactions are possible with sulfinic acids, sulfonyl chlorides, sulfonyl hydrazides, etc.[24-25] So, the insertion of SO_2 functionalities in organic molecules at ambient conditions *via* multicomponent reaction strategies can be a topic of interest.

Quinoline[26-31] and sulfone[32-34] skeletons have exhibited a broad spectrum in medicinal chemistry, natural products, bioactive molecules, and functional materials. For example, bioactive drugs like SB-742457[35] and RGH-618[36] having 3-sulfonylquinolines core are common for the treatment of diseases like Alzheimer and anxiety, respectively (Figure 1d).[37] Various reaction strategies have been developed to synthesize 3-arylsulfonylquinolines from *N*-propargylanilines,[37-41] using metal-catalyst, visible-light photocatalyst, electrochemical cell, peroxide reagents, etc.

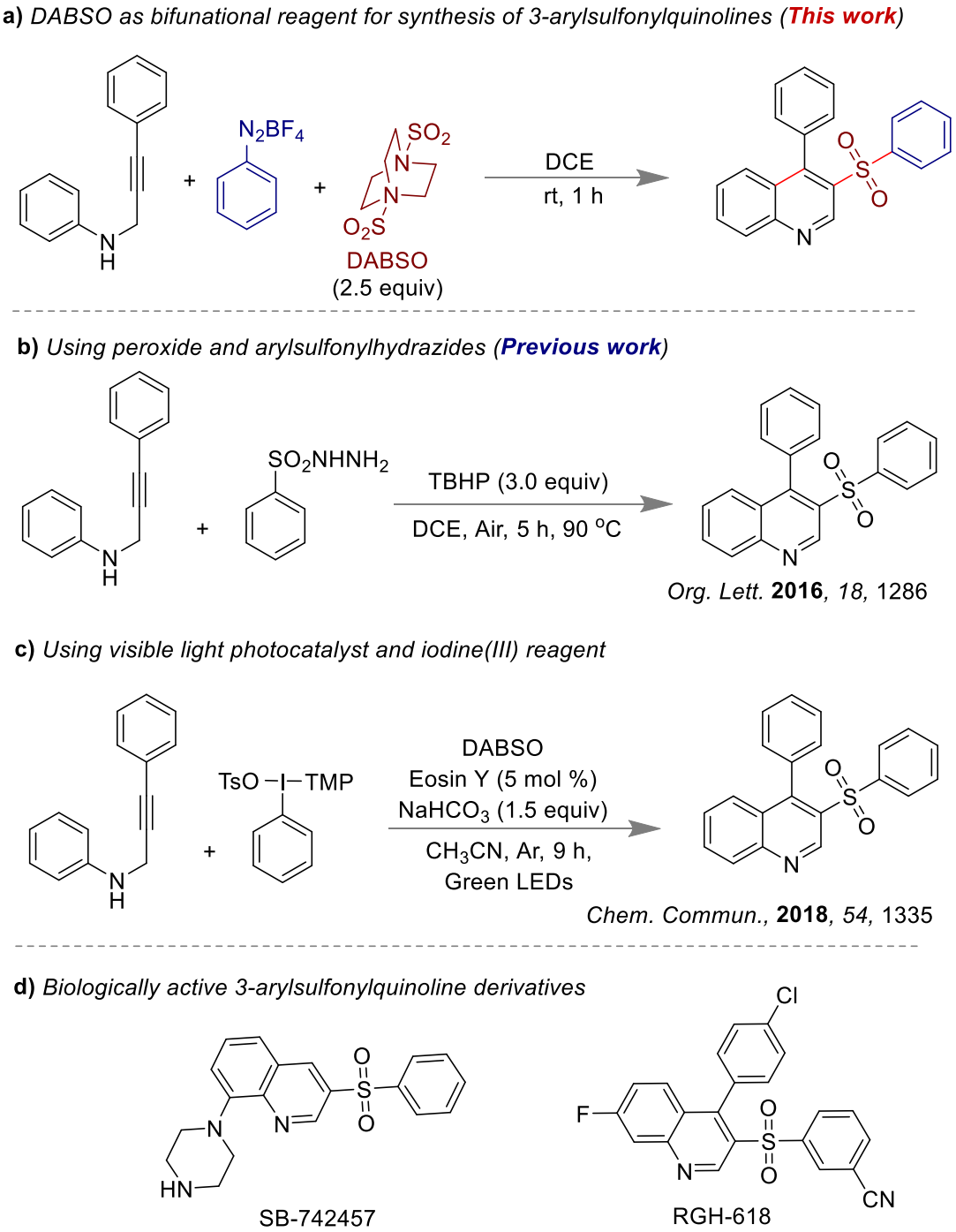

Figure 3.1. The synthesis of 3-arysulfonylquinolines. a) Cascaded synthesis by directly mixing diazonium tetrafluoroborate, *N*-propargylamine, and DABSO. b) Using peroxide.[38] c) Using visible-light photocatalyst.[37] d) Bioactive quinoline derivatives.

Tang and co-workers reported tertbutyl-hydroperoxide mediated synthesis of 3-arylsulfonylquinolines from aryl sulfonyl hydrazides as a sulfone source (Figure 1b).[38] Later, Zhang and co-workers developed a visible-light-induced strategy for a similar synthesis, using iodine(III) reagent as an aryl source and DABSO as a sulfur dioxide source (Figure 1c).[37] Recently, the Wang group reported the synthesis of 3-arylsulfonylquinolines from aryl sulfinic acid using the electro-oxidation technique.[39] In this study, we have shown that the aryl diazonium tetrafluoroborate and DABSO reacted with *N*-propargylanilines under ambient conditions to afford 3-arylsulfonylquinolines in the absence of any external additives or catalysts (Figure 1a).

3.3 RESULT AND DISCUSSION

In continuation of our efforts on controlling reactivities of various alkenes[42-43] and alkynes[44-47] for C-S bond formation reactions,[48-49] we have also investigated the reactivity of *N*-phenylpropargylamine as internal alkynes. The reaction conditions were optimized using *N*-phenylpropargylamine **1a** and diazonium salt **2a** (Table 1). Delightfully, propargyl amine **1a** was reacted with diazonium salt (1.5 equiv) and DABSO (2.5 equiv) at 60 ºC in CH_3CN for 1 h, 3-arylsulfonylquinoline **3aa** was isolated in 52% yield (entry 1). Other solvents like DMSO, DMF, dioxane, and THF did not have any better impact on the outcome of the reaction (entries 2-5). Again, the reaction at room temperature confirmed that heating was not essential for this transformation (entry 6). Interestingly, using 3.0 equiv of diazonium salt in an inert atmosphere led to better yields (entry 7). The yield of the reaction was maximum in the presence of 3.0 equiv of diazonium salt **2a** under the inert atmosphere in DCE (entry 8). The excess amount of DABSO might be required due to the volatile nature of SO_2 (see supporting information).[50] However, the yield of **3aa** was comparatively low at 30 min of reaction time (entry 9). No

significant improvement of the yield was noted when 3.0 equiv of DABSO was employed in the reaction mixture (entry 10). Again, addition of 1.5 equiv of DABSO produced very low yield (entry 11).

Table 3.1. The reaction condition optimization.[a]

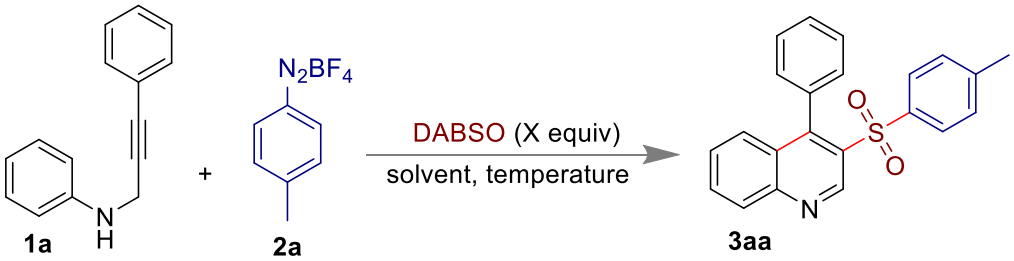

entry	diazonium (equiv)	DABSO (equiv)	solvent	temp (ºC)	yield[a] (%)
1	1.5	2.5	CH_3CN	60	52
2	1.5	2.5	DMSO	60	27
3	1.5	2.5	DMF	60	0
4	1.5	2.5	Dioxane	60	0
5	1.5	2.5	THF	60	31
6	1.5	2.5	CH_3CN	30	50
7	3.0	2.5	CH_3CN	60	70 [c]
8	3.0	2.5	DCE	60	82 [c]
9	3.0	2.5	DCE	30	72 [d]
10	3.0	3.0	DCE	30	80
11	3.0	1.5	DCE	30	35

[a]Isolated yields after column chromatography, [b]Reaction conditions: **1a** (0.29 mmol, 1.0 equiv), **2a** (0.87 mmol, 3.0 equiv) and DABSO (0.73 mmol, 2.5 equiv) in 1.5 mL of DCE under inert atmosphere for 1 h; [c]at inert atmosphere; [d]at 30 min.

The substrate scope with various *N*-propargyl aromatic amines in the presence of *p*-tolyl diazonium tetrafluoroborate and DABSO is shown in Figure 2. The -Me, -Et, -^{i}pr substituted propargyl amines produced corresponding sulfonylquinolines **3ba-3da** in fair yields (64-72%). Again, halogens containing *N*-propargylamines were reacted efficiently to provide analogous quinoline derivatives **3ea-3ga** with 74-85% yields. By looking at para substituent in phenyl group of *N*-propargylamines, it was confirmed that no spiro-intermediate was formed during the reaction.[45] The 3-methyl/fluoro/chloro-*N*-(3-phenylprop-2-yn-1-yl) anilines afforded products **3ha**, **3ia** and **3ja** with 74%, 75% and 74% yields, respectively. In contrast, dihalo substituted sulfonylquinolines **3ka** and **3la** were isolated in 80% and 84% yields, respectively. On the other hand, substituents on another aromatic ring of *N*-propargylamines were also varied, and compounds **3ma-3qa** were produced in good to excellent yields (77-87%). Again, heteroaromatic substituted *N*-propargyl amines with thiophene and pyridine moieties were effective under this reaction condition to deliver **3ra** and **3sa** with 76% and 72% yields, respectively. Alkyl *N*-propargyl **1t** also produced compound **3ta** with 49% yield.

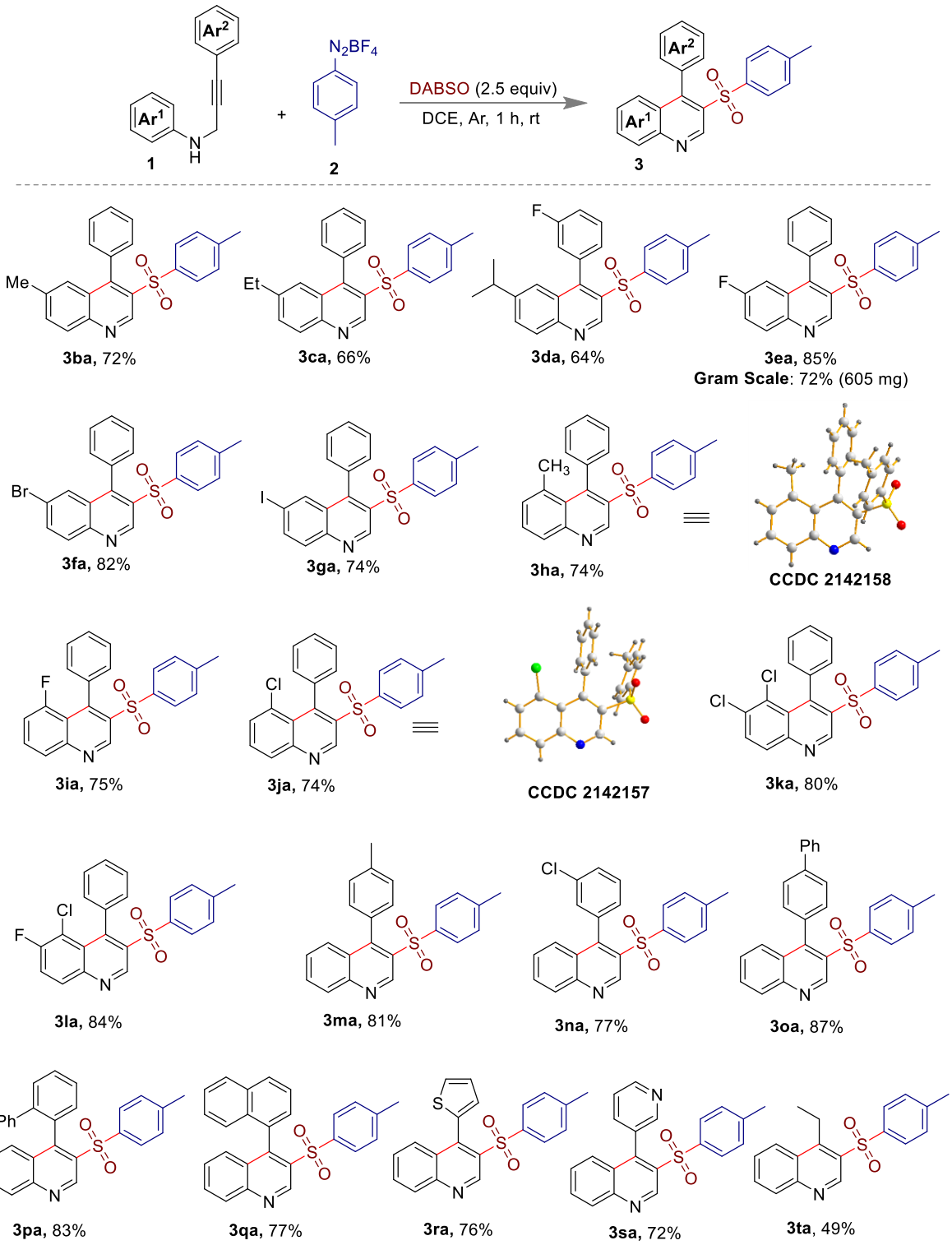

Figure 3.2. Substrate scope for various *N*-propargylamines using *p*-tolyldiazonium salt and DABSO. Ellipsoids of crystal **3ha** and **3ja** are drawn at the 30% and 50% probability level respectively.

Using various aryldiazonium tetrafluoroborates the substrate scope is shown in Figure 3a . The -Me, -Et, -^{i}pr, and -OEt substituted diazonium salts were also well productive to give the corresponding 3-arylsulfonylquinolines **3aa-3af** with a range of 82-86% yields. Halo substituted diazonium salts like -Br and -Cl have also afforded the products **3ag**, **3ah,** and **3ai** with 77%, 74%, and 69% yields. Naphthalene containing polycyclic diazonium tetrafluoroborate and 3-quinoline diazonium tetrafluoroborate resulted in the products **3aj** and **3ak** with 80% and 76% yields, respectively. Again, one-pot synthesis of arylsulfonylquinoline **3aa** was also carried out from *p*-toluidine using *tert*-butyl nitrite (TBN), which showed 52% of the product (Figure 3b).

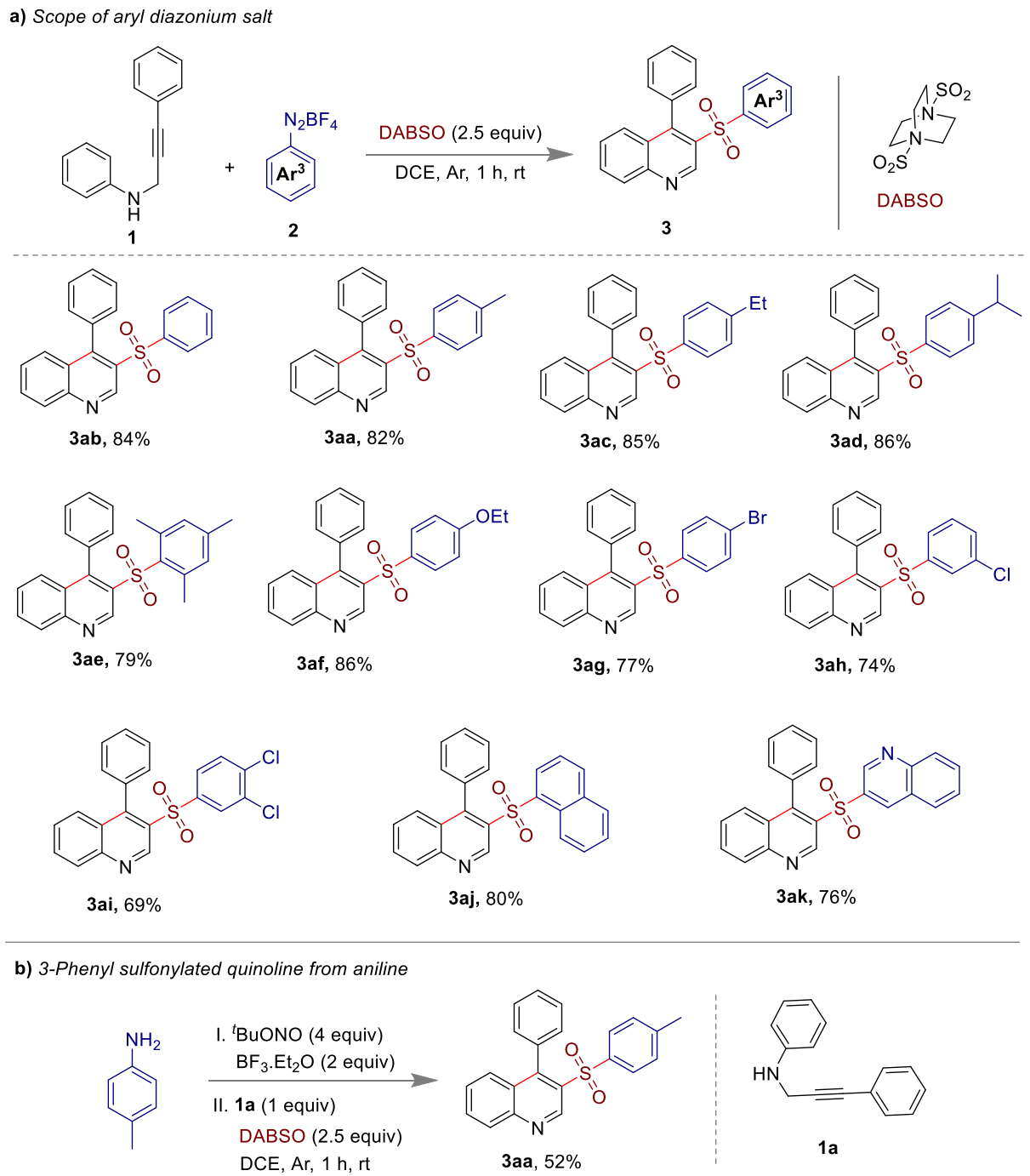

Figure 3.3. a) The substrates scope for various diazonium salts using propargylamine and DABSO. b) One-pot synthesis of arylsulfonylquinoline **3aa** from *p*-toluidine.

The control experiments (Figure 4) helped to establish the reaction mechanism. The reaction with TEMPO (Figure 4a), confirmed the involvement of the radical pathway. The *N*-

propargylamine **1a** was neither oxidized to **4** nor **4'** in the absence of diazonium salt (Figure 4b). This fact indicates that oxidation or aromatization was not at the initial step over the addition of aryl sulfonyl radical to *N*-propargylamine **1a** (Figure 5a, *vide infra*). The cyclization reaction failed with **4** instead of **1a** (Figure 4c). This observation suggested that amine oxidation to imine could not occur at the reaction's beginning.

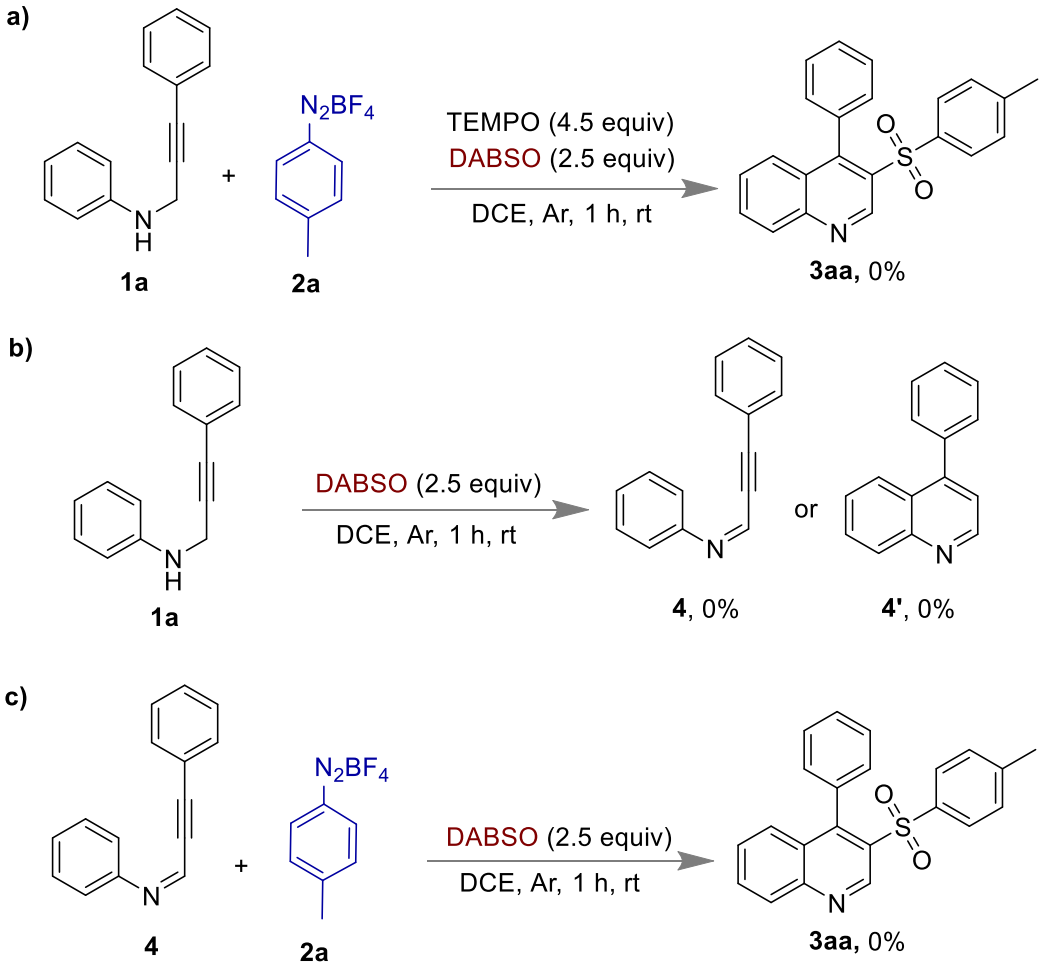

Figure 3.4. Control experiments. a) Radical trapping experiment with TEMPO. b) Reaction in the absence of diazonium salt. c) The reaction of compound **4** with diazonium **2a** and DABSO.

Based on control experiments and literature reports,[51-52] a plausible mechanism is proposed in Figure 5a. Initially, the aryl diazonium tetrafluoroborate and DABSO formed a complex **I** *via* electrostatic interaction. However, complex **I** evolved N_2 and furnished intermediate **II**. As a

result, aryl radical and sulfur dioxide, which were assumed to be formed *in-situ,* reacted to generate aryl sulfonyl radical. Following, sulfonyl radical attacked to triple bond of *N*-propargylamine **1** to form intermediate **III**, which instantly underwent intramolecular cyclization to generate cyclized intermediate **IV**. Finally, the rearomatization followed by oxidation of **IV** was occurred with the help of intermediate **II** to give 3-aryl sulfonyl quinoline.[52]

Although there was a possibility of forming product **3** or **3'** from *meta* substituted *N*-phenylpropargylamine, only product 3 was formed exclusively. (Figure 5b). The attack of vinyl radical was more favorable to the substituted side (green arrow) but the reason of regioselectivity was still unclear.

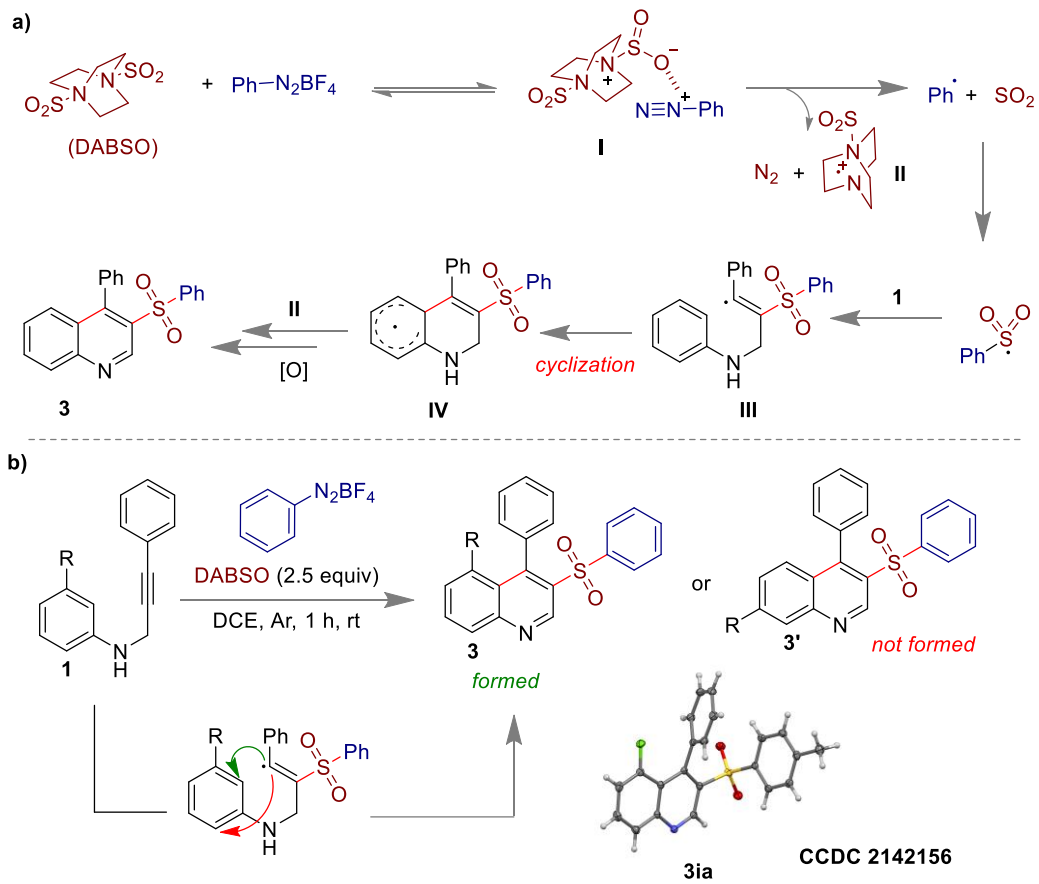

Figure 3.5. a) Plausible mechanism. b) Regioselectivity in the cyclization process. Ellipsoids of crystal **3ia** are drawn at the 50% probability level, respectively.

We have also explored various cross-coupling reactions on the synthesized molecules (Figure 6). Compounds **5**, **6**, and **7** were obtained from corresponding halo-substituted quinolines **3fa** and **3ga** in 78%, 88%, and 51% yields, respectively.

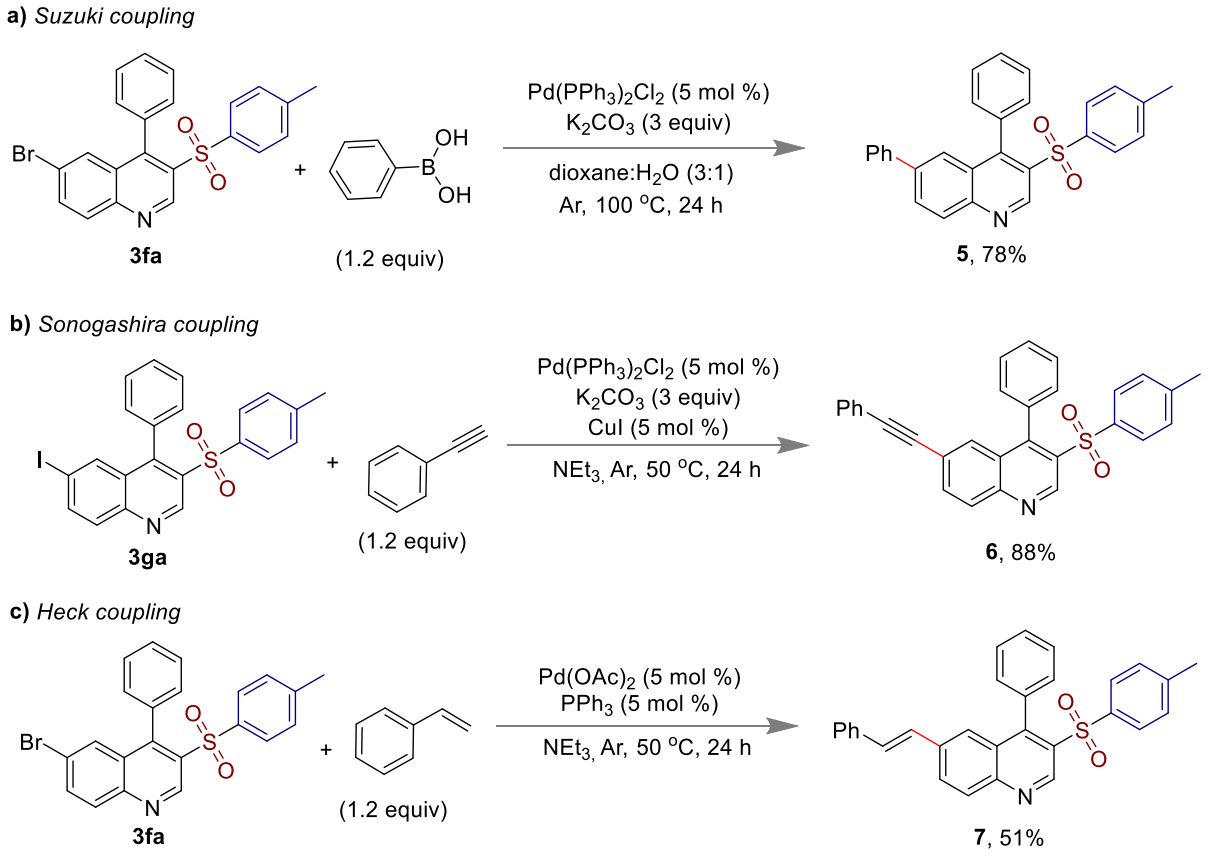

Figure 3.6. Chemical modifications. a) Suzuki coupling with phenyl boronic acid. b) Sonogashira coupling with phenyl acetylene. c) Heck coupling with styrene.

3.4 CONCLUSION

In summary, we have developed a one-pot and sustainable protocol for synthesizing 3-arylsulfonylquinoline from diazonium tetrafluoroborate, *N*-propargylamine, and DABSO without any external additives. This metal-free unique reaction strategy offers an excellent guideline on controlling the three-component reaction in a single step *via* a cascade process.

Thus, we believe that the newly developed synthetic route will help to identify many quinolines and sulfones frameworks in nitrogen-based heterocycle synthesis and sulfur chemistry.

3.5 EXPERIMENTAL SECTION

All the chemicals were purchased from commercial sources and used as received. All the reactions were generally carried out under an open atmosphere unless otherwise noted. The reactions were monitored by TLC on aluminum sheets pre-coated with silica gel. Chromatographic purifications of the compounds were performed using silica gel (Mesh 230-400) and ethyl acetate/hexane as eluent. The ^{1}H and ^{13}C spectra of the compounds were recorded on Bruker 400 MHz and 700 MHz instruments at 25 ºC. The chemical shift value (δ, ppm) was reported with respect to the residual chloroform (7.26 for ^{1}H and 77.16 ppm for ^{13}C) and DMSO-d_6 (2.50 for ^{1}H and 39.52 ppm for ^{13}C). Mass spectra were recorded as ESI-TOF (HRMS). Infrared spectra were recorded on neat solids using KBr pellets and described in wavenumber (cm^{-1}). Digital melting point apparatus was used to record the compound's melting point in degree centigrade (°C) and are uncorrected.

Representative experimental procedure for the synthesis of products 4-phenyl-3-tosylquinoline 3aa.

In an oven-dried 25 mL round-bottomed flask, DABSO (0.73 mmol, 2.5 equiv) and freshly prepared diazonium salt **2a** (0.87 mmol, 3.0 equiv) were taken under argon atmosphere. To this 1.0 mL DCE was then added and the reaction mixture was degassed. After stirring the whole solution for 2 minutes, *N*-(3-phenylprop-2-yn-1-yl) aniline **1a** (0.29 mmol, 1.0 equiv), was dissolved in 0.5 mL DCE at argon and the solution was allowed to be injected into the reaction mixture in a dropwise manner. Following, the reaction mixture was stirred under an inert

atmosphere for 1 hour. After that, the crude mixture was diluted in DCE, washed with brine solution, dried over anhydrous sodium sulfate (Na_2SO_4) and concentrated on a high vacuum. The organic residue is purified by column chromatography on silica gel to isolate the desired products 4-phenyl-3-tosylquinoline **3aa**.

Experimental procedure for the gram scale synthesis of 3ea.

In an oven-dried 50 mL round-bottomed flask, DABSO (5.5 mmol, 2.5 equiv) and freshly prepared diazonium salt **2a** (6.6 mmol, 3.0 equiv) were taken under argon atmosphere. To this 6.0 mL DCE was then added, and the reaction mixture was degassed. After stirring the whole solution for 2 minutes, 4-fluoro-N-(3-phenylprop-2-yn-1-yl) aniline **1e** (2.2 mmol, 1.0 equiv) was dissolved in 2 mL DCE at argon, and the solution was allowed to be injected into the reaction mixture in a dropwise manner. Following, the reaction mixture was stirred under an inert atmosphere for 1 hour. After that, the crude mixture was diluted in DCE, washed with brine solution, dried over anhydrous sodium sulfate (Na_2SO_4), and concentrated in a high vacuum. The organic residue is purified by column chromatography on silica gel to isolate the desired product **3ea** with 72% yield (605 mg).

Experimental procedure for the synthesis of 3aa from aniline.

^{t}BuONO (1.16 mmol, 4.0 equiv) was added dropwise to a solution of arylamine (0.58 mmol, 2 equiv) and BF_3Et_2O (0.58 mmol) in DCE (1.5 mL) under 0°C. After 10 minutes the above mixture was added to a solution of N-(3-phenylprop-2-yn-1-yl)aniline **1a** (0.29 mmol, 1 equiv) and DABSO (0.72 mmol, 2.5 equiv) in DCE under argon atmosphere *via* syringe. Then the reaction mixture was stirred at room temperature for 1 h. After that, the crude mixture was diluted in DCE, and organic content was washed with saturated brine solution, dried over

Na_2SO_4, and evaporated to dryness. The crude mixture was further purified by column chromatography using the hexane-EtOAc mixture as eluent.

Representative procedure for the synthesis of N-(prop-2-yn-1-yl)aniline.

In a 100 mL round-bottomed flask, a solution of compound aniline (3.2 g, 34.4 mmol, 4.1 equiv), potassium carbonate (2.44 g, 17.64 mmol, 2.1 equiv), and N, N - dimethylformamide (DMF, 50 mL) were stirred for 5 min at room temperature. A solution of propargyl bromide (1.24 g, 80% solution in toluene). The reaction mixture is kept at room temperature for 12 h. After that, the crude mixture was diluted in Ethyl Acetate, and the combined filtrate is transferred to a funnel and washed with brine solution. The aqueous phase is extracted three times with ethyl acetate. The combined organic phases dried over anhydrous sodium sulfate (Na_2SO_4), filtered and concentrated by rotary evaporation to give a dark brown oil. The residue is purified by column chromatography on silica to afford the N-(prop-2-yn-1-yl) aniline as light-yellow oil.

Representative procedure for the synthesis of N-(3-phenylprop-2-yn-1-yl)aniline.[38]

An oven-dried 100-mL round-bottomed flask equipped with a magnetic stirring bar, N-(2-propynyl) aniline (1.19 g, 3.84 mmol, 1.0 equiv), triethylamine (10 mL), iodobenzene (1.0 g, 5.0 mmol, 1.2 equiv) and bis(triphenylphosphine)palladium dichloride (53 mg, 0.08 mmol, 0.02 equiv) were charged with argon. Copper iodide (16 mg, 0.08 mmol, 0.02 equiv) is then added in a single portion to the flask. The reaction mixture was stirred at room temperature for 6 h. After completion, the reaction mixture was concentrated under reduced pressure. After that, the crude mixture was diluted in DCM, and organic content was washed with saturated brine solution, dried over Na_2SO_4, and evaporated to dryness. The crude mixture was further purified by column chromatography using the hexane-EtOAc mixture as eluent.

Synthesis of 4,6-diphenyl-3-tosylquinoline 5.

A 20 mL Schlenk tube holding a magnetic bar was charged with 6-bromo-4-phenyl-3-tosylquinoline **3fa** (0.137 mmol, 1.0 equiv), phenylboronic acid (0.165 mmol, 1.2 equiv), K_2CO_3 (0.412 mmol, 3.0 equiv), and $Pd(PPh_3)_2Cl_2$ (0.06 mmol, 5 mg) in dioxane/H_2O (1.5 mL/0.5 mL) under inert atmosphere. Then the reaction mixture was placed into a preheated oil bath at 100 °C for 24 h. After that, the crude mixture was diluted in EtOAc, and organic content was washed with saturated brine solution, dried over Na_2SO_4, and evaporated to dryness. The crude mixture was further purified using the hexane-EtOAc mixture as eluent by column chromatography.

Synthesis of 4-phenyl-6-(phenylethynyl)-3-tosylquinoline 6.

A 20 mL Schlenk tube holding a magnetic bar was charged with 6-iodo-4-phenyl-3-tosylquinoline **3ga** (0.12 mmol, 1.0 equiv), phenylacetylene (0.15 mmol, 1.2 equiv), CuI (5 mol %, 2 mg), and $Pd(PPh_3)_2Cl_2$ (5 mol %, 5 mg) in triethylamine (5 mL) under an inert atmosphere. Then the reaction mixture was stirred into a preheated oil bath at 50 °C for 24 h. The mixture was cooled to room temperature, and the solvent was evaporated to dryness. After that, the crude mixture was diluted in EtOAc, and organic content was washed with saturated brine solution, dried over Na_2SO_4, and evaporated to dryness. The crude mixture was further purified by column chromatography using the hexane-EtOAc mixture as eluent.

Synthesis of (E)-4-phenyl-6-styryl-3-tosylquinoline 7.

6-bromo-4-phenyl-3-tosylquinoline **3ea** (0.14 mmol, 1.0 equiv), styrene (0.16 mmol, 1.2 equiv), PPh_3 (0.007 mmol, 2 mg), and $Pd(OAc)_2$ (5 mol %, 2 mg) in triethylamine (5 mL) were placed in a 20 mL Schlenk tube under an inert atmosphere. Then the reaction mixture was stirred into an oil bath at 50 °C for 24 h. The mixture was cooled to room temperature, and

solvent was evaporated to dryness. After that, the crude mixture was further purified by column chromatography using the hexane-EtOAc mixture as eluent.

Crystal measurement

Crystals of compounds **3ga, 3ia, 3ja,** and **3ha** were achieved after slow evaporation of $CHCl_3$. The crystals data were collected with a Bruker SMART D8 goniometer equipped with an APEX CCD detector and an INCOATEC micro source (Mo-Kα radiation, λ = 0.71073 Å). SAINT+[53] and SADABS[54] were used to integrate the intensities and correct the absorption. The structure was resolved by direct methods and refined on F^2 with SHELXL-97.[55] ORTEP drawing of the compounds **3ga, 3ia, 3ja, and 3ha** showing ellipsoid contour at the 50% probability level.

Compound 3ga (CCDC 2142154)

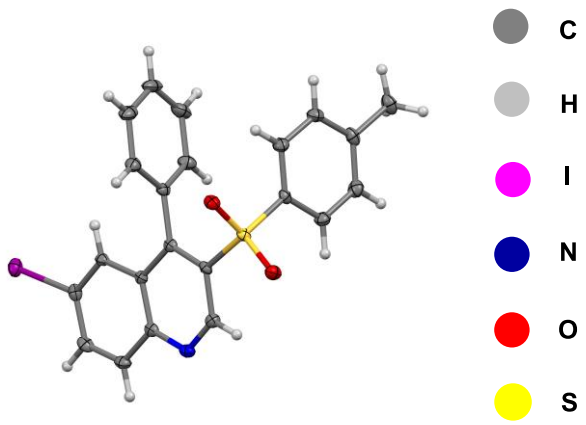

Fig.3.7. Crystal structure of **3ga** (CCDC 2142154). Ellipsoids are drawn at the 50% probability level.

Crystallographic Data for 3ga

Empirical formula	$C_{22}H_{16}INO_2S$
Formula weight	485.32
Temperature/K	100.00(10)

Crystal system	Triclinic
Space group	P-1
a/Å	10.53529(13)
b/Å	10.60349(14)
c/Å	35.6484(4)
α/°	91.4305(10)
β/°	92.3985(10)
γ/°	105.9716(11)
Volume/Å3	3822.47(8)
Z	8
ρcalcg/cm^3	1.687
μ/mm^{-1}	1.802
F(000)	1920.0
Crystal size/mm^3	0.2 × 0.1 × 0.1
Radiation	MoKα (λ = 0.71073)
Reflections collected	77819
Independent reflections	18659 [R_{int} = 0.0444, R_{sigma} = 0.0383]
Goodness-of-fit on F2	1.050
Final R indexes [I>=2σ (I)]	R_1 = 0.0308, wR_2 = 0.0594
Final R indexes [all data]	R_1 = 0.0382, wR_2 = 0.0613
Largest diff. peak/hole / e Å^{-3}	0.61/-0.69

Compound 3ia (CCDC 2142156)

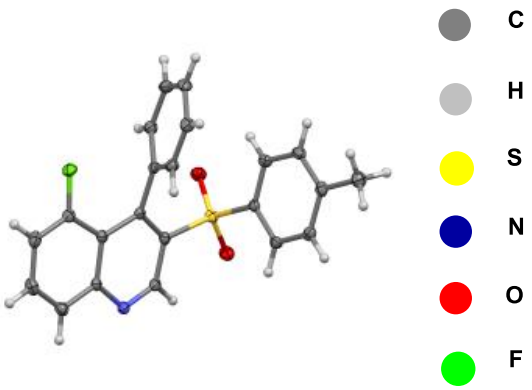

Fig. 3.8. Crystal structure of **3ia** (CCDC 2142156). Ellipsoids are drawn at the 50% probability level.

Crystallographic Data for 3ia

Empirical formula	$C_{22}H_{16}FNO_2S$
Formula weight	377.43
Temperature/K	100.00(10)
Crystal system	Monoclinic
Space group	$P2_1/n$
a/Å	9.2148(3)
b/Å	18.5404(6)
c/Å	13.1351(6)
α/°	90
β/°	107.433(4)
γ/°	90
Volume/Å3	2141.01(15)
Z	4

ρcalcg/cm^3	1.541
μ/mm^{-1}	0.556
F(000)	1016.0
Crystal size/mm^3	0.2 × 0.1 × 0.1
Radiation	MoKα (λ = 0.71073)
Reflections collected	22249
Independent reflections	5217 [R_{int} = 0.0501, R_{sigma} = 0.0449]
Goodness-of-fit on F2	1.059
Final R indexes [I>=2σ (I)]	R_1 = 0.0373, wR_2 = 0.0880
Final R indexes [all data]	R_1 = 0.0503, wR_2 = 0.0931
Largest diff. peak/hole / e Å^{-3}	0.45/-0.39

Compound 3ja (CCDC 2142157)

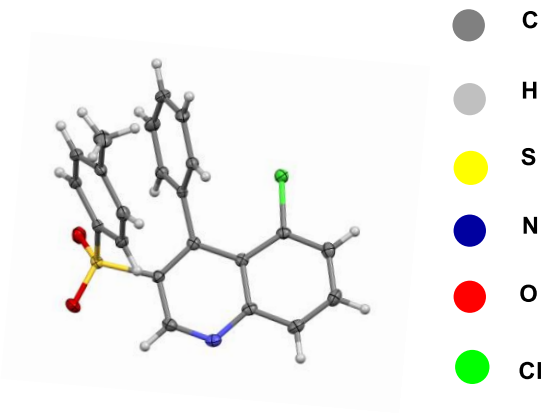

Fig. 3.9. Crystal structure of **3ja** (CCDC 2142157). Ellipsoids are drawn at the 50% probability level.

Crystallographic Data for 3ja

Empirical formula	$C_{22}H_{16}ClNO_2S$
Formula weight	393.87
Temperature/K	100.00(10)
Crystal system	Monoclinic
Space group	$P2_1/c$
a/Å	10.2909(6)
b/Å	18.1352(8)
c/Å	10.0347(6)
α/°	90
β/°	108.468(6)
γ/°	90
Volume/Å3	1776.29(18)
Z	4
ρcalcg/cm^3	1.473
μ/mm^{-1}	0.351
F(000)	816.0
Crystal size/mm^3	0.2 × 0.2 × 0.1
Radiation	MoKα (λ = 0.71073)
Reflections collected	18673
Independent reflections	4251 [R_{int} = 0.0588, R_{sigma} = 0.0504]
Goodness-of-fit on F2	1.059
Final R indexes [I>=2σ (I)]	R_1 = 0.0393, wR_2 = 0.0941
Final R indexes [all data]	R_1 = 0.0521, wR_2 = 0.0996

Largest diff. peak/hole / e $Å^{-3}$	0.45/-0.51

Compound 3ha (CCDC 2142158)

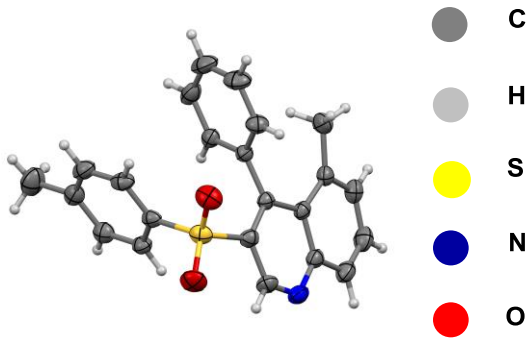

Fig. 3.10. Crystal structure of **3ha** (CCDC 2142158). Ellipsoids are drawn at the 30% probability level.

Crystallographic Data for 3ha

Empirical formula	$C_{23}H_{19}NO_2S$
Formula weight	373.45
Temperature/K	297.95(10)
Crystal system	Monoclinic
Space group	$P2_1/c$
a/Å	10.3272(11)
b/Å	18.7427(19)
c/Å	10.0833(9)
α/°	90
β/°	108.653(11)
γ/°	90
Volume/Å3	1849.2(3)
Z	4

ρcalcg/cm^3	1.341
μ/mm^{-1}	0.193
F(000)	784.0
Crystal size/mm^3	0.2 × 0.1 × 0.1
Radiation	MoKα (λ = 0.71073)
Reflections collected	18773
Independent reflections	4441 [R_{int} = 0.0480, R_{sigma} = 0.0457]
Goodness-of-fit on F2	1.051
Final R indexes [I>=2σ (I)]	R_1 = 0.0457, wR_2 = 0.1144
Final R indexes [all data]	R_1 = 0.0797, wR_2 = 0.1277
Largest diff. peak/hole / e Å^{-3}	0.20/-0.24

NMR CHARACTERIZATION DATA

6-Methyl-4-phenyl-3-tosylquinoline (3ba):[41] R_f = 0.5 (10% ethyl acetate in hexane); yellow solid; yield 72 % (73 mg); ^{1}H NMR (400 MHz, $CDCl_3$) δ 9.71 (s, 1H), 8.10 (d, *J* = 8.6 Hz, 1H), 7.65 (dd, *J* = 8.6, 1.8 Hz, 1H), 7.48-7.44 (m, 1H), 7.34 (t, *J* = 7.8 Hz, 2H), 7.20 (d, *J* = 8.2 Hz, 2H), 7.05 (d, *J* = 7.8 Hz, 3H), 6.95-6.93 (m, 2H), 2.36 (s, 3H), 2.35 (s, 3H); ^{13}C{^{1}H} NMR (100 MHz, $CDCl_3$) δ 149.2, 148.5, 147.1, 144.1, 138.3, 138.2, 134.7, 132.9, 132.8, 130.2, 129.5, 129.4, 128.7, 128.1, 127.8, 127.7, 126.1, 21.9, 21.7.

6-Ethyl-4-phenyl-3-tosylquinoline (3ca): R_f = 0.55 (10% ethyl acetate in hexane); light yellow semi solid; yield 66% (65 mg); ^{1}H NMR (400 MHz, $CDCl_3$) δ 9.71 (s, 1H), 8.12 (d, *J* = 8.6 Hz, 1H), 7.67 (d, *J* = 7.8 Hz, 1H), 7.45 (t, *J* = 7.4 Hz, 1H), 7.33 (t, *J* = 7.6 Hz, 2H), 7.19 (d, *J* = 8.0 Hz, 2H), 7.05-7.02 (m, 3H), 6.94 (d, *J* = 7.2 Hz, 2H), 2.63 (q, *J* = 7.6 Hz, 2H), 2.33 (s, 3H), 1.12 (t, *J* = 7.6 Hz, 3H); ^{13}C{^{1}H} NMR (100 MHz, $CDCl_3$) δ 149.3, 148.7, 147.0, 144.3, 144.0, 138.1, 133.5, 132.8, 132.6, 130.1, 129.5, 129.3, 128.6, 127.9, 127.7, 127.6, 124.9, 29.0, 21.6, 15.4; IR (KBr) ῡ 3415, 3031, 2961, 1651, 672; HRMS (ESI/Q-TOF) m/z: $[M + H]^+$ calcd for $C_{24}H_{22}NO_2S$ 388.1371; found 388.1364.

4-(3-Fluorophenyl)-6-isopropyl-3-tosylquinoline (3da): R_f = 0.45 (10% ethyl acetate in hexane); reddish oily liquid; yield 64% (72 mg); ^{1}H NMR (400 MHz, $CDCl_3$) δ 9.71 (s, 1H), 8.16 (d, *J* = 8.6 Hz, 1H), 7.75 (dd, *J* = 8.8, 1.8 Hz, 1H), 7.39-7.34 (m, 1H), 7.27-7.25 (m, 2H), 7.19-7.15 (m, 1H), 7.10 (d, *J* = 8.0 Hz, 2H), 7.05 (d, *J* = 1.8 Hz, 1H), 6.86 (d, *J* = 7.6 Hz, 1H), 6.54-6.51 (m, 1H), 2.95-2.85 (m, 1H), 2.37 (s, 3H), 1.16 (d, *J* = 7.0 Hz, 6H); ^{13}C{^{1}H} NMR (100 MHz, $CDCl_3$) δ 162.1 (d, $^1J_{C\text{-}F}$ = 247.5 Hz), 149.2, 148.9, 147.6 (d, $^4J_{C\text{-}F}$ = 1.8 Hz), 144.5, 138.1, 134.9 (d, $^3J_{C\text{-}F}$ = 8.2 Hz), 132.7, 132.1, 129.8, 129.6, 129.5, 129.4, 128.0, 127.2, 126.3 (d, $^4J_{C\text{-}F}$ = 3.0 Hz), 123.3, 117.2 (d, $^2J_{C\text{-}F}$ = 22.8 Hz), 115.8 (d, $^2J_{C\text{-}F}$ = 20.8 Hz), 34.4, 23.8, 21.7; ^{19}F NMR (377 MHz, $CDCl_3$) δ -113.1; IR (KBr) ῡ 3396, 2960, 2922, 1583, 681; HRMS (ESI/Q-TOF) m/z: $[M + H]^+$ calcd for $C_{25}H_{23}FNO_2S$ 436.166; 436.1370.

6-Fluoro-4-phenyl-3-tosylquinoline (3ea):[41] R_f = 0.45 (10% ethyl acetate in hexane); light yellow solid; yield 85% (86 mg); ^{1}H NMR (400 MHz, $CDCl_3$) δ 9.74 (s, 1H), 8.22 (m, 1H), 7.64-7.56 (m, 1H), 7.59 (m, 1H), 7.48 (m, 2H), 7.21 (m, 2H), 7.06 (d, *J* = 8.0 Hz, 2H), 6.96-6.93 (m, 2H), 6.91 (d, *J* = 2.8 Hz, 1H), 2.36 (s, 3H); ^{13}C{^{1}H} NMR (100 MHz, $CDCl_3$) δ 161.2

(d, $^{1}J_{C\text{-}F}$ = 250.7 Hz), 149.3 (d, $^{3}J_{C\text{-}F}$ = 5.9 Hz), 147.3 (d, $^{4}J_{C\text{-}F}$ = 2.7 Hz), 147.1, 144.4, 137.8, 133.6, 132.4, 132.4 (d, $^{3}J_{C\text{-}F}$ = 3.8 Hz), 130.02, 129.5, 129.0, 128.8 (d, $^{3}J_{C\text{-}F}$ = 9.6 Hz), 128.1, 128.0, 122.6 (d, $^{2}J_{C\text{-}F}$ = 26.0 Hz), 110.9 (d, $^{2}J_{C\text{-}F}$ = 23.7 Hz), 21.7; ^{19}F NMR (377 MHz, $CDCl_3$) δ -109.7.

6-Bromo-4-phenyl-3-tosylquinoline (3fa):[41] R_f = 0.40 (10% ethyl acetate in hexane); pale yellow solid; yield 82% (75 mg); ^{1}H NMR (400 $CDCl_3$) δ 9.77 (s, 1H), 8.08 (d, *J* = 9.0 Hz, 1H), 7.87 (dd, *J* = 9.0, 2.2 Hz, 1H), 7.51-7.46 (m, 1H), 7.45 (d, *J* = 8.0 Hz, 1H), 7.37-7.33 (m, 2H), 7.20-7.18 (m, 2H), 7.06 (d, *J* = 8.0 Hz, 2H), 6.95-6.93 (m, 2H), 2.36 (s, 3H); ^{13}C{^{1}H} NMR (100 MHz, $CDCl_3$) δ 149.1, 148.4, 148.2, 144.4, 137.7, 135.8, 133.7, 132.0, 131.4, 130.1, 129.5, 129.5, 129.1, 128.9, 128.1, 128.0, 122.5, 21.7.

6-Iodo-4-phenyl-3-tosylquinoline (3ga): R_f = 0.45 (10% ethyl acetate in hexane); pale yellow solid; yield 74% (65 mg); mp 164-167 ºC; ^{1}H NMR (400 MHz, $CDCl_3$) δ 9.76 (s, 1H), 8.04 (d, *J* = 8.9 Hz, 1H), 7.92 (d, *J* = 8.9 Hz, 1H), 7.66 (d, *J* = 1.8 Hz, 1H), 7.48 (t, *J* = 7.6 Hz, 1H), 7.35 (t, *J* = 7.8 Hz, 2H), 7.18 (d, *J* = 8.2 Hz, 2H), 7.05 (d, *J* = 8.2 Hz, 2H), 6.94-6.92 (m, 2H), 2.35 (s, 3H); ^{13}C{^{1}H} NMR (100 MHz, $CDCl_3$) δ 148.8, 148.8, 148.4, 144.4, 141.0, 137.7, 136.1, 133.5, 131.9, 131.3, 130.1, 129.4, 129.3, 129.1, 128.1, 128.0, 94.2, 21.7; IR (KBr) ῡ 3303, 3054, 2935, 1644, 690; HRMS (ESI/Q-TOF) m/z: $[M + H]^+$ calcd for $C_{22}H_{17}INO_2S$ 486.0019; found 485.9992.

5-Methyl-4-phenyl-3-tosylquinoline (3ha): R_f = 0.7 (20% ethyl acetate in hexane); red solid; yield 74% (75 mg); mp 144-147 ºC; ^{1}H NMR (700 MHz, $CDCl_3$) δ 9.87 (s, 1H), 8.32 (d, *J* = 7.3 Hz, 1H), 7.80-7.76 (m, 1H), 7.44-7.42 (m, 1H), 7.38-7.37 (m, 2H), 7.26-7.25 (m, 2H), 7.20 (d, *J* = 7.8 Hz, 1H), 7.13 (d, *J* = 7.7 Hz, 1H), 7.04 (d, *J* = 7.6 Hz, 1H), 6.95 (d, *J* = 7.1 Hz, 2H),

2.35 (s, 3H), 1.75 (s, 3H); $^{13}C\{^1H\}$ NMR (175 MHz, $CDCl_3$) δ 144.4, 138.9, 137.7, 133.1, 130.5, 129.9, 129.8, 129.6, 129.5, 129.2, 128.3, 127.96, 127.9, 127.6, 127.4, 127.0, 123.0, 24.0, 21.7; IR (KBr) ῡ 3402, 3060, 2929, 1484, 668; HRMS (ESI/Q-TOF) m/z: $[M + H]^+$ calcd for $C_{23}H_{20}NO_2S$ 374.1209; found 374.1220.

8-Fluoro-4-phenyl-3-tosylquinoline (3ia): R_f = 0.45 (10% ethyl acetate in hexane); pale yellow solid; yield 75% (75 mg); mp 136-140 ºC; ^1H NMR (400 MHz, $CDCl_3$) δ 9.81 (s, 1H), 8.05 (d, *J* = 8.5 Hz, 1H), 7.75 (td, *J* = 8.0, 5.2 Hz, 1H), 7.39 (t, *J* = 7.5 Hz, 1H), 7.23 (t, *J* = 7.8 Hz, 2H), 7.15 (d, *J* = 8.2 Hz, 2H), 7.10-7.07 (m, 1H), 7.05 (d, *J* = 8.2 Hz, 2H), 6.94-6.92 (m, 2H), 2.35 (s, 3H); $^{13}C\{^1H\}$ NMR (100 MHz, $CDCl_3$) δ 159.4 (d, $^1J_{C\text{-}F}$ = 263.5 Hz), 151.0, 148.7, 147.89 (d, $^4J_{C\text{-}F}$ = 2.5 Hz), 144.3, 137.9, 134.5 (d, $^3J_{C\text{-}F}$ = 4.0 Hz), 134.2, 132.3 (d, $^2J_{C\text{-}F}$ = 9.8 Hz), 129.4, 129.0 (d, $^4J_{C\text{-}F}$ = 3.5 Hz), 128.3, 127.9, 127.2, 126.4 (d, $^3J_{C\text{-}F}$ = 4.4 Hz), 118.0 (d, $^3J_{C\text{-}F}$ = 7.5 Hz), 113.6 (d, $^2J_{C\text{-}F}$ = 22.3 Hz), 21.7; ^{19}F NMR (377 MHz, $CDCl_3$) δ -104.2; IR (KBr) ῡ 3381, 3013, 2919, 1647, 670; HRMS (ESI/Q-TOF) m/z: $[M + H]^+$ calcd for $C_{22}H_{17}FNO_2S$ 378.0959; found 378.0956.

8-Chloro-4-phenyl-3-tosylquinoline (3ja): R_f = 0.45 (10% ethyl acetate in hexane); pale yellow solid; yield 74% (72 mg); mp 162-164 ºC; ^1H NMR (400 MHz, $CDCl_3$) δ 9.86 (s, 1H), 8.18 (dd, *J* = 8.4, 1.3 Hz, 1H), 7.70 (dd, *J* = 8.4, 7.6 Hz, 1H), 7.56 (dd, *J* = 7.5, 1.3 Hz, 1H), 7.40-7.35 (m, 1H), 7.20-7.15 (m, 2H), 7.13-7.10 (m, 2H), 7.03 (d, *J* = 8.2 Hz, 2H), 6.92-6.90 (m, 2H), 2.35 (s, 3H); $^{13}C\{^1H\}$ NMR (100 MHz, $CDCl_3$) δ 151.6, 149.8, 148.4, 144.1, 138.0, 134.9, 133.6, 132.8, 131.9, 131.7, 130.9, 130.2, 129.4, 128.7, 127.8, 127.1, 124.5, 21.7; IR (KBr) ῡ 3402, 3058, 2922, 1596, 689; HRMS (ESI/Q-TOF) m/z: $[M + Na]^+$ calcd for $C_{22}H_{16}ClNO_2SNa$ 416.0482; found 416.0475.

6,7-Dichloro-4-phenyl-3-tosylquinoline (3ka): R_f = 0.5 (10% ethyl acetate in hexane); pale yellow solid; yield 80% (73 mg); mp 151-155 ºC; ^{1}H NMR (400 MHz, $CDCl_3$) δ 9.85 (s, 1H), 8.11 (d, *J* = 9.0 Hz, 1H), 7.87 (d, *J* = 9.0 Hz, 1H), 7.38 (t, *J* = 7.6 Hz, 1H), 7.18 (t, *J* = 7.8 Hz, 2H), 7.10 (d, *J* = 8.2 Hz, 2H), 7.02 (d, *J* = 8.2 Hz, 2H), 6.89-6.87 (m, 2H), 2.35 (s, 3H); ^{13}C{^{1}H} NMR (100 MHz, $CDCl_3$) δ 150.0, 149.6, 148.5, 144.3, 137.8, 135.7, 135.6, 133.6, 133.4, 130.8, 130.4, 130.3, 129.4, 128.8, 127.8, 127.3, 125.6, 21.7; IR (KBr) ῡ 3403, 3059, 2919, 1595, 695; HRMS (ESI/Q-TOF) m/z: $[M + H]^+$ calcd for $C_{22}H_{16}Cl_2NO_2S$ 428.0279; found 428.0266.

7-Chloro-6-fluoro-4-phenyl-3-tosylquinoline (3la): R_f = 0.5 (10% ethyl acetate in hexane); pale yellow solid; yield 84% (81 mg); mp 174-176 ºC; ^{1}H NMR (400 MHz, $CDCl_3$) δ 9.82 (s, 1H), 8.18 (dd, *J* = 9.2, 5.6 Hz, 1H), 7.66 (t, *J* = 8.6 Hz, 1H), 7.38 (t, *J* = 7.6 Hz, 1H), 7.18 (t, *J* = 7.8 Hz, 2H), 7.11 (d, *J* = 8.2 Hz, 2H), 7.03 (d, *J* = 8.0 Hz, 2H), 6.89 (d, *J* = 7.2 Hz, 2H), 2.34 (s, 3H); ^{13}C{^{1}H} NMR (100 MHz, $CDCl_3$) δ 158.19 (d, $^1J_{C\text{-}F}$ = 250.4 Hz), 149.5 (d, $^3J_{C\text{-}F}$ = 6.6 Hz), 148.1, 147.7 (d, $^3J_{C\text{-}F}$ = 2.6 Hz), 144.3, 137.8, 135.4, 133.0, 131.2 (d, $^3J_{C\text{-}F}$ = 8.9 Hz), 130.8, 129.4, 128.8, 127.8, 127.2, 125.1, 121.9 (d, $^2J_{C\text{-}F}$ = 26.9 Hz), 117.9 (d, $^2J_{C\text{-}F}$ = 20.0 Hz), 21.7; ^{19}F NMR (377 MHz, $CDCl_3$) δ -104.9; IR (KBr) ῡ 3412, 3065, 2927, 1485, 697; HRMS (ESI/Q-TOF) m/z: $[M + Na]^+$ calcd for $C_{22}H_{15}ClFNO_2SNa$ 434.0388; found 434.0384.

4-(*p*-Tolyl)-3-tosylquinoline (3ma):[41] R_f = 0.5 (10% ethyl acetate in hexane); pale yellow solid; yield 81% (82 mg); ^{1}H NMR (400 MHz, $CDCl_3$) δ 9.76 (s, 1H), 8.20 (d, *J* = 8.6 Hz, 1H), 7.82-7.78 (m, 1H), 7.46-7.42 (m, 1H), 7.37 (dd, *J* = 8.4, 0.8 Hz, 1H), 7.24 (d, *J* = 8.4 Hz, 2H), 7.15 (d, *J* = 8.0 Hz, 2H), 7.06 (d, *J* = 8.0 Hz, 2H), 6.85 (d, *J* = 8.0 Hz, 2H), 2.47 (s, 3H), 2.35 (s, 3H); ^{13}C{^{1}H} NMR (100 MHz, $CDCl_3$) δ 150.3, 149.8, 148.0, 144.1, 138.7, 138.2, 133.0, 132.2, 130.1, 129.8, 129.7, 129.3, 128.4, 128.1, 127.7, 127.8, 127.7, 21.7, 21.6.

4-(3-Chlorophenyl)-3-tosylquinoline (3na): R_f = 0.5 (10% ethyl acetate in hexane); pale yellow solid; yield 77% (76 mg); mp 134-136 ºC; ^{1}H NMR (400 MHz, $CDCl_3$) δ 9.80 (s, 1H), 8.23 (d, *J* = 8.4 Hz, 1H), 7.86-7.82 (m, 1H) 7.51-7.47 (m, 1H), 7.45-7.43 (m, 1H), 7.38 (t, *J* = 7.8 Hz, 1H), 7.31 (d, *J* = 8.4 Hz, 1H), 7.26-7.23 (m, 2H), 7.12-7.10 (m, 3H), 6.59 (t, *J* = 1.6 Hz, 1H), 2.39 (s, 3H); ^{13}C{^{1}H} NMR (100 MHz, $CDCl_3$) δ 149.9, 148.0, 147.8, 144.7, 137.8, 134.5, 134.0, 132.9, 132.5, 130.0, 129.6, 129.5, 129.4, 129.0, 128.8, 128.3, 128.0, 127.2, 127.2, 21.7; IR (KBr) ῡ 3393, 3068, 2919, 1683, 680; HRMS (ESI/Q-TOF) m/z: $[M + Na]^+$ calcd for $C_{22}H_{16}ClNO_2SNa$ 416.0482; found 416.0490.

4-([1,1'-Biphenyl]-4-yl)-3-tosylquinoline (3oa):[56] R_f = 0.45 (10% ethyl acetate in hexane); pale yellow solid; yield 87% (80 mg); ^{1}H NMR (700 MHz, $CDCl_3$) δ 9.82 (s, 1H), 8.23 (d, *J* = 8.5 Hz, 1H), 7.84 (t, *J* = 7.5 Hz, 1H), 7.69 (d, *J* = 7.6 Hz, 2H), 7.56 (d, *J* = 7.8 Hz, 2H), 7.53 (t, *J* = 7.5 Hz, 2H), 7.50-7.44 (m,3H), 7.25 (d, *J* = 7.9 Hz, 2H), 7.04 (d, *J* = 7.8 Hz, 4H), 2.36 (s, 3H); ^{13}C{^{1}H} NMR (175 MHz, $CDCl_3$) δ 149.9, 149.7, 147.9, 144.2, 141.7, 140.4, 138.1, 133.1, 132.3, 131.7, 130.7, 129.9, 129.3, 129.2, 128.1, 128.0, 127.6, 127.5, 127.2×2, 126.4, 21.7.

4-([1,1'-Biphenyl]-2-yl)-3-tosylquinoline (3pa): R_f = 0.45 (10% ethyl acetate in hexane); light yellow solid; yield 83% (76 mg); mp 184-188 ºC; ^{1}H NMR (700 MHz, $CDCl_3$) δ 9.56 (s, 1H), 8.05 (d, *J* = 8.5 Hz, 1H), 7.70 (t, *J* = 7.5 Hz, 1H), 7.61 (t, *J* = 7.6 Hz, 1H), 7.52 (d, *J* = 7.7 Hz, 1H), 7.43 (d, *J* = 8.1 Hz, 2H), 7.39-7.34 (m, 3H), 7.18 (d, *J* = 8.1 Hz, 2H), 6.98-6.90 (m, 5H), 6.89 (d, *J* = 7.6 Hz, 1H), 2.36 (s, 3H); ^{13}C{^{1}H} NMR (175 MHz, $CDCl_3$) δ 149.8, 149.2, 148.6, 144.7, 142.2, 140.2, 138.6, 132.9, 132.1, 131.7, 130.4, 130.3, 129.7, 129.63, 129.60, 128.9, 128.5, 127.8, 127.8, 127.7, 127.2, 127.0, 126.6, 21.7; IR (KBr) ῡ 3393, 3057, 2911, 1564, 675; HRMS (ESI/Q-TOF) m/z: $[M + H]^+$ calcd for $C_{28}H_{22}NO_2S$ 436.1366; found 436.1389.

4-(Naphthalen-1-yl)-3-tosylquinoline (3qa): R_f = 0.45 (10% ethyl acetate in hexane); pale yellow solid; yield 77% (73 mg); mp 132-134 ºC; ^{1}H NMR (700 MHz, $CDCl_3$) δ 9.92 (s, 1H), 8.26 (d, *J* = 8.4 Hz, 1H), 7.99 (d, *J* = 8.1 Hz, 1H), 7.80 (t, *J* = 9.7 Hz, 2H), 7.61 (t, *J* = 7.5 Hz, 1H), 7.43 (d, *J* = 6.9 Hz, 1H), 7.32 (t, *J* = 7.5 Hz, 2H), 7.08 (d, *J* = 8.5 Hz, 1H), 6.94 (d, *J* = 7.9 Hz, 2H), 6.88 (t, *J* = 7.5 Hz, 1H), 6.62 (d, *J* = 7.9 Hz, 2H), 6.32 (d, *J* = 8.5 Hz, 1H), 2.08 (s, 3H); ^{13}C{^{1}H} NMR (175 MHz, $CDCl_3$) δ 149.7, 148.5×2, 148.0, 143.8, 136.6, 134.1, 132.9, 132.3, 131.6, 129.9, 129.8, 129.7, 128.9, 128.15, 128.12, 127.9, 127.7, 127.6, 126.3, 125.6, 125.5, 125.1, 21.4. IR (KBr) ῡ 3365, 3056, 2924, 1497, 705; HRMS (ESI/Q-TOF) m/z: [M + Na]$^+$ calcd for $C_{26}H_{19}NO_2SNa$ 432.1029; found 432.1019.

4-(Thiophen-2-yl)-3-tosylquinoline (3ra):[41] R_f = 0.35 (5% ethyl acetate in hexane); yellow solid; yield 76% (78 mg); ^{1}H NMR (700 MHz, $CDCl_3$) δ 9.79 (s, 1H), 8.20 (d, *J* = 8.8 Hz, 1H), 7.83 (t, *J* = 7.6 Hz, 1H), 7.59 (d, *J* = 8.5 Hz, 1H), 7.52-7.50 (m, 2H), 7.33 (d, *J* = 8.1 Hz, 2H), 7.14-7.12 (m, 1H), 7.11 (d, *J* = 8.1 Hz, 2H), 7.02 (d, *J* = 3.4 Hz, 1H), 2.36 (s, 3H); ^{13}C{^{1}H} NMR (175 MHz, $CDCl_3$) δ 149.8, 147.9, 144.3, 143.2, 137.7, 134.4, 132.5, 131.9, 131.6, 129.8, 129.5, 128.8, 128.6, 128.2, 128.0, 127.3, 126.9, 21.7.

4-(Pyridin-3-yl)-3-tosylquinoline (3sa): R_f = 0.5 (20% ethyl acetate in hexane); pale yellow solid; yield 72% (74 mg); mp 132-135ºC; ^{1}H NMR (400 MHz, $CDCl_3$) δ 9.79 (s, 1H), 8.75-8.73 (m, 1H), 8.25 (d, *J* = 8.4 Hz, 1H), 7.99 (d, *J* = 1.7 Hz, 1H), 7.88-7.84 (m, 1H), 7.60-7.58 (m, 1H), 7.53-7.49 (m, 1H), 7.44-7.41 (m, 1H), 7.29 (d, *J* = 8.6 Hz, 1H), 7.23 (d, *J* = 8.4 Hz, 2H), 7.13 (d, *J* = 8.2 Hz, 2H), 2.36 (s, 3H); ^{13}C{^{1}H} NMR (100 MHz, $CDCl_3$) δ 150.0, 149.9, 149.5, 148.0, 146.0, 144.9, 138.2, 138.0, 133.3, 132.6, 130.1, 129.8, 129.3, 128.5, 127.8, 127.3, 126.9, 122.8, 21.8 ; IR (KBr) ῡ 3397, 3046, 2928, 1610, 705; HRMS (ESI/Q-TOF) m/z: [M + H]$^+$ calcd for $C_{21}H_{17}N_2O_2S$ 361.1005; found 361.1030.

4-ethyl-3-tosylquinoline (3ta): R_f = 0.65 (20% ethyl acetate in hexane); reddish yellow solid; yield 49% (38 mg); mp 142-146 ºC; ^{1}H NMR (400 MHz, $CDCl_3$) δ 9.54 (s, 1H), 8.18-8.11 (m, 2H), 7.85-7.82 (m, 3H), 7.65 (t, *J* = 7.6 Hz, 1H), 7.33-7.31 (m, 2H), 3.44 (q, *J* = 7.6 Hz, 2H), 2.41 (s, 3H), 1.16 (t, *J* = 7.4 Hz, 3H); ^{13}C NMR (100 MHz, $CDCl_3$) δ 152.7, 148.6, 144.7, 138.9, 132.1×2, 130.7, 130.2, 130.1, 128.0, 127.8, 126.6, 124.9, 22.3, 21.8, 15.2; IR (KBr) ῡ 3306, 3078, 1628, 749; HRMS (ESI/Q-TOF) m/z: $[M + Na]^+$ calcd for $C_{18}H_{17}NO_2SNa$ 334.0872; found 334.0843.

4-Phenyl-3-tosylquinoline (3aa):[41] R_f = 0.35 (20% ethyl acetate in hexane); pale yellow solid; yield 84% (88 mg); ^{1}H NMR (700 MHz, $CDCl_3$) δ 9.7 8 (s, 1H), 8.21 (d, *J* = 8.4 Hz, 1H), 7.83-7.80 (m, 1H), 7.47-7.44 (m, 2H), 7.34 (t, *J* = 7.8 Hz, 3H), 7.21 (d, *J* = 8.4 Hz, 2H), 7.05 (d, *J* = 8.1 Hz, 2H), 6.96-6.95 (m, 2H), 2.35 (s, 3H); ^{13}C{^{1}H} NMR (175 MHz, $CDCl_3$) δ 150.0, 149.8, 147.9, 144.2, 138.1, 132.8, 132.8, 132.3, 130.2, 129.8, 129.4, 128.8, 128.1, 128.0, 127.8, 127.6, 127.6, 21.7.

4-Phenyl-3-(phenylsulfonyl)quinoline (3ab):[41] R_f = 0.40 (10% ethyl acetate in hexane); yellow solid; yield 82% (82 mg); ^{1}H NMR (700 MHz, $CDCl_3$) δ 9.81 (s, 1H), 8.22 (d, *J* = 8.5 Hz, 1H), 7.83 (t, *J* = 7.6 Hz, 1H), 7.47-7.44 (m, 3H), 7.34-7.31 (m, 5H), 7.27-7.24 (m, 2H), 6.94 (d, *J* = 7.5 Hz, 2H); ^{13}C{^{1}H} NMR (175 MHz, $CDCl_3$) δ 150.2, 150.0, 147.9, 141.0, 133.1, 132.6, 132.5, 132.4, 130.2, 129.8, 128.9, 128.8, 128.7, 128.0, 127.8, 127.6, 127.5.

3-((4-Ethylphenyl)sulfonyl)-4-phenylquinoline (3ac): R_f = 0.45 (10% ethyl acetate in hexane); pale red solid; yield 85% (92 mg); mp 123-129 ºC; ^{1}H NMR (400 MHz, $CDCl_3$) δ 9.79 (s, 1H), 8.22 (d, *J* = 8.4 Hz, 1H), 7.84-7.80 (m, 1H), 7.47-7.43 (m, 2H), 7.34-7.30 (m,

3H), 7.24-7.22 (m, 2H), 7.07 (d, *J* = 8.5 Hz, 2H), 6.96-6.94 (m, 2H), 2.64(q, *J* = 7.6 Hz, 2H), 1.20 (t, *J* = 7.6 Hz, 3H); $^{13}C\{^{1}H\}$ NMR (100 MHz, $CDCl_3$) δ 150.3, 150.0, 149.8, 147.9, 138.2, 132.8, 132.8, 132.3, 130.2, 129.8, 128.7, 128.3, 128.2, 127.9, 127.8, 127.7, 127.6, 28.9, 15.4; IR (KBr) ῡ 3369, 3060, 2917, 1596, 666; HRMS (ESI/Q-TOF) m/z: $[M + H]^+$ calcd for $C_{23}H_{.20}NO_2S$ 374.1209; found 374.1232.

3-((4-Isopropylphenyl)sulfonyl)-4-phenylquinoline (3ad): R_f = 0.45 (10% ethyl acetate in hexane); pale yellow solid; yield 86% (96 mg); mp 124-126 ºC; ^{1}H NMR (700 MHz, $CDCl_3$) δ 9.79 (s, 1H), 8.21 (d, *J* = 8.5 Hz, 1H), 7.82-7.80 (m, 1H), 7.45-7.43 (m, 2H), 7.33-7.29 (m, 3H), 7.24-7.23 (m, 2H), 7.09 (d, *J* = 8.4 Hz, 2H), 6.95-6.93 (m, 2H), 2.92-2.86 (m, 1H), 1.21 (s, 3H), 1.20 (s, 3H); $^{13}C\{^{1}H\}$ NMR (175 MHz, $CDCl_3$) δ 154.8, 149.9, 149.8, 147.8, 138.2, 132.8, 132.7, 132.3, 130.1, 129.8, 128.7, 128.1, 127.9, 127.8, 127.6, 127.5, 126.9, 34.3, 23.7; IR (KBr) ῡ 3423, 2957, 2916, 1652, 665; HRMS (ESI/Q-TOF) m/z: $[M + H]^+$ calcd for $C_{24}H_{22}NO_2S$ 388.1366; found 388.1338.

3-(Mesitylsulfonyl)-4-phenylquinoline (3ae): R_f = 0.45 (10% ethyl acetate in hexane); pale yellow solid; yield 79% (89 mg); mp 164-166 ºC; ^{1}H NMR (400 MHz, $CDCl_3$) δ 9.76 (s, 1H), 8.22 (d, *J* = 8.5 Hz, 1H), 7.82-7.79 (m, 1H), 7.44 (t, *J* = 7.7 Hz, 1H), 7.35 (t, *J* = 7.3 Hz, 1H), 7.22-7.18 (m, 3H), 6.82 (d, *J* = 7.7 Hz, 2H), 6.68 (s, 2H), 2.24 (s, 3H), 2.12 (s, 6H); $^{13}C\{^{1}H\}$ NMR (100 MHz, $CDCl_3$) δ 149.3, 148.9, 147.8, 143.3, 139.5, 134.9, 134.3, 132.8, 132.0, 131.8, 129.7, 129.2, 128.5, 127.9, 127.8, 127.6, 127.4, 22.2, 21.0; IR (KBr) ῡ 3391, 3061, 2918, 1602, 1440, 670; HRMS (ESI/Q-TOF) m/z: $[M + H]^+$ calcd for $C_{24}H_{22}NO_2S$ 388.1366; found 388.1394.

3-((4-Ethoxyphenyl)sulfonyl)-4-phenylquinoline (3af): R_f = 0.60 (20% ethyl acetate in hexane); pale yellow solid; yield 86% (97 mg); mp 154-156 ºC; ^{1}H NMR (400 MHz, $CDCl_3$) δ 9.78 (s, 1H), 8.21 (d, *J* = 8.4 Hz, 1H), 7.81 (t, *J* = 7.2 Hz, 1H), 7.48-7.43 (m, 2H), 7.40-7.31 (m, 3H), 7.22 (d, *J* = 8.8 Hz, 2H), 6.99 (d, *J* = 7.3 Hz, 2H), 6.69 (d, *J* = 8.9 Hz, 2H), 4.02 (q, *J* = 7.0 Hz, 2H), 1.41 (t, *J* = 7.0 Hz, 3H); ^{13}C{^{1}H} NMR (100 MHz, $CDCl_3$) δ 162.8, 149.8, 147.9, 133.1, 132.9, 132.3, 132.2, 132.1, 130.3, 130.2, 129.8, 128.8, 127.9, 127.8, 127.7, 127.5, 114.4, 64.2, 14.6; IR (KBr) ῡ 3004, 1645, 1275, 764; HRMS (ESI/Q-TOF) m/z: $[M + H]^+$ calcd for $C_{23}H_{20}NO_3S$ 390.1158; found 390.1175.

3-((4-Bromophenyl)sulfonyl)-4-phenylquinoline (3ag):[41] R_f = 0.65 (20% ethyl acetate in hexane); brown solid; yield 77% (95 mg); ^{1}H NMR (400 MHz, DMSO) δ 9.63 (s, 1H), 8.22 (d, *J* = 8.4 Hz, 1H) 8.00-7.95 (m, 1H), 7.65-7.63 (m, 1H), 7.62-7.58 (m, 2H), 7.53-7.49 (m, 2H), 7.38 (t, *J* = 7.7 Hz, 2H), 7.28-7.25 (m, 2H), 6.97-6.95 (m, 2H); ^{13}C{^{1}H} NMR (100 MHz, DMSO) δ 149.7, 149.3, 147.0, 139.6, 133.0, 132.2, 132.0, 131.4, 129.6, 129.4, 129.3, 128.9, 128.7, 127.9, 127.7, 127.1, 126.8.

3-((3-Chlorophenyl)sulfonyl)-4-phenylquinoline (3ah):[41] R_f = 0.65 (20% ethyl acetate in hexane); pale red solid; yield 74% (82 mg); ^{1}H NMR (400 MHz, DMSO) δ 9.66 (s, 1H), 8.23 (d, *J* = 8.4 Hz, 1H), 7.97 (t, *J* = 7.7 Hz, 1H), 7.72-7.59 (m, 2H), 7.46 (d, *J* = 8.0 Hz, 2H), 7.41-7.36(m, 2H), 7.27 (d, *J* = 8.4 Hz, 1H), 7.15-7.11 (m, 2H), 6.95 (d, *J* = 7.4 Hz, 2H); ^{13}C{^{1}H} NMR (100 MHz, DMSO) δ 149.8, 149.3, 146.9, 141.9, 133.8, 133.7, 133.6, 133.1, 131.7, 131.3, 131.2, 129.7, 129.4, 129.0, 128.7, 127.7, 127.1, 126.7, 126.2.

3-((3,4-Dichlorophenyl)sulfonyl)-4-phenylquinoline (3ai): R_f = 0.65 (20% ethyl acetate in hexane); pale red solid; yield 69% (83 mg); mp 126-130 ºC; ^{1}H NMR (400 MHz, DMSO) δ

9.66 (s, 1H), 8.24 (d, *J* = 8.4 Hz, 1H), 8.01-7.97 (m, 1H), 7.69 (d, *J* = 8.5 Hz, 1H), 7.68-7.63 (m, 1H), 7.55 (t, *J* = 7.5 Hz, 1H), 7.43-7.38 (m, 3H), 7.33-7.32 (m, 1H), 7.28 (d, *J* = 8.4 Hz, 1H), 7.00 (d, *J* = 7.1 Hz, 2H); $^{13}C\{^{1}H\}$ NMR (100 MHz, DMSO) δ 149.8, 149.4, 146.9, 140.2, 137.1, 133.2, 132.0, 131.7, 131.6, 131.1, 129.8, 129.37, 129.32, 129.1, 128.7, 127.7, 127.5, 127.1, 126.7; IR (KBr) ῡ 3406, 2917, 2850, 1559, 673; HRMS (ESI/Q-TOF) m/z: $[M + H]^+$ calcd for $C_{21}H_{14}Cl_2NO_2S$ 414.0117; found 414.0113.

3-(Naphthalen-1-ylsulfonyl)-4-phenylquinoline (3aj):[41] R_f = 0.55 (20% ethyl acetate in hexane); pale yellow solid; yield 80% (91 mg); ^{1}H NMR (700 MHz, $CDCl_3$) δ 10.06 (s, 1H), 8.27-8.22 (m, 2H), 7.91 (d, *J* = 8.0 Hz, 1H), 7.83 (d, *J* = 7.0 Hz, 1H), 7.80 (t, *J* = 7.3 Hz, 1H), 7.44 (d, *J* = 6.8 Hz, 3H), 7.41-7.39 (m, 1H), 7.34 (t, *J* = 7.0 Hz, 1H), 7.22 (d, *J* = 8.3 Hz, 1H), 7.15-7.11 (m, 3H), 6.63 (d, *J* = 6.9 Hz, 2H); $^{13}C\{^{1}H\}$ NMR (175 MHz, $CDCl_3$) δ 149.8, 149.7, 147.7, 134.9, 134.6, 133.8, 133.0, 132.3, 130.6×2, 129.9, 129.7, 129.1, 128.6, 128.5, 127.9, 127.8, 127.7, 127.5, 127.4, 126.7, 124.4, 123.7.

4-Phenyl-3-(quinolin-3-ylsulfonyl)quinoline (3ak): R_f = 0.65 (20% ethyl acetate in hexane); pale yellow solid; yield 76% (88 mg); mp 160-166 ºC; ^{1}H NMR (700 MHz, $CDCl_3$) δ 9.90 (s, 1H), 8.75 (s, 1H), 8.24 (d, *J* = 8.5 Hz, 1H), 8.10 (d, *J* = 8.4 Hz, 1H), 7.95 (s, 1H), 7.87-7.83 (m, 2H), 7.68 (d, *J* = 8.1 Hz, 1H), 7.65-7.63 (m, 1H), 7.47-7.44 (m, 1H), 7.42 (t, *J* = 7.4 Hz, 1H), 7.31 (d, *J* = 8.5 Hz, 1H), 7.22 (t, *J* = 7.5 Hz, 2H), 6.92 (d, *J* = 7.5 Hz, 2H); $^{13}C\{^{1}H\}$ NMR (175 MHz, $CDCl_3$) δ 150.3, 150.2, 149.3, 147.5, 146.9, 137.9, 133.8, 132.9, 132.8, 132.3, 131.9, 130.3, 129.9, 129.7, 129.4, 129.3, 128.3, 128.2, 128.0, 127.5, 127.4, 126.0; IR (KBr) ῡ 3309, 3063, 2924, 1566, 760; HRMS (ESI/Q-TOF) m/z: $[M + Na]^+$ calcd for $C_{24}H_{16}N_2O_2SNa$ 419.0825; found 419.084.

4,6-Diphenyl-3-tosylquinoline 5: R_f = 0.45 (20% ethyl acetate in hexane); white solid; yield 78% (47 mg); mp 135-140 ºC; ^{1}H NMR (400 MHz, $CDCl_3$) δ 9.78 (s, 1H), 8.28 (d, *J* = 8.7 Hz, 1H), 8.08 (d, *J* = 8.7 Hz, 1H), 7.48-7.44 (m, 3H), 7.42-7.39 (m, 3H), 7.37-7.33 (m, 3H), 7.22 (d, *J* = 8.1 Hz, 2H), 7.06 (d, *J* = 8.1 Hz, 2H), 7.00 (d, *J* = 7.6 Hz, 2H), 2.36 (s, 3H); ^{13}C NMR (100 MHz, $CDCl_3$) δ 150.1, 149.2, 147.8, 144.2, 140.7, 139.8, 138.0, 133.2, 132.6, 132.1, 130.2, 130.1, 129.4, 129.1, 128.9, 128.2, 128.1, 127.9, 127.8, 127.5, 125.0, 21.7; IR (KBr) ῡ 3401, 3060, 2927, 1562, 646; HRMS (ESI/Q-TOF) m/z: $[M + H]^+$ calcd for $C_{28}H_{22}NO_2S$ 436.1366; found 436.1370.

4-Phenyl-6-(phenylethynyl)-3-tosylquinoline 6: R_f = 0.45 (20% ethyl acetate in hexane); white solid; yield 88% (50 mg); mp 166-170 ºC; ^{1}H NMR (700 MHz, $CDCl_3$) δ 9.76 (s, 1H), 8.17 (d, *J* = 8.7 Hz, 1H), 7.90 (d, *J* = 8.7 Hz, 1H), 7.51-7.47 (m, 4H), 7.37 (t, *J* = 7.6 Hz, 2H), 7.32 (d, *J* = 6.4 Hz, 3H), 7.21 (d, *J* = 8.1 Hz, 2H), 7.07 (d, *J* = 8.1 Hz, 2H), 6.98 (d, *J* = 7.5 Hz, 2H), 2.36 (s, 3H); ^{13}C NMR (175 MHz, $CDCl_3$) δ 149.5, 149.2, 148.4, 144.3, 137.9, 135.0, 133.6, 132.4, 131.8, 130.4, 130.2, 130.0, 129.4, 129.0×2, 128.6, 128.1, 127.9, 127.6, 123.3, 122.5, 91.9, 88.6, 21.7; IR (KBr) ῡ 3398, 3021, 2919, 1556, 645; HRMS (ESI/Q-TOF) m/z: $[M + H]^+$ calcd for $C_{30}H_{22}NO_2S$ 460.1366; found 460.1367.

(*E*)-4-Phenyl-6-styryl-3-tosylquinoline 7: R_f = 0.45 (20% ethyl acetate in hexane); yellow solid; yield 51% (32 mg); mp 161-166 ºC; ^{1}H NMR (700 MHz, $CDCl_3$) δ 9.72 (s, 1H), 8.18 (d, *J* = 8.8 Hz, 1H), 8.11 (d, *J* = 8.7 Hz, 1H), 7.50 (t, *J* = 7.5 Hz, 1H), 7.45 (d, *J* = 7.7 Hz, 2H), 7.37 (t, *J* = 7.6 Hz, 2H), 7.33 (t, *J* = 7.5 Hz, 2H), 7.27-7.21 (m, 4H), 7.10 (d, *J* = 16.3 Hz, 1H), 7.06 (d, *J* = 8.0 Hz, 2H), 7.02-6.98 (m, 3H), 2.36 (s, 3H); ^{13}C NMR (175 MHz, $CDCl_3$) δ 149.7, 149.5, 147.6, 144.2, 138.1, 137.0, 136.7, 133.3, 132.7, 131.3, 130.3, 130.2, 129.5, 129.4, 128.9, 128.8, 128.4, 128.1, 128.0, 127.9, 127.5, 126.8, 125.7, 21.7; IR (KBr) ῡ 3417, 2957, 2850,

1463, 665; HRMS (ESI/Q-TOF) m/z: $[M + H]^+$ calcd for $C_{30}H_{24}NO_2S$ 462.1522; found 462.1506.

(Z)-3-Phenyl-N-(p-tolyl)prop-2-yn-1-imine 4:[57] R_f = 0.55 (5% ethyl acetate in hexane); yellow solid; yield 51% (312 mg); ^{1}H NMR (700 MHz, $CDCl_3$) δ 7.95 (s, 1H), 7.59 (d, *J* = 7.3 Hz, 2H), 7.41 (t, *J* = 7.2 Hz, 1H), 7.37 (t, *J* = 7.4 Hz, 2H), 7.20 (d, *J* = 8.0 Hz, 2H), 7.14 (d, *J* = 8.1 Hz, 2H), 2.37 (s, 3H); ^{13}C NMR (175 MHz, $CDCl_3$) δ 148.5, 142.7, 137.5, 132.6, 130.0, 129.9, 128.6, 121.6, 120.9, 94.6, 87.8, 21.2.

N-(3-phenylprop-2-yn-1-yl)aniline 1a:[58] R_f = 0.55 (5 % ethyl acetate in hexane); red oilly; yield 80% (382 mg); ^{1}H NMR (400 MHz, $CDCl_3$) δ 7.43-7.40 (m, 2H), 7.31-7.26 (m, 4H), 7.24 (dd, *J* = 7.1, 1.4 Hz, 1H), 6.81 (t, *J* = 7.3 Hz, 1H), 6.77-6.74 (m, 2H), 4.17 (s, 2H), 3.97 (s, 1H).

4-Methyl-N-(3-phenylprop-2-yn-1-yl)aniline 1b:[58] R_f = 0.5 (5% ethyl acetate in hexane); reddish liquid; yield 65% (300 mg); ^{1}H NMR (400 MHz, $CDCl_3$) δ 7.40-7.38 (m, 3H), 7.29-7.27 (m, 3H), 7.04 (d, *J* = 8.2 Hz, 2H), 6.67 (d, *J* = 8.4 Hz, 2H), 4.13 (s, 2H), 2.27 (s, 3H).

4-Ethyl-N-(3-phenylprop-2-yn-1-yl)aniline 1c: R_f = 0.45 (5% ethyl acetate in hexane); reddish liquid; yield 77% (347 mg); ^{1}H NMR (700 MHz, CDCl3) δ 7.41-7.40(m, 2H), 7.30-7.29 (m, 3H), 7.08 (d, J = 8.1 Hz, 2H), 6.70 (d, J = 8.3 Hz, 2H), 4.14 (s, 2H), 3.85 (s, 1H), 2.58 (q, J = 7.6 Hz, 2H), 1.22 (t, J = 7.6 Hz, 3H); ^{13}C{^{1}H} NMR (100 MHz, $CDCl_3$) δ 145.2, 134.5, 131.8, 128.7, 128.4, 128.3, 123.1, 113.9, 86.7, 83.3, 35.0, 28.1, 16.0; IR (KBr) ῡ 3365, 3031, 2961, 1651, 690; HRMS (ESI/Q-TOF) m/z: $[M + H]^+$ calcd for $C_{17}H_{18}N$ 236.1434; found 236.1433.

N-(3-(3-Fluorophenyl)prop-2-yn-1-yl)-4-isopropylaniline 1d: R_f = 0.45 (20% ethyl acetate in hexane); oily red; yield 80% (370 mg); ^{1}H NMR (400 MHz, $CDCl_3$) δ 7.33-7.24 (m, 1H), 7.22 (t, *J* = 8.6 Hz, 1H), 7.14 (d, *J* = 6.6 Hz, 3H), 7.03 (t, *J* = 8.6 Hz, 1H), 6.73 (d, *J* = 7.6 Hz, 2H), 4.16 (s, 2H), 3.88 (s, 1H), 2.92-2.82 (m, 1H), 1.27 (d, *J* = 6.9 Hz, 6H); ^{13}C{^{1}H} NMR (100 MHz, $CDCl_3$) δ 162.4 (d, *J* = 246.3 Hz), 145.1, 139.3, 129.9 (d, *J* = 8.7 Hz), 127.7 (d, *J* = 2.9 Hz), 127.2 , 124.9 (d, *J* = 9.5 Hz), 118.6 (d, *J* = 22.7 Hz), 115.6 (d, *J* = 21.2 Hz), 113.8, 87.9, 82.1, 34.9, 33.3, 24.3; IR (KBr) ῡ 3419, 2957, 1634, 772; HRMS (ESI/Q-TOF) m/z: [M + H]$^+$ calcd for $C_{18}H_{19}FN$ 268.1496; found 268.1496.

4-Fluoro-N-(3-phenylprop-2-yn-1-yl)aniline 1e:[59] R_f = 0.45 (5% ethyl acetate in hexane); oily red; yield 60% (274 mg); ^{1}H NMR (700 MHz, $CDCl_3$) δ 7.40-7.37 (m, 2H), 7.31-7.27 (m, 3H), 6.95-6.92 (m, 2H), 6.69-6.67 (m, 2H), 4.12 (s, 2H), 3.86 (s, 1H).

4-Bromo-N-(3-phenylprop-2-yn-1-yl)aniline 1f:[58] R_f = 0.4 (5% ethyl acetate in hexane); brown solid; yield 77% (320 mg); ^{1}H NMR (400 MHz, $CDCl_3$) δ 7.41-7.37 (m, 2H), 7.31-7.28 (m, 5H), 6.64-6.59 (m, 2H), 4.12 (s, 2H), 4.00 (s, 1H).

4-Iodo-N-(3-phenylprop-2-yn-1-yl)aniline 1g: R_f = 0.55 (5% ethyl acetate in hexane); yellow solid; yield 75% (294 mg); mp 154-156 ºC; ^{1}H NMR (400 MHz, $CDCl_3$) δ 7.90-7.89 (m, 1H), 7.49-7.46 (m, 2H), 7.40-7.36 (m, 2H), 7.32-7.27 (m, 2H), 6.54-5.40 (m, 2H), 4.12 (s, 2H), 4.02 (s, 1H); ^{13}C{^{1}H} NMR (100 MHz, $CDCl_3$) δ 146.8, 145.9, 137.9, 131.8, 128.5, 128.4, 122.8, 115.9, 85.8, 83.7, 34.4; IR (KBr) ῡ 3400, 3054, 2917, 1683, 671; HRMS (ESI/Q-TOF) m/z: [M + H]$^+$ calcd for $C_{15}H_{13}IN$ 334.0087; found 334.0076.

3-Methyl-N-(3-phenylprop-2-yn-1-yl)aniline 1h:[58] R_f = 0.55 (10 % ethyl acetate in hexane); oily red ; yield 66% (500 mg); ^{1}H NMR (400 MHz, $CDCl_3$) δ 7.43-7.41 (m, 2H), 7.31-7.29 (m, 3H), 7.16-7.12 (m, 1H), 6.63 (d, *J* = 7.5 Hz, 1H), 6.57 (d, *J* = 5.4 Hz, 2H), 4.15 (s, 2H), 3.91 (s, 1H), 2.33 (s, 3H).

3-Fluoro-N-(3-phenylprop-2-yn-1-yl)aniline 1i: R_f = 0.4 (5% ethyl acetate in hexane); oily red; yield 60% (275 mg); ^{1}H NMR (700 MHz, $CDCl_3$) δ 7.41-7.39 (m, 1H), 7.32-7.28 (m, 3H), 7.15 (dd, *J* = 14.9, 8.1 Hz, 3H), 6.50-6.43 (m, 2H), 4.14 (s, 2H), 4.10 (s, 1H); ^{13}C{^{1}H} NMR (100 MHz, $CDCl_3$) δ 164.1 (d, *J* = 242.6 Hz), 149.0 (d, *J* = 10.7 Hz), 131.9, 130.4 (d, *J* = 10.1 Hz), 128.5, 128.4, 122.8, 109.5 (d, *J* = 2.3 Hz), 105.0 (d, *J* = 21.6 Hz), 100.4 (d, *J* = 25.5 Hz), 85.8, 83.7, 34.6; IR (KBr) ῡ 3415, 3061, 2928, 1626, 690; HRMS (ESI/Q-TOF) m/z: $[M + H]^+$ calcd for $C_{15}H_{13}FN$ 226.1027; found 226.1031.

3-Chloro-N-(3-phenylprop-2-yn-1-yl)aniline 1j: R_f = 0.4 (5% ethyl acetate in hexane); oily red; yield 56% (250 mg); ^{1}H NMR (400 MHz, $CDCl_3$) δ 7.43-7.41 (m, 2H), 7.32-7.26 (m, 3H), 7.14 (t, *J* = 8.0 Hz, 1H), 6.77 (d, *J* = 7.9 Hz, 1H), 6.73-6.72 (m, 1H), 6.61-6.59 (m, 1H), 4.14 (s, 2H), 4.06 (s, 1H); ^{13}C{^{1}H} NMR (100 MHz, $CDCl_3$) δ 148.3, 135.1, 131.8, 130.3, 128.5, 128.4, 122.8, 118.4, 113.4, 111.9, 85.8, 83.7, 34.4; IR (KBr) ῡ 3417, 3058, 2931, 1652, 675; HRMS (ESI/Q-TOF) m/z: $[M + H]^+$ calcd for $C_{15}H_{13}ClN$ 242.0731; found 242.0743.

3,4-Dichloro-N-(3-phenylprop-2-yn-1-yl)aniline 1k: R_f = 0.45 (5% ethyl acetate in hexane); oily red; yield 50% (207 mg); ^{1}H NMR (400 MHz, $CDCl_3$) δ 7.41-7.38 (m, 2H), 7.32-7.28 (m, 3H), 7.24 (d, *J* = 8.7 Hz, 1H), 6.81 (d, *J* = 2.7 Hz, 1H), 6.57-6.54 (m, 1H), 4.11 (s, 2H), 4.06 (s, 1H); ^{13}C{^{1}H} NMR (100 MHz, $CDCl_3$) δ 146.7, 132.9, 131.8, 130.7, 128.6, 128.5, 122.6,

121.2, 114.8, 113.4, 85.3, 83.9, 34.5; IR (KBr) ῡ 3415, 3072, 2957, 1682, 688; HRMS (ESI/Q-TOF) m/z: $[M + H]^+$ calcd for $C_{15}H_{12}Cl_2N$ 276.0341; found 276.0327.

3-Chloro-4-fluoro-N-(3-phenylprop-2-yn-1-yl)aniline 1l: R_f = 0.4 (10% ethyl acetate in hexane); oily red; yield 80% (342 mg); ^{1}H NMR (400 MHz, $CDCl_3$) δ 7.40-7.38 (m, 2H), 7.32-7.28 (m, 3H), 7.00 (t, *J* = 8.9 Hz, 1H), 6.76-6.74 (m, 1H), 6.58-6.54 (m, 1H), 4.11 (s, 2H), 3.92 (s, 1H); ^{13}C{^{1}H} NMR (100 MHz, $CDCl_3$) δ 151.73 (d, *J* = 238.6 Hz), 144.1, 131.8, 128.5, 128.5, 122.7, 121.3 (d, *J* = 18.6 Hz), 117.0 (d, *J* = 22.2 Hz), 114.9, 113.1 (d, *J* = 6.4 Hz), 85.6, 83.8, 35.0; IR (KBr) ῡ 3414, 3070, 2928, 1652, 681; HRMS (ESI/Q-TOF) m/z: $[M + Na]^+$ calcd for $C_{15}H_{12}ClFN$ 260.0637; found 260.0635.

***N*-(3-(p-Tolyl)prop-2-yn-1-yl)aniline 1m:**[58] R_f = 0.65 (5% ethyl acetate in hexane); yellow solid; yield 74% (380 mg); ^{1}H NMR (400 MHz, $CDCl_3$) δ 7.33 (d, *J* = 8.0 Hz, 2H), 7.27-7.24 (m, 2H), 7.12 (d, *J* = 7.8 Hz, 2H), 6.82 (t, *J* = 7.3 Hz, 1H), 6.77-6.75 (m, 2H), 4.16 (s, 2H), 3.97 (s, 1H), 2.36 (s, 3H).

***N*-(3-(3-Chlorophenyl)prop-2-yn-1-yl)aniline 1n:** R_f = 0.45 (5% ethyl acetate in hexane); oily red; yield 73% (470 mg); ^{1}H NMR (400 MHz, $CDCl_3$) δ 7.38 (t, *J* = 1.6 Hz, 1H), 7.29-7.27 (m, 1H), 7.26-7.20 (m, 4H), 6.82-6.79 (m, 1H), 6.75-6.72 (m, 2H), 4.15 (s, 2H), 3.95 (s, 1H); ^{13}C{^{1}H} NMR (100 MHz, $CDCl_3$) δ 147.1, 134.2, 131.7, 129.9, 129.6, 129.4, 128.6, 124.7, 118.7, 113.7, 87.9, 82.0, 34.5; IR (KBr) ῡ 3412, 2922, 1633, 680; HRMS (ESI/Q-TOF) m/z: $[M + H]^+$ calcd for $C_{15}H_{13}ClN$ 242.0731; found 242.0718.

***N*-(3-([1,1'-Biphenyl]-4-yl)prop-2-yn-1-yl)aniline 1o:** R_f = 0.55 (20% ethyl acetate in hexane); yellow solid; yield 78% (510 mg); mp 95-98 ºC; ^{1}H NMR (400 MHz, $CDCl_3$) δ 7.57 (d, 7.9 Hz, 2H), 7.53 (d, 8.2 Hz, 2H), 7.49-7.42 (m, 4H), 7.35 (t, *J* = 7.3 Hz, 1H), 7.26-7.22 (m, 2H), 6.82-6.75 (m, 3H), 4.18 (s, 2H), 3.99 (s, 1H); ^{13}C{^{1}H} NMR (100 MHz, $CDCl_3$) δ 147.3, 141.1, 140.5, 132.3, 129.4, 129.0, 127.8, 127.1, 127.1, 121.9, 118.6, 113.7, 87.2, 83.3, 34.8; IR (KBr) ῡ 3410, 3052, 2916, 1601, 692; HRMS (ESI/Q-TOF) m/z: $[M + H]^+$ calcd for $C_{21}H_{18}N$ 284.1434; found 284.1434.

***N*-(3-([1,1'-biphenyl]-2-yl)prop-2-yn-1-yl)aniline 1p:** R_f = 0.55 (20% ethyl acetate in hexane); oily red; yield 76% (500 mg); ^{1}H NMR (700 MHz, $CDCl_3$) δ 7.53-7.51 (m, 3H), 7.36-7.35 (m, 5H), 7.28-7.26 (m, 1H), 7.20 (t, *J* = 7.7 Hz, 2H), 6.78 (t, *J* = 7.3 Hz, 1H), 6.64 (d, *J* = 8.2 Hz, 2H), 4.03 (s, 2H), 3.81 (s, 1H); ^{13}C{^{1}H} NMR (175 MHz, $CDCl_3$) δ 147.3, 144.1, 140.6, 133.3, 129.6, 129.4, 129.3, 128.6, 128.0, 127.5, 127.1, 121.3, 118.5, 113.6, 89.5, 83.0, 34.6; IR (KBr) ῡ 3397, 3046, 2928, 1610, 713; HRMS (ESI/Q-TOF) m/z: $[M + H]^+$ calcd for $C_{21}H_{18}N$ 284.1434; found 284.1433.

***N*-(3-(Naphthalen-1-yl)prop-2-yn-1-yl)aniline 1q:** R_f = 0.45 (5% ethyl acetate in hexane); oily red; yield 80% (500 mg); ^{1}H NMR (700 MHz, $CDCl_3$) δ 8.18 (d, *J* = 3.6 Hz, 1H), 7.83-7.79 (m, 2H), 7.64-7.63 (m, 1H), 7.51-7.49 (m, 2H), 7.41-7.38 (m, 1H), 7.29-7.25 (m, 2H), 6.85 (t, *J* = 8.6 Hz, 3H), 4.32 (d, *J* = 5.0 Hz, 2H), 4.06 (s, 1H); ^{13}C{^{1}H} NMR (175 MHz, $CDCl_3$) δ 147.3, 133.5, 133.2, 130.5, 129.4, 128.8, 128.3, 126.9, 126.5, 126.3, 125.3, 120.6, 118.8, 114.1, 91.6, 81.5, 35.0; IR (KBr) ῡ 3400, 2960, 1733, 1520, 770; HRMS (ESI/Q-TOF) m/z: $[M + H]^+$ calcd for $C_{19}H_{16}N$ 258.1277; found 258.1274.

***N*-(3-(Thiophen-2-yl)prop-2-yn-1-yl)aniline 1r:**[58] R_f = 0.65 (5% ethyl acetate in hexane); oil liquid; yield 86% (420 mg); ^{1}H NMR (700 MHz, $CDCl_3$) δ 7.24-7.21 (m, 3H), 7.17 (d, *J* = 3.4 Hz, 1H), 6.95-6.94 (m, 1H), 6.80 (t, *J* = 7.3 Hz, 1H), 6.73 (d, *J* = 7.9 Hz, 2H), 4.17 (s, 2H), 3.95 (s, 1H).

***N*-(3-(Pyridin-3-yl)prop-2-yn-1-yl)aniline 1s:** R_f = 0.45 (20% ethyl acetate in hexane); yellow solid; yield 86% (420 mg); mp 120-124 ºC; ^{1}H NMR (400 MHz, $CDCl_3$) δ 8.60 (d, *J* = 1.6 Hz, 1H), 8.49-8.47 (m, 1H), 7.65-7.62 (m, 1H), 7.26-7.17 (m, 3H), 6.78 (t, *J* = 7.4 Hz, 1H), 6.72 (d, *J* = 7.7 Hz, 2H), 4.15 (s, 2H), 3.98 (s, 1H); ^{13}C{^{1}H} NMR (100 MHz, $CDCl_3$) δ 152.5, 148.7, 147.0, 138.8, 129.4, 123.1, 120.2, 118.8, 113.7, 90.1, 80.1, 34.6; IR (KBr) ῡ 3394, 3054, 2920, 1602, 670; HRMS (ESI/Q-TOF) m/z: $[M + H]^+$ calcd for $C_{14}H_{13}N_2$ 209.1073; found 209.1084.

***N*-(Pent-2-yn-1-yl)aniline 1t:**[60] R_f = 0.45 (5% ethyl acetate in hexane); colourless liquid; yield 51% (150 mg); ^{1}H NMR (400 MHz, $CDCl_3$) δ 7.23-7.19 (m, 2H), 6.77 (t, *J* = 7.2 Hz, 1H), 6.68 (d, *J* = 7.8 Hz, 2H), 3.90-3.89 (m, 3H), 2.22-2.17 (m, 2H), 1.13 (t, *J* = 7.4 Hz, 3H).

3.6 NOTES AND REFERENCES

(1) Aubert, S.; Bezagu, M.; Spivey, A. C.; Arseniyadis, S. Spatial and Temporal Control of Chemical Processes. *Nat. Rev. Chem.* **2019**, *3*, 706-722.

(2) Manna, M. S.; Tamer, Y. T.; Gaszek, I.; Poulides, N.; Ahmed, A.; Wang, X.; Toprak, F. C. R.; Woodard, D. R.; Koh, A. Y.; Williams, N. S., et al. A Trimethoprim Derivative Impedes Antibiotic Resistance Evolution. *Nat. Commun.* **2021**, *12*, 2949.

(3) Ghosh, P.; Mondal, S.; Hajra, A. Tert-Butyl Hydroperoxide-Mediated Oxo-Sulfonylation of 2h-Indazoles with Sulfinic Acid toward Indazol-3(2h)-Ones. *Org. Lett.* **2020**, *22*, 1086-1090.

(4) Chen, J.; Li, J.; Plutschack, M. B.; Berger, F.; Ritter, T. Regio- and Stereoselective Thianthrenation of Olefins to Access Versatile Alkenyl Electrophiles. *Angew. Chem. Int. Ed.* **2020**, *59*, 5616-5620.

(5) Jarvis, C. L.; Richers, M. T.; Breugst, M.; Houk, K. N.; Seidel, D. Redox-Neutral A-Sulfenylation of Secondary Amines: Ring-Fused N,S-Acetals. *Org. Lett.* **2014**, *16*, 3556-3559.

(6) Sahoo, H.; Singh, S.; Baidya, M. Radical Cascade Reaction of Aryl Alkynoates at Room Temperature: Synthesis of Fully Substituted A,B-Unsaturated Acids with Chalcogen Functionality. *Org. Lett.* **2018**, *20*, 3678-3681.

(7) Ye, S.; Li, X.; Xie, W.; Wu, J. Photoinduced Sulfonylation Reactions through the Insertion of Sulfur Dioxide. *Eur. J. Org. Chem.* **2020**, 1274-1287.

(8) Emmett, E. J.; Willis, M. C. The Development and Application of Sulfur Dioxide Surrogates in Synthetic Organic Chemistry. *Asian J. Org. Chem.* **2015**, *4*, 602-611.

(9) Wang, M.; Jiang, X. The Same Oxidation-State Introduction of Hypervalent Sulfur Via Transition-Metal Catalysis. *Chem. Rec.* **2021**, *21*, 3338-3355.

(10) Zeng, D.; Wang, M.; Deng, W.-P.; Jiang, X. The Same Oxygenation-State Introduction of Hypervalent Sulfur under Transition-Metal-Free Conditions. *Org. Chem. Front.* **2020**, *7*, 3956-3966.

(11) Hofman, K.; Liu, N.-W.; Manolikakes, G. Radicals and Sulfur Dioxide: A Versatile Combination for the Construction of Sulfonyl-Containing Molecules. *Chem. Eur. J.* **2018**, *24*, 11852-11863.

(12) Deeming, A. S.; Russell, C. J.; Hennessy, A. J.; Willis, M. C. Dabso-Based, Three-Component, One-Pot Sulfone Synthesis. *Org. Lett.* **2014**, *16*, 150-153.

(13) Yuan, Y.; Cao, Y.; Lin, Y.; Li, Y.; Huang, Z.; Lei, A. Electrochemical Oxidative Alkoxysulfonylation of Alkenes Using Sulfonyl Hydrazines and Alcohols with Hydrogen Evolution. *ACS Catal.* **2018**, *8*, 10871-10875.

(14) Bertrand, M. P. Recent Progress in the Use of Sulfonyl Radicals in Organic Synthesis. A Review. *Organic Preparations and Procedures International* **1994**, *26*, 257-290.

(15) Blum, S. P.; Hofman, K.; Manolikakes, G.; Waldvogel, S. R. Advances in Photochemical and Electrochemical Incorporation of Sulfur Dioxide for the Synthesis of Value-Added Compounds. *Chem. Commun.* **2021**, *57*, 8236-8249.

(16) Seyed Hashtroudi, M.; Fathi Vavsari, V.; Balalaie, S. Dabso as a So2 Gas Surrogate in the Synthesis of Organic Structures. *Org. Biomol. Chem.* **2022**, *20*, 2149-2163.

(17) Meng, Y.; Wang, M.; Jiang, X. Multicomponent Reductive Cross-Coupling of an Inorganic Sulfur Dioxide Surrogate: Straightforward Construction of Diversely Functionalized Sulfones. *Angew. Chem. Int. Ed.* **2020**, *59*, 1346-1353.

(18) Li, K.; Wang, M.; Jiang, X. Full-Spectrum Fluoromethyl Sulfonation Via Modularized Multicomponent Coupling. *CCS Chem.* **2021**, *3*, 1735-1743.

(19) Van Mileghem, S.; De Borggraeve, W. M. A Convenient Multigram Synthesis of Dabso Using Sodium Sulfite as So2 Source. *Organic Process Research & Development* **2017**, *21*, 785-787.

(20) Emmett, E. J.; Willis*, M. C., Dabco-Bis(Sulfur Dioxide), Dabso, as an Easy-to-Handle Source of So2: Sulfonamide Preparation. In *Organic Syntheses*, pp 125-136.

(21) Kumar, M.; Ahmed, R.; Singh, M.; Sharma, S.; Thatikonda, T.; Singh, P. P. Functionalization of Alkynes and Alkenes Using a Cascade Reaction Approach: Synthesis of B-Keto Sulfones under Metal-Free Conditions. *J. Org. Chem.* **2020**, *85*, 716-725.

(22) Lo, P. K. T.; Oliver, G. A.; Willis, M. C. Sulfinamide Synthesis Using Organometallic Reagents, Dabso, and Amines. *J. Org. Chem.* **2020**, *85*, 5753-5760.

(23) Ye, S.; Yang, M.; Wu, J. Recent Advances in Sulfonylation Reactions Using Potassium/Sodium Metabisulfite. *Chem. Commun.* **2020**, *56*, 4145-4155.

(24) Mulina, O. M.; Ilovaisky, A. I.; Parshin, V. D.; Terent'ev, A. O. Oxidative Sulfonylation of Multiple Carbon-Carbon Bonds with Sulfonyl Hydrazides, Sulfinic Acids and Their Salts. *Adv. Synth. Catal.* **2020**, *362*, 4579-4654.

(25) Zhu, J.; Yang, W.-C.; Wang, X.-d.; Wu, L. Photoredox Catalysis in C–S Bond Construction: Recent Progress in Photo-Catalyzed Formation of Sulfones and Sulfoxides. *Adv. Synth. Catal.* **2018**, *360*, 386-400.

(26) Lilienkampf, A.; Mao, J.; Wan, B.; Wang, Y.; Franzblau, S. G.; Kozikowski, A. P. Structure-Activity Relationships for a Series of Quinoline-Based Compounds Active against Replicating and Nonreplicating Mycobacterium Tuberculosis. *J. Med. Chem.* **2009**, *52*, 2109-2118.

(27) Narwal, S.; Kumar, S.; Verma, P. K. Synthesis and Therapeutic Potential of Quinoline Derivatives. *Research on Chemical Intermediates* **2017**, *43*, 2765-2798.

(28) Afzal, O.; Kumar, S.; Haider, M. R.; Ali, M. R.; Kumar, R.; Jaggi, M.; Bawa, S. A Review on Anticancer Potential of Bioactive Heterocycle Quinoline. *Eur. J. Med. Chem.* **2015**, *97*, 871-910.

(29) Michael, J. P. Quinoline, Quinazoline and Acridone Alkaloids. *Natural Product Reports* **2008**, *25*, 166-187.

(30) Andries, K.; Verhasselt, P.; Guillemont, J.; Göhlmann, H. W.; Neefs, J. M.; Winkler, H.; Van Gestel, J.; Timmerman, P.; Zhu, M.; Lee, E., et al. A Diarylquinoline Drug Active on the Atp Synthase of Mycobacterium Tuberculosis. *Science* **2005**, *307*, 223-227.

(31) Dutta, U.; Modak, A.; Bhaskararao, B.; Bera, M.; Bag, S.; Mondal, A.; Lupton, D. W.; Sunoj, R. B.; Maiti, D. Catalytic Arene Meta-C–H Functionalization Exploiting a Quinoline-Based Template. *ACS Catal.* **2017**, *7*, 3162-3168.

(32) Ettari, R.; Nizi, E.; Di Francesco, M. E.; Dude, M.-A.; Pradel, G.; Vičík, R.; Schirmeister, T.; Micale, N.; Grasso, S.; Zappalà, M. Development of Peptidomimetics with a Vinyl Sulfone Warhead as Irreversible Falcipain-2 Inhibitors. *J. Med. Chem.* **2008**, *51*, 988-996.

(33) Alba, A.-N. R.; Companyó, X.; Rios, R. Sulfones: New Reagents in Organocatalysis. *Chemical Society Reviews* **2010**, *39*, 2018-2033.

(34) Murphy, A. R.; Fréchet, J. M. J. Organic Semiconducting Oligomers for Use in Thin Film Transistors. *Chem. Rev.* **2007**, *107*, 1066-1096.

(35) Maher-Edwards, G.; Dixon, R.; Hunter, J.; Gold, M.; Hopton, G.; Jacobs, G.; Hunter, J.; Williams, P. Sb-742457 and Donepezil in Alzheimer Disease: A Randomized, Placebo-Controlled Study. *International Journal of Geriatric Psychiatry* **2011**, *26*, 536-544.

(36) Fu, T.-t.; Tu, G.; Ping, M.; Zheng, G.-x.; Yang, F.-y.; Yang, J.-y.; Zhang, Y.; Yao, X.-j.; Xue, W.-w.; Zhu, F. Subtype-Selective Mechanisms of Negative Allosteric Modulators Binding to Group I Metabotropic Glutamate Receptors. *Acta Pharmacol. Sin.* **2021**, *42*, 1354-1367.

(37) Sun, D.; Yin, K.; Zhang, R. Visible-Light-Induced Multicomponent Cascade Cycloaddition Involving N-Propargyl Aromatic Amines, Diaryliodonium Salts and Sulfur Dioxide: Rapid Access to 3-Arylsulfonylquinolines. *Chem. Commun.* **2018**, *54*, 1335-1338.

(38) Zhang, L.; Chen, S.; Gao, Y.; Zhang, P.; Wu, Y.; Tang, G.; Zhao, Y. Tert-Butyl Hydroperoxide Mediated Cascade Synthesis of 3-Arylsulfonylquinolines. *Org. Lett.* **2016**, *18*, 1286-1289.

(39) Liu, J.; Wang, M.; Li, L.; Wang, L. Electrooxidative Tandem Cyclization of N-Propargylanilines with Sulfinic Acids for Rapid Access to 3-Arylsulfonylquinoline Derivatives. *Green Chem.* **2021**, *23*, 4733-4740.

(40) Li, L.; Zhang, X.-G.; Hu, B.-L.; Zhang, X.-H. Copper-Catalyzed Electrophilic Cyclization of N-Propargylamines with Sodium Sulfinate for the Synthesis of 3-Sulfonated Quinolines. *Chem. Asian J.* **2019**, *14*, 4358-4364.

(41) Zhang, Y.; Chen, W.; Jia, X.; Wang, L.; Li, P. A Visible-Light-Induced Oxidative Cyclization of N-Propargylanilines with Sulfinic Acids to 3-Sulfonated Quinoline Derivatives without External Photocatalysts. *Chem. Commun.* **2019**, *55*, 2785-2788.

(42) Pramanik, M.; Choudhuri, K.; Mal, P. N-Iodosuccinimide as Bifunctional Reagent in (E)-Selective C(Sp2)−H Sulfonylation of Styrenes. *Asian J. Org. Chem.* **2019**, *8*, 144-150.

(43) Choudhuri, K.; Mandal, A.; Mal, P. Aerial Dioxygen Activation Vs. Thiol-Ene Click Reaction within a System. *Chem. Commun.* **2018**, *54*, 3759-3762.

(44) Choudhuri, K.; Pramanik, M.; Mandal, A.; Mal, P. S−H···Π Driven Anti-Markovnikov Thiol-Yne Click Reaction. *Asian J. Org. Chem.* **2018**, *7*, 1849–1855.

(45) Pramanik, M.; Mathuri, A.; Sau, S.; Das, M.; Mal, P. Chlorinative Cyclization of Aryl Alkynoates Using Ncs and 9-Mesityl-10-Methylacridinium Perchlorate Photocatalyst. *Org. Lett.* **2021**, *23*, 8088-8092.

(46) Pramanik, M.; Mathuri, A.; Mal, P. Sulfur···Oxygen Interaction-Controlled (Z)-Selective Anti-Markovnikov Vinyl Sulfides. *Chem. Commun.* **2021**, *57*, 5698-5701.

(47) Pramanik, M.; Choudhuri, K.; Chakraborty, S.; Ghosh, A.; Mal, P. (Z)-Selective Anti-Markovnikov or Markovnikov Thiol–Yne-Click Reactions of an Internal Alkyne by Amide Hydrogen Bond Control. *Chem. Commun.* **2020**, *56*, 2991-2994.

(48) Choudhuri, K.; Pramanik, M.; Mal, P. Noncovalent Interactions in C–S Bond Formation Reactions. *J. Org. Chem.* **2020**, *85*, 11997-12011.

(49) Pramanik, M.; Choudhuri, K.; Mal, P. Metal-Free C–S Coupling of Thiols and Disulfides. *Org. Biomol. Chem.* **2020**, *18*, 8771-8792.

(50) Nair, A. M.; Halder, I.; Khan, S.; Volla, C. M. R. Metal Free Sulfonylative Spirocyclization of Alkenyl and Alkynyl Amides Via Insertion of Sulfur Dioxide. *Adv. Synth. Catal.* **2020**, *362*, 224-229.

(51) Zheng, D.; An, Y.; Li, Z.; Wu, J. Metal-Free Aminosulfonylation of Aryldiazonium Tetrafluoroborates with Dabco·(So2)2 and Hydrazines. *Angew Chem Int Ed* **2014**, *53*, 2451-2454.

(52) Chen, Z.; Liu, N.-W.; Bolte, M.; Ren, H.; Manolikakes, G. Visible-Light Mediated 3-Component Synthesis of Sulfonylated Coumarins from Sulfur Dioxide. *Green Chem.* **2018**, *20*, 3059-3070.

(53) SAINT+, Bruker AXS Inc., Madison, Wisconsin, USA, 1999 (Program for Reduction of Data collected on Bruker CCD Area Detector Diffractometer V. 6.02.)

(54) Sheldrick, G. In *Sadabs, Program for Empirical Absorption Correction of Area Detector Data*, 1996.

(55) Sheldrick, G. A Short History of Shelx. *Acta Crystallogr. Sect. A* **2008**, *64*, 112-122.

(56) Yuan, J.-M.; Li, J.; Zhou, H.; Xu, J.; Zhu, F.; Liang, Q.; Liu, Z.; Huang, G.; Huang, J. Synthesis of 3-Sulfonylquinolines by Visible-Light Promoted Metal-Free Cascade Cycloaddition Involving N-Propargylanilines and Sodium Sulfinates. *New J. Chem.* **2020**, *44*, 3189-3193.

(57) Dahlkamp, J. M.; Tolzmann, M.; Lucchesi, R.; Daniliuc, C.-G.; Wibbeling, B.; Uhl, W.; Würthwein, E.-U. Chemoselective Hydroalumination of 1-Aza-but-1-En-3-Ynes (C-Iminoalkynes): Formation of Propargylamines by Imine Reduction and of 5-Aluminazoles and 1-Aza-Butadienes by Anti-Michael Attack. *Organometall.* **2018**, *37*, 1346-1357.

(58) Yuan, B.; Zhang, F.; Li, Z.; Yang, S.; Yan, R. Agno2 as the No Source for the Synthesis of Substituted Pyrazole N-Oxides from N-Propargylamines. *Org. Lett.* **2016**, *18*, 5928-5931.

(59) Zhu, D.; Wu, Z.; Luo, B.; Du, Y.; Liu, P.; Chen, Y.; Hu, Y.; Huang, P.; Wen, S. Heterocyclic Iodoniums for the Assembly of Oxygen-Bridged Polycyclic Heteroarenes with Water as the Oxygen Source. *Org. Lett.* **2018**, *20*, 4815-4818.

(60) Liu, M.; Tang, T.; Apolinar, O.; Matsuura, R.; Busacca, C. A.; Qu, B.; Fandrick, D. R.; Zatolochnaya, O. V.; Senanayake, C. H.; Song, J. J., et al. Atom-Economical Cross-Coupling of Internal and Terminal Alkynes to Access 1,3-Enynes. *J. Am. Chem. Soc.* **2021**, *143*, 3881-3888.

NMR Spectrum of Selected Compounds

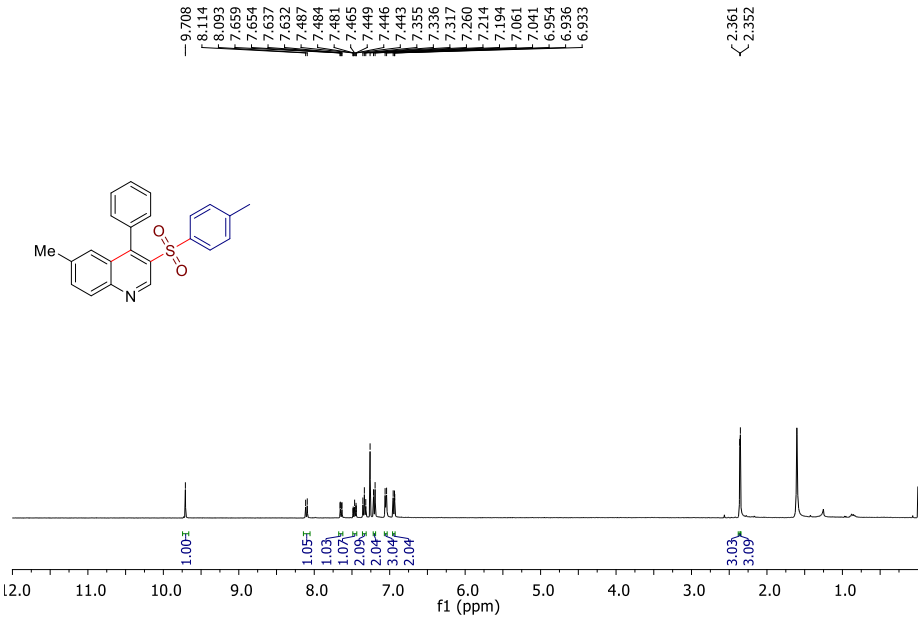

Fig. 3.11. ^{1}H NMR (400 MHz, $CDCl_3$) spectrum of 6-methyl-4-phenyl-3-tosylquinoline (**3ba**)

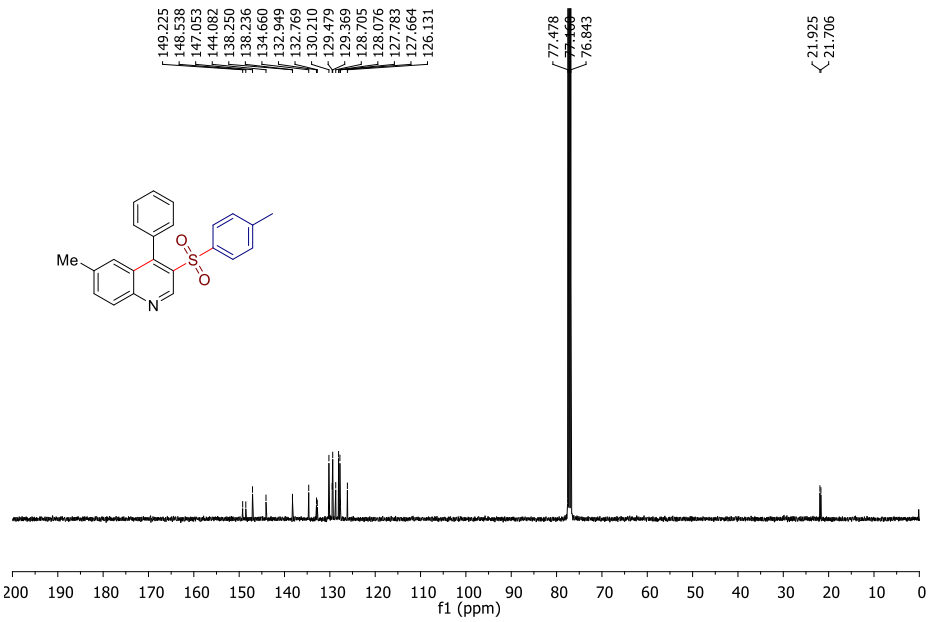

Fig. 3.12. ^{13}C{^{1}H} NMR (100 MHz, $CDCl_3$) spectrum of 6-methyl-4-phenyl-3-tosylquinoline (**3ba**)

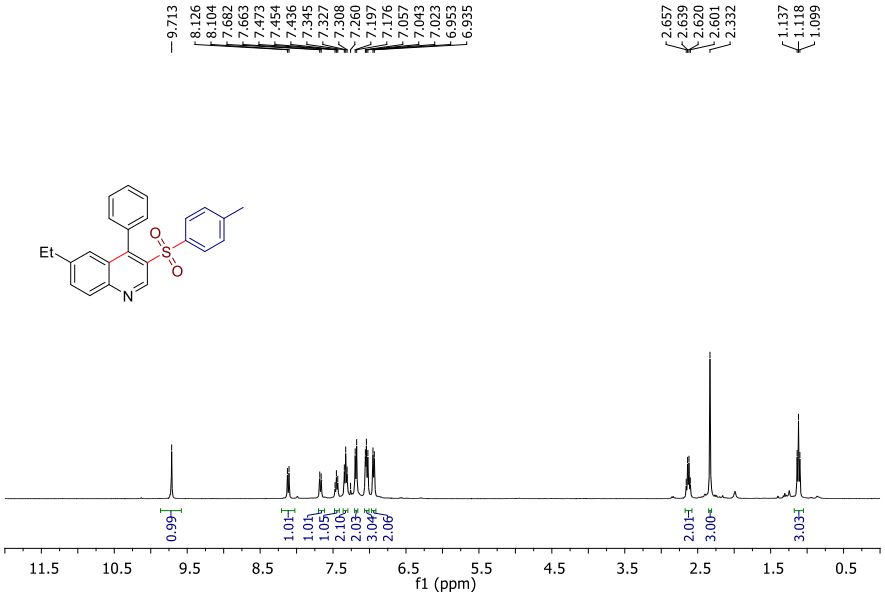

Fig.3.13 . ^{1}H NMR (400 MHz, $CDCl_3$) spectrum of 6-ethyl-4-phenyl-3-tosylquinoline (**3ca**)

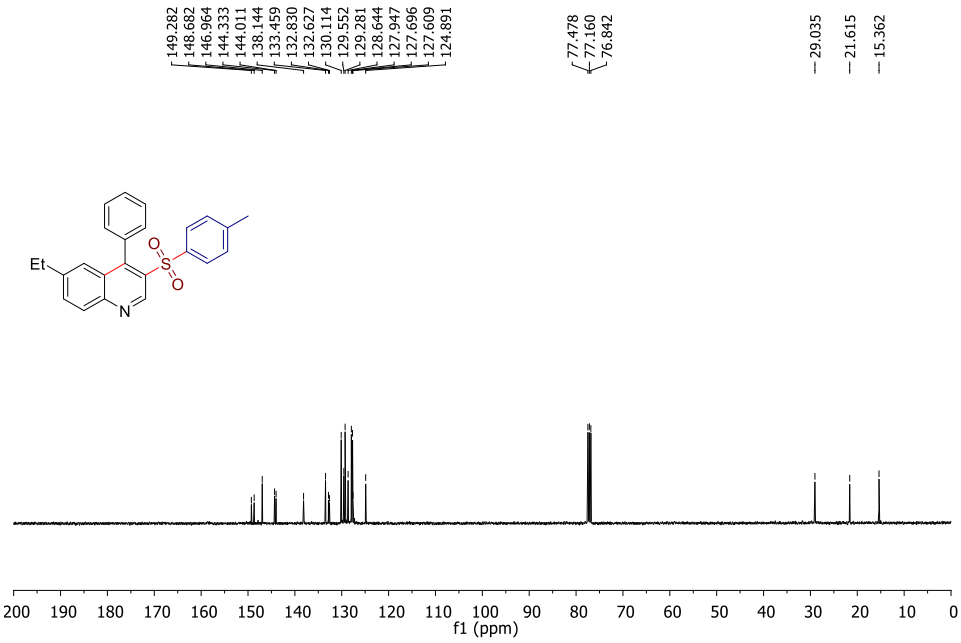

Fig. 3.14. ^{13}C{^{1}H} NMR (100 MHz, $CDCl_3$) spectrum of 6-ethyl-4-phenyl-3-tosylquinoline (**3ca**)

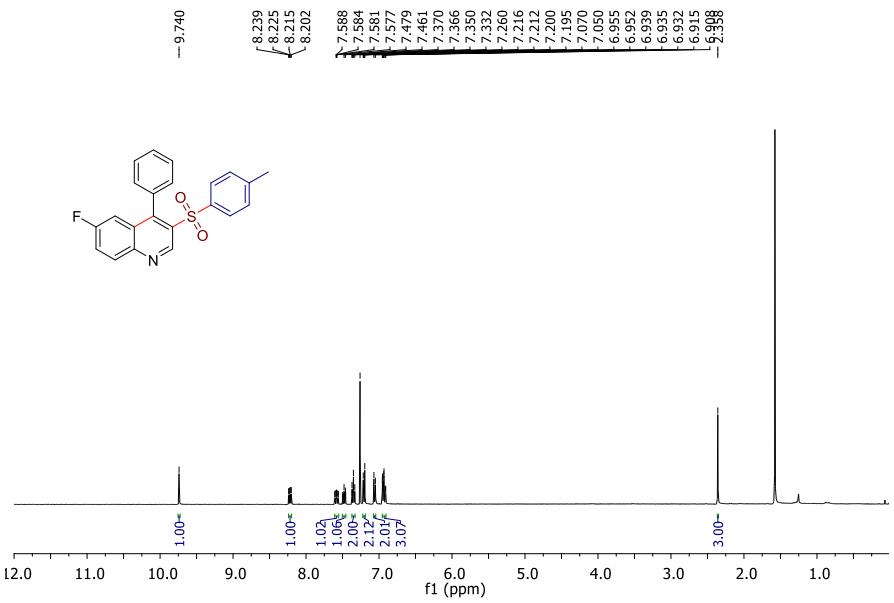

Fig. 3.15. ^{1}H NMR (400 MHz, $CDCl_3$) spectrum of 6-fluoro-4-phenyl-3-tosylquinoline (**3ea**)

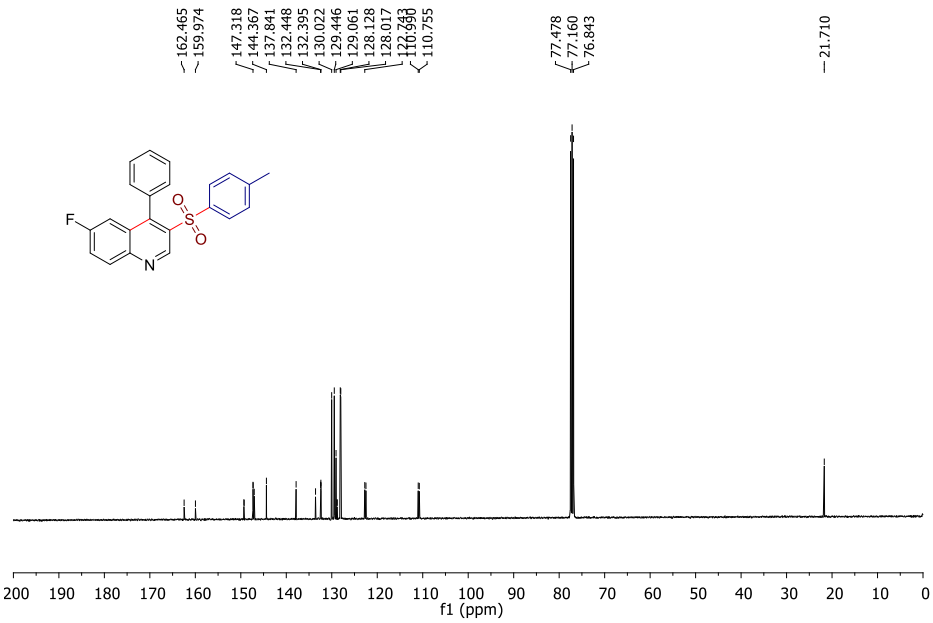

Fig. 3.16. ^{13}C{^{1}H} NMR (100 MHz, $CDCl_3$) spectrum of 6-fluoro-4-phenyl-3-tosylquinoline (**3ea**)

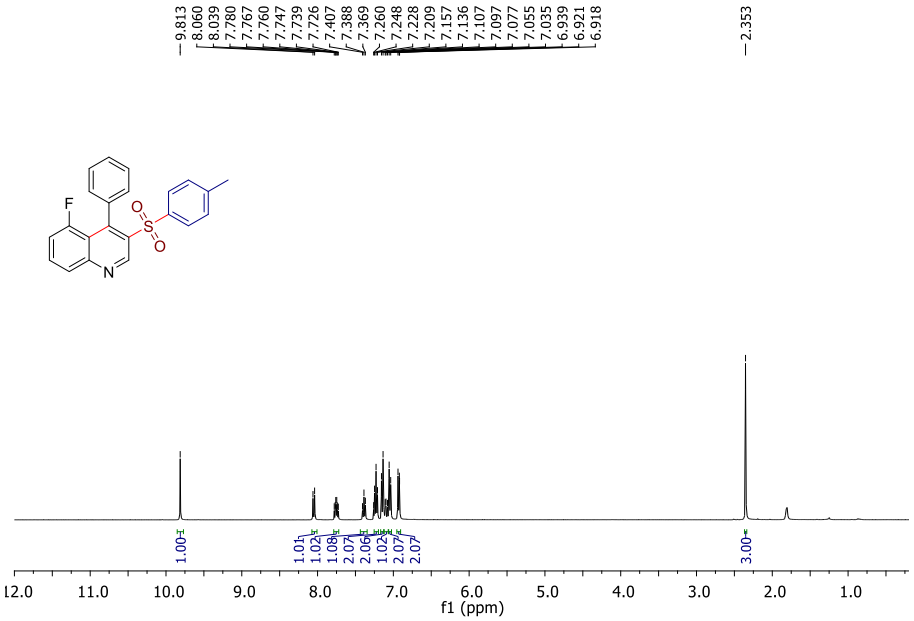

Fig. 3.17. ^{1}H NMR (400 MHz, $CDCl_3$) spectrum of 5-fluoro-4-phenyl-3-tosylquinoline (**3ia**)

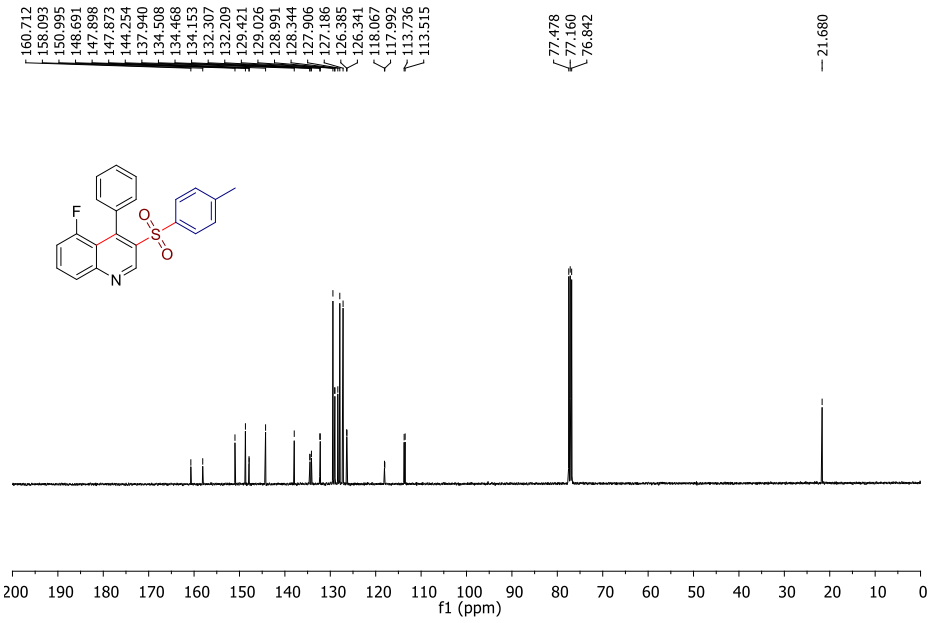

Fig. 3.18. ^{13}C{^{1}H} NMR (100 MHz, $CDCl_3$) spectrum of 5-fluoro-4-phenyl-3-tosylquinoline (**3ia**)

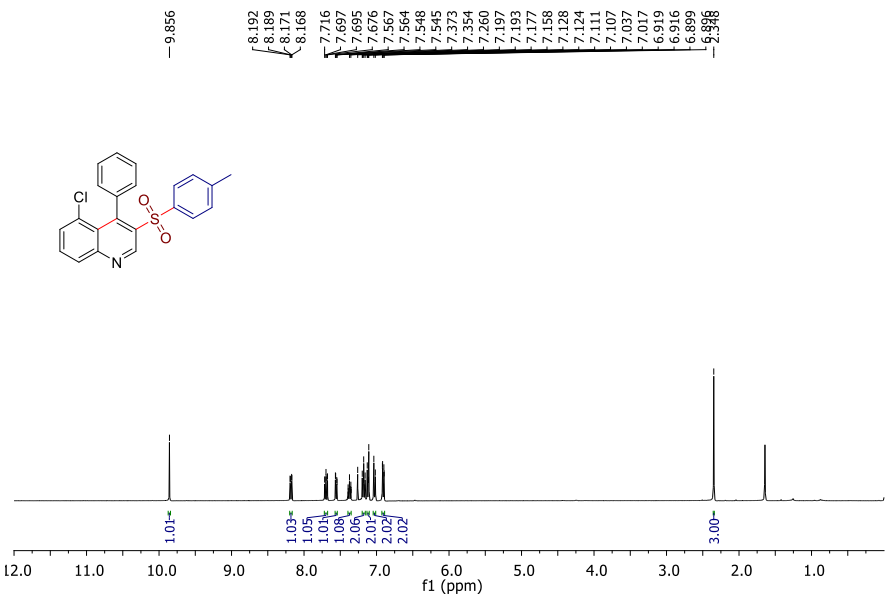

Fig. 3.19. ^{1}H NMR (400 MHz, $CDCl_3$) spectrum of 5-chloro-4-phenyl-3-tosylquinoline (**3ja**)

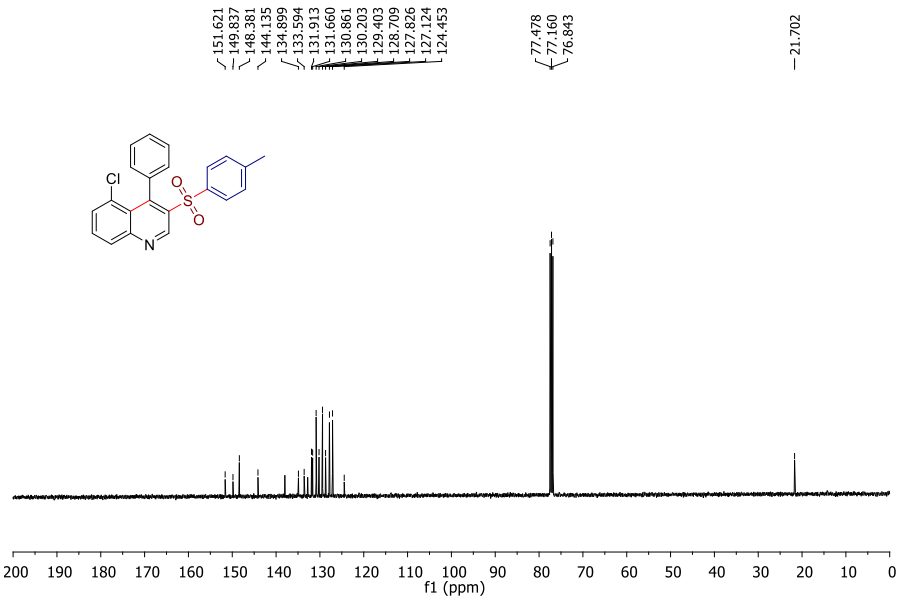

Fig. 3.20. ^{13}C{^{1}H} NMR (100 MHz, $CDCl_3$) spectrum of 5-chloro-4-phenyl-3-tosylquinoline (**3ja**)

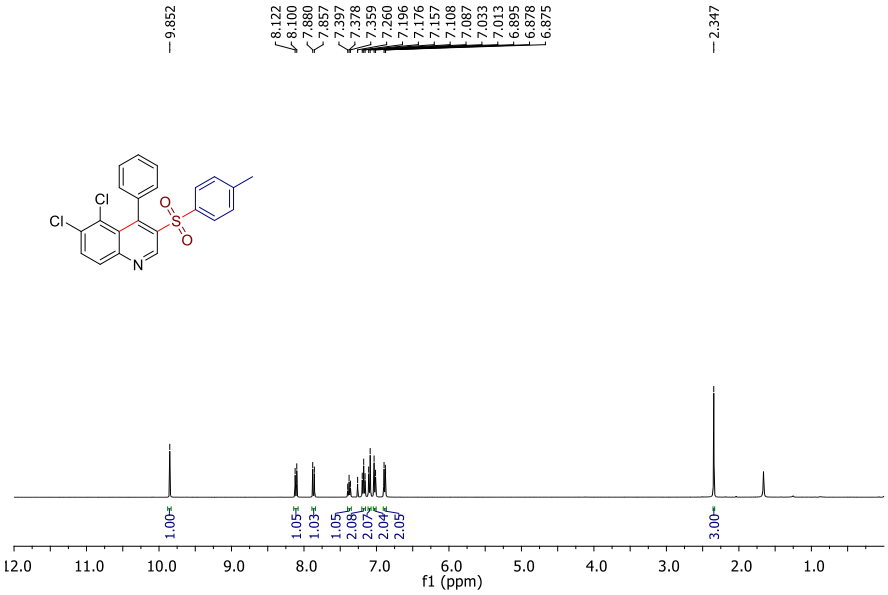

Fig. 3.21. ^{1}H NMR (400 MHz, $CDCl_3$) spectrum of 5,6-dichloro-4-phenyl-3-tosylquinoline (**3ka**)

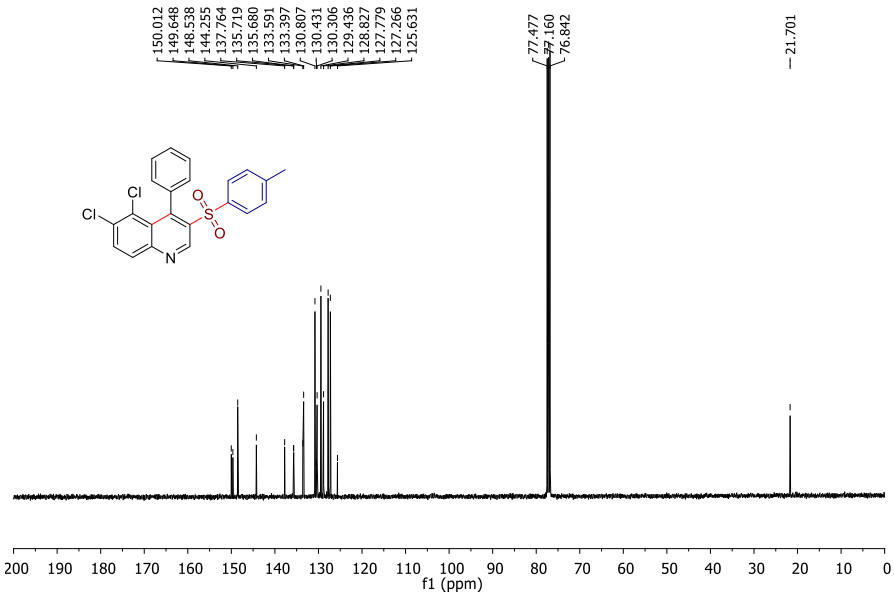

Fig.3.22. ^{13}C{^{1}H} NMR (100 MHz, $CDCl_3$) spectrum of 5,6-dichloro-4-phenyl-3-tosylquinoline (**3ka**)

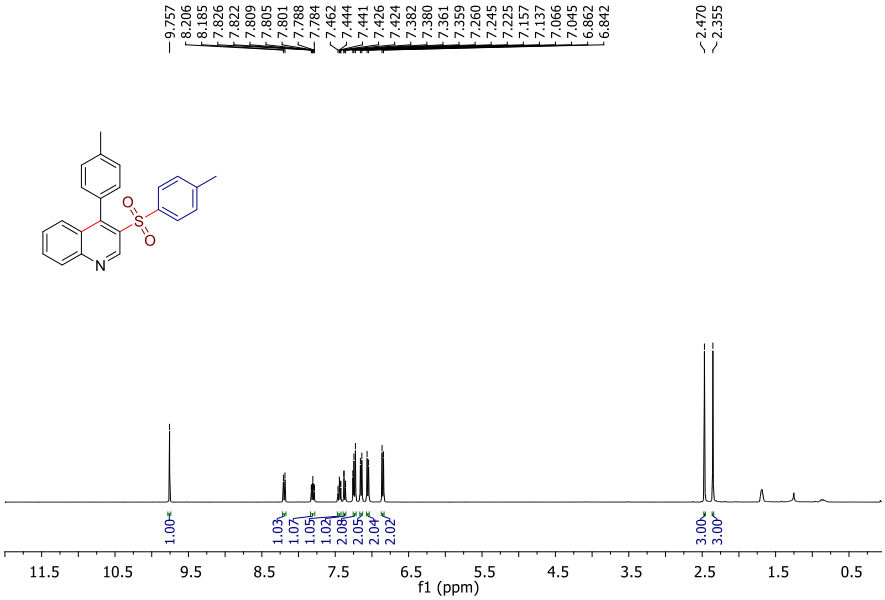

Fig. 3.23. ^{1}H NMR (400 MHz, $CDCl_3$) spectrum of 4-(p-tolyl)-3-tosylquinoline (**3ma**)

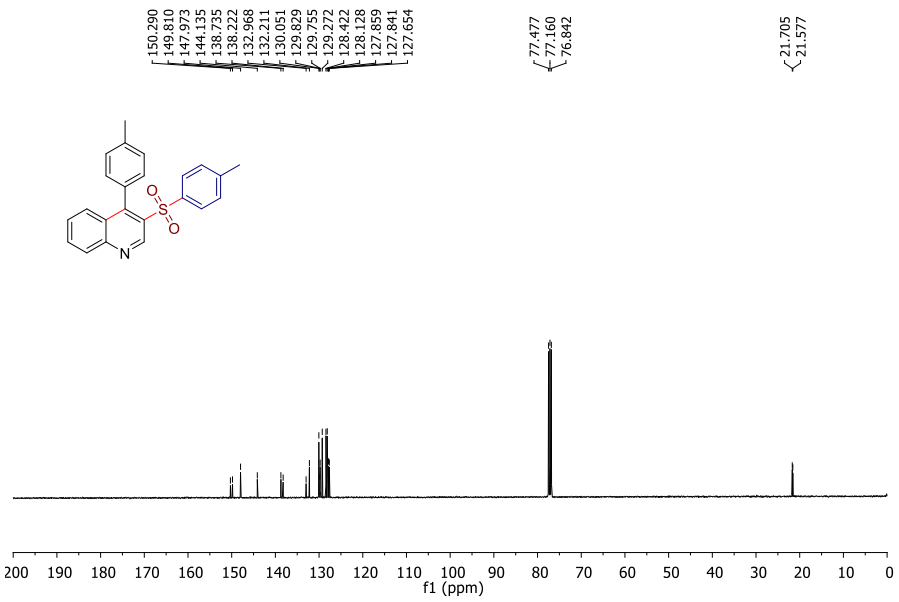

Fig. 3.24. ^{13}C{^{1}H} NMR (100 MHz, $CDCl_3$) spectrum of 4-(p-tolyl)-3-tosylquinoline (**3ma**)

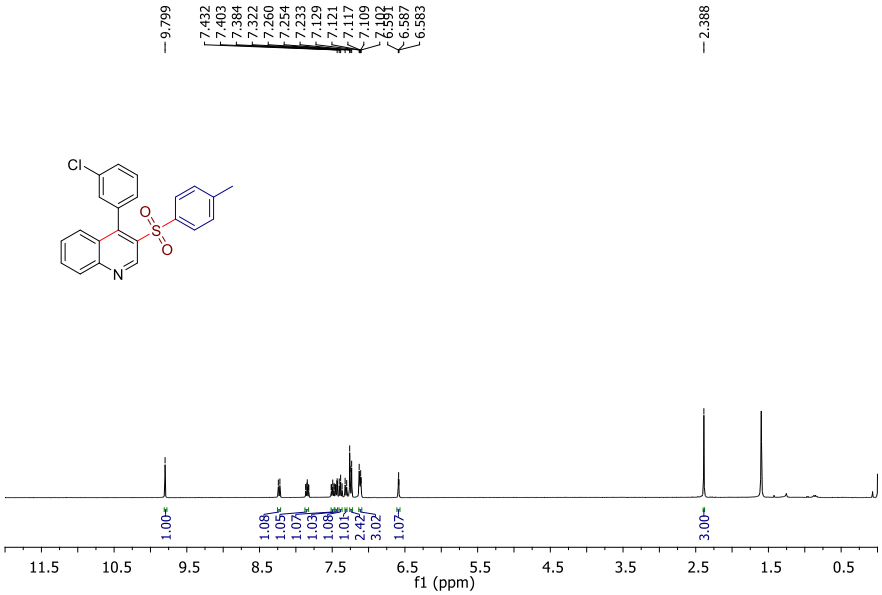

Fig. 3.25. ^{1}H NMR (400 MHz, $CDCl_3$) spectrum of 4-(3-chlorophenyl)-3-tosylquinoline (**3na**)

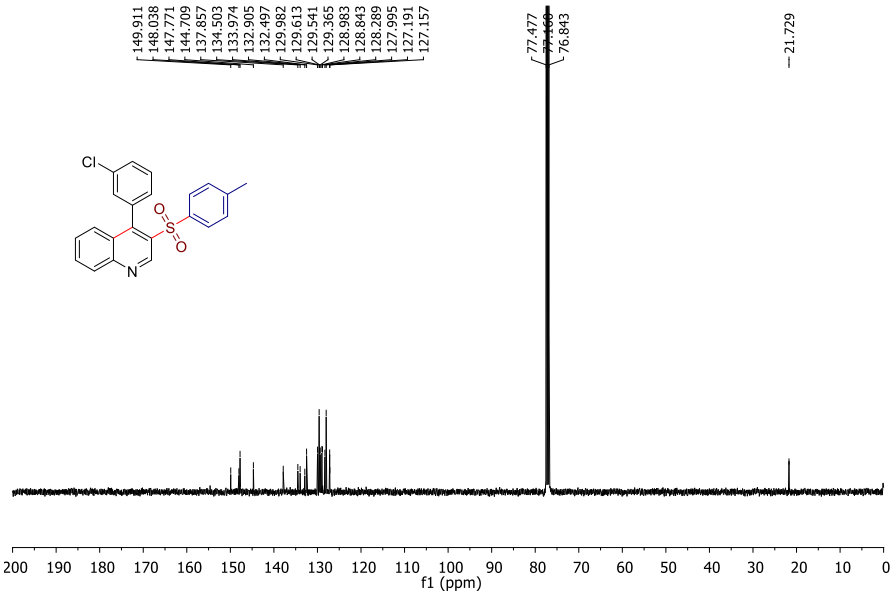

Fig. 3.26. ^{13}C{^{1}H} NMR (100 MHz, $CDCl_3$) spectrum of 4-(3-chlorophenyl)-3-tosylquinoline (**3na**)

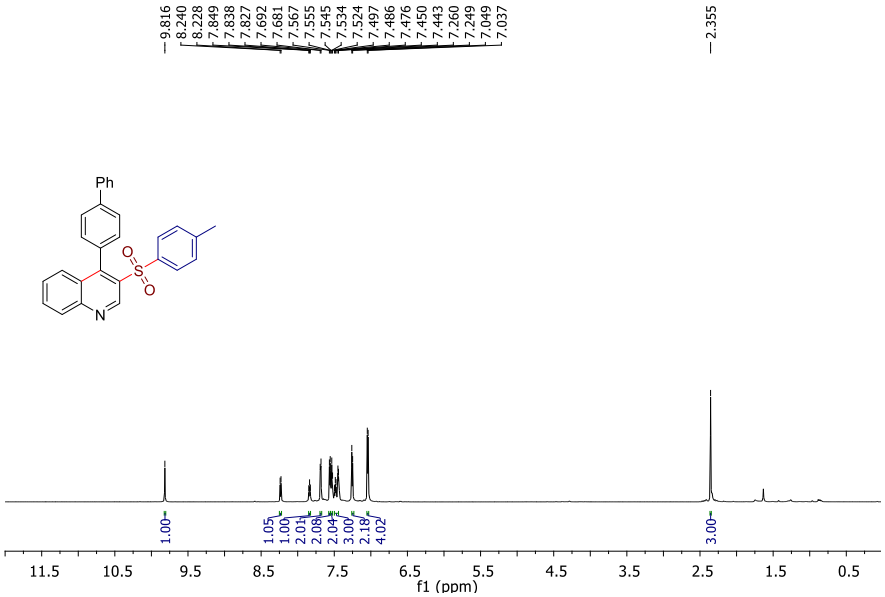

Fig. 3.27. ^{1}H NMR (700 MHz, $CDCl_3$) spectrum of 4-([1,1'-biphenyl]-4-yl)-3-tosylquinoline (**3oa**)

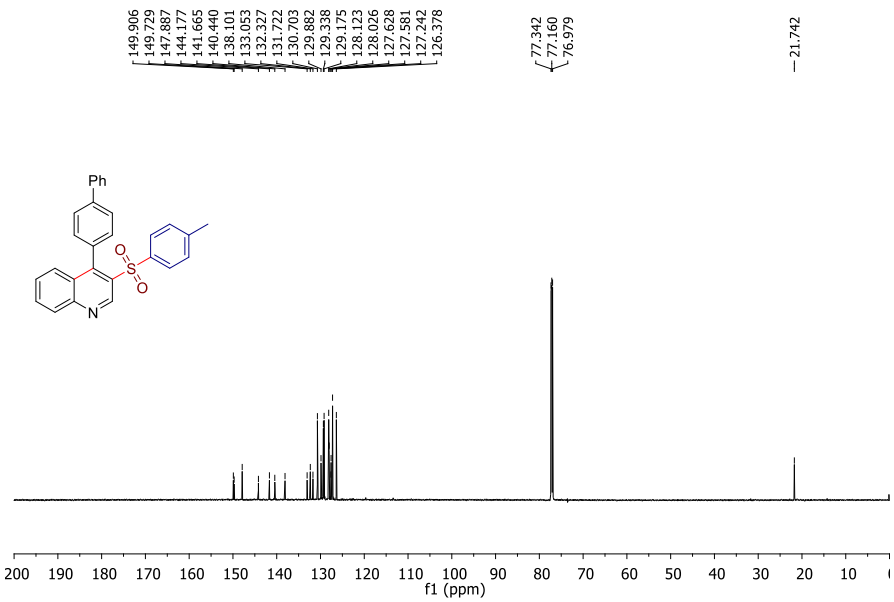

Fig. 3.28. ^{13}C{^{1}H} NMR (175 MHz, $CDCl_3$) spectrum of 4-([1,1'-biphenyl]-4-yl)-3-tosylquinoline (**3oa**)

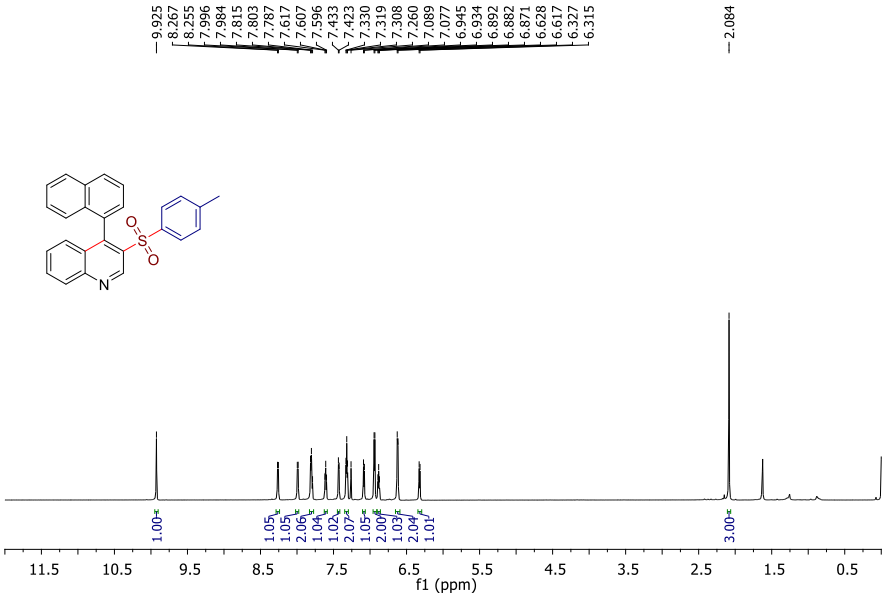

Fig. 3.29. ^{1}H NMR (700 MHz, $CDCl_3$) spectrum of 4-(naphthalen-1-yl)-3-tosylquinoline (**3qa**)

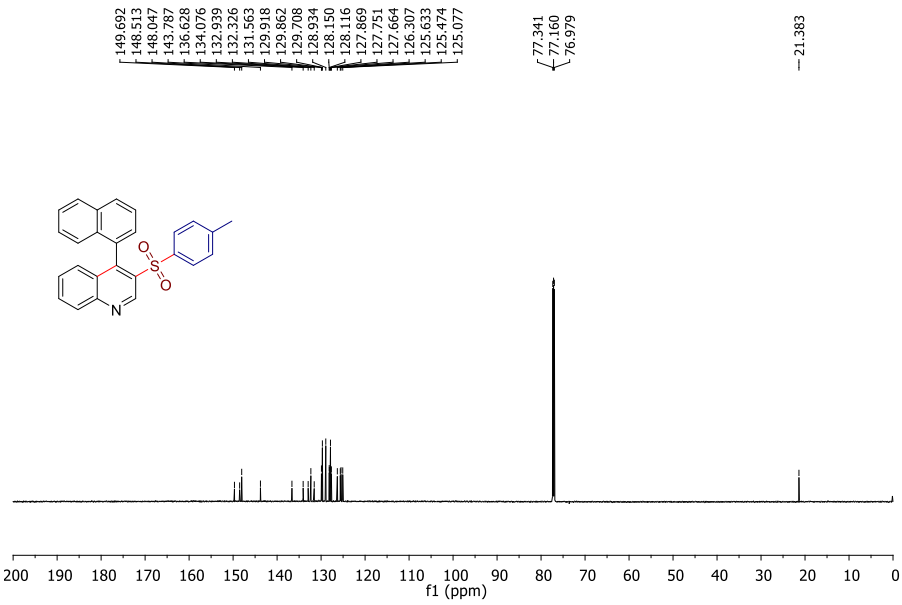

Fig. 3.30. ^{13}C{^{1}H} NMR (175MHz, $CDCl_3$) spectrum of 4-(naphthalen-1-yl)-3-tosylquinoline (**3qa**)

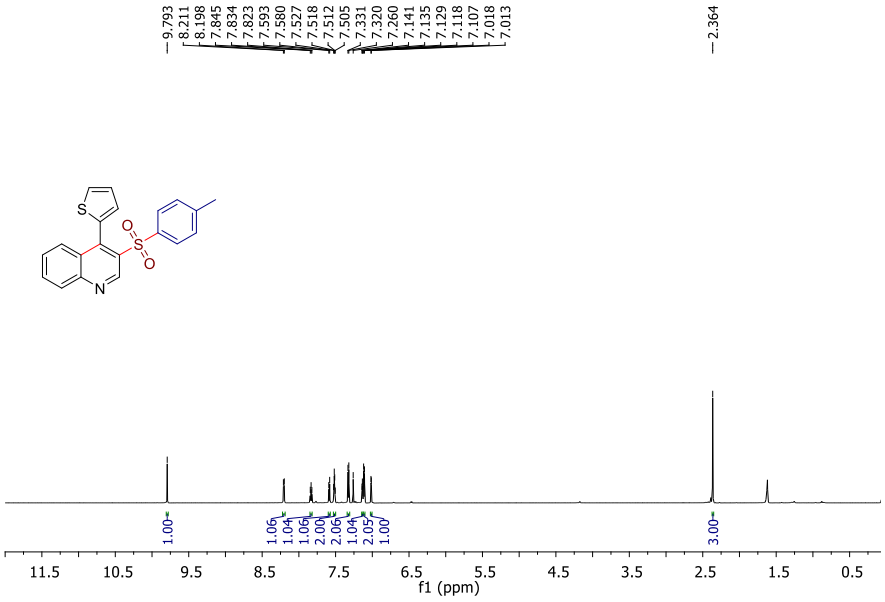

Fig. 3.31. ^{1}H NMR (700 MHz, $CDCl_3$) spectrum of 4-(thiophen-2-yl)-3-tosylquinoline (**3ra**)

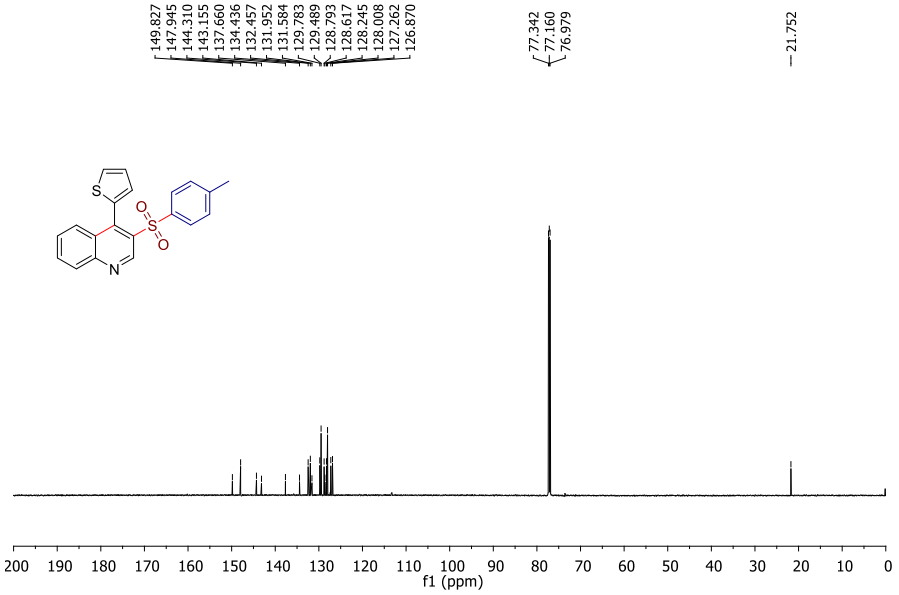

Fig. 3.32. ^{13}C{^{1}H} NMR (175 MHz, $CDCl_3$) spectrum of 4-(thiophen-2-yl)-3-tosylquinoline (**3ra**)

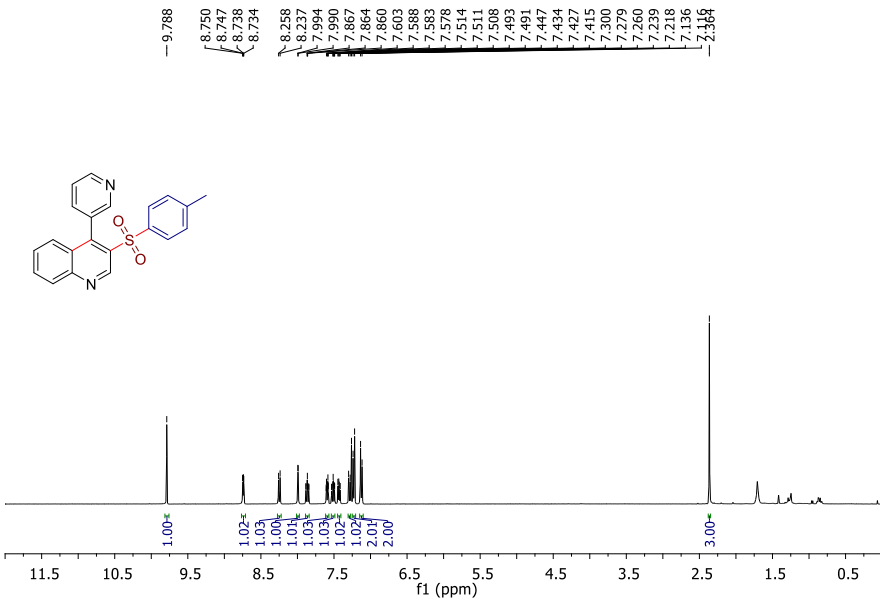

Fig. 3.33. ^{1}H NMR (400 MHz, $CDCl_3$) spectrum of 4-(pyridin-3-yl)-3-tosylquinoline (**3sa**)

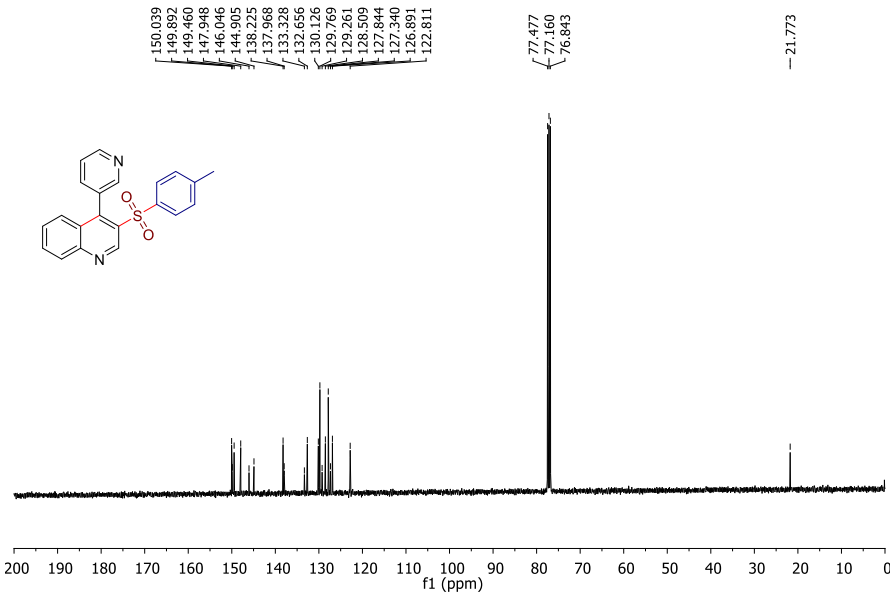

Fig.3.34. ^{13}C{^{1}H} NMR (100 MHz, $CDCl_3$) spectrum of 4-(pyridin-3-yl)-3-tosylquinoline (**3sa**)

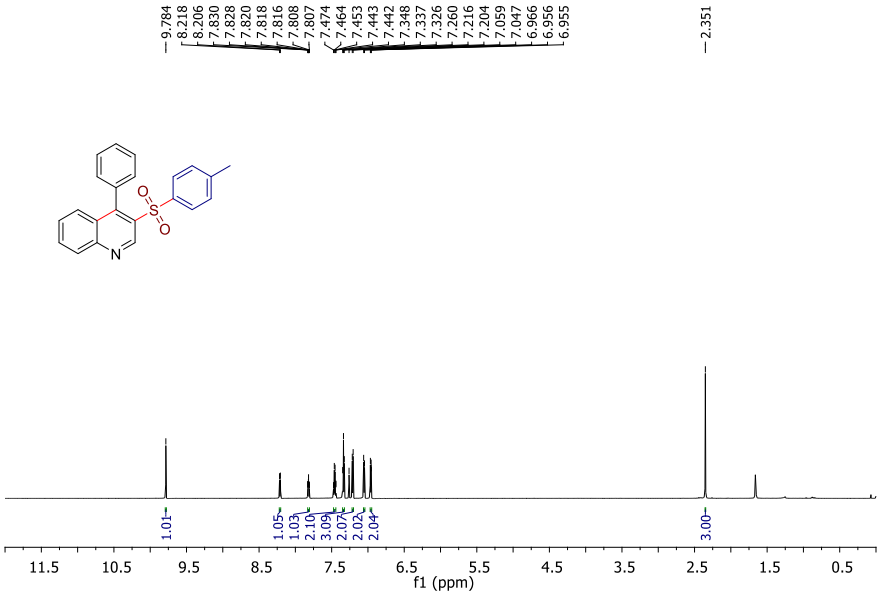

Fig.3.35. ^{1}H NMR (700 MHz, $CDCl_3$) spectrum of 4-phenyl-3-tosylquinoline (**3aa**)

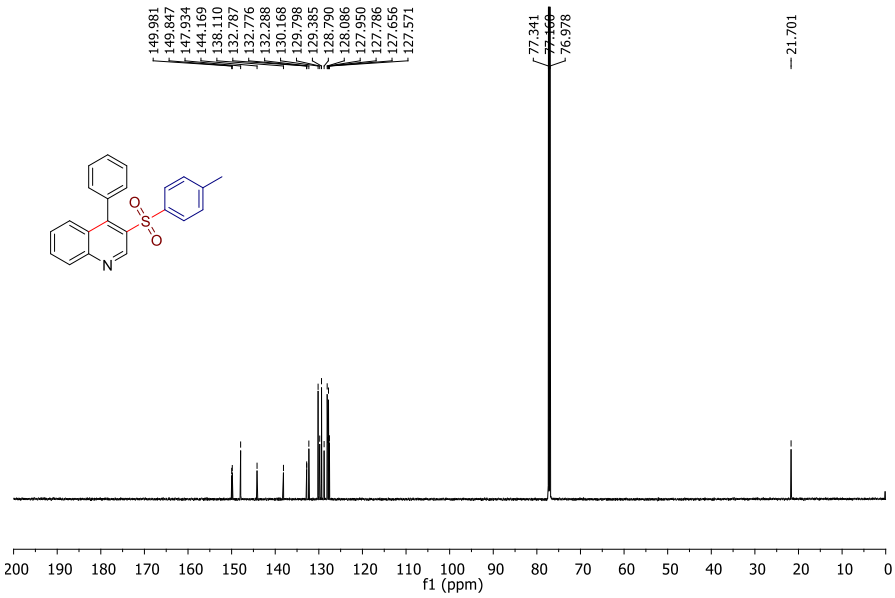

Fig. 3.36. ^{13}C{^{1}H} NMR (175 MHz, $CDCl_3$) spectrum of 4-phenyl-3-tosylquinoline (**3aa**)

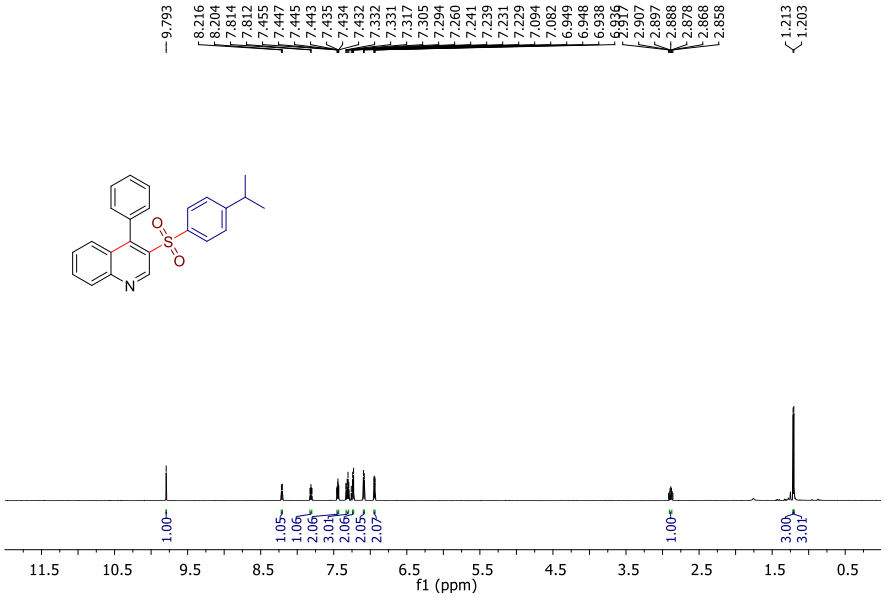

Fig. 3.37. ^{1}H NMR (700 MHz, $CDCl_3$) spectrum of 3-((4-isopropylphenyl)sulfonyl)-4-phenylquinoline (**3ad**)

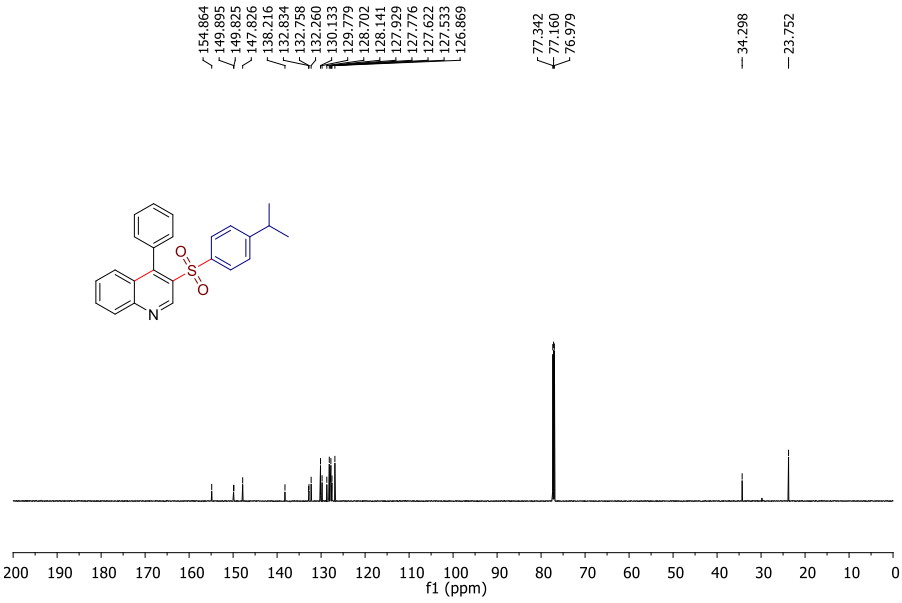

Fig. 3.38. ^{13}C{^{1}H} NMR (175 MHz, $CDCl_3$) spectrum of 3-((4-isopropylphenyl)sulfonyl)-4-phenylquinoline (**3ad**)

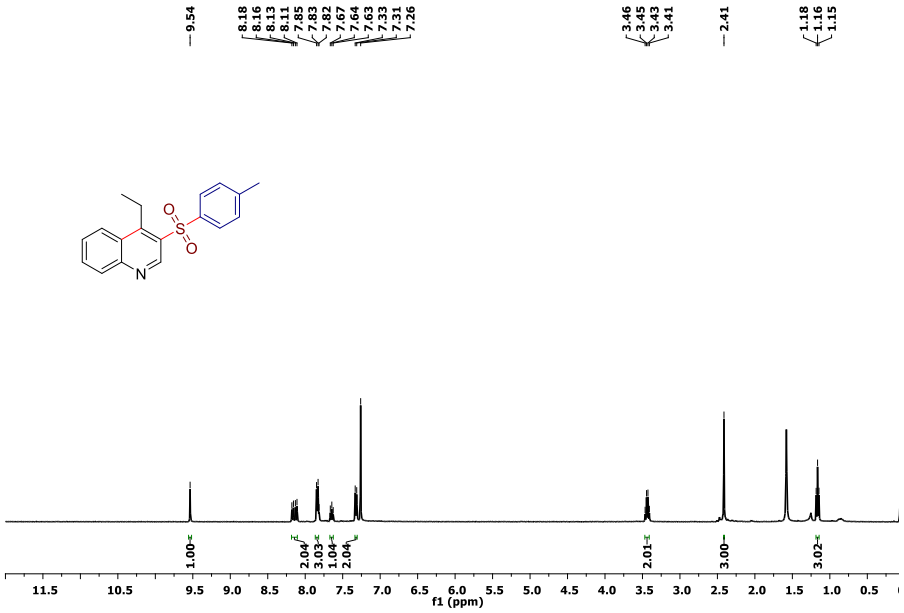

Fig. 339. ^{1}H NMR (400 MHz, $CDCl_3$) spectrum of 4-ethyl-3-tosylquinoline (**3ta**)

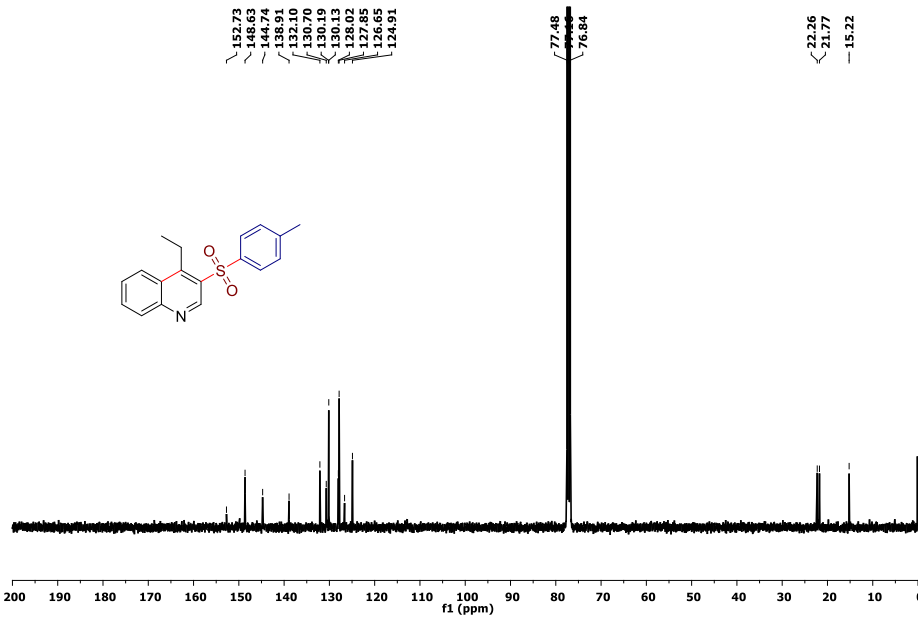

Fig. 3.40. ^{13}C{^{1}H} NMR (100 MHz, $CDCl_3$) spectrum of 4-ethyl-3-tosylquinoline (**3ta**)

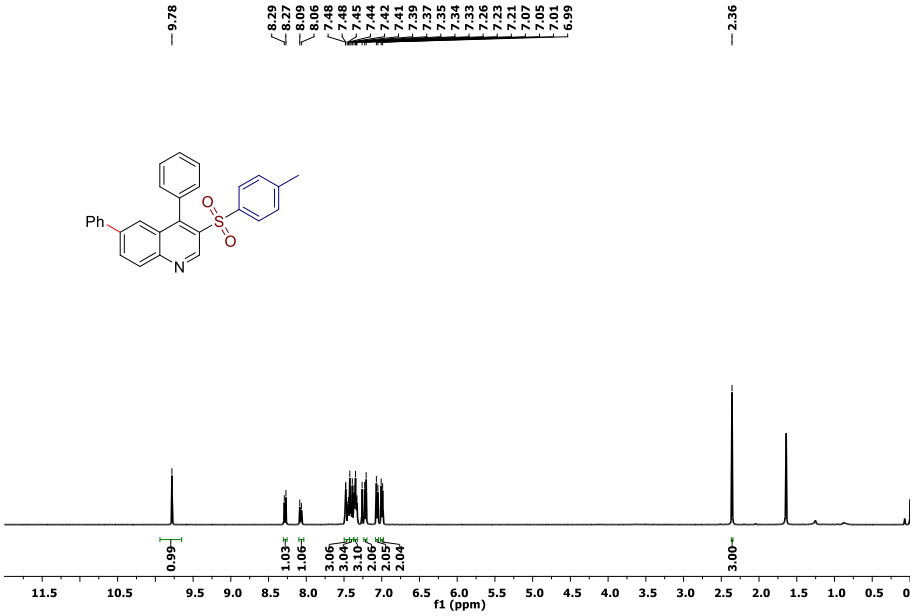

Fig. 3.41. ^{1}H NMR (400 MHz, $CDCl_3$) spectrum of 4,6-diphenyl-3-tosylquinoline **(5)**

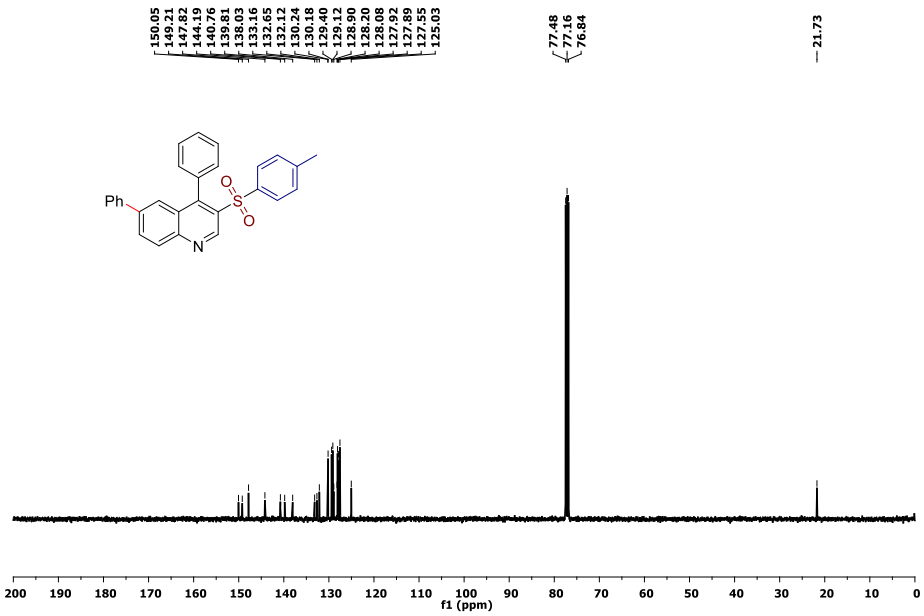

Fig. 3.42. ^{13}C{^{1}H} NMR (100 MHz, $CDCl_3$) spectrum of 4,6-diphenyl-3-tosylquinoline **(5)**

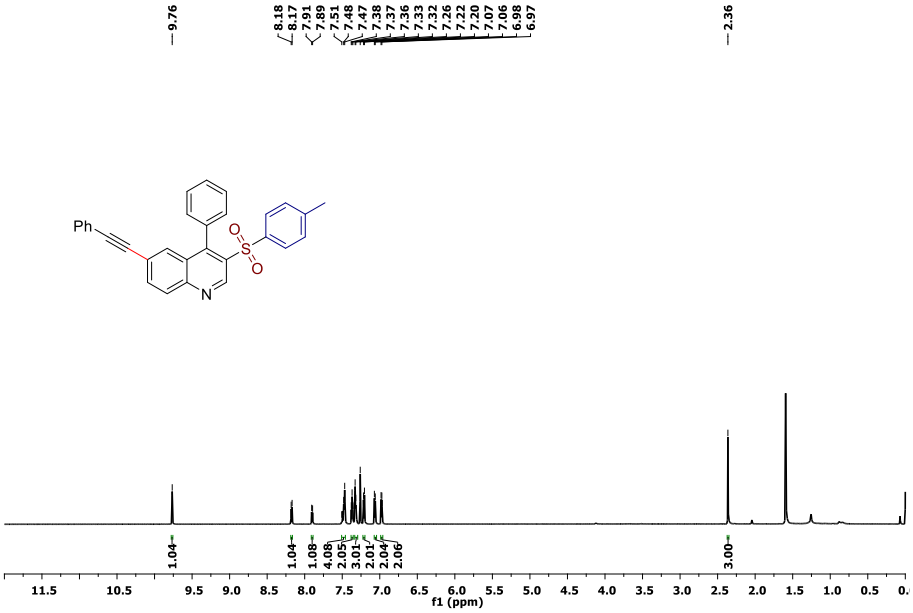

Fig. 3.43. ^{1}H NMR (700 MHz, $CDCl_3$) spectrum of 4-phenyl-6-(phenylethynyl)-3-tosylquinoline **(6)**

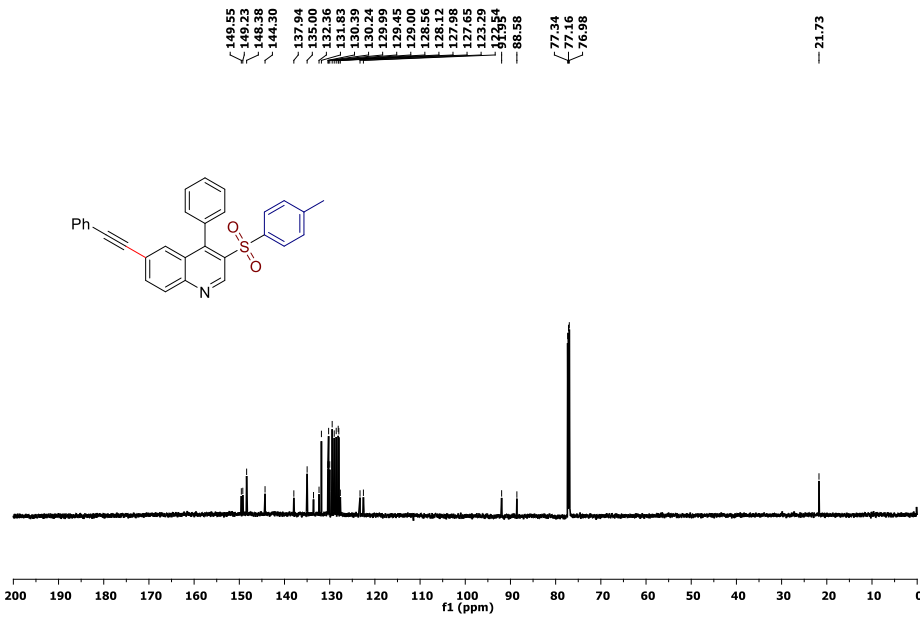

Fig. 3.44. ^{13}C{^{1}H} NMR (175 MHz, $CDCl_3$) spectrum of 4-phenyl-6-(phenylethynyl)-3-tosylquinoline **(6)**

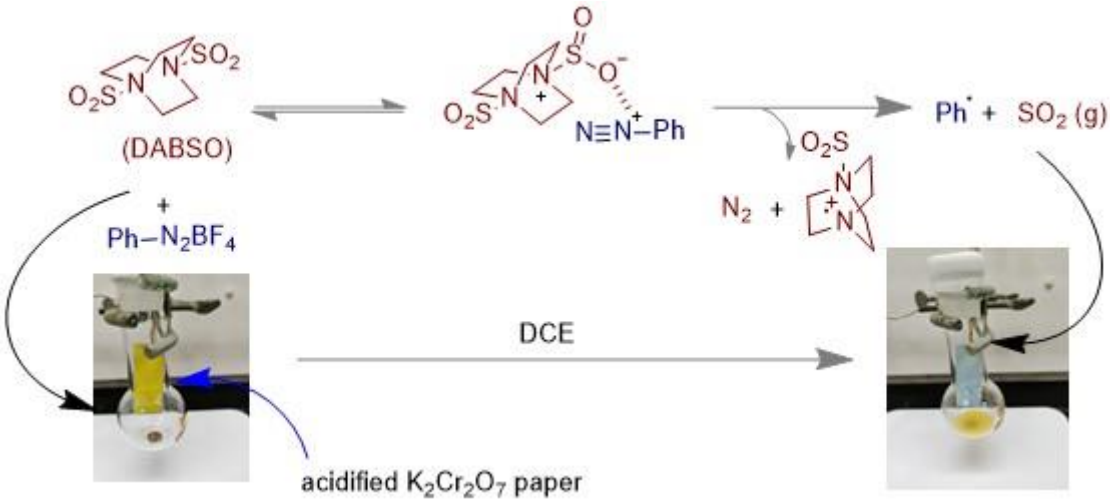

Fig. 3.45. Detection of SO_2 gas: acidified $K_2Cr_2O_7$ paper becomes green from orange yellow.

CHAPTER 4

C-H Chalcogenation by a Bromide Rich and Environmentally Benign Orthorhombic $CsPbBr_3$ under Visible Light, Polar Media and Aerobic Condition

4.1 ABSTRACT

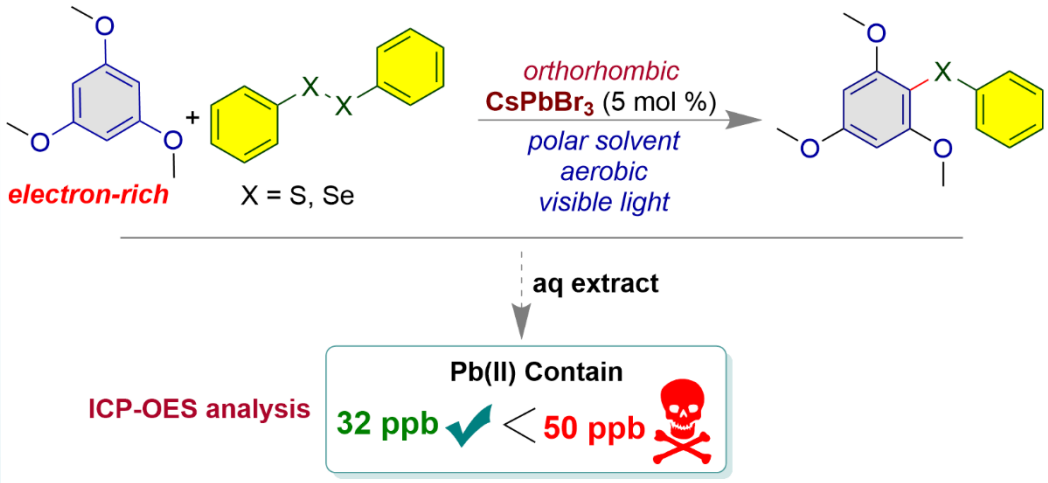

The stability of $CsPbBr_3$ nanocrystals (NCs) in open air remains challenging and can vary depending on the specific material and conditions. Generally, perovskites are prone to degradation due to oxygen, moisture, polar solvent, and light exposure. In this work, we have aimed to develop strategies to improve the stability of $CsPbBr_3$ perovskite and broaden its potential applications in organic synthesis. An orthorhombic $CsPbBr_3$ perovskite nano-crystal (NC) obtained from bromide precursor dibromoisocyanuric acid, can work efficiently as a visible light photocatalyst (blue LED, 5 mol % and TON ~ 18.11) under O_2 atmosphere and in acetonitrile (dielectric constant ε ~ 37.5). The synthesis of diaryl sulfides and a diaryl selenide were achieved *via* template-free C-H functionalization of electron-rich arenes. The electron-rich arenes also helped to enhance the stability of the $CsPbBr_3$ perovskites photocatalyst within the reaction system. The orthorhombic and bromide-rich $CsPbBr_3$ NC displayed superior

photocatalytic activity than cubic $CsPbBr_3$ NCs and was found to be environmentally benign. After the reaction, only 32 ppb of Pb(II) was leached out (ICP-OES analysis) which is quite lower than the maximum permissible limit for drinking water of humans (50 ppb).

4.2 INTRODUCTION

The lead halide perovskite $CsPbBr_3$ nanocrystals (NCs) are the materials that have gained significant attention recently due to their exceptional optoelectronic properties.[1] They have shown promising potential for various applications which include solar cells,[2-5] light-emitting diodes,[6-7] lasers,[8-9] and photodetectors.[10] In addition, the perovskites are widely used as photocatalysts for H_2 generation, CO_2 reduction, N_2 fixation, dye degradation, etc.[11-14] This is due to its high absorption coefficient, tunable bandgap, and high photoluminescence quantum yield. In addition, $CsPbBr_3$ perovskite has a relatively low cost and is simple to synthesize, making it a promising material for large-scale applications.[15]

In recent times, the $CsPbBr_3$ perovskite NCs also have been explored as photocatalysts in organic synthesis.[16-21] Photocatalysis has gained interest as a green and sustainable alternative to traditional chemical synthesis methods, which often rely on high temperatures and/or harsh chemicals.[22-23] However, there are still some challenges associated with $CsPbBr_3$ perovskite, such as its long-term stability[24] and the toxicity of lead. Nevertheless, ongoing research is aimed at addressing these issues and developing more efficient and stable perovskite-based photocatalysts. The major challenges for practical utilization of the perovskites NCs as photocatalysts in organic synthesis is the instability of perovskites towards light,[25-30] moisture,[25-26, 28-29] O_2 atmosphere,[25-28] and polar solvent.[31-32]

The C-H chalcogenation is a valuable strategy for synthesizing chalcogen-containing compounds, which have a wide range of applications, including pharmaceuticals, materials science, and catalysis.[33-35] The C-H chalcogenation process can be carried out using various

methods, including transition-metal catalysis,[36] photoredox catalysis,[37] and organocatalysis.[38] In recent years, significant progress has been made in the development of more efficient methods for C-H chalcogenation.[39-40] Maiti and co-workers have reported a ligand-assisted palladium-catalyzed C-H activation approach for the synthesis of chalcogens. This method utilizes palladium catalysts, which can functionalize the C-H bond of arenes and mediate the reaction with chalcogens like diaryl disulfide and diaryl diselenide (Figure 1a).[41] Lei and co-workers have identified the C-H functionalization of electron-rich arenes using stoichiometric oxidants, such as 2,3-dichloro-5,6-dicyano-1,4-benzoquinone (DDQ).[42]

4.3 RESULT AND DISCUSSION

To the best of our knowledge, C-H chalcogenation of arenes using visible light photocatalysis is hitherto unknown. Herein, we report the synthesis of diaryl sulfides and diaryl selenide (Figure 1c) under visible light (blue LED) using $CsPbBr_3$ NCs as photocatalyst. Moreover, the synthesis of the $CsPbBr_3$ perovskites was achieved by using hot injection methods.[43-44] The green-fluorescent orthorhombic $CsPbBr_3$ (DBIA-$CsPbBr_3$) NC was synthesized using dibromoisocyanuric acid as the bromide-precursor (Figure 1b).[45] Orthorhombic $CsPbBr_3$ perovskite is known for its high stability and improved performance in optoelectronic devices, compared to its cubic counterpart.[46] This is due to its more ordered crystal structure and improved optical properties. The cubic $CsPbBr_3$ perovskites DBHT-$CsPbBr_3$, NBS-$CsPbBr_3$ and NBA-$CsPbBr_3$ were obtained using bromide-precursors 1,3-dibromo-5,5-dimethyl hydantoin (DBHT),[47] *N*-bromosuccinimide (NBS)[48] and *N*-bromoacetamide (NBA), respectively. The use of the *N*-bromoacetamide (NBA) precursor for the synthesis of NBA-$CsPbBr_3$ NC is indeed a relatively novel approach.

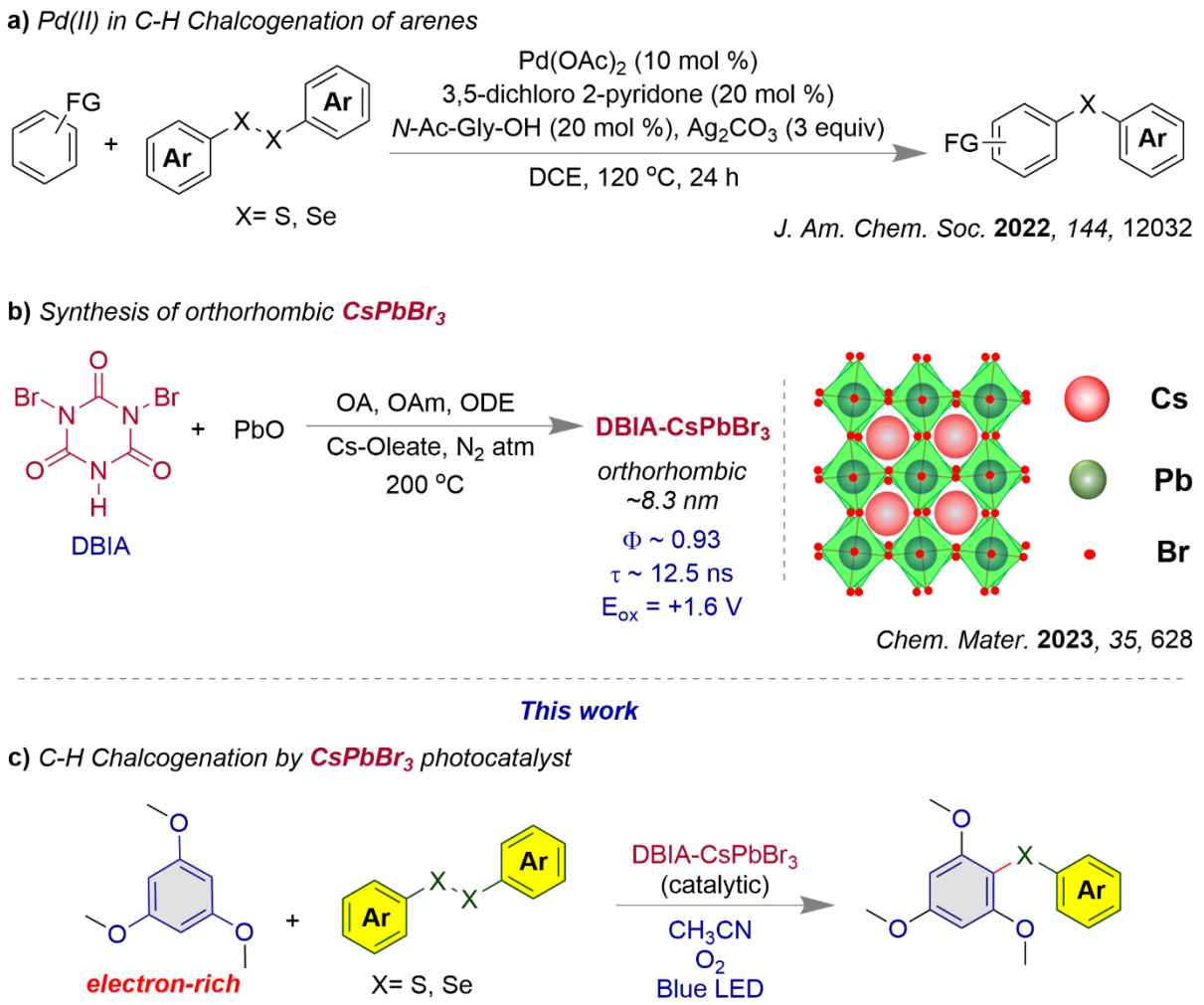

Figure 4.1. The C-H chalcogenation reactions. a) Pd(II) catalyzed Maiti's report.[41] b) The synthesis of orthorhombic DBIA-$CsPbBr_3$.[45] c) The DBIA-$CsPbBr_3$ as visible light photocatalyst for C-H chalcogenation.

The PXRD pattern showed that the structure of the newly synthesized NBA-$CsPbBr_3$ is also cubic, similar to the DBHT-$CsPbBr_3$[47] and NBS-$CsPbBr_3$,[48] whereas DBIA-$CsPbBr_3$ is orthorhombic (Figure 2a). The images from transmission electron microscopy (TEM) demonstrate the morphologies of the $CsPbBr_3$ NCs and average edge length (8 ~ 8.4 nm) (supporting information). However, the TEM image of the newly synthesized NBA-$CsPbBr_3$ is shown in Figure 2b. In the photophysical study, the colloidal suspension of NCs in hexane exhibited significant broad absorption bands in the visible region (up to 525 nm) (Figure 2c).

All the $CsPbBr_3$ NCs suspension displayed intense green photoluminescence with a comparable quantum yield near unity (Φ ~ 0.92 to 0.99) (Figure 2c).[45, 47-48]

The other factors that can influence the colloidal stability of $CsPbBr_3$ perovskite NCs, are the presence of various aromatic molecules, which can prevent particle aggregation and improve the long-term stability of the NCs.[49-50] We have also established that the electron-rich arenes like methoxy benzenes also been shown to increase the stability of the $CsPbBr_3$ perovskite (supporting information). The fluorescence quenching experiments that were performed with 1,3,5-trimethoxy benzene **1a** (*vide infra*) in acetonitrile under aerobic conditions can provide information about the relative stability of the $CsPbBr_3$ NCs in the presence of electron-rich arenes (Figure 2d). The experiments involved adding **1a** to a solution of $CsPbBr_3$ NCs in acetonitrile and measuring the fluorescence intensity of the solution after 24 h, which remained unchanged with DBIA-$CsPbBr_3$. Contrastingly, NBS-$CsPbBr_3$, DBHT-$CsPbBr_3$ and NBA-$CsPbBr_3$ NCs showed quenching of the fluorescence intensity in acetonitrile in the presence of **1a** (Figure 2d). It is indeed interesting that under aerobic conditions and in polar solvent acetonitrile, the $CsPbBr_3$ NCs showed degradation, and among them, DBIA-$CsPbBr_3$ exhibited better stability in the absence of electron rich arenes.

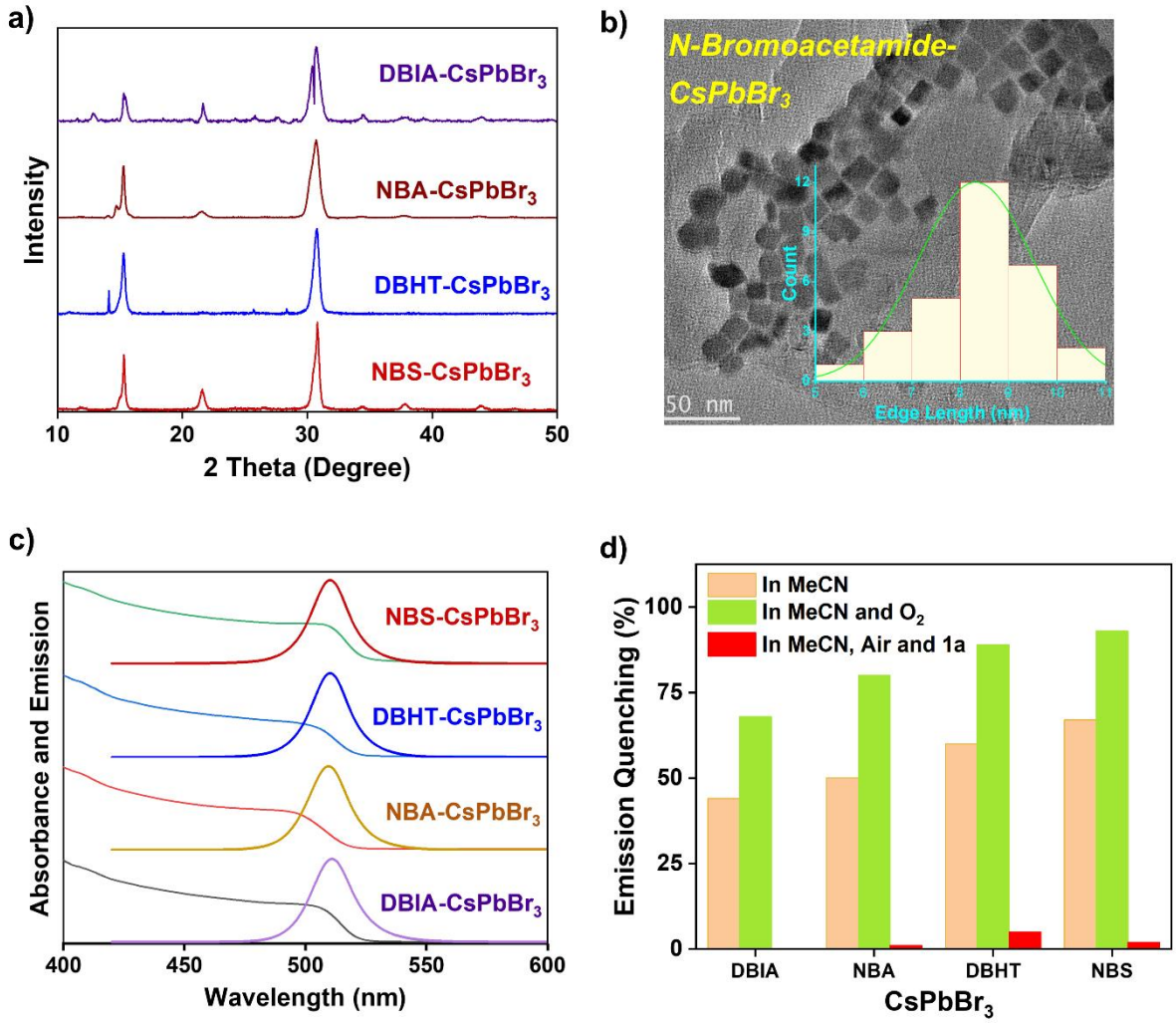

Figure 4.2. a) PXRD of all the $CsPbBr_3$ NCs. b) TEM image of NBA-$CsPbBr_3$. c) Absorption and emission spectra of all the $CsPbBr_3$ NCs. d) Relative stability of the $CsPbBr_3$ NCs in the presence of electron-rich arene 1,3,5-trimethoixy benzene (**1a**).

The information of optimized reaction conditions provided in Figure 3a and the detail of optimization is given in the supporting information. The synthesis of phenyl(2,4,6-trimethoxyphenyl)sulfane **3aa** was achieved from electron-rich 1,3,5-trimethoxybenzene **1a** (0.35 mmol) and 1,2-diphenyldisulfane **2a** (0.43 mmol) using DBIA-$CsPbBr_3$ (5 mol %) in dry acetonitrile (dielectric constant $\varepsilon \sim 37.5$) and O_2 (aerobic) atmosphere under blue LED ($\lambda \sim 450$ - 455 nm). The results presented in Figure 3b indicate that the yield of compound **3aa** using

the DBIA-$CsPbBr_3$ photocatalyst was found to be the highest among the photocatalysts tested, with a yield of approximately 88%. This is higher compared to the yields obtained using NBS-$CsPbBr_3$ (57%), DBHT-$CsPbBr_3$ (51%), and NBA-$CsPbBr_3$ (75%) photocatalysts. These results suggest that the DBIA-CsPbBr3 photocatalyst is more effective in promoting the reaction to produce **3aa** than the other photocatalysts.

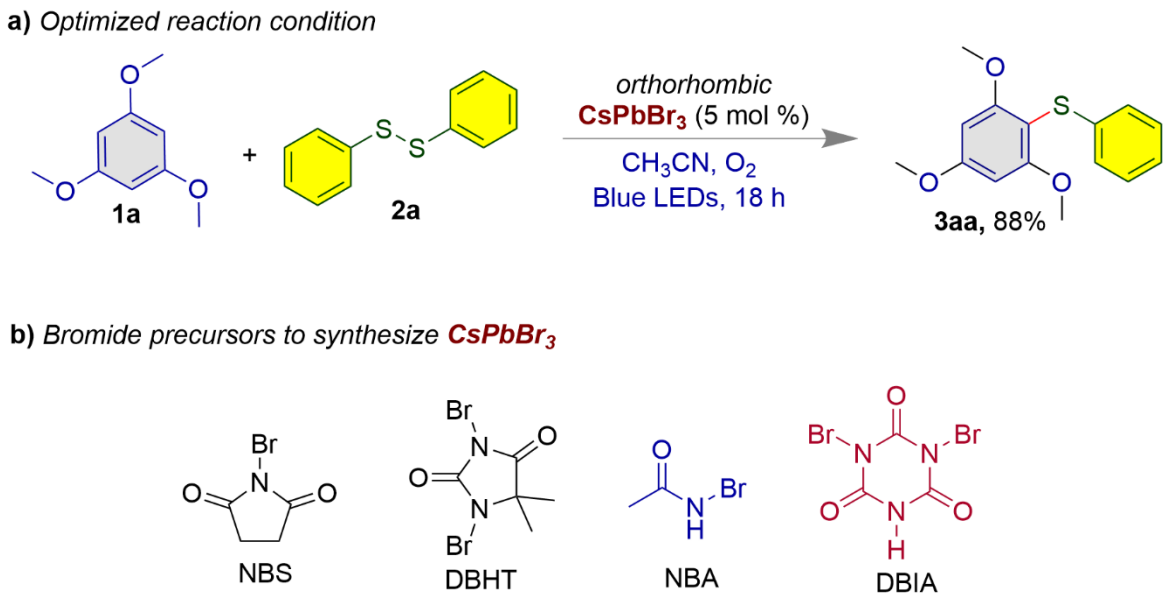

Br – source	Crystal Pattern	Edge Length (nm)	τ (ns)	Φ_{fl}	Yield of 3aa (%)
NBS	Cubic[48]	8.4	9.7	99	57
DBHT	Cubic[47]	8	7.4	92	51
NBA	Cubic (**new**)	8.4	10.2	92	75
DBIA	Orthorhombic[45]	8.3	12.5	93	88

Figure 4.3. a) The optimized reaction condition. b) Bromide-precursors used for the synthesis of $CsPbBr_3$ NCs and the properties of the NCs.

The photoluminescence lifetime studies were also conducted for the $CsPbBr_3$ NCs ($\tau \sim 7$ to 12.5 ns) (Figure 3b).[45, 47-48, 51] Redox potentials of the $CsPbBr_3$ NCs are determined through cyclic voltammetry (CV) experiments (oxidation potentials, $E_{ox} = +1.6$ V and the reduction potentials, $E_{red} = -1.15 \sim -1.25$V) (Figure S8, supporting information).

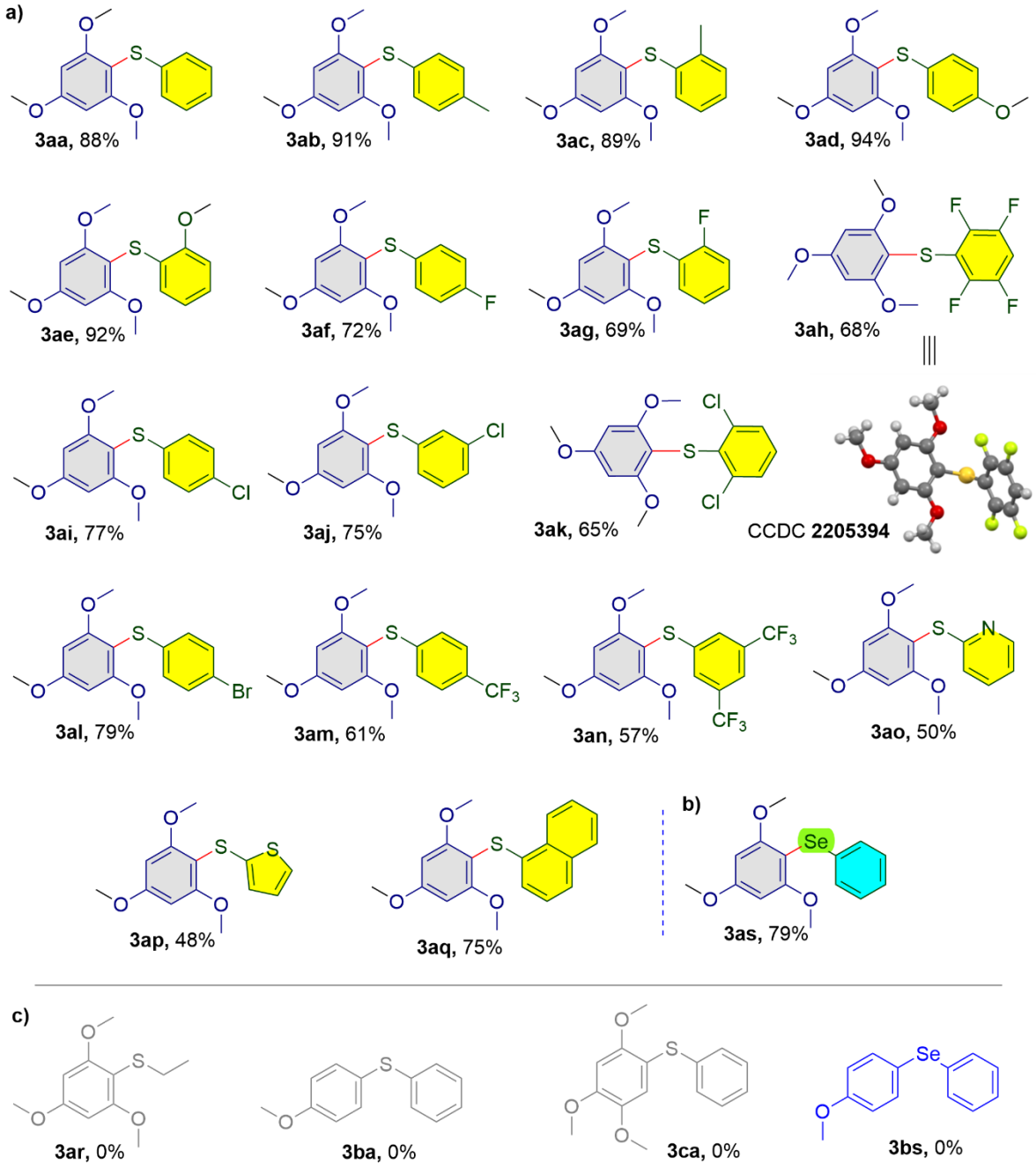

Figure 4.4. The products from the reactions with a) various disulfides b) and a diselenide. c) Unsuccessful attempts.

The reaction efficiency of different disulfides in the presence of electron-rich arenes is shown in Figure 4a. A variety of disulfides and diselenides were subjected to the reaction under standard conditions. The -Me, and -OMe groups at the *para*- and *ortho*-positions of disulfide produced the corresponding phenyl sulfanes **3aa-3ae** with high yields (88% to 94%). Again, -F containing diaryl disulfides produced thioethers **3af**, **3ag**, and **3ah** with 72%, 69%, and 68% yield, respectively. Next, thioethers **3ai-3ak** having –Cl substituent were synthesized with 65-75% yields. 4-Dibromodiaryl disulfide resulted in **3al** with 79% yield. Compounds **3am** and **3an** were synthesized with 61% and 57% yields, respectively. Furthermore, 1,2-di(thiophen-2-yl)disulfane and 1,2-di(pyridin-2-yl)disulfane reacted well to produce the corresponding thioethers **3ao** and **3ap** with 50% and 48% yields, respectively. Polyaromatic containing disulfide yielded the corresponding diaryl sulfide **3aq** with 75% yield. The coupling reaction between aliphatic disulfide and trimethoxybenzene to produce compound **3ar** failed. The sluggish reaction was observed with anisole under the standard condition. On the other hand, the successful coupling of diaryl diselenide (Figure 4b) with 1,3,5-trimethoxybenzene **1a** to produce **3as** in 79% yield indicates that the reaction conditions were also favorable for this system. The structure of the substrates shown in Figure 4c, which could not be isolated.

The control experiments shown in Figure 5 provided important information about the reaction mechanism. The energy potential diagram shown in Figure 5a, obtained from CV (cyclic voltammetry) experiments, for the photocatalyst (PC) and the reactants **1a** and **2a**. The observation of a lowering of photoluminescence intensity with increasing addition of disulfide suggests that the disulfide quenches the photoluminescence of $CsPbBr_3$ in acetonitrile with a quenching constant of $k_q = 7.52 \times 10^{12}\ s^{-1}\ M^{-1}$ (Figure 5b). The results presented in Figure 5c demonstrate the visual change before and after the reaction under visible light and UV light. The fact that the $CsPbBr_3$ remains crystalline even after the reaction, as shown in Figure S10

(supporting information), suggests that the material retains its structural integrity and is likely to remain catalytically active. The observation of a strong signal in EPR in the trapping experiment in the presence of 5,5-dimethyl-1-pyrroline-*N*-oxide (DMPO, Figure 5d) provides evidence for a radical-based pathway in the reaction.[52] The radical-based mechanism was further supported by the experiments using 1,1-diphenylethylene, 2,2,6,6-tetramethylpiperidine 1-oxyl radical (TEMPO), and butylated hydroxytoluene (BHT) as radical scavengers (Figure 5e). In the light On-OFF-ON experiment (Figure 5f), the reaction was done under three different conditions: once with the light turned on (ON), once with the light turned off (OFF), and once with the light turned on again (ON). By comparing the results of the three conditions, it was established that visible light is indeed essential for the reaction.

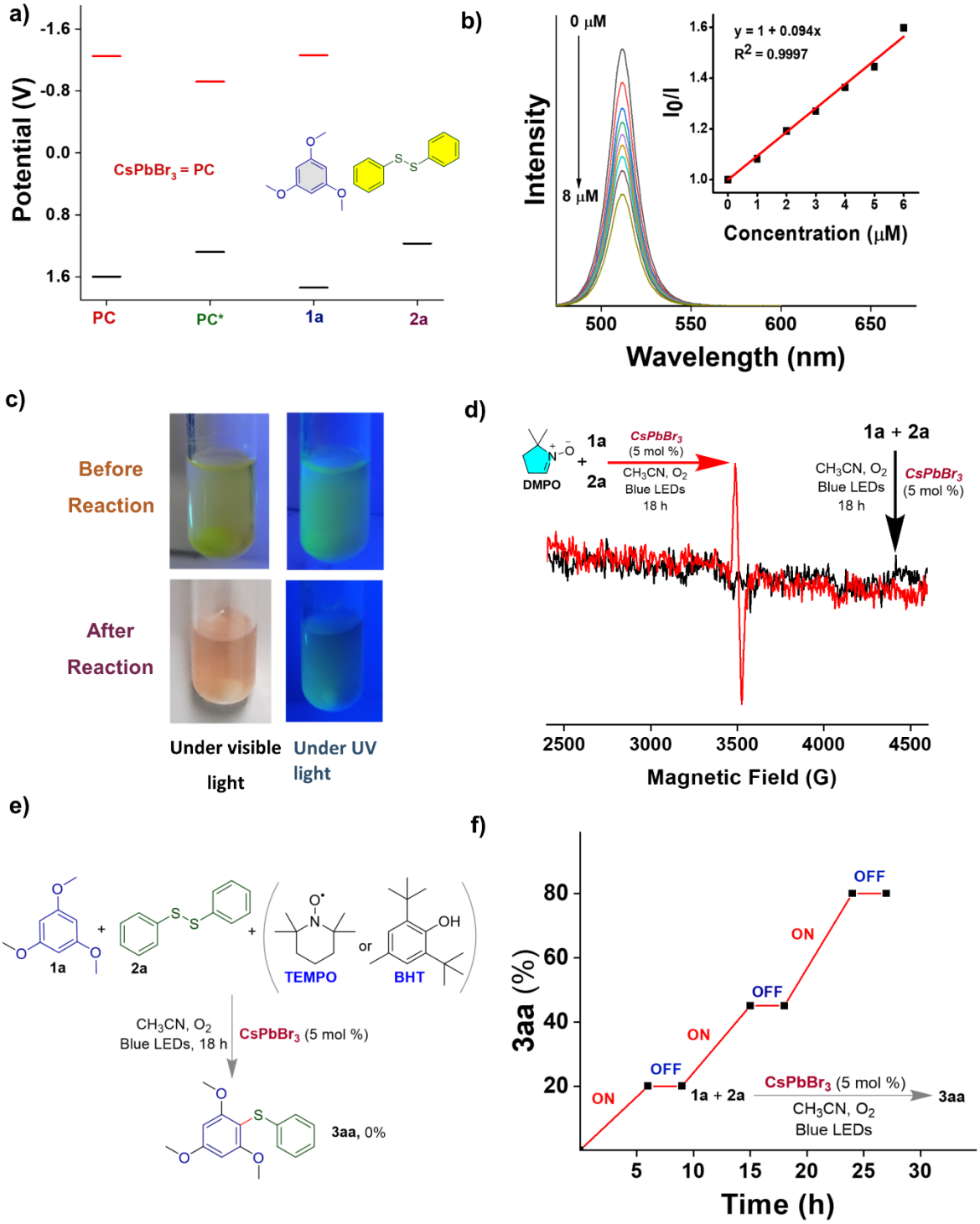

Figure 4.5.control experiments a) Energy potential diagram of the reactants (**1a** and **2a**) and photocatalyst (PC). b) Fluorescence quenching experiment of DBIA-$CsPbBr_3$ upon addition of **2a** in acetonitrile and Stern-Volmer quenching plot (inset). c) Photograph of the reaction

mixture before and after irradiation. d) EPR study in the presence of DMPO. e) Radical trapping experiments with TEMPO and BHT. f) The light ON-OFF-ON experiment.

A plausible reaction mechanism is shown in Figure 6a. The presence of a strong absorption band in the visible region of the DBIA-$CsPbBr_3$ NCs makes them susceptible to photochemical excitation after absorption of visible light (blue LED). The disulfide radical cation can be generated through the hole transfer (HT) process from the valence band (VB) of the $CsPbBr_3$ perovskite to the disulfide moiety. The comparison of the redox potentials can provide insights into the driving force for the hole transfer process and the photocatalytic activity of the DBIA-$CsPbBr_3$ NCs (E_{ox} = +1.17 V of disulfide < E^*_{red} = +1.28 V of $CsPbBr_3$) (Figure 5a). The disulfide radical cation generated can react with electron-rich arenes to form intermediate **I**, a radical cation. The superoxide radical anion can be generated through an electron transfer process[53] from the conduction band of the perovskite to molecular oxygen. In this process, the electrons in the conduction band of the perovskite are transferred to molecular oxygen (O_2), forming superoxide radical anions ($O_2^{-\cdot}$). These superoxide radical anions can then react with intermediate **I**, leading to deprotonation and led to the formation of product **3aa** and by-product hydrogen peroxide (H_2O_2). The formation of hydrogen peroxide (H_2O_2) was confirmed by UV-vis spectroscopy through the detection of tri-iodide (I_3^-) in the reaction medium. The detection of tri-iodide is typically performed by adding potassium iodide (KI) and dilute acid to the reaction mixture, which can then be monitored by UV-vis spectroscopy. The appearance of a peak in the UV-vis spectrum at a wavelength of 359 nm was indicative of the formation of tri-iodide, which confirms the presence of hydrogen peroxide in the reaction medium.[54]

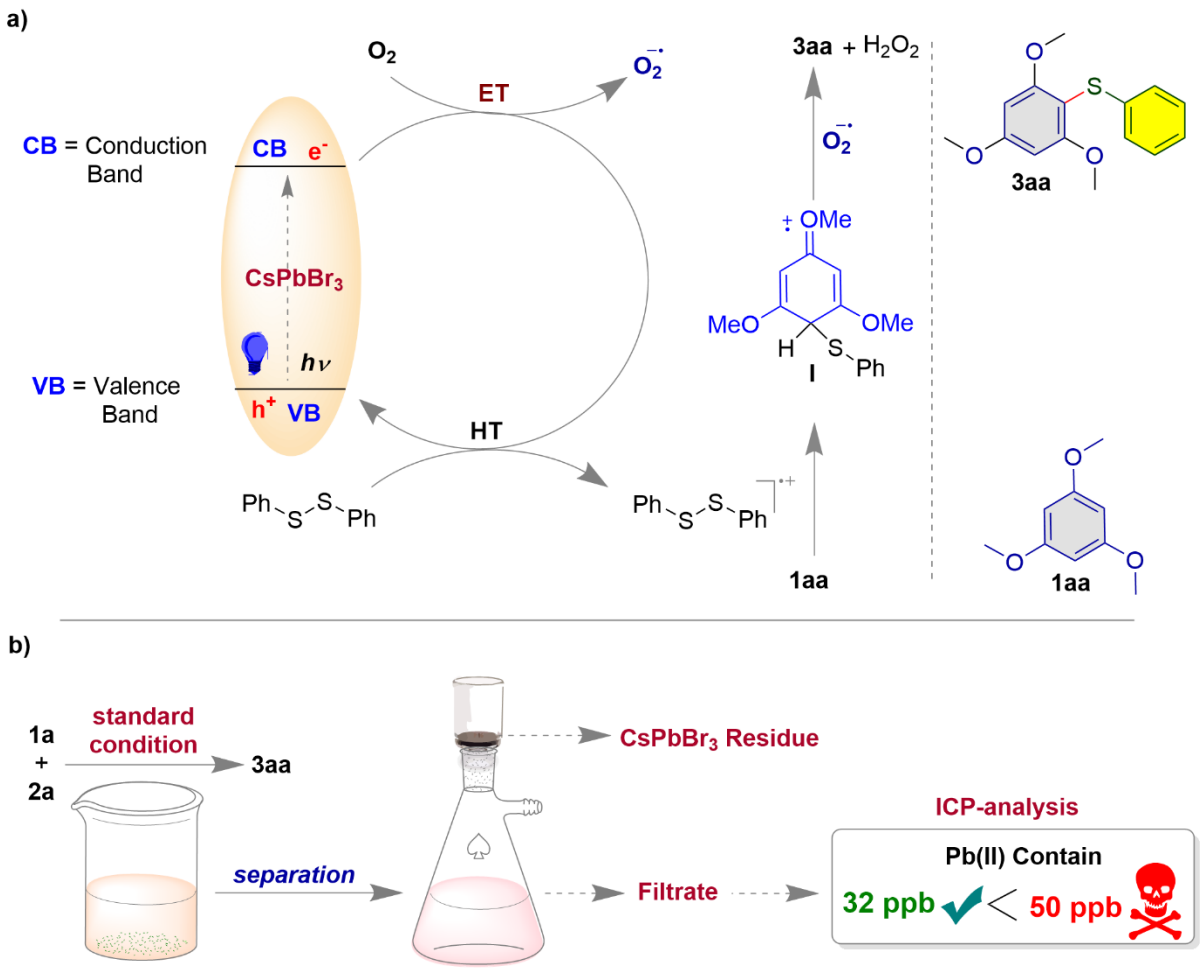

Figure 4.6. a) Plausible reaction mechanism. b) The lead leaching experiment after the reaction.

The Turn Over Number (TON) measures the catalytic efficiency of the catalyst and in this case, the TON of DBIA-$CsPbBr_3$ NC is 18.11.[55] The perovskite NCs were recovered from the reaction mixture through simple centrifugation (Figure 6b) and the low level of Pb leaching, as indicated by the ICP-OES (inductively coupled plasma optical emission spectrometry) analysis of the filtrate, is also encouraging compare to the previous report.[17] The fact that only 32 ppb (parts per billion) of Pb was leached, shows that this photocatalyst is relatively safe and can be used without significant environmental concern. The maximum allowable amount of lead in

drinking water is set at 50 ppb (parts per billion).[56] So, it is possible that DBIA-$CsPbBr_3$ NCs are considered to be environmentally benign visible light photocatalysts.

This is likely due to the unique crystal structure of orthorhombic DBIA-$CsPbBr_3$ perovskite nanocrystals (NCs), which allows for a more efficient transfer of electrons and holes compared to other cubic $CsPbBr_3$ NCs. This leads to a longer photoluminescence lifetime and quantum yields (Φ) compare to the cubic NCs. Importantly, the specific properties of perovskite NCs can also be influenced by other factors such as the modified synthetic methods,[57-60] surface treatment,[5] post-synthetic modifications,[61] etc. The photoluminescence quenching study was carried out of these perovskites in acetonitrile (ACN) and under O_2 atmosphere where orthorhombic $CsPbBr_3$ displayed more stable behavior compare to the cubic $CsPbBr_3$ perovskites (Figure 2d, and Figures S4 and S5, supporting information). The intrinsic stability of orthorhombic DBIA-$CsPbBr_3$ perovskite can be attributed to the fewer crystal defects[62] and higher bromide ion ratios,[63] as these factors contributed to the stability of the orthorhombic $CsPbBr_3$ perovskite. A perovskite NC with fewer crystal defects is less prone to degradation, while a higher bromide ion ratio can improve the overall stability of the material. In addition, we have shown that the electron rich arenes can improve the stability of the perovskite NCs within the reaction system.

Derivatization of the synthesized compounds (diaryl sulfides) is shown in Figure 7. *meta*-Chloroperoxybenzoic acid (*m*CPBA) was used for the oxidation of diaryl sulfide **3aa** into the corresponding sulfoxide (Figure 7a).[64] The Suzuki (Figure 7b)[65] and Sonogashira (Figure 7c)[66] cross-coupling reactions were performed on the compound **3aj**.

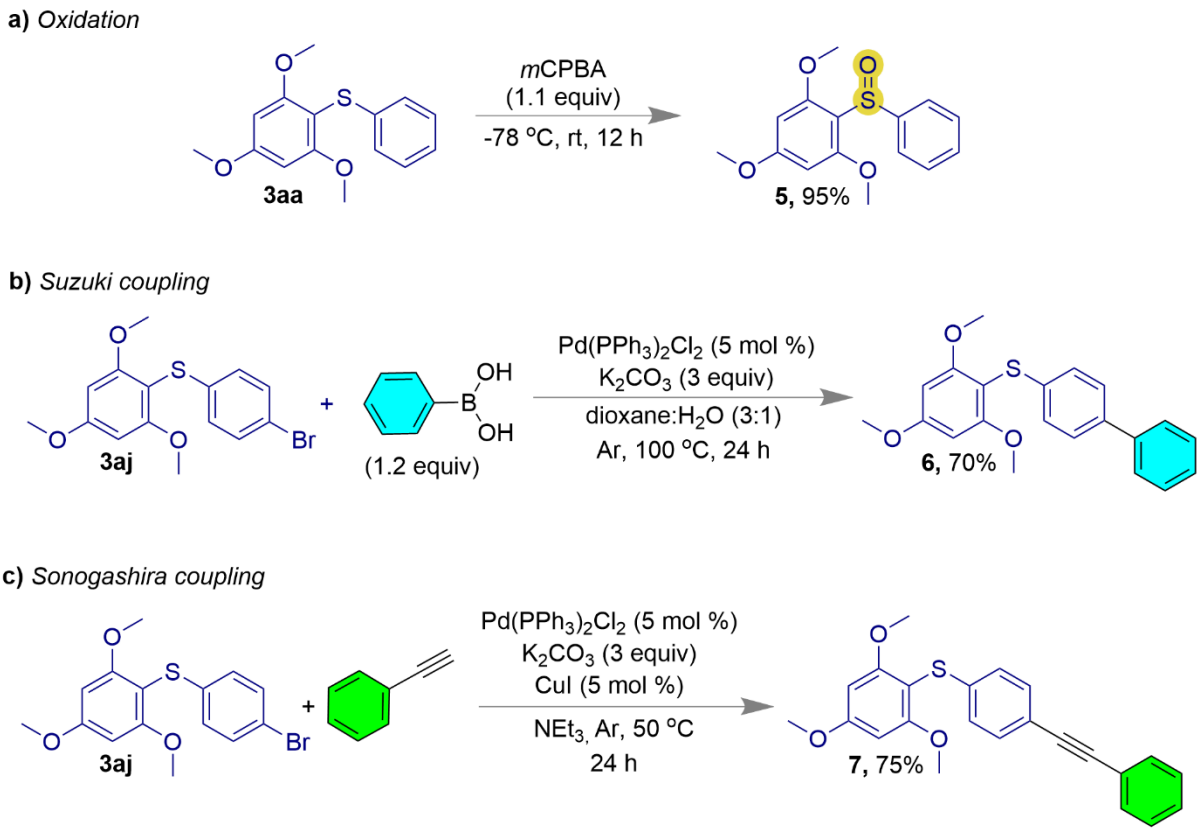

Figure 4.7. Synthetic utilities of the diaryl sulfides. a) Oxidation of **3aa** using *m*CPBA. b) The Suzuki and c) Sonogashira cross-coupling reactions of **3aj**.

4.4. CONCLUSION

In conclusion, the use of an orthorhombic $CsPbBr_3$ perovskite nanocrystal (NC) as visible light photocatalysis, for the synthesis of diaryl sulfides and a diaryl selenide has been reported here. Compared to the cubic-perovskites (NBS-$CsPbBr_3$, DBHT-$CsPbBr_3$ and DBA-$CsPbBr_3$) the orthorhombic DBIA-$CsPbBr_3$ is found to be an efficient visible light photocatalyst under blue LEDs, aerobic condition and in polar solvent like acetonitrile (dielectric constant $\varepsilon \sim 37.5$). The intrinsic stability of the orthorhombic $CsPbBr_3$ was due to the fewer crystal defect and higher bromide ion ratios. In addition, one of the reactants 1,3,5-trimethoxy benzene also helped to increase the stability of the DBIA-$CsPbBr_3$ NC within the reaction system. Due to low lead leaching after the reaction, this NC can also be considered as an environmentally benign

photocatalyst. We anticipate that the results of this work have the potential to provide new insights and guidelines for the fields of synthetic organic and material chemistry.

4.5. EXPERIMENTAL SECTION

Chemicals. All the reagents were purchased from commercially available sources and used without further purification. All organic solvents were also received commercially and purified.

Synthesis of DBIA-$CsPbBr_3$ NCs. $CsPbBr_3$ NCs were synthesized according to the literature procedure.[45] Pre-dried Cs_2CO_3 (195 mg, 0.6 mmol), ODE (9 mL), and OA (1.0 mL) were taken in a two-necked 50 mL round-bottom flask (RB). The reaction mixture was dried under vacuum for 30 min at 120 °C and then transferred to the N_2 atmosphere for 1 h, maintaining the same temperature to become a clear solution. In another three-necked 25 mL RB, PbO (44 mg, 0.3 mmol), DBIA (174 mg, 0.6 mmol) and ODE (5 mL, pre-dried) were added respectively. The reaction mixture was kept under vacuum for 30 min at elevated temperature (~120 °C) followed by to the N_2 environment at 130 °C. After 10 min, 1.0 mL OA and 1.0 mL OLA were injected to the reaction mixture and temperature of the reaction mixture was raised to ~200 °C. Then, cesium-oleate (~0.8 mL) solution (preheated at 100 °C) was swiftly injected into the reaction mixture. Subsequently, the reaction was quenched in an ice bath. After that, 3 mL of MeOAc was added to the mixture and centrifuged for 10 min at 6500 rpm. The supernatant was discarded, and the precipitation was dispersed in hexane and kept in the refrigerator for 30 min. The suspension was again centrifuged for 10 min at 6500 rpm. Finally, the supernatant containing the NCs and precipitation were separated and both were stored for future experiments.

Synthesis of NBA-$CsPbBr_3$ NCs. NBA-$CsPbBr_3$ NCs was synthesized using the same procedure as previous using NBA (83 mg, 0.6 mmol).[45]

Synthesis of DBHT-$CsPbBr_3$ NCs. NBA-$CsPbBr_3$ NCs was synthesized following the literature procedure using DBHT (172 mg, 0.6 mmol).[47]

Synthesis of NBS-$CsPbBr_3$ NCs. NBA-$CsPbBr_3$ NCs was synthesized following the literature procedure using NBS (107 mg, 0.6 mmol).[48]

Powder X-ray Diffraction Measurement (PXRD). PXRD pattern was collected using Bruker Davinci D8 diffractometer (Cu-Ka radiation; λ=0.15418 nm). A thin film of the sample was prepared by drop-casting the concentrated suspension of NCs onto a thin quartz plate.

Transmission Electron Microscopy (TEM). TEM images were captured by JEOL (JEM-2100) operating at an accelerating voltage of 200 kV. The sample was prepared on a carbon-coated copper grid by drop-casting the dilute suspension of NCs in hexane.

Energy Dispersive X-ray Spectroscopy (EDX). Energy dispersive X-ray spectra were recorded by Oxford instruments X-MaxN SDD (50 mm2) system and INCA analysis software attached with Carl Zeiss FESEM instrument.

Absorption and Photoluminescence Measurements. UV-VIS absorption and steady-state photoluminescence (PL) spectrum of a colloidal suspension of NCs were recorded with JascoV-730 spectrophotometer and Edinburgh spectrofluorometer FS5 with SC-25 cuvette holder, respectively.

Absolute quantum yield was measured by using an integrating sphere (SC-30).

Time-Correlated Single-Photon Counting. PL decay measurement was carried out through TCSPC method using Edinburgh Instruments (Model OB-920), decorated with 405 nm laser as the excitation source. IRF was determined using a scatter ludox solution. The lifetime profile was fitted with exponential decay function according to the equation, $I(t) = \sum_{i=1}^{n} \alpha_i \exp(-\frac{\tau_i}{t})$ and the average fluorescence lifetime was determined using equation $\tau_{av} = \frac{\sum \alpha_i \tau_i^2}{\sum \alpha_i \tau_i}$; where α_i and τ_i are amplitude and lifetime of ith component respectively.

Photoluminescence Quenching Study. Photoluminescence quenching study of $CsPbBr_3$ was conducted using disulfide as quencher. Through Stern-Volmer kinetics, rate of quenching (k_q) was determined using the equation $I_0/I = 1 + k_q\tau$ [*quencher*], where I_0 is the initial PL intensity without the quencher, I is the intensity after addition of the quencher, and τ is the lifetime of the $CsPbBr_3$. Probe sample was prepared by suspending $CsPbBr_3$ NCs in DCE of concentration 0.5 mg mL^{-1}. Then 20 μL of the concentrate solution was diluted to make a total volume 2 mL. Quencher of concentration of 1 mM was added to the probe suspension in an incremental way of 2 μL maintaining the total volume of 2 mL. Lifetime of $CsPbBr_3$ is ~ 12.5 ns.

Nuclear Magnetic Resonance (NMR) Measurements. NMR spectra were recorded on 400 MHz and 700 MHz (BRUKER® ULTRASHIELD) instruments at 25 °C. The chemical shift values are reported in parts per million (ppm) for residual chloroform (7.26 ppm for ^1H and 77.16 ppm for ^{13}C). The peak patterns are designated as follows: s: singlet; d: doublet; t: triplet; q: quartet; m: multiplet; dd: doublet of doublets; td: triplet of doublets; brs: broad singlet. The

coupling constants (*J*) are reported in hertz (Hz). Samples solutions were prepared by dissolving in $CDCl_3$.

High-resolution Mass Spectra (HR-MS). HR-MS were recorded on a TOF Q-II (Bruker) (time of flight) mass spectrometer. Clear solutions of samples were prepared after dissolving in methanol or acetonitrile.

Fourier Transform Infrared Spectroscopy (FTIR). FTIR analysis data were collected from Thermo Scientific (NICOLET iS5) instrument under transmittance mode and reported in wavenumber (cm^{-1}). A thin layer of the compounds on the surface of the KBr pallet was prepared using dichloromethane as a solvent to record the data.

Electron Paramagnetic Resonance (EPR). EPR spectrum was recorded with a Bruker System EMX-microX at 298K and 9.4335 GHz. Typical EPR spectrometer parameters are shown as follows, scan range: 100 G; centre field set: 3480.00 G; time constant: 0.16 ms; scan time: 128.22 s; modulation amplitude: 20.0 G; modulation frequency: 100 kHz; receiver gain: 2.00×10^2; microwave power: $7.14e^{-001}$ mW; g = 2.007092. A description of sample preparation is given later.

Cyclic Voltammetry (CV). Cyclic voltametric data were investigated on the CorrTest Electrochemical Station (Model: CS310, S/N: 1711458) in dry and oxygen-free DCM: hexane (1:4) solution containing 0.1 M tetrabutylammonium hexafluorophosphate as a supporting electrolyte with a decoration of a glassy carbon electrode, a Ag/AgCl electrode and a platinum wire as the working electrode, reference electrode, and counter electrode, respectively using a

scan rate 100 mV/s. Redox potential was referenced against ferrocene/ferrocenium (Fc/Fc^+).

Melting Points. Melting points (mp) of the compounds were determined using a digital melting point apparatus and are uncorrected.

Photoreactor. This photoreactor used obtained from commercial source (Model No.-LED Photochemical reactor CN302, CRYOANO VL- PHOTON). Quartz tubes (LUZCHEM) The intensity of the blue LED is (417 x 100) lx (measured by Sigma-Digital Lux Meter 101, Model: 20036176). Distance between quartz tube and light source was approximately 4.2 cm.

General procedure for the synthesis of 3aa. In an oven dried quartz tube 1,3,5-trimethoxybenzene (0.35 mmol), chalcogens (0.43 mmol), and $CsPbBr_3$ (5 mol %) were dissolved in 2.0 mL dry acetonitrile. After that, the reaction mixture was irradiated by visible light (450-455 nm) for 18 h in the presence of an oxygen balloon. After completion of the reaction, unreacted NCs (photocatalysts) were filtered off, and supernatant acetonitrile was removed under reduced pressure. Then, the crude mixture was diluted in dichloromethane (CH_2Cl_2) and washed with brine solution. The resulting organic solution was dried over anhydrous sodium sulfate and concentrated to obtain a crude mixture which was further purified by silica-gel column chromatography using ethyl acetate and hexane as the eluent to afford the pure product.

The calculation of Turn Over Number (TON). Turn Over Number is calculated by the equation, TON = total mol of product/total mol of catalyst

Molecular weight of $CsPbBr_3$ catalysis is calculated as 579.8 g mol^{-1}

Pb(II) leaching experiment. Pb(II) concentration was estimated using ICP-OES spectrometer (Themo SCIENTIFIC, iCAP 7000 SERIES with autosampler TELEDYNE CETAC TECHNOLOGIES, ASX-280). First 10 mg (5 mol %) $CsPbBr_3$ was dissolved in Millipore water (10% HNO_3) and Pb(II) concentration was determined. Again, after the reaction the solid was separated and the organic solvent was removed from the filtrate followed by the residue was dissolved in Millipore water (10% HNO_3). Then initial and final concentration of Pb(II) was estimated and leaching was calculated.

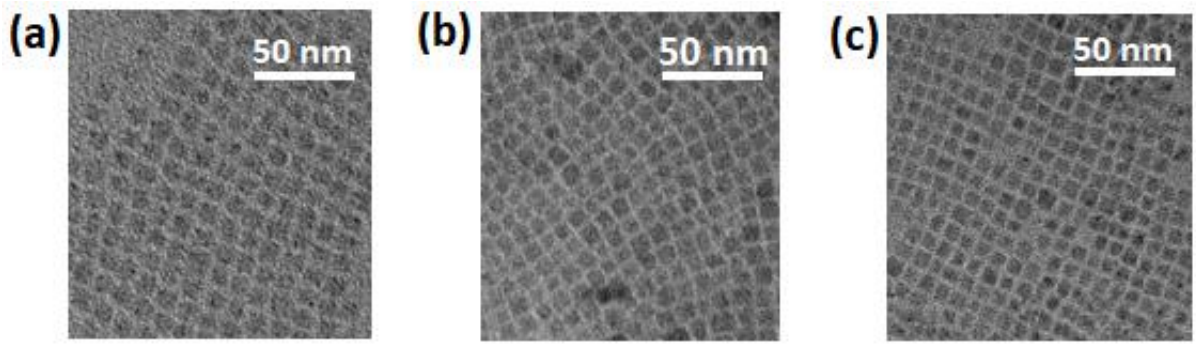

Fig. 4.8. TEM images of (a) NBS-$CsPbBr_3$, (b) DBHT-$CsPbBr_3$, (c) DBIA-$CsPbBr_3$

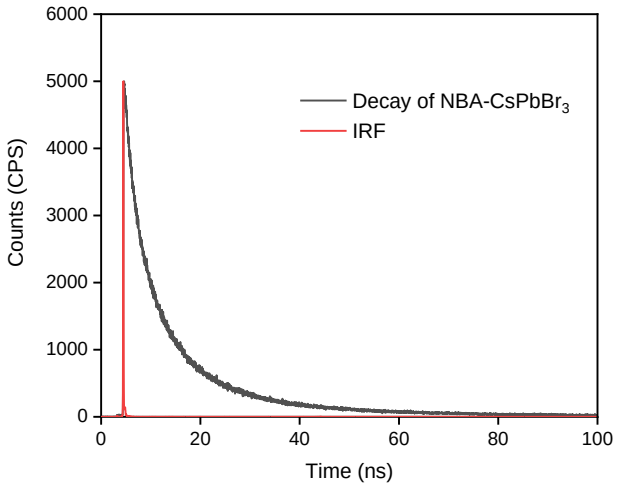

Fig. 4.9. PL lifetime decay of NBA-$CsPbBr_3$

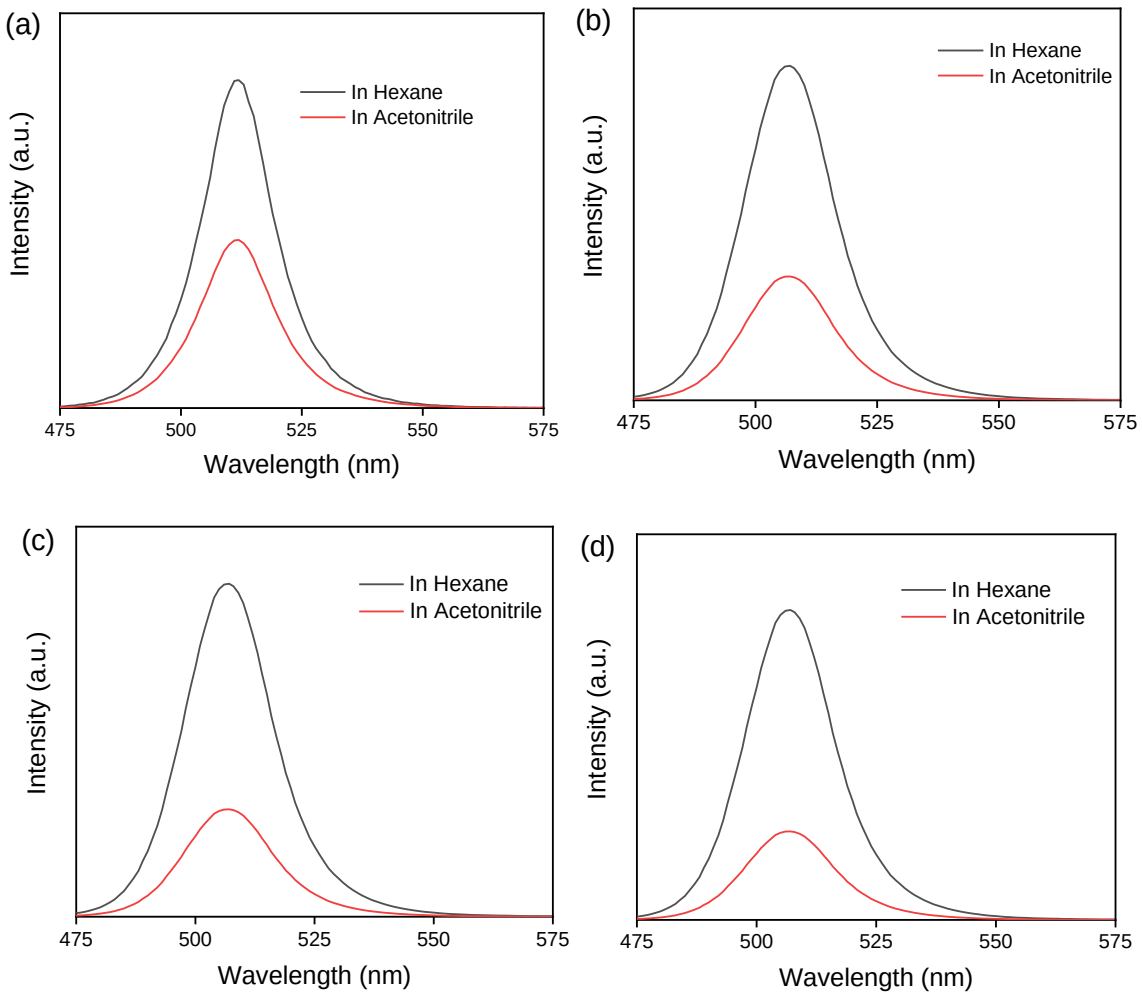

Fig. 4.10. PL spectra of (a) DBIA-$CsPbBr_3$, (b) NBA-$CsPbBr_3$, (c) DBHT-$CsPbBr_3$, (d) NBS-$CsPbBr_3$ in Hexane and Acetonitrile

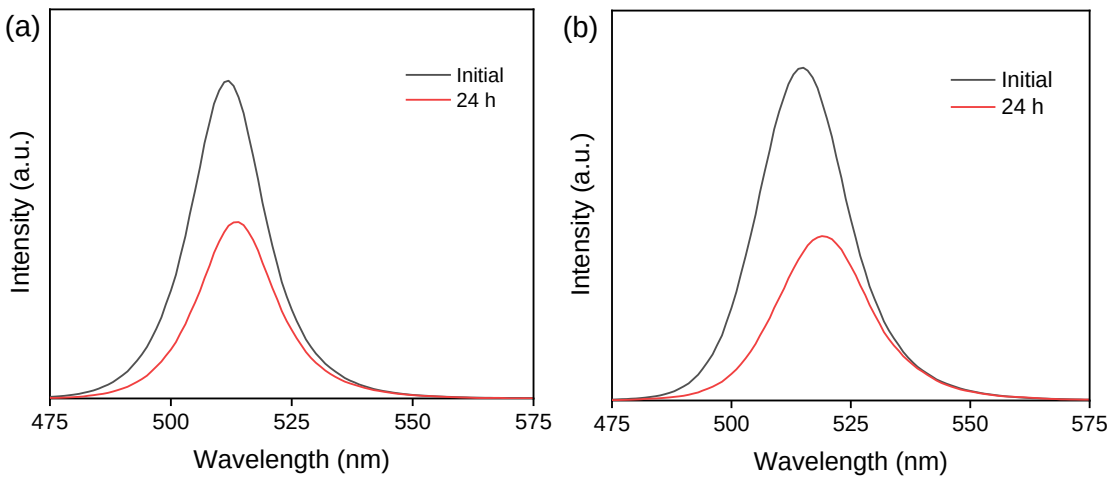

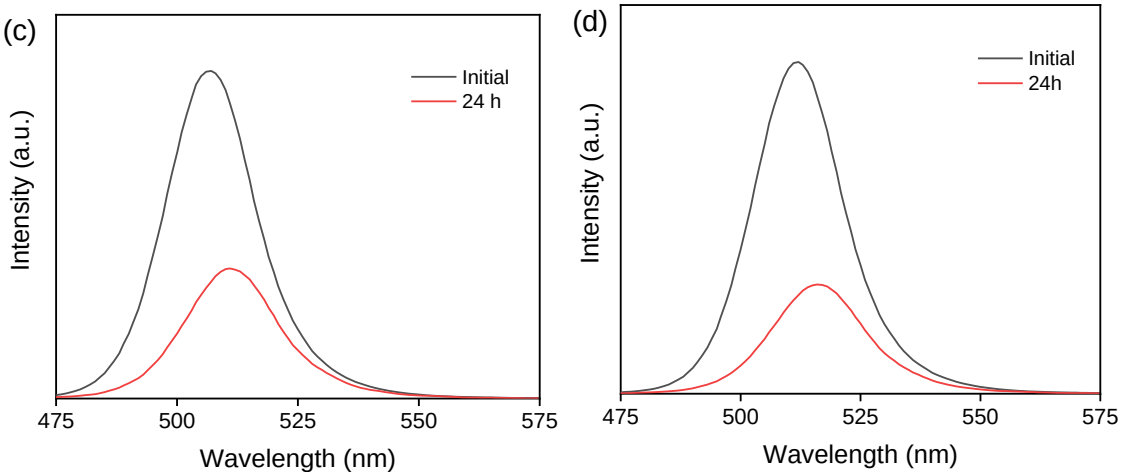

Fig. 4.11. PL quenching of $CsPbBr_3$s in ACN obtained from (a) DBIA, (b) NBA, (c) DBHT, (d) NBS

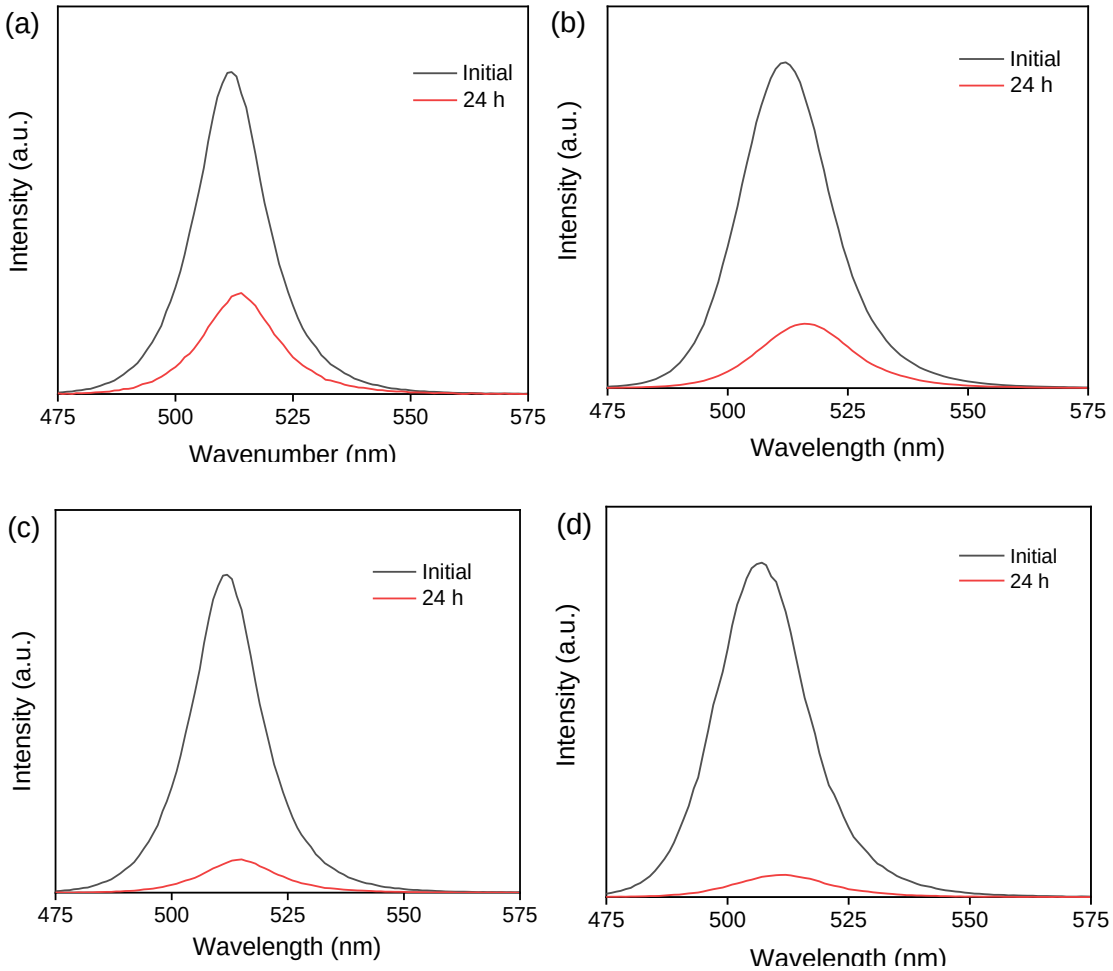

Fig. 4.12. PL quenching of $CsPbBr_3$s in ACN and O_2 atmosphere obtained from (a) DBIA, (b) NBA, (c) DBHT, (d) NBS

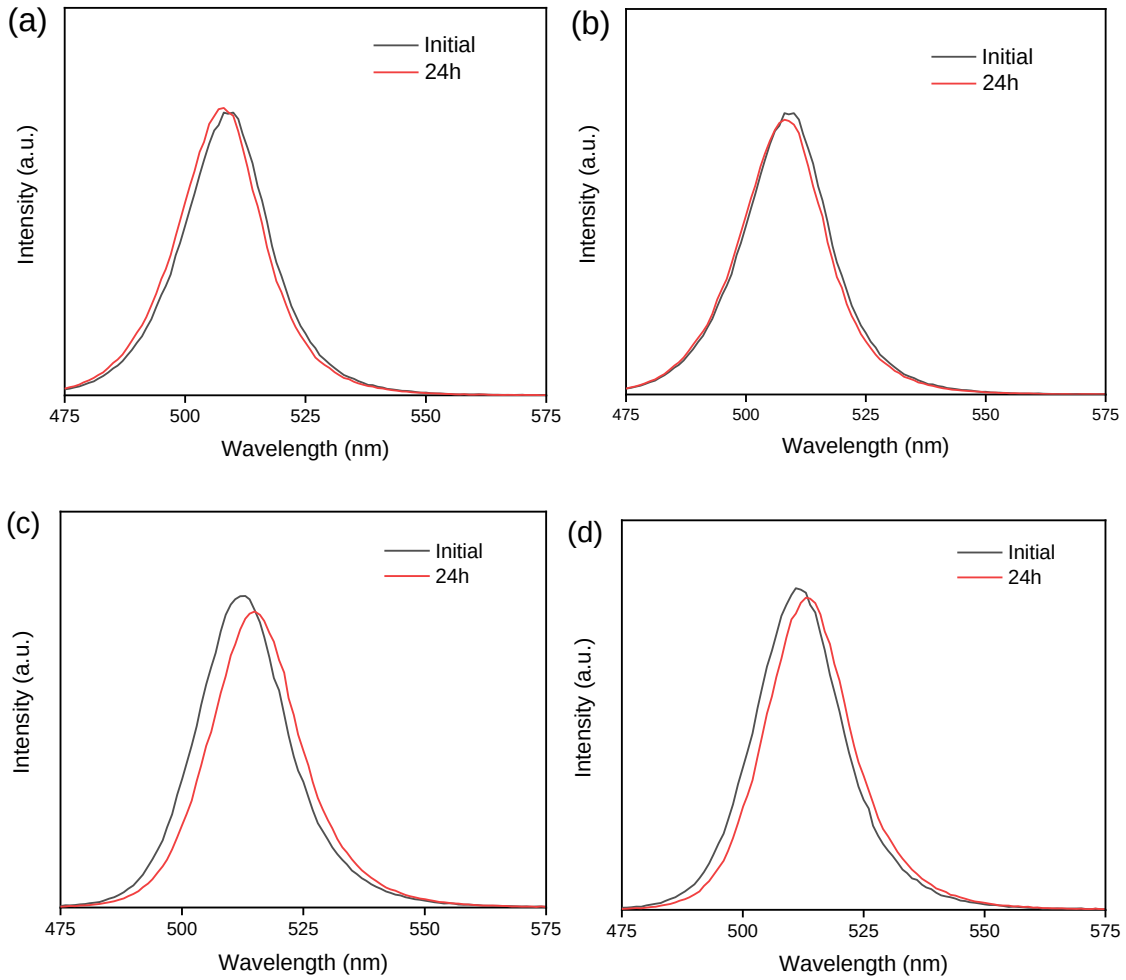

Fig. 4.13. PL quenching of $CsPbBr_3$s in ACN and 1,3,5-Trimethoxybenzene obtained from (a) DBIA, (b) NBA, (c) DBHT, (d) NBS

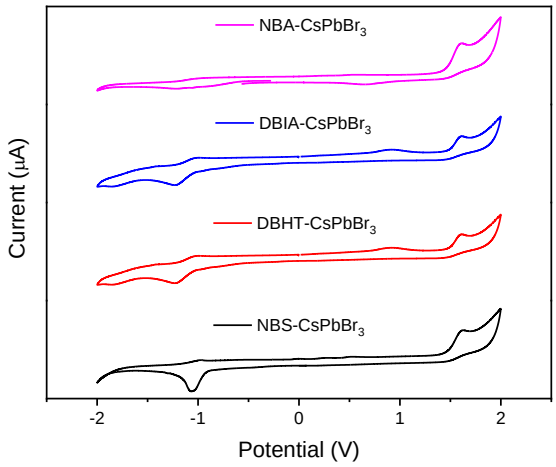

Fig. 4.14. Cyclic voltammetry of $CsPbBr_3$

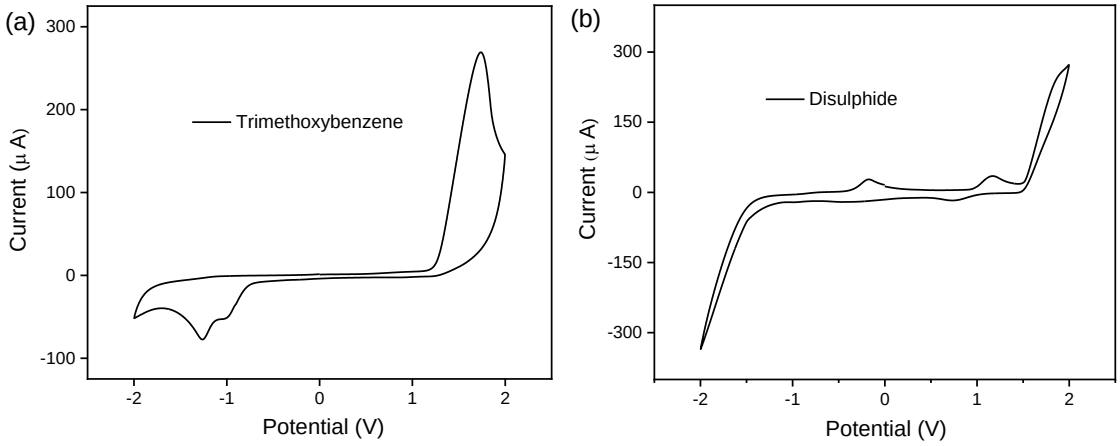

Fig. 4.15. Cyclic voltammetry of (a) TMB and (b) Disulphide

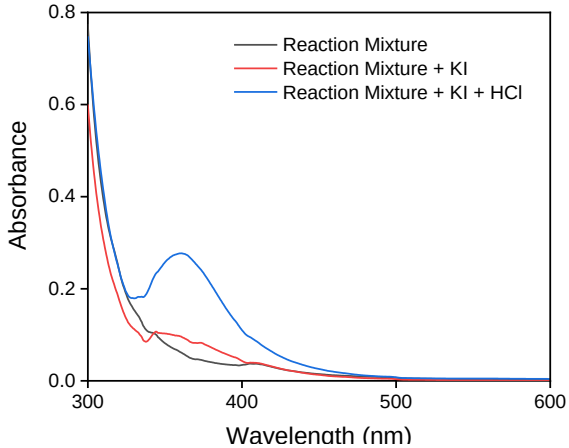

Fig. 4.16. UV-Vis spectroscopy for H_2O_2 generation

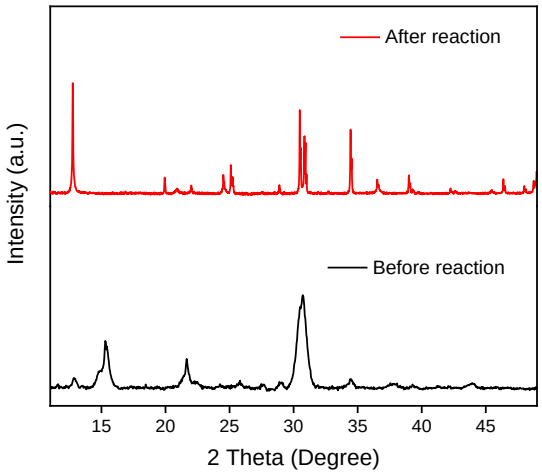

Fig. 4.17. PXRD of DBIA-$CsPbBr_3$ before and after reaction

Synthesis

Representative procedure for the preparation of Phenyl(2,4,6-trimethoxyphenyl)sulfane (3aa).

In an oven dried quartz tube 1,3,5-trimethoxybenzene **1a** (0.35 mmol, 60 mg), 1,2-diphenyldisulfane (0.43 mmol, 94 mg), and $CsPbBr_3$ (5 mol %, 0.0178 mmol) were dissolved in 2.0 mL dry acetonitrile solvent. After that, the reaction mixture was irradiated by visible light (wavelength 450-455 nm) for 18 h in the presence of an oxygen balloon. After completion of the reaction, acetonitrile was removed under reduced pressure. Then, the crude mixture was diluted in dichloromethane (CH_2Cl_2) and extracted with brine solution. The resulting organic solution was dried over anhydrous sodium sulfate and concentrated to obtain a crude mixture which was further purified by silica-gel column chromatography using distilled ethyl acetate and hexane as the eluent to afford the pure product.

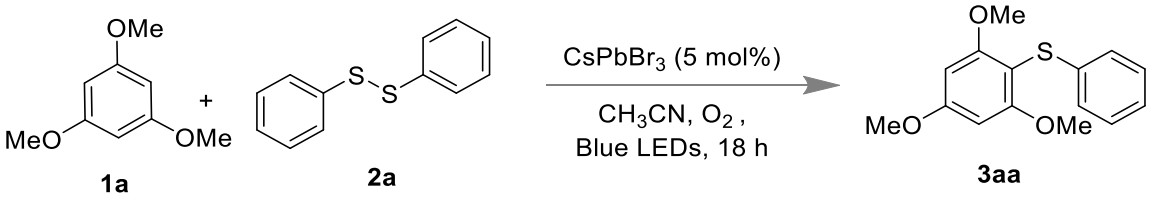

Scheme 4.1. Synthesis of **3aa**.

Synthetic procedure for compound 5. A 20 mL Schlenk tube holding a magnetic bar was charged with a 2 mL DCM solution of phenyl(2,4,6-trimethoxyphenyl)sulfane **3aa** (60 mg, 0.217 mmol) and *m*CPBA(41 mg, 0.24 mmol) was added under argon atmosphere and stirred at -78 °C for 12 h. After the completion of the reaction, solution was quenched with H_2O and then extracted with DCM, dried over Na_2SO_4 and concentrated in rotary evaporator. The crude

mixture was further purified by column chromatography to afford 1,3,5-trimethoxy-2-(phenylsulfinyl)benzene **5** (35 mg, 67%) as a white solid.

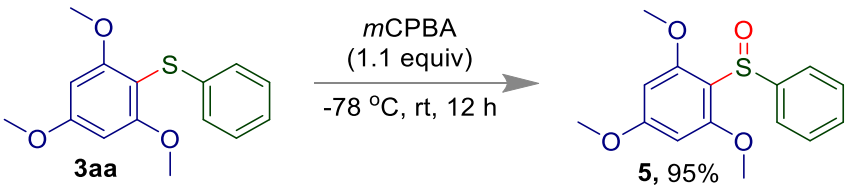

Scheme 4.2. Synthesis of compound **5**

Synthetic procedure for compound 6. A 20 mL Schlenk tube holding a magnetic bar was charged with (4-bromophenyl)(2,4,6-trimethoxyphenyl)sulfane **3 al** (0.169 mmol, 60 mg), phenyl boronic acid (0.203 mmol, 25 mg), K_2CO_3 (0.507 mmol, 70 mg), and $Pd(PPh_3)_2Cl_2$ (0.08 mmol, 6 mg) in dioxane/H_2O (1.5 mL/0.5 mL) under inert atmosphere. Then the reaction mixture was placed into a preheated oil bath at 100 °C for 24 h. After that, the crude mixture was extracted with EtOAc, dried over Na_2SO_4 and concentrated in rotary evaporator. The crude mixture was further purified by column chromatography to afford **6** (29 mg, 52%) as a white solid.

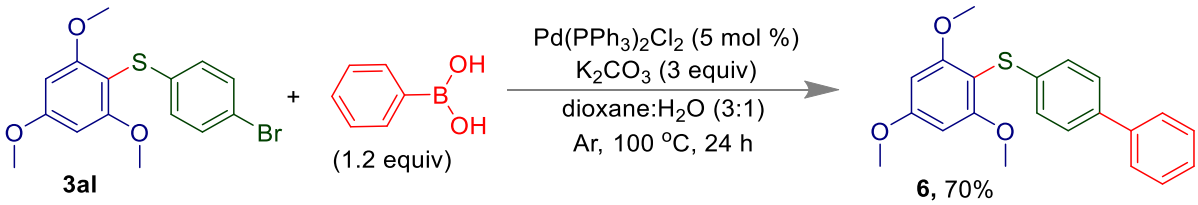

Scheme 4.3. Synthesis of compound **6**

Table 4.1. The Reaction Condition Optimization[b]

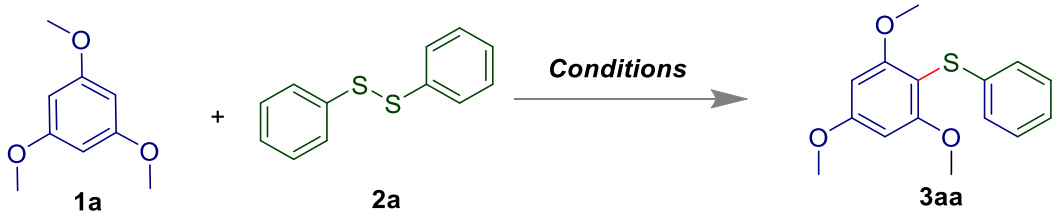

entry	2a (equiv)	$CsPbBr_3$ (mol%)	solvent	light source	yield[a] (%)
1	1.2	3 (DBIA-$CsPbBr_3$)	CH_3CN	Blue LED	75
2	1.2	3 (DBIA-$CsPbBr_3$)	DMSO	Blue LED	0
3	1.2	3 (DBIA-$CsPbBr_3$)	DMF	Blue LED	0
4	1.2	3 (DBIA-$CsPbBr_3$)	Toluene	Blue LED	0
5	1.2	3 (DBIA-$CsPbBr_3$)	THF	Blue LED	0
6	1.2	3 (DBIA-$CsPbBr_3$)	MeOH	Blue LED	30
7	1.2	3 (DBIA-$CsPbBr_3$)	DCE	Blue LED	70
8	0.6	3 (DBIA-$CsPbBr_3$)	CH_3CN	Blue LED	40
9	0.6	5 (DBIA-$CsPbBr_3$)	CH_3CN	Blue LED	50
10	1.2	5 (DBIA-$CsPbBr_3$)	CH_3CN	Blue LED	80
11	1.2	5 (DBIA-$CsPbBr_3$)	CH_3CN	Blue LED	88[c]
12	1.2	5 (NBA-$CsPbBr_3$)	CH_3CN	Blue LED	75
13	1.2	5 (DBHT-$CsPbBr_3$)	CH_3CN	Blue LED	51
14	1.2	5 (NBS-$CsPbBr_3$)	CH_3CN	Blue LED	57

[a]Isolated yields after column chromatography, [b]Reaction conditions: **1a** (60 mg, 0.35 mmol), **2a** (94 mg, 0.43 mmol) and $CsPbBr_3$ (5 mol%) in 1.5 mL of CH_3CN for 18 h, [c]In dry CH_3CN.

Radical trapping experiment with TEMPO/BHT/Diphenylethelene. In an oven dried quartz tube 1,3,5-trimethoxybenzene **1a** (0.35 mmol, 60 mg), 1,2-diphenyldisulfane **2a** (0.43

mmol, 94 mg), and $CsPbBr_3$ (5 mol %, 0.0178 mmol) were dissolved in 2.0 mL dry acetonitrile (ACN) solvent and TEMPO (1.07 mmol, 167 mg) were dissolved in 1.0 mL dry acetonitrile (ACN) solvent. After that, the reaction mixture was irradiated by Blue LEDs light for 18 h in the presence of an oxygen balloon. The reaction was monitored by TLC. After the reaction time, no desired product was found. The same experiment was carried out using BHT (235 mg, 1.07 mmol) and 1,1-diphenylethylene (193 mg, 1.07 mmol). However, the addition of BHT led to no product formation whereas diphenylethylene reduced the yield of the product **3aa** giving only 10% (5 mg).

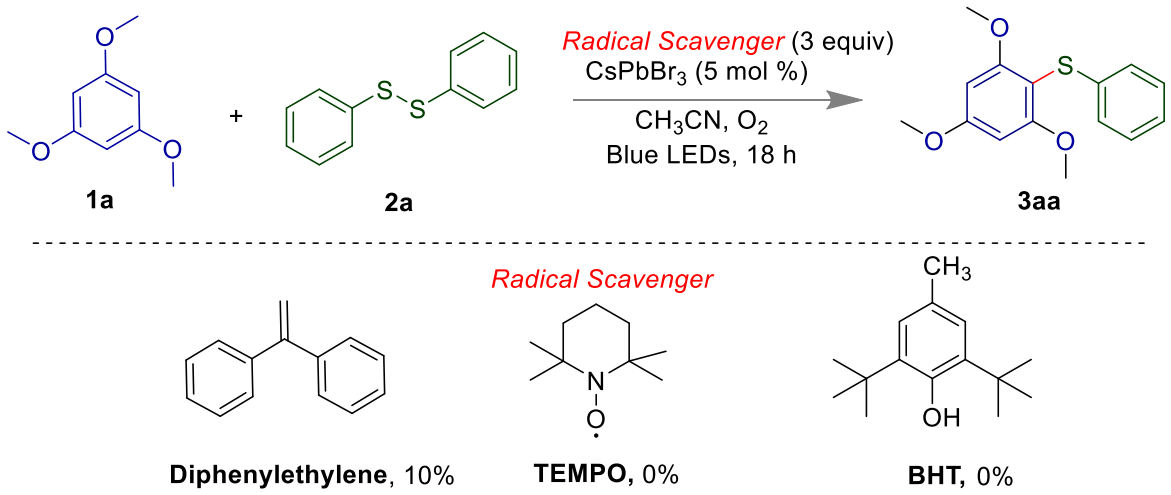

Scheme 4.4. Various radical scavengers under standard condition.

Light ON-OFF-ON Experiment. In an oven dried quartz tube 1,3,5-trimethoxybenzene **1a** (0.35 mmol, 60 mg), 1,2-diphenyldisulfane **2a** (0.43 mmol, 94 mg), and $CsPbBr_3$ (5 mol %, 0.0178 mmol) were dissolved in 2.0 mL dry acetonitrile (ACN) solvent. After that, the reaction mixture was irradiated by Blue LEDs light for 18 h in the presence of an oxygen balloon. Successive progress of the reaction was monitored every 6 h and 3 h in the presence of light and absence of light by ^1H NMR experiment using $CDCl_3$ as an internal standard.

Spin-trapping experiment in the presence DMPO.[52] A mixture of 1,3,5-trimethoxybenzene **1a** (0.35 mmol, 60 mg), 1,2-diphenyldisulfane **2a** (0.43 mmol, 94 mg), and $CsPbBr_3$ (5 mol %, 0.0178 mmol) were dissolved in 2.0 mL dry acetonitrile (ACN) solvent. After that, the reaction mixture was irradiated by Blue LEDs light for 2 h in the presence of an oxygen balloon. Afterwards, 300 μL solution was quickly transferred into EPR tube to analyze EPR no signal was observed. Then 5,5-dimethyl-1- pyrroline-N-oxide (DMPO) (20 μL) was add to the reaction mixture. Afterwards, 300 μL solution was quickly transferred into EPR tube to analyze EPR. Appearance of sharp signal indicated the presence of radical intermediate.

Crystal measurement

Crystals of compound **3ah** was achieved after slow evaporation of $CHCl_3$ and water mixture (1:0.5). The crystals data were collected with Bruker SMART D8 goniometer equipped with an APEX CCD detector and with an INCOATEC micro source (Mo-Kα radiation, λ = 0.71073 Å). ORTEP drawing of the compound **3ah** show ellipsoid contour at the 50% probability level.

Compound 3ah (CCDC 2205394)

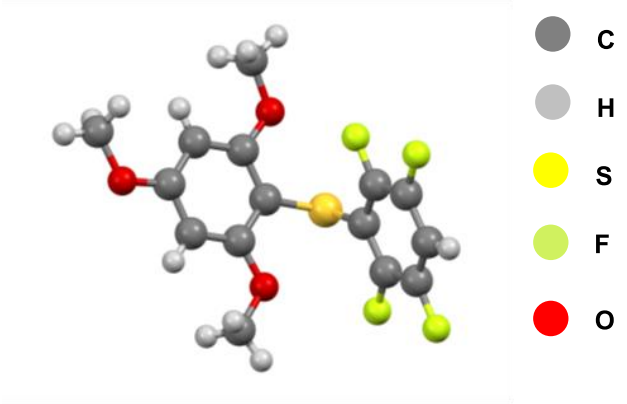

Fig. 4.18. Crystal structure of **3ah** (CCDC 2205394). Ellipsoids are drawn at the 50% probability level.

Crystallographic Data for (3ah)

Empirical formula	$C_{15}H_{12}F_4O_3S$
Formula weight	348.31
Temperature/K	100.00(10)
Crystal system	triclinic
Space group	P-1
a/Å	6.9500(4)
b/Å	9.8071(6)
c/Å	11.6221(5)
α/°	90.667(4)
β/°	105.074(4)
γ/°	107.794(5)
Volume/Å3	724.72(7)
Z	2
ρcalcg/cm^3	1.596
μ/mm^{-1}	0.280

F(000)	356.0
Crystal size/mm^3	0.2 × 0.1 × 0.1
Radiation	Mo Kα (λ = 0.71073)
Reflections collected	13243
Independent reflections	3515 [R_{int} = 0.0378, R_{sigma} = 0.0319]
Goodness-of-fit on F2	0.992
Final R indexes [I>=2σ (I)]	R_1 = 0.0313, wR_2 = 0.0803
Final R indexes [all data]	R_1 = 0.0356, wR_2 = 0.0827
Largest diff. peak/hole / e Å^{-3}	0.36/-0.31

CHARATERIZATION DATA

Phenyl(2,4,6-trimethoxyphenyl)sulfane (3aa): R_f = 0.45 (5% ethyl acetate in hexane); white solid; yield 88% (43 mg); ^{1}H NMR (400 MHz, $CDCl_3$) δ 7.18-7.13 (m, 2H), 7.05-7.01 (m, 3H), 6.22 (s, 2H), 3.87 (s, 3H), 3.81 (s, 6H); ^{13}C NMR (100 MHz, $CDCl_3$) δ 163.1, 162.7, 138.8, 128.6, 125.8, 124.5, 98.9, 91.3, 56.4 , 55.6.

***p*-Tolyl(2,4,6-trimethoxyphenyl)sulfane (3ab):**[67] R_f = 0.5 (5% ethyl acetate in hexane); white solid; yield 91% (95 mg); ^{1}H NMR (400 MHz, $CDCl_3$) δ 6.98-6.93 (m, 4H), 6.21 (s, 2H), 3.86 (s, 3H), 3.81 (s, 6H), 2.25 (s, 3H); ^{13}C NMR (100 MHz, $CDCl_3$) δ 162.9, 162.6, 135.1, 134.2, 129.4, 126.1, 99.5, 91.3, 56.4, 55.5, 21.0.

***o*-Tolyl(2,4,6-trimethoxyphenyl)sulfane (3ac):**[68] R_f = 0.45 (5% ethyl acetate in hexane); white solid; yield 89% (92 mg); ^{1}H NMR (400 MHz, $CDCl_3$) δ 7.10-7.08 (m, 1H), 6.97-6.91 (m, 2H), 6.59- 6.56 (m, 1H), 6.23 (s, 2H), 3.88 (s, 3H), 3.80 (s, 6H), 2.46 (s, 3H); ^{13}C NMR

(100 MHz, $CDCl_3$) δ 163.1, 162.7, 137.7, 134.84, 129.8, 126.1, 124.6, 124.2, 98.5, 91.4, 56.4, 55.5, 20.1.

(4-Methoxyphenyl)(2,4,6-trimethoxyphenyl)sulfane(3ad):[68] R_f = 0.55 (10% ethyl acetate in hexane); white solid; yield 94% (105 mg); ^{1}H NMR (700 MHz, $CDCl_3$) δ 7.07-7.06 (m, 2H), 6.74-6.72 (m, 2H), 6.19 (s, 2H), 3.85 (s, 3H), 3.81 (s, 6H), 3.74 (s, 3H); ^{13}C NMR (175 MHz, $CDCl_3$) δ 162.7, 162.4, 157.6, 129.3, 128.68, 114.3, 100.7, 91.3, 56.4, 55.5, 55.4.

(2-Methoxyphenyl)(2,4,6-trimethoxyphenyl)sulfane (3ae):[68] R_f = 0.55 (10% ethyl acetate in hexane); white solid; yield 92% (100 mg); ^{1}H NMR (700 MHz, $CDCl_3$) δ 7.02-7.00 (m, 1H), 6.80-6.79 (m, 1H), 6.72-6.70 (m, 1H), 6.48-6.47 (m, 1H), 6.23 (s, 2H), 3.90 (s, 3H), 3.88 (s, 3H), 3.79 (s, 6H); ^{13}C NMR (175 MHz, $CDCl_3$) δ 163.1, 163, 155.6, 127.3, 124.9, 124.8, 120.9, 109.9, 97.4, 91.3, 56.4, 55.7, 55.5.

(4-Fluorophenyl)(2,4,6-trimethoxyphenyl)sulfane (3af):[68] R_f = 0.5 (5% ethyl acetate in hexane); white solid; yield 72% (76 mg); ^{1}H NMR (700 MHz, $CDCl_3$) δ 7.03-7.01 (m, 2H), 6.87-6.85 (m, 2H), 6.20 (s, 2H), 3.86 (s, 3H), 3.81 (s, 6H); ^{13}C NMR (175 MHz, $CDCl_3$) δ 163, 162.4, 160.88 (d, J = 243.2 Hz), 133.72 (d, J = 3.0 Hz), 127.97 (d, J = 7.7 Hz), 115.63 (d, J = 22.0 Hz), 99.4, 91.3, 56.4, 55.5.

(2-Fluorophenyl)(2,4,6-trimethoxyphenyl)sulfane (3ag): R_f = 0.4 (5% ethyl acetate in hexane); white solid; yield 69% (73 mg); mp 115-118 ºC; ^{1}H NMR (700 MHz, $CDCl_3$) δ 7.05-6.96 (m, 2H), 6.89-6.87 (m, 1H), 6.68-6.65 (m, 1H), 6.22 (s, 2H), 3.87 (s, 3H), 3.81 (s, 6H); ^{13}C NMR (175 MHz, $CDCl_3$) δ 163.2, 162.8, 159.60 (d, J = 243.6 Hz), 127.42 (d, J = 2.7 Hz), 126.10 (d, J = 16.7 Hz), 125.81 (d, J = 7.4 Hz), 124.17 (d, J = 3.4 Hz), 115.16 (d, J = 21.2 Hz),

96.9, 91.4, 56.4, 55.5; IR (KBr) ῡ 2967, 2940, 1582, 815; HRMS (ESI/Q-TOF) m/z: $[M + Na]^+$ calcd for $C_{15}H_{15}FO_3SNa$ 317.0607; found 317.0624.

(2,3,5,6-Tetrafluorophenyl)(2,4,6-trimethoxyphenyl)sulfane (3ah): R_f = 0.4 (5% ethyl acetate in hexane); white solid; yield 68% (85 mg); mp 102-104 ºC; ^{1}H NMR (700 MHz, $CDCl_3$) δ 6.92-6.87 (m, 1H), 6.12 (s, 2H), 3.82 (s, 9H); ^{13}C NMR (175 MHz, $CDCl_3$) δ 162.7, 161.6, 146.9(m), 146.30 (m), 145.5(m), 144.9 (m), 117.4, 104.3(m), 98.0, 91.0, 56.1, 55.3; IR (KBr) ῡ 2916, 2847, 2359, 1584, 709; HRMS (ESI/Q-TOF) m/z: $[M + Na]^+$ calcd for $C_{15}H_{12}F_4O_3SNa$ 371.0341; found 371.0319.

(4-Chlorophenyl)(2,4,6-trimethoxyphenyl)sulfane (3ai):[67] R_f = 0.4 (5% ethyl acetate in hexane); white solid; yield 77% (85 mg); ^{1}H NMR (400 MHz, $CDCl_3$) δ 7.28-7.26 (m, 2H), 6.90-6.89 (m, 2H), 6.23 (s, 2H), 3.89 (s, 3H), 3.82 (s, 6H); ^{13}C NMR (100 MHz, $CDCl_3$) δ 163.3, 162.5, 138.2, 131.5, 127.4, 117.9, 98.2, 91.3, 56.4, 55.6.

(3-Chlorophenyl)(2,4,6-trimethoxyphenyl)sulfane (3aj):[68] R_f = 0.45 (5% ethyl acetate in hexane); white solid; yield 75% (82 mg); ^{1}H NMR (700 MHz, $CDCl_3$) δ 7.09-7.06 (m, 1H), 7.00-6.99 (m, 1H), 6.93-6.92 (m, 2H), 6.22 (s, 2H), 3.88 (s, 3H), 3.81 (s, 6H). ^{13}C NMR (175 MHz, $CDCl_3$) δ 163.4, 162.6, 141.2, 134.5, 129.6, 125.2, 124.6, 123.8, 97.7, 91.4, 56.4, 55.6.

(2,6-Dichlorophenyl)(2,4,6-trimethoxyphenyl)sulfane (3ak): R_f = 0.4 (5% ethyl acetate in hexane); white solid; yield 65% (80 mg); mp 85-90 ºC; ^{1}H NMR (700 MHz, $CDCl_3$) δ 7.27-7.26 (m, 2H), 7.06-7.03 (m, 1H), 6.10 (s, 2H), 3.80 (s, 3H), 3.73 (s, 6H); ^{13}C NMR (175 MHz, $CDCl_3$) δ 161.8, 160.9, 139.2, 134.4, 128.4, 128.1, 101.5, 91.3, 56.1, 55.4; IR (KBr) ῡ 2921,

2848, 2360, 1582, 731; HRMS (ESI/Q-TOF) m/z: $[M + Na]^+$ calcd for $C_{15}H_{14}Cl_2O_3SNa$ 366.9859; found 366.9838.

(4-Bromophenyl)(2,4,6-trimethoxyphenyl)sulfane (3al):[67] R_f = 0.45 (5% ethyl acetate in hexane); white solid; yield 79% (100 mg); ^{1}H NMR (400 MHz, $CDCl_3$) δ 7.12-7.10 (m, 2H), 6.95-6.94 (m, 2H), 6.21 (s, 2H), 3.87 (s, 3H), 3.81 (s, 6H); ^{13}C NMR (175 MHz, $CDCl_3$) δ 163.1, 162.4, 137.4, 130.0, 128.5, 126.9, 98.3, 91.2, 56.3, 55.4.

(4-(Trifluoromethyl)phenyl)(2,4,6-trimethoxyphenyl)sulfane (3am):[69] R_f = 0.5 (5% ethyl acetate in hexane); white solid; yield 61% (75 mg); ^{1}H NMR (700 MHz, $CDCl_3$) δ 7.38-7.37 (m, 2H), 7.06-7.05 (m, 2H), 6.23 (s, 2H), 3.89 (s, 3H), 3.81 (s, 6H); ^{13}C NMR (176 MHz, $CDCl_3$) δ 163.6, 162.7, 144.3, 127.6, 126.3, 125.4 (q, *J* = 3.7 Hz), 125.2, 97.1, 91.4, 56.5, 55.6.

(3,5-Bis(trifluoromethyl)phenyl)(2,4,6-trimethoxyphenyl)sulfane (3an): R_f = 0.4 (5% ethyl acetate in hexane); white solid; yield 57% (84 mg); mp 88-91 ºC; ^{1}H NMR (400 MHz, $CDCl_3$) δ 7.50 (s, 1H), 7.38 (s, 2H), 6.24 (s, 2H), 3.90 (s, 3H), 3.81 (s, 6H); ^{13}C NMR (175 MHz, $CDCl_3$) δ 163.9, 162.5, 142.7, 131.7 (q, *J* = 33.1 Hz), 125.3, 124.2, 122.6, 118.0 (q, *J* = 3.7 Hz), 95.9, 91.5, 56.4, 55.6; IR (KBr) ῡ 2918, 2850, 2360, 1582, 736; HRMS (ESI/Q-TOF) m/z: $[M\ ]^+$ calcd for $C_{17}H_{14}F_6O_3S$ 412.0568; found 412.0562.

2-((2,4,6-Trimethoxyphenyl)thio)pyridine (3ao): R_f = 0.6 (30% ethyl acetate in hexane); white solid; yield 50% (49 mg); mp 120-125 ºC; ^{1}H NMR (400 MHz, $CDCl_3$) δ 8.36-8.35 (m, 1H), 7.38-7.34 (m, 1H), 6.92-6.88 (m, 1H), 6.72 (d, *J* = 8.0 Hz, 1H), 6.23 (s, 2H), 3.87 (s, 3H), 3.80 (s, 6H); ^{13}C NMR (100 MHz, $CDCl_3$) δ 163.3, 162.5, 161.9, 149.4, 136.2, 119.5, 119.0,

97.9, 91.4, 56.4, 55.6; IR (KBr) ῡ 2920, 2848, 2364, 1582, 761; HRMS (ESI/Q-TOF) m/z: [M + H]$^+$ calcd for $C_{14}H_{16}NO_3S$ 278.0851; found 278.0828.

2-((2,4,6-Trimethoxyphenyl)thio)thiophene (3ap):[70] R_f = 0.5 (5% ethyl acetate in hexane); white solid; yield 48% (49 mg); ^{1}H NMR (700 MHz, $CDCl_3$) δ 7.15 (m, 1H), 7.12-7.10 (m, 1H), 6.86-6.85 (m, 1H), 6.14 (s, 2H), 3.88 (s, 6H), 3.82 (s, 3H); ^{13}C NMR (175 MHz, $CDCl_3$) δ 162.8, 161.9, 137.2, 130.6, 127.2, 126.9, 102.8, 91.2, 56.3, 55.5.

Naphthalen-1-yl(2,4,6-trimethoxyphenyl)sulfane(3aq):[67] R_f = 0.45 (5% ethyl acetate in hexane); white solid; yield 75% (87 mg); ^{1}H NMR (700 MHz, $CDCl_3$) δ 8.46 (d, *J* = 8.4 Hz, 1H), 7.80 (d, *J* = 8.0 Hz, 1H), 7.56 (d, *J* = 8.1 Hz, 1H), 7.53 (t, *J* = 7.5 Hz, 1H), 7.48 (t, *J* = 7.4 Hz, 1H), 7.21 (t, *J* = 7.7 Hz, 1H), 6.84 (d, *J* = 7.3 Hz, 1H), 6.25 (s, 2H), 3.89 (s, 3H), 3.79 (s, 6H); ^{13}C NMR (175 MHz, $CDCl_3$) δ 163.18, 162.8, 135.8, 133.8, 131.2, 128.3, 126.0, 125.8, 125.7, 125.0, 124.6, 122.5, 98.3, 91.5, 56.4, 55.5.

Phenyl(2,4,6-trimethoxyphenyl)selane (3as):[71] R_f = 0.5 (5% ethyl acetate in hexane); white solid; yield 79% (91 mg); ^{1}H NMR (700 MHz, $CDCl_3$) δ 7.21-7.19 (m, 2H), 7.13 (t, *J* = 7.5 Hz, 2H), 7.09-7.07 (m, 1H), 6.21 (s, 2H), 3.86 (s, 3H), 3.78 (s, 6H); ^{13}C NMR (176 MHz, $CDCl_3$) δ 163.2, 162.2, 133.8, 129.2, 128.8, 125.4, 97.7, 91.5, 56.4, 55.6.

1,3,5-Trimethoxy-2-(phenylsulfinyl)benzene (5):[72] R_f = 0.5 (40% ethyl acetate in hexane); white solid; yield 95% (60 mg); ^{1}H NMR (700 MHz, $CDCl_3$) δ 7.54 (d, *J* = 7.8 Hz, 2H), 7.38-7.36 (t, *J* = 7.6 Hz, 2H), 7.33-7.31 (t, *J* = 7.2 Hz, 1H), 6.04 (s, 2H), 3.79 (s, 3H), 3.67 (s, 6H); ^{13}C NMR (176 MHz, $CDCl_3$) δ 165.2, 161.5, 145.4, 129.0, 128.1, 124.3, 112.8, 91.3, 56.0, 55.6.

[1,1'-Biphenyl]-4-yl(2,4,6-trimethoxyphenyl)sulfane (6):[73] R_f = 0.5 (5% ethyl acetate in hexane); white solid; yield 70% (42 mg); ^{1}H NMR (700 MHz, $CDCl_3$) δ 7.33-7.26 (m, 6H), 7.05-7.03 (m, 3H), 6.22 (s, 2H), 3.88 (s, 3H), 3.81 (s, 6H); ^{13}C NMR (176 MHz, $CDCl_3$) δ 163.1, 162.7, 137.7, 137.1, 131.4, 126.9, 126.59, 126.58, 126.5, 126.1, 98.7, 91.4, 56.5, 55.6.

(4-(Phenylethynyl)phenyl)(2,4,6-trimethoxyphenyl)sulfane (7): R_f = 0.5 (5% ethyl acetate in hexane); white solid; yield 75% (48 mg); mp 127-131 ºC; ^{1}H NMR (400 MHz, $CDCl_3$) δ 7.50-7.48 (m, 2H), 7.32-7.26 (m, 5H), 6.98-6.96 (m, 2H), 6.23 (s, 2H), 3.89 (s, 3H), 3.81 (s, 6H); ^{13}C NMR (100 MHz, $CDCl_3$) δ 163.3, 162.6, 139.9, 131.8, 131.6, 128.4, 128.2, 125.4, 123.6, 119.0, 98.0, 91.4, 89.7, 89.2, 56.5, 55.6; IR (KBr) ῡ 3100, 2928, 1589, 1226, 728; HRMS (ESI/Q-TOF) m/z: $[M + Na]^+$ calcd for $C_{23}H_{20}O_3SNa$ 399.1031; found 399.1048.

4.6 NOTES AND REFERENCES

(1) Fu, Y.; Zhu, H.; Chen, J.; Hautzinger, M. P.; Zhu, X. Y.; Jin, S. Metal Halide Perovskite Nanostructures for Optoelectronic Applications and the Study of Physical Properties. *Nat. Rev. Mater.* **2019**, *4*, 169-188.

(2) Al-Ashouri, A.; Köhnen, E.; Li, B.; Magomedov, A.; Hempel, H.; Caprioglio, P.; Márquez, J. A.; Morales Vilches, A. B.; Kasparavicius, E.; Smith, J. A., et al. Monolithic Perovskite/Silicon Tandem Solar Cell with >29% Efficiency by Enhanced Hole Extraction. *Science* **2020**, *370*, 1300-1309.

(3) Lu, H.; Liu, Y.; Ahlawat, P.; Mishra, A.; Tress, W. R.; Eickemeyer, F. T.; Yang, Y.; Fu, F.; Wang, Z.; Avalos, C. E., et al. Vapor-Assisted Deposition of Highly Efficient, Stable Black-Phase Fapbi3 Perovskite Solar Cells. *Science* **2020**, *370*, eabb8985.

(4) Jeong, J.; Kim, M.; Seo, J.; Lu, H.; Ahlawat, P.; Mishra, A.; Yang, Y.; Hope, M. A.; Eickemeyer, F. T.; Kim, M., et al. Pseudo-Halide Anion Engineering for A-Fapbi3 Perovskite Solar Cells. *Nature* **2021**, *592*, 381-385.

(5) Garai, R.; Gupta, R. K.; Hossain, M.; Iyer, P. K. Surface Recrystallized Stable 2d–3d Graded Perovskite Solar Cells for Efficiency Beyond 21%. *J. Mater. Chem. A* **2021**, *9*, 26069-26076.

(6) Kim, H.; Zhao, L.; Price, J. S.; Grede, A. J.; Roh, K.; Brigeman, A. N.; Lopez, M.; Rand, B. P.; Giebink, N. C. Hybrid Perovskite Light Emitting Diodes under Intense Electrical Excitation. *Nat. Commun.* **2018**, *9*, 4893.

(7) Cho, H.; Jeong, S.-H.; Park, M.-H.; Kim, Y.-H.; Wolf, C.; Lee, C.-L.; Heo, J. H.; Sadhanala, A.; Myoung, N.; Yoo, S., et al. Overcoming the Electroluminescence Efficiency Limitations of Perovskite Light-Emitting Diodes. *Science* **2015**, *350*, 1222-1225.

(8) Zhang, Q.; Shang, Q.; Su, R.; Do, T. T. H.; Xiong, Q. Halide Perovskite Semiconductor Lasers: Materials, Cavity Design, and Low Threshold. *Nano Lett.* **2021**, *21*, 1903-1914.

(9) Zhizhchenko, A.; Syubaev, S.; Berestennikov, A.; Yulin, A. V.; Porfirev, A.; Pushkarev, A.; Shishkin, I.; Golokhvast, K.; Bogdanov, A. A.; Zakhidov, A. A., et al. Single-Mode Lasing from Imprinted Halide-Perovskite Microdisks. *ACS Nano* **2019**, *13*, 4140-4147.

(10) Deng, W.; Huang, L.; Xu, X.; Zhang, X.; Jin, X.; Lee, S.-T.; Jie, J. Ultrahigh-Responsivity Photodetectors from Perovskite Nanowire Arrays for Sequentially Tunable Spectral Measurement. *Nano Lett.* **2017**, *17*, 2482-2489.

(11) Kumar, A.; Kumar, A.; Krishnan, V. Perovskite Oxide Based Materials for Energy and Environment-Oriented Photocatalysis. *ACS Catal.* **2020**, *10*, 10253-10315.

(12) Sun, Q.-M.; Xu, J.-J.; Tao, F.-F.; Ye, W.; Zhou, C.; He, J.-H.; Lu, J.-M. Boosted Inner Surface Charge Transfer in Perovskite Nanodots@Mesoporous Titania Frameworks for Efficient and Selective Photocatalytic Co2 Reduction to Methane. *Angew. Chem. Int. Ed.* **2022**, *61*, e202200872.

(13) Huang, H.; Pradhan, B.; Hofkens, J.; Roeffaers, M. B. J.; Steele, J. A. Solar-Driven Metal Halide Perovskite Photocatalysis: Design, Stability, and Performance. *ACS Energy Lett.* **2020**, *5*, 1107-1123.

(14) Cardenas-Morcoso, D.; Gualdrón-Reyes, A. F.; Ferreira Vitoreti, A. B.; García-Tecedor, M.; Yoon, S. J.; Solis de la Fuente, M.; Mora-Seró, I.; Gimenez, S. Photocatalytic and Photoelectrochemical Degradation of Organic Compounds with

All-Inorganic Metal Halide Perovskite Quantum Dots. *J. Phys. Chem. Lett.* **2019**, *10*, 630-636.

(15) Quan, L. N.; Rand, B. P.; Friend, R. H.; Mhaisalkar, S. G.; Lee, T.-W.; Sargent, E. H. Perovskites for Next-Generation Optical Sources. *Chem. Rev.* **2019**, *119*, 7444-7477.

(16) Gurung, B.; Pradhan, S.; Sharma, D.; Bhujel, D.; Basel, S.; Chettri, S.; Rasaily, S.; Pariyar, A.; Tamang, S. Cspbbr3 Perovskite Quantum Dots as a Visible Light Photocatalyst for Cyclisation of Diamines and Amino Alcohols: An Efficient Approach to Synthesize Imidazolidines, Fused-Imidazolidines and Oxazolidines. *Catal. Sci. Technol.* **2022**, *12*, 5891-5898.

(17) Shi, A.; Sun, K.; Chen, X.; Qu, L.; Zhao, Y.; Yu, B. Perovskite as Recyclable Photocatalyst for Annulation Reaction of N-Sulfonyl Ketimines. *Org. Lett.* **2022**, *24*, 299-303.

(18) Wu, W.-B.; Wong, Y.-C.; Tan, Z.-K.; Wu, J. Photo-Induced Thiol Coupling and C–H Activation Using Nanocrystalline Lead-Halide Perovskite Catalysts. *Catal. Sci. Technol.* **2018**, *8*, 4257-4263.

(19) Wang, K.; Lu, H.; Zhu, X.; Lin, Y.; Beard, M. C.; Yan, Y.; Chen, X. Ultrafast Reaction Mechanisms in Perovskite Based Photocatalytic C–C Coupling. *ACS Energy Lett.* **2020**, *5*, 566-571.

(20) Zhu, X.; Lin, Y.; Sun, Y.; Beard, M. C.; Yan, Y. Lead-Halide Perovskites for Photocatalytic A-Alkylation of Aldehydes. *J. Am. Chem. Soc.* **2019**, *141*, 733-738.

(21) Li, Y.; Wang, T.; Wang, Y.; Deng, Z.; Zhang, L.; Zhu, A.; Huang, Y.; Zhang, C.; Yuan, M.; Xie, W. Tunable Photocatalytic Two-Electron Shuttle between Paired Redox Sites on Halide Perovskite Nanocrystals. *ACS Catal.* **2022**, *12*, 5903-5910.

(22) Tlili, A.; Lakhdar, S. Acridinium Salts and Cyanoarenes as Powerful Photocatalysts: Opportunities in Organic Synthesis. *Angew. Chem. Int. Ed.* **2021**, *60*, 19526-19549.

(23) Chan, A. Y.; Perry, I. B.; Bissonnette, N. B.; Buksh, B. F.; Edwards, G. A.; Frye, L. I.; Garry, O. L.; Lavagnino, M. N.; Li, B. X.; Liang, Y., et al. Metallaphotoredox: The Merger of Photoredox and Transition Metal Catalysis. *Chem. Rev.* **2022**, *122*, 1485-1542.

(24) Steele, J. A.; Braeckevelt, T.; Prakasam, V.; Degutis, G.; Yuan, H.; Jin, H.; Solano, E.; Puech, P.; Basak, S.; Pintor-Monroy, M. I., et al. An Embedded Interfacial Network Stabilizes Inorganic Cspbi3 Perovskite Thin Films. *Nat. Commun.* **2022**, *13*, 7513.

(25) Boyd, C. C.; Cheacharoen, R.; Leijtens, T.; McGehee, M. D. Understanding Degradation Mechanisms and Improving Stability of Perovskite Photovoltaics. *Chem. Rev.* **2019**, *119*, 3418-3451.

(26) Mateker, W. R.; McGehee, M. D. Progress in Understanding Degradation Mechanisms and Improving Stability in Organic Photovoltaics. *Adv. Mater.* **2017**, *29*, 1603940.

(27) Zhang, Z.; Tian, X.; Wang, C.; Jin, J.; Jiang, Y.; Zhou, Q.; Zhu, J.; Xu, J.; He, R.; Huang, Y., et al. Revealing Superoxide-Induced Degradation in Lead-Free Tin Perovskite Solar Cells. *Energy Environ. Sci.* **2022**, *15*, 5274-5283.

(28) Wang, R.; Mujahid, M.; Duan, Y.; Wang, Z.-K.; Xue, J.; Yang, Y. A Review of Perovskites Solar Cell Stability. *Adv. Funct. Mater.* **2019**, *29*, 1808843.

(29) Otero-Martínez, C.; Fiuza-Maneiro, N.; Polavarapu, L. Enhancing the Intrinsic and Extrinsic Stability of Halide Perovskite Nanocrystals for Efficient and Durable Optoelectronics. *ACS Appl. Mater. Interfaces* **2022**, *14*, 34291-34302.

(30) Slotcavage, D. J.; Karunadasa, H. I.; McGehee, M. D. Light-Induced Phase Segregation in Halide-Perovskite Absorbers. *ACS Energy Lett.* **2016**, *1*, 1199-1205.

(31) Kim, B. J.; Kim, D. H.; Kwon, S. L.; Park, S. Y.; Li, Z.; Zhu, K.; Jung, H. S. Selective Dissolution of Halide Perovskites as a Step Towards Recycling Solar Cells. *Nat. Commun.* **2016**, *7*, 11735.

(32) Akkerman, Q. A.; Rainò, G.; Kovalenko, M. V.; Manna, L. Genesis, Challenges and Opportunities for Colloidal Lead Halide Perovskite Nanocrystals. *Nat. Mater.* **2018**, *17*, 394-405.

(33) Boudreault, P.-L. T.; Najari, A.; Leclerc, M. Processable Low-Bandgap Polymers for Photovoltaic Applications. *Chem. Mater.* **2011**, *23*, 456-469.

(34) Qiu, R.; Reddy, V. P.; Iwasaki, T.; Kambe, N. The Palladium-Catalyzed Intermolecular C-H Chalcogenation of Arenes. *J. Org. Chem.* **2015**, *80*, 367-374.

(35) Zhao, C.; Rakesh, K. P.; Ravidar, L.; Fang, W.-Y.; Qin, H.-L. Pharmaceutical and Medicinal Significance of Sulfur (Svi)-Containing Motifs for Drug Discovery: A Critical Review. *Eur. J. Med. Chem.* **2019**, *162*, 679-734.

(36) Gandeepan, P.; Koeller, J.; Ackermann, L. Expedient C–H Chalcogenation of Indolines and Indoles by Positional-Selective Copper Catalysis. *ACS Catal.* **2017**, *7*, 1030-1034.

(37) Sharma, U. K.; Gemoets, H. P. L.; Schröder, F.; Noël, T.; Van der Eycken, E. V. Merger of Visible-Light Photoredox Catalysis and C–H Activation for the Room-Temperature C-2 Acylation of Indoles in Batch and Flow. *ACS Catal.* **2017**, *7*, 3818-3823.

(38) Qin, Y.; Zhu, L.; Luo, S. Organocatalysis in Inert C–H Bond Functionalization. *Chem. Rev.* **2017**, *117*, 9433-9520.

(39) Pramanik, M.; Choudhuri, K.; Mal, P. Metal-Free C–S Coupling of Thiols and Disulfides. *Org. Biomol. Chem.* **2020**, *18*, 8771-8792.

(40) Choudhuri, K.; Pramanik, M.; Mal, P. Noncovalent Interactions in C–S Bond Formation Reactions. *J. Org. Chem.* **2020**, *85*, 11997-12011.

(41) Sinha, S. K.; Panja, S.; Grover, J.; Hazra, P. S.; Pandit, S.; Bairagi, Y.; Zhang, X.; Maiti, D. Dual Ligand Enabled Nondirected C–H Chalcogenation of Arenes and Heteroarenes. *J. Am. Chem. Soc.* **2022**, *144*, 12032-12042.

(42) Huang, Z.; Zhang, D.; Qi, X.; Yan, Z.; Wang, M.; Yan, H.; Lei, A. Radical-Radical Cross-Coupling for C-S Bond Formation. *Org Lett* **2016**, *18*, 2351-2354.

(43) Protesescu, L.; Yakunin, S.; Bodnarchuk, M. I.; Krieg, F.; Caputo, R.; Hendon, C. H.; Yang, R. X.; Walsh, A.; Kovalenko, M. V. Nanocrystals of Cesium Lead Halide Perovskites (Cspbx3, X = Cl, Br, and I): Novel Optoelectronic Materials Showing Bright Emission with Wide Color Gamut. *Nano Lett.* **2015**, *15*, 3692-3696.

(44) Vighnesh, K.; Wang, S.; Liu, H.; Rogach, A. L. Hot-Injection Synthesis Protocol for Green-Emitting Cesium Lead Bromide Perovskite Nanocrystals. *ACS Nano* **2022**, *16*, 19618-19625.

(45) Manna, A.; Dinda, T. K.; Ghosh, S.; Mal, P. Cspbbr3 in the Activation of the C–Br Bond of Cbrx3 (X = Cl, Br) under Sunlight. *Chem. Mater.* **2023**, *35*, 628-637.

(46) Zhang, B.; Altamura, D.; Caliandro, R.; Giannini, C.; Peng, L.; De Trizio, L.; Manna, L. Stable Cspbbr3 Nanoclusters Feature a Disk-Like Shape and a Distorted Orthorhombic Structure. *J. Am. Chem. Soc.* **2022**, *144*, 5059-5066.

(47) Mahankudo, S. K.; Das, A.; Mishra, K.; Barai, M.; Mal, P.; Ghosh, S. Synthesis of Cs/Methylammonium/Formamidinium Pbbr3 Perovskite Nanocrystals with Green Emissions: Implications for Display Applications. *ACS Appl. Nano Mater.* **2022**, *5*, 4360-4366.

(48) Paul, S.; Samanta, A. N-Bromosuccinimide as Bromide Precursor for Direct Synthesis of Stable and Highly Luminescent Green-Emitting Perovskite Nanocrystals. *ACS Energy Lett.* **2020**, *5*, 64-69.

(49) Kim, J.; Yun, A. J.; Gil, B.; Lee, Y.; Park, B. Triamine-Based Aromatic Cation as a Novel Stabilizer for Efficient Perovskite Solar Cells. *Adv. Funct. Mater.* **2019**, *29*, 1905190.

(50) Dutt, V. G. V.; Akhil, S.; Mishra, N. Enhancement of Photoluminescence and the Stability of Cspbx3 (X = Cl, Br, and I) Perovskite Nanocrystals with Phthalimide Passivation. *Nanoscale* **2021**, *13*, 14442-14449.

(51) Imran, M.; Caligiuri, V.; Wang, M.; Goldoni, L.; Prato, M.; Krahne, R.; De Trizio, L.; Manna, L. Benzoyl Halides as Alternative Precursors for the Colloidal Synthesis of Lead-Based Halide Perovskite Nanocrystals. *J. Am. Chem. Soc.* **2018**, *140*, 2656-2664.

(52) Wang, H.; Li, Y.; Tang, Z.; Wang, S.; Zhang, H.; Cong, H.; Lei, A. Z-Selective Addition of Diaryl Phosphine Oxides to Alkynes Via Photoredox Catalysis. *ACS Catal.* **2018**, *8*, 10599-10605.

(53) Liang, G.; Wang, J.-H.; Lei, T.; Cheng, Y.-Y.; Zhou, C.; Chen, Y.-J.; Ye, C.; Chen, B.; Tung, C.-H.; Wu, L.-Z. Direct C–H Thiolation for Selective Cross-Coupling of Arenes with Thiophenols Via Aerobic Visible-Light Catalysis. *Org. Lett.* **2021**, *23*, 8082-8087.

(54) Ang, D.; Harmonis; Yuk; Ung; Ei, S. N.; On, A.; Eon; Ong, J. J. C.; Yuseok Determination of Triiodide Ion Concentration Using Uv-Visible Spectrophotometry. *Asian J. Chem.* **2014**, *26*, 4084-4086.

(55) Zhu, X.; Lin, Y.; San Martin, J.; Sun, Y.; Zhu, D.; Yan, Y. Lead Halide Perovskites for Photocatalytic Organic Synthesis. *Nat. Commun.* **2019**, *10*, 2843.

(56) Kumar, M.; Puri, A. A Review of Permissible Limits of Drinking Water. *Indian J. Occup. Environ. Med.* **2012**, *16*, 40-44.

(57) Bera, S.; Behera, R. K.; Pradhan, N. A-Halo Ketone for Polyhedral Perovskite Nanocrystals: Evolutions, Shape Conversions, Ligand Chemistry, and Self-Assembly. *J. Am. Chem. Soc.* **2020**, *142*, 20865-20874.

(58) Dutta, A.; Behera, R. K.; Pal, P.; Baitalik, S.; Pradhan, N. Near-Unity Photoluminescence Quantum Efficiency for All Cspbx3 (X=Cl, Br, and I) Perovskite

Nanocrystals: A Generic Synthesis Approach. *Angew. Chem. Int. Ed.* **2019**, *58*, 5552-5556.

(59) Pradhan, N. Tips and Twists in Making High Photoluminescence Quantum Yield Perovskite Nanocrystals. *ACS Energy Lett.* **2019**, *4*, 1634-1638.

(60) Stelmakh, A.; Aebli, M.; Baumketner, A.; Kovalenko, M. V. On the Mechanism of Alkylammonium Ligands Binding to the Surface of Cspbbr3 Nanocrystals. *Chem. Mater.* **2021**, *33*, 5962-5973.

(61) Shamsi, J.; Urban, A. S.; Imran, M.; De Trizio, L.; Manna, L. Metal Halide Perovskite Nanocrystals: Synthesis, Post-Synthesis Modifications, and Their Optical Properties. *Chem. Rev.* **2019**, *119*, 3296-3348.

(62) Bera, S.; Saha, A.; Mondal, S.; Biswas, A.; Mallick, S.; Chatterjee, R.; Roy, S. Review of Defect Engineering in Perovskites for Photovoltaic Application. *Mater. Adv.* **2022**, *3*, 5234-5247.

(63) Akhil, S.; Palabathuni, M.; Biswas, S.; Singh, R.; Mishra, N. Highly Stable Amine-Free Cspbbr3 Perovskite Nanocrystals for Perovskite-Based Display Applications. *ACS Appl. Nano Mater.* **2022**, *5*, 13561-13572.

(64) Pramanik, M.; Mathuri, A.; Mal, P. Sulfur···Oxygen Interaction-Controlled (Z)-Selective Anti-Markovnikov Vinyl Sulfides. *Chem. Commun.* **2021**, *57*, 5698-5701.

(65) Martin, R.; Buchwald, S. L. Palladium-Catalyzed Suzuki−Miyaura Cross-Coupling Reactions Employing Dialkylbiaryl Phosphine Ligands. *Acc. Chem. Res.* **2008**, *41*, 1461-1473.

(66) Chinchilla, R.; Nájera, C. The Sonogashira Reaction: A Booming Methodology in Synthetic Organic Chemistry. *Chem. Rev.* **2007**, *107*, 874-922.

(67) Parumala, S. K. R.; Peddinti, R. K. Iodine Catalyzed Cross-Dehydrogenative C–S Coupling by C(Sp2)–H Bond Activation: Direct Access to Aryl Sulfides from Aryl Thiols. *Green Chem.* **2015**, *17*, 4068-4072.

(68) Wang, X.-X.; Chen, C.; Shi, H.-Z.; Zhang, G.-W.; Tang, Y.; Zhang, C.-G.; Wu, M.-Y.; Feng, S. Metal-and Oxidant-Free Electrochemical Synthesis of Aryl Sulfides. *J. Electrochem. Soc.* **2021**, *168*, 015501.

(69) Feng, Q.; Chen, D.; Hong, M.; Wang, F.; Huang, S. Phenyliodine(Iii) Bis(Trifluoroacetate) (Pifa)-Mediated Synthesis of Aryl Sulfides in Water. *J. Org. Chem.* **2018**, *83*, 7553-7558.

(70) Mino, T.; Yoshizawa, E.; Watanabe, K.; Abe, T.; Hirai, K.; Sakamoto, M. Palladium-Catalyzed Decarboxylative Coupling of Benzoic Acid Derivatives Using Hydrazone Ligands. *Tetrahedron Lett.* **2014**, *55*, 3184-3188.

(71) Guo, Y.; Bao, H.; Chen, L.; Shi, J.; Li, Y. Diverse Synthesis of Triarylselenonium Salts and O-(Alkoxy)Aryl Aryl Selanes Via Insertion of Benzyne into the Se═O Bond. *Org. Lett.* **2022**, *24*, 6999-7003.

(72) Pradhan, S.; Patel, S.; Chatterjee, I. Nitrosoarene-Catalyzed Regioselective Aromatic C–H Sulfinylation with Thiols under Aerobic Conditions. *Chem. Commun.* **2020**, *56*, 5054-5057.

(73) Ravi, C.; Semwal, R.; Kumar, R.; Reddy, N. N. K.; Adimurthy, S. Iodine-Catalyzed One-Pot Decarboxylative Sulfenylation of Electron-Rich Arenes and Indoles. *ChemistrySelect* **2018**, *3*, 6116-6121.

NMR Spectrum of Selected Compounds

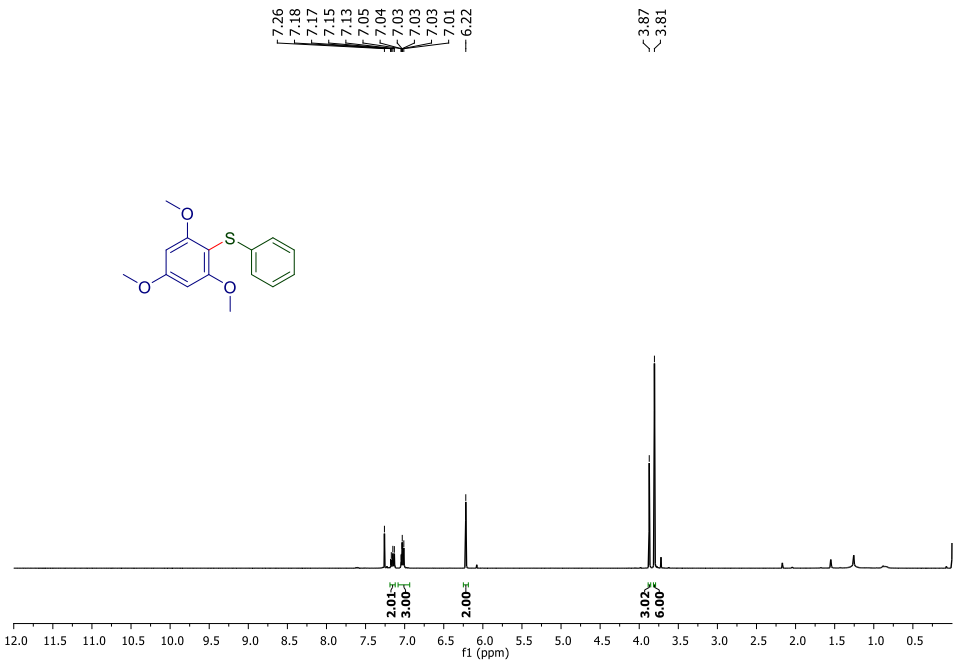

Fig. 4.19. ^{1}H NMR(400 MHz, $CDCl_3$) spectrum of phenyl(2,4,6-trimethoxyphenyl)sulfane (**3aa**)

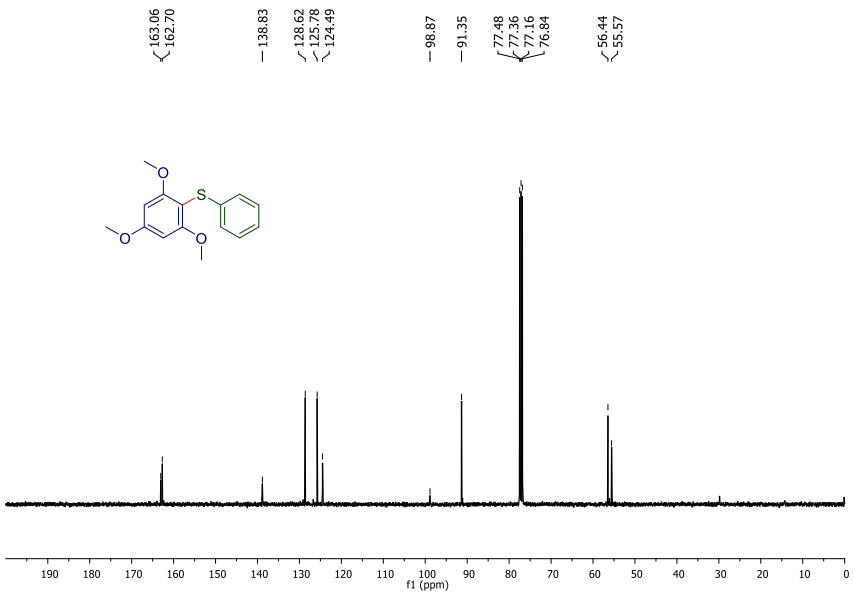

Fig. 4.20. $^{13}C\{^{1}H\}$ NMR (100 MHz, $CDCl_3$) spectrum of phenyl(2,4,6-trimethoxyphenyl)sulfane (**3aa**)

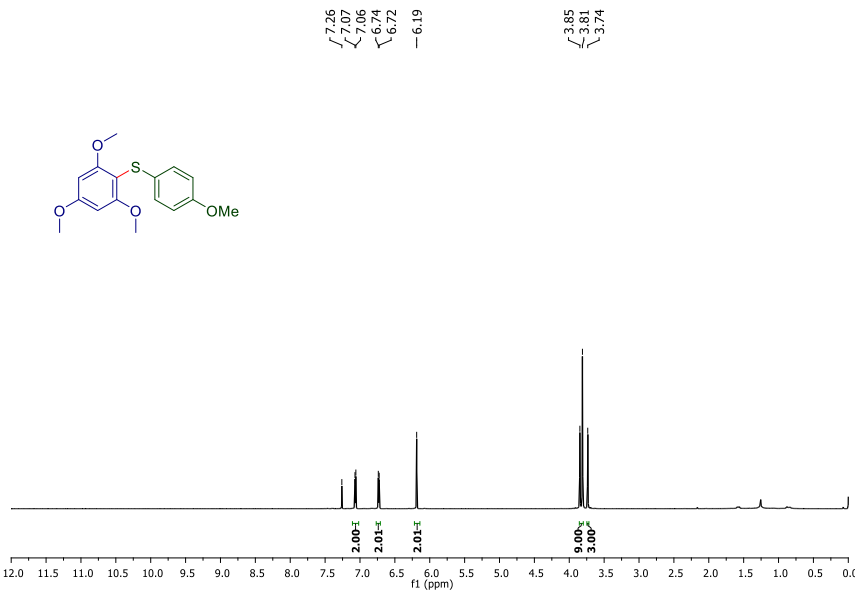

Fig. 4.21. ^{1}H NMR(700 MHz, $CDCl_3$) spectrum of (4-methoxyphenyl)(2,4,6-trimethoxyphenyl)sulfane (**3ad**)

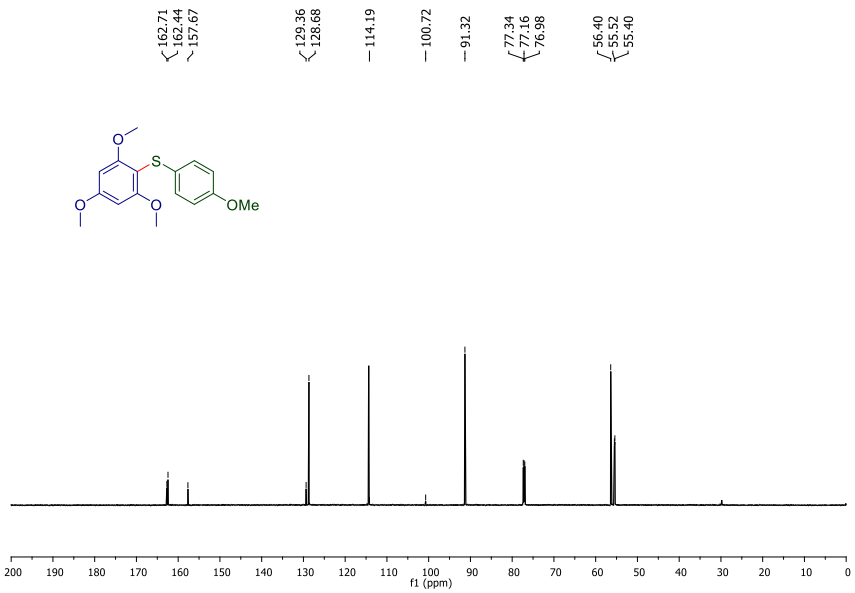

Fig. 4.22. $^{13}C\{^{1}H\}$ NMR (175 MHz, $CDCl_3$) spectrum of (4-methoxyphenyl)(2,4,6-trimethoxyphenyl)sulfane (**3ad**)

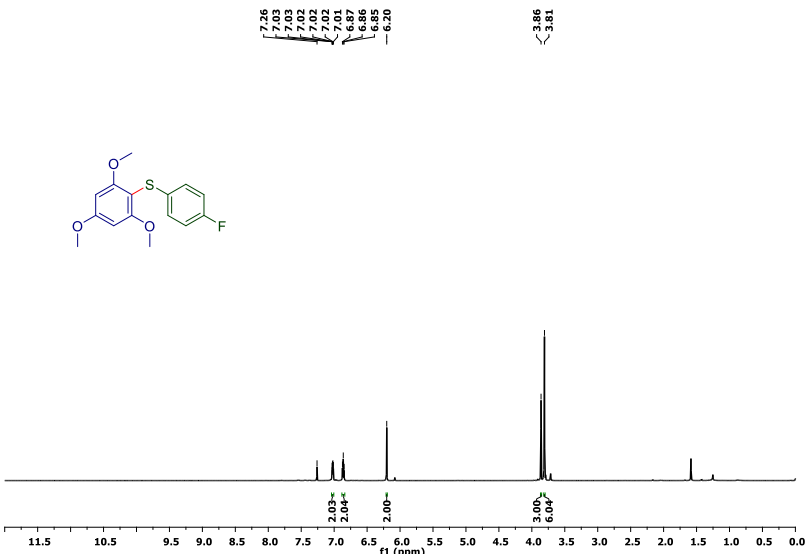

Fig. 4.23. ^{1}H NMR(700 MHz, $CDCl_3$) spectrum of (4-fluorophenyl)(2,4,6-trimethoxyphenyl)sulfane (**3af**)

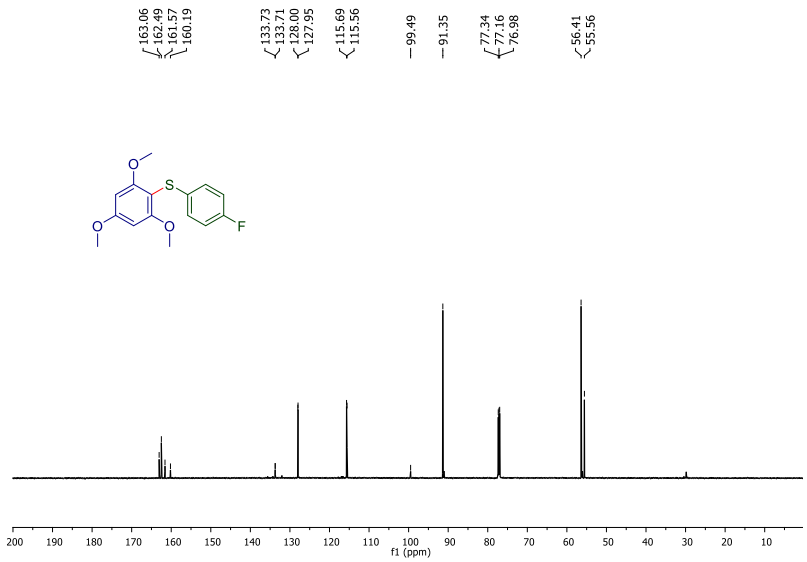

Fig. 4.24. $^{13}C\{^{1}H\}$ NMR (175 MHz, $CDCl_3$) spectrum of (4-fluorophenyl)(2,4,6-trimethoxyphenyl)sulfane (**3af**)

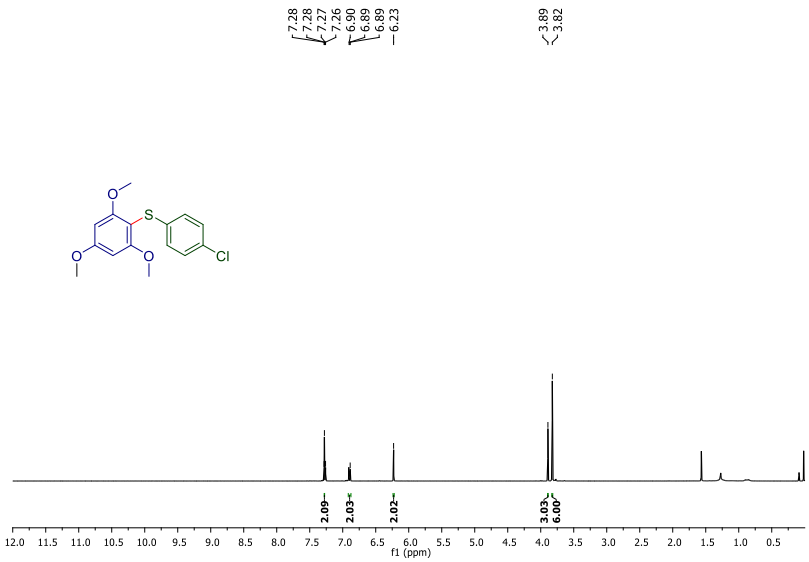

Fig. 4.25. ^{1}H NMR(700 MHz, $CDCl_3$) spectrum of (4-chlorophenyl)(2,4,6-trimethoxyphenyl)sulfane (**3ai**)

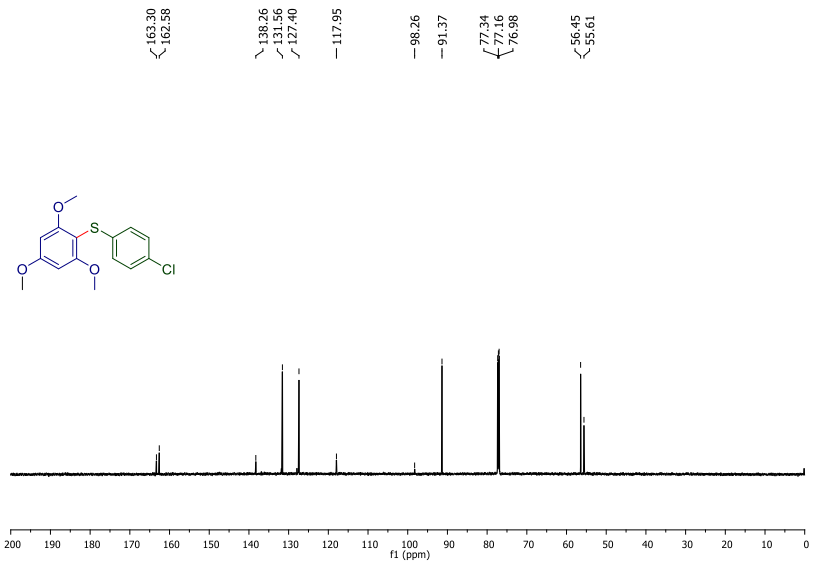

Fig. 4.26. $^{13}C\{^{1}H\}$ NMR (175 MHz, $CDCl_3$) spectrum of (4-chlorophenyl)(2,4,6-trimethoxyphenyl)sulfane (**3ai**)

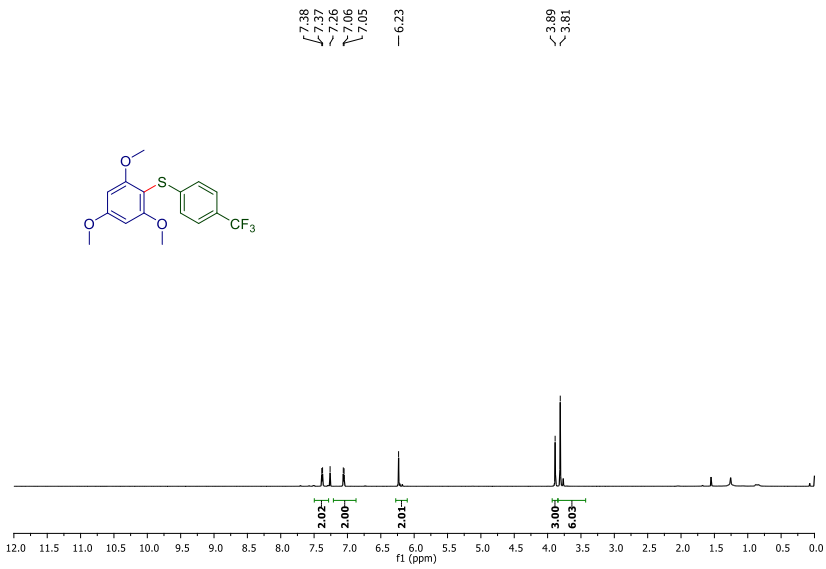

Fig. 4.27. ^{1}H NMR(700 MHz, $CDCl_3$) spectrum of (4-(trifluoromethyl)phenyl)(2,4,6-trimethoxyphenyl)sulfane (**3am**)

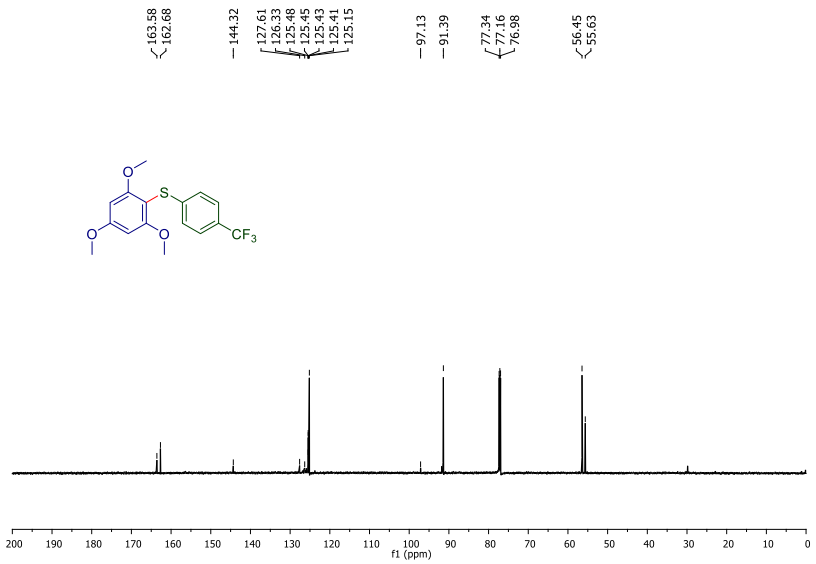

Fig. 4.28. $^{13}C\{^{1}H\}$ NMR (175 MHz, $CDCl_3$) spectrum of (4-(trifluoromethyl)phenyl)(2,4,6-trimethoxyphenyl)sulfane (**3am**)

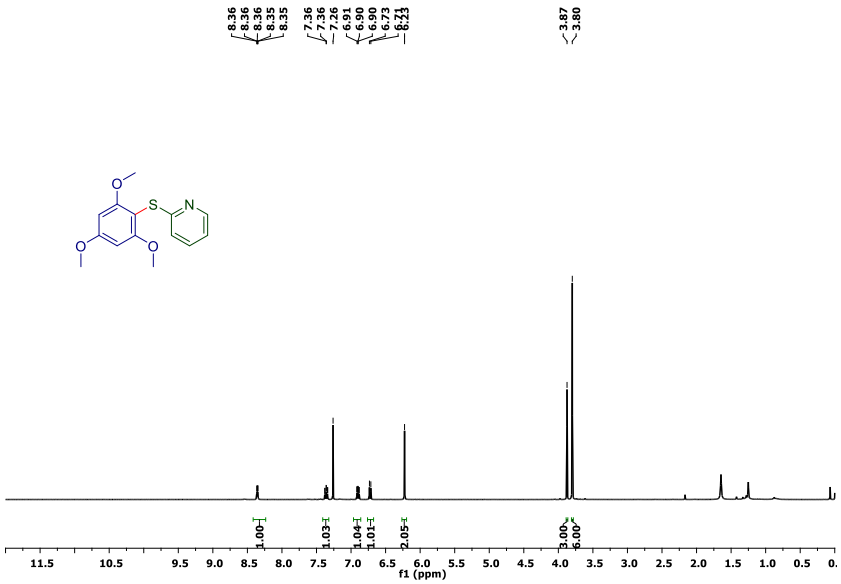

Fig. 4.29. ^{1}H NMR(400 MHz, $CDCl_3$) spectrum of 2-((2,4,6-trimethoxyphenyl)thio)pyridine (**3ao**)

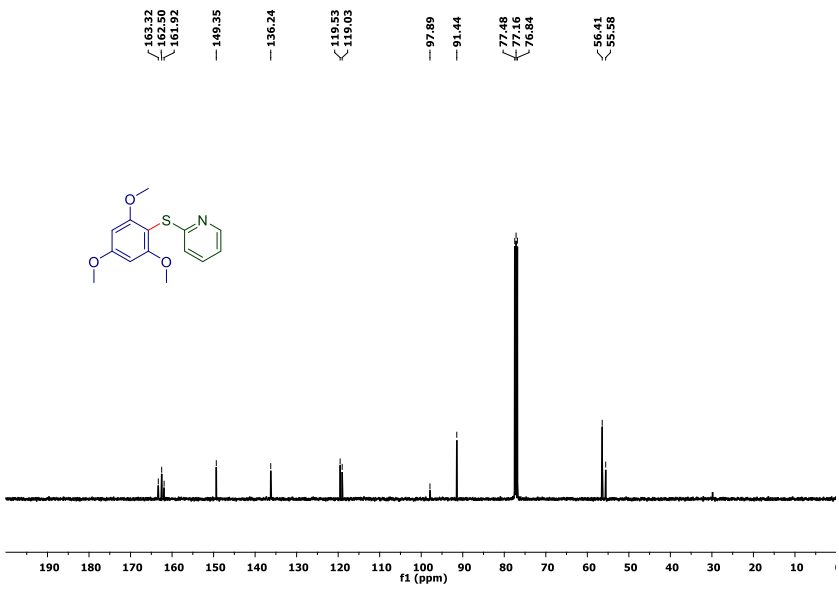

Fig. 4.30. $^{13}C\{^{1}H\}$ NMR (100 MHz, $CDCl_3$) spectrum of 2-((2,4,6-trimethoxyphenyl)thio)pyridine (**3ao**)

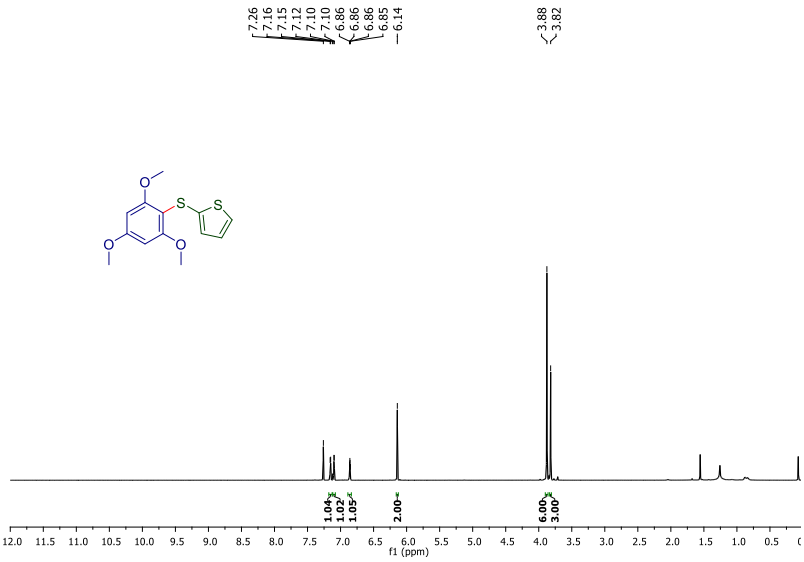

Fig. 4.31. ^{1}H NMR(700 MHz, $CDCl_3$) spectrum of 2-((2,4,6-trimethoxyphenyl)thio)thiophene (**3ap**)

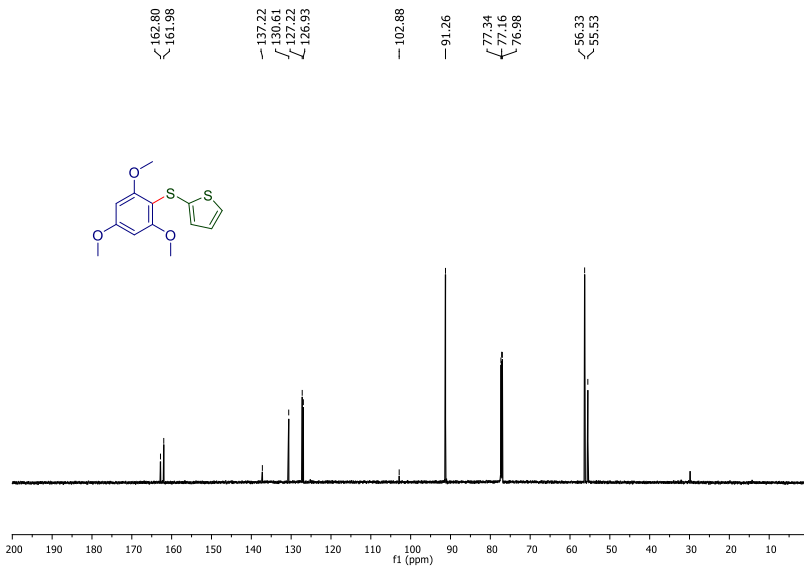

Fig. 4.32. $^{13}C\{^{1}H\}$ NMR (175 MHz, $CDCl_3$) spectrum of 2-((2,4,6-trimethoxyphenyl)thio)thiophene (**3ap**)

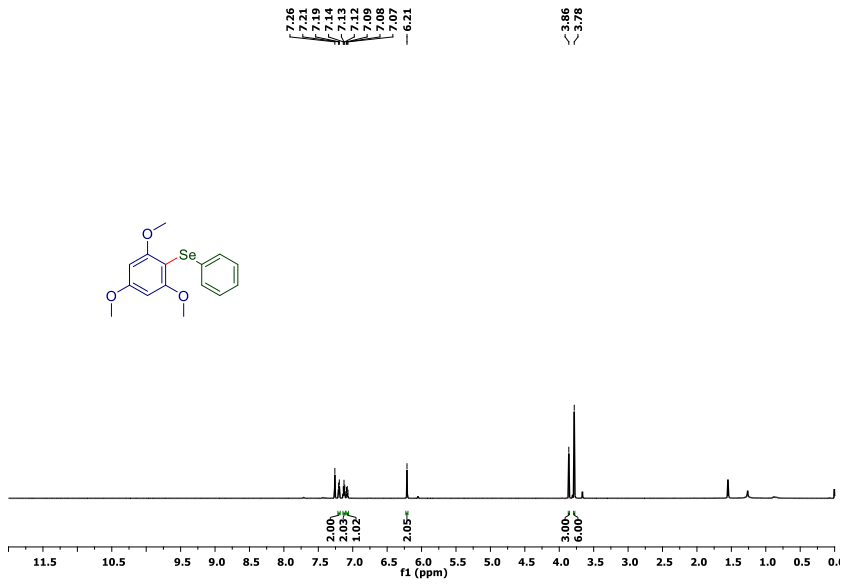

Fig. 4.33. ^{1}H NMR(700 MHz, $CDCl_3$) spectrum of phenyl(2,4,6-trimethoxyphenyl)selane (**3as**)

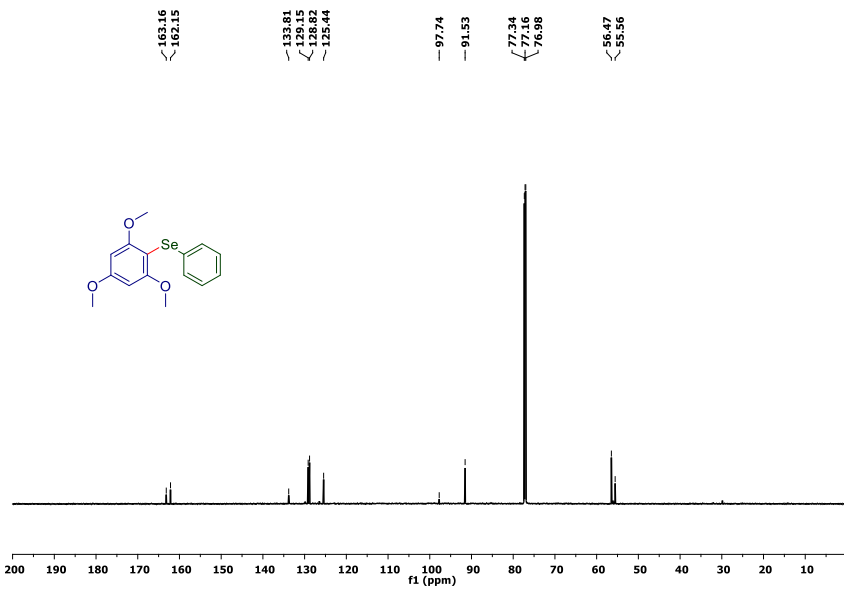

Fig. 4.34. $^{13}C\{^{1}H\}$ NMR (175 MHz, $CDCl_3$) spectrum of phenyl(2,4,6-trimethoxyphenyl)selane (**3as**)

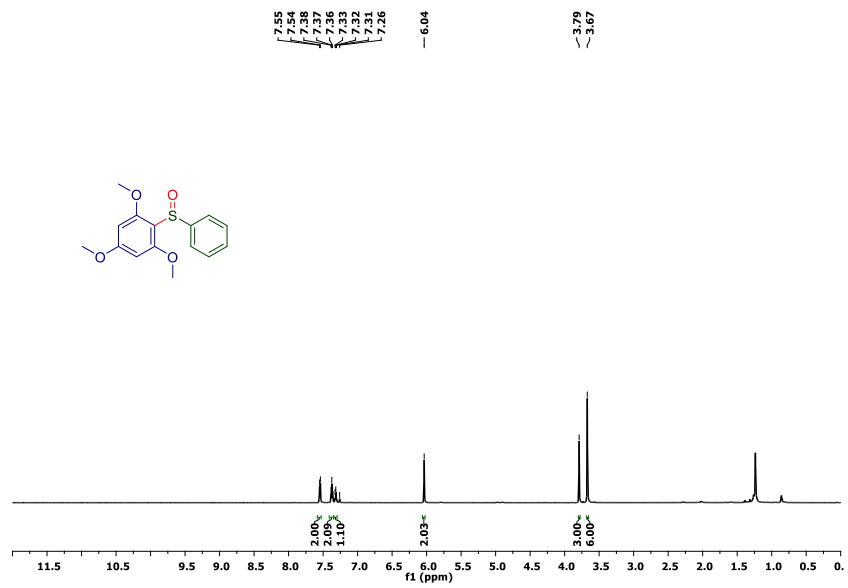

Fig. 4.35. ^{1}H NMR(700 MHz, $CDCl_3$) spectrum of 1,3,5-trimethoxy-2-(phenylsulfinyl)benzene (**5**)

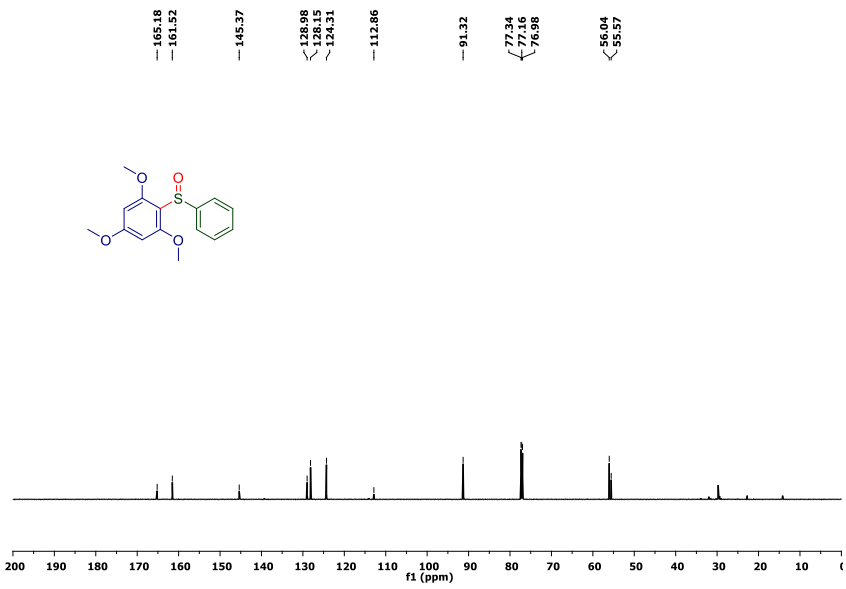

Fig. 4.36. $^{13}C\{^{1}H\}$ NMR (175 MHz, $CDCl_3$) spectrum of 1,3,5-trimethoxy-2-(phenylsulfinyl)benzene (**5**)

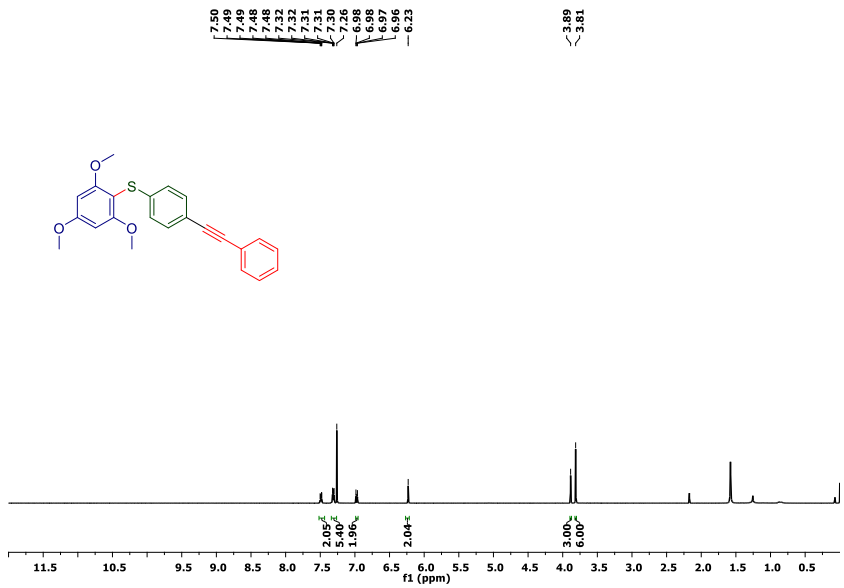

Fig. 4.37. ^{1}H NMR(400 MHz, $CDCl_3$) spectrum of (4-(phenylethynyl)phenyl)(2,4,6-trimethoxyphenyl)sulfane (**7**)

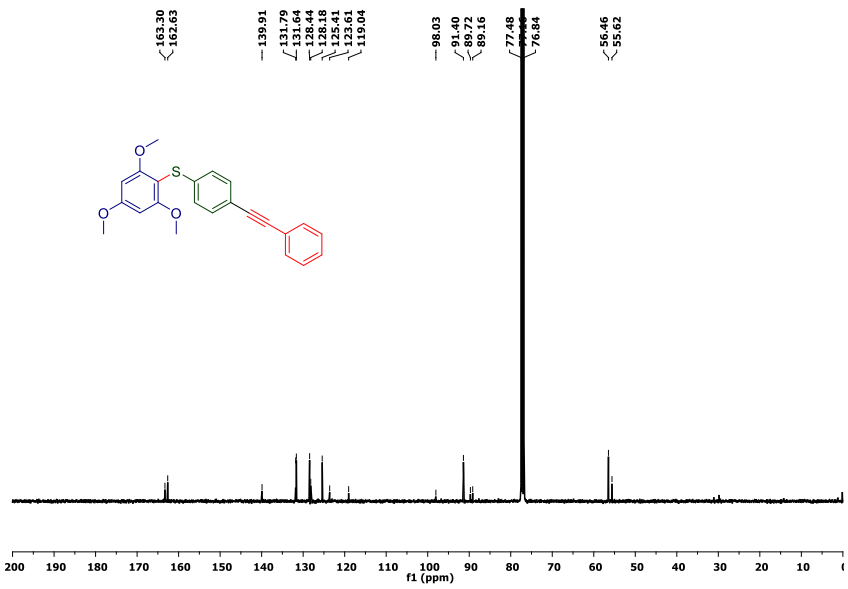

Fig. 4.38. $^{13}C\{^{1}H\}$ NMR (100 MHz, $CDCl_3$) spectrum of (4-(phenylethynyl)phenyl)(2,4,6-trimethoxyphenyl)sulfane (**7**)

CHAPTER 5

Chemodivergent Chalcogenation of Aryl Alkynoates or *N*-Arylpropynamides using 9-Mesityl-10-Methylacridinium Perchlorate Photocatalyst

5.1 ABSTRACT

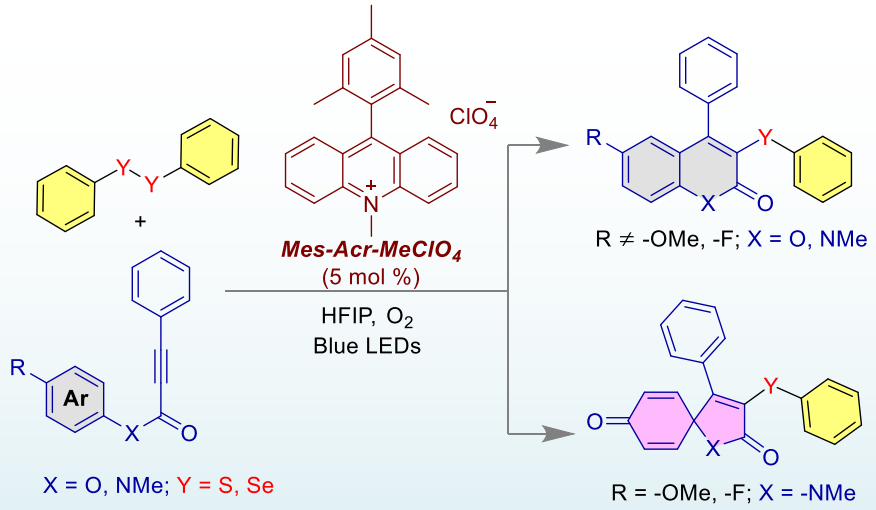

Herein we report a cascaded chalcogenation of aryl alkynoates or *N*-arylpropynamides using 9-mesityl-10-methylacridinium perchlorate as a visible light photocatalyst to obtain selectively, either 3-sulfenylated/selenylated coumarins or spiro[4,5]trienones. In a radical initiated process, the spiro-cyclization reaction was favored due to the presence of -OMe or -F substituent at the para position of the aryl group, that helped to stabilize the allylic radical intermediate formed during the reaction. Otherwise, 6-endo-trig cyclization led to 3-sulfenylated/selenylated coumarins.

5.2 INTRODUCTION

The broadening of photocatalytic organic transformation has been a fascinating area of research in recent years.[1] This approach to organic synthesis offers several advantages, including high atom economy, step economy, and unconventional synthesis strategies.[2] One of the most exciting developments in this area has been the use of organic dyes as photocatalysts.[3-6] These dyes are less expensive, readily accessible, and less toxic than transition metal complexes, making them excellent alternatives for use in photocatalysis.[7-8] Overall, the use of organic dyes as photocatalysts has greatly expanded the scope of photocatalytic organic transformations, offering a promising and sustainable approach to organic synthesis.

Chemodivergent reactions are reactions in which different products are formed from the same starting materials by altering the reaction conditions.[9] In addition, regiodivergent reactions have applications in the synthesis of complex organic molecules, as they allow for the selective formation of specific regioisomers.[10] These chemodivergent reactions represent an attractive area of research for the synthetic community, and the exploration of visible light-triggered chemodivergent reactions may offer exciting avenues for the development of new synthetic methods in organic synthesis.[11-13] However, visible-light-triggered chemodivergent reactions in organic synthesis remains largely unexplored.

Radical addition to activated alkynes for cascade cyclization has become an important tool in organic synthesis.[14-17] Arylalkynoates are a particularly useful class of precursors for these reactions, as they can undergo regio- and stereocontrolled radical additions to produce highly substituted cyclic products with a high degree of structural complexity.[18] Additionally, arylalkynoates can be easily synthesized from simple starting materials, making them readily accessible for use in organic synthesis.[19] Chang and co-workers have developed a Lewis acid mediated synthesis of 3-sulfenylated coumarins from arylalkynoates and N-

sulfanylsuccinimides using boron trifluoride etherate as a catalyst.[20] Baidya *et al.*, reported a peroxide-mediated synthesis of tetra-substituted α,β-unsaturated acids with chalcogen functionality.[21] Srimani's group has reported a visible light-induced synthesis of tetra-substituted α,β-unsaturated acids and diselenide olefins (Figure 1a).[22]

5.3 RESULT AND DISCUSSION

Herein we report an unprecedented visible light-induced cascaded chalcogenation of arylalkynoates and *N*-arylpropiolamides to afford 3-sulfenylated/selenylated coumarins or spiro[4,5]trienones (Figure 1b). A one-pot synthesis of C-S/C-Se, C-C, and C=O bonds has been shown using 9-mesityl-10-methylacridinium perchlorate as a photocatalyst, molecular oxygen as a terminal oxidant and carbonyl oxygen source, disulfide as a sulfenyl source, diselenide as a selenyl source, and blue light irradiation in HFIP solvent. The product selectivity of the reaction could be switched from 3-sulfenylated/selenylated coumarins to spiro[4,5]trienones by using different substituents on the aryl group of *N*-arylpropiolamides *via* either 6-endo-trig or 5-exo-trig cyclization pathways.

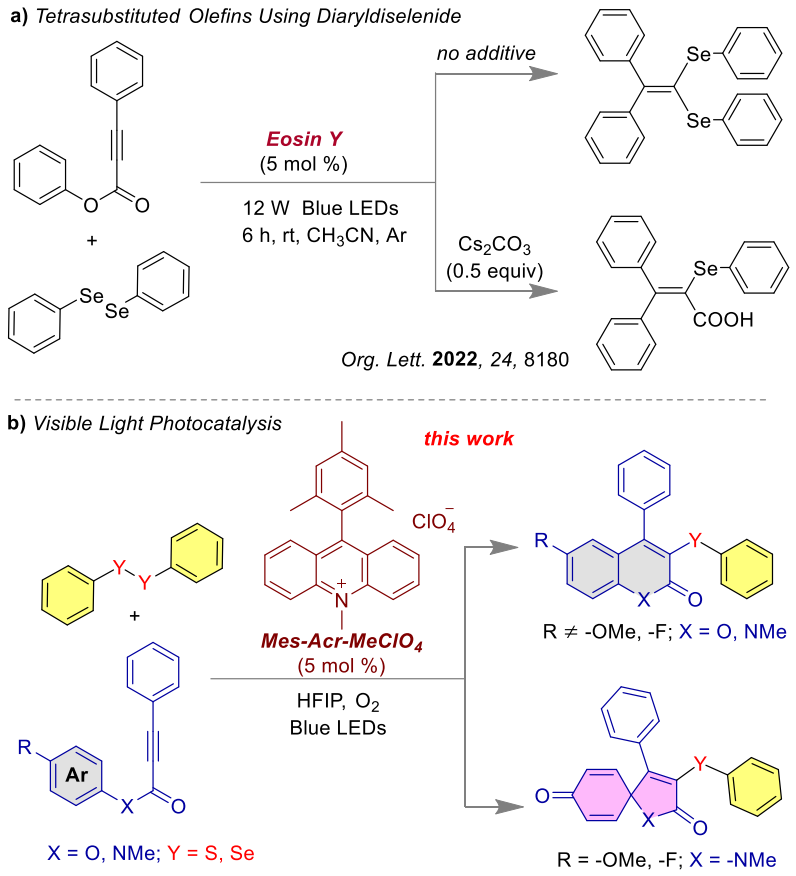

Figure 5.1. a) Tetra substituted selenylation using visible light photocatalyst.[22] b) Our work is based on photocatalytic chalcogenation of aryl alkynoates or *N*-phenyl propynamides.

Organochalcogenides containing C-S or C-Se bonds have a wide range of applications in the synthesis of bioactive molecules and functional materials.[23] For example, 3-sulfenylated coumarins have demonstrated significant biological activity, including hepatoprotective properties and estrogenic effects.[24] After establishing the optimal reaction conditions, the substrate scope was evaluated by using different arylpropiolates and diaryldisulfides or diaryldiselenides (Figure 2). The optimized reaction condition was established by the use of **1a** (0.270 mmol, 1 equiv), **2a** (0.29 mmol, 1.1 equiv), and 9-mesityl-10-methylacridinium perchlorate or Mes-Acr-MeClO$_4$ (0.013 mmol 5 mol %), in 1.5 mL of HFIP under O$_2$

atmosphere for 24 h using blue LEDs (entry 8, Table S1, supporting information). In the study, bis(4-methoxyphenyl)disulfide was chosen as the sulfenylating agent, which reacted with *para*-Me, -Et, -^{t}Bu substituted phenyl propiolates to produce a series of 3-sulfenylated coumarin derivatives (**3aa-3da**) with good yields ranging from 77% to 85%. The X-ray structure of the compound **3da** is shown in the Figure 2, in which the position of the *tert*-butyl group remains at the *para*-position. This suggested that the cyclization reaction proceeded through the 6-endo-trig mode rather than the 5-exo-trig mode (spiro cyclization). Benzo[d][1,3]dioxol-5-yl-3-phenylpropiolate reacted to yield the 3-sulfenylated coumarin derivative **3ea** with a yield of 49%. Phenyl 3-(thiophen-3-yl)propiolate reacted to yield the 3-sulfenylated coumarin derivative **3fa** with a yield of 52%. The use of other diaryl disulfides with different substituents, including bis(4-bromophenyl)disulfide and bis(4-chlorophenyl)disulfide, in the radical cascade cyclization reaction with para-substituted phenylpropiolates resulted in the formation of 3-sulfenylated coumarin derivatives **3ab, 3ac**, and **3ad** with yields of 72%, 63%, and 67%, respectively. The radical-mediated cascade cyclization was also observed for aliphatic diethyldisulfide with phenylpropiolate which yielded 3-sulfenylated coumarin **3ae** with 92% yield. Unfortunately, no product was found when alkyl-substituted propiolate **1g** was allowed to irradiate under the standard reaction conditions. On the other hand, diaryl diselenide with different types of aryl substituted propiolates was tested in which selenylation products **3ax**, **3cx**, **3hx**, **3ix** and **3jx** were achieved in 73%, 67%, 72%, 66% and 70% yields, respectively.

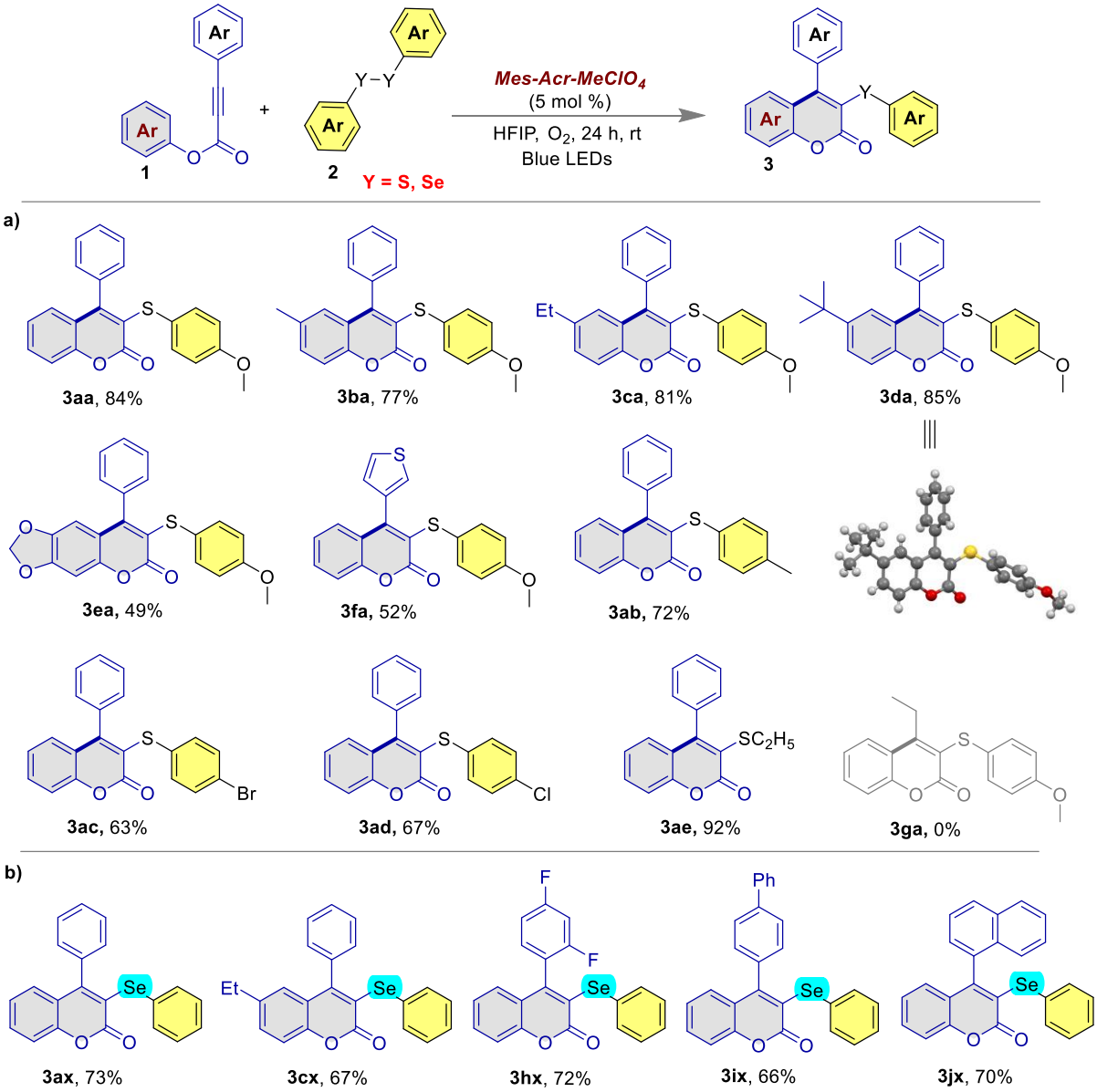

Figure 5.2. Reaction scope for various alkynoate with a) disulfides and b) diselenide.

The reaction appears to produce two different compounds, quinolinones **5** and azaspiro[4,5]trienones **6**, depending on the specific aryl substituent present in the propiolamide reactant (Figure 3). In the reaction bis(4-methoxyphenyl)disulfide was reacted with various propiolamides, including *N*-methyl phenylpropiolamide and propiolamides with electron-donating groups (-Et, -iPr, -tBu) at the para position of the phenyl ring, and 3-sulfenylated quinolinones (**5aa-5da**) were isolated with yields ranging from 81% to 88% (Figure 3b). The

X-ray crystal structure analysis of the compound **5ca** suggests the involvement of a 6-endo-trig cyclization mode in the reaction mechanism, and this is attributed to the non-migratory nature of the -^{i}Pr group.[25] The 3-sulfenylated quinolinone **5ea** having dichloro substituents was isolated with 78% yield. The propiolamides with –naphthalene and biphenyl substituent were also efficient to the reaction condition to afford *N*-quinoline **5ga** with 70% yields. Further, the diphenyl disulfide and disulfides containing different substituents (-Me, -Cl, and -F) on the phenyl ring were used as the disulfide reactant and the reaction also resulted in the synthesis of 3-sulfenylated quinolinones (**5af, 5ab, 5ad, 5ag,** and **5ah**) with yields ranging from 62% to 77%, depending on the nature of the substituent.

In Figure 3a, the results from *para* -OMe or -F substituents on *N*-phenyl of propiolamides are shown. The 3-sulfenyl azaspiro[4,5] trienones (**6ha-6hk**) were formed *via* 5-*exo-trig* cyclization when various disulfides were coupled with for R = -OMe in *N*-phenyl of propiolamides. The electron-donating sulfenyl sources, such as bis(4-methoxyphenyl)disulfide and bis(4-methylphenyl)disulfide, were used to synthesize spiro products **6ha-6hf** with yields ranging from 71% to 92%. On the other hand, electron-withdrawing sulfenyl sources, such as disulfides with halogens, -NO_2 and -CF_3 substituents, were used to synthesize spiro products **6hc-6hk** with yields ranging from 44% to 78% for R = -OMe in *N*-phenyl of propiolamides. Again, 3-selenyl azaspiro[4,5]trienones **6hx** was also found in 79% yield when R = -OMe in *N*-phenyl of propiolamides was taken as the alkyne partner (Figure 3c). When the reaction was performed using propiolamides with a fluorine (-F) substituent on the *N*-phenyl group, the spiro products **6hb, 6hf, 6hg**, and **6hh** were synthesized with yields ranging from 60% to 75%. This observation indicated that oxygen of –OMe is not the oxygen source of the spirocyclic product. However, the diphenyl diselenide led to **5ax** and **5dx** with yields of 86% and 89%, respectively (Figure 3d).

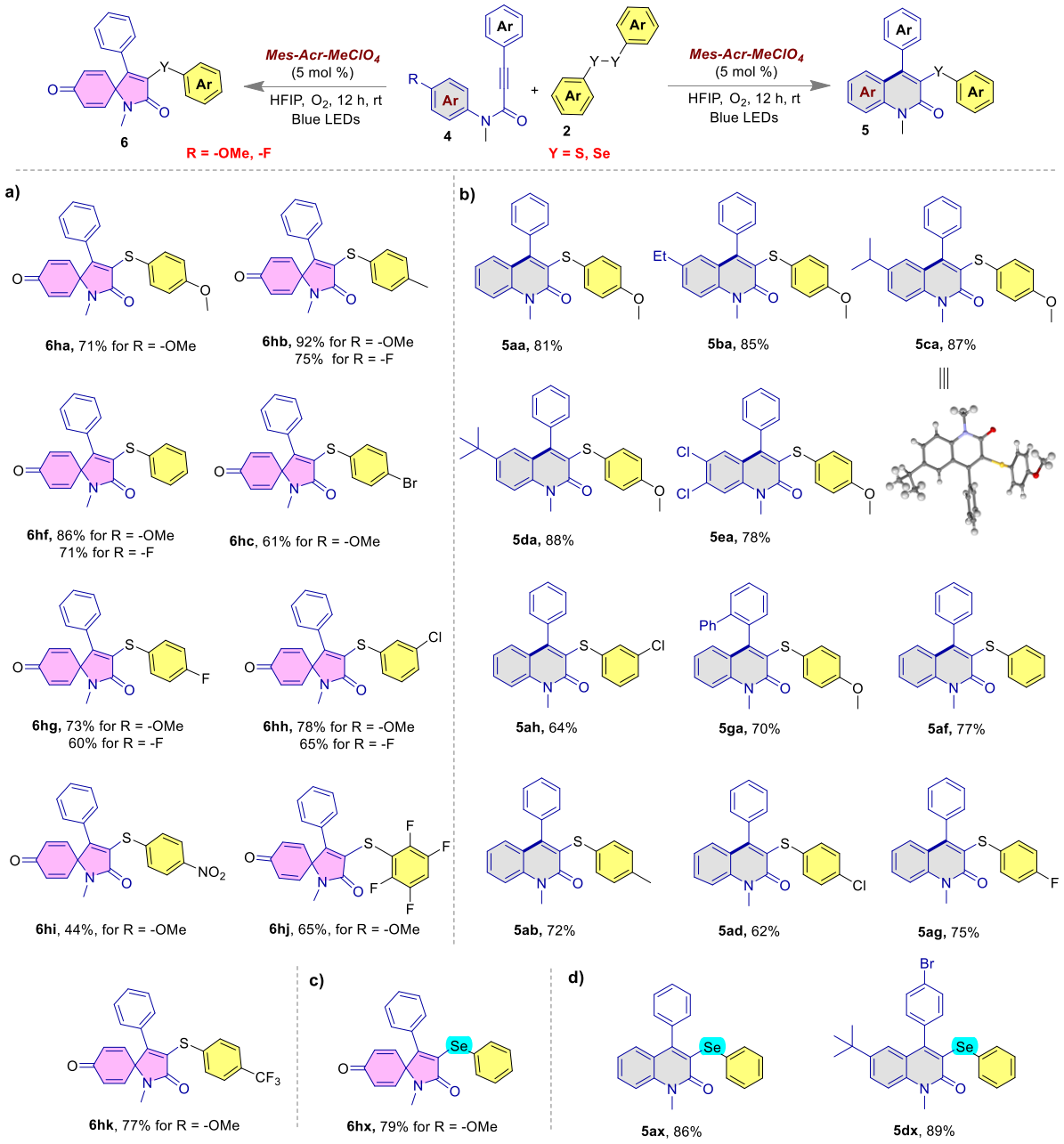

Figure 5.3. Reaction scope for various alkynamides with disulfides and diselenides.

The control experiments shown in Figure 4, helped to understand the divergent reactivity of the alkynamides and arylpropiolates with chalcogens under the standard condition. The addition of various types of quenchers like TEMPO as a radical inhibitor, DABCO as a singlet oxygen quencher, and *p*-benzoquinone as a superoxide radical anion scavenger in the reaction medium no product formation could be observed (Figure 4a). These facts suggest that radical

species, singlet oxygen, or superoxide radical anions might be involved in the reaction pathway.[25] The absence of an EPR signal when the experiment was carried out in the presence of DMPO under standard condition, but in the absence of disulfide **2f** suggests that there were no free radicals present in the reaction medium at that time. However, the detection of an EPR signal when the experiment was repeated in the presence of both disulfide and DMPO suggests that a sulfur-centered radical was present in the reaction medium (Figure 4b).[26] In the light ON-OFF-ON experiment (Figure 4c), the preservation of the progress of the reaction upon irradiation with light, followed by no further conversion upon removal of the light source, provides evidence for the requirement of light in the reaction. The fluorescence quenching and Stern-Volmer studies of disulfide with Mes-Acr-MeClO_4 provide evidence for a reliable single electron transfer (SET) process between the disulfide and the excited state of Mes-Acr-MeClO_4 (Figure 4d and Figure 4e).

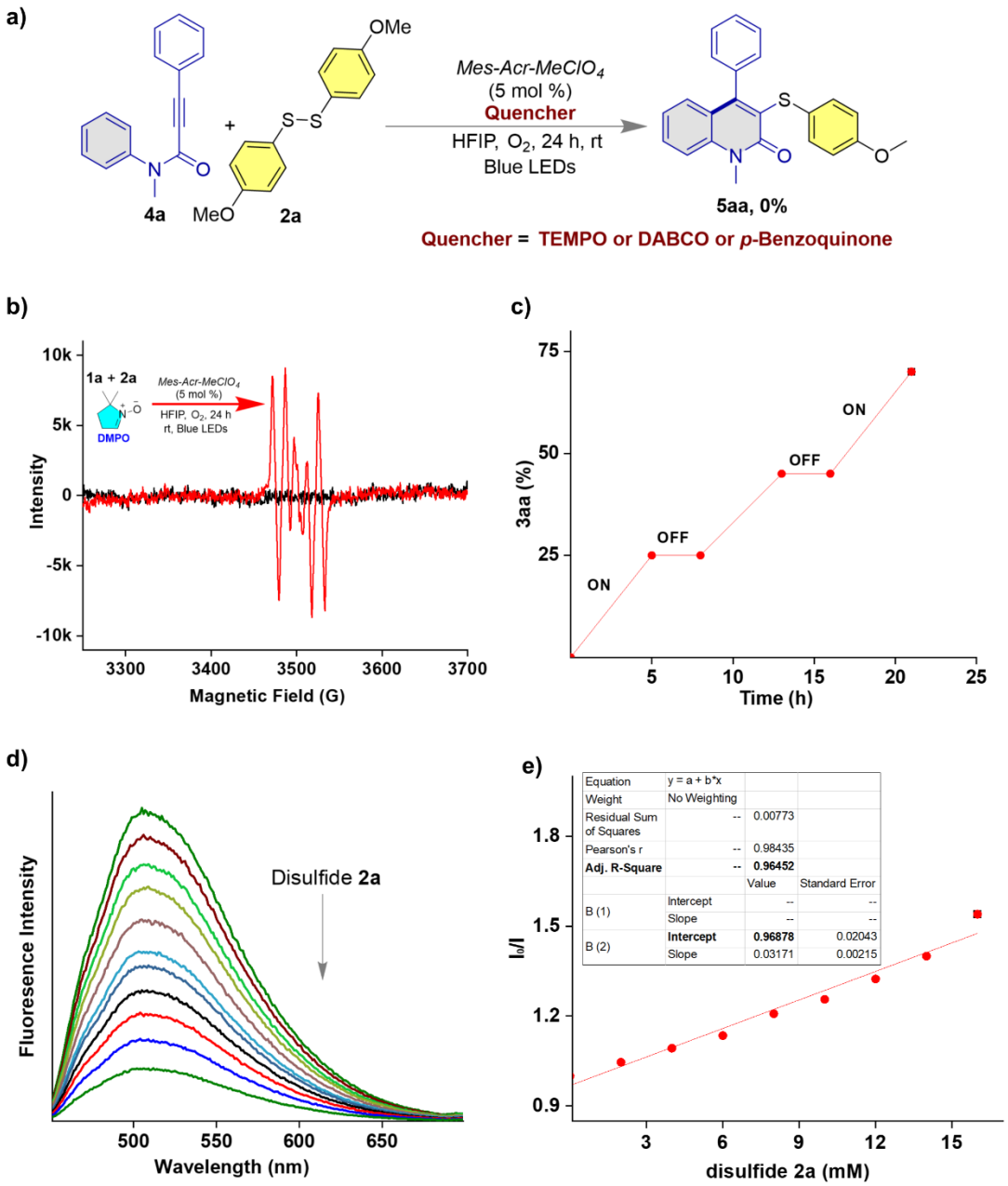

Figure 5.4. Control experiments. a) Radical trapping experiments using TEMPO, DABCO and *p*-benzoquinone. b) EPR experiments with (red) and without (black) using the disulfide. c) Light ON-OFF-ON experiment. d) Fluorescence quenching experiment of Mes-Acr-ClO_4 by disulfide **2a**. e) Stern-Volmer plot of **2a**.

In order to understand the mechanism, the redox properties of propiolate esters, disulfides, and Mes-Acr-$MeClO_4$ (PC or photocatalyst) were compared.[27] The excited state reduction potential

of Mes-Acr-MeClO$_4$ is = +2.06 V vs. SCE (charge transfer singlet state), and the oxidation potentials of propiolate ester **1a**, and disulfide **2f** were found to be +0.65 V *vs.* SCE and +1.56 V *vs.* SCE, respectively.[28] Due to the lower oxidation potential of **1a** and **2f** than the excited state reduction potential of Mes-Acr-MeClO$_4$, it is anticipated that Mes-Acr-MeClO$_4$ with propiolate ester **1a** and disulfide **2f** might experience reductive quenching. However, the excited state Mes-Acr-MeClO$_4$ (**PC***) could oxidize the disulfide **2f** to disulfide radical cation **I** and the **PC** were reduced to **PC**$^{\bullet-}$. Again **PC** was regenerated in the presence of molecular oxygen, which was reduced to $O_2^{\bullet-}$ by **PC**$^{\bullet-}$. The next step was the nucleophilic addition of the thiyl radical generated from intermediate **I** to the alkyne of propiolamide **4**. The strong H-bonding[29] between the carbonyl oxygen of propiolamide **4** and HFIP, could help the activation of carbonyl group.[30] Next, the vinyl radical intermediate **II** led to either 5-exo-trig or 6-endo-trig mode of cyclization to generate intermediate **III** and **V** depending upon the *para*-substitution of the phenyl group of propiolamides. The key factor that facilitated the spiro-cyclization reaction was the presence of either a methoxy (-OMe) or fluorine (-F) substituent at the para position of the aryl group. These substituents helped to stabilize the allylic-type radical intermediate **V**, which was formed during the reaction.[31] However, in the absence of a stabilizing substituent such as -OMe or -F at the para-position of the aryl group, the chalcogenide radical underwent 6-endo-trig cyclization to obtain 3-sulfenylated/selenylated coumarins **5** *via* the formation of a six-membered intermediate **III**. The $O_2^{\bullet-}$ also might have helped for the conversion of **III** to the intermediate **IV**. The spirocyclic 3-sulfenyl azaspiro[4,5]trienones **6** were produced in the presence of molecular oxygen *via* the removal of –OMe or –F substituent. Note that intermediate **I** also reacted with $O_2^{\bullet-}$ to produce *p*-anisyl sulfonothioate **10** as a side product, which was confirmed by X-ray analysis (CCDC 2243014). Overall, the new C-S/C-Se, C-C, and C=O bonds were formed in a single step.

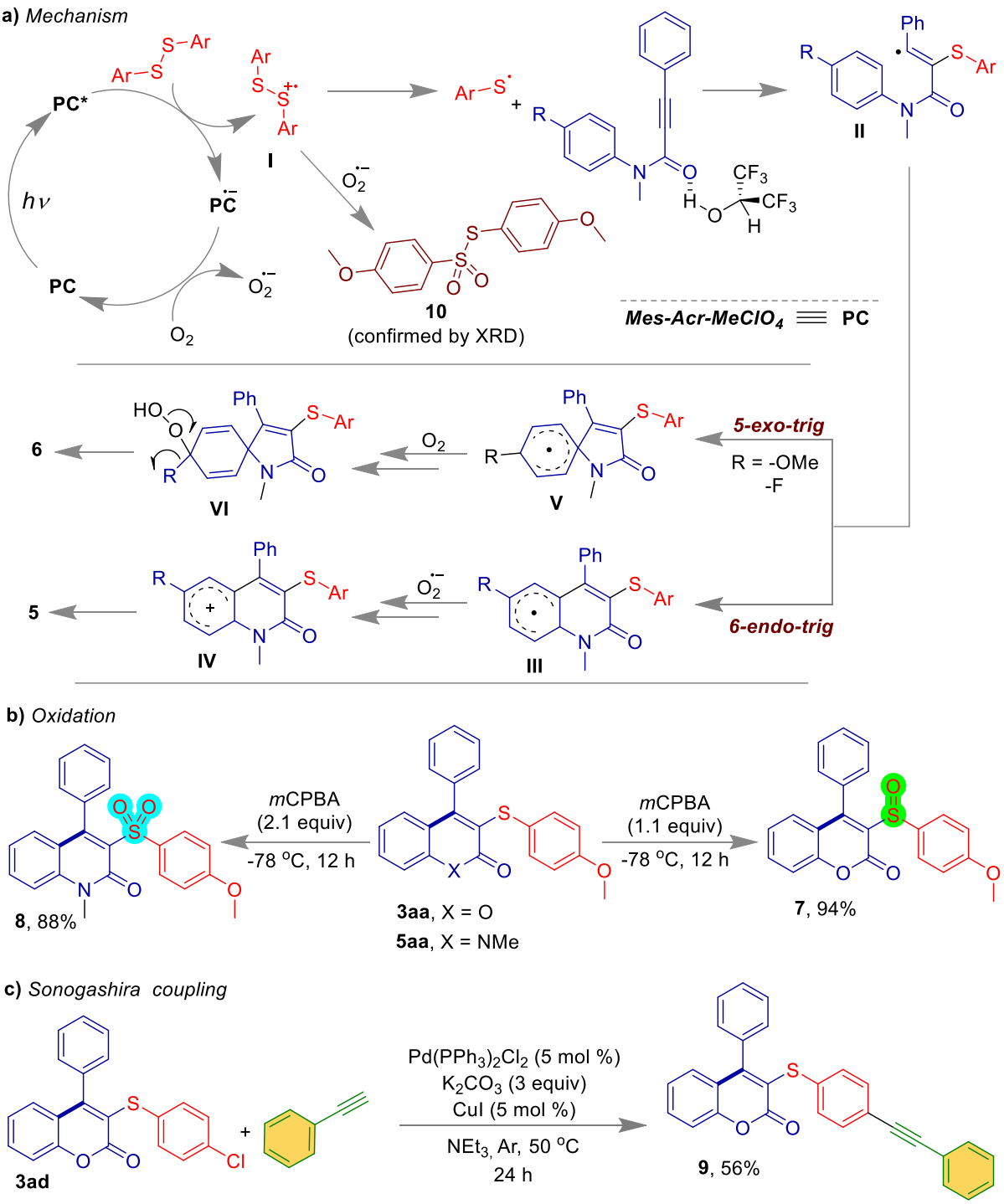

Figure 5.5. a) Plausible mechanism. b) Oxidation of **3aa** and **5aa**. c) Sonogashira coupling of **3ad**.

The synthetic utility of the methodology is demonstrated in Figures 5b and 5c. The 3-sulfenylated coumarin and quinolinone (**3aa** and **5aa**) were oxidized to corresponding sulfoxide **7** and sulfone **8** and in the sequential addition of 1.1 equiv and 2.1 equiv of *m*CPBA (Figures 5b). Again, Sonogashira coupling of **3ad** with phenylacetylene directed C-C coupling product **9** with 56% yield (Figures 5c).

5.4. CONCLUSION

In conclusion, we have established an unprecedented reaction strategy for the chemodivergent cascaded chalcogenation of arylalkynoates and *N*-arylpropiolamides to afford a wide range of 3-sulfenylated/selenylated coumarins or spiro[4,5]trienones using 9-mesityl-10-methylacridinium perchlorate photocatalyst. The formation of multiple bonds like C-S/C-Se, C-C, and C=O bonds were achived in a single step. The reaction involved obtaining of the products *via* 6-endo-trig or 5-exo-trig (spiro) mode of cyclization by choosing appropriate substituents on the aryl of *N*-arylpropiolamides. Overall, this research represents an important contribution to the field of organic chemistry and highlights the ongoing efforts to develop new methods for the efficient and sustainable synthesis of complex molecules.

5.5. EXPERIMENTAL SECTION

General Aspects. All chemicals were obtained from commercial sources. Mainly, all the reactions were carried out under aerobic conditions unless otherwise noted. The reactions were monitored by TLC on aluminium sheets pre-coated with silica gel. Chromatographic purifications of the compounds were performed using silica gel (Mesh 230-400) and ethyl acetate and hexane as eluent. ^{1}H and ^{13}C spectra were recorded on Bruker 400 and 700 MHz instruments at 25 ºC. The chemical shift value (δ, ppm) was reported to the residual chloroform (7.26 for ^{1}H and 77.16 ppm for ^{13}C). Mass spectra were recorded as ESI-TOF (HRMS). Infrared

spectra were recorded on neat solids using KBr pellets and described in wavenumber (cm^{-1}). Digital melting point apparatus was used to record the Melting Point of the compound in degree centigrade (°C) and are uncorrected.

SYNTHESIS

Synthesis of Phenyl 3-phenylpropiolate derivatives.[21] In a 25 mL round-bottomed flask, a solution of 3-phenylpropiolic acid (5.85 mmol, 1.1 equiv, 854 mg) was made by the addition of 5 mL CH_2Cl_2 (DCM); followed by the solution was allowed to stir at 0 °C. After that, a mixture of 4-dimethylaminopyridine (0.53 mmol, 0.1 equiv, 65 mg) and DCC (5.85 mmol, 1.1 equiv, 1205 mg) in 5 mL CH_2Cl_2 was slowly added to the 3-phenylpropiolic acid solution. Again, a solution of phenol (5.32 mmol, 1.0 equiv, 500 mg) in 5 mL CH_2Cl_2 was then added to dropwise. Afterward, the reaction mixture was stirred at room temperature for another 4 to 12 h. Then, the crude mixture was diluted in DCM (CH_2Cl_2) and extracted with brine and dried over in Na_2SO_4, and concentrated under rotary-evaporator. Finally, the crude residue was purified by column chromatography to afford the desired 3-phenylpropiolate derivatives.

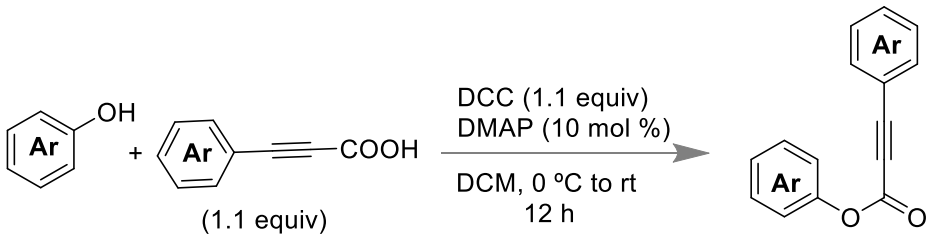

Scheme 5.1. Synthesis of phenyl 3-phenylpropiolate.

Synthesis of N,3-diphenylpropiolamide derivatives. In a 25 mL round-bottomed flask, a solution of 3-phenylpropiolic acid (5.91 mmol, 1.1 equiv, 0.863 g) was made by the addition of 5 mL CH_2Cl_2 (DCM); followed by the solution was allowed to stir at 0 °C. After that, a

mixture of 4-dimethylaminopyridine (0.54 mmol, 0.1 equiv, 65 mg) and dicyclohexylcarbodiimide (5.91 mmol, 1.1 equiv, 1.218 g) in 5 mL CH_2Cl_2 was slowly added to the 3-phenylpropiolic acid solution. Again, a solution of aniline (5.37 mmol, 1.0 equiv, 0.5 g) in 5 mL CH_2Cl_2 was then added to dropwise. Afterward, the reaction mixture was stirred at room temperature for another 4 to 12 h. Then, the crude mixture was diluted in DCM (CH_2Cl_2) and extracted with brine and dried over in Na_2SO_4, and concentrated under rotary-evaporator. Finally, the crude residue was purified by column chromatography to afford the desired N,3-diphenylpropiolamide derivatives.

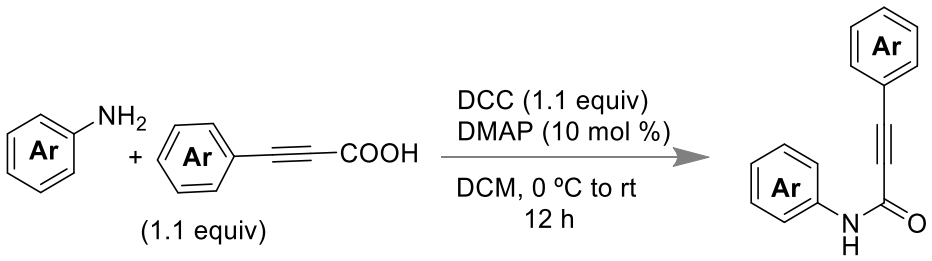

Scheme 5.2. Synthesis of N,3-diphenylpropiolamide.

Synthesis of N-methyl-N,3-diphenylpropiolamide

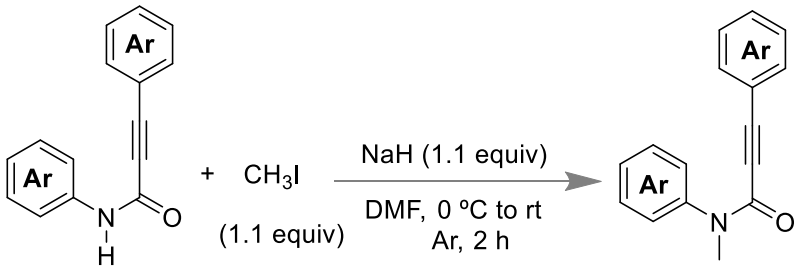

Scheme 5.3. Synthesis of N-methyl-N,3-diphenylpropiolamide

In a 25 mL round-bottomed flask, a solution of N,3-diphenylpropiolamide (2.26 mmol, 1.0 equiv, 0.5 g) was made by the addition of 2 mL dry DMF, followed by the solution was allowed to stir at 0 °C. After that, NaH (2.5 mmol, 1.0 equiv, 57 mg) was added under argon atmosphere.

After 10 minutes CH_3I (2.5 mmol, 1.1 equiv, 0.355 g) was added to reaction mixture. The reaction was proceeded for 2 hours under argon atmosphere. After completion of reaction mixture have been extracted with EtOAc and the combining organic layers have been washed with H_2O and brine dried over in Na_2SO_4, and concentrated under rotary-evaporator. Finally, the crude residue was purified by column chromatography to afford the desired N-methyl-N,3-diphenylpropiolamide derivatives.

Representative procedure for the preparation of 1-methyl-4-phenyl-3 (phenylthio)quinolin-2(1H)-one.

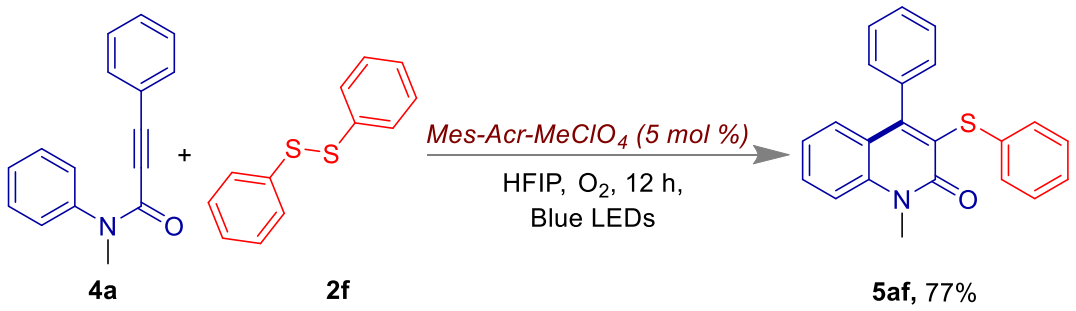

Scheme 5.4. Synthesis of 1-methyl-4-phenyl-3-(phenylthio)quinolin-2(1H)-one.

In an oven dried quartz tube N,3-diphenylpropiolamide **4a** (0.255 mmol, 60 mg), disulfide **2f** (0.306 mmol, 80 mg), and Mes-Acr-$MeClO_4$ (5 mol %, 0.0128 mmol, 5 mg) were dissolved in 1.5 mL hexafluoro-2-propanol (HFIP) solvent. After that, the reaction mixture was irradiated by blue LEDs light for 12 h in the presence of an oxygen balloon. After completion of the reaction, HFIP was removed under reduced pressure. Then, the crude mixture was diluted in DCM (CH_2Cl_2) and extracted with brine. The resulting organic solution was dried over anhydrous sodium sulphate and concentrated to obtain a crude mixture which was further purified by silica-gel column chromatography using ethyl acetate and hexane as the eluent to afford the pure product.

Synthesis of 1-methyl-4-phenyl-3-(phenylselanyl)quinolin-2(1H)-one

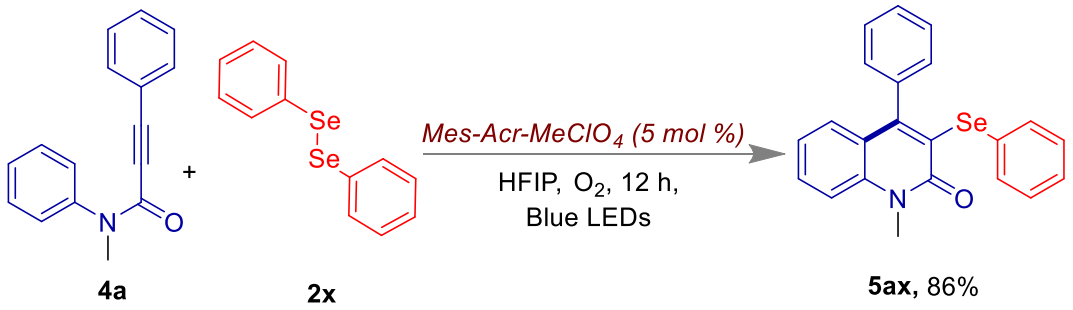

Scheme 5.5. Synthesis of 1-methyl-4-phenyl-3-(phenylselanyl)quinolin-2(1H)-one.

In an oven dried quartz tube N,3-diphenylpropiolamide **4a** (0.255 mmol, 60 mg), diselenide **2x** (0.306 mmol, 95 mg), and Mes-Acr-$MeClO_4$ (5 mol %, 0.0128 mmol, 5 mg) were dissolved in 1.5 mL Hexafluoro-2-propanol (HFIP) solvent. After that, the reaction mixture was irradiated by Blue LEDs light for 12 h in the presence of an oxygen balloon. After completion of the reaction, HFIP was removed under reduced pressure. Then, the crude mixture was diluted in DCM (CH_2Cl_2) and extracted with brine. The resulting organic solution was dried over anhydrous sodium sulphate and concentrated to obtain a crude mixture which was further purified by silica-gel column chromatography using ethyl acetate and hexane as the eluent to afford the pure product.

Synthesis of 3-((4-methoxyphenyl)thio)-4-phenyl-2H-chromen-2-one

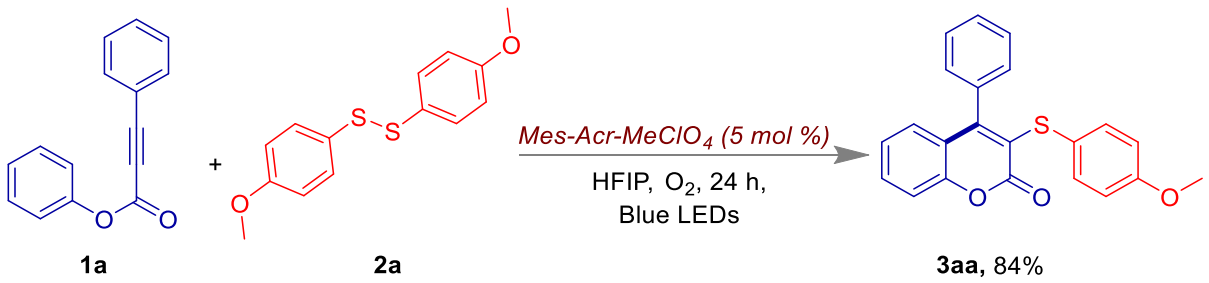

Scheme 5.6. Synthesis of 3-((4-methoxyphenyl)thio)-4-phenyl-2H-chromen-2-one.

In an oven dried quartz tube phenyl 3-phenylpropiolate **1a** (0.27 mmol, 60 mg), disulfide **2a** (0.30 mmol, 82 mg), and Mes-Acr-$MeClO_4$ (5 mol %, 0.0135 mmol, 6 mg) were dissolved in 1.5 mL HFIP. After that, the reaction mixture was irradiated by Blue LEDs light for 24 h in the presence of an oxygen balloon. After completion of the reaction, HFIP was removed under reduced pressure. Then, the crude mixture was diluted in DCM (CH_2Cl_2) and extracted with brine. The resulting organic solution was dried over anhydrous sodium sulphate and concentrated to obtain a crude mixture which was further purified by silica-gel column chromatography using ethyl acetate and hexane as the eluent to afford the pure product.

Synthesis of 4-phenyl-3-(phenylselanyl)-2H-chromen-2-one

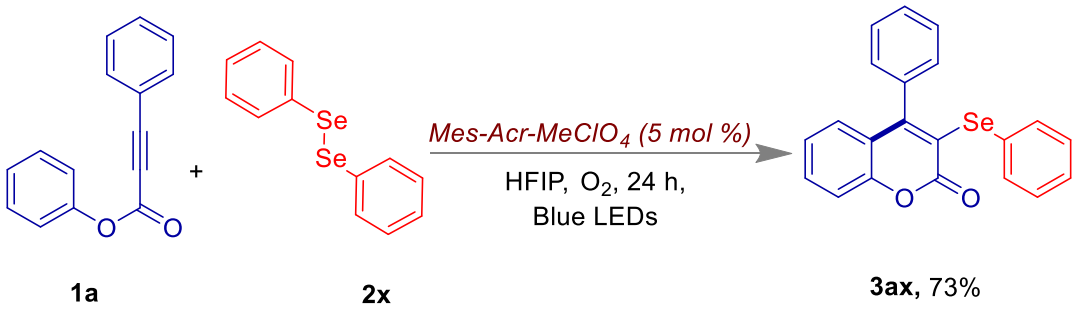

Scheme 5.7. Synthesis of 4-phenyl-3-(phenylselanyl)-2H-chromen-2-one.

In an oven dried quartz tube phenyl 3-phenylpropiolate **1a** (0.27 mmol, 60 mg), diselenide (0.324 mmol, 71 mg), and Mes-Acr-$MeClO_4$ (5 mol %, 0.0135 mmol, 6 mg) were dissolved in 1.5 mL HFIP. After that, the reaction mixture was irradiated by blue LEDs light for 24 h in the presence of an oxygen balloon. After completion of the reaction, HFIP was removed under reduced pressure. Then, the crude mixture was diluted in DCM (CH_2Cl_2) and extracted with brine. The resulting organic solution was dried over anhydrous sodium sulphate and

concentrated to obtain a crude mixture which was further purified by silica-gel column chromatography using ethyl acetate and hexane as the eluent to afford the pure product.

Synthesis of 1-methyl-4-phenyl-3-(phenylthio)-1-azaspiro[4.5]deca-3,6,9-triene-2,8-dione

Scheme 5.8. Synthesis of 1-methyl-4-phenyl-3-(phenylthio)-1-azaspiro[4.5]deca-3,6,9-triene-2,8-dione.

In an oven dried quartz tube N-(4-methoxyphenyl)-N-methyl-3-phenylpropiolamide **4h** (0.225 mmol, 60 mg), disulfide **2f** (0.27 mmol, 59 mg), and Mes-Acr-$MeClO_4$ (5 mol %, 0.0112 mmol, 5 mg) were dissolved in 1.5 mL HFIP. After that, the reaction mixture was irradiated by blue LEDs light for 12 h in the presence of an oxygen balloon. After completion of the reaction, HFIP was removed under reduced pressure. Then, the crude mixture was diluted in DCM (CH_2Cl_2) and extracted with brine. The resulting organic solution was dried over anhydrous sodium sulphate and concentrated to obtain a crude mixture which was further purified by silica-gel column chromatography using ethyl acetate and hexane as the eluent to afford the pure product.

Synthesis of 1-methyl-4-phenyl-3-(phenylthio)-1-azaspiro[4.5]deca-3,6,9-triene-2,8-dione

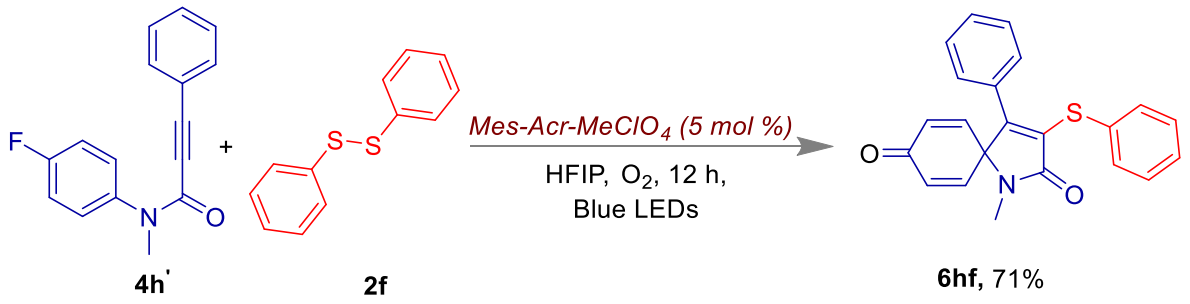

Scheme 5.9. Synthesis of 1-methyl-4-phenyl-3-(phenylthio)-1-azaspiro[4.5]deca-3,6,9-triene-2,8-dione.

In an oven dried quartz tube N-(4-fluorophenyl)-N-methyl-3-phenylpropiolamide **4h´** (0.237 mmol, 60 mg), disulfide (0.29 mmol, 62 mg), and Mes-Acr-$MeClO_4$ (5 mol %, 0.0118 mmol, 5 mg) were dissolved in 1.5 mL HFIP. After that, the reaction mixture was irradiated by blue LEDs light for 12 h in the presence of an oxygen balloon. After completion of the reaction, HFIP was removed under reduced pressure. Then, the crude mixture was diluted in DCM (CH_2Cl_2) and extracted with brine. The resulting organic solution was dried over anhydrous sodium sulphate and concentrated to obtain a crude mixture which was further purified by silica-gel column chromatography using ethyl acetate and hexane as the eluent to afford the pure product.

Synthesis of 1-methyl-4-phenyl-3-(phenylselanyl)-1-azaspiro[4.5]deca-3,6,9-triene-2,8-dione

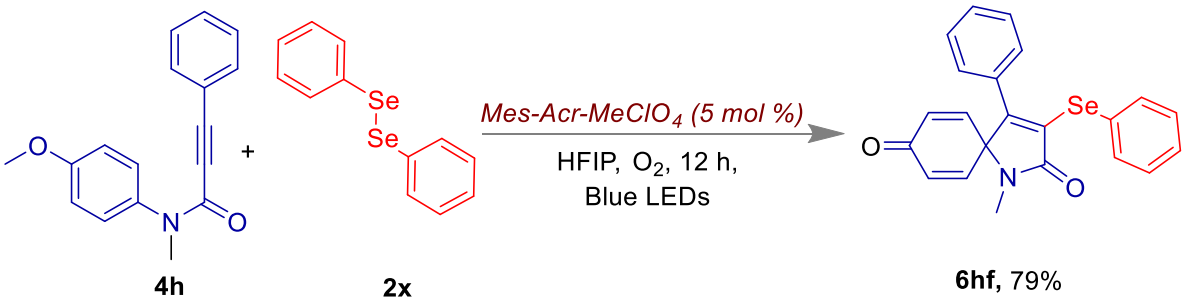

Scheme 5.10. Synthesis of 1-methyl-4-phenyl-3-(phenylselanyl)-1-azaspiro[4.5]deca-3,6,9-triene-2,8-dione.

In an oven dried quartz tube N-(4-methoxyphenyl)-N-methyl-3-phenylpropiolamide **4h** (0.226 mmol, 60 mg), diselenide (0.27 mmol, 85 mg), and Mes-Acr-MeClO$_4$ (5 mol %, 0.0113 mmol, 5 mg) were dissolved in 1.5 mL HFIP. After that, the reaction mixture was irradiated by Blue LEDs light for 12 h in the presence of an oxygen balloon. After completion of the reaction, HFIP was removed under reduced pressure. Then, the crude mixture was diluted in DCM (CH_2Cl_2) and extracted with brine. The resulting organic solution was dried over anhydrous sodium sulphate and concentrated to obtain a crude mixture which was further purified by silica-gel column chromatography using ethyl acetate and hexane as the eluent to afford the pure product.

Synthetic procedure for compound 7. A 15 mL Schlenk tube holding a magnetic bar was charged with a 2 mL DCM solution of 3-((4-methoxyphenyl)thio)-4-phenyl-2H-chromen-2-one **3aa** (60 mg, 0.17 mmol) and *m*CPBA(32 mg, 0.19 mmol) was added under argon atmosphere and stirred at -78 °C for 12 h. Then, the crude mixture was diluted in DCM (CH_2Cl_2) and extracted with brine. The resulting organic solution was dried over anhydrous sodium sulphate and concentrated to obtain a crude mixture which was further purified by

silica-gel column chromatography using ethyl acetate and hexane as the eluent to afford the pure product.

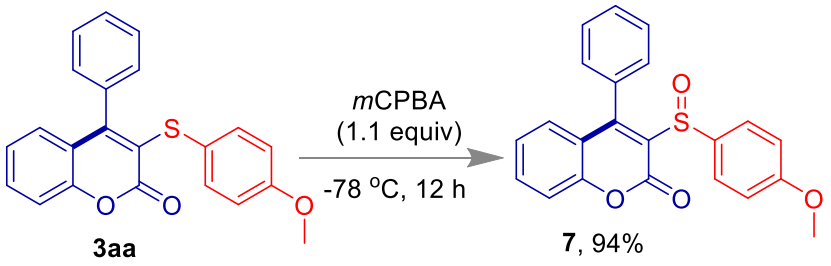

Scheme 5.11. Synthesis of compound **7.**

Synthetic procedure for compound 8. A 15 mL Schlenk tube holding a magnetic bar was charged with a 2 mL DCM solution of 3-((4-methoxyphenyl)thio)-1-methyl-4-phenylquinolin-2(1H)-one **5aa** (60 mg, 0.16 mmol) and *m*CPBA(59 mg, 0.34 mmol) was added under argon atmosphere and stirred at -78 °C for 12 h. Then, the crude mixture was diluted in DCM (CH_2Cl_2) and extracted with brine. The resulting organic solution was dried over anhydrous sodium sulphate and concentrated to obtain a crude mixture which was further purified by silica-gel column chromatography using ethyl acetate and hexane as the eluent to afford the pure product.

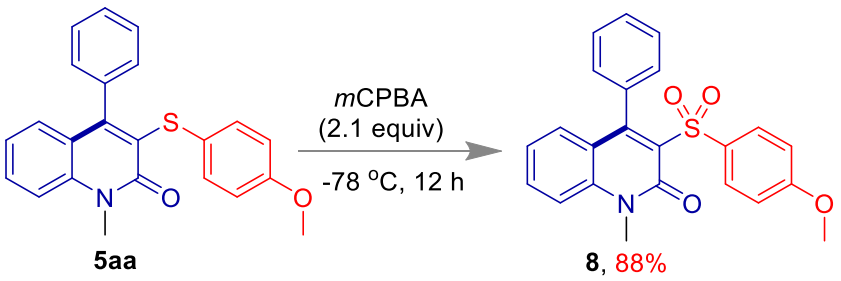

Scheme 5.12. Synthesis of compound **8.**

Synthetic procedure for compound 9. A 15 mL Schlenk tube holding a magnetic bar was charged with 3-((4-chlorophenyl)thio)-4-phenyl-2H-chromen-2-one **3ad** (0.165 mmol, 60 mg),

phenyl acetylene (0.20 mmol, 20 mg), K_2CO_3 (0.50 mmol, 68 mg), and $Pd(PPh_3)_2Cl_2$ (0.08 mmol, 6 mg) and CuI (0.08 mmol) in NEt_3 under inert atmosphere. Then the reaction mixture was placed into a preheated oil bath at 50 °C for 24 h. Then, the crude mixture was diluted in DCM (CH_2Cl_2) and extracted with brine. The resulting organic solution was dried over anhydrous sodium sulphate and concentrated to obtain a crude mixture which was further purified by silica-gel column chromatography using ethyl acetate and hexane as the eluent to afford the pure product.

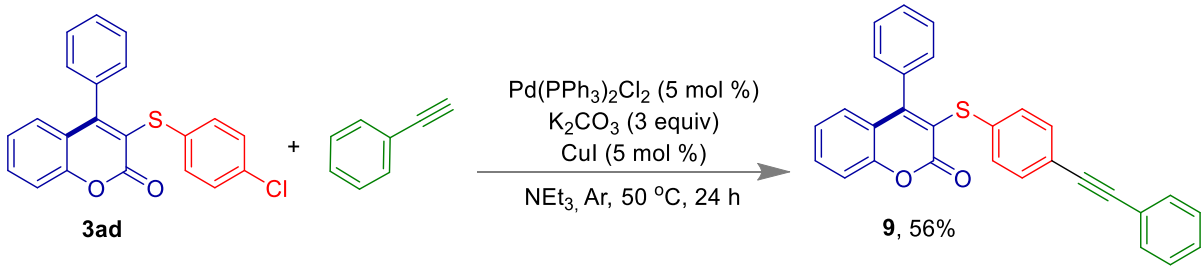

Scheme 5.13. Synthesis of compound **9.**

Table 5.1. Reaction Condition Optimization.[a]

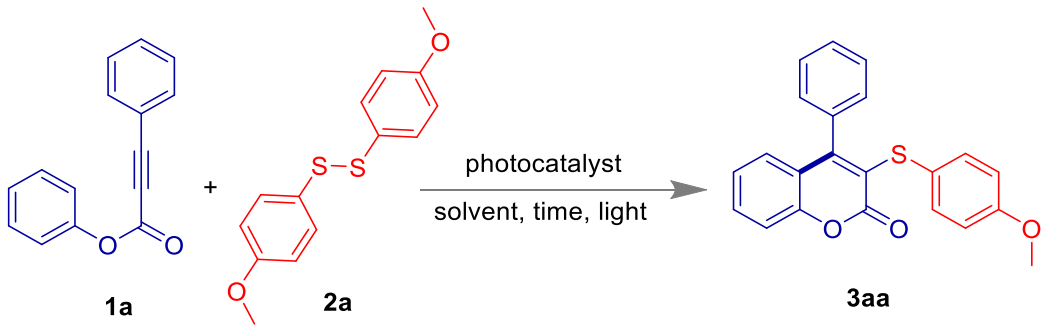

entry	catalyst	Solvent	light source	yield (%)[a]
1	-	HFIP(1.5 ml)	Blue LED	0
2	Mes-Acr-$MeClO_4$	CH_3CN	Blue LED	0
3	Mes-Acr-$MeClO_4$	MeOH	Blue LED	0
4	Mes-Acr-$MeClO_4$	DCM	Blue LED	0

5	Mes-Acr-$MeClO_4$	Toluene	Blue LED	0
6	Mes-Acr-$MeClO_4$	HFIP (0.5 ml)	Blue LED (3W)	30
7	Mes-Acr-$MeClO_4$	TFE	Blue LED	0
8	Mes-Acr-$MeClO_4$	HFIP (1.5 ml)	Blue LED	84
9	Mes-Acr-$MeClO_4$	HFIP:DCM	Blue LED	0
10	Mes-Acr-$MeBF_4$	HFIP (1.5 ml)	Blue LED	81
11	Eosin Y	HFIP	Blue LED	0
12	$Ru(bpy)_3(PF_6)_2$	HFIP	Blue LED	0
13	Rose Bengal	HFIP	Blue LED	0
14	Mes-Acr-$MeClO_4$	HFIP	White LED	75
15	Mes-Acr-$MeClO_4$	HFIP	green LED	0
16	Mes-Acr-$MeClO_4$	HFIP (1.5 ml)	Blue LED	56[b]
17	Mes-Acr-$MeClO_4$	HFIP (1.5 ml)	Blue LED	0[c]
18	Mes-Acr-$MeClO_4$	HFIP (1.5 ml)	Blue LED	0[d]

[a]Reaction Conditions: **1a** (0.270 mmol, 1 equiv), **2a** (0.29 mmol, 1.1 equiv), and Mes-Acr-$MeClO_4$ (0.013 mmol 5 mol %), in 1.5 mL HFIP under O_2 atmosphere for 24 h using Blue LEDs, [b]after 12 h, [c]Ar atmosphere, [d] thiophenol instead of disulfide **2a**.

Radical trapping experiment with TEMPO/DABCO/*p*-Benzoquinone. In an oven dried quartz tube N-methyl-N,3-diphenylpropiolamide **4a** (0.25 mmol, 60 mg), 1,2-bis(4-methoxyphenyl)disulfane **2a** (0.31 mmol, 85 mg), and PC (5 mol %, 0.0128 mmol, 5 mg) were dissolved in 1.0 mL Hexafluoro-2-propanol (HFIP) solvent and TEMPO (0.53 mmol, 84 mg) were dissolved in 1.0 mL HFIP. After that, the reaction mixture was irradiated by blue LEDs light for 12 h in the presence of an oxygen balloon. The reaction was monitored by TLC.

After the reaction time, no desired product was found. The same experiment was carried out using DABCO (0.54 mmol, 60 mg) and *p*-Benzoquinone (0.54 mmol, 58 mg). However, the addition of DABCO and *p*-benzoquinone led to no product formation.

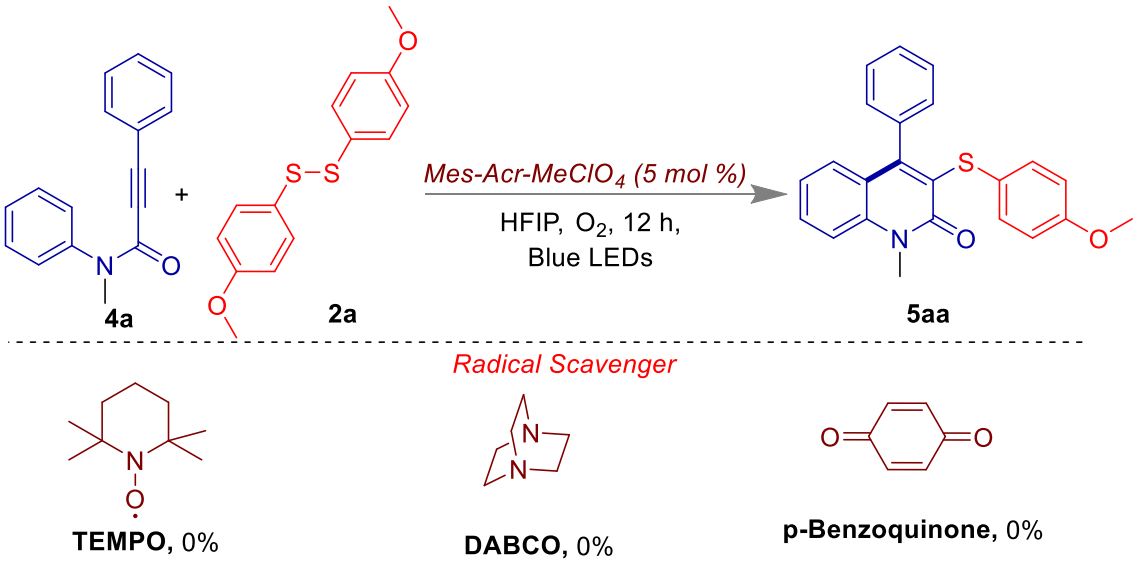

Scheme 5.14. Various radical scavengers under standard condition.

Light ON-OFF-ON experiment. phenyl 3-phenylpropiolate **1a** (0.27 mmol, 60 mg), disulfide **2a** (0.32 mmol, 90 mg) and Mes-Acr-MeClO$_4$ (5 mol %, 0.0135 mmol, 6 mg) were dissolved in 1.5 mL HFIP. After that, the reaction mixture was irradiated by Blue LEDs light for 24 h in the presence of an oxygen balloon. Successive progress of the reaction was monitored every 5 h and 3 h in the presence of light and absence of light by ^{1}H NMR experiment.

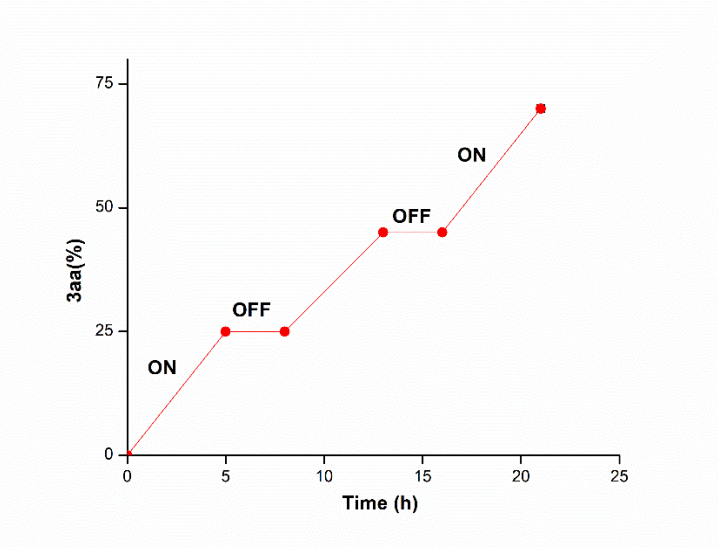

Figure 5.6. Conversion of **3aa** *vs.* time in the presence and absence of light.

EPR Experiments. EPR spectra was recorded at 298 K using EPR spectrometer derived at 9.4335 GHz. Typical spectrometer parameters are shown as follows, scan range: 100 G; center field set: 3480.00 G; time constant: 0.16 ms; scan time: 122.88 s; modulation amplitude: 20.0 G; modulation frequency: 100 kHz; receiver gain: 2.00×10^{2} ; microwave power: $7.14e^{-001}$ mW; g = 2.00686.

Spin-trapping experiment in the presence DMPO.[32] A mixture of phenyl 3-phenylpropiolate **1a** (0.27 mmol, 60 mg), disulfide **2a** (0.32 mmol, 90 mg) and Mes-Acr-$MeClO_4$ (5 mol %, 0.0135 mmol, 6 mg) were dissolved in 2.0 mL HFIP. After that, the reaction mixture was irradiated by Blue LEDs light for 2.5 h in the presence of an oxygen balloon. Afterward, 20 µL 5,5-dimethyl-1-pyrroline-N-oxide (DMPO) solution was quickly poured into EPR tube and 200 µL reaction mixture was appended to analyse EPR. A sharp signal appeared, indicating the presence of an unpaired electron in the reaction pathway. A similar experiment was performed without disulfide; which shows no signal.

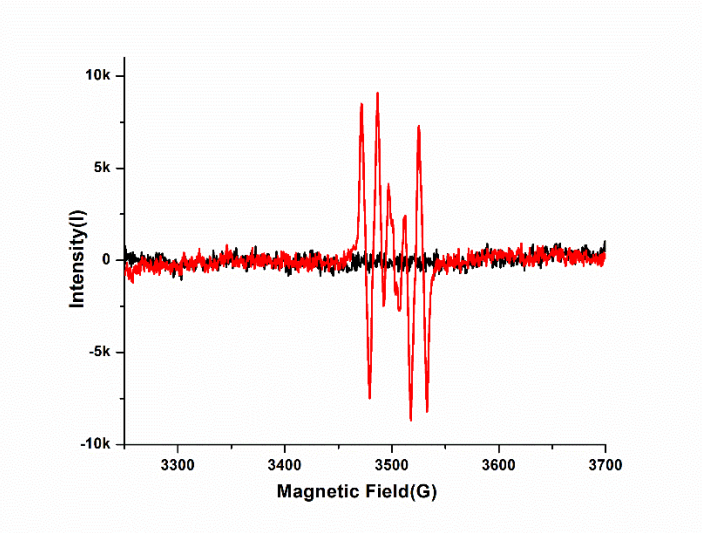

Figure 5.7. EPR experiment under the standard condition with catalyst (red signal) and without disulfide (black line).

Fluorescence quenching study.[26] The maximum emission of the photocatalyst Mes-Acr-$MeClO_4$ (4×10^{-4} M in HFIP) was observed at 512 nm upon excitation wavelength at 360 nm. Following, the addition of **2a** (4×10^{-4} M in HFIP) led to the gradual decrease of fluorescence intensity, as shown below.

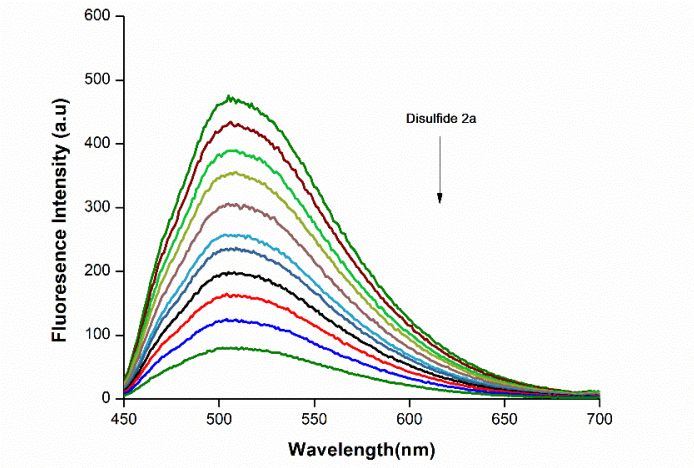

Figure 5.8. Fluorescence spectra of Mes-Acr-$MeClO_4$ upon gradual addition of disulfide **2a**.

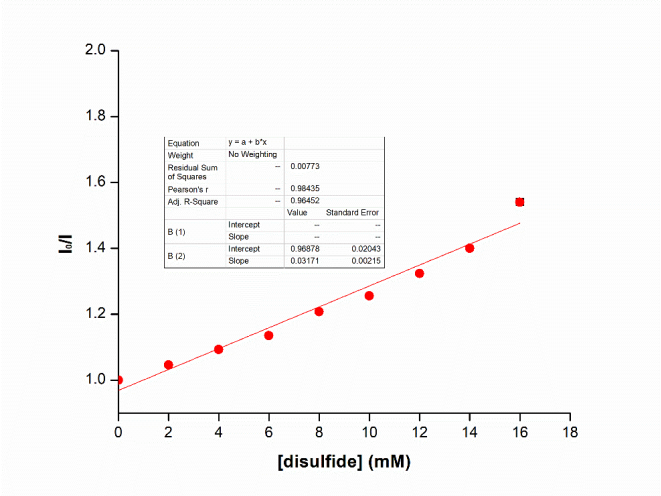

Figure 5.8. Stern-Volmer plot for disufide **2a**.

Crystal measurement. Crystals of compound **3da, 5ca** and **10** were isolated after slow evaporation of $CHCl_3$ and water mixture (1 : 0.5). The crystals data were collected with Bruker SMART D8 goniometer equipped with an APEX CCD detector and with an INCOATEC micro source (Cu-Kα radiation, λ = 0.71073 Å). SAINT+[33] and SADABS[34] were used to integrate the intensities and to correct the absorption respectively The structure was resolved by direct methods and refined on F^2 with SHELXL-97.[35] ORTEP drawing of the compound **3da, 5ca** and **10** show ellipsoid contour at the 50% probability level.

Compound 3da (CCDC 2242733)

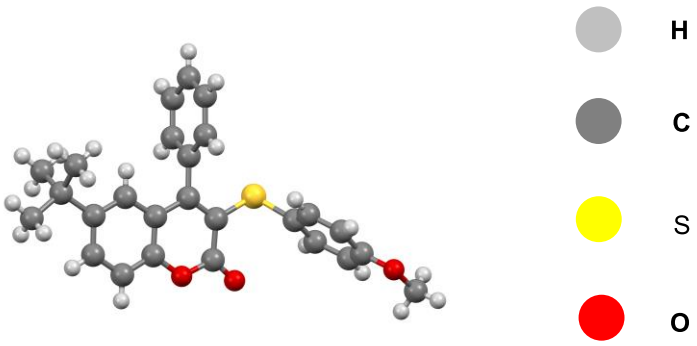

Figure 5.9. Crystal structure of **3da** (CCDC 2242733). Ellipsoids are drawn at the 50% probability level.

Crystallographic Data for (3da)

Empirical formula	$C_{26}H_{24}O_3S$
Formula weight	416.51
Temperature/K	100.00(10)
Crystal system	triclinic
Space group	P-1
a/Å	9.6252(4)
b/Å	9.9045(5)
c/Å	12.1084(5)
α/°	67.542(4)
β/°	79.963(3)

γ/°	83.716(3)
Volume/Å3	1049.29(9)
Z	2
ρcalcg/cm^3	1.318
μ/mm^{-1}	0.180
F(000)	440.0
Crystal size/mm^3	0.2 × 0.1 × 0.1
Radiation	Mo Kα (λ = 0.71073)
Reflections collected	18897
Independent reflections	5104 [R_{int} = 0.0528, R_{sigma} = 0.0528]
Goodness-of-fit on F2	1.064
Final R indexes [I>=2σ (I)]	R_1 = 0.0424, wR_2 = 0.0980
Final R indexes [all data]	R_1 = 0.0584, wR_2 = 0.1047
Largest diff. peak/hole / e Å^{-3}	0.37/-0.31

Compound 5ca (CCDC 2242836)

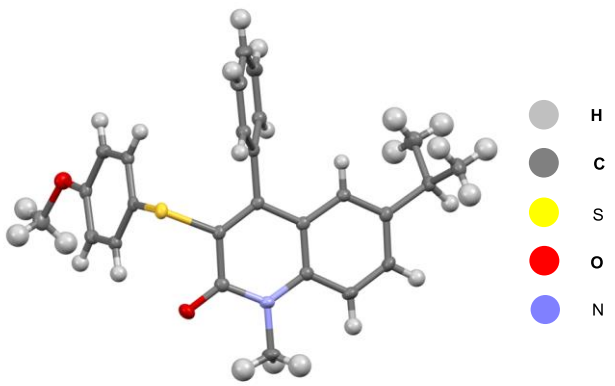

Figure 5.10. Crystal structure of **5ca** (CCDC 2242836). Ellipsoids are drawn at the 50% probability level.

Crystallographic Data for (5ca)

Empirical formula	$C_{50}H_{44}N_4O_4S_2$
Formula weight	829.01
Temperature/K	100.00(10)
Crystal system	monoclinic
Space group	I2/a
a/Å	19.4773(5)
b/Å	11.7691(3)
c/Å	38.0602(10)
α/°	90
β/°	100.270(3)
γ/°	90
Volume/Å3	8584.8(4)
Z	8
ρcalcg/cm^3	1.283
μ/mm^{-1}	0.175
F(000)	3488.0
Crystal size/mm^3	0.2 × 0.1 × 0.1
Radiation	Mo Kα (λ = 0.71073)
Reflections collected	42297
Independent reflections	10333 [R_{int} = 0.0434, R_{sigma} = 0.0387]
Goodness-of-fit on F2	1.065
Final R indexes [I>=2σ (I)]	R_1 = 0.0387, wR_2 = 0.0925

Final R indexes [all data]	R_1 = 0.0506, wR_2 = 0.0977
Largest diff. peak/hole / e Å^{-3}	0.33/-0.30

Anisylsulfonothioate **(10) (CCDC 2243014)**

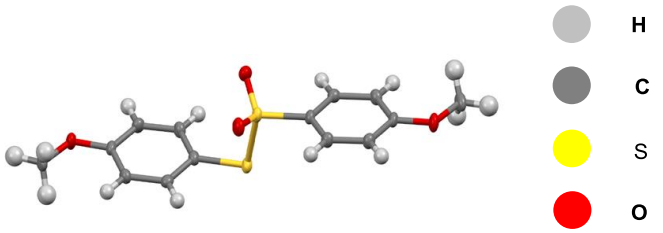

Figure 5.11. Crystal structure of **10** (CCDC 2243014). Ellipsoids are drawn at the 50% probability level.

Crystallographic Data for 10

Empirical formula	$C_{14}H_{14}O_4S_2$
Formula weight	310.37
Temperature/K	101(1)
Crystal system	monoclinic
Space group	$P2_1/n$
a/Å	7.5750(7)
b/Å	20.1043(17)
c/Å	9.5891(8)
α/°	90
β/°	106.570(9)

γ/°	90
Volume/Å3	1399.7(2)
Z	4
ρcalcg/cm^3	1.473
μ/mm^{-1}	0.390
F(000)	648.0
Crystal size/mm^3	0.2 × 0.2 × 0.1
Radiation	Mo Kα (λ = 0.71073)
Reflections collected	12095
Independent reflections	3392 [R_{int} = 0.0615, R_{sigma} = 0.0441]
Goodness-of-fit on F2	1.162
Final R indexes [I>=2σ (I)]	R_1 = 0.0745, wR_2 = 0.1914
Final R indexes [all data]	R_1 = 0.0894, wR_2 = 0.1989
Largest diff. peak/hole / e Å^{-3}	1.67/-0.47

CHARATERIZATION DATA

3-((4-Methoxyphenyl)thio)-4-phenyl-2H-chromen-2-one (3aa).[20] R_f = 0.45 (5% ethyl acetate in hexane); yellow solid; yield 84% (82 mg); ^{1}H NMR (400 MHz, $CDCl_3$) δ 7.53-7.49 (m, 4H), 7.37 (d, *J* = 8.3 Hz, 1H), 7.26-7.13 (m, 5H), 7.07 (d, *J* = 8.0 Hz, 1H), 6.74 (d, *J* = 8.5 Hz, 2H), 3.75 (s, 3H); ^{13}C{^{1}H} NMR (100 MHz, $CDCl_3$) δ 159.5, 159.4, 157.5, 153.3, 135.1, 133.2, 132.0, 129.1, 128.7, 128.6, 128.2, 124.9, 124.4, 123.5, 120.7, 116.9, 114.6, 55.4.

3-((4-Methoxyphenyl)thio)-6-methyl-4-phenyl-2H-chromen-2-one (3ba). R_f = 0.45 (10% ethyl acetate in hexane); yellow solid; yield 77% (73 mg); mp 145-148 ºC; ^{1}H NMR (700 MHz, $CDCl_3$) δ 7.55-7.51 (m, 3H), 7.33-7.32 (m, 1H), 7.28-7.25 (m, 3H), 7.21 (d, *J* = 8.7 Hz, 1H), 6.84 (s, 1H), 6.75 (d, *J* = 8.7 Hz, 2H), 3.76 (s, 3H), 2.28 (s, 3H); ^{13}C{^{1}H} NMR (176 MHz, $CDCl_3$) δ 159.7, 159.3, 157.6, 151.5, 135.2, 134.4, 134.1, 133.1, 129.0, 128.6, 128.5, 127.7, 125.0, 123.3, 120.4, 116.6, 114.6, 55.4, 21.0; IR (KBr) ῡ 3015, 2916, 1736, 1492, 712; HRMS (ESI/Q-TOF) m/z: $[M + H]^+$ calcd for $C_{24}H_{18}O_3S$ 375.1049; found 375.1036.

6-Ethyl-3-((4-methoxyphenyl)thio)-4-phenyl-2H-chromen-2-one (3ca). R_f = 0.5 (10% ethyl acetate in hexane); yellow solid; yield 81% (75 mg); mp 142-145 ºC; ^{1}H NMR (700 MHz, $CDCl_3$) δ 7.53 -7.55 (m, 3H), 7.36-7.34 (m, 1H), 7.29-7.28 (m, 1H), 7.26-7.24 (m, 2H), 7.20-7.18 (m, 2H), 6.84 (s, 1H), 6.74-6.72 (m, 2H), 3.75 (s, 3H), 2.55 (q, *J* = 7.6 Hz, 2H), 1.12 (t, *J* = 7.6 Hz, 3H); ^{13}C{^{1}H} NMR (176 MHz, $CDCl_3$) δ 159.7, 159.3, 157.8, 151.6, 140.6, 135.3, 133.1, 131.9, 129.0, 128.63, 128.62, 126.7, 125.1, 123.3, 120.5, 116.8, 114.6, 55.4, 28.4, 15.8; IR (KBr) ῡ 2920, 1588,1181, 740; HRMS (ESI/Q-TOF) m/z: $[M + H]^+$ calcd for $C_{24}H_{21}O_3S$ 389.1206; found 389.1209.

6-(*tert*-Butyl)-3-((4-methoxyphenyl)thio)-4-phenyl-2H-chromen-2-one (3da). R_f = 0.5 (10% ethyl acetate in hexane); yellow solid; yield 85% (76 mg); mp 155-159 ºC; ^{1}H NMR (700 MHz, $CDCl_3$) δ 7.57-7.50 (m, 4H), 7.31-7.26 (m, 3H), 7.20-7.19 (m, 2H), 7.04 (s, 1H), 6.74 (d, *J* = 8.8 Hz, 2H), 3.75 (s, 3H), 1.19 (s, 9H); ^{13}C{^{1}H} NMR (176 MHz, $CDCl_3$) δ 159.8, 159.3, 158.1, 151.4, 147.4, 135.2, 133.0, 129.7, 129.1, 128.7, 128.5, 125.2, 124.3, 123.1, 120.1, 116.4, 114.7, 55.4, 34.7, 31.3; IR (KBr) ῡ 2922, 1712, 1598, 711; HRMS (ESI/Q-TOF) m/z: $[M + H]^+$ calcd for $C_{26}H_{25}O_3S$ 417.1519; found 417.1498.

7-((4-Methoxyphenyl)thio)-8-phenyl-6H-[1,3]dioxolo[4,5-g]chromen-6-one (3ea). R_f = 0.4 (20 % ethyl acetate in hexane); white solid; yield 49% (45 mg); mp 158-161 ºC; ^{1}H NMR (400 MHz, $CDCl_3$) δ 7.50-7.49 (m, 3H), 7.21-7.17 (m, 4H), 6.85 (s, 1H), 6.75-6.73 (m, 2H), 6.40 (s, 1H), 6.02 (s, 2H), 3.75 (s, 3H); ^{13}C{^{1}H} NMR (100 MHz, $CDCl_3$) δ 160.08, 159.29, 158.4, 151.4, 150.7, 144.7, 135.6, 132.9, 129.0, 128.7, 128.4, 125.4, 119.8, 114.7, 114.6, 105.5, 102.5, 98.8942, 55.4; IR (KBr) ῡ 2946, 1590, 1482,699 ; HRMS (ESI/Q-TOF) m/z: $[M + H]^+$ calcd for $C_{23}H_{16}O_5S$ 404.0727; found 404.0718.

3-((4-Methoxyphenyl)thio)-4-(thiophen-3-yl)-2H-chromen-2-one (3fa). R_f = 0.45 (10% ethyl acetate in hexane); yellow solid; yield 52% (50 mg); mp 132-135 ºC; ^{1}H NMR (400 MHz, $CDCl_3$) δ 7.50-7.32 (m, 4H), 7.26-7.10 (m, 5H), 6.76-6.74 (m, 2H), 3.76 (s, 3H); ^{13}C{^{1}H} 10 MHz, $CDCl_3$) δ 159.4, 153.1, 153.0, 135.8, 134.6, 133.1, 132.1, 128.5, 127.8, 126.3, 126.1, 124.9, 124.5, 124.1, 120.7, 116.9, 114.7, 55.5; IR (KBr) ῡ 2960, 1725, 1599, 1245,658 ; HRMS (ESI/Q-TOF) m/z: $[M + H]^+$ calcd for $C_{20}H_{15}O_3S_2$ 367.0463; found 367.0445.

4-Phenyl-3-(*p*-tolylthio)-2H-chromen-2-one (3ab).[20] R_f = 0.45 (10% ethyl acetate in hexane); yellow solid; yield 72% (67 mg); ^{1}H NMR (700 MHz, $CDCl_3$) δ 7.54-7.50 (m, 4H), 7.39 (d, *J* = 8.3 Hz, 1H), 7.27-7.26 (m, 2H), 7.19-7.17 (m, 1H), 7.13-7.09 (m, 3H), 7.0 (d, *J* = 7.9 Hz,

2H), 2.28 (s, 3H); $^{13}C\{^{1}H\}$ NMR (176 MHz, $CDCl_3$) δ 159.3, 158.4, 153.4, 137.0, 135.1, 132.1, 131.2, 130.1, 129.8, 129.1, 128.6, 128.5, 128.2, 124.4, 122.6, 120.7, 116.9, 21.2.

3-((4-Bromophenyl)thio)-4-phenyl-2H-chromen-2-one (3ac).[20] R_f = 0.4 (10% ethyl acetate in hexane); yellow solid; yield 63% (70mg); ^{1}H NMR (400 MHz, $CDCl_3$) δ 7.51-7.43 (m, 4H), 7.35-7.33 (m, 1H), 7.26-7.24 (m, 2H), 7.19-7.11 (m, 3H), 7.05-7.03 (m, 1H), 7.01-6.99 (m, 2H); $^{13}C\{^{1}H\}$ NMR (100 MHz, $CDCl_3$) δ 159.4, 159.2, 153.5, 134.8, 134.2, 132.6, 132.1, 131.1, 129.3×2, 128.8, 128.4, 124.6, 121.4, 121.0, 120.5, 117.1.

3-((4-Chlorophenyl)thio)-4-phenyl-2H-chromen-2-one (3ad).[20] R_f = 0.4 (10% ethyl acetate in hexane); yellow solid; yield 67% (66 mg); ^{1}H NMR (400 MHz, $CDCl_3$) δ 7.51-7.43 (m, 4H), 7.35-7.33 (m, 1H), 7.19-7.14 (m, 3H), 7.12-7.07 (m, 3H), 7.05-7.03 (m, 2H); $^{13}C\{^{1}H\}$ NMR (100 MHz, $CDCl_3$) δ 159.3, 153.5, 134.9, 133.4, 133.0, 132.6, 131.0, 129.3, 129.2, 128.8, 128.4, 128.3, 124.6, 123.7, 121.6, 120.5, 117.1.

3-(Ethylthio)-4-phenyl-2H-chromen-2-one (3ae).[20] R_f = 0.6 (5 % ethyl acetate in hexane); white solid; yield 89% (70 mg); ^{1}H NMR (700 MHz, $CDCl_3$) δ 7.55-7.48 (m, 3H), 7.39-7.38 (m, 1H), 7.26- 7.24 (m, 3H), 7.15 (t, *J* = 7.6 Hz, 1H), 7.02 (d, *J* = 8.0 Hz, 1H), 2.95 (q, *J* = 7.4 Hz, 2H), 1.14 (t, *J* = 7.4 Hz, 3H); $^{13}C\{^{1}H\}$ NMR (176 MHz, $CDCl_3$) δ 159.6, 156.8, 153.0, 135.5, 131.5, 129.0, 128.7, 128.7, 127.8, 124.4, 122.6, 120.8, 116.8, 27.6, 15.2.

4-Phenyl-3-(phenylselanyl)-2H-chromen-2-one (3ax).[36] R_f = 0.6 (10% ethyl acetate in hexane); white solid; yield 73% (75 mg); ^{1}H NMR (700 MHz, $CDCl_3$) δ 7.53-7.51 (m, 1H), 7.46-7.45 (m, 3H), 7.38-7.37 (m, 1H), 7.33-7.32 (m, 2H), 7.20-7.14 (m, 6H), 7.06 (d, *J* = 8.0

Hz, 1H); $^{13}C\{^{1}H\}$ NMR (176 MHz, $CDCl_3$) δ 159.7, 159.1, 153.6, 136.4, 133.0, 132.1, 130.4, 129.2, 129.0, 128.6, 128.4, 128.1, 127.5, 124.4, 120.9, 120.6, 116.9.

6-Ethyl-4-phenyl-3-(phenylselanyl)-2H-chromen-2-one (3cx).[36] R_f = 0.45 (5% ethyl acetate in hexane); white solid; yield 67% (65 mg); ^{1}H NMR (700 MHz, $CDCl_3$) δ 7.46-7.45 (m, 3H), 7.37-7.36 (m, 1H), 7.31-7.30 (m, 3H), 7.18-7.13 (m, 5H), 6.83 (s, 1H), 2.55 (q, 7.6 Hz, 2H), 1.12 (t, *J* = 7.6 Hz, 3H); $^{13}C\{^{1}H\}$ NMR (176 MHz, $CDCl_3$) δ 159.9, 159.4, 151.9, 140.6, 136.5, 132.8, 132.0, 130.6, 129.1, 128.9, 128.6, 128.4, 127.4, 126.7, 120.6, 120.3, 116.8, 28.4, 15.8.

4-(2,4-Difluorophenyl)-3-(phenylselanyl)-2H-chromen-2-one (3hx). R_f = 0.4 (5% ethyl acetate in hexane); white solid; yield 72% (70 mg); mp 155-158 ºC; ^{1}H NMR (400 MHz, $CDCl_3$) δ 7.55-7.51 (m, 1H), 7.40-7.37 (m, 1H), 7.33-7.31 (m, 2H), 7.23-7.12 (m, 5H), 6.99-6.95 (m, 2H), 6.85-6.79 (m, 1H); $^{13}C\{^{1}H\}$ NMR (176 MHz, $CDCl_3$) δ 164.40 (d, *J* = 11.8 Hz), 163.69 (dd, *J* = 252.2, 11.8 Hz), 162.97 (d, *J* = 11.9 Hz), 159.83 (d, *J* = 12.9 Hz), 159.31 (s), 160.1 (dd, *J* = 252.0, 12.8 Hz), 158.4 (d, *J* = 12.8 Hz), 153.3, 152.0, 133.4, 132.3, 131.2 (dd, *J* = 9.7, 4.5 Hz), 129.5, 129.2, 127.9, 126.8, 124.7, 123.6, 120.0, 117.1, 112.0 (dd, *J* = 21.2, 4.0 Hz), 104.6 (t, *J* = 25.3 Hz); IR (KBr) ῡ 3018, 1710, 1597, 737; HRMS (ESI/Q-TOF) m/z: $[M + H]^+$ calcd for $C_{21}H_{13}F_2O_2Se$ 415.0045; found 415.0076.

4-([1,1'-biphenyl]-4-yl)-3-(phenylselanyl)-2H-chromen-2-one (3ix).[37] R_f = 0.4 (5% ethyl acetate in hexane); white solid; yield 66% (60 mg); ^{1}H NMR (400 MHz, $CDCl_3$) δ 7.67-7.63 (m, 4H), 7.55-7.48 (m, 3H), 7.43-7.39 (m, 2H), 7.33-7.31 (m, 2H), 7.24-7.18 (m, 3H), 7.17-7.11(m, 4H); $^{13}C\{^{1}H\}$ NMR (100 MHz, $CDCl_3$) δ 159.8, 158.5, 153.6, 141.7, 140.4, 135.0, 133.2, 132.1, 130.4, 129.1, 129.0, 128.9, 127.9, 128.0, 127.6, 127.3, 127.2, 124.4, 121.2, 120.6, 117.0.

4-(Naphthalen-1-yl)-3-(phenylselanyl)-2H-chromen-2-one (3jx).[37] R_f = 0.4 (5% ethyl acetate in hexane); white solid; yield 70% (65 mg); ^{1}H NMR (400 MHz, $CDCl_3$) δ 7.97-7.91 (m, 2H), 7.57-7.47 (m, 3H), 7.42-7.35 (m, 3H), 7.30-7.28 (m, 1H), 7.25-7.22 (m, 2H), 7.11-7.00(m, 4H), 6.80-6.77 (m, 1H); ^{13}C{^{1}H} NMR (100 MHz, $CDCl_3$) δ 159.5, 157.5, 153.4, 133.9, 133.6, 133.5, 132.1, 130.5, 129.5, 129.3, 128.9, 128.7, 128.0, 127.7, 127.0, 126.6, 126.4, 125.4, 125.2, 124.5, 122.6, 120.9, 116.9.

3-((4-Methoxyphenyl)thio)-1-methyl-4-phenylquinolin-2(1H)-one (5aa).[38] R_f = 0.45 (20% ethyl acetate in hexane); white solid; yield 81% (77 mg); ^{1}H NMR (400 MHz, $CDCl_3$) δ 7.57-7.39 (m, 5H), 7.26-7.09 (m, 6H), 6.73-6.71 (m, 2H), 3.79 (s, 3H), 3.74 (s, 3H); ^{13}C{^{1}H} NMR (176 MHz, $CDCl_3$) δ 162.3, 160.6, 158.8, 154.2, 139.8, 137.1, 132.1, 130.9, 129.0, 128.5, 128.3, 127.7, 126.7, 122.2, 121.6, 114.5, 114.3, 55.4, 30.8.

6-Ethyl-3-((4-methoxyphenyl)thio)-1-methyl-4-phenylquinolin-2(1H)-one (5ba). R_f = 0.45 (20% ethyl acetate in hexane); white solid; yield 85% (82 mg); mp 160-162 ºC; ^{1}H NMR (400 MHz, $CDCl_3$) δ 7.48-7.32 (m, 5H), 7.26-7.15 (m, 4H), 6.95 (s, 1H), 6.71 (d, *J* = 8.2 Hz, 2H), 3.78 (s, 3H), 3.74 (s, 3H), 2.56 (q, *J* = 7.4 Hz, 2H), 1.13 (t, *J* = 7.5 Hz, 3H); ^{13}C{^{1}H} NMR (100 MHz, $CDCl_3$) δ 160.5, 158.7, 154.2, 138.2, 138.1, 137.2, 131.9, 131.1, 129.0, 128.4, 128.3, 127.5, 127.4, 126.9, 121.5, 114.5, 114.4, 55.4, 30.8, 28.3, 15.9; IR (KBr) ῡ 2926, 1715, 1640, 667; HRMS (ESI/Q-TOF) m/z: $[M + H]^+$ calcd for $C_{25}H_{24}NO_2S$ 402.1522; found 402.1549.

6-Isopropyl-3-((4-methoxyphenyl)thio)-1-methyl-4-phenylquinolin-2(1H)-one (5ca). R_f = 0.45 (10% ethyl acetate in hexane); white solid; yield 87% (78 mg); mp 125-130 ºC; ^{1}H NMR

(400 MHz, $CDCl_3$) δ 7.48-7.45 (m, 4H), 7.36-7.34 (m, 1H), 7.26-7.14 (m, 4H), 6.98 (s, 1H), 6.72-6.71 (m, 1H), 3.78 (s, 3H), 3.74 (s, 3H), 2.87-2.77 (m, 1H), 1.14 (s, 6H); $^{13}C\{^1H\}$ NMR (100 MHz, $CDCl_3$) δ 160.5, 158.6, 154.3, 142.8, 138.2, 137.2, 131.8, 131.7, 129.4, 129.0, 128.4, 128.3, 127.0, 126.3, 121.4, 114.5, 114.4, 55.4, 33.5, 30.8, 24.1; IR (KBr) ῡ 2930, 1785, 1649, 721; HRMS (ESI/Q-TOF) m/z: $[M + H]^+$ calcd for $C_{26}H_{25}NO_2S$ 415.1599; found 415.1606.

6-(*tert*-Butyl)-3-((4-methoxyphenyl)thio)-1-methyl-4-phenylquinolin-2(1H)-one (5da). R_f = 0.45 (10% ethyl acetate in hexane); white solid; yield 88% (81 mg); mp 150-155 ºC; ^1H NMR (700 MHz, $CDCl_3$) δ 7.62-7.60 (m, 1H), 7.48-7.45 (m, 3H), 7.35-7.34 (m, 1H), 7.23-7.22 (m, 2H), 7.16-7.15 (m, 3H), 6.71 (d, *J* = 8.7 Hz, 2H), 3.78 (s, 3H), 3.73 (s, 3H), 1.19 (s, 9H); $^{13}C\{^1H\}$ NMR (176 MHz, $CDCl_3$) δ 160.6, 158.7, 154.5, 145.1, 137.9, 137.1, 131.9, 129.0, 128.8, 128.4, 128.3, 127.3, 127.0, 125.1, 121.2, 114.5, 114.1, 55.4, 34.4, 31.3, 30.8; IR (KBr) ῡ 2959, 1641, 1492, 816, 692; HRMS (ESI/Q-TOF) m/z: $[M + H]^+$ calcd for $C_{27}H_{28}ClNO_2S$ 430.1835; found 430.1819.

6,7-Dichloro-3-((4-methoxyphenyl)thio)-1-methyl-4-phenylquinolin-2(1H)-one (5ea). R_f = 0.45 (20% ethyl acetate in hexane); white solid; yield 78% (68 mg); mp 170-173 ºC; ^1H NMR (400 MHz, $CDCl_3$) δ 7.52-7.48 (m, 4H), 7.19-7.17 (m, 5H), 6.72-6.70 (d, *J* = 8.4 Hz, 1H), 3.74 (s, 3H), 3.73 (s, 3H); $^{13}C\{^1H\}$ NMR (100 MHz, $CDCl_3$) δ 160.1, 159.0, 151.9, 138.7, 136.0, 135.0, 134.3, 132.7, 129.7, 129.5, 128.9, 128.8, 126.3, 125.8, 121.3, 116.0, 114.6, 55.4, 31.1; IR (KBr) ῡ 2921, 1725, 1529, 1171, 734; HRMS (ESI/Q-TOF) m/z: $[M + H]^+$ calcd for $C_{23}H_{17}Cl_2NO_2S$ 441.0367; found 441.0357.

4-([1,1'-Biphenyl]-2-yl)-3-((4-methoxyphenyl)thio)-1-methylquinolin-2(1H)-one (5ga). R_f = 0.45 (20% ethyl acetate in hexane); white solid; yield 70% (60 mg); mp 166-170 ºC; ^{1}H NMR (400 MHz, $CDCl_3$) δ 7.55-7.50 (m, 3H), 7.46-7.42 (m, 1H), 7.35-7.28 (m, 3H), 7.18-7.10 (m, 6H), 6.89-6.87 (m, 2H), 6.66-6.64 (m, 2H), 3.73 (s, 3H), 3.69 (s, 3H); ^{13}C{^{1}H} NMR (100 MHz, $CDCl_3$) δ 160.1, 158.6, 153.3, 141.6, 140.7, 139.6, 135.4, 131.5, 130.7, 130.6, 129.7, 129.0, 128.9, 128.9, 128.2, 127.6, 127.3, 127.2, 126.5, 122.3, 122.1, 114.4, 114.3, 55.3, 30.7; IR (KBr) ῡ 2917, 1728, 1495, 735; HRMS (ESI/Q-TOF) m/z: $[M + H]^+$ calcd for $C_{29}H_{24}NO_2S$ 449.1501; found 450.1528.

1-Methyl-4-phenyl-3-(phenylthio)quinolin-2(1H)-one (5af).[38] R_f = 0.4 (20% ethyl acetate in hexane); white solid; yield 77% (72 mg); ^{1}H NMR (700 MHz, $CDCl_3$) δ 7.60-7.58 (m, 1H), 7.45-7.42 (m, 4H), 7.23-7.20 (m, 3H), 7.17-7.14 (m, 4H), 7.13-7.09 (m, 2H), 3.81 (s, 3H); ^{13}C{^{1}H} NMR (176 MHz, $CDCl_3$) δ 160.5, 155.6, 140.1, 137.0, 136.7, 131.3, 129.1, 128.8, 128.7, 128.6, 128.5, 128.4, 126.2, 126.0, 122.3, 121.5, 114.4, 30.9.

.

1-Methyl-4-phenyl-3-(p-tolylthio)quinolin-2(1H)-one (5ab).[38] R_f = 0.35 (10% ethyl acetate in hexane); white solid; yield 72% (70 mg); ^{1}H NMR (700 MHz, $CDCl_3$) δ 7.58-7.56 (m, 1H), 7.46-7.41 (m, 4H), 7.26-7.19 (m, 3H), 7.13-7.08 (m, 3H), 6.98 (d, *J* = 7.7 Hz, 2H), 3.80 (s, 3H), 2.26 (s, 3H); ^{13}C{^{1}H} NMR (176 MHz, $CDCl_3$) δ 160.5, 155.0, 140.0, 137.1, 136.0, 132.9, 131.1, 129.7, 129.1, 128.9, 128.5, 128.4, 128.3, 126.7, 122.2, 121.5, 114.3, 30.8, 21.2.

3-((4-Chlorophenyl)thio)-1-methyl-4-phenylquinolin-2(1H)-one (5ad).[38] R_f = 0.4 (10% ethyl acetate in hexane); white solid; yield 62% (60 mg); ^{1}H NMR (700 MHz, $CDCl_3$) δ 7.61-7.59 (m, 1H), 7.47-7.43 (m, 4H), 7.22-7.20 (m, 3H), 7.15-7.12 (m, 3H), 7.10-7.08 (m, 2H),

3.81 (s, 3H); $^{13}C\{^{1}H\}$ NMR (176 MHz, $CDCl_3$) δ 160.3, 155.7, 140.1, 136.8, 135.2, 132.0, 131.5, 130.0, 129.5, 129.2, 129.0, 128.7, 128.5, 125.8, 122.4, 121.4, 114.4, 30.9.

3-((4-Fluorophenyl)thio)-1-methyl-4-phenylquinolin-2(1H)-one (5ag).[39] R_f = 0.45 (10% ethyl acetate in hexane); white solid; yield 75% (68 mg); ^{1}H NMR (400 MHz, $CDCl_3$) δ 7.60-7.56 (m, 1H), 7.49-7.41 (m, 4H), 7.26-7.17 (m, 4H), 7.16-7.10 (m, 2H), 6.89-6.84 (m, 2H), 3.80 (s, 3H); $^{13}C\{^{1}H\}$ NMR (100 MHz, $CDCl_3$) δ 161.8 (d, *J* = 245.7 Hz), 160.5, 155.0, 139.9, 136.9, 131.5 (d, *J* = 8.0 Hz), 131.4, 131.3, 129.1, 128.8, 128.5, 128.4, 126.7, 122.3, 121.5, 115.9 (d, *J* = 22.0 Hz), 114.4, 30.8.

3-((3-Chlorophenyl)thio)-1-methyl-4-phenylquinolin-2(1H)-one (5ah). R_f = 0.45 (10% ethyl acetate in hexane); white solid; yield 64% (62 mg); mp 142-145 ºC; ^{1}H NMR (700 MHz, $CDCl_3$) δ 7.62-7.60 (m, 1H), 7.45-7.44 (m, 4H), 7.21-7.13 (m, 4H), 7.10-7.04 (m, 4H), 3.82 (s, 3H); $^{13}C\{^{1}H\}$ NMR (176 MHz, $CDCl_3$) δ 160.3, 156.1, 140.2, 138.8, 136.7, 134.6, 131.6, 129.8, 129.2, 128.7, 128.6, 128.5, 128.0, 126.5, 126.2, 125.3, 122.4, 121.4, 114.5, 30.9; IR (KBr) $\bar{\upsilon}$ 2919, 1623, 1071, 699; HRMS (ESI/Q-TOF) m/z: $[M + Na]^+$ calcd for $C_{22}H_{16}ClNOSNa$ 400.0558; found 400.0539.

1-Methyl-4-phenyl-3-(phenylselanyl)quinolin-2(1H)-one (5ax).[36] R_f = 0.45 (10% ethyl acetate in hexane); white solid; yield 86% (86 mg); ^{1}H NMR (700 MHz, $CDCl_3$) δ 7.57-7.55 (m, 1H), 7.42-7.39 (m, 4H), 7.28-7.26 (m, 2H), 7.17-7.13 (m, 4H), 7.11-7.08 (m, 3H), 3.82 (s, 3H); $^{13}C\{^{1}H\}$ NMR (176 MHz, $CDCl_3$) δ 160.7, 155.1, 140.0, 138.2, 132.3, 131.9, 131.0, 128.9, 128.87, 128.8, 128.4, 128.2, 126.8, 126.4, 122.2, 121.7, 114.3, 31.0.

4-(4-Bromophenyl)-6-(tert-butyl)-1-methyl-3-(phenylselanyl)quinolin-2(1H)-one (5dx). R_f = 0.45 (10% ethyl acetate in hexane); white solid; yield 89% (76 mg); mp 171-175 ºC; ^{1}H NMR (400 MHz, $CDCl_3$) δ 7.64-7.61 (m, 1H), 7.48-7.45 (m, 2H), 7.38-7.35 (m, 1H), 7.22-7.20 (m, 2H), 7.14-7.12 (m, 1H), 7.10-7.07 (m, 3H), 6.99-6.97 (m, 2H), 3.82 (s, 3H), 1.19 (s, 9H); ^{13}C NMR (176 MHz, $CDCl_3$) δ 160.7, 153.4, 145.2, 137.9, 136.8, 132.7, 131.8, 131.5, 130.7, 129.0, 128.8, 127.0, 126.9, 124.3, 122.3, 120.9, 114.2, 34.5, 31.3, 30.9; IR (KBr) ῡ 2919, 1651, 1526, 726; HRMS (ESI/Q-TOF) m/z: $[M + H]^+$ calcd for $C_{26}H_{25}BrNOSe$ 526.0281; found 526.0313.

3-((4-Methoxyphenyl)thio)-1-methyl-4-phenyl-1-azaspiro[4.5]deca-3,6,9-triene-2,8-dione (6ha).[40] R_f = 0.35 (10 % ethyl acetate in hexane); white solid; yield 71% (70 mg); ^{1}H NMR (400 MHz, $CDCl_3$) δ 7.28-7.21 (m, 7H), 7.16-7.14 (m, 2H), 6.70-6.68 (m, 2H), 6.50-6.47 (m, 2H), 6.45-6.42 (m, 2H), 3.74 (s, 1H), 2.87 (s, 3H); ^{13}C NMR (100 MHz, $CDCl_3$) δ 184.1, 168.0, 159.9, 150.3, 145.4, 134.7, 133.7, 133.2, 130.8, 129.5, 128.4, 128.3, 121.2, 114.6, 67.8, 55.4, 26.4.

.

1-Methyl-4-phenyl-3-(p-tolylthio)-1-azaspiro[4.5]deca-3,6,9-triene-2,8-dione (6hb).[40] R_f = 0.45 (10 % ethyl acetate in hexane); white solid; yield 92% (77 mg); ^{1}H NMR (400 MHz, $CDCl_3$) δ 7.28-7.21 (m, 5H), 7.16-7.14 (m, 2H), 6.70-6.68 (m, 2H), 6.50-6.47 (m, 2H), 6.45-6.42 (m, 2H), 3.74 (s, 3H), 2.87 (s, 3H); ^{13}C{^{1}H} NMR (100 MHz, $CDCl_3$) δ 184.1, 168.0, 159.9, 150.3, 145.4, 134.7, 133.7, 133.2, 130.8, 129.5, 128.4, 128.3, 121.2, 114.6, 67.8, 55.4, 26.4.

1-Methyl-4-phenyl-3-(phenylthio)-1-azaspiro[4.5]deca-3,6,9-triene-2,8-dione (6hf).[40] R_f = 0.4 (10% ethyl acetate in hexane); white solid; yield 86% (70 mg); ^{1}H NMR (700 MHz, $CDCl_3$)

δ 7.76-7.75 (m, 2H), 7.51-7.44 (m, 3H), 7.46-7.38 (m, 3H), 7.28-7.26 (m, 2H), 6.51-6.48 (m, 2H), 6.47-6.44 (m, 2H), 2.81 (s, 3H); $^{13}C\{^{1}H\}$ NMR (176 MHz, $CDCl_3$) δ 183.5, 164.7, 159.8, 143.4, 143.3, 141.4, 139.4, 134.2, 134.0, 131.4, 130.9, 129.3, 128.8, 128.6, 128.6, 125.2, 68.2, 26.1.

3-((4-Bromophenyl)thio)-1-methyl-4-phenyl-1-azaspiro[4.5]deca-3,6,9-triene-2,8-dione (6hc).[40] R_f = 0.45 (10% ethyl acetate in hexane); white solid; yield 61% (60 mg); ^{1}H NMR (700 MHz, $CDCl_3$) δ 7.42-7.32 (m, 4H), 7.30-7.25 (m, 3H), 7.20-7.15(m, 2H), 6.51-6.50 (m, 2H), 6.48-6.46 (m, 2H), 2.96 (s, 3H); $^{13}C\{^{1}H\}$ NMR (176 MHz, $CDCl_3$) δ 183.8, 167.6, 158.1, 145.0, 144.2, 133.45, 132.9, 132.2, 132.0, 130.8, 130.3, 130.0, 128.8, 128.6, 128.2, 127.8, 67.9, 27.2.

3-((4-Fluorophenyl)thio)-1-methyl-4-phenyl-1-azaspiro[4.5]deca-3,6,9-triene-2,8-dione (6hg).[40] R_f = 0.45 (10% ethyl acetate in hexane); white solid; yield 73% (62 mg); ^{1}H NMR (700 MHz, $CDCl_3$) δ 7.36-7.29(m, 3H), 7.26-7.24 (m, 2H), 7.17-7.16 (m, 2H), 6.86 (t, *J* = 8.5 Hz, 2H), 6.50 (d, *J* = 10.0 Hz, 2H), 6.46 (d, *J* = 10.0 Hz, 2H), 2.88 (s, 3H); $^{13}C\{^{1}H\}$ NMR (176 MHz, $CDCl_3$) δ 184.0, 167.7, 162.7 (d, *J* = 248.9 Hz), 151.7, 145.1, 144.2, 134.3 (d, *J* = 8.6 Hz), 133.4, 132.8, 130.6, 129.8, 128.8, 128.5, 128.3, 126.2 (d, *J* = 3.3 Hz), 116.2 (d, *J* = 21.9 Hz), 67.9, 26.4.

3-((3-Chlorophenyl)thio)-1-methyl-4-phenyl-1-azaspiro[4.5]deca-3,6,9-triene-2,8-dione (6hh).[40] R_f = 0.45 (10% ethyl acetate in hexane); white solid; yield 78% (70 mg); ^{1}H NMR (700 MHz, $CDCl_3$) δ 7.32-7.25 (m, 4H), 7.21-7.17 (m, 3H), 7.13-7.09 (m, 2H), 6.50 (d, *J* = 10.0 Hz, 2H), 6.46 (d, *J* = 10.0 Hz, 2H), 2.88 (s, 3H); $^{13}C\{^{1}H\}$NMR (176 MHz, $CDCl_3$) δ

184.0, 167.5, 153.5, 144.9, 144.2, 134.7, 133.6, 133.5, 131.6, 130.8, 130.5, 130.3, 130.0, 129.1, 128.8, 128.5, 128.1, 128.0, 68.0, 26.5.

1-Methyl-3-((4-nitrophenyl)thio)-4-phenyl-1-azaspiro[4.5]deca-3,6,9-triene-2,8-dione (6hi). R_f = 0.45 (30% ethyl acetate in hexane); white solid; yield 44% (40 mg); mp 141-145 ºC; ^{1}H NMR (700 MHz, $CDCl_3$) δ 8.09-8.08 (m, 2H), 7.38-7.32(m, 4H), 7.31-7.26 (m, 3H), 6.57-6.53 (m, 4H), 2.93 (s, 3H); ^{13}C{^{1}H} NMR (176 MHz, $CDCl_3$) δ 183.7, 167.0, 157.1, 146.5, 144.4, 142.3, 141.7, 133.8, 131.0, 130.6, 130.4, 129.6, 129.1, 128.8, 128.0, 124.2, 68.1, 26.6; IR (KBr) ῡ 2917, 1512, 1334, 852, 734; HRMS (ESI/Q-TOF) m/z: $[M + H]^+$ calcd for $C_{22}H_{17}N_2O_4S$ 405.0943; found 405.0909.

1-Methyl-4-phenyl-3-((2,3,5,6-tetrafluorophenyl)thio)-1-azaspiro[4.5]deca-3,6,9-triene-2,8-dione (6hj). R_f = 0.45 (10% ethyl acetate in hexane); white solid; yield 65% (63 mg); mp 171-176 ºC; ^{1}H NMR (700 MHz, $CDCl_3$) δ 7.32-7.26 (m, 3H), 7.21-7.20 (d, *J* = 7.4 Hz, 1H), 6.95-6.90 (m, 1H), 6.50 (d, *J* = 10.2 Hz, 2H), 6.46 (d, *J* = 10.2 Hz, 2H), 2.88 (s, 3H); ^{13}C{^{1}H} NMR (176 MHz, $CDCl_3$) δ 183.9, 166.7, 150.1, 147.2, 146.5, 145.8, 145.0, 144.6, 133.6, 130.1, 130.0, 129.2, 128.6, 127.9, 110.6 (t, *J* = 19.1 Hz), 106.9 (t, *J* = 22.9 Hz), 68.0, 26.4; IR (KBr) ῡ 2919, 1663, 919, 709; HRMS (ESI/Q-TOF) m/z: $[M + H]^+$ calcd for $C_{22}H_{14}F_4NO_2S$ 432.0645; found 432.0681.

1-Methyl-4-phenyl-3-((4-(trifluoromethyl)phenyl)thio)-1-azaspiro[4.5]deca-3,6,9-triene-2,8-dione (6hk). R_f = 0.45 (10% ethyl acetate in hexane); white solid; yield 77% (75 mg); mp 148-151 ºC; ^{1}H NMR (400 MHz, $CDCl_3$) δ 7.45-7.43 (m, 2H), 7.37-7.29 (m, 3H), 7.28-7.21 (m, 4H), 6.56-6.48 (m, 4H), 2.92 (s, 3H); ^{13}C{^{1}H} NMR (100 MHz, $CDCl_3$) δ 183.9, 167.4, 155.1, 144.7, 144.2, 137.3, 133.6, 133.5, 130.9, 130.5, 130.3, 130.1, 128.9, 128.7, 128.1, 127.8,

125.9 (q, J = 3.6 Hz), 68.1, 26.5; IR (KBr) ῡ 2917, 1547, 1222, 771; HRMS (ESI/Q-TOF) m/z: $[M + H]^+$ calcd for $C_{23}H_{17}F_3NO_2S$ 428.0947; found 428.0932.

1-Methyl-4-phenyl-3-(phenylselanyl)-1-azaspiro[4.5]deca-3,6,9-triene-2,8-dione (6hx).[41] R_f = 0.45 (10% ethyl acetate in hexane); white solid; yield 79% (73 mg); ^{1}H NMR (700 MHz, $CDCl_3$) δ 7.39 (d, J = 7.3 Hz, 2H), 7.28-7.26 (m, 1H), 7.22-7.18 (m, 3H), 7.13-7.11(m, 4H), 6.54-6.52 (m, 2H), 6.46-6.44 (m, 2H), 2.92 (s, 3H); ^{13}C{^{1}H} NMR (176 MHz, $CDCl_3$) δ 184.1, 168.9, 154.2, 145.2, 134.0, 133.2, 131.3, 130.3, 129.5, 129.1, 128.6, 128.3, 128.1, 128.0, 127.2, 126.7, 69.2, 26.5.

3-((4-Methoxyphenyl)sulfinyl)-4-phenyl-2H-chromen-2-one (7). R_f = 0.4 (50% ethyl acetate in hexane); white solid; yield 94% (59 mg); mp 160-163 ºC; ^{1}H NMR (700 MHz, $CDCl_3$) δ 7.61-7.57 (m, 6H), 7.5-7.50 (m, 1H), 7.36-7.32 (m, 2H), 7.21-7.19 (m, 1H), 7.14-7.13 (m, 1H), 6.97-6.95 (m, 2H), 3.82 (s, 3H); ^{13}C{^{1}H} NMR (176 MHz, $CDCl_3$) δ 161.9, 158.3, 154.8, 154.3, 134.0, 132.7, 132.1, 130.0, 129.3, 129.1, 128.8, 128.6, 127.1, 124.8, 119.9, 117.2, 114.5, 55.6; IR (KBr) ῡ 3000, 1677, 1529, 702; HRMS (ESI/Q-TOF) m/z: $[M + H]^+$ calcd for $C_{22}H_{17}O_4S$ 377.0835; found 377.0847.

3-((4-Methoxyphenyl)sulfonyl)-1-methyl-4-phenylquinolin-2(1H)-one (8). R_f = 0.4 (5% ethyl acetate in hexane); white solid; yield 88% (55 mg); mp 160-165 ºC; ^{1}H NMR (400 MHz, $CDCl_3$) δ 8.00-7.97 (m, 2H), 7.64-7.54 (m, 4H), 7.38-7.33 (m, 3H), 7.13-7.12 (m, 2H), 6.96-6.94 (m, 2H), 3.84 (s, 3H), 3.70 (s, 3H); ^{13}C{^{1}H} NMR (100 MHz, $CDCl_3$) δ 163.3, 157.4, 154.3, 140.7, 134.6, 133.4, 133.0, 131.4, 130.7, 130.0, 128.4, 128.0, 127.9, 122.5, 121.1, 114.1,

113.5, 55.6, 30.0; IR (KBr) ῡ 3063, 2917, 1650, 1543, 1010, 755; HRMS (ESI/Q-TOF) m/z: $[M + H]^+$ calcd for $C_{23}H_{20}NO_4S$ 406.1122; found 406.1113.

4-Phenyl-3-((4-(phenylethynyl)phenyl)thio)chroman-2-one (9). R_f = 0.45 (10% ethyl acetate in hexane); white solid; yield 56% (40 mg); mp 165-170 ºC; ^{1}H NMR (700 MHz, $CDCl_3$) δ 7.59 (t, *J* = 8.8 Hz, 1H), 7.54 (dd, *J* = 21.7, 7.3 Hz, 1H), 7.44 (d, *J* = 8.2 Hz, 1H), 7.31 (t, *J* = 9.1 Hz, 1H), 7.25 (dd, *J* = 15.1, 7.6 Hz, 1H); ^{13}C{^{1}H} NMR (176 MHz, $CDCl_3$) δ 159.6, 156.4, 153.0, 134.5, 132.2, 131.9, 129.5×2, 129.3, 128.9, 128.6, 128.4×2, 127.7, 124.7×2, 122.6, 117.2, 111.4×2, 98.9, 83.9; IR (KBr) ῡ 2917, 2845, 1720, 1600, 690; HRMS (ESI/Q-TOF) m/z: $[M + H]^+$ calcd for $C_{29}H_{19}O_2S$ 432.1106; found 432.1129.

S-(4-Methoxyphenyl) 4-methoxybenzenesulfonothioate (10).[42] R_f = 0.55 (10% ethyl acetate in hexane); white solid; ^{1}H NMR (700 MHz, $CDCl_3$) δ 7.51 (d, *J* = 8.2 Hz, 2H), 7.28-7.26 (m, 2H), 6.88-6.84 (m, 4H), 3.87 (s, 3H), 3.83 (s, 3H); ^{13}C{^{1}H} NMR (176 MHz, $CDCl_3$) δ 163.7, 162.4, 138.5, 135.1, 130.1, 119.1, 115.0, 114.0, 55.8, 55.6.

5.6 NOTES AND REFERENCES

(1) Pan, P.; Liu, S.; Lan, Y.; Zeng, H.; Li, C.-J. Visible-Light-Induced Cross-Coupling of Aryl Iodides with Hydrazones Via an Eda-Complex. *Chem. Sci.* **2022**, *13*, 7165-7171.

(2) Marzo, L.; Pagire, S. K.; Reiser, O.; König, B. Visible-Light Photocatalysis: Does It Make a Difference in Organic Synthesis? *Angew. Chem. Int. Ed.* **2018**, *57*, 10034-10072.

(3) Romero, N. A.; Nicewicz, D. A. Organic Photoredox Catalysis. *Chem. Rev.* **2016**, *116*, 10075-10166.

(4) Sahoo, A. K.; Rakshit, A.; Dahiya, A.; Pan, A.; Patel, B. K. Visible-Light-Mediated Synthesis of Thio-Functionalized Pyrroles. *Org. Lett.* **2022**, *24*, 1918-1923.

(5) Das, S.; Parida, S. K.; Mandal, T.; Hota, S. K.; Roy, L.; De Sarkar, S.; Murarka, S. An Organophotoredox-Catalyzed Redox-Neutral Cascade Involving N-(Acyloxy)Phthalimides and Maleimides. *Org. Chem. Front.* **2021**, *8*, 2256-2262.

(6) Vanderghinste, J.; Das, S. Applications of Photoredox Catalysis for the Radical-Induced Cleavage of C–C Bonds. *Synthesis* **2022**, *54*, 3383-3398.

(7) Patel, R. I.; Sharma, A.; Sharma, S.; Sharma, A. Visible Light-Mediated Applications of Methylene Blue in Organic Synthesis. *Org. Chem. Front.* **2021**, *8*, 1694-1718.

(8) Sharma, S.; Sharma, A. Recent Advances in Photocatalytic Manipulations of Rose Bengal in Organic Synthesis. *Org. Biomol. Chem.* **2019**, *17*, 4384-4405.

(9) Beletskaya, I. P.; Nájera, C.; Yus, M. Chemodivergent Reactions. *Chem. Soc. Rev.* **2020**, *49*, 7101-7166.

(10) Bera, S. K.; Mal, P. Regiodivergent C–N Coupling of Quinazolinones Controlled by the Dipole Moments of Tautomers. *Org. Lett.* **2022**, *24*, 3144-3148.

(11) Yu, B.; Huang, R.; Li, R.; Zhang, H.; Huang, H. Silver-Catalyzed Chemodivergent Assembly of Aminomethylated Isochromenes and Naphthols. *Chem. Commun.* **2022**, *58*, 3969-3972.

(12) Qi, Z.; Wang, S. Chemodivergent Synthesis of Oxazoles and Oxime Ethers Initiated by Selective C–N/C–O Formation of Oximes and Diazo Esters. *Org. Lett.* **2021**, *23*, 8549-8553.

(13) Li, M.-B.; Inge, A. K.; Posevins, D.; Gustafson, K. P. J.; Qiu, Y.; Bäckvall, J.-E. Chemodivergent and Diastereoselective Synthesis of Γ-Lactones and Γ-Lactams: A Heterogeneous Palladium-Catalyzed Oxidative Tandem Process. *J. Am. Chem. Soc.* **2018**, *140*, 14604-14608.

(14) Pramanik, M.; Mathuri, A.; Mal, P. Sulfur···Oxygen Interaction-Controlled (Z)-Selective Anti-Markovnikov Vinyl Sulfides. *Chem. Commun.* **2021**, *57*, 5698-5701.

(15) Pramanik, M.; Mathuri, A.; Mal, P. Tbuoli-Promoted Terminal Alkyne Functionalizations by Aliphatic Thiols and Alcohols. *Org. Biomol. Chem.* **2022**, *20*, 2671-2680.

(16) Yi, H.; Zhang, G.; Wang, H.; Huang, Z.; Wang, J.; Singh, A. K.; Lei, A. Recent Advances in Radical C-H Activation/Radical Cross-Coupling. *Chem. Rev.* **2017**, *117*, 9016-9085.

(17) Dénès, F.; Pichowicz, M.; Povie, G.; Renaud, P. Thiyl Radicals in Organic Synthesis. *Chem. Rev.* **2014**.

(18) Singh, J.; Sharma, A. Visible Light-Induced Synthesis of Functionalized Coumarins. *Adv. Synth. Catal.* **2021**, *363*, 3411-3438.

(19) Maja, M.; Melita, L.; Marija, K. Green Chem. Approaches to the Synthesis of Coumarin Derivatives. *Current Organic Chemistry* **2020**, *24*, 4-43.

(20) Gao, W.-C.; Liu, T.; Zhang, B.; Li, X.; Wei, W.-L.; Liu, Q.; Tian, J.; Chang, H.-H. Synthesis of 3-Sulfenylated Coumarins: Bf3·Et2o-Mediated Electrophilic Cyclization of Aryl Alkynoates Using N-Sulfanylsuccinimides. *J. Org. Chem.* **2016**, *81*, 11297-11304.

(21) Sahoo, H.; Singh, S.; Baidya, M. Radical Cascade Reaction of Aryl Alkynoates at Room Temperature: Synthesis of Fully Substituted A,B-Unsaturated Acids with Chalcogen Functionality. *Org. Lett.* **2018**, *20*, 3678-3681.

(22) Roy, M.; Jamatia, R.; Samanta, A.; Mohar, K.; Srimani, D. Change in the Product Selectivity in the Visible Light-Induced Selenium Radical-Mediated 1,4-Aryl Migration Process. *Org. Lett.* **2022**, *24*, 8180-8185.

(23) Beletskaya, I. P.; Ananikov, V. P. Transition-Metal-Catalyzed C−S, C−Se, and C−Te Bond Formation Via Cross-Coupling and Atom-Economic Addition Reactions. *Chem. Rev.* **2011**, *111*, 1596-1636.

(24) Refouvelet, B.; Guyon, C.; Jacquot, Y.; Girard, C.; Fein, H.; Bévalot, F.; Robert, J.-F.; Heyd, B.; Mantion, G.; Richert, L., et al. Synthesis of 4-Hydroxycoumarin and 2,4-Quinolinediol Derivatives and Evaluation of Their Effects on the Viability of Hepg2 Cells and Human Hepatocytes Culture. *Eur. J. Med. Chem.* **2004**, *39*, 931-937.

(25) Pramanik, M.; Mathuri, A.; Sau, S.; Das, M.; Mal, P. Chlorinative Cyclization of Aryl Alkynoates Using Ncs and 9-Mesityl-10-Methylacridinium Perchlorate Photocatalyst. *Org. Lett.* **2021**, *23*, 8088-8092.

(26) Pramanik, M.; Choudhuri, K.; Mathuri, A.; Mal, P. Dithioacetalization or Thioetherification of Benzyl Alcohols Using 9-Mesityl-10-Methylacridinium Perchlorate Photocatalyst. *Chem. Commun.* **2020**, *56*, 10211-10214.

(27) Ohkubo, K.; Mizushima, K.; Iwata, R.; Souma, K.; Suzuki, N.; Fukuzumi, S. Simultaneous Production of P-Tolualdehyde and Hydrogen Peroxide in Photocatalytic Oxygenation of P-Xylene and Reduction of Oxygen with 9-Mesityl-10-Methylacridinium Ion Derivatives. *Chem. Commun.* **2010**, *46*, 601-603.

(28) Roth, H. G.; Romero, N. A.; Nicewicz, D. A. Experimental and Calculated Electrochemical Potentials of Common Organic Molecules for Applications to Single-Electron Redox Chemistry. *Synlett* **2016**, *27*, 714-723.

(29) Colomer, I.; Batchelor-McAuley, C.; Odell, B.; Donohoe, T. J.; Compton, R. G. Hydrogen Bonding to Hexafluoroisopropanol Controls the Oxidative Strength of Hypervalent Iodine Reagents. *J. Am. Chem. Soc.* **2016**, *138*, 8855-8861.

(30) Ghosh, S.; Qu, Z.-W.; Pradhan, S.; Ghosh, A.; Grimme, S.; Chatterjee, I. Hfip-Assisted Single C−F Bond Activation of Trifluoromethyl Ketones Using Visible-Light Photoredox Catalysis. *Angew. Chem. Int. Ed.* **2022**, *61*, e202115272.

(31) Zhang, N.; Zuo, H.; Xu, C.; Pan, J.; Sun, J.; Guo, C. Visible Light Induced the High-Efficiency Spirocyclization Reaction of Propynamide and Thiophenols Via Recyclable Catalyst Pd/Zro2. *Chin. Chem. Lett.* **2020**, *31*, 337-340.

(32) Wang, H.; Li, Y.; Tang, Z.; Wang, S.; Zhang, H.; Cong, H.; Lei, A. Z-Selective Addition of Diaryl Phosphine Oxides to Alkynes Via Photoredox Catalysis. *ACS Catal.* **2018**, *8*, 10599-10605.

(33) SAINT+, Bruker AXS Inc., Madison, Wisconsin, USA, 1999 (Program for Reduction of Data collected on Bruker CCD Area Detector Diffractometer V. 6.02.)

(34) SADABS, Bruker AXS, Madison, Wisconsin, USA, 2004

(35) Sheldrick, G. A Short History of Shelx. *Acta Crystallogr. A* **2008**, *64*, 112-122.

(36) Hua, J.; Fang, Z.; Xu, J.; Bian, M.; Liu, C.; He, W.; Zhu, N.; Yang, Z.; Guo, K. Electrochemical Oxidative Cyclization of Activated Alkynes with Diselenides or Disulfides: Access to Functionalized Coumarins or Quinolinones. *Green Chem.* **2019**, *21*, 4706-4711.

(37) Fang, J.-D.; Yan, X.-B.; Zhou, L.; Wang, Y.-Z.; Liu, X.-Y. Synthesis of 3-Organoselenyl-2h-Coumarins from Propargylic Aryl Ethers Via Oxidative Radical Cyclization. *Adv. Synth. Catal.* **2019**, *361*, 1985-1990.

(38) Gao, W. C.; Liu, T.; Cheng, Y. F.; Chang, H. H.; Li, X.; Zhou, R.; Wei, W. L.; Qiao, Y. Alcl3-Catalyzed Intramolecular Cyclization of N-Arylpropynamides with N-Sulfanylsuccinimides: Divergent Synthesis of 3-Sulfenyl Quinolin-2-Ones and Azaspiro[4,5]Trienones. *J Org Chem* **2017**, *82*, 13459-13467.

(39) Wu, W.; An, Y.; Li, J.; Yang, S.; Zhu, Z.; Jiang, H. Iodine-Catalyzed Cascade Annulation of Alkynes with Sodium Arylsulfinates: Assembly of 3-Sulfenylcoumarin and 3-Sulfenylquinolinone Derivatives. *Org. Chem. Front.* **2017**, *4*, 1751-1756.

(40) Wei, W.; Cui, H.; Yang, D.; Yue, H.; He, C.; Zhang, Y.; Wang, H. Visible-Light-Enabled Spirocyclization of Alkynes Leading to 3-Sulfonyl and 3-Sulfenyl Azaspiro[4,5]Trienones. *Green Chem.* **2017**, *19*, 5608-5613.

(41) Yu, K.; Kong, X.; Yang, J.; Li, G.; Xu, B.; Chen, Q. Electrochemical Oxidative Halogenation of N-Aryl Alkynamides for the Synthesis of Spiro[4.5]Trienones. *J. Org. Chem.* **2021**, *86*, 917-928.

(42) Cao, L.; Luo, S.-H.; Jiang, K.; Hao, Z.-F.; Wang, B.-W.; Pang, C.-M.; Wang, Z.-Y. Disproportionate Coupling Reaction of Sodium Sulfinates Mediated by Bf3·Oet2: An Approach to Symmetrical/Unsymmetrical Thiosulfonates. *Org. Lett.* **2018**, *20*, 4754-4758.

NMR Spectra of Selected Compounds

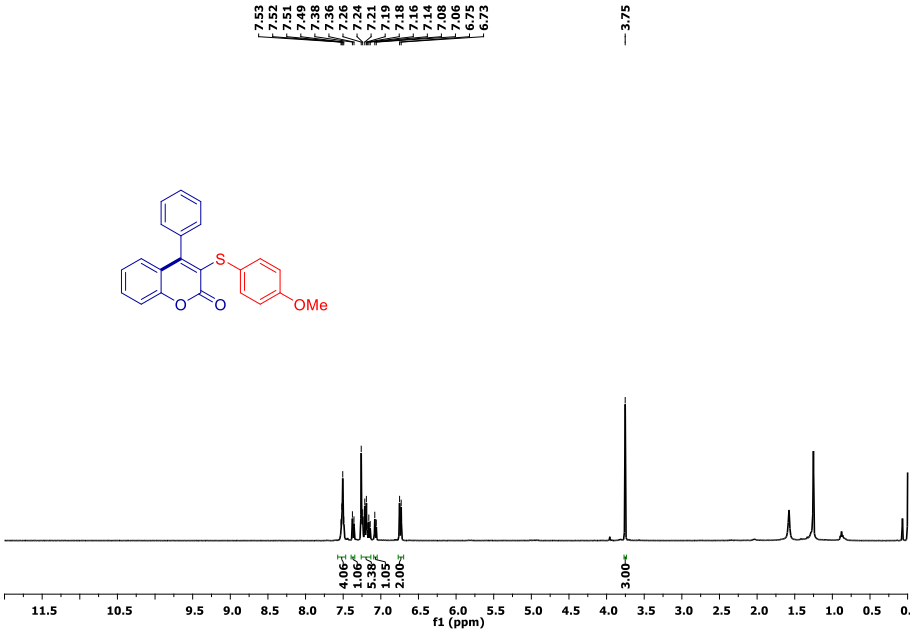

Figure 5.12. ^{1}H NMR(400 MHz, $CDCl_3$) spectrum of 3-((4-Methoxyphenyl)thio)-4-phenyl-2H-chromen-2-one (**3aa**).

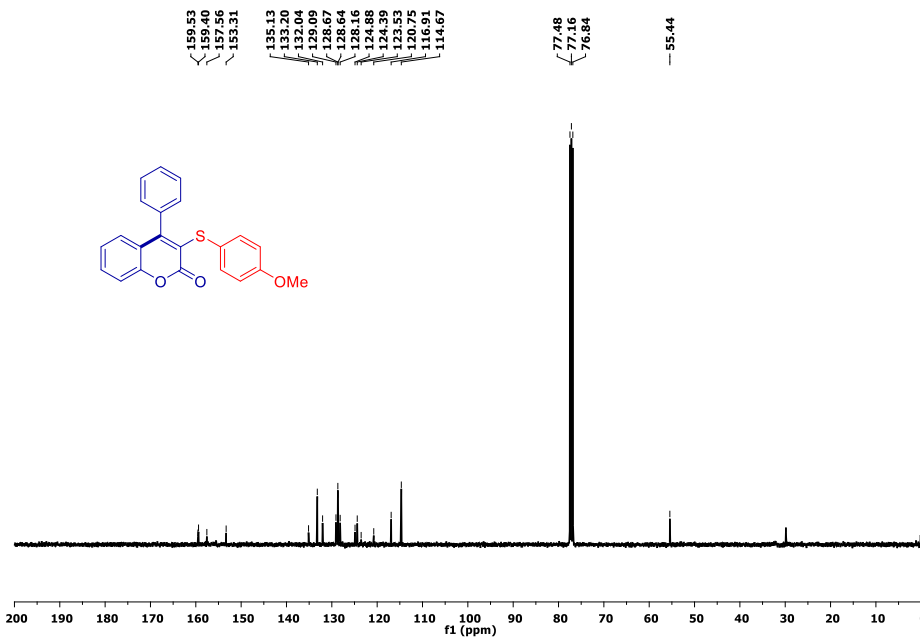

Figure 5.13. $^{13}C\{^{1}H\}$ NMR (100 MHz, $CDCl_3$) spectrum of 3-((4-Methoxyphenyl)thio)-4-phenyl-2H-chromen-2-one (**3aa**).

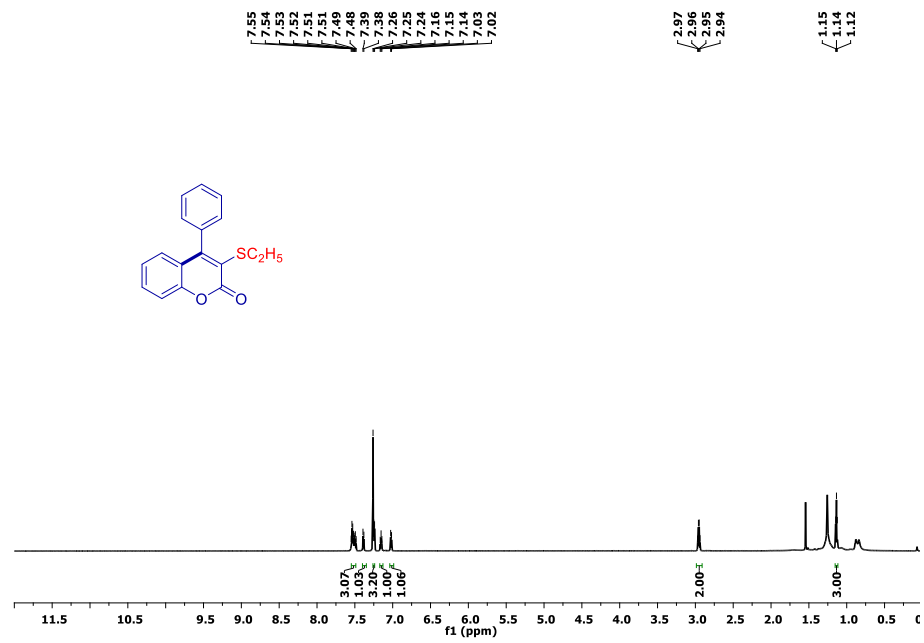

Figure 5.14. ^{1}H NMR(700 MHz, $CDCl_3$) spectrum of 3-(Ethylthio)-4-phenyl-2H-chromen-2-one (**3ae**).

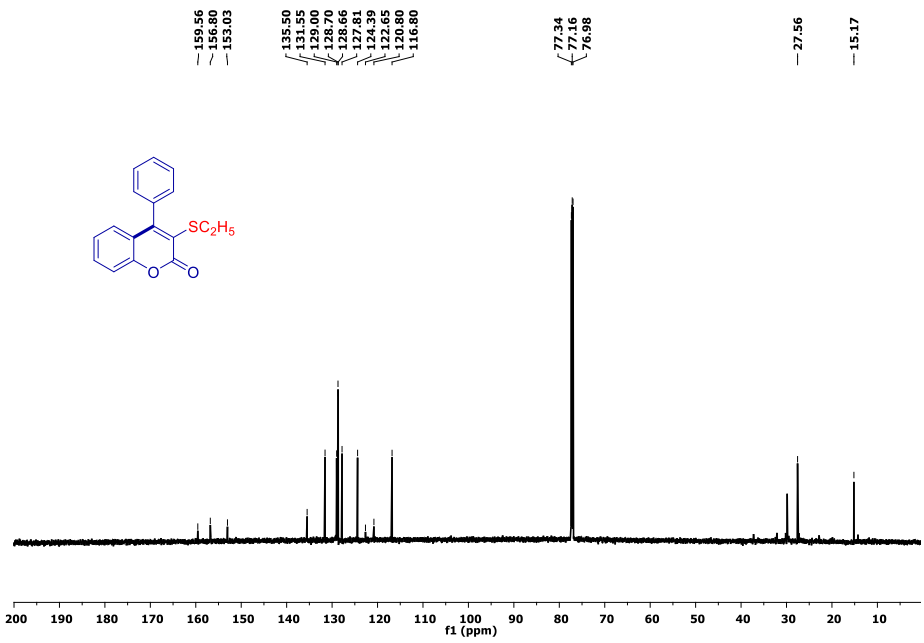

Figure 5.15. $^{13}C\{^{1}H\}$ NMR (175 MHz, $CDCl_3$) spectrum of 3-(Ethylthio)-4-phenyl-2H-chromen-2-one (**3ae**).

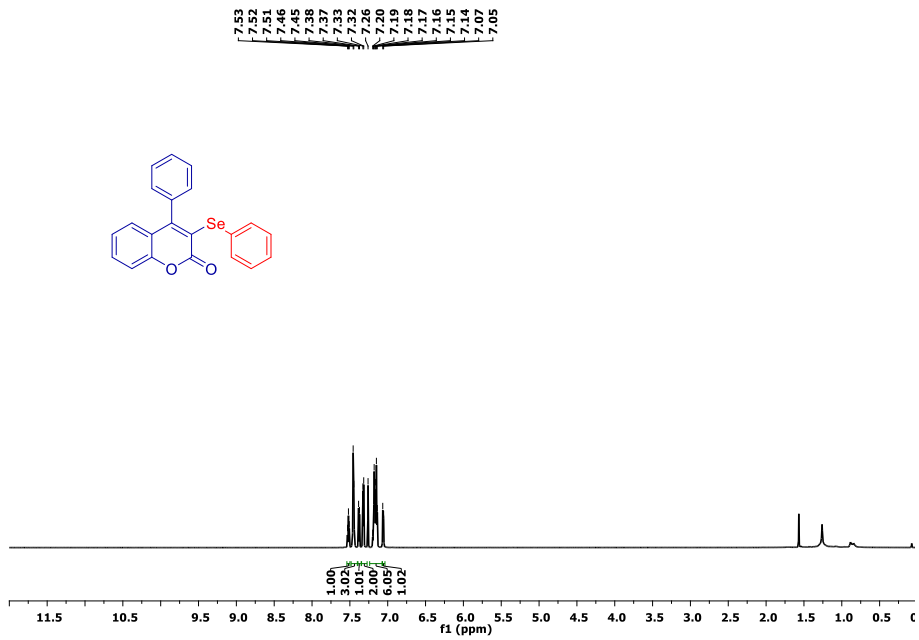

Figure 5.16. ^{1}H NMR(700 MHz, $CDCl_3$) spectrum of 4-Phenyl-3-(phenylselanyl)-2H-chromen-2-one (**3ax**).

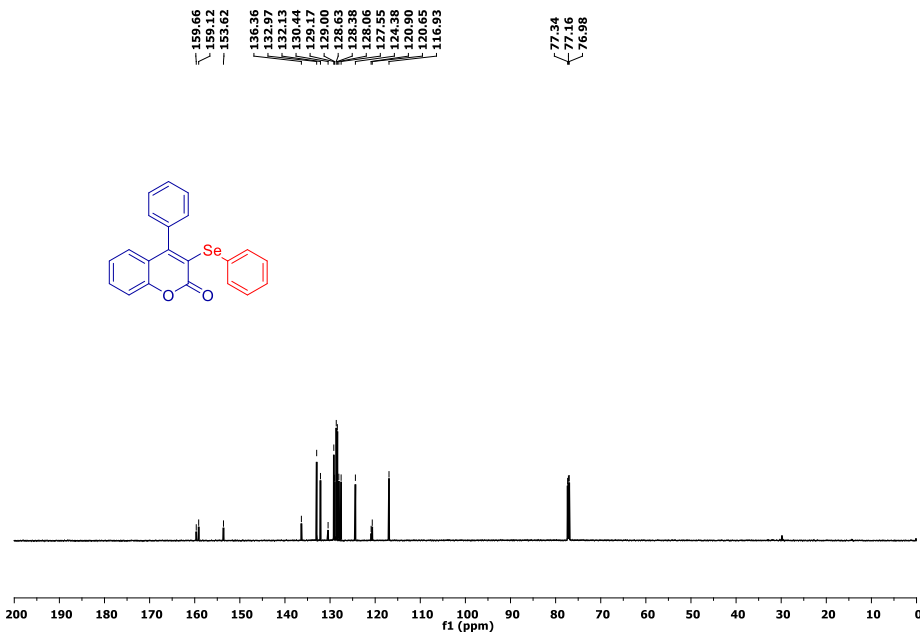

Figure 5.17. $^{13}C\{^{1}H\}$ NMR (175 MHz, $CDCl_3$) spectrum of 4-Phenyl-3-(phenylselanyl)-2H-chromen-2-one (**3ax**).

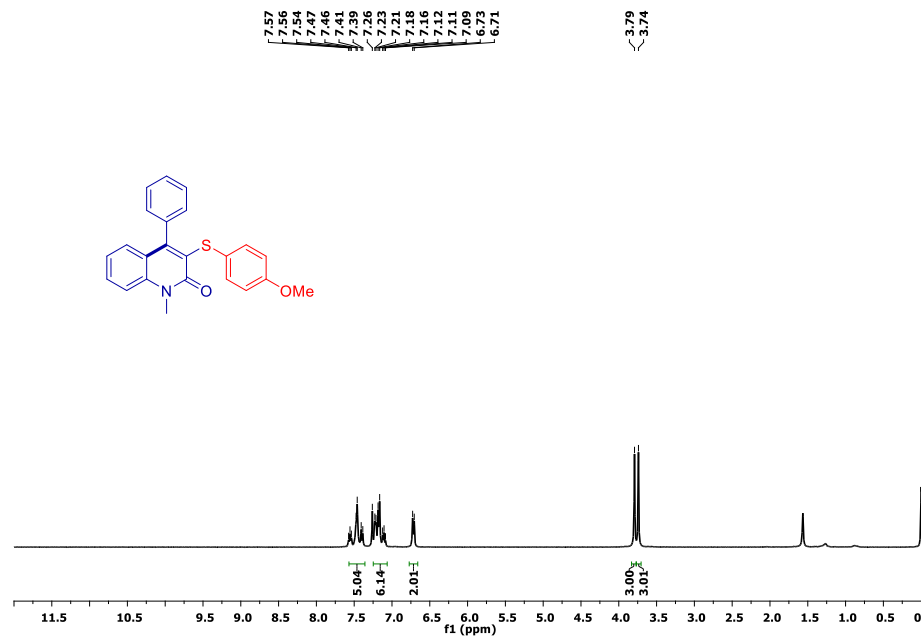

Figure 5.18. ^{1}H NMR(400 MHz, $CDCl_3$) spectrum of 3-((4-Methoxyphenyl)thio)-1-methyl-4-phenylquinolin-2(1H)-one (**5aa**).

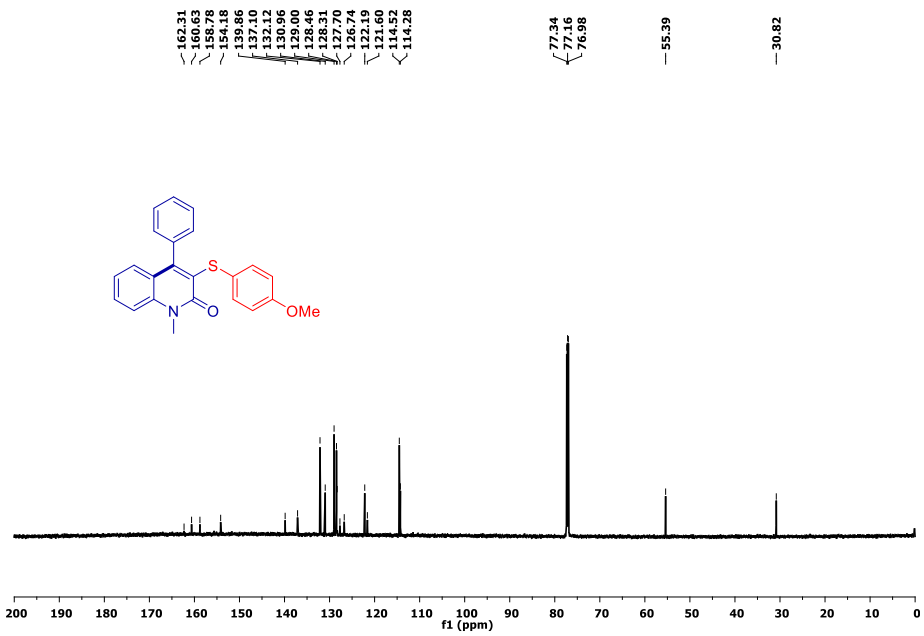

Figure 5.19. $^{13}C\{^{1}H\}$ NMR (100 MHz, $CDCl_3$) spectrum of 3-((4-Methoxyphenyl)thio)-1-methyl-4-phenylquinolin-2(1H)-one (**5aa**).

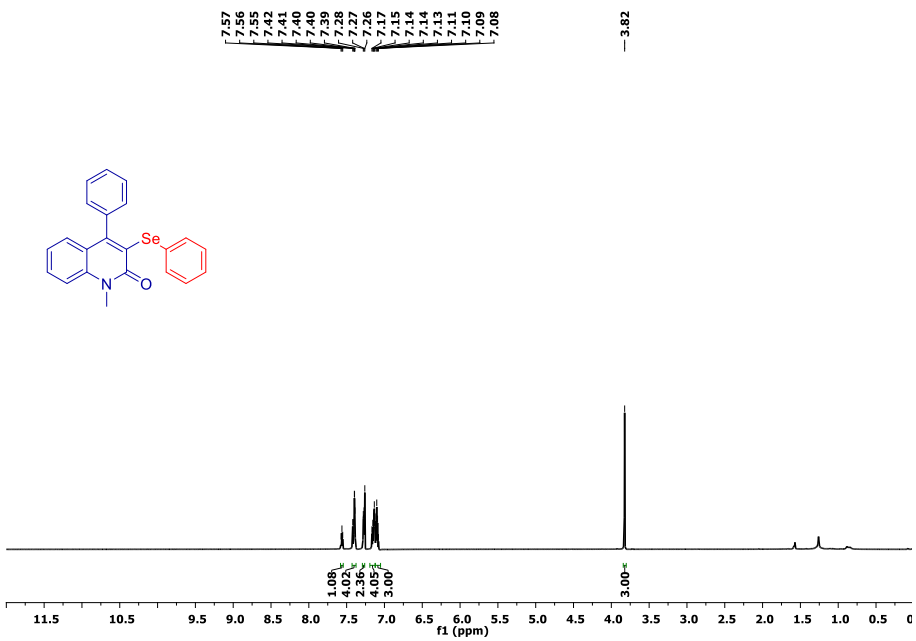

Figure 5.20. ^{1}H NMR(700 MHz, $CDCl_3$) spectrum of 1-Methyl-4-phenyl-3-(phenylselanyl)quinolin-2(1H)-one (**5ax**).

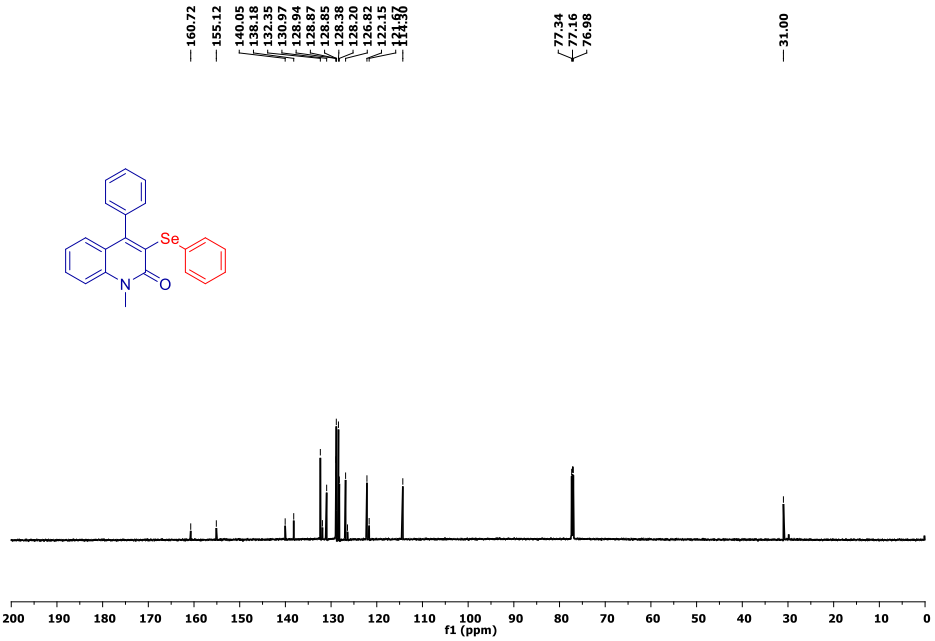

Figure 5.21. $^{13}C\{^{1}H\}$ NMR (175 MHz, $CDCl_3$) spectrum of 1-Methyl-4-phenyl-3-(phenylselanyl)quinolin-2(1H)-one (**5ax**).

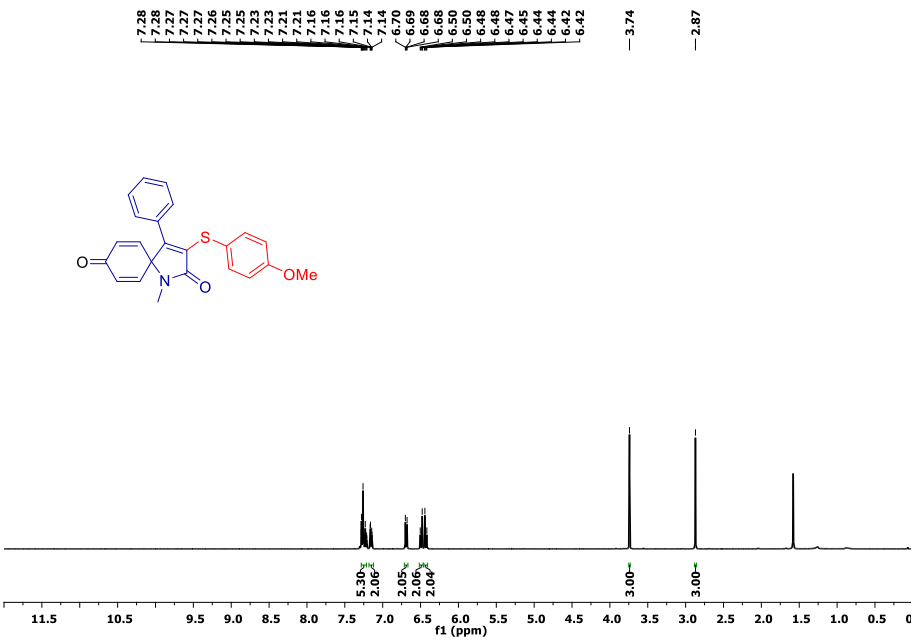

Figure 5.22. ^{1}H NMR(400 MHz, $CDCl_3$) spectrum of 3-((4-Methoxyphenyl)thio)-1-methyl-4-phenyl-1-azaspiro[4.5]deca-3,6,9-triene-2,8-dione (**6ha**).

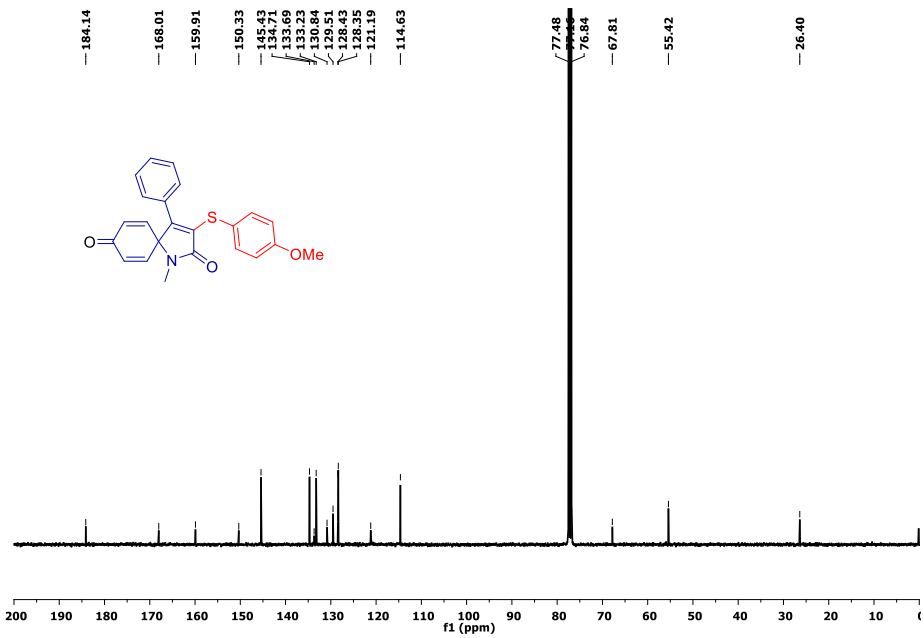

Figure 5.23. $^{13}C\{^{1}H\}$ NMR (100 MHz, $CDCl_3$) spectrum of 3-((4-Methoxyphenyl)thio)-1-methyl-4-phenyl-1-azaspiro[4.5]deca-3,6,9-triene-2,8-dione (**6ha**).

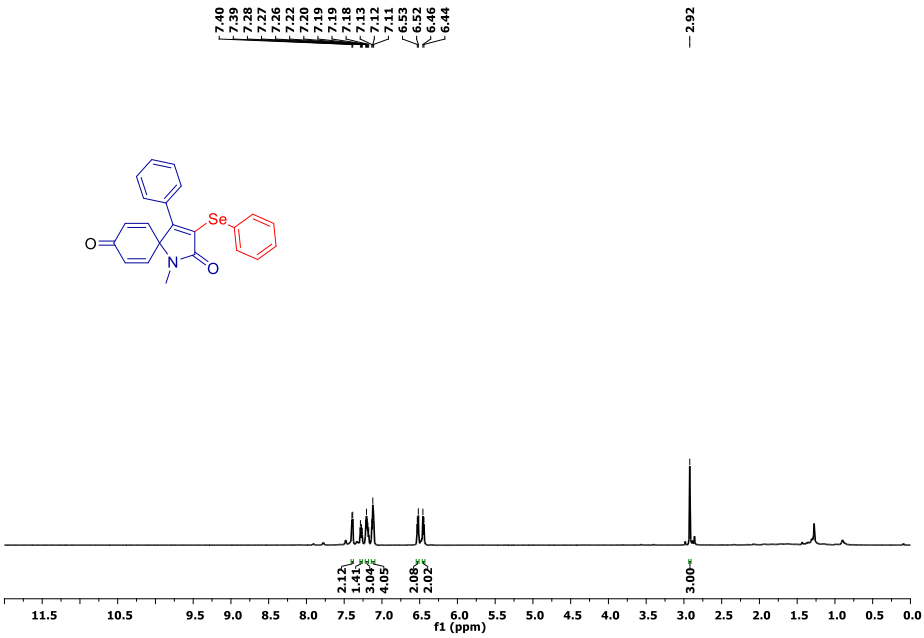

Figure 5.24. ^{1}H NMR (700 MHz, $CDCl_3$) spectrum of 1-methyl-4-phenyl-3-(phenylselanyl)-1-azaspiro[4.5]deca-3,6,9-triene-2,8-dione (**6hx**).

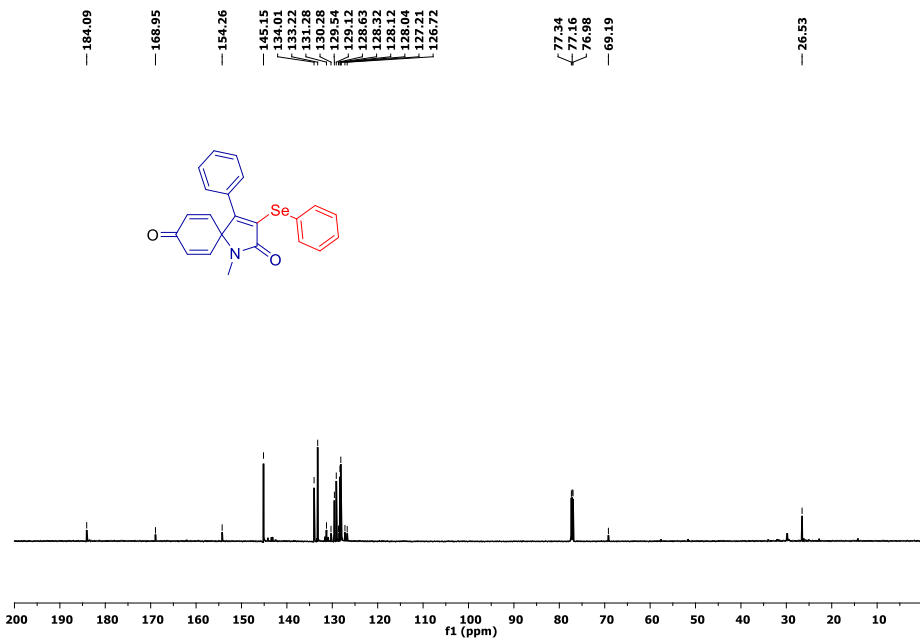

Figure 5.25. $^{13}C\{^{1}H\}$ NMR (176 MHz, $CDCl_3$) spectrum of 1-methyl-4-phenyl-3-(phenylselanyl)-1-azaspiro[4.5]deca-3,6,9-triene-2,8-dione (**6hx**).

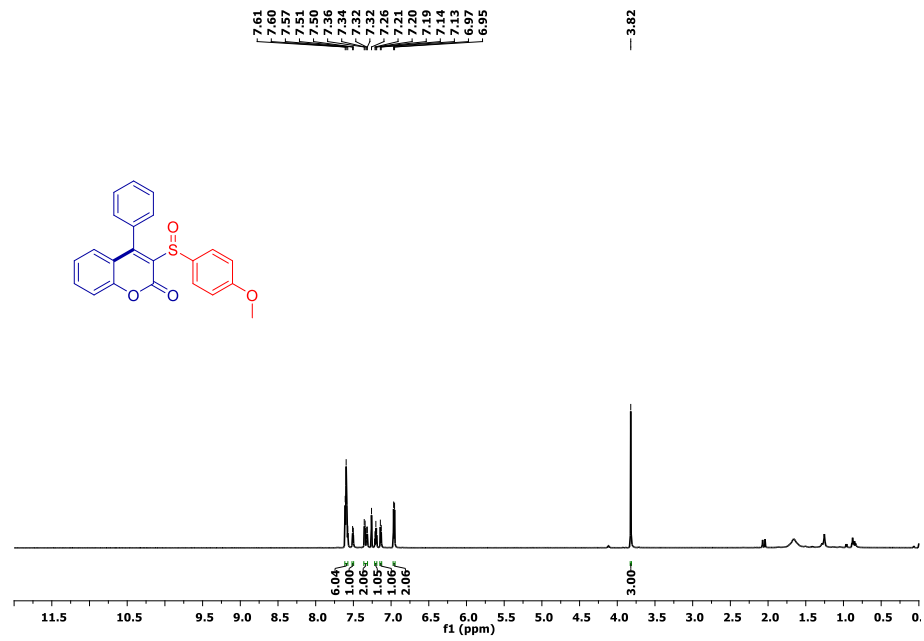

Figure 5.26. ^{1}H NMR (700 MHz, $CDCl_3$) spectrum of 3-((4-methoxyphenyl)sulfinyl)-4-phenyl-2H-chromen-2-one (**7**).

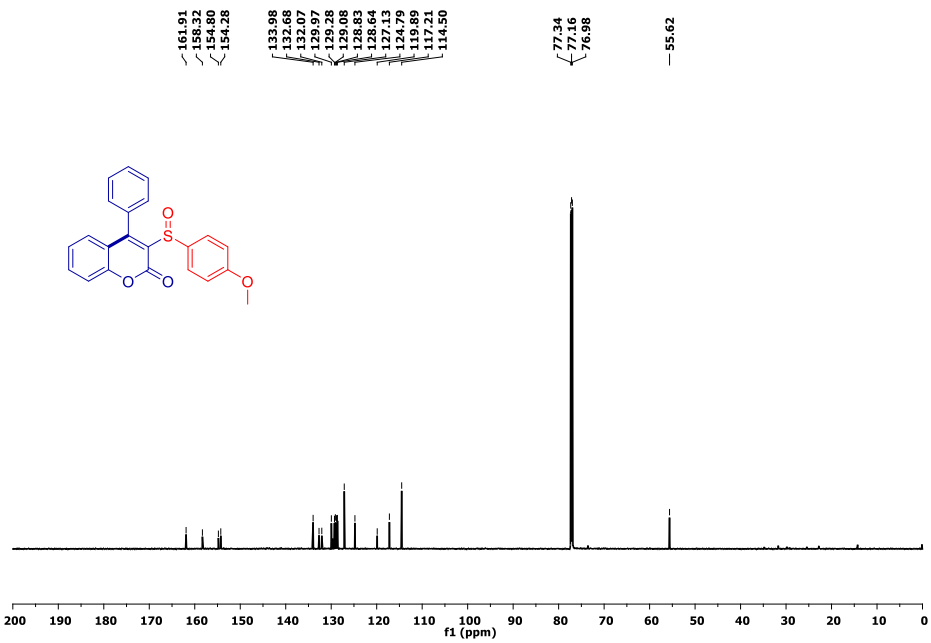

Figure 5.27. $^{13}C\{^{1}H\}$ NMR (176 MHz, $CDCl_3$) spectrum of 3-((4-methoxyphenyl)sulfinyl)-4-phenyl-2H-chromen-2-one (**7**).

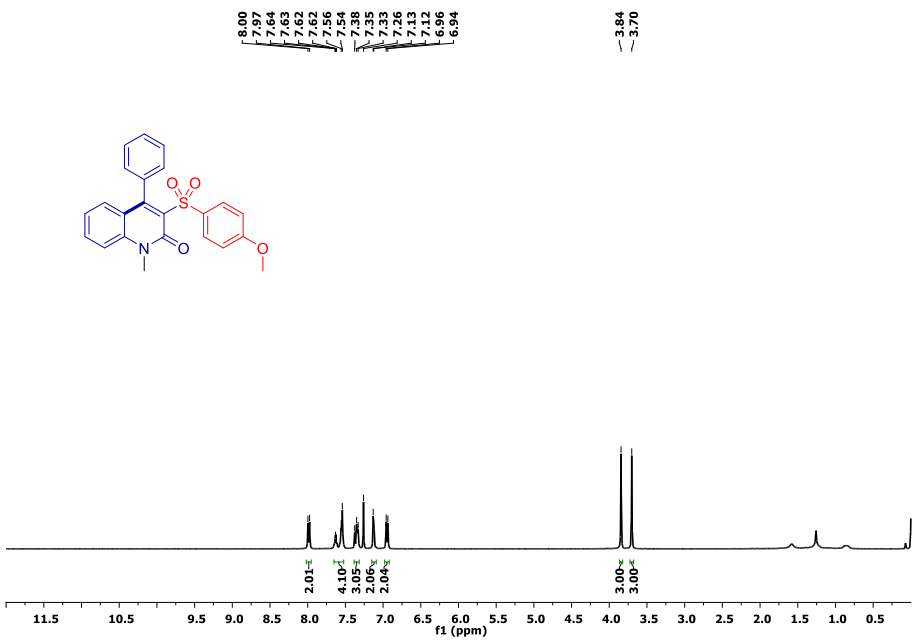

Figure 5.28. ^{1}H NMR (400 MHz, $CDCl_3$) spectrum of 3-((4-methoxyphenyl)sulfonyl)-1-methyl-4-phenylquinolin-2(1H)-one (**8**).

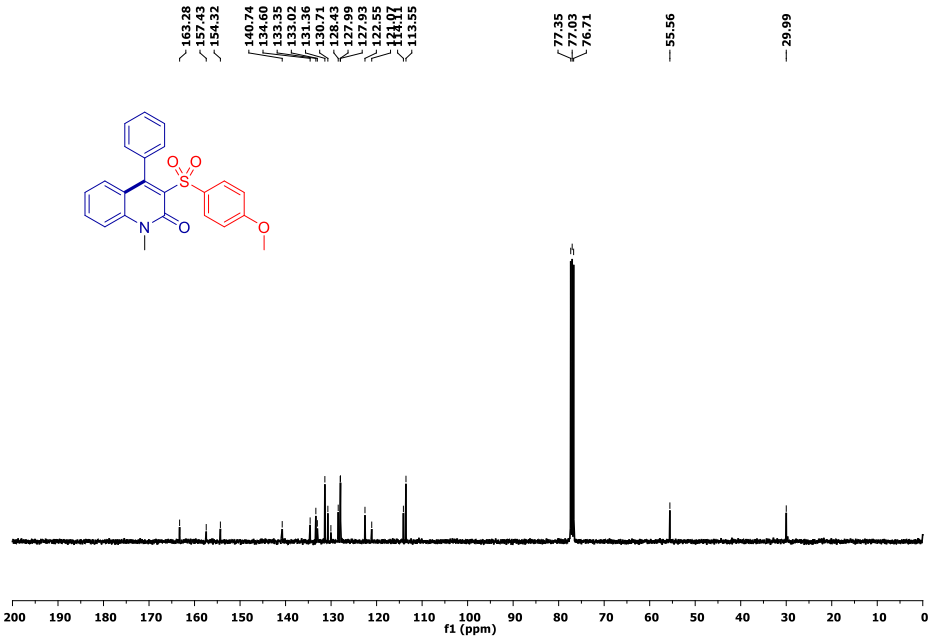

Figure 5.29. $^{13}C\{^{1}H\}$ NMR (100 MHz, $CDCl_3$) spectrum of 3-((4-methoxyphenyl)sulfonyl)-1-methyl-4-phenylquinolin-2(1H)-one (**8**).

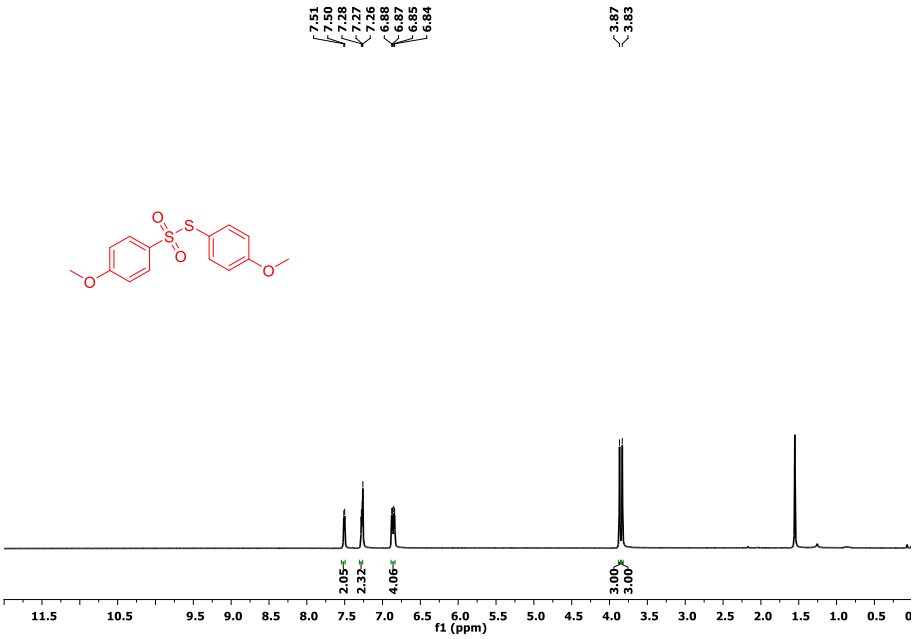

Figure 5.30. ^{1}H NMR (700 MHz, $CDCl_3$) spectrum of S-(4-methoxyphenyl) 4-methoxybenzenesulfonothioate (**10**).

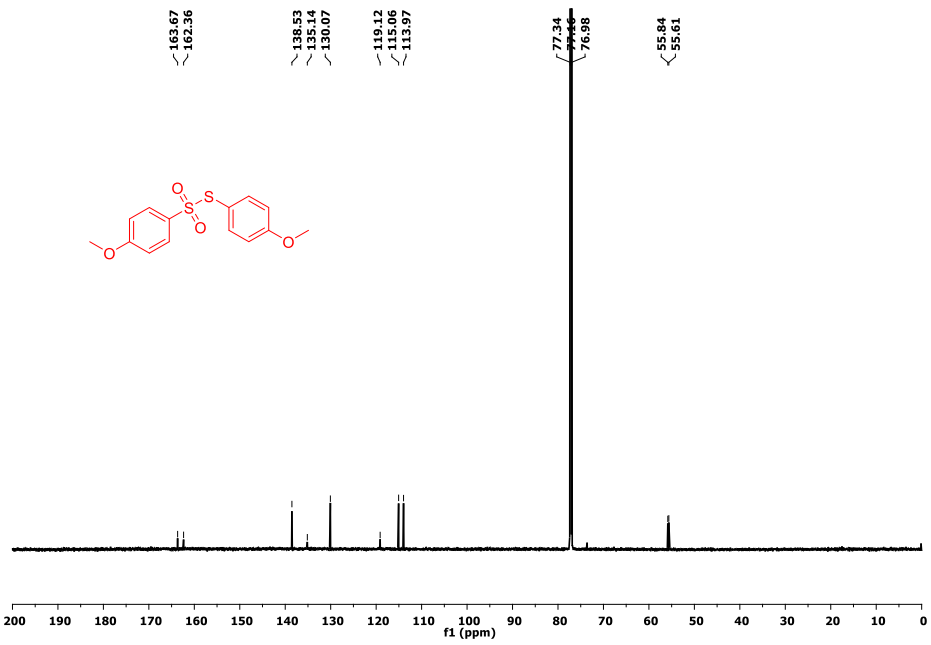

Figure 5.31. $^{13}C\{^{1}H\}$ NMR (176 MHz, $CDCl_3$) spectrum of S-(4-methoxyphenyl) 4-methoxybenzenesulfonothioate (**10**).

CHAPTER 6

Disulfide Metathesis *via* Sulfur…Iodine Interaction and Photoswitchability

6.1 ABSTRACT

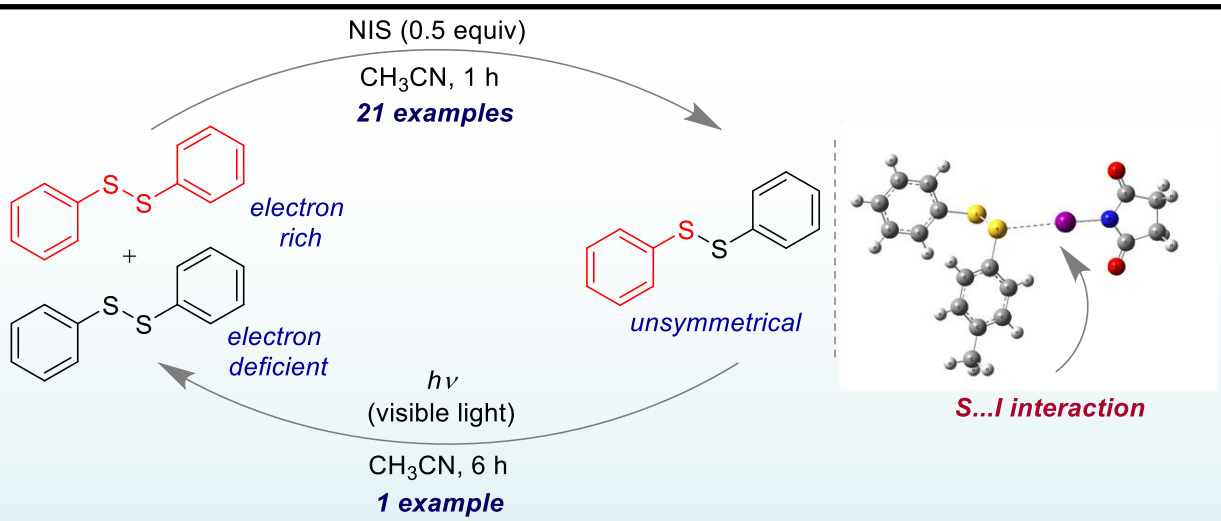

The idea of constitutional dynamic chemistry (CDC) and dynamic combinatorial chemistry (DCC) is widespread in literature using the chemistry of disulfides. The synthesis of unsymmetrical diaryl disulfides is challenging due to the presence of a weak S-S bond. We report herein the synthesis of unsymmetrical diaryl disulfides from two symmetrical disulfides *via* a cross-metathesis reaction which was controlled by a weak sulfur…iodine (S…I) interaction. The unsymmetrical disulfides were stable in acetonitrile solution in the presence of *N*-iodosuccinimide (NIS), and found to be photoswitachable reversibly to the symmetrical disulfides under visible light irradiation.

.

6.2 INTRODUCTION

The concept of constitutional dynamic chemistry (CDC)[1] and dynamic combinatorial chemistry (DCC)[2] is also well-known in disulfides chemistry.[3] Due to the presence of weak S-S bonds, the formation of many products is possible in the equilibrium.[3] Among the disulfides, unsymmetrical disulfides are challenging to synthesize due to the chemoselectivity factor.[4] The synthesis of unsymmetrical disulfides is known using thiols as cross dehydrogenating coupling partners. However, the use of thiols for synthesis of unsymmetrical disulfides have less practical utility because of their unpleasant odors.[5-8] In addition, disulfide exchange reactions are also reported by using thiolate ions,[9] solid-state exchange processes in the presence of a basic catalyst,[10] irradiation by UV light,[10] etc. The disulfide exchange methodology is also popularly used for the construction of various supramolecular architectures.[11]

Disulfides are ubiquitously found in many organic and inorganic compounds of biological importance.[12] Selective examples of disulfides used as drugs are shown in Figure 1a. The cleavage and recombination of organo-disulfides or polysulfides generally lead to the disulfide exchange process. The exchange process is adapted to generate, alter, and degrade biologically active materials and substances.[4] The sulfur-sulfur (S-S) bond in disulfides is easily cleavable in a reversible way using various chemical processes.[13-14] The S-S bonds cleavage is known to occur both heterolytically and homolytically. During the homolytic cleavage, the sulfenyl radicals are mainly generated through heating, photolysis, and oxidation processes. On the other hand, heterolytic cleavage requires ionic scission to produce sulfenium ion (cation)[15] either under acidic/electrophilic conditions or from the mercaptides under basic/nucleophilic conditions.[16]

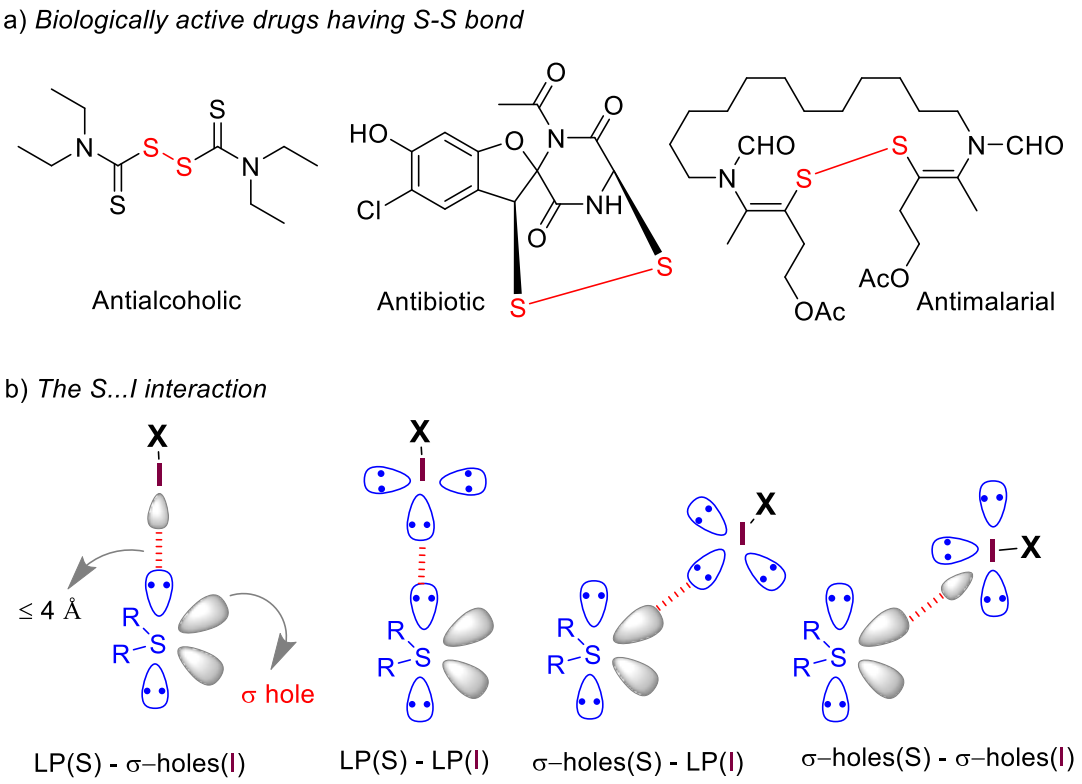

Figure 6.1. a) Examples of disulfides in natural products and drugs. b) Types of S…I interaction.

Small molecule system chemistry has gained significant attention in supramolecular chemistry because it has revolutionized the constitution of complex molecular architectures.[17-18] The noncovalent or weak interactions have a substantial effects in the organic systems to obtain the selectivities in the product formation by mimicking biological phenomena.[19] The use of noncovalent interactions like chalcogen bonding,[20] hydrophobic effect,[21] halogen bonding,[22-23] anion-π,[24] cation-π,[25] S-H…π,[26] S..O,[27] etc., which have utilities in organic synthesis is emerging at a fast pace.[28]

The sulfur iodine (S…I) interaction[29-31] is identified in various crystals.[32] Besides, the use of the S…I interaction to design and synthesize organic molecules is relatively less explored.[33] From the analysis of various crystals, the S…I interaction can be rationalized as follows (Figure 1b).[31] Generally, four types of possible S...I interactions are expected to form in which σ-holes

and lone pairs of atoms (sulfur and iodine) are involved. The required angle and distance for the interaction is anticipated as <180 ^{o} and <4 Å, respectively. However, in most of the cases, noncovalent interaction within S...I interaction is originated from the delocalization of the electron of divalent sulfur to σ*orbital (σ hole) of iodine.

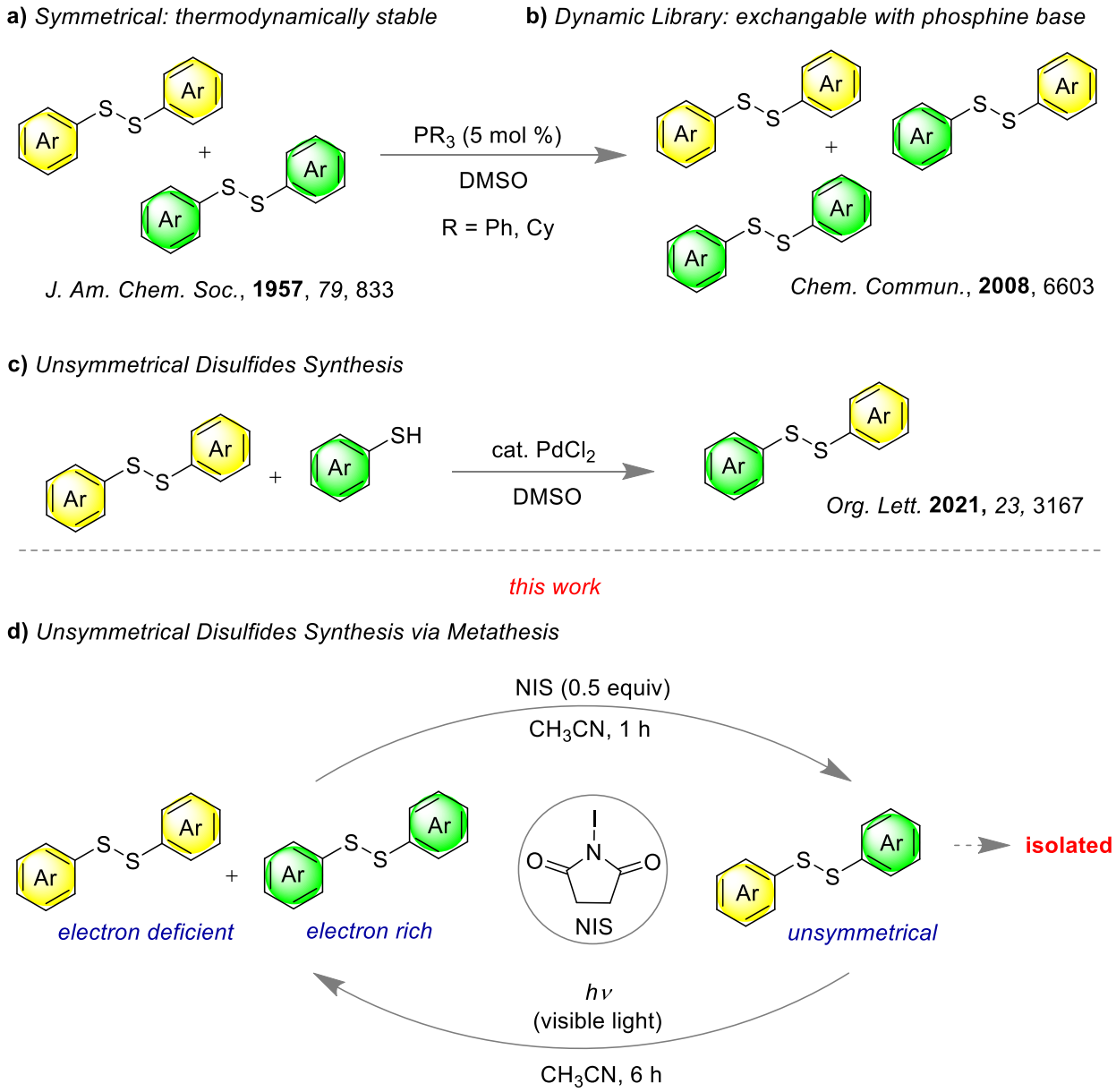

Figure 6.2. a) The symmetrical disulfides are non-exchangeable under any additive-free condition.[10] b) A dynamic combinatorial library from the reaction between disulfides and phosphines.[34] c) $PdCl_2$ catalyzed synthesis of unsymmetrical disulfides *via* a thiols-disulfides

exchange reported by Tan and Xu with coworkers.[35] d) Our approach to synthesize unsymmetrical disulfides from two different symmetrical disulfides using *N*-iodosuccinimide (NIS) and the reverse reaction initiated by visible light.

6.3 RESULT AND DISCUSSION

The hypervalent iodine reagents are known since 1886, and their use in bringing effective organic transformations *via* an oxidative pathway in organic synthesis has become popular.[36-37] In the context of our research focus on developing iodine-based reagents in organic synthesis,[36-39] we propose herein the use of *N*-iodosuccinimide (NIS)[40-41] as an efficient reagent for the promotion of a disulfide metathesis reaction (Figure 2). In Figure 2a, a mixture of two symmetrical disulfides is shown, which are stable and non-exchangeable under any additive-free condition.[10] The reversible disulfide metathesis process or a dynamic combinatorial library is obtainable from a reaction between disulfides and phosphines (Figure 2b).[34] Recently, Tan and Xu with coworkers reported $PdCl_2$ catalyzed synthesis of unsymmetrical disulfides *via* a thiols-disulfides exchange method (Figure 2c).[35] In this work (Figure 2d), we have shown the synthesis of unsymmetrical diaryl disulfides from two symmetrical diaryl disulfides with different electronic frameworks (electron-rich and electron-deficient) *via* a cross-metathesis reaction. NIS helped to promote the reaction in acetonitrile at room temperature. Again, the switching of unsymmetrical to symmetrical diaryl disulfides was possible in the absence of NIS under visible light irradiation.

Table 6.1. Optimization of the reaction condition[a]

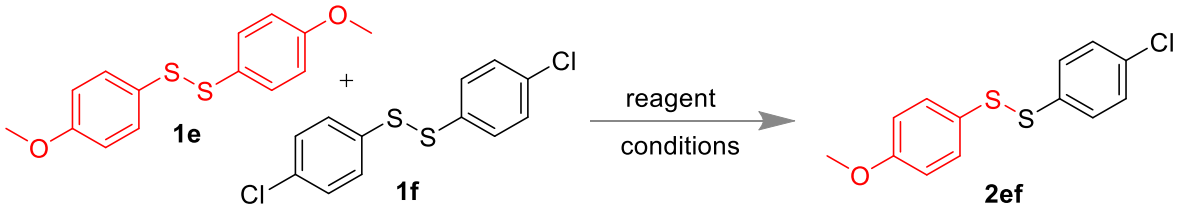

entry	catalyst (equiv)	solvent	yield (%)[b]
1	NIS (0.2)	MeCN	65
2	NIS (0.2)	MeCN	58
3	NIS (0.5)	MeCN	80
4	NIS (1.0)	MeCN	79
5	NIS (0.5)	EtOH	42
6	NIS (0.5)	THF	62
7	NIS (0.5)	CH_2Cl_2	49
8	NIS (0.5)	DMF	55
9	NIS (0.5)	DMSO	32
10	NIS (0.5)	EtOH/H_2O	45
11	NIS (0.5)	1,4-Dioxane	38
12	I_2 (0.5)	MeCN	59
13	NBS (0.5)	MeCN	67
14	PIDA (0.5)	MeCN	46
15	NIS (1.0)	MeCN	79[c]
16	--------	MeCN	0

[a]Reaction conditions: **1e** (0.209 mmol), **1f** (0.209 mmol), room temperature, 1 h, [b]Isolated yields after column chromatography, [c]at argon atmosphere.

We have demonstrated here a new strategy for the synthesis of unsymmetrical disulfides by using a mixture of symmetrical disulfides as starting materials.[15] The reaction condition was optimized using two symmetrical disulfides **1e** and **1f** (Table 1). We have also used NIS, phenyl iodine diacetate (PIDA) and iodine, *N*-bromosuccinimide (NBS), etc., as reagents. Solvents like CH_3CN, DMSO, DMF, EtOH-water, and 1,4-dioxane were also screened. The use of 0.5

equiv NIS in acetonitrile was found to be optimum. The reaction took 1 h at room temperature and open atmosphere for completion (monitored by TLC). However, no product was found when the reaction was carried out in the absence of NIS.

We attempted to examine the scopes of various unsymmetrical disulfides synthesis with the optimized condition (Figure 3). To our preliminary study, pyridine-based disulfides were allowed to react with diaryl disulfides having methyl groups at the -*para* or -*ortho* position. Notably, both the unsymmetrical disulfides (**2ag** and **2bg**) were isolated in 75% and 74% yields, respectively. Diaryl disulfides having -OMe, -Me and -Cl groups were also well-tolerated to give 82% of **2bd**, and 80% of **2ef**. Next, a series of aliphatic disulfides were also used for the metathesis process. The diaryl disulfides having -OMe substituent at -*ortho* or -*meta* position of the phenyl ring were coupled with cyclopentyl, cyclohexyl, isobutyl and diphenylethyl disulfide to offer the respective unsymmetrical disulfides (**2ch**-**2dh**) with 64%-84% yields. In addition, dodecyl disulfide reacted smoothly with -*meta* and -*para* methoxy substituted disulfides to produce **2do** and **2eo** with 71% and 82% yields, respectively. On the other hand, disulfides having furan and pyridine cores showed good reactivity under standard reaction conditions to deliver **2mn**-**2gq** with 54-95% yields. Interestingly, the yield of pyridine substituted disulfide **2gn** was higher than furan substituted disulfide **2mn**, possibly due to the thiyl radical stabilization by the pyridine. Moreover, other pyridine-containing aliphatic disulfides also result.

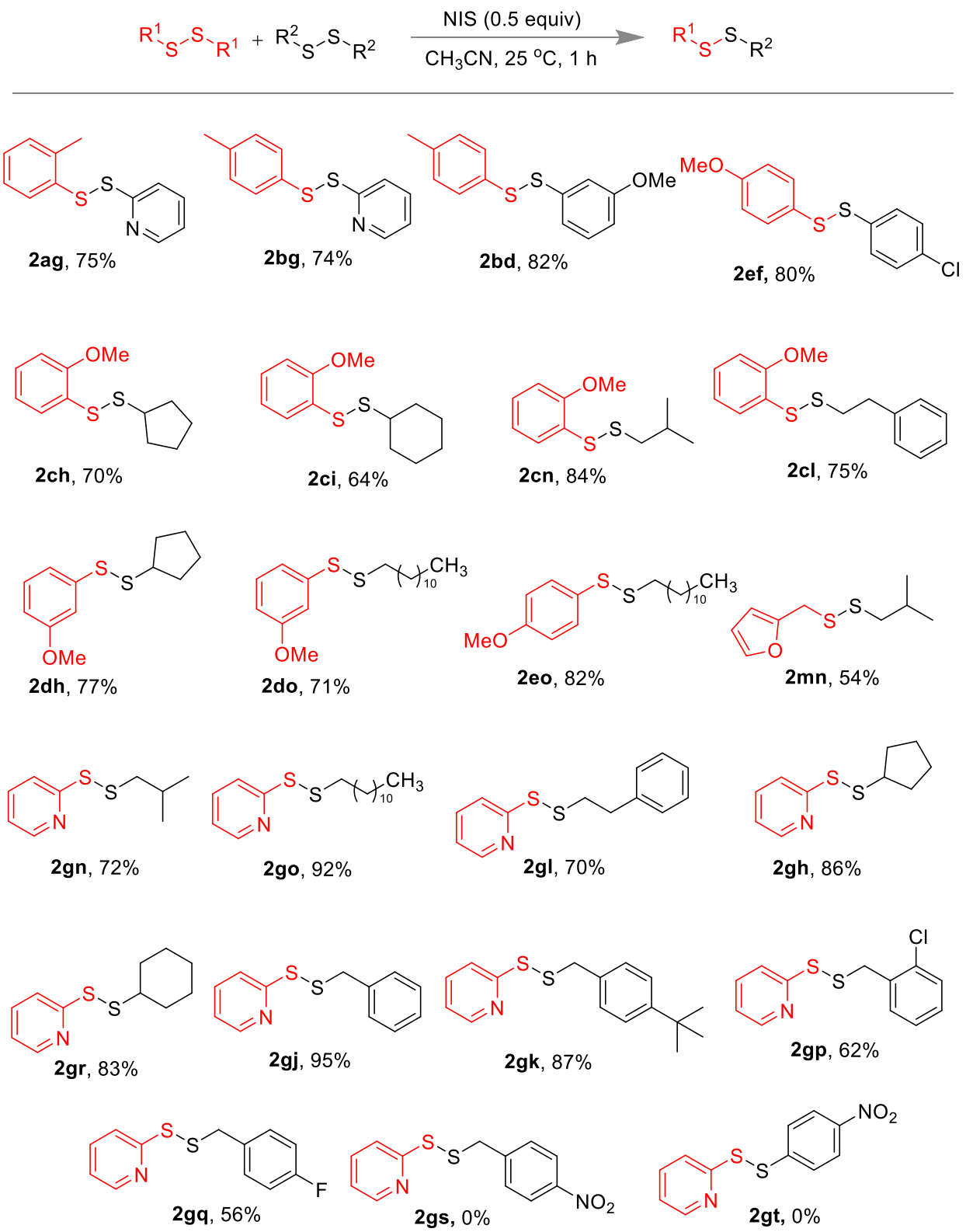

Figure 6.3. Unsymmetrical disulfides synthesis *via* metathesis.

in **2go-2gr** with near quantitative yields. Next, the substituted benzyl mercaptans were used, keeping pyridine-containing disulfides unchanged. Next, the substituted benzyl mercaptans were used, keeping pyridine-containing disulfides unchanged. Compound **2gj** was isolated in 95% yield and benzyl mercaptan disulfide having –^{t}Bu group also showed 87% of **2gk**. The disulfides containing –Cl and –F substituted benzyl mercaptans **1p** and **1q** led to lower yields (ca. 62% and 56%, respectively). Nitro-substituted disulfides (**1s** and **1t**) were ineffective for this metathesis reaction.

The control experiments (Figure 4) helped to establish the mechanism of the reaction. UV-Vis and fluorescence studies of disulfide 1f and NIS were carried out to understand the role of NIS in the reaction medium. A significant red shift from 245 nm to 360 nm was observed when NIS was added to the disulfide 1f in MeCN. Also, a sharp redshift from 245 nm to 341 nm was observed for disulfide 1e upon addition of NIS in same concentration of MeCN solution (supporting information). However, small redshift was found at 470 nm upon the addition of NIS to unsymmetrical disulfide 2ef. Also, fluorescence measurements suggested that the addition of NIS to disulfide 1f, 1e and 2ef displayed a gradual decrease in the fluorescence intensity. Notably, the addition of disulfide 1f in NIS solution showed appreciable color change (Figure 4a). In the UV-Vis absorption spectra a strong charge transfer band was appeared near 400 nm (Figure 4b). The charge transfer complex formation might be due to the S…I interaction between sulfur of disulfides and iodine of NIS. Time-dependent fluorescence spectra of disulfide 1f and NIS is shown in Figure 4c. The EPR experiment (Figure 4d) was performed with DMPO.[27, 42] No signal appeared when the reaction was done without NIS, and a strong signal was detected in the presence of NIS and DMPO. As the spectra gives a broad spectrum, we are unable to signify which radical was present. This observation we believed in the involvement of a radical pathway.

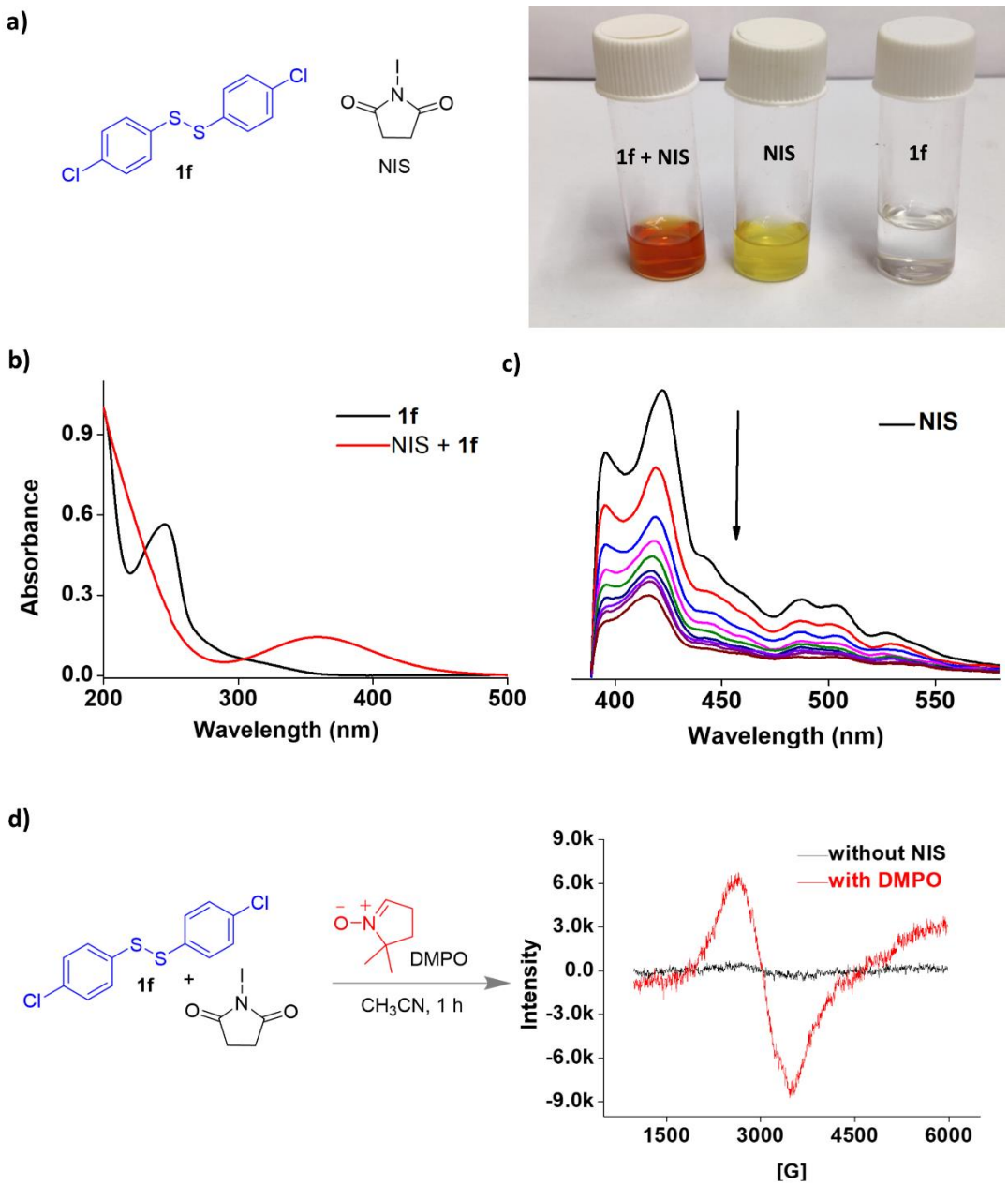

Figure 6.4. a) The color change after adding disulfide **1f** into NIS in MeCN solvent. b) UV-Vis absorption spectrum of disulfide **1f** and NIS in 2×10^{-4} M MeCN. c) Time-dependent fluorescence spectrum of disulfide **1f** and NIS in 2×10^{-4} M MeCN (every 10 min intervals). d) EPR spectra of the reaction of **1f** with DMPO.

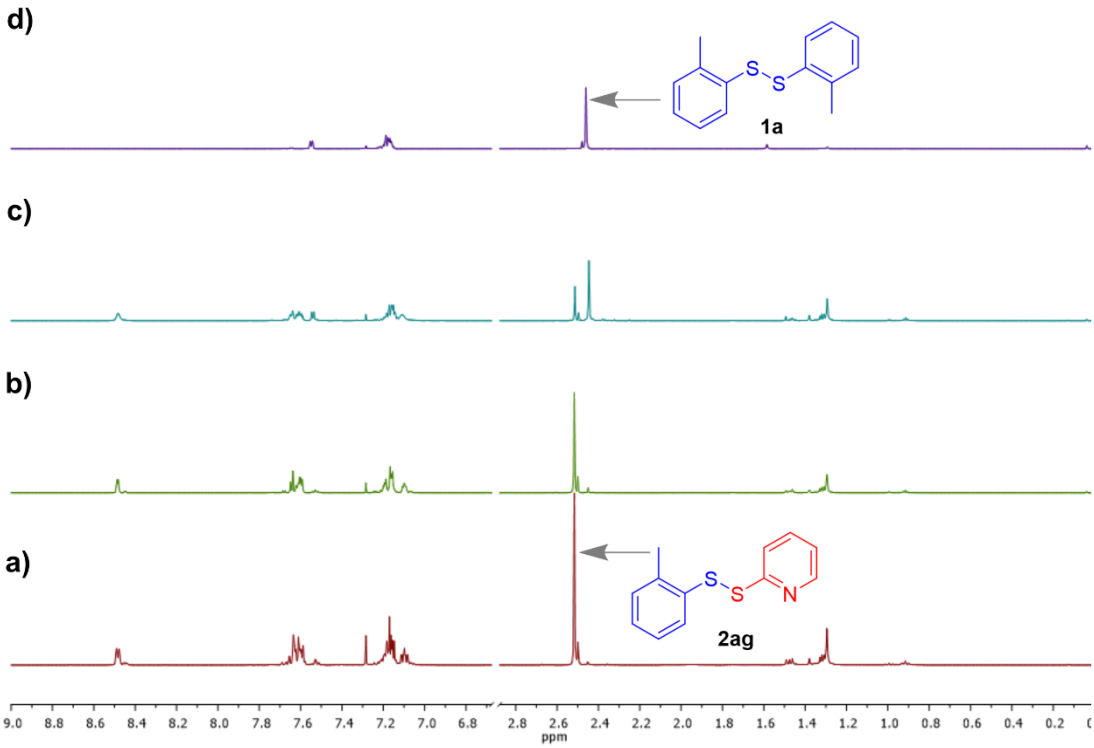

Figure 6.5. ^{1}H NMR spectra in CD_3CN a) of the compound **2ag**. The conversion of unsymmetrical disulfide **2ag** to symmetrical disulfide **1a** is shown after b) 3 h and c) 6 h irradiation under the visible light (white LED). d) The ^{1}H NMR spectrum of the compound **1a** as reference.

Reversibility of the reaction from unsymmetrical disulfides to symmetrical disulfides was observed with irradiation of visible light. A time-dependent proton NMR study of unsymmetrical disulfide **2ag** under visible light indicated that unsymmetrical disulfide **2ag** was cleaved homolytically to produce symmetrical disulfides (Figure 5). The symmetrical disulfides **1a** and **1g** were isolated in 38% and 45% yields, respectively.

a) *Plausible mechanism*

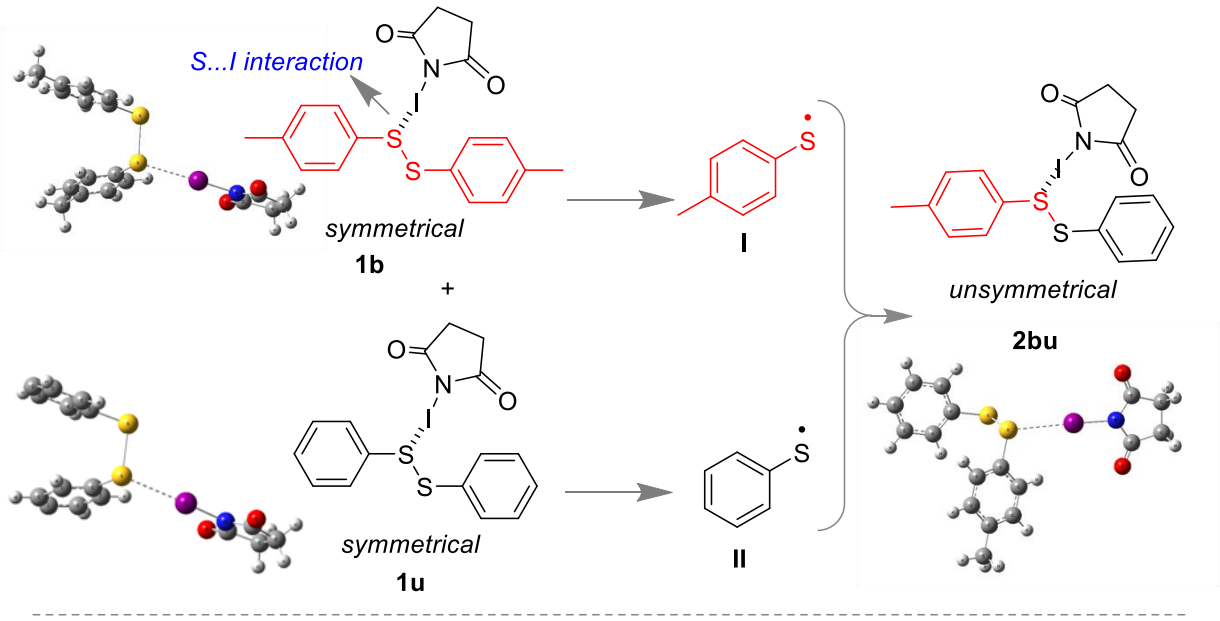

b) *S...I interactions*

disulfides	S...I distance (Å)	S...I-N bond angle (°)	$E_{lp(O1)-\sigma^*(NIS)}$ (kcal/mol)	$E_{lp(O2)-\sigma^*(NIS)}$ (kcal/mol)
1u	3.262	176.33	0.81	11.70
1b	3.224	178.10	0.97	13.21
2bu	3.233	177.99	0.94	12.81

Figure 6.6. a) Plausible mechanism and b) S...I interactions from calculated bond distance and second-order perturbation energy using b3lyp/LanL2DZ DFT theory.

Based on the literature evidence and control experiments, a plausible mechanism is proposed in Figure 6. Geometry optimizations and NBO analysis of 1b, 1u, and 2bu with NIS were done using Density Functional Theory (b3lyp/LanL2DZ level).[43] The optimized bond distances (S…I), angles (S…I-N) and second-order perturbation energy $E_{lp(O)-\sigma^*(NIS)}$ are tabulated below, which showed that diphenyl disulfides having dimethyl group as electron-donating partner exhibited stronger second-order perturbation energy $E_{lp(O)-\sigma^*(NIS)}$ and shorter S…I distance than

diphenyl disulfides. This observation indicated that electron-donating substituent (-Me group) on disulfide linkage helps to enhance the donating ability of sulfur lone pair, as a result, S…I interaction is favored in between sulfur of 1b and iodine of NIS. However, second-order perturbation energy for unsymmetrical disulfide 2bu with NIS was also found to be approximately half of the average of two symmetrical disulfides 1b and 1u with NIS, suggesting that S…I interaction is responsible for the stability of product 2bu. When NIS was added to the mixture of symmetrical disulfides, due to the S…I interaction with one of the sulfur atoms *via* charge transfer complexation,[44-45] the corresponding aryl ring becomes electron deficient. As a result, a dynamic combinational library was generated after homolytic cleavage of the S-S bonds. Next, a new S-S bond was formed to compensate for the electronic imbalance, leading to an iodide (from NIS) coordinated unsymmetrical disulfide. Thus, the unsymmetrical disulfide was found to be stable for a longer time in solution in the presence of NIS. This hypothesis was further supported when nitro-derivatives failed to produce unsymmetrical disulfides (Figure 3). Due to the high electron deficiency by the nitro-group, the electronic imbalance could not be compensated. Furthermore, the weak S-S bond tends to homolytic cleavage faster under visible light like Se-Se or Te-Te bonds,[46] promoting the unsymmetrical disulfides for symmetrization.

6.4 CONCLUSION

In conclusion, we could perceive that cross-metathesis between two symmetrical disulfides led to the formation of an unsymmetrical disulfide as a product using *N*-iodosuccinimide (NIS) as a reaction promoter. However, the current methodology could explore a new synthetic route for generating a new S-S bond *via* disulfide exchange or S-S bond cleavage. We foresee that the conceptualization of cross-metathesis in building S-S bonds will contribute to making a

variety of sulfur-containing architectures in organic chemistry. The presented work can also be considered as one of the important additions in the research area of supramolecular catalysis.[47-48]

6.5 EXPERIMENTAL SECTION

General Aspects. All the chemicals were purchased from commercial sources and used as received. All the reactions were generally carried out under an open atmosphere unless otherwise noted. The reactions were monitored by TLC on aluminum sheets pre-coated with silica gel. Chromatographic purifications of the compounds were performed using silica gel (Mess 230-400) and ethyl acetate/hexane as eluent. The ^{1}H and ^{13}C spectra of the compounds were recorded on Bruker 400 MHz and 700 MHz instruments at 25 ºC. The chemical shift value (δ, ppm) were reported with respect to the residual chloroform (7.26 for ^{1}H and 77.16 ppm for ^{13}C). Mass spectra were recorded as ESI-TOF (HRMS). Infrared spectra were recorded on neat solids using KBr pellets and described in wavenumber (cm^{-1}). Digital melting point apparatus was used to record the compound's melting point in degree centigrade (°C) and are uncorrected.

Synthesis

Representative procedure for the synthesis of unsymmetrical diaryldisulfide (2ef)

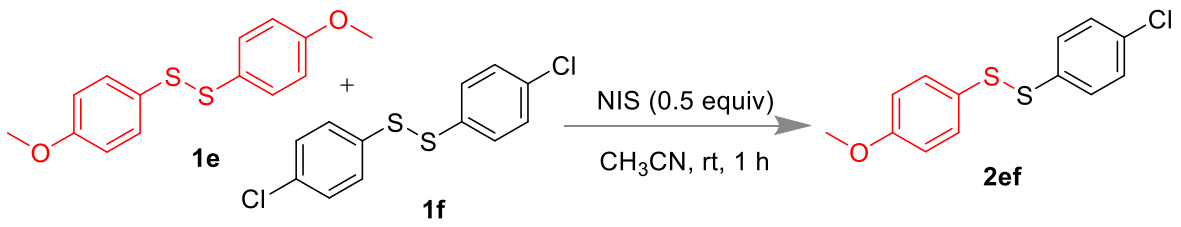

Scheme 6.1 synthesis of unsymmetrical diaryldisulfide

In a 10 mL round-bottomed flask, a solution of compound **1e** (58 mg, 0.209 mmol) and **1f** (60 mg, 0.209 mmol) were prepared in 1.5 mL CH_3CN. Next, *N*-iodosuccinimide (NIS) (24 mg, 0.105 mmol) was added to the solution, and content was allowed to stir at room temperature for 1 h. After completion, the reaction mixture was concentrated under reduced pressure. After that, the crude mixture was diluted in DCM, and organic content was washed with saturated $(NH_4)_2S_2O_8$ solution, dried over Na_2SO_4, and evaporated to dryness. The crude mixture was further purified by column chromatography using the hexane-EtOAc mixture as eluent.

Procedure for the synthesis of symmetrical diaryldisulfide using visible light.

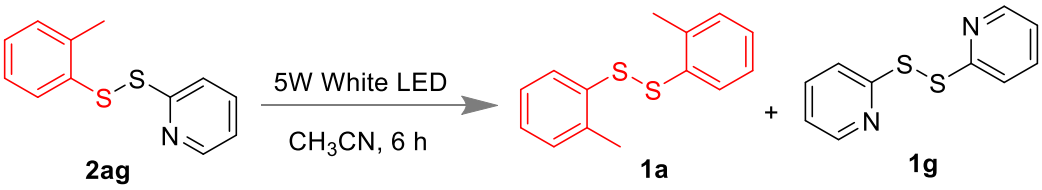

Scheme 6.2 synthesis of symmetrical diaryldisulfide using visible light.

In an oven dried quartz tube unsymmetrical disulfide **2ag** (0.2439 mmol, 60 mg) was dissolved in 0.5 mL acetonitrile (CH_3CN) solvent. Then the reaction mixture was irradiated by 5W white LEDs light for 6 h. After completion of the reaction, acetonitrile (CH_3CN) was removed under reduced pressure. Then, the crude mixture purified by silica-gel column chromatography using distilled ethyl acetate and hexane as the eluent to afford **1a** with 38% (16 mg) and **1g** with 45% (17 mg) yields, respectively.

EPR Experiments. EPR spectra was recorded at 298 K using EPR spectrometer derived at 9.4335 GHz. Typical spectrometer parameters are shown as follows, g = 2.9898; scan range: 100 G; center field set: 3480.00 G; time constant: 0.16 ms; scan time: 122.88 s; modulation

amplitude: 20.0 G; modulation frequency: 100 kHz; receiver gain: 2.00×10^{2}; microwave power: $7.14e^{-001}$ mW.

Experiment in presence DMPO.[42] A mixture compound **1e** (58 mg, 0.209 mmol) , **1f** (60 mg, 0.209 mmol) , N-iodosuccinimide (NIS) (24 mg, 0.105 mmol) and DMPO (20 µL) were stirred in 1.0 mL CH_3CN for 60 min. Afterwards, 300 µL solution was quickly transferred into EPR tube to analyze EPR. Appearance of sharp signal indicated the presence of radical intermediate. A similar experiment was conducted without NIS but no signal was observed. As the spectra gives a broad spectrum, we are unable to signify which radical was present. This observation we believed in the involvement of a radical pathway.

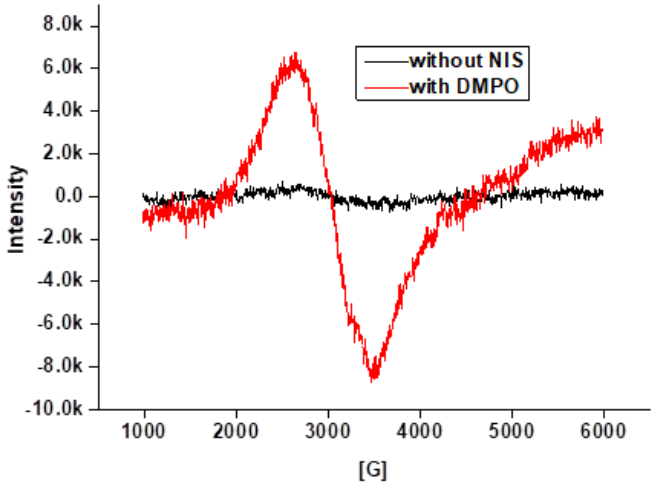

Fig. 6.7. a) EPR spectrum of the reaction under the standard condition with DMPO (red); b) EPR spectrum of the reaction without NIS and with DMPO.

UV experiment. UV experiments were carried out for the solution of disulfide **1f (**2×10^{-4} M in MeCN which shows absorption at 245 nm. Following addition of NIS (2×10^{-4} M in MeCN) showed significant red shift from 245 nm to 360 nm.

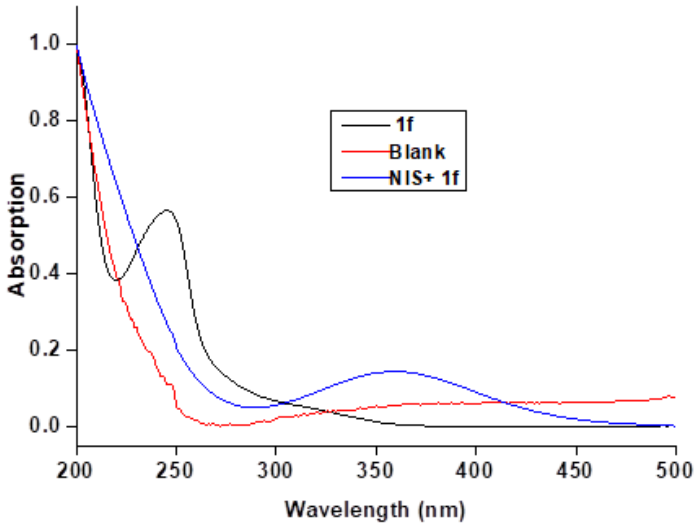

Fig. 6.8. UV spectrum of disulfide **1f** and NIS in MeCN.

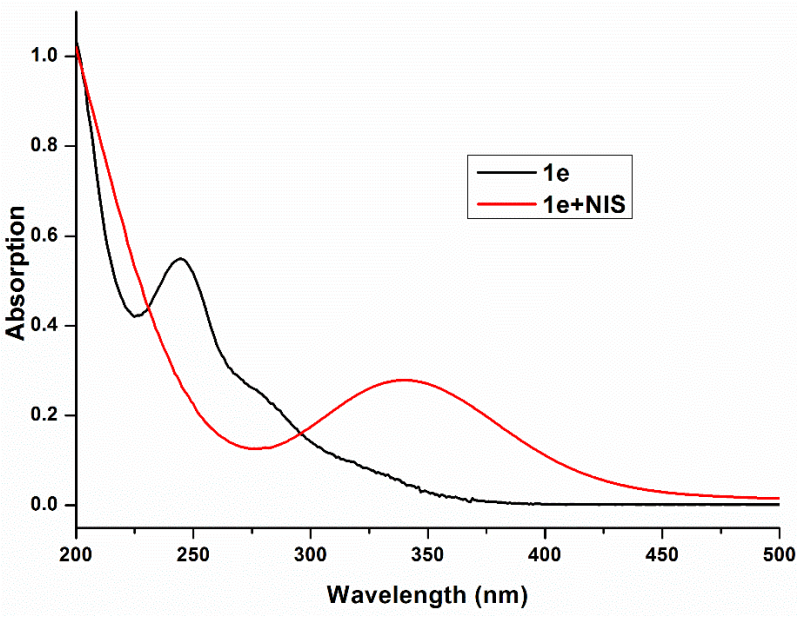

Fig. 6.9. UV spectrum of disulfide **1e** and NIS in MeCN.

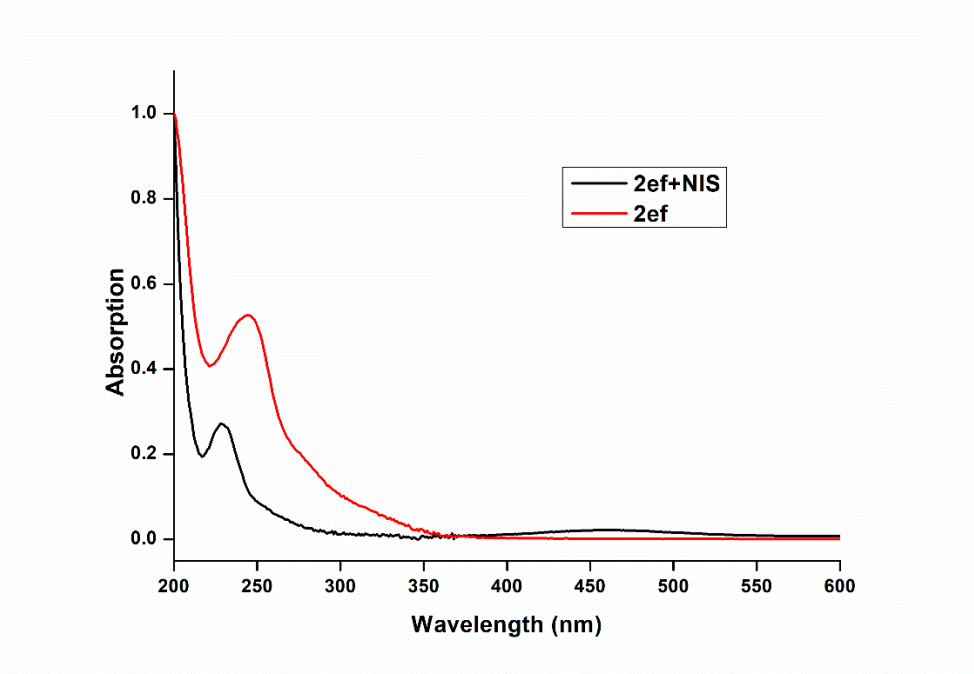

Fig. 6.10. UV spectrum of disulfide **2ef** and NIS in MeCN.

Fluorescence quenching studies. The addition of NIS (2×10^{-4} M in MeCN) to disulfide at 360 nm in room temperature shows maximum emission at 418 nm. Following gradual decrese in fluorescence intensity was observed with every 10 mins time intervals.

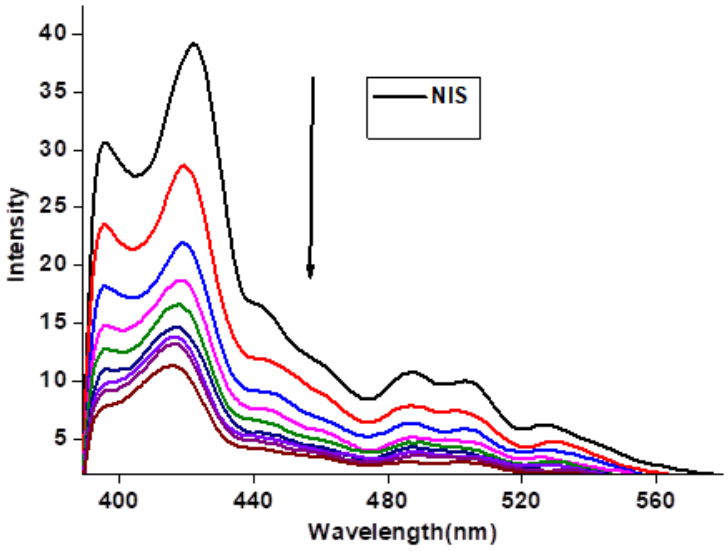

Fig. 6.11. Time-dependent Fluorescence spectrum of disulfide **1f** and NIS in MeCN (every 10 min intervals).

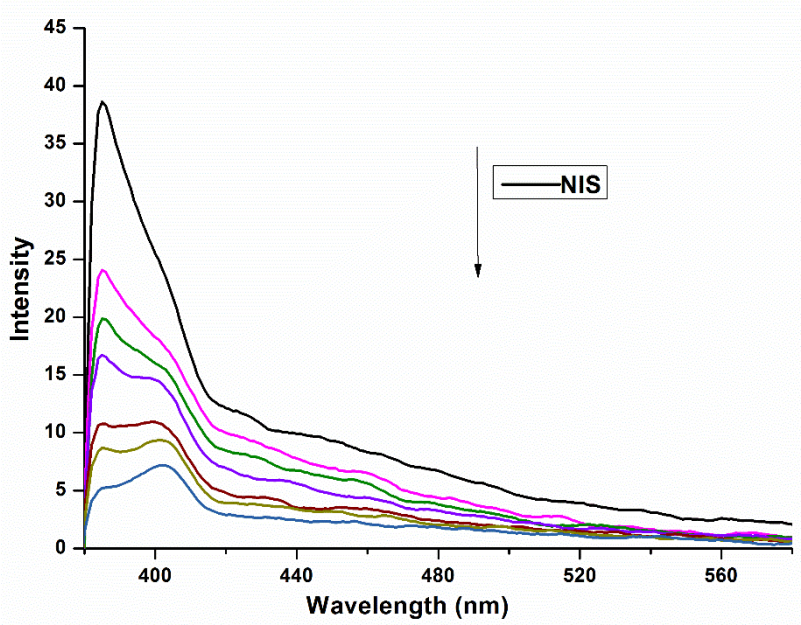

Fig. 6.12. Time-dependent Fluorescence spectrum of disulfide **1e** and NIS in MeCN (every 10 min intervals).

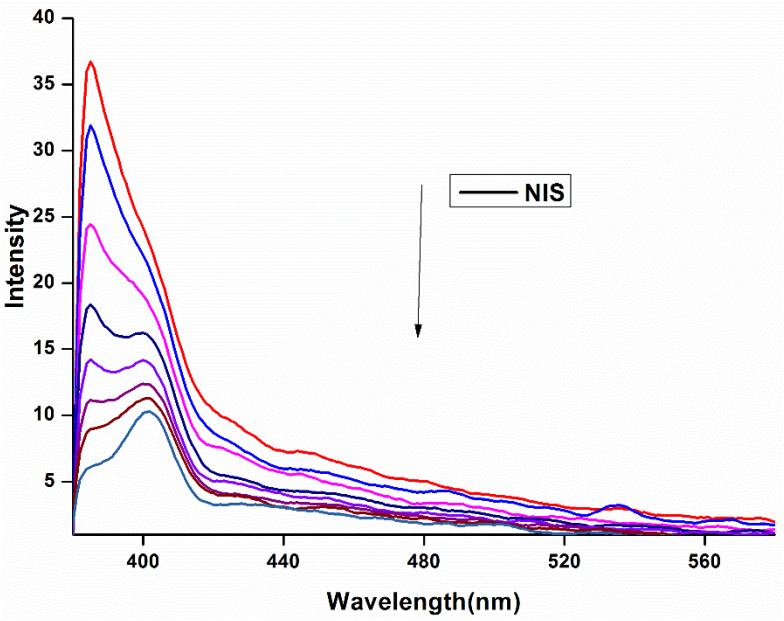

Fig. 6.13. Time-dependent Fluorescence spectrum of disulfide **2ef** and NIS in MeCN (every 10 min intervals).

Theoretical Investigations

All calculations were performed using software package Gaussian 09 ver. D01. The geometry of all the disulfides and NIS were optimized by density functional theory (DFT) at RB3LYP/LanL2DZ level.

XYZ Coordinates and Thermochemical Data of disulfide (2bu) (Energies in Hartree)

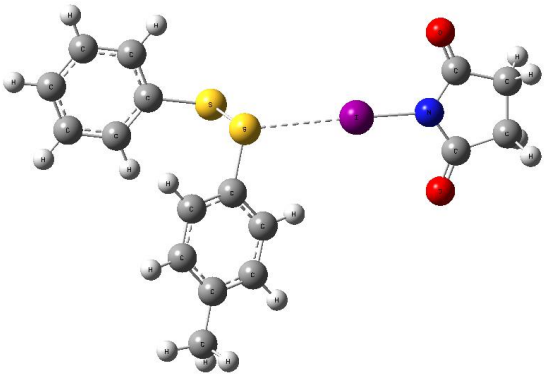

Fig. 6.14. Thermochemical Data of disulfide

Sum of electronic and zero-point Energies = -893.805937

Sum of electronic and thermal Energies = -893.781657

Sum of electronic and thermal Enthalpies = -893.780713

Sum of electronic and thermal Free Energies = -893.870846

C	1.32174	-0.74962	0.53955
C	0.48047	-1.28147	-0.45272
C	-0.45653	-0.45079	-1.1036
C	-0.54465	0.91155	-0.74608
C	0.30111	1.43388	0.24737
C	1.24375	0.61311	0.90857
H	2.0446	-1.39785	1.03071
H	0.54869	-2.32989	-0.72871

H	-1.26533	1.55093	-1.24784
H	0.22869	2.48712	0.51094
C	-4.42945	-2.49561	-2.5101
C	-4.33294	-3.85822	-2.86647
C	-5.36111	-1.6578	-3.16046
C	-5.17259	-4.38136	-3.86743
H	-3.61075	-4.49378	-2.36223
C	-6.19849	-2.1858	-4.16077
H	-5.42552	-0.61017	-2.88117
C	-6.10525	-3.54666	-4.51507
H	-5.09855	-5.43139	-4.13929
H	-6.91702	-1.53987	-4.65929
H	-6.75304	-3.95273	-5.28861
C	2.13165	1.17468	2.00336
H	2.34199	2.23872	1.84398
H	1.6474	1.07972	2.98612
H	3.08835	0.64193	2.05758
S	-1.50173	-1.11995	-2.45323
S	-3.387	-1.82713	-1.1526
C	4.05329	-3.4161	-6.12757
C	3.40354	-4.80669	-5.94098
H	4.15726	-3.12518	-7.17805
H	5.04473	-3.33711	-5.66963
H	3.14432	-5.29309	-6.88716
H	4.03164	-5.50551	-5.37874

I	0.47354	-2.29966	-3.86624
N	2.03239	-3.16751	-4.90577
C	3.11481	-2.42194	-5.43614
C	2.11529	-4.56136	-5.1489
O	1.28708	-5.40317	-4.7795
O	3.25302	-1.1958	-5.34396

XYZ Coordinates and Thermochemical Data of disulfide (1b) (Energies in Hartree)

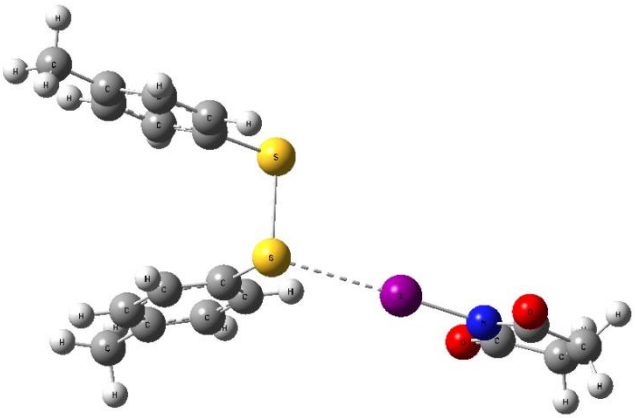

Fig. 6.15.

Sum of electronic and zero-point Energies = -933.091097

Sum of electronic and thermal Energies = -933.064908

Sum of electronic and thermal Enthalpies = -933.063964

Sum of electronic and thermal Free Energies = -933.159256

C	-2.13394	1.47759	0.62612
C	-1.86543	0.12961	0.33917
C	-2.74246	-0.60445	-0.48848
C	-3.88788	0.0244	-1.01881

C	-4.14703	1.37656	-0.72633
C	-3.27622	2.12441	0.09664
H	-1.4509	2.03412	1.26528
H	-0.9854	-0.35616	0.75118
H	-4.56456	-0.54041	-1.65366
H	-5.03278	1.85181	-1.14285
C	-5.11935	-3.60468	0.33783
C	-5.59572	-4.65313	-0.47878
C	-6.01972	-2.6283	0.81185
C	-6.95834	-4.72124	-0.81054
H	-4.90126	-5.40279	-0.84747
C	-7.38405	-2.70671	0.47468
H	-5.65357	-1.81984	1.43815
C	-7.87538	-3.75221	-0.33774
H	-7.3148	-5.53401	-1.4408
H	-8.0698	-1.94888	0.84805
C	-3.54191	3.58876	0.39315
H	-4.56884	3.87152	0.13584
H	-3.3821	3.81767	1.45446
H	-2.86554	4.23542	-0.18391
S	-2.36639	-2.3483	-0.92888
S	-3.35211	-3.5426	0.83722
C	-9.34997	-3.85102	-0.68235
H	-9.83646	-4.64785	-0.10179
H	-9.87744	-2.91526	-0.46564

H	-9.49803	-4.08683	-1.74378
C	1.49807	-8.6358	0.49859
C	0.28196	-9.59005	0.53336
H	2.09623	-8.73119	-0.41358
H	2.17712	-8.76964	1.34704
H	0.20033	-10.21886	-0.35937
H	0.28089	-10.2577	1.40126
I	-1.76452	-5.72287	0.7107
N	-0.49282	-7.34697	0.61641
C	0.91743	-7.2192	0.55587
C	-0.95352	-8.68731	0.60956
O	-2.13945	-9.03711	0.65676
O	1.54002	-6.14991	0.55166

XYZ Coordinates and Thermochemical Data of disulfide (1u) (Energies in Hartree)

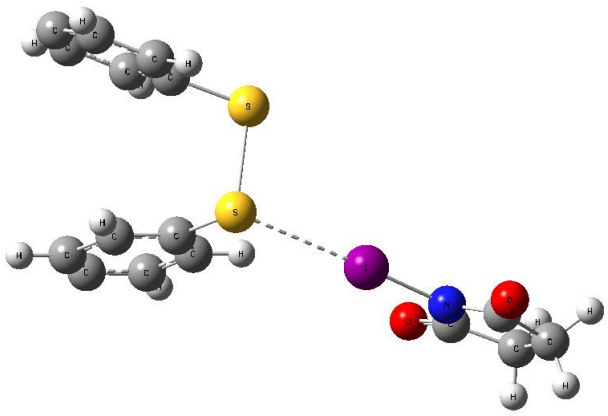

Fig. 6.16. Thermochemical Data of disulfide

Sum of electronic and zero-point Energies = -853.095286

Sum of electronic and thermal Energies = -853.072786

Sum of electronic and thermal Enthalpies = -853.071841

Sum of electronic and thermal Free Energies = -853.156339

C	-3.274	0.49583	0.80713
C	-2.68306	-0.75716	0.4972
C	-3.28851	-1.60611	-0.45573
C	-4.47771	-1.22385	-1.11605
C	-5.08049	0.02952	-0.82638
C	-4.45008	0.8074	0.13477
H	-2.81567	1.15468	1.54066
H	-1.76863	-1.06479	0.99845
H	-4.93327	-1.88745	-1.84638
H	-5.99227	0.33288	-1.33543
C	-5.18064	-4.63308	0.31353
C	-5.65375	-5.56403	-0.63769
C	-6.06349	-3.72795	0.94412
C	-7.03212	-5.59335	-0.97597
H	-4.96273	-6.25385	-1.11593
C	-7.44794	-3.7465	0.62585
H	-5.68549	-3.01639	1.67353
C	-7.84604	-4.66851	-0.33216
H	-7.40453	-6.30547	-1.70846
H	-8.13404	-3.05712	1.1119
S	-2.50694	-3.21505	-0.88498

S	-3.40121	-4.61553	0.77974
C	1.76608	-8.80892	-1.05608
C	0.45292	-9.62497	-1.03578
H	2.36833	-8.98165	-1.95408
H	2.40953	-9.00356	-0.1918
H	0.32114	-10.25387	-1.92243
H	0.36197	-10.27612	-0.16015
I	-1.16381	-5.55641	-0.94855
N	-0.07473	-7.3101	-0.99621
C	1.34198	-7.33701	-1.0282
C	-0.67828	-8.59249	-0.99677
O	-1.89593	-8.81082	-0.97066
O	2.07717	-6.34176	-1.03198

CHARATERIZATION DATA

2-(*o*-Tolyldisulfaneyl)pyridine (2ag). R_f = 0.5 (5% ethyl acetate in hexane); colorless liquid;

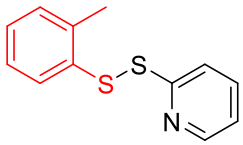

yield 75% (43 mg); ^{1}H NMR (700 MHz, $CDCl_3$) δ 8.46 (dd, *J* = 4.8, 0.4 Hz, 1H), 7.62-7.56 (m, 3H), 7.17-7.13 (m, 3H), 7.01-6.99 (m, 1H), 2.49 (s, 3H); ^{13}C NMR (100 MHz, $CDCl_3$) δ 159.7, 149.6, 137.3, 136.7, 134.6, 130.5, 127.4, 127.3, 126.9, 120.9, 119.8, 20.0; IR (KBr) ῡ 3046, 2921, 2348, 1573, 1445, 674, 484; HRMS (ESI/Q-TOF) m/z: $[M + H]^+$ calcd for $C_{12}H_{12}NS_2$ 234.0406; found 234.0381.

2-(*p*-Tolyldisulfaneyl)pyridine (2bg).[49] R_f = 0.5 (5% ethyl acetate in hexane); colorless liquid; yield 74% (42 mg); ^{1}H NMR (400 MHz, $CDCl_3$) δ 8.45 (d, *J* = 4.2 Hz, 1H), 7.67 (d, *J* = 8.2 Hz, 1H), 7.61-7.57 (m, 1H), 7.42 (d, *J* = 8.2 Hz, 2H), 7.10 (d, *J* = 8.2 Hz, 2H), 7.08-7.05 (m, 1H), 2.30 (s, 3H); ^{13}C NMR (100 MHz, $CDCl_3$) δ 160.0, 149.6, 137.7, 137.3, 132.8, 130.0, 128.2, 120.8, 119.7, 21.1.

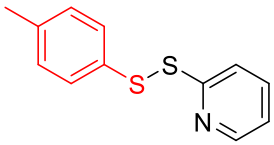

1-(3-Methoxyphenyl)-2-(*p*-tolyl)disulfane (2bd).[50] R_f = 0.5 (2% ethyl acetate in hexane); colorless liquid; yield 82% (44 mg); ^{1}H NMR (400 MHz, $CDCl_3$) δ 7.41-7.38 (m, 2H), 7.23-7.18 (m, 1H), 7.11 (d, *J* = 8.0 Hz, 2H), 7.09-7.07 (m, 2H), 6.77-6.74 (m, 1H), 3.77(s, 3H), 2.32 (s, 3H); ^{13}C NMR (100 MHz, $CDCl_3$) δ 160.2, 138.7, 137.7, 133.7, 130.0(×2), 128.6, 119.7, 113.2, 112.6, 55.4, 21.2.

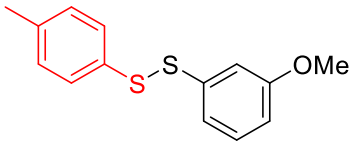

1-(4-Chlorophenyl)-2-(4-methoxyphenyl)disulfane (2ef).[51] R_f = 0.5 (2% ethyl acetate in hexane); colorless liquid; yield 80% (35 mg); ^{1}H NMR (400 MHz, $CDCl_3$) δ 7.45-7.38 (m, 4H), 7.29-7.26 (m, 2H), 6.85-6.82 (m, 2H), 3.79 (s, 3H); ^{13}C NMR (100 MHz, $CDCl_3$) δ 160.2, 136.2, 133.6, 132.3, 130.0, 129.3, 127.7, 114.9, 55.5.

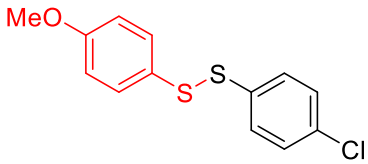

1-Cyclopentyl-2-(2-methoxyphenyl)disulfane (2ch).[49] R_f = 0.6 (2% ethyl acetate in hexane); colorless liquid; yield 70% (36 mg); ^{1}H NMR (400 MHz, $CDCl_3$) δ 7.74 (dd, *J* = 7.8, 1.6 Hz, 1H), 7.21-7.17 (m, 1H), 7.01-6.97 (m, 1H), 6.85 (d, *J* = 8.0 Hz, 1H), 3.89 (s, 3H), 3.36-3.30 (m, 1H), 1.98-1.91 (m, 2H), 1.77-1.66 (m, 4H), 1.61-

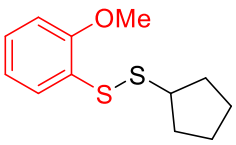

1.55 (m, 2H); ^{13}C NMR (100 MHz, $CDCl_3$) δ 156.4, 127.5,127.4, 126.0, 121.2, 110.7, 56.0, 50.0, 32.9, 24.8.

1-Cyclohexyl-2-(2-methoxyphenyl)disulfane (2ci). R_f = 0.5 (in hexane); colorless liquid; yield 64% (35 mg); ^{1}H NMR (400 MHz, $CDCl_3$) δ 7.73 (dd, *J* = 7.8, 1.6 Hz, 1H), 7.20-7.16 (m, 1H), 6.99 (td, *J* = 7.6, 1.0 Hz, 1H), 6.85-6.83 (m, 1H), 3.89 (s, 3H), 2.83-2.76 (m, 1H), 2.06-2.02 (m, 2H), 1.78-1.75 (m, 2H), 1.45-1.31 (m, 3H), 1.29-1.24 (m, 3H); ^{13}C NMR (100 MHz, $CDCl_3$) δ 156.3, 127.3, 127.2, 126.4, 121.3, 110.6, 56.0, 49.7, 32.8, 26.2, 25.7. IR (KBr) ῡ 2925, 2348, 1236, 746, 588; HRMS (ESI/Q-TOF) m/z: $[M + Na]^+$ calcd for $C_{13}H_{18}OS_2Na$ 277.0691; found 277.0668.

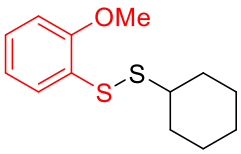

1-Isobutyl-2-(2-methoxyphenyl)disulfane (2cn). R_f = 0.7 (hexane); colorless liquid; yield 84% (41 mg); ^{1}H NMR (400 MHz, $CDCl_3$) δ 7.71 (dd, *J* = 7.6, 1.4 Hz, 1H), 7.23-7.19 (m, 1H), 7.02-6.98 (m, 1H), 6.86 (dd, *J* = 8.0, 0.5 Hz, 1H), 3.89 (s, 3H), 2.64 (d, *J* = 6.8 Hz, 2H), 2.04-1.90 (m, 1H), 1.01 (d, *J* = 6.8 Hz, 6H); ^{13}C NMR (100 MHz, $CDCl_3$) δ 156.7, 127.8, 127.7, 125.7, 121.3, 110.8, 56.0, 48.1, 28.2, 21.9; IR (KBr) ῡ 3085, 2957, 1473, 748, 674; HRMS (ESI/Q-TOF) m/z: $[M]^+$ calcd for $C_{11}H_{16}OS_2$ 228.0637; found 228.0619.

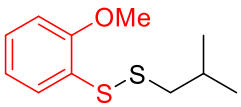

1-(2-Methoxyphenyl)-2-phenethyldisulfane (2cl). R_f = 0.3 (in hexane); colorless liquid; yield 75% (45 mg) ^{1}H NMR (400 MHz, $CDCl_3$) δ 7.70 (dd, *J* = 7.6, 1.6 Hz, 1H), 7.31-7.28 (m, 2H), 7.26-7.23 (m, 1H), 7.22-7.18 (m, 3H), 7.01-6.97 (m, 1H), 6.88 (dd, *J* = 8.0, 0.8 Hz, 1H), 3.91 (s, 3H), 3.05-2.96 (m, 4H); ^{13}C NMR (100 MHz, $CDCl_3$) δ 156.9, 140.1, 128.8, 128.6, 128.3, 128.0, 126.5,

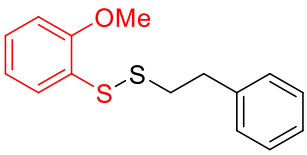

125.3, 121.4, 110.9, 56.0, 39.8, 35.5; IR (KBr) ῡ 3061, 2929, 2348, 1602, 699; HRMS (ESI/Q-TOF) m/z: $[M + Na]^+$ calcd for $C_{15}H_{16}OS_2Na$ 299.0535; found 299.0544.

1-Cyclopentyl-2-(3-methoxyphenyl)disulfane (2dh). R_f = 0.5 (in hexane); colorless liquid;

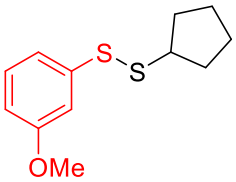

yield 77% (40 mg); ^{1}H NMR (400 MHz, $CDCl_3$) δ 7.22 (t, *J* = 7.8 Hz, 1H), 7.14-7.09 (m, 2H), 6.75-6.72 (m, 1H), 3.82 (s, 3H), 3.37-3.30 (m, 1H), 1.97-1.90 (m, 2H), 1.78-1.64 (m, 4H), 1.61-1.54 (m, 2H); ^{13}C NMR (100 MHz, $CDCl_3$) δ 160.2, 139.6, 129.9, 119.3, 112.5, 112.2, 55.5, 50.5, 32.9, 24.8; IR (KBr) ῡ 2955, 2347, 1588, 684; HRMS (ESI/Q-TOF) m/z: $[M + H]^+$ calcd for $C_{12}H_{17}OS_2$ 241.0715; found 241.0744.

1-Dodecyl-2-(3-methoxyphenyl)disulfane (2do).[52] R_f = 0.6 (in hexane); colorless liquid;

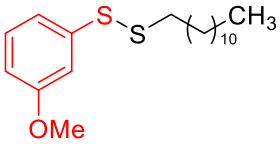

yield 71% (36 mg); ^{1}H NMR (400 MHz, $CDCl_3$) δ 7.22 (t, *J* = 7.8 Hz, 1H), 7.13-7.12 (m, 1H), 7.11-7.09 (m, 1H), 6.75 (dd, *J* = 8.2, 0.8 Hz, 1H), 3.82 (s, 3H), 2.75 (t, *J* = 7.2 Hz, 2H), 1.71-1.63 (m, 2H), 1.31-1.26 (m, 18H), 0.91-0.87 (m, 3H); ^{13}C NMR (100 MHz, $CDCl_3$) δ 160.3, 139.3, 129.9, 119.6, 112.7, 112.6, 55.5, 39.3, 32.1, 29.8, 29.74, 29.71, 29.6, 29.5, 29.3, 29.0, 28.6, 22.8, 14.2.

1-Dodecyl-2-(4-methoxyphenyl)disulfane (2eo).[13] R_f = 0.4 (5% ethyl acetate in hexane); colorless liquid; yield 82% (26 mg); NMR (400 MHz, $CDCl_3$) δ 7.49-7.45 (m, 2H), 6.88-6.84

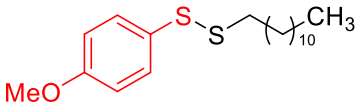

(m, 2H), 3.80 (s, 3H), 2.73 (t, *J* = 7.2, 2H), 1.69-1.62 (m, 2H), 1.33-1.24 (m, 18H), 0.90-0.88 (m, 3H); ^{13}C NMR (100 MHz, $CDCl_3$) δ 159.6, 131.8, 128.7, 114.8, 55.5, 39.0, 32.1, 29.79, 29.78, 29.73, 29.6, 29.5, 29.3, 28.9, 28.6, 22.8, 14.3.

2-(Cyclopentyldisulfaneyl)pyridine (2gh).[50] R_f = 0.6 (5% ethyl acetate in hexane); colorless

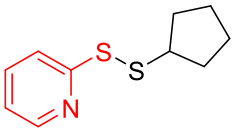

liquid; yield 86% (50 mg); ^{1}H NMR (400 MHz, $CDCl_3$) δ 8.43-8.41 (m, 1H), 7.74 (d, *J* = 8.0 Hz, 1H), 7.63-7.59 (m, 1H), 7.05-7.02 (m, 1H), 3.40-3.33 (m, 1H), 1.97-1.90 (m, 2H), 1.79-1.63 (m, 2H), 1.60-1.54 (m, 2H), 1.27-1.23 (m, 2H); ^{13}C NMR (100 MHz, $CDCl_3$) δ 161.2, 149.5, 137.0, 120.5, 119.6, 50.4, 32.9, 24.8.

2-(Dodecyldisulfaneyl)pyridine (2go).[53] R_f = 0.7 (5% ethyl acetate in hexane); colorless

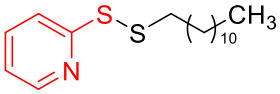

liquid; yield 92% (43 mg); ^{1}H NMR (400 MHz, $CDCl_3$) δ 8.45 (dd, *J* = 4.8, 0.8 Hz, 1H), 7.72 (d, *J* = 8.0 Hz, 1H), 7.64-7.60 (m, 1H), 7.07-7.04 (m, 1H), 2.78 (t, *J* = 7.2, 2H), 1.71-1.64 (m, 2H), 1.41-1.24 (m, 18H), 0.88-0.85 (m, 3H); ^{13}C NMR (100 MHz, $CDCl_3$) δ 160.9, 149.7, 137.0, 120.6, 119.7, 39.2, 32.0, 30.3, 29.7, 29.7, 29.6, 29.5, 29.3, 29.1, 28.6, 22.8, 14.2.

2-(Benzyldisulfaneyl)pyridine (2gj).[54] R_f = 0.3 (2% ethyl acetate in hexane); colorless liquid;

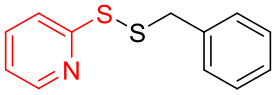

yield 95% (54 mg); ^{1}H NMR (400 MHz, $CDCl_3$) δ 8.43-8.41 (m, 1H), 7.50-7.48 (m, 2H), 7.31-7.26 (m, 3H), 7.24-7.18 (m, 2H), 7.03-6.99 (m, 1H), 4.01 (s, 2H);^{13}C NMR (100 MHz, $CDCl_3$) δ 160.1, 149.5, 136.8, 136.6, 129.4, 128.6, 127.7, 120.5, 119.6, 43.9.

2-((4-(*tert*-Butyl)benzyl)disulfaneyl)pyridine (2gk). R_f = 0.5 (5% ethyl acetate in hexane);

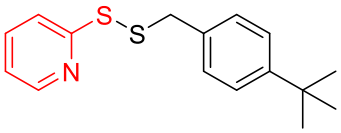

colorless liquid; yield 87% (42 mg); ^{1}H NMR (400 MHz, $CDCl_3$) δ 8.41-8.39 (m, 1H), 7.47-7.46 (m, 2H), 7.27-7.21(m, 4H), 7.01-6.97 (m, 1H), 4.00 (s, 2H), 1.27 (s, 9H); ^{13}C NMR (100 MHz, $CDCl_3$) δ 160.4, 150.7, 149.5, 136.8, 133.5, 129.2, 125.6, 120.5, 119.6, 43.6, 31.4, 29.8; IR (KBr) ῡ 2960, 2924, 2348, 1574, 758; HRMS (ESI/Q-TOF) m/z: $[M + H]^+$ calcd for $C_{16}H_{20}NS_2$ 290.1032; found 290.1051.

2-(Isobutyldisulfaneyl)pyridine (2gn).[55] R_f = 0.7 (5% ethyl acetate in hexane); colorless

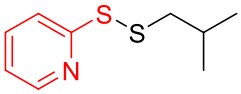

liquid; yield 72% (39 mg); ^{1}H NMR (400 MHz, $CDCl_3$) δ 8.42 (d, *J* =4.6 Hz, 1H), 7.70 (d, *J* = 8.2 Hz, 1H), 7.62-7.58 (m, 1H), 7.04-7.01 (m, 1H), 2.67 (d, *J* = 6.8 Hz, 2H), 1.98-1.89 (m, 1H), 0.98 (d, *J* = 6.8 Hz, 6H); ^{13}C NMR (100 MHz, $CDCl_3$) δ 160.8, 149.6, 137.0, 120.5, 119.6, 48.4, 28.2, 21.8.

2-(Cyclohexyldisulfaneyl)pyridine (2gr).[56] R_f = 0.6 (5% ethyl acetate in hexane); colorless

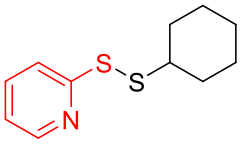

liquid; yield 83% (49 mg); ^{1}H NMR (400 MHz, $CDCl_3$) δ 8.43 (d, *J* = 4.6 Hz, 1H), 7.77 (d, *J* = 8.1 Hz, 1H), 7.63 (t, *J* = 7.8 Hz, 1H), 7.06-7.03 (m, 1H), 2.87-2.81 (m, 1H), 2.05 (d, *J* = 11.3 Hz, 2H), 1.77-1.74 (m, 2H), 1.44-1.35 (m, 3H), 1.34-1.16 (m, 3H); ^{13}C NMR (100 MHz, $CDCl_3$) δ 161.6, 149.4, 137.0, 120.4, 119.5, 50.1, 32.8, 26.2, 25.6.

2-((4-Fluorobenzyl)disulfaneyl)pyridine(2gq). R_f = 0.55 (5% ethyl acetate in hexane);

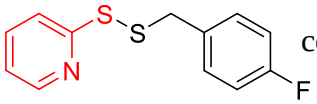

colorless liquid; yield 56% (30 mg); ^{1}H NMR (700 MHz, $CDCl_3$) δ 8.42 (d, *J* = 4.2 Hz, 1H), 7.51 (dd, *J* = 7.9, 7.5 Hz, 1H), 7.45 (d, *J* = 8.0 Hz, 1H), 7.25-7.23 (m, 2H), 7.04-7.01 (m, 1H), 6.91 (t, *J* = 8.6 Hz, 2H), 3.98 (s, 2H); ^{13}C NMR (176 MHz, $CDCl_3$) δ 162.37 (d, $^1J_{CF}$ = 246.5 Hz), 159.9, 149.6, 136.8, 132.5 (d, $^4J_{CF}$ = 3.2 Hz), 131.1 (d, $^3J_{CF}$ = 8.2 Hz), 120.7, 119.7, 115.5 (d, $^2J_{CF}$ = 21.5 Hz), 42.8, IR (KBr) ῡ 2923, 2352, 1508, 759; HRMS (ESI/Q-TOF) m/z: $[M + Na]^+$ calcd for $C_{12}H_{10}ClNS_2Na$ 289.9835; found 289.9815.

2-((2-Chlorobenzyl)disulfaneyl)pyridine (2gp). R_f = 0.5 (5% ethyl acetate in hexane);

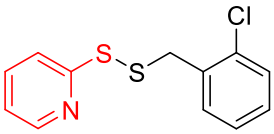

colorless liquid; yield 62% (31 mg); ^{1}H NMR (700 MHz, $CDCl_3$) δ 8.39 (d, *J* = 4.5 Hz, 1H), 7.51-7.47 (m, 2H), 7.33 (d, *J* = 7.9 Hz, 1H), 7.13-7.10 (m, 2H), 7.07 (t, *J* = 7.4 Hz, 1H), 7.02-6.97 (m, 1H), 4.13 (s, 2H); ^{13}C NMR (176 MHz, $CDCl_3$) δ 160.2, 149.5, 136.9, 134.4, 131.9, 129.7, 129.2, 126.8, 120.6, 119.4, 41.5; IR (KBr) ῡ 2927, 2348, 1518, 749; HRMS (ESI/Q-TOF) m/z: $[M + Na]^+$ calcd for $C12H_{10}ClNS_2Na$ 289.9835; found 289.9815.

2-(Phenethyldisulfaneyl)pyridine (2gl).[54] R_f = 0.3 (2% ethyl acetate in hexane); colorless

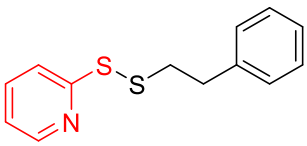

liquid; yield 70% (38 mg); ^{1}H NMR (400 MHz, $CDCl_3$) δ 8.48-8.46 (m, 1H), 7.68-7.66 (m, 1H), 7.63-7.59 (m, 1H), 7.30-7.27 (m, 2H), 7.23-7.17 (m, 3H), 7.09-7.06 (m, 1H), 3.08-2.99 (m, 4H); ^{13}C NMR (100 MHz, $CDCl_3$) δ 160.4, 149.7, 139.7, 137.1, 128.7, 128.6, 126.6, 120.7, 119.7, 40.1, 35.4.

2-((Isobutyldisulfaneyl)methyl)furan (2mn). R_f = 0.5 (2% ethyl acetate in hexane);colorless

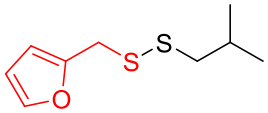

liquid; yield 54% (29 mg); ^{1}H NMR (400 MHz, $CDCl_3$) δ 7.39 (d, *J* = 1.4 Hz, 1H), 6.33-6.32 (m, 1H), 6.27 (d, *J* = 3.0, 1H), 3.89 (s, 2H), 2.34 (d, *J* = 6.8 Hz, 2H), 1.89-1.79 (m, 1H), 0.94 (d, *J* = 6.8 Hz, 6H); ^{13}C NMR (100 MHz, $CDCl_3$) δ 150.7, 142.5, 110.9, 108.5, 48.4, 36.0, 28.1, 21.8; IR (KBr) ῡ 2956, 2924, 2348, 1463, 736; HRMS (ESI/Q-TOF) m/z: $[M + H]^+$ calcd for $C_9H_{15}OS_2$ 203.0559; found 203.0543.

1,2-Di-o-tolyldisulfane (1a).[57] R_f = 0.7 (hexane); white solid; yield 38% (16 mg); ^{1}H NMR

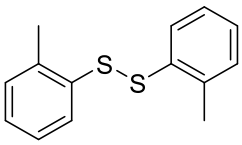

(700 MHz, $CDCl_3$) δ 7.53-7.51 (m, 2H), 7.17 (d, *J* = 7.0 Hz, 3H), 7.16-7.12 (m, 3H), 2.44 (s, 6H); ^{13}C NMR (176 MHz, $CDCl_3$) δ 137.5, 135.6, 130.4, 128.8, 127.5, 126.8, 20.1.

1,2-Di(pyridin-2-yl)disulfane (1g).[57] R_f = 0.5 (5% ethyl acetate in hexane); white solid; yield 45% (17 mg); ^{1}H NMR (700 MHz, $CDCl_3$) δ 8.43 (d, *J* = 4.8 Hz, 2H), 7.60-7.56 (m, 4H), 7.09-7.07 (m, 2H); ^{13}C NMR (176 MHz, $CDCl_3$) δ 158.9, 149.6, 137.5, 121.2, 119.7.

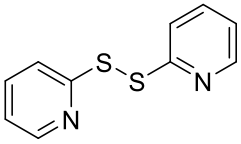

6.6 NOTES AND REFERENCES

(1) Lehn, J. M. Constitutional Dynamic Chemistry: Bridge from Supramolecular Chemistry to Adaptive Chemistry. *Top. Curr. Chem.* **2012**, *322*, 1-32.

(2) Diemer, S. L.; Kristensen, M.; Rasmussen, B.; Beeren, S. R.; Pittelkow, M. Simultaneous Disulfide and Boronic Acid Ester Exchange in Dynamic Combinatorial Libraries. *International Journal of Molecular Sciences* **2015**, *16*, 21858-21872.

(3) Belenguer, A. M.; Friščić, T.; Day, G. M.; Sanders, J. K. M. Solid-State Dynamic Combinatorial Chemistry: Reversibility and Thermodynamic Product Selection in Covalent Mechanosynthesis. *Chem. Sci.* **2011**, *2*, 696-700.

(4) Wang, M.; Jiang, X. Sulfur–Sulfur Bond Construction. *Top. Curr. Chem.* **2018**, *376*, 14.

(5) Qiu, X.; Yang, X.; Zhang, Y.; Song, S.; Jiao, N. Efficient and Practical Synthesis of Unsymmetrical Disulfides Via Base-Catalyzed Aerobic Oxidative Dehydrogenative Coupling of Thiols. *Org. Chem. Front.* **2019**, *6*, 2220-2225.

(6) Hunter, R.; Caira, M.; Stellenboom, N. Inexpensive, One-Pot Synthesis of Unsymmetrical Disulfides Using 1-Chlorobenzotriazole. *J. Org. Chem.* **2006**, *71*, 8268-8271.

(7) Ren, S.; Luo, N.; Liu, K.; Liu, J.-B. Synthesis of Unsymmetrical Disulfides Via the Cross-Dehydrogenation of Thiols. *J. Chem. Res.* **2020**, *45*, 365-373.

(8) Vandavasi, J. K.; Hu, W.-P.; Chen, C.-Y.; Wang, J.-J. Efficient Synthesis of Unsymmetrical Disulfides. *Tetrahedron* **2011**, *67*, 8895-8901.

(9) Fernandes, P. A.; Ramos, M. J. Theoretical Insights into the Mechanism for Thiol/Disulfide Exchange. *Chem. Eur. J.* **2004**, *10*, 257-266.

(10) Fava, A.; Iliceto, A.; Camera, E. Kinetics of the Thiol-Disulfide Exchange. *J. Am. Chem. Soc* **1957**, *79*, 833-838.

(11) Black, S. P.; Stefankiewicz, A. R.; Smulders, M. M.; Sattler, D.; Schalley, C. A.; Nitschke, J. R.; Sanders, J. K. M. Generation of a Dynamic System of Three-Dimensional Tetrahedral Polycatenanes. *Angew. Chem. Int. Ed.* **2013**, *52*, 5749-5752.

(12) Fass, D.; Thorpe, C. Chemistry and Enzymology of Disulfide Cross-Linking in Proteins. *Chem. Rev.* **2018**, *118*, 1169-1198.

(13) Sattler, L. E.; Otten, C. J.; Hilt, G. Alternating Current Electrolysis for the Electrocatalytic Synthesis of Mixed Disulfide Via Sulfur–Sulfur Bond Metathesis Towards Dynamic Disulfide Libraries. *Chem. Eur. J.* **2020**, *26*, 3129-3136.

(14) Kanemoto, K.; Furuhashi, K.; Morita, Y.; Komatsu, T.; Fukuzawa, S.-i. Acid-Mediated Sulfonylthiolation of Arenes Via Selective Activation of Ss-Morpholino Dithiosulfonate. *Org. Lett.* **2021**, *23*, 1582-1587.

(15) Parida, A.; Choudhuri, K.; Mal, P. Unsymmetrical Disulfides Synthesis Via Sulfenium Ion. *Chem. Asian J.* **2019**, *14*, 2579-2583.

(16) Mandal, B.; Basu, B. Recent Advances in S–S Bond Formation. *RSC Adv* **2014**, *4*, 13854-13881.

(17) Ashkenasy, G.; Hermans, T. M.; Otto, S.; Taylor, A. F. Systems Chemistry. *Chem. Soc. Rev.* **2017**, *46*, 2543-2554.

(18) Sarma, R. J.; Otto, S.; Nitschke, J. R. Disulfides, Imines, and Metal Coordination within a Single System: Interplay between Three Dynamic Equilibria. *Chem. Eur. J.* **2007**, *13*, 9542-9546.

(19) Riley, K. E.; Hobza, P. Noncovalent Interactions in Biochemistry. *WIREs Comput. Mol. Sci.* **2011**, *1*, 3-17.

(20) Vogel, L.; Wonner, P.; Huber, S. M. Chalcogen Bonding: An Overview. *Angew. Chem., Int. Ed.* **2019**, *58*, 1880-1891.

(21) Raynal, M.; Ballester, P.; Vidal-Ferran, A.; van Leeuwen, P. W. N. M. Supramolecular Catalysis. Part 1: Non-Covalent Interactions as a Tool for Building and Modifying Homogeneous Catalysts. *Chem. Soc. Rev.* **2014**, *43*, 1660-1733.

(22) Twum, K.; Rissanen, K.; Beyeh, N. K. Recent Advances in Halogen Bonded Assemblies with Resorcin[4]Arenes. *Chem. Rec.* **2021**, *21*, 386-395.

(23) Nandy, A.; Kazi, I.; Guha, S.; Sekar, G. Visible-Light-Driven Halogen-Bond-Assisted Direct Synthesis of Heteroaryl Thioethers Using Transition-Metal-Free One-Pot C–I Bond Formation/C–S Cross-Coupling Reaction. *J. Org. Chem.* **2021**, *86*, 2570-2581.

(24) Giese, M.; Albrecht, M.; Rissanen, K. Anion−Π Interactions with Fluoroarenes. *Chem. Rev.* **2015**, *115*, 8867-8895.

(25) Dougherty, D. A. The Cation−Π Interaction. *Acc. Chem. Res.* **2013**, *46*, 885-893.

(26) Choudhuri, K.; Mandal, A.; Mal, P. Aerial Dioxygen Activation Vs. Thiol-Ene Click Reaction within a System. *Chem. Commun.* **2018**, *54*, 3759-3762.

(27) Pramanik, M.; Mathuri, A.; Mal, P. Sulfur···Oxygen Interaction-Controlled (Z)-Selective Anti-Markovnikov Vinyl Sulfides. *Chem. Commun.* **2021**, *57*, 5698-5701.

(28) Mahadevi, A. S.; Sastry, G. N. Cooperativity in Noncovalent Interactions. *Chem. Rev.* **2016**, *116*, 2775-2825.

(29) Näther, C.; Bolte, M. Investigations on the Interaction between Sp 2 -Sulfur Atoms and Iodine Molecules Using the Cambridge Structural Database. *Phosphorus Sulfur Silicon Relat. Elem.* **2003**, *178*, 453-464.

(30) Arman, H. D.; Gieseking, R. L.; Hanks, T. W.; Pennington, W. T. Complementary Halogen and Hydrogen Bonding: Sulfur···Iodine Interactions and Thioamide Ribbons. *Chem. Commun.* **2010**, *46*, 1854-1856.

(31) Bartashevich, E.; Mukhitdinova, S.; Yushina, I.; Tsirelson, V. Electronic Criterion for Categorizing the Chalcogen and Halogen Bonds: Sulfur–Iodine Interactions in Crystals. *Acta Crystallogr. B* **2019**, *75*, 117-126.

(32) Fukuroi, K.; Takahashi, K.; Mochida, T.; Sakurai, T.; Ohta, H.; Yamamoto, T.; Einaga, Y.; Mori, H. Synergistic Spin Transition between Spin Crossover and Spin-Peierls-Like Singlet Formation in the Halogen-Bonded Molecular Hybrid System: [Fe(Iqsal)2][Ni(Dmit)2]·Ch3 Cn·H2 O. *Angew. Chem. Int. Ed.* **2014**, *53*, 1983-1986.

(33) Wodrich, M. D.; Caramenti, P.; Waser, J. Alkynylation of Thiols with Ethynylbenziodoxolone (Ebx) Reagents: A- or B- Π-Addition? *Org. Lett.* **2016**, *18*, 60-63.

(34) Caraballo, R.; Rahm, M.; Vongvilai, P.; Brinck, T.; Ramström, O. Phosphine-Catalyzed Disulfide Metathesis. *Chem. Commun.* **2008**, 6603-6605.

(35) Guo, J.; Zha, J.; Zhang, T.; Ding, C.-H.; Tan, Q.; Xu, B. Pdcl2/Dmso-Catalyzed Thiol–Disulfide Exchange: Synthesis of Unsymmetrical Disulfide. *Org. Lett.* **2021**, *23*, 3167-3172.

(36) Bal, A.; Maiti, S.; Mal, P. Strategies to Control Hypervalent Iodine - Primary Amine Reactions. *Chem. Asian J.* **2020**, *15*, 624-635.

(37) Maiti, S.; Alam, M. T.; Bal, A.; Mal, P. Nitrenium Ions from Amine-Iodine(Iii) Combinations. *Adv. Synth. Catal.* **2019**, *361*, 4401-4425.

(38) Maiti, S.; Achar, T. K.; Mal, P. An Organic Intermolecular Dehydrogenative Annulation Reaction. *Org. Lett.* **2017**, *19*, 2006-2009.

(39) Bera, S. K.; Alam, M. T.; Mal, P. C–N Coupling Via Antiaromatic Endocyclic Nitrenium Ions. *J. Org. Chem.* **2019**, *84*, 12009-12020.

(40) Pramanik, M.; Choudhuri, K.; Mal, P. N-Iodosuccinimide as Bifunctional Reagent in (E)-Selective C(Sp2)−H Sulfonylation of Styrenes. *Asian J. Org. Chem.* **2019**, *8*, 144-150.

(41) Alam, M. T.; Maiti, S.; Mal, P. An Intramolecular C(Sp2)–H Amidation Using N-Iodosuccinimide. *Eur. J. Org. Chem.* **2018**, 4178-4186.

(42) Pramanik, M.; Choudhuri, K.; Mathuri, A.; Mal, P. Dithioacetalization or Thioetherification of Benzyl Alcohols Using 9-Mesityl-10-Methylacridinium Perchlorate Photocatalyst. *Chem. Commun.* **2020**, *56*, 10211-10214.

(43) Koohi, M.; Bastami, H. A Density Functional Theory Perspective on 2,2,9,9-Tetrahalostannacyclonona-3,5,7-Trienylidenes. *J. Phys. Org. Chem.* **2020**, *33*, e4031.

(44) Liu, B.; Lim, C. H.; Miyake, G. M. Visible-Light-Promoted C-S Cross-Coupling Via Intermolecular Charge Transfer. *J. Am. Chem. Soc.* **2017**, *139*, 13616-13619.

(45) Sundaravelu, N.; Nandy, A.; Sekar, G. Visible Light Mediated Photocatalyst Free C–S Cross Coupling: Domino Synthesis of Thiochromane Derivatives Via Photoinduced Electron Transfer. *Org. Lett.* **2021**, *23*, 3115-3119.

(46) Liu, C.; Xia, J.; Ji, S.; Fan, Z.; Xu, H. Visible-Light-Induced Metathesis Reaction between Diselenide and Ditelluride. *Chem. Commun.* **2019**, *55*, 2813-2816.

(47) Pramanik, M.; Choudhuri, K.; Mal, P. Metal-Free C–S Coupling of Thiols and Disulfides. *Org. Biomol. Chem.* **2020**, *18*, 8771-8792.

(48) Choudhuri, K.; Pramanik, M.; Mal, P. Noncovalent Interactions in C–S Bond Formation Reactions. *J. Org. Chem.* **2020**, *85*, 11997-12011.

(49) Dethe, D. H.; Srivastava, A.; Dherange, B. D.; Kumar, B. V. Unsymmetrical Disulfide Synthesis through Photoredox Catalysis. *Adv. Synth. Catal.* **2018**, *360*, 3020-3025.

(50) Wang, Y.; Deng, J.; Chen, J.; Cao, F.; Hou, Y.; Yang, Y.; Deng, X.; Yang, J.; Wu, L.; Shao, X., et al. Dechalcogenization of Aryl Dichalcogenides to Synthesize Aryl Chalcogenides Via Copper Catalysis. *ACS Catal.* **2020**, *10*, 2707-2712.

(51) Wang, D.; Liang, X.; Xiong, M.; Zhu, H.; Zhou, Y.; Pan, Y. Synthesis of Unsymmetrical Disulfides Via Pph3-Mediated Reductive Coupling of Thiophenols with Sulfonyl Chlorides. *Org. Biomol. Chem.* **2020**, *18*, 4447-4451.

(52) Yoshida, S.; Nagai, A.; Uchida, K.; Hosoya, T. Enhancing the Synthetic Utility of 3-Haloaryne Intermediates by Their Efficient Generation from Readily Synthesizable Ortho-Iodoaryl Triflate-Type Precursors. *Chem. Lett.* **2017**, *46*, 733-736.

(53) Du, Y.; He, W.; Zhou, W.; Li, X. Disulfide Phosphatidylcholines: Alternative Phospholipids for the Preparation of Functional Liposomes. *Chem. Commun.* **2019**, *55*, 8434-8437.

(54) Biscans, A.; Rouanet, S.; Vasseur, J.-J.; Dupouy, C.; Debart, F. A Versatile Post-Synthetic Method on a Solid Support for the Synthesis of Rna Containing Reduction-Responsive Modifications. *Org. Biomol. Chem.* **2016**, *14*, 7010-7017.

(55) Sheppard, J. G.; McAleer, J. P.; Saralkar, P.; Geldenhuys, W. J.; Long, T. E. Allicin-Inspired Pyridyl Disulfides as Antimicrobial Agents for Multidrug-Resistant Staphylococcus Aureus. *Eur. J. Med. Chem.* **2018**, *143*, 1185-1195.

(56) Oka, M.; Katsube, D.; Tsuji, T.; Iida, H. Phototropin-Inspired Chemoselective Synthesis of Unsymmetrical Disulfides: Aerobic Oxidative Heterocoupling of Thiols Using Flavin Photocatalysis. *Org. Lett.* **2020**, *22*, 9244-9248.

(57) Song, L.; Li, W.; Duan, W.; An, J.; Tang, S.; Li, L.; Yang, G. Natural Gallic Acid Catalyzed Aerobic Oxidative Coupling with the Assistance of Mnco3 for Synthesis of Disulfanes in Water. *Green Chem.* **2019**, *21*, 1432-1438.

NMR Spectrum of Selected Compounds

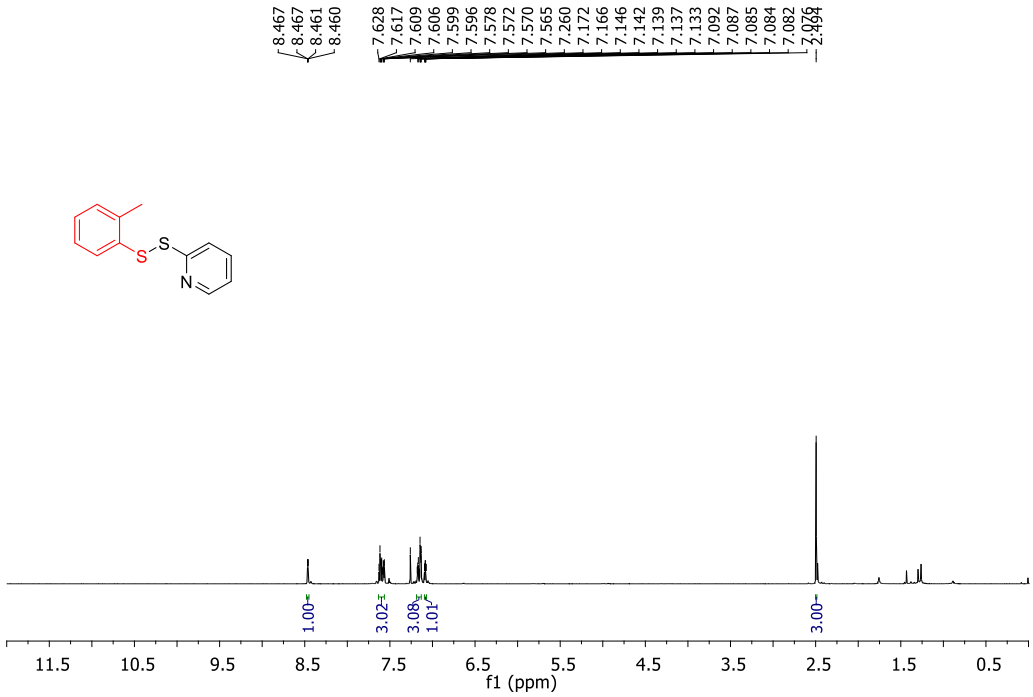

Fig. 6.17. ^{1}H NMR spectrum of 2-(o-tolyldisulfaneyl)pyridine **(2ag)**

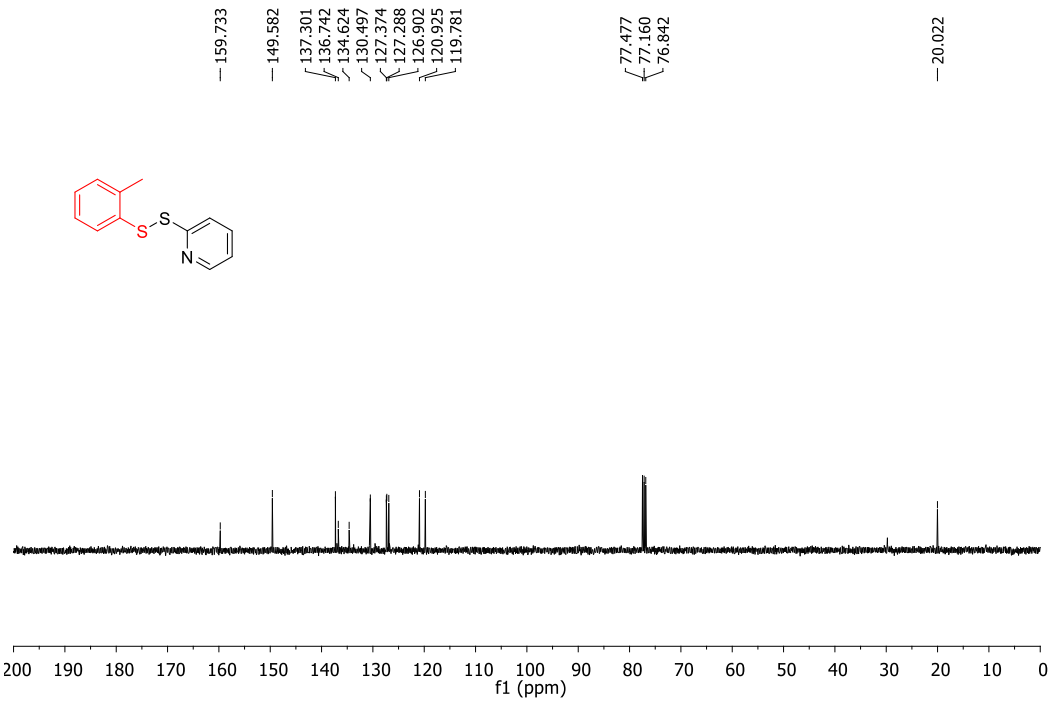

Fig. 6.18. ^{13}C NMR spectrum of 2-(o-tolyldisulfaneyl)pyridine **(2ag)**

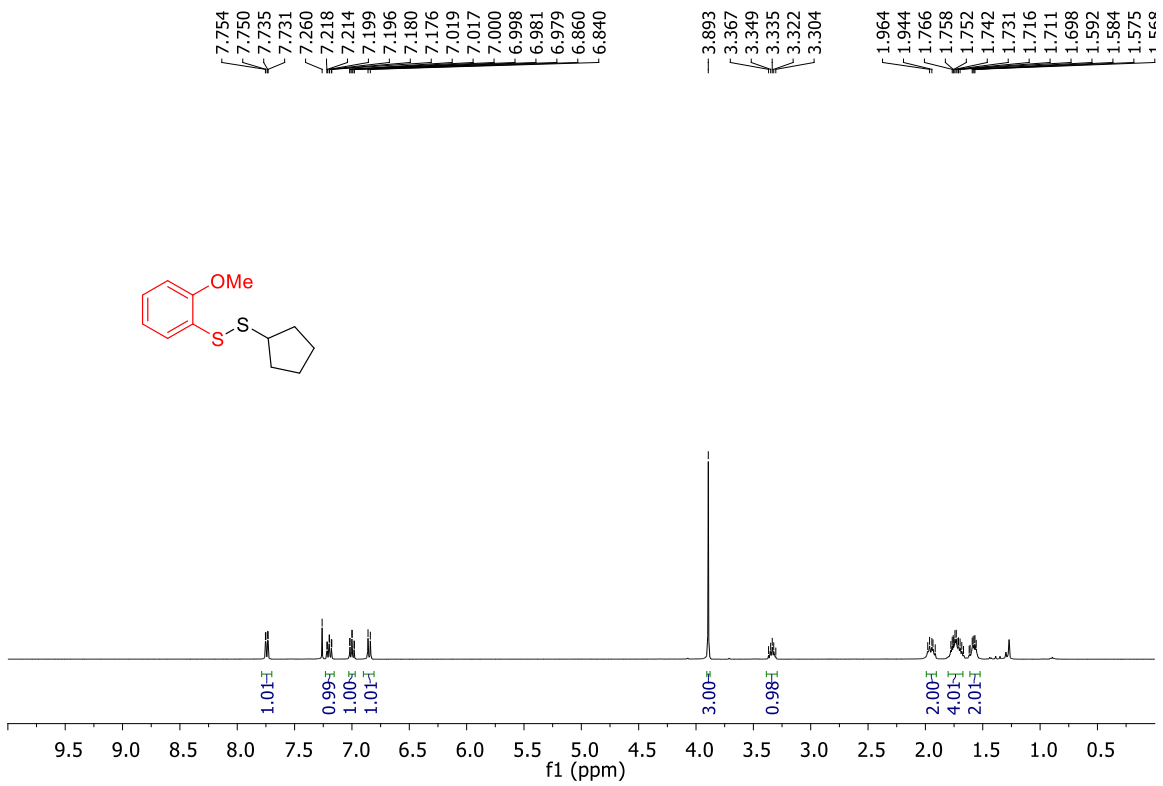

Fig.6.19. ^{1}H NMR spectrum of1-cyclopentyl-2-(2-methoxyphenyl)disulfane **(2ch)**

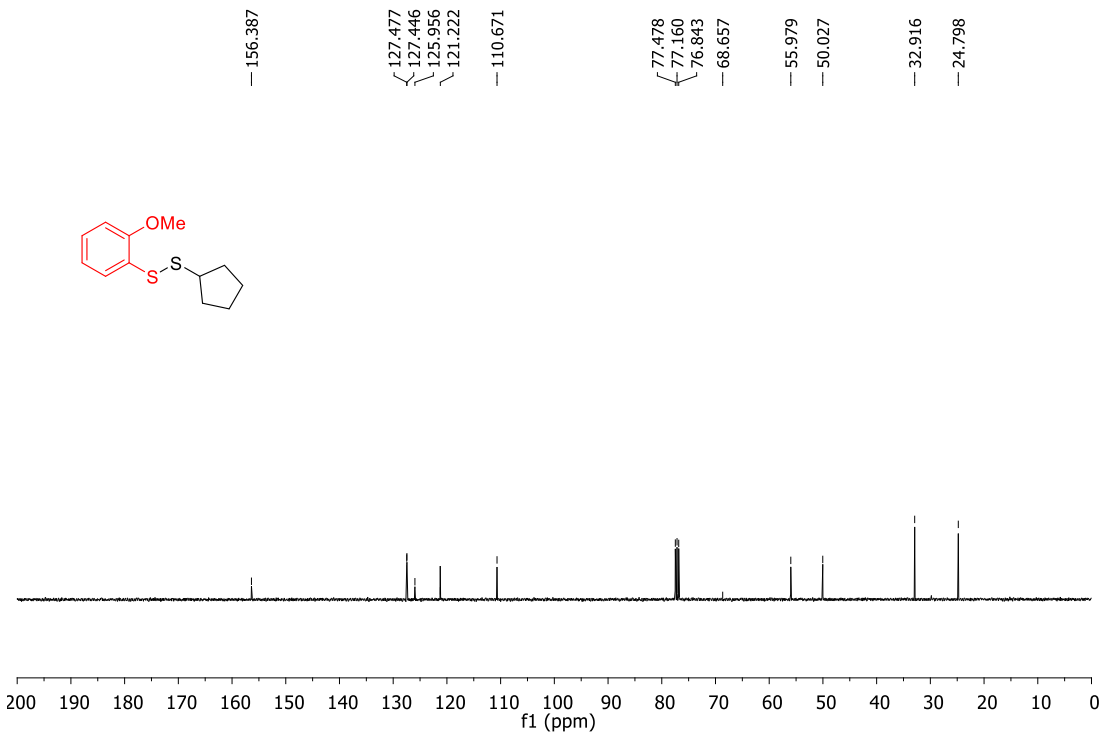

Fig. 6.20. ^{13}C NMR spectrum of 1-cyclopentyl-2-(2-methoxyphenyl)disulfane **(2ch)**

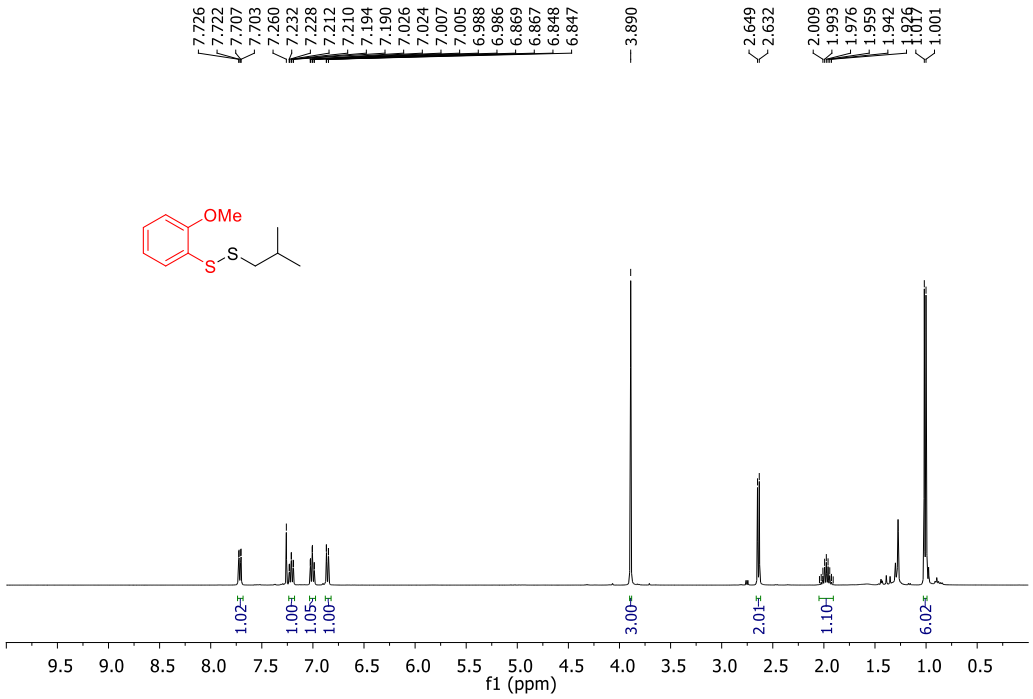

Fig. 6.21. ^{1}H NMR spectrum of 1-isobutyl-2-(2-methoxyphenyl)disulfane **(2cn)**

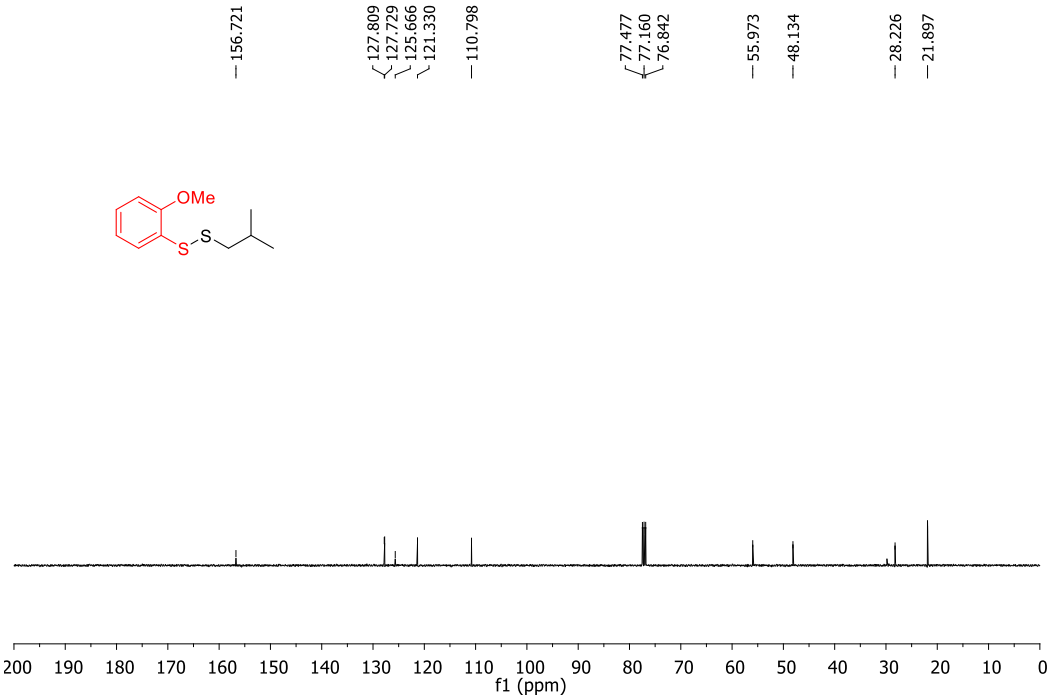

Fig. 6.22. ^{13}C NMR spectrum of 1-isobutyl-2-(2-methoxyphenyl)disulfane **(2cn)**

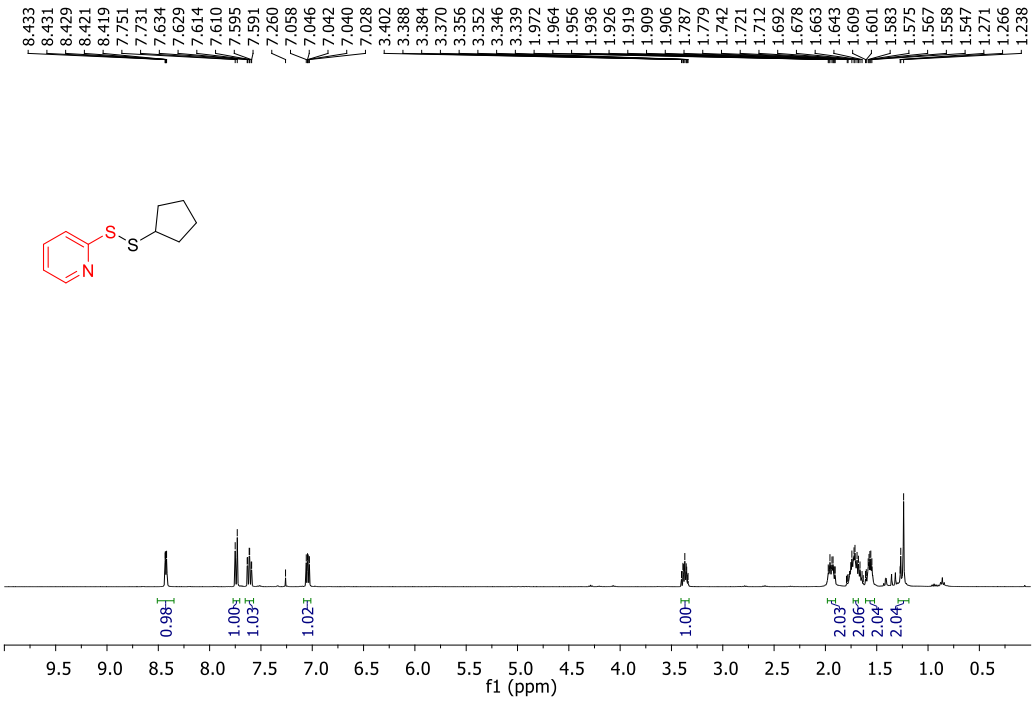

Fig. 6.23. ^{1}H NMR spectrum of 2-(cyclopentyldisulfaneyl)pyridine **(2gh)**

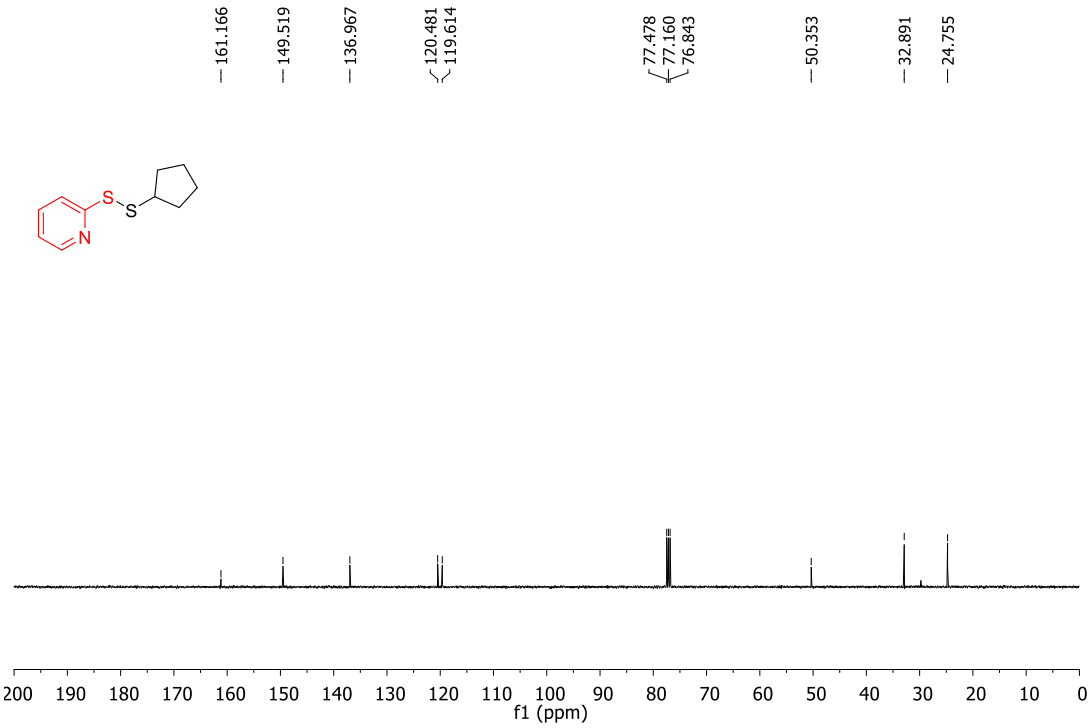

Fig. 6.24. ^{13}C NMR spectrum of 2-(cyclopentyldisulfaneyl)pyridine **(2gh)**

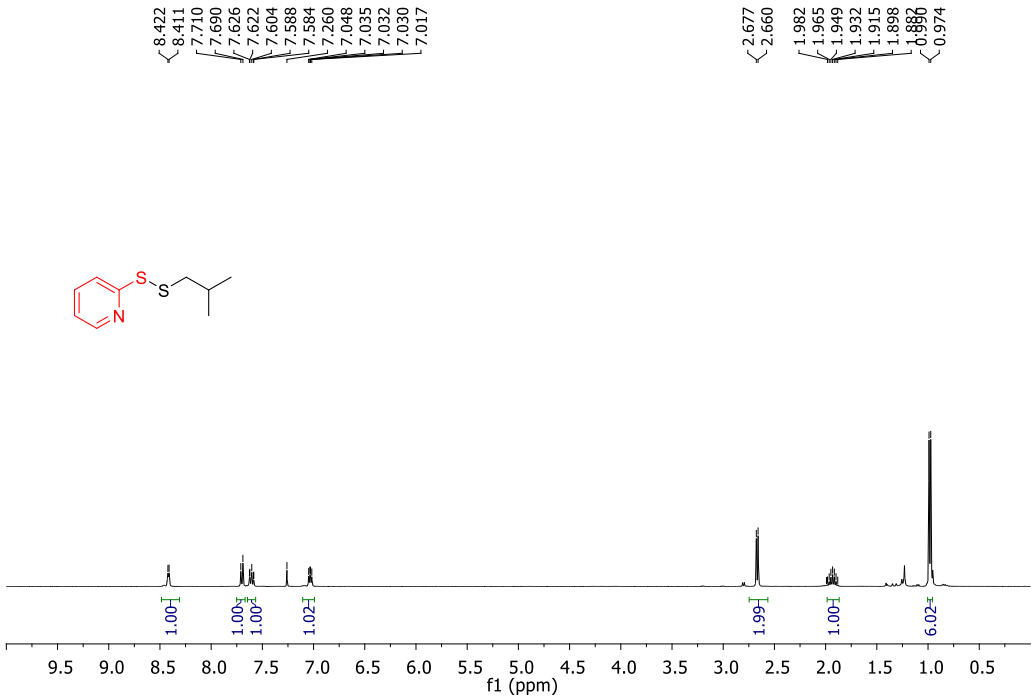

Fig. 6.25. ^{1}H NMR spectrum of 2-(isobutyldisulfaneyl)pyridine **(2gn)**

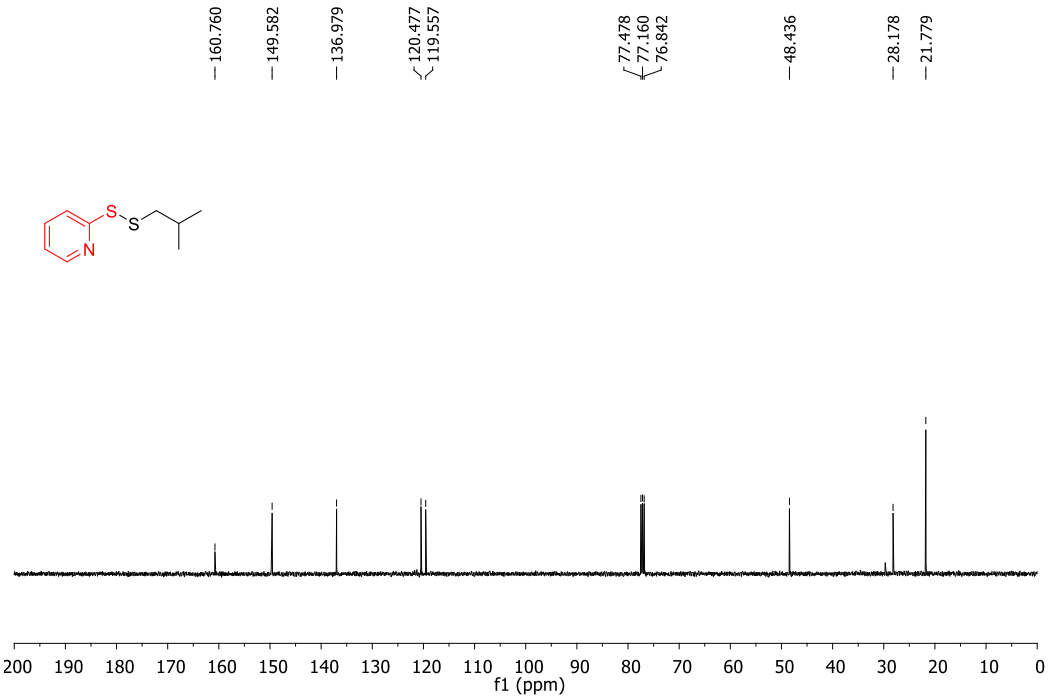

Fig. 6.26. ^{13}C NMR spectrum of 2-(isobutyldisulfaneyl)pyridine **(2gn)**

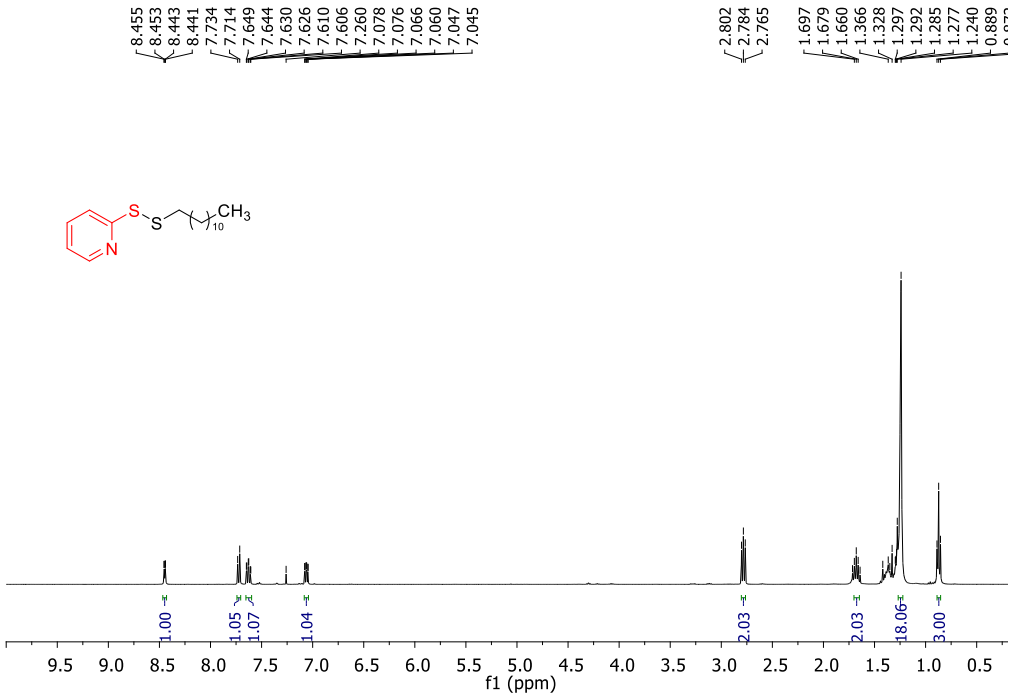

Fig. 6.27. ^{1}H NMR spectrum of 2-(dodecyldisulfaneyl)pyridine **(2go)**

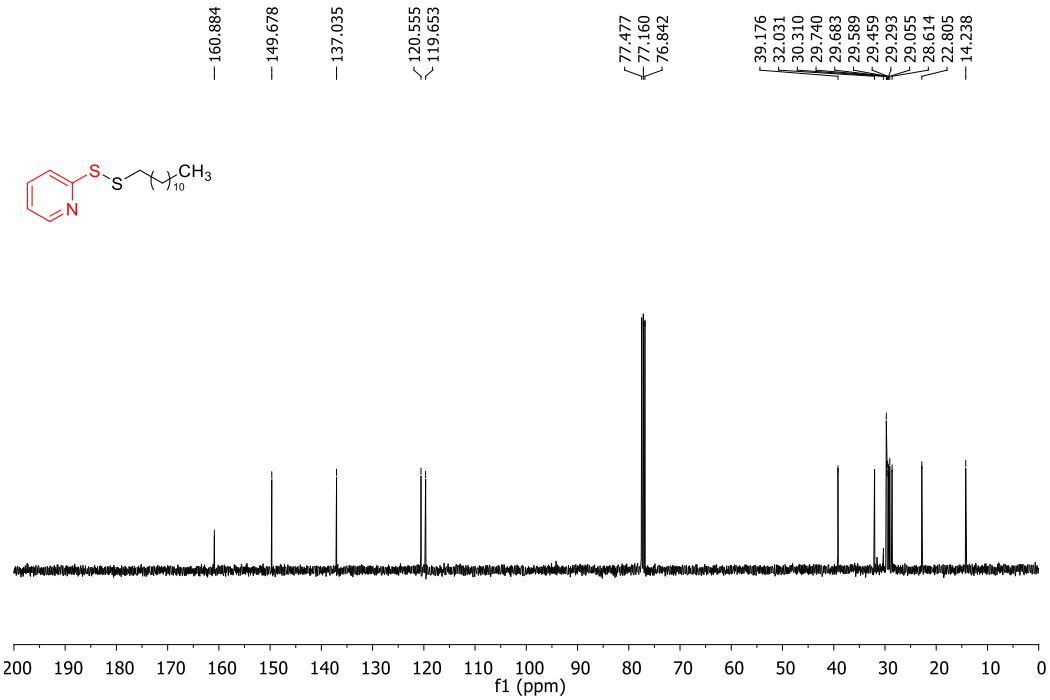

Fig. 6.28. ^{13}C NMR spectrum of 2-(dodecyldisulfaneyl)pyridine **(2go)**

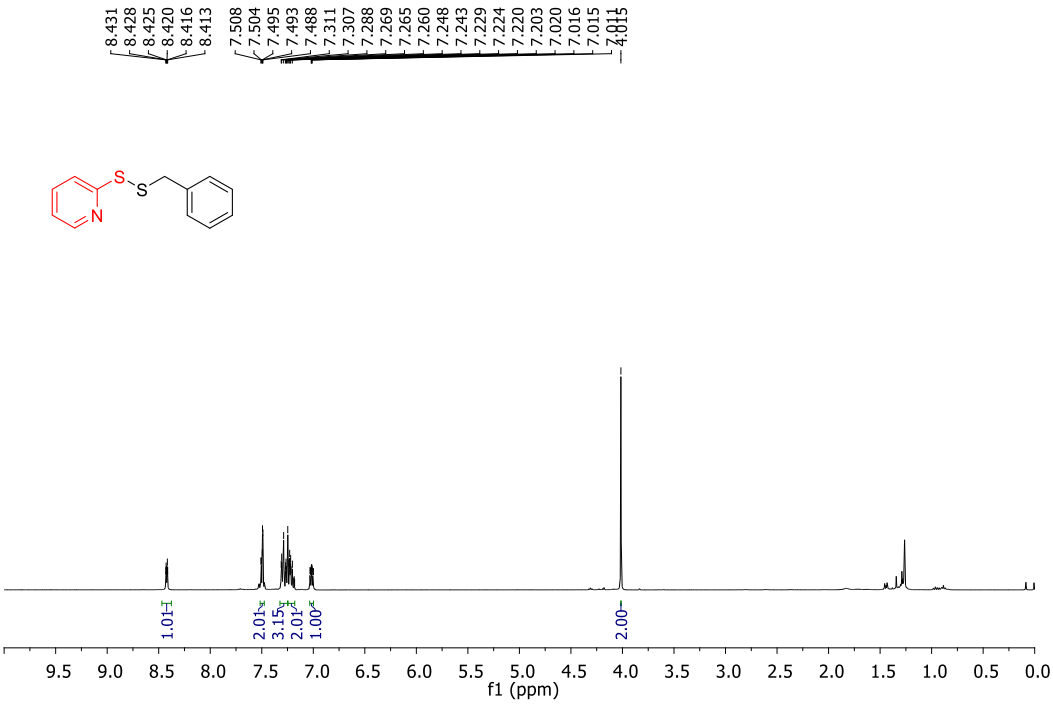

Fig. 6.29. ^{1}H NMR spectrum of 2-(benzyldisulfaneyl)pyridine **(2gj)**

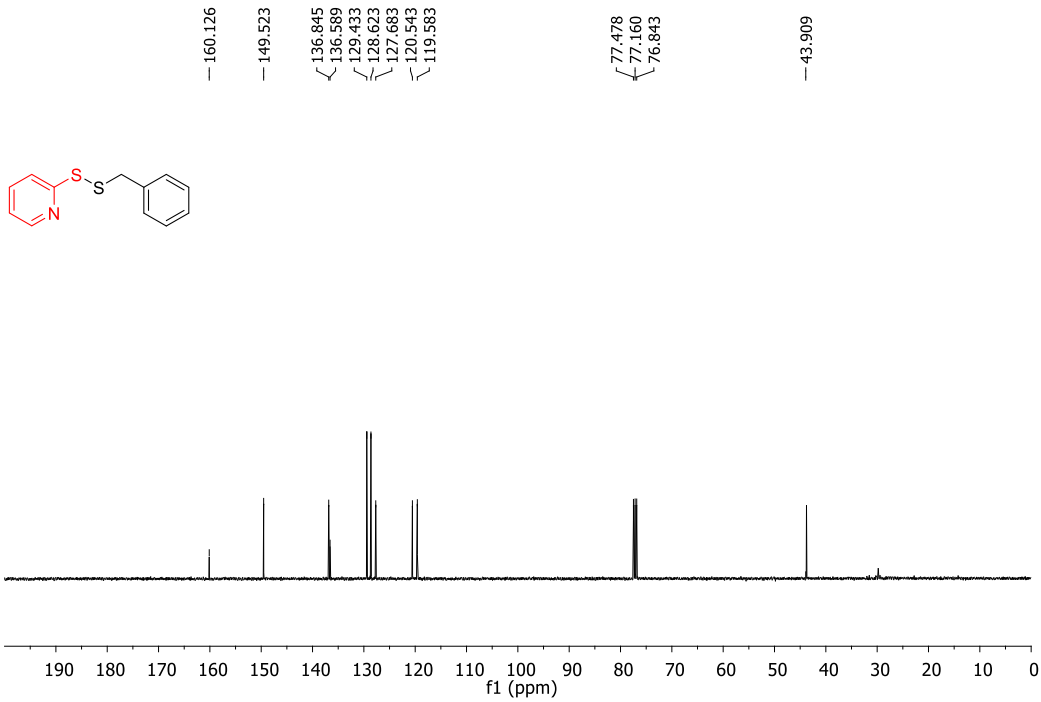

Fig. 6.30. ^{13}C NMR spectrum of 2-(benzyldisulfaneyl)pyridine **(2gj)**

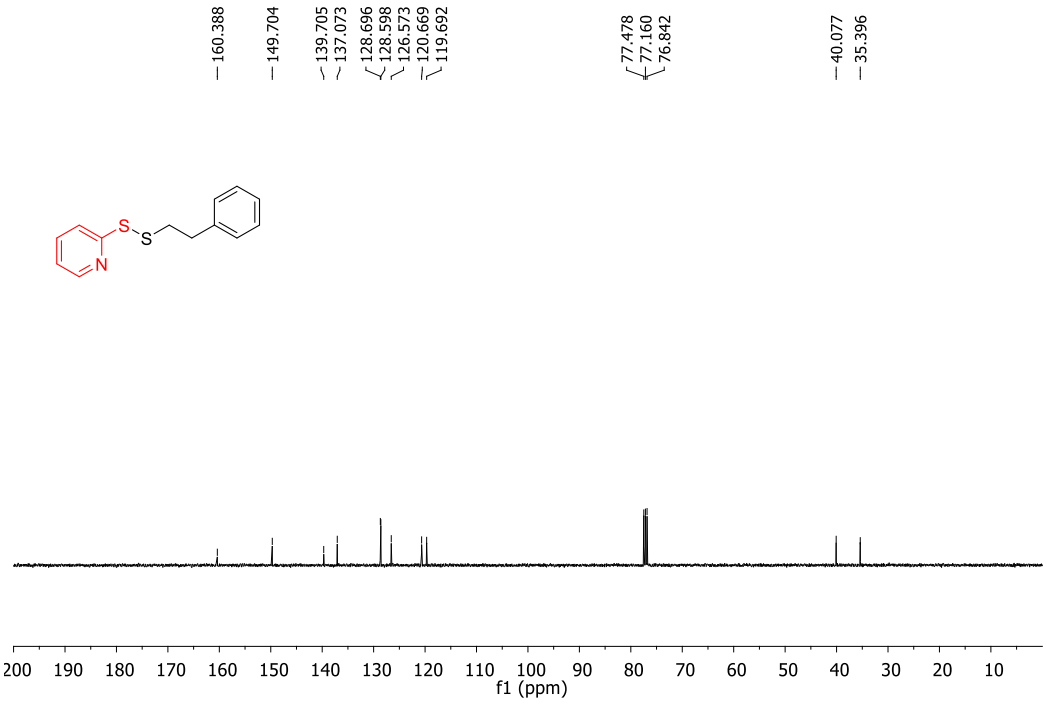

Fig. 6.31. ^{13}C NMR spectrum of 2-(phenethyldisulfaneyl) pyridine **(2gl)**

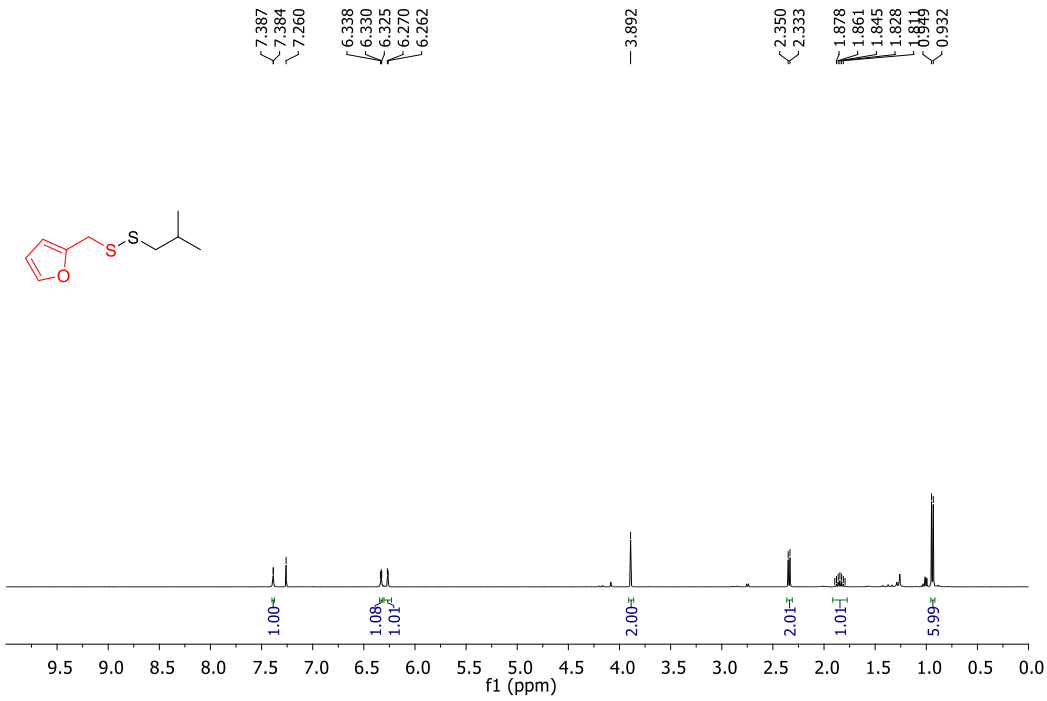

Fig. 6.32. ^{1}H NMR spectrum of 2-((isobutyldisulfaneyl) methyl) furan **(2mn)**

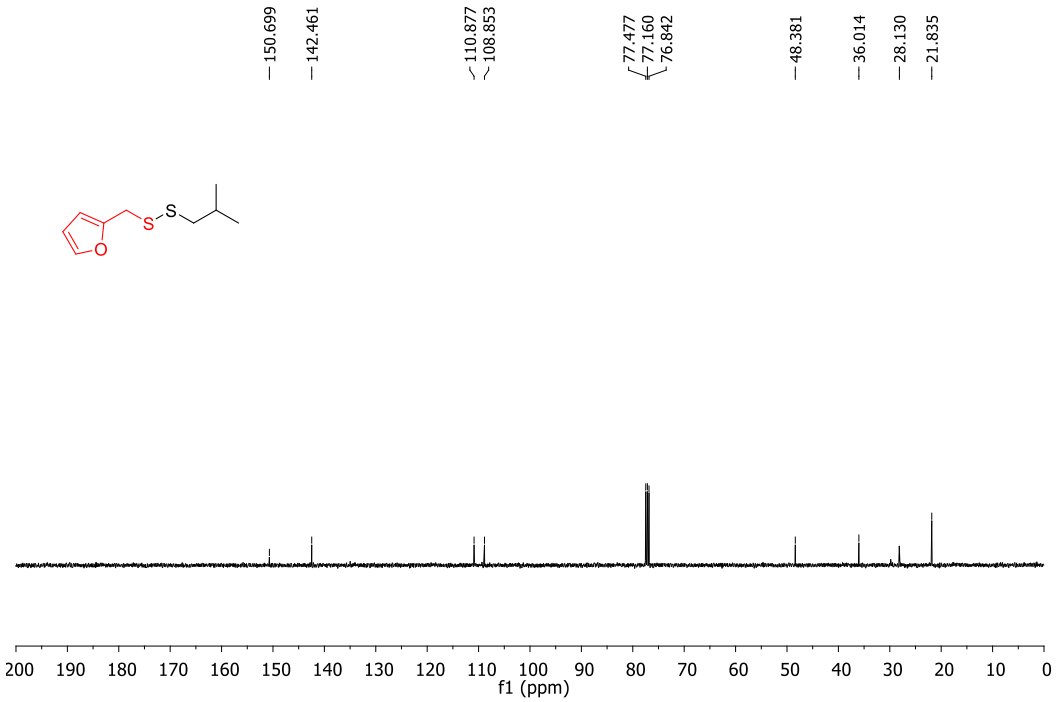

Fig. 6.33. ^{13}C NMR spectrum of 2-((isobutyldisulfaneyl) methyl)furan **(2mn)**

Thesis at a Glance

Reactivity of Alkynes

J. Org. Chem. **2022**, *87 (10), 6812-6823*

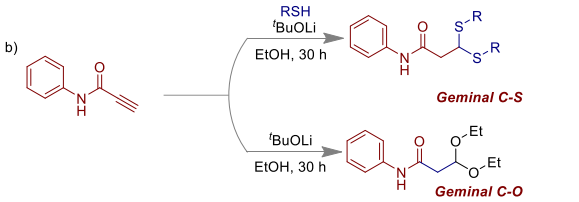

Org. Biomol. Chem. **2022**, **20,** 2671

Disulfide Methathesis

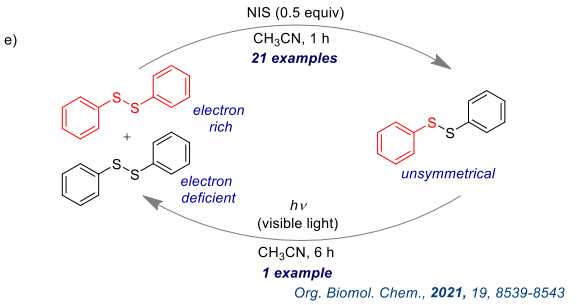

Org. Biomol. Chem., ***2021,*** *19, 8539-8543*

Visible Light Photocatalyst

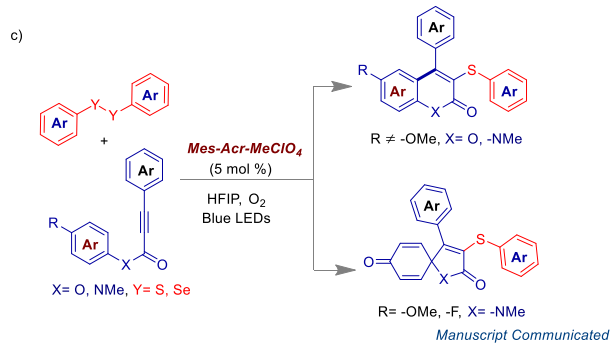

Manuscript Communicated

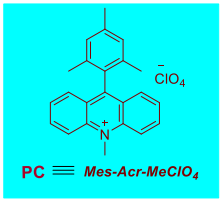

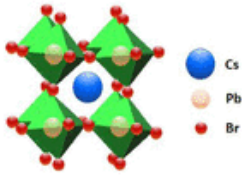

Manuscript Communicated

Overall Work

Reactivity of Alkynes

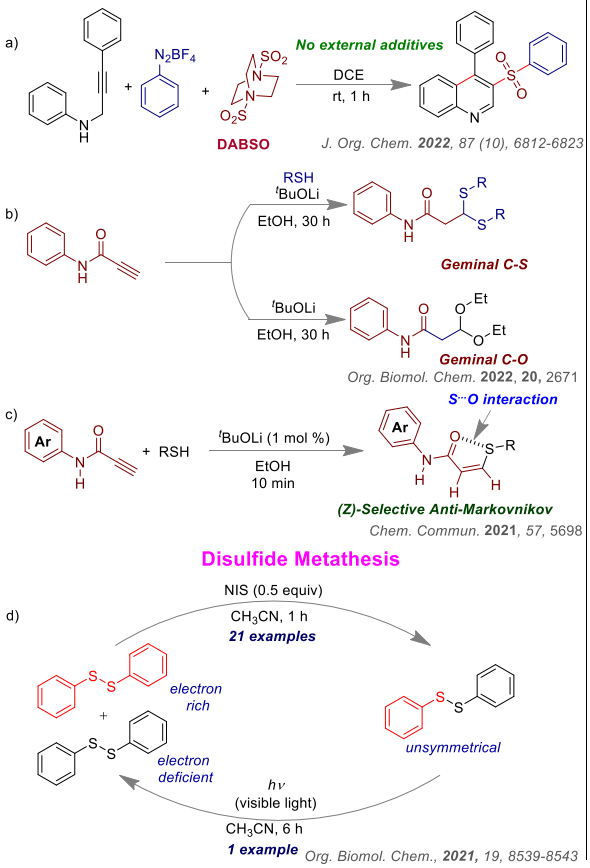

Disulfide Metathesis

Visible Light Photocatalyst

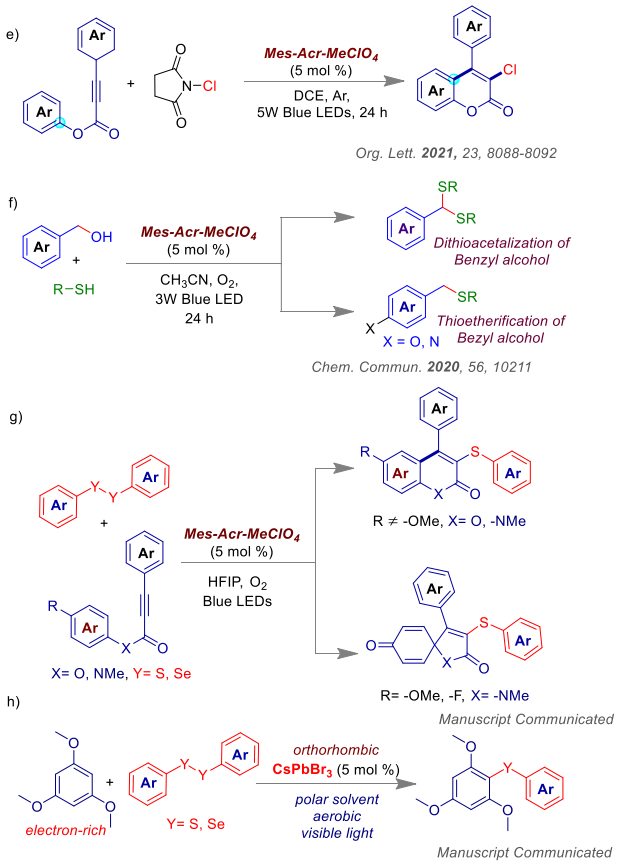

Conclusion and Future Prospect

Organosulfur compounds are omnipresent in bioactive molecules and natural products. Their substantial utilization is recognized in diverse pharmaceuticals, agrochemicals, pesticides, medical chemistry, and material science fields. Therefore, finding mild, sustainable, and step-economic strategies for the synthesis of organosulfur compounds has become an essential topic of research in synthetic organic chemistry. To achieve environmentally benign methods, chemists have rendered unremitting efforts to replace harsh reaction conditions with mild reagents. In this regard, the major focus of this thesis is to introduce mild and sustainable protocols towards the synthesis of organosulfur compounds. We have shown that 1 mol % of lithium *tert*-butoxide (^{t}BuOLi) was sufficient for generating thiyl radical to conduct an addition reaction between *N*-phenylpropiolamide and aliphatic thiol in ethanol. In continuation, we explored a cascaded oxidative sulfonylation reaction of *N*-propargylamine *via* a three-component coupling reaction using *N*-propargylamine, diazonium tetrafluoroborate, and DABSO under an argon atmosphere in dichloroethane (DCE) which delivered 3-arylsulfonylquinolines with good to excellent yields. Next, we disclosed two unprecedented visible light-induced organic transformations. DBIA-$CsPbBr_3$ nano-crystals (NC) was utilized as visible light photocatalyst for C-H chalcogenation reaction. Following, we achieved a visible-light promoted cascaded chalcogenation of arylalkynoates and *N*-arylpropiolamides using 9-mesityl-10-methylacridinium perchlorate as visible-light photocatalyst which furnished 3-sulfenylated/selenylated coumarins or spiro[4,5]trienones. Finally, we discussed the synthesis of unsymmetrical diaryl disulfides from two symmetrical disulfides *via* a cross-metathesis reaction controlled by a weak sulfur…iodine (S…I) interaction. The unsymmetrical disulfides were stable in acetonitrile solution in the presence of *N*-iodosuccinimide (NIS), and were reversibly converted to the symmetrical disulfides under visible light irradiation. In summary, these simple, cost-effective, and sustainable protocols are anticipated to contribute

significantly to the research areas like cascade cyclization reactions, visible-light photocatalysis, Moreover, we have shown the gram-scale synthesis for each protocol, so the synthesis of these compounds can be scaled up at the industry level and our protocols might get commercial importance and have significant applications in medicinal chemistry, pharmaceutical industries and other fields.